48th International Symposium CIB W062

Water supply and drainage for buildings

CIB W062
Leuven / 2023

29th to 31th August 2023

Leuven, Belgium

Intentionally blank page

The 48th International Symposium CIB W062 is hosted by

Main sponsors

Sponsors

SYMPOSIUM WELCOME

Dear colleagues and professionals,

The 48th International Symposium on Water Supply and Drainage for Buildings, CIB W062, is organised by the Belgian CIB Member Buildwise with the support of the International Council for Research and Innovation in Buildings and Construction (CIB) and in particular, the Chair of CIB W062, Professor Lynne Jack from Heriot-Watt University, Scotland.

This Symposium will take place in Leuven, Belgium from 29th to 31st of August 2023.

The purpose of this Symposium is to disseminate global research and innovation in water supply and drainage for buildings which will contribute to the ongoing progression of this field of expertise.

The proceedings contain 43 papers, presented in nine technical sessions. The sessions cover topics that are important to our profession, including "Health and Hygiene","Sizing" and "Low water consumption in buildings" amongst others.

We thank all the authors for their contributions and presentations and hope they will enjoy our country, in particular Leuven. Our appreciation is also extended to our international scientific committee and to our sponsors for supporting this event.

We encourage each one of you to contribute your insights, and make the most of this invaluable platform. Together, we can build a stronger foundation for advancements in water supply and drainage practices that will benefit communities worldwide.

We also encourage any CIB Non Members attending, to embrace membership and continue to contribute to the ongoing success of CIB W062 in 2024.

I genuinely look forward to meeting all of you, and together, let's make this symposium a resounding success!
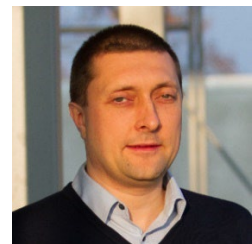
Bart Bleys
48th CIB W062 Organising Chairman

International Scientific Committee
L. Jack, Co-ordinator of CIBW62, Heriot Watt University, Scotland
A. Silva Afonso, University of Aveiro and Chair of ANQIP, Portugal
B. Bleys, Buildwise, Belgium
C. L. Cheng, Taiwan University of Science and Technology, Taiwan
P. DeMarco, IAPMO, USA
M. Nekrep, Univresity of Maribor, Slovenia
L. H. Oliveira, University of Sao Paulo, Brazil
M. Otsuka, Kanto Gakuin University, Japan
L. T. Wong, Hong Kong Polytechnic University, China
M. S. O Ilha, University of Campinas, Brazil
O. M. Goncalves, University of Sao Paulo, Brazil
Z. Vranayova, Technical University of Kosice, Slovakia

Table of Contents

PROGRAM DAY 1 – TUESDAY 29th AUGUST

08:30 - 09:00	**REGISTRATION**
09:00 - 09:15	**SYMPOSIUM COMMENCES** **OPENING ADDRESS** Bart Ingelare – CGO Buildwise and CIB Board Member
09:15 - 10:45	**TECHNICAL SESSION 1 – SIZING I** *Chairs: L.B. Jack and L.T. Wong*
	Application of dynamic cold and hot water supply loads calculation method in buildings - Effects of introducing cold and hot water-saving plumbing fixtures in an apartment complex **H. Takata, S. Murakawa, D. Ikeda, K. Sakamoto**
	Examination of unit model applied to dynamic cold and hot water supply loads calculation method - as an example of toilet flushing water supply system in the office building **S. Murakawa, D. Ikeda, K. Sakamoto, H. Takata**
	Implementation of sustainability and circularity solutions in the building water cycle: The need to review sizing methods **A. Silva-Afonso, C. Pimentel-Rodrigues**
	Pipe sizing research in Australia; a decade on. **T. Roberts**
	Towards a better understanding of hot water demand in nursing homes **T. Delwiche, M. Guarini, C. Jacques, B. Poncelet, B. Bleys**
10:45 - 11:15	**COFFEE BREAK**
11:15 - 13:00	**TECHNICAL SESSION 2 – DRAINAGE** *Chairs: W. van der Schee and K. Dinne*
	The impact of current and future extreme rainfall events on historic buildings **D.A. Kelly and J.J. Claridge**
	Modification of the Building Drainage System airflow and pressure regime due to airflow from the sewer network. **K.S.Sharif, M.Gormley**
	A hybrid particle-polygon technique for the simulation of solid transport in a building drainage system **M.C.B. Teixeira, L. S. Pereira, R.A. Amaro Jr, L.Y. Cheng, L.H. Oliveira**
	Studies on High-pressure Washing of Drainage Pipe in Apartment Building Part 1 : Cleaning Performance in Actual Piping and Piping with Pseudo-Dirt **Y. Nishimura, T. Mitsunaga, K. Sakaue, K. Sakai**
	Study on simulation of building drainage systems by CFD Part 1 : Verification based on existing experimental results **S. Iwamoto, R. Fujimoto, K. Sakaue, T. Mitsunaga**
	Study on suitability of hybrid feed-forward-PSO ANN model for predicting pressure profile data in the building drainage system **I. Mahapatra, M. Gormley**

13:00 - 14:00	**LUNCH**
14:00 - 15:30	**TECHNICAL SESSION 3 – MISCELLANEOUS** *Chairs: B. Bleys and L.H. Oliveira*
	Experimental study of the heat transfer coefficient between human skin and the flowing water during showering **L.T. Wong, C.W. Poon, K.W. Mui, D. Zhang**
	Current Circumstances and Issues Surrounding Disposable Underwear Crushing/Disposal Systems to be Installed at Care and Nursing Homes **Y. Ino, M. Otsuka, A. Kimura, M. Maki**
	Aqua container house for natural disasters and non-sanitary areas Part 2 : Suitability evaluation by water use experiment **M. Hashimoto, H. Iizuka, K. Sakaue, T. Mitsunaga**
	Role of Discharge Water Temperature Upon Hydraulic Performance of High-Rise Wastewater Drainage Stacks **C. Stewart**
	Study on the performance and quality evaluation of unit bathrooms in Taiwan **C. Lo, C. Cheng**
15:30 - 16:00	**COFFEE BREAK**
16:00 - 17:15	**TECHNICAL SESSION 4 – HEALTH & HYGIENE I** *Chairs: C. Cheng and D. Kelly*
	Analysis of the possibility of dispersion of SARS-CoV-2 in bathrooms, using computational fluid dynamics (CFD) **L. S. Vieira, L.H. Oliveira, F.A. Kurokawa**
	Designing a lead measuring protocol in de domestic drinking water installation **M. Blokker, A. Dash**
	Study on Hand Washing for Preventing COVID-19 in Various Countries, Regulatory Trends, and Issues **M. Itabashi, M. Otsuka**
	Climate change - underestimated risk factor for domestic water hygiene **F. Schmidt**
17:15 - 18:30	**FREE TIME**
18:30 - 22:30	**SOCIAL PROGRAM**

PROGRAM DAY 2 – WEDNESDAY 30th AUGUST

08:30 - 10:00	**TECHNICAL SESSION 5 – ENERGY AND GHG EMISSIONS REDUCTION** *Chairs: M. Gormley and S. Murakawa*
	Advanced building facilities embodying the transition to carbon neutrality **K. Osako, U. Roslan, K. Shibata, N. Aizawa, M. Otsuka**
	Impact of domestic hot water safety advices on energy consumption and the energy transition in The Netherlands **A. Moerman, F. Oesterholt**
	Study on Energy Efficiency Evaluation Indicators for Building Hot Water Systems in Taiwan **H. Huang, C. Cheng**
	The energy saving efficiency of hot water transmission pipeline between PU-insulated and uninsulated stainless pipes. **M. C. Jeffrey Lee**
	Climate resilience design of potable water installations in buildings - hygienic safe temperature reduction of potable water hot (PWH) **C. Schauer**
10:00 - 10:30	**COFFEE BREAK**
10:30 - 11:30	**TECHNICAL SESSION 6 - LOW WATER CONSUMPTION BUILDINGS I** *Chairs: A. Silva-Afonso and M. Otsuka*
	Research of water saving design and near zero water consumption feasibility for office buildings **W. Chang, C. Cheng, K. Sadahico**
	Study on water balance and environmental performance evaluation in buildings Part 3 : Water Balance and CO2 Emissions by Precipitation Characteristics of Rainwater Utilization Buildings **J. Oyagi, T. Nishikawa**
	Towards the Feasibility of Near-Zero Water Consumption Buildings **Sadahico Kawamura, Cheng-Li Cheng**
11:30 - 12:30	**TECHNICAL SESSION 7 – LOW WATER CONSUMPTION BUILDINGS II** *Chairs: H. Kose and B. Bleys*
	Economic feasibility of implementing rainwater harvesting systems for sustainable urban water management: A case study in Goiânia, Brazil. **L.M. Gonçalves, M. A. S. Campos**
	CO2 Emissions from Water Supply Facilities and Rainwater Utilization Facilities in Japan **U. Takeuchi, T. Mitsunaga**
	Navigating Modern Crises through Sustainable and Resilient Urban Development (How to do more with Less?) **H. Nekrep, M. Nekrep Perc, T. P. Nekrep**

12:30 - 14:00	**LUNCH**
14:00 - 15:45	**TECHNICAL SESSION 8 – HEALTH & HYGIENE II** *Chairs: L.B. Jack and M. Nekrep*
	Study on Evaporation Phenomenon of Trap Seal Water Part 2 : Indoor and outdoor evaporation rates by regions **T. Mitsunaga, K. Sakaue**
	Improving the Environment of Toilet Spaces in Evacuation Centers —Organizing the Problem of Evacuation Toilets based on Previous Studies and the Thermal Environment of Temporary Toilets— **H. Yamaguchi**
	Risk Assessment to Contaminant Spreading through Building Drainage System in Residential Building **Y Lin, C. Cheng**
	The Transport of a Model Viral Pathogen on Bioaerosols through a Full-Scale Building Drainage Test Rig under Realistic Conditions **T. Dight, M. Gormley**
	Trends in Studies, and Reviews Thereof, in Relation to Droplets on and around Toilets that Can Cause Infections **A. Kimura, M. Otsuka**
	Vertical bioaerosol transmission in toilet environment **Tsang TW, Mui KW, Wong LT, Wong YS**
15:45 - 16:15	**COFFEE BREAK**
16:15 - 17:45	**TECHNICAL SESSION 9 – SIZING II** *Chairs: M.C. Jeffrey Lee and C. Pimentel-Rodrigues*
	An international review of design requirements for the single stack drainage configuration **J. S. Lansing**
	Modeling Study of "Zero Water Building" **H. Kose**
	Comparison and Assessment of Building Drainage Design Codes for use in Tall Buildings **S. A. Mohammed, M. Gormley, C. Stewart, D.A. Kelly and D.P Campbell**
	DHW production for collective residential buildings: development of a sizing method **B. Poncelet, B. Bleys**
	The need for a new approach to the assessment of water demand loading, post-Covid, for office buildings **L.B. Jack, S. Fernandez, S. Dass and C. Rogers**
17:45 - 18:30	**FREE TIME**
18:30 - 22:00	**SOCIAL PROGRAM**

PROGRAM DAY 3 – THURSDAY 31th AUGUST

TECHNICAL VISITS

09:00 - 09:45	**TRIP TO BUILDWIZE LIMELETTE**
09:45 - 10:15	**ARRIVAL AND WELCOME**
10:15 - 12:30	**TECHNICAL VISIT BUILDWISE LIMELETTE**
	Water tower visit
	Experience lab exploration
	Acoustic lab exploration
12:30 - 13:30	**LUNCH**
14:00 - 14:45	**TRIP TO BUILDWISE ZAVENTEM**
14:45 - 16:00	**TECHNICAL VISIT BUILDWISE ZAVENTEM**
	Green walls and efficient heating system
	Virtual reality
	Drones flight
16:00 - 17:00	**ROOFTOP DRINK**
17:00 - 17:45	**TRIP TO PARK-INN LEUVEN**
17:45 - 18:30	**FREE TIME**
18:30 - 23:00	**SOCIAL PROGRAM**

TECHNICAL SESSION 1 – SIZING I

Application of dynamic cold and hot water supply loads calculation method in buildings - Effects of introducing cold and hot water-saving plumbing fixtures in an apartment complex

**Hiroshi Takata (1), Saburo Murakawa (2),
Daisuke Ikeda (3), Kazuhiko Sakamoto (4)**

(1) h.takata.h5@it-hiroshima.ac.jp
(2) saburo.murakawa@gmail.com
(3) daisuke.ikeda225@gmail.com
(4) ksakamoto@archi.ous.ac.jp

(1) Hiroshima Institute of Technology, Japan
(2) Hiroshima University, Japan
(3) Tokyo Tatemono Co., Ltd, Japan
(4) Okayama University of Science, Japan

Abstract

Accurate prediction of cold and hot water supply loads is the basis for the optimal design of cold and hot water supply systems for buildings. However, it has been pointed out that these existing prediction methods in this field do not necessarily reflect the actual situation in the circumstances where water saving and energy saving are progressing in recent years, and they show excessive values. Therefore, through the CIB-W062 symposium, etc., the authors have proposed a dynamic calculation method for cold and hot water supply loads by simulation technique that applies the Monte Carlo method in order to solve various problems with the conventional calculation method. Moreover, in April 2020, the authors published a book titled "New Calculation Method for Cold and Hot Water Supply Loads in Buildings, and Application to Practical Design", summarizing the series of research results [1]. The calculation program named MSWC (Murakawa's Simulation for Water Consumption) can be downloaded free of charge from the website of Shokokusha Co., Ltd. (https://www.shokokusha.co.jp/DL/321490/).

In this paper, after giving an overview of the MSWC program, the authors present a model of cold and hot water usage for each number of households set for an apartment complex, and show that these models can be easily changed according to the water usage manners and customs of the country. As the calculation results, the authors show the cold and hot water supply loads when conventional standard plumbing fixtures and water-saving

plumbing fixtures are installed for four-person households, and clarify the effect of installing cold and hot water-saving fixtures. In addition, this program shows that a series of loads can be grasped from instantaneous loads to hourly loads and daily loads.

Keywords

Cold and hot water supply loads; Dynamic calculation method; Monte Carlo simulation technique; MSWC program; Apartment complex; Cold and hot water-saving plumbing fixtures

1 Introduction

The MSWC program is a new calculation method for cold and hot water supply loads in buildings developed by the authors. The program simulates people's water usage behavior in buildings by simulation technique that applies the Monte Carlo method and can calculate the cold and hot water supply loads on a time-series basis.

As we have already presented at past CIB-W062 symposiums, this program incorporates calculation models of various building types such as apartment complex, office building, hotel, and restaurant and so on [2] - [10].

In this paper, the authors present a model for calculating the cold and hot water supply loads in an apartment complex and explain that the setting conditions can be easily changed according to water usage manners and customs. Especially in Japan, it is expected that changes in living time, home time and the number of hands washing times are occurring due to the COVID-19 pandemic, so it is possible to change the calculation conditions due to such changes in habits. The purpose of this study is to examine the effects of installing water-saving plumbing fixtures that have become popular in recent years. In addition, this program shows that a series of loads can be grasped from instantaneous loads to hourly loads and daily loads.

2 Calculation model for apartment complex for MSWC program

In the case of apartment, most of the cold and hot water used in the building are generated by the living activities of the residents. Therefore, it is important to grasp the number of household members in order to accurately predict the amount of water used. In addition, the lifestyle of the residents and the specifications of the installed plumbing fixtures also affect the amount of water used. The authors have established the calculation model shown below based on the results of previous research and analysis. However, it is also possible for designers to set their own models by referring to these models according to the characteristics of the building they are targeting.

2.1 Setting up cold and hot water usage models

Tables 1 shows the calculation models for cold and hot water supply loads per dwelling unit of apartment for summer and winter. Household composition ranges from one to five people. These models demonstrate summer and winter variations for water usage, taking

into account the temperature-dependent factors. Water and hot water are used for "Bathing", "Bathing & Shower", "Shower", "Bathtub hot water filling", "Wash basin using cold water", "Wash basin using hot water", "Kitchen etc. using cold water", "Kitchen etc. using hot water". "Washing machine", "WC-feces", and "WC-urine". These uses can be added or deleted as needed when calculating. Note that the model shown here is not classified by day of the week but assumes an average daily load. Therefore, the frequency of using the toilet is slightly lower values in this model because of assuming that there are people in the family who go out during the day. It is possible to change the usage frequency and the usage frequency ratio when there are many families who spend time in the house during the daytime.

Table 1 - Cold and hot water supply loads calculation model

(a) Summer

		Bathing	Bathing & Shower	Shower	Bathtub hot water filling	Wash basin (Cold water)	Wash basin (Hot water)	Kitchen, etc. (Cold water)	Kitchen, etc. (Hot water)	Washing machine	WC-feces	WC-urine
Water usage frequency per day [times/flat/day]	5 people	1.0	1.0	3.0	1.0	7.0	7.0	10.0	10.0	2.0	4.0	11.0
	4 people	0.8	0.8	2.4	1.0	6.0	6.0	8.0	8.0	1.8	3.0	9.0
	3 people	0.6	0.6	1.8	0.8	5.0	5.0	6.0	6.0	1.6	2.0	7.0
	2 people	0.4	0.4	1.2	0.6	4.0	4.0	4.0	4.0	1.2	1.5	5.0
	1 people	0.2	0.2	0.6	0.4	3.0	3.0	2.0	2.0	0.8	1.0	2.5
Average water discharge time (Distribution*, phase)	[s]	180	420	480	600	40	30	100	60	500	50	35
		Exp.	Exp.	Exp.	Erl.15	Hyp.5	Exp.	Hyp.5	Hyp.2	Exp.	Exp.	Exp.
Average discharge flow rate (Distribution*, phase)	[L/min]	9	9	8.5	14	12	8.5	12	8	12	10	10
		Erl.7	Erl.7	Erl.7	Erl.20	Erl.4	Erl.10	Erl.3	Erl.4	Erl.5	Erl.6	Erl.6
Operating temperature	[°C]	40	40	40	40	22	36	22	37	22	22	22
Ratio of water and hot water usage		1.00	1.00	1.00	1.00	0.80	0.20	0.80	0.20	1.00	1.00	1.00

*Note: Exp., Hyp. and Erl. mean exponential distribution, hyperexponential distribution and erlang distribution respectively.

(b) Winter

		Bathing	Bathing & Shower	Shower	Bathtub hot water filling	Wash basin (Cold water)	Wash basin (Hot water)	Kitchen, etc. (Cold water)	Kitchen, etc. (Hot water)	Washing machine	WC-feces	WC-urine
Water usage frequency per day [times/flat/day]	5 people	2.0	2.0	1.0	1.0	7.0	7.0	10.0	10.0	1.6	4.0	11.0
	4 people	1.7	1.7	0.6	1.0	6.0	6.0	8.0	8.0	1.4	3.0	9.0
	3 people	1.2	1.2	0.6	1.0	5.0	5.0	6.0	6.0	1.2	2.0	7.0
	2 people	0.8	0.8	0.4	0.8	4.0	4.0	4.0	4.0	0.8	1.5	5.0
	1 people	0.3	0.3	0.4	0.5	3.0	3.0	2.0	2.0	0.6	1.0	2.5
Average water discharge time (Distribution*, phase)	[s]	180	420	480	600	30	40	60	100	500	50	35
		Exp.	Exp.	Exp.	Erl.15	Hyp.5	Exp.	Hyp.5	Hyp.2	Exp.	Exp.	Exp.
Average discharge flow rate (Distribution*, phase)	[L/min]	9	9	8.5	14	12	8.5	12	8	12	10	10
		Erl.7	Erl.7	Erl.7	Erl.20	Erl.4	Erl.10	Erl.3	Erl.4	Erl.5	Erl.6	Erl.6
Operating temperature	[°C]	41	41	41	42	12	37	12	38	12	12	12
Ratio of water and hot water usage		1.00	1.00	1.00	1.00	0.40	0.60	0.30	0.70	1.00	1.00	1.00

*Note: Exp., Hyp. and Erl. mean exponential distribution, hyperexponential distribution and erlang distribution respectively.

The usage behavior of cold and hot water for each purpose in Table 1 is shown as values per dwelling unit, and the number of dwelling units to be calculated is set in the calculation program. Here, "Bathing", "Bathing & Shower", and "Shower" are set according to the bathing style. In other words, "Bathing" means using the bathtub but not using the shower, and assumes the use of hot water from the bathtub faucet and the use of hot water added to the bathtub. "Bathing & Shower" refers to the combined use of a bathtub and a shower. "Shower" refers to the use of shower only, and does not use hot water from the bathtub faucet. It is set so that the total number of times of these bathing behavior matches the number of household members. In this case, all members of the household use hot water in the bathroom once a day. If there is a change in behavior within the family, it is necessary to increase or decrease the frequency. The water discharge duration time and water discharge flow rate are set based on the survey results. The water supply and operating temperature for each use are set as different depending on the season. Also, it is not assumed that only water is used in the bathroom. Therefore,

the "Ratio of water and hot water usage" in the bathroom is set to "1.00" for each bathing behavior, and the usage of fixture is based on the set temperature of hot water.

In the wash basin, "Wash basin using cold water" and "Wash basin using hot water" are set assuming that cold water is used and hot water is also used. The frequency of use per day for both is assumed to be the same, but this each frequency is multiplied by the "Ratio of cold and hot water usage" to calculate the frequency of use of cold water or hot water, respectively. The ratio of hot water usage in summer is set to 0.20, but if there is no use of hot water in some areas, the ratio can be modified to 1.00 for cold water use and 0.00 for hot water use.

The conditions for "Kitchen, etc." are set assuming the use of cold water and hot water in the same way as the "Wash basin". The frequency of use in this model includes water use activities such as sweeping up, as well as cooking and washing dishes. For "Washing machine", the frequency of water usage per day is set according to the number of household members. Here, the water discharge duration time is 500 seconds, the water discharge flow rate is 12 L/min, and the amount of water used per washing is 100 L. In washing machines, the standard amount of water used varies depending on the washing method, and in recent years water saving has been progressing. Therefore, if a water-saving washing machine is used, it is possible to set the water discharge duration time to be short. This calculation model does not consider the use of hot water or the reuse of leftover hot water in the bathtub. The "Toilet" has a system that allows the flushing of the toilet bowl to be switched between feces and urine.

It is easy to grasp the average amount of water and hot water used for each purpose from the values of water usage shown in Table 1. Here, the daily water consumption of the entire dwelling unit is 250-275L for a one-person household and 815-958L for a five-person household. In addition, the intermediate period, which is considered as an annual average model, is based on the average values of summer and winter.

2.2 Setting up hourly water usage frequency models

For this calculation method, it is necessary to know the frequency of water usage on an hourly basis. For apartment, the daily frequency of water usage given by the number of household members shown in Table 1 should be assigned to the hourly values. For that purpose, it is necessary to set the ratio of each hourly period to the daily usage frequency for each usage or appliance. Based on the results of past surveys, the authors have set the fluctuation patterns shown in Figures 1 (a) to (h), taking into account the effect of the number of household members. Here, there are slight differences in usage time between small and large households depending on the season. Slight differences are set for each occurrence pattern of usage frequency. In addition, two patterns are set in consideration of the number of people in a household for "Wash basin", "Kitchen, etc.", and "Washing machine". For the intermediate season, the average pattern of summer and winter is used. In the calculation program, the "Hourly water usage frequency" for each use is calculated by multiplying the water usage frequency per day shown in Table 1 by the hourly water usage frequency ratio shown in Figure 1. This value is calculated automatically, but the value per dwelling unit is small depending on the time of day. Therefore, in terms of accuracy in calculation, it is desirable that this program should be calculated for 10 or more dwelling units, and the average value per dwelling unit should be calculated from the results.

(a) Bathing

(b) Bathing & Shower

(c) Shower

(d) Bathtub hot water filling

(e) Wash basin

(f) Kitchen, etc.

(g) Washing machine

(h) WC-feces and WC-urine
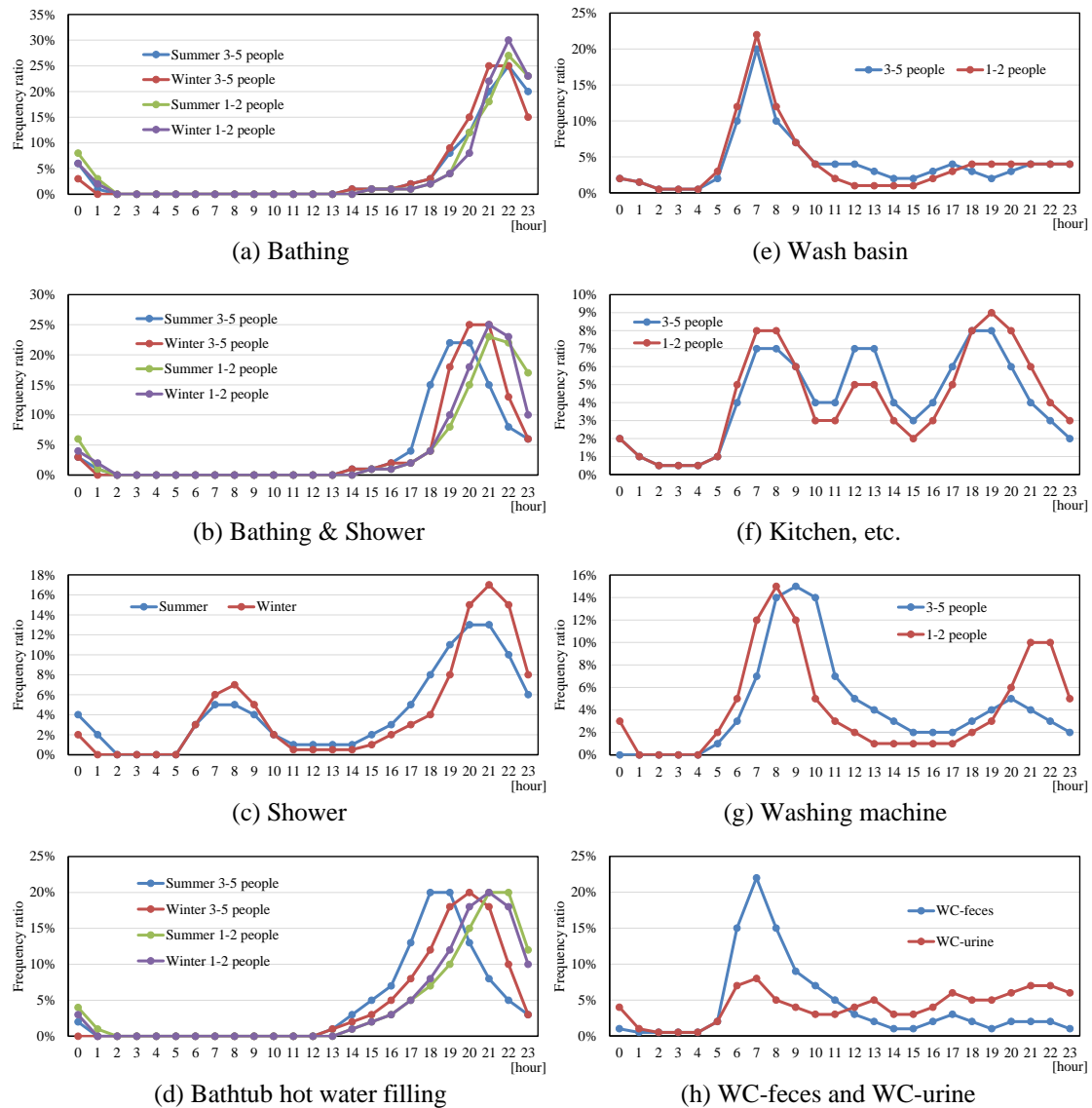
Figure 1 – Frequency ratio of cold and hot water usage in each usage or appliance

3 Examination of the effects of introducing water-saving and hot water-saving equipment

3.1 Setting the Calculation Model

In recent years, water saving of facilities and equipment in homes has been progressing, and water saving in toilet bowls and washing machines has been remarkable. In addition, amid the demand for energy conservation, hot water-saving fixtures such as shower heads and mixer faucets are also becoming widespread. Here, the authors create a cold and hot water load calculation model that incorporates these water-saving fixtures and compare it with the standard model presented earlier. In the case of apartments, it is possible that the household composition of the occupants differs depending on the type of room, etc., but here we consider only the winter season of four-person households.

Table 2 shows the water-saving and super-water-saving types of calculation models. Since the standard type has the same conditions as the model shown in Table 1(b), it is omitted here. The water-saving type and the super-water-saving type are shown in the table with background colors on the applications and numerical values for which the setting values are changed compared to the standard type.

Table 2 - Water-saving and super-water-saving types of calculation models for cold and hot water supply loads; Winter, Four- person households

(a) Water-saving type

		Bathing	Bathing & Shower	Shower	Bathtub hot water filling	Wash basin (Cold water)	Wash basin (Hot water)	Kitchen, etc. (Cold water)	Kitchen, etc. (Hot water)	Washing machine	WC-feces	WC-urine
Water usage frequency per day	[times/flat/day]	1.7	1.7	0.6	1.0	6.0	6.0	8.0	8.0	1.4	3.0	9.0
Average water discharge time (Distribution*, phase)	[s]	180	360	420	600	30	40	60	100	450	36	27
		Exp.	Exp.	Exp.	Erl.15	Hyp.5	Exp.	Hyp.5	Hyp.2	Exp.	Exp.	Exp.
Average discharge flow rate (Distribution*, phase)	[L/min]	9	7	6.5	14	10	8	12	8	12	10	10
		Erl.7	Erl.7	Erl.7	Erl.20	Erl.4	Erl.10	Erl.3	Erl.4	Erl.5	Erl.6	Erl.6
Operating temperature	[°C]	41	41	41	42	12	37	12	38	12	12	12
Ratio of water and hot water usage		1.00	1.00	1.00	1.00	0.50	0.50	0.30	0.70	1.00	1.00	1.00

*Note: Exp., Hyp. and Erl. mean exponential distribution, hyperexponential distribution and erlang distribution respectively.

(b) Super-water-saving type

		Bathing	Bathing & Shower	Shower	Bathtub hot water filling	Wash basin (Cold water)	Wash basin (Hot water)	Kitchen, etc. (Cold water)	Kitchen, etc. (Hot water)	Washing machine	WC-feces	WC-urine
Water usage frequency per day	[times/flat/day]	1.7	1.7	0.6	1.0	6.0	6.0	8.0	8.0	1.4	3.0	9.0
Average water discharge time (Distribution*, phase)	[s]	180	300	360	600	30	40	60	100	400	41	31
		Exp.	Exp.	Exp.	Erl.15	Hyp.5	Exp.	Hyp.5	Hyp.2	Exp.	Exp.	Exp.
Average discharge flow rate (Distribution*, phase)	[L/min]	9	7	6.5	14	9	7	12	8	12	7	7
		Erl.7	Erl.7	Erl.7	Erl.20	Erl.4	Erl.10	Erl.3	Erl.4	Erl.5	Erl.6	Erl.6
Operating temperature	[°C]	41	41	41	42	12	37	12	38	12	12	12
Ratio of water and hot water usage		1.00	1.00	1.00	1.00	0.60	0.40	0.30	0.70	1.00	1.00	1.00

*Note: Exp., Hyp. and Erl. mean exponential distribution, hyperexponential distribution and erlang distribution respectively.

In the water-saving and super-water-saving types, water-saving fixtures and appliances are installed in shower heads, washbasin faucets, washing machines, and toilet bowls. In addition, since users' awareness of water conservation is also increasing, the water discharge duration time is set short for the water-saving type and the super-water-saving type.

In anticipation of the introduction of a single-lever faucet with a hot water saving function and the improvement of water conservation awareness on the user side, the ratio of hot water used is lowered for the water-saving type and the super-water-saving type, and the discharge flow rate is shortened.

Regarding washing machines, the standard type used water was set at 100 L/times, but since the water saving of fully automatic washing machines has progressed in recent years, the standard water consumption is 90 L/times for the water-saving type, and 80 L/times for the super water-saving type.

Furthermore, for toilet bowls that are becoming water-saving, the amount of water flushed per times was 8.3 L for large and 5.8 L for small for standard types, but 6.0 L for large and 4.5 L for small for water-saving types, and 4.8 L for large and 3.6 L for super-water-saving types.

Figure 2 shows the ratio of frequency of water usage in each usage in winter for a four-person household. When calculating the load, the same conditions are used for any of the standard type, water-saving type, and super-water-saving type using the frequency ratio shown in Figure 2. The hot water supply temperature and the water supply temperature are set at 60°C and 12°C respectively.

(a) Bathing, Bathing & Shower,
Shower, Bathtub hot water filling

(b) Wash basin, Kitchen, etc., Washing machine,
WC-feces, WC-urine
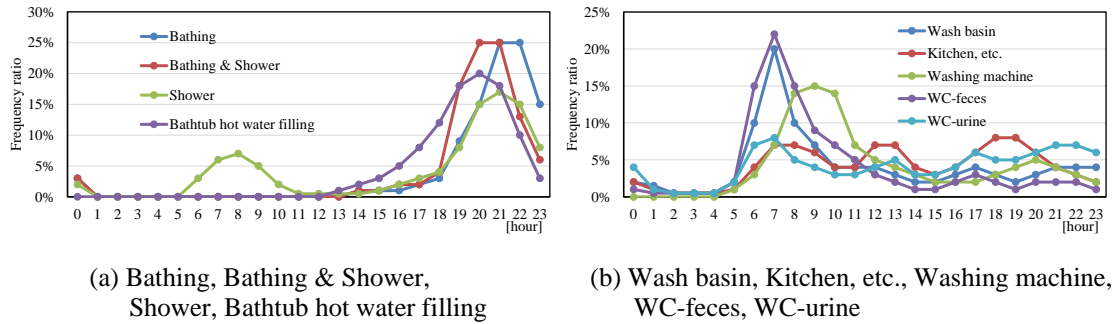
Figure 2 - Ratio of frequency of water usage; Winter, Four-person households

3.2 Calculation of instantaneous cold and hot water supply loads

Using the above-mentioned standard, water-saving, and super-water-saving types of calculation models for cold and hot water supply loads, these loads were calculated by changing the number of dwelling units in the apartment complex to 30, 100, 300, 500, and 1000 in winter. All households are four-person households.

As a result of calculating the instantaneous maximum flow rate in the standard type, the values obtained by aggregating each time zone at 1 minute intervals and 5 second intervals are shown in Figure 3 (a) and (b), respectively. These represent the calculated results for 100 households.

In the case of an apartment complex, a tank-type toilet bowl is assumed instead of a flush valve, so the discharge flow rate is set at 14 L / min or less for all water usage category. Therefore, it is rare for a large amount of cold and hot water to be generated in a short time, and there is no significant difference between the 1 minute values and the 5 second values of the instantaneous maximum flow rate in each time zone.

(a) 1 minute values
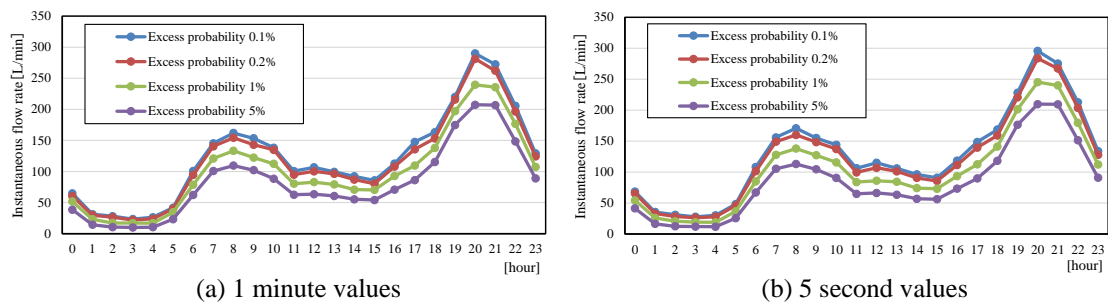
(b) 5 second values

Figure 3 - Instantaneous maximum flow rate; Standard type, 100 households

Figure 4 shows the instantaneous maximum flow rates which are 5 second values of the water-saving type and the super-water-saving type. It can be seen that the values of the water-saving type and the super-water-saving type are smaller than the standard type of Figure 3(b) for the instantaneous maximum flow rate at 20 o'clock, which is the peak load generation time zone. When comparing the water-saving type and the super-water-saving type, there is no significant difference at 20 o'clock, but the instantaneous maximum flow rate of the super-water-saving type decreases around 8 o'clock, which is the peak load generation time in the morning.

(a) Water-saving type

(b) Super-water-saving type
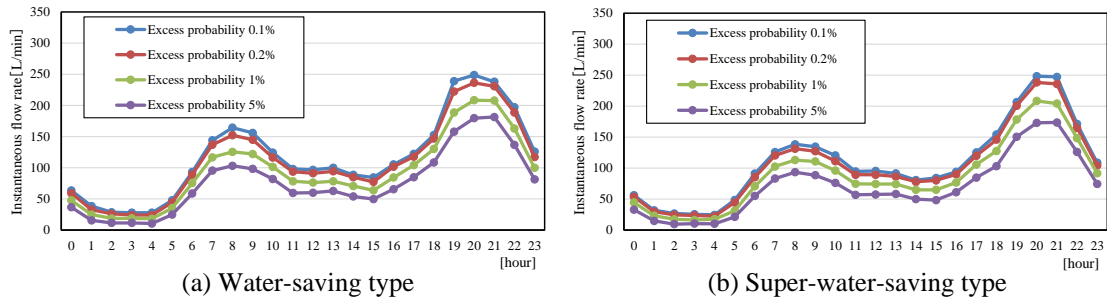
Figure 4 - Instantaneous maximum flow rate; Water-saving and Super-water-saving types, 5 second values, 100 households

Figure 5 shows the calculation results of the instantaneous maximum load using the standard, water-saving, and super-water-saving types of calculation models. The instantaneous maximum load is set to an excess probability of 0.2 at the aggregation time interval of 5 seconds. The horizontal axis is the number of dwelling units, and an approximate formula is shown in the Figure 5 from the calculation results of 30, 100, 300, 500, and 1000 units.

The aggregation targets the time periods when the following peaks occurred; the water supply amount peaked at 20:00 time zone, the hot water supply amount peaked at 21:00 time zone, and the hot water supply heat peaked at 21:00 time zone. From the Figure 5(a), the instantaneous maximum flow rate for 1,000 dwelling units shows that the instantaneous maximum flow rate of the water-saving type and the super-water-saving type is 13% less (1,543 L/min) and 19% less (1,446 L/min), respectively, compared to the standard type (1,779 L/min). The amount of hot water supply and the amount of hot water heat show the same ratio, and the instantaneous flow rate of the water-saving type and the super-water-saving type is 15% lower and 18%, respectively, compared to the standard type.

(a) Water supply; 20:00

(b) Hot water supply; 21:00

(c) Hot water heat; 21:00
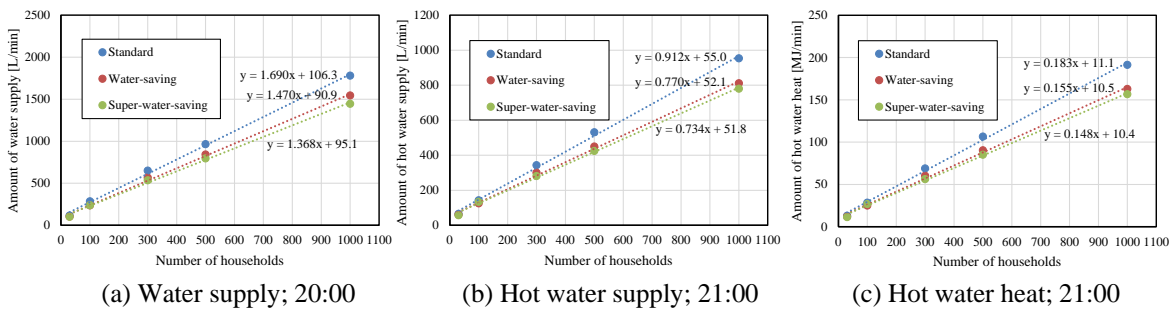
Figure 5 - Instantaneous maximum loads; Excess probability of 0.2%

3.3 Calculation of hourly and daily cold and hot water supply loads

Figure 6 and Figure 7 show the hourly and daily maximum cold and hot water supply loads using the standard, water-saving, and super-water-saving types of calculation models. The hourly maximum loads are an excess probability of 0.2% at the time when the peak load occurs as well as the instantaneous maximum flow rate. The daily maximum

loads are values with an excess probability of 0.2% based on calculation results from 100 simulation trials.

From the hourly maximum cold and hot water supply loads shown in Figure 6, for 1,000 dwelling units, the water supply amount is 93.9m³/h for the standard type, 78.1m³/h for the water-saving type, and 74.3m³/h for the super-water-saving type, which is 17% less for the water-saving type and 21% less for the super-water-saving type than the standard type. The amount of hot water supply and heat consumption are 15% lower for the water-saving type and 18% less for the super-water-saving type than the standard type.

Similarly, the daily maximum cold and hot water supply loads shown in Figure 7, for 1,000 dwelling units, the water supply amount is 701.6m³/d for the standard type, 616.0m³/d for the water-saving type, and 571.8m³/d for the super-water-saving type, which is 12% less for the water-saving type and 19% less for the super-water-saving type than the standard type. The amount of hot water supply and heat consumption are 12% lower for water-saving type and 16% less for the super-water-saving type than standard type.

(a) Water supply; 20:00	(b) Hot water supply; 21:00	(c) Hot water heat; 21:00
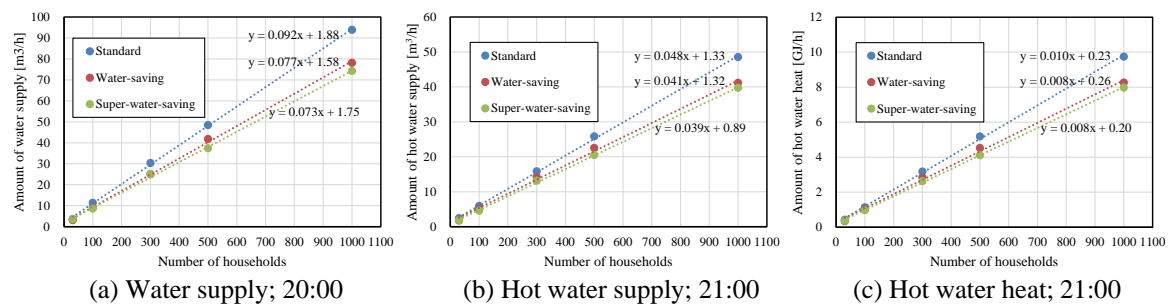
**Figure 6 - Hourly maximum cold and hot water supply loads;
Excess probability of 0.2%**

(a) Water supply	(b) Hot water supply	(c) Hot water heat

**Figure 7 - Daily maximum cold and hot water supply loads;
Excess probability of 0.2%**

4 Conclusion

In this paper, the authors explained the calculation model of cold and hot water supply loads of an apartment complex in a newly developed dynamic calculation method for cold and hot water supply loads.

In addition, in order to examine the effect of introducing water-saving appliances, which have become popular in recent years, the authors changed the discharge duration time and water discharge flow rate of the appliances, and set up calculation models for water-saving type and super-water-saving type. Based on these resu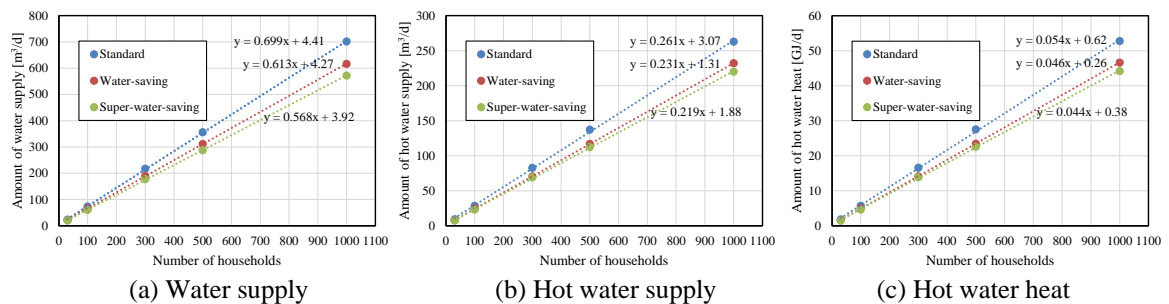lts, the authors simulated a series of loads from instantaneous load to hourly and daily loads, and clarified the effect of introducing water-saving equipment in apartment complex as the difference in cold and hot water supply loads by number of households.

This new dynamic calculation method can not only change the specifications of the equipment, but also change the detailed settings according to lifestyles, so it is expected to be able to respond to future changes due to social factors such as the declining birthrate and aging population.

In the future, the authors would like to improve the accuracy of this calculation model and build calculation models for various buildings.

5 References

1. S. Murakawa, D. Ikeda, K. Sakamoto and H. Takata: New Calculation Method for Cold and Hot Water Supply Loads in Building, and Application to Plumbing Design (In Japanese), Shokokusha Co.Ltd, (2020)

2. D. Ikeda, S. Murakawa, K. Sakamoto, H. Takata: Dynamic calculation method for cold and hot water supply loads by simulation and application to optimum design of the central hot water supply system in a business hotel, Proceedings of the CIB-W062 International Symposium on Water Supply and Drainage for Buildings (Taiwan), pp.1-14 (2022)

3. S. Murakawa, H. Takata, K. Sakamoto: Effect of setting up the water saving bowls in the toilets of office buildings based on the analysis of simulation technique, Proceedings of the CIB-W062 International Symposium on Water Supply and Drainage for Buildings (São Paulo, Brazil), C-10, pp.409-424 (2014)

4. H. Takata, S. Shimada, S. Murakawa, D. Ikeda: Calculation of the loads of hot water consumption in Japanese hot spring hotel, Proceedings of the CIB-W062 International Symposium on Water Supply and Drainage for Buildings (Online), H-2, pp.1-12 (2021)

5. S. Murakawa, D. Ikeda, K. Sakamoto, H. Takata: Verification on the dynamic calculation method for cold and hot water supply loads, and a simple calculation method for the instantaneous maximum flow rates, Proceedings of the CIB-W062 International Symposium on Water Supply and Drainage for Buildings (Online), A-1, pp.1-17 (2021)

6. K. Sakamoto, S. Murakawa, D. Ikeda, H. Takata: Design of water supply systems in buildings based on the estimation of instantaneous flow rates by the dynamic calculation method, Proceedings of the CIB-W062 International Symposium on Water Supply and Drainage for Buildings (Online), A-4, pp.1-10 (2021)

7. S. Murakawa, Y. Koshikawa, H. Takata, and A. Tanaka: Calculation for the Cold and Hot Water Demands in the Guest Rooms of City Hotel; Proceedings of the CIB/W062 International Symposium on Water Supply and Drainage for Buildings (Brno), B-1, pp.73-85 (2007)

8. H. Takata, S. Murakawa, C. Saito, M. Abe, and K. Toyosada: Development of the Calculating Method for the Loads of Cold and Hot Water Consumption in a Business Hotel (Part 1) Cold and hot water demands through the attributes of guests and plumbing fixtures, Proceedings of the CIB-W062 International Symposium on Water Supply and Drainage for Buildings (Beijing), B-6, pp.330-339 (2015)

9. S. Murakawa, H. Takata, C. Saito, M. Abe, and K. Toyosada: Development of the Calculating Method for the Loads of Cold and Hot Water Consumption in a Business Hotel (Part 2) Dynamic estimation for the loads of cold and hot water demands, Proceedings of the CIB-W062 International Symposium on Water Supply and Drainage for Buildings (Beijing), B-7, pp.340-352 (2015)

10. S. Murakawa, D. Nishina, H. Takata: Development of the Calculating Method for the Loads of Water Consumption in Restaurant, Proceedings of the CIB-W062 International Symposium on Water Supply and Drainage for Buildings (Paris, France), 1S-7, pp.1-14 (2004)

6 Presentation of Authors

Dr. Hiroshi Takata is an Associate Professor at the Department of Architecture and Design, Faculty of Environmental Studies, Hiroshima Institute of Technology. His special field is planning cold and hot water supply systems. Recently, he has been studying the housing environment and living behaviour, and researching building systems and environmental simulation.

Dr. Saburo Murakawa is the Emeritus Professor of Hiroshima University. His special fields are water environment engineering of building and city, and sanitary plumbing engineering of building services. He is now spreading the new dynamic calculation method for cold and hot water consumption in buildings, which has been called MSWC program developed with his colleagues. In addition, he is engaged in study to spread the harvesting of rainwater in buildings and urban areas.

Mr. Daisuke Ikeda had worked as a design engineer at Sogo Setsubi Consulting Co., Ltd, after completing master program at Hiroshima University. After that, he has been mainly engaged in building management work as a property manager at Tokyo Tatemono Co., Ltd. In addition to practical work, he is researching and developing a new dynamic calculation method of cold and hot water supply loads jointly with Dr. S. Murakawa et al.

Dr. Kazuhiko Sakamoto is the Professor of Okayama University of Science. His special fields are environmental and facility planning. He was engaged in building services designer at Takenaka Corporation for a long time after graduating from Kyoto University. He is studying how to reflect MSWC calculations in water supply system design. He has devised MSPS program and is researching appropriate pump capacity setting method and energy saving system.

Examination of unit model applied to dynamic cold and hot water supply loads calculation method - as an example of toilet flushing water supply system in an office building

Saburo Murakawa (1), Daisuke Ikeda (2), Kazuhiko Sakamoto (3), Hiroshi Takata (4)

(1) saburo.murakawa@gmail.com, Hiroshima University, Japan
(2) daisuke.ikeda225@gmail.com. Tokyo Tatemono Co., Ltd, Japan
(3) ksakamoto@archi.ous.ac.jp, Okayama University of Science, Japan
(4) h.takata.h5@it-hiroshima.ac.jp, Hiroshima Institute of Technology, Japan

Abstract

The dynamic cold and hot water supply loads calculation method applying the simulation method proposed by the authors consists of calculation models based on fairly detailed data analysis such as people's water usage behaviour. In order to popularize this calculation method widely, setting up simpler models are required. One way to do this is to utilize BEMS (Building Energy Management System) data, which has been installed in the operation management of large buildings. This data is often recorded hourly with respect to the amount of water used as well as the energy consumption of various equipment installed in the buildings. Therefore, if it is possible to establish a method of treating the target system or the entire building as a single unit model by utilizing the data measured in BEMS, the scope of application of the dynamic calculation method will be expected to greatly expanded utilization.

In this paper, the authors clarify the validity of the setting model by comparing the calculated value by the unit model and each fixture usage model for the water supply load of the toilet flushing system, taking the T-building as an example. In addition, the average water discharge flow rate and average water discharge duration time for each unit, which greatly affect the calculation results in the unit model setting are shown based on the relationship of the number of employees in the office and the male/female composition ratio. By setting up such the unit models, the highly accurate prediction method of the water supply loads of the toilet flushing system can be expected to be used when considering the effective use of water resources such as rainwater.

Keywords

Dynamic calculation method; Water supply loads; Monte Carlo simulation technique; MSWC program; Office building; Toilet flushing system; BEMS data; Unit model

1 Introduction

Accurate prediction of the cold and hot water supply loads is the basis for the optimal design of the cold and hot water supply systems for buildings. However, it has been pointed out that these past prediction methods in this field do not necessarily reflect the actual situation in the circumstances where water saving and energy saving are progressing in recent years, and they show excessive values. In addition, in the prediction of the design consumption unit and the instantaneous maximum flow rate shown in the conventional method, there is no relationship between the two. Moreover, it is difficult to apply to the evaluation of the energy consumption of equipment systems over time because load fluctuations cannot be grasped.

Therefore, through the CIB-W062 symposium, etc., the authors have proposed a dynamic calculation method for cold and hot water supply loads by simulation technique that applies the Monte Carlo method in order to solve various problems with the conventional calculation method [1- 5]. And, in April 2020, the authors published a book titled "New Calculation Method for Cold and Hot Water Supply Loads in Buildings, and Application to Practical Design" [6], summarizing the series of research results. It consists of a developed calculation program that is called "MSWC; Murakawa's Simulation for Water Consumption". And, users can download it for free from the publisher's website.

The MSWC program developed based on the analysis data has been used to simulate the occurrence of instantaneous flow rate fluctuations, which is the water supply loads of the building, throughout the day using a personal computer. Then, a method of obtaining the instantaneous, hourly, and daily loads as occurrence probability values by statistical processing has been shown. The authors have proposed the calculation results from the built models for the design of seven kinds of buildings which are apartments, office buildings, accommodations, restaurants, large kitchen facilities, hospitals, and welfare facilities for the elderly. In addition, the authors have proposed a method for setting the original calculation models according to the characteristics of the building targeted by the designer. And, it has shown how to utilize existing data recorded by "BEMS; Building Energy Management System". The method has shown how to treat several plumbing fixtures as a unit. Also, the authors have proposed an optimal design method for cold and hot water supply systems using these calculation results. The subprogram "MSPS; Murakawa's Simulation for Pump System" has been developed to apply to the selection of pump specifications for booster pump water supply system [8].

By the way, the developed calculation method is based on the models fairly detailed data analysis such as people's water usage behavior. Therefore, in order to popularize the calculation method widely, setting up simpler models are required. One way to do this is to utilize BEMS data, which has been installed in the operation management of large buildings. This data is often recorded hourly with respect to the amount of water used as well as the energy consumption of various equipment installed in the buildings. If it is possible to establish a method of treating the target system or the entire building as a single unit model by utilizing the data measured in BEMS, the scope of application of the dynamic calculation method will be expected to greatly expanded utilization.

In this paper, as for the water supply load of the toilet flushing system, taking the T-building as an example, the authors clarify the validity of calculation results by the unit model set based on the BEMS data by comparison with the calculation results of using each fixture usage model. In addition, the average water discharge flow rate and average water discharge duration time for each unit model, which greatly affect the calculation results in the unit model setting are shown based on the relationship of the number of employees in the office and the male/female composition. By setting up such the unit models, the highly accurate prediction method of the water supply load of the toilet flushing system can be expected to be used when considering the effective use of water resources such as rainwater. As for the T-building, which is the subject of this paper, the results of the analysis of the cold and hot water supply loads have already been presented at the CIB-W062 symposium [9,10].

2 Creation of calculation models using recorded data

2.1 Outline of the target office building

The target office building "T-building" is a company building located in Tokyo. **Table 1** shows an outline of the target building. The company includes a convenience store and an employee cafeteria. The number of registered employees is confirmed to be around 1,860 to 1,900. Here, the assumed number of people is 1,900, and the male to female ratio is 4:1. The women's toilet bowls are equipped with simulated sound running water devices from the viewpoint of saving water. The water supply system adopts a booster pump system with a water receiving tank. The capacity of the pump is 500L/min, the head is 60m, and two pumps are operated in parallel.

Table 1 - Over view of the subject building "T-building"

Building name	T-building
Building application	Office
Ownership form	Own Building
Completion	October 2014
Total floor area	29,747 m^2
Office area	24,269 m^2
Ratio of effective office area	81.6 %
Number of seats	2,347 seats
Employed enrollment	1,900 people (assumed value)
Gender ratio	Male : Female = 4 : 1
Construction	S and CFT structure
Scale	The ground 7th Floor, penthouse second floor
Water supply system	Receiving tank and booster pomp system, Rainwater harvesting system
Number of plumbing fixtures	Male's water closet : 41
	Uriral : 47
	Female's water closet (with device of imitative sounds) : 39
	Washbasin : 56
	Small washbasin for brushing teeth : 21
	Sink for cleaning : 16

Figure 1 shows the water supply system diagram and measurement points by BEMS. In the T-building, a rainwater utilization system is adopted for the gray water system, and water is supplied to the toilet flushing system on each floor from a rainwater utilization tank equipped with a tap water supply device. The measurement points are M① to M⑪ shown in Figure 1, and the office water supply system and rainwater utilization system, which are not directly measured, are calculated by subtracting the data of the measurement points before and after. The measurement data is the integrated value for each hour, and the recording unit is m^3. Among the measured values for each system, here the authors show the toilet flushing system for each floor at measurement point ③.
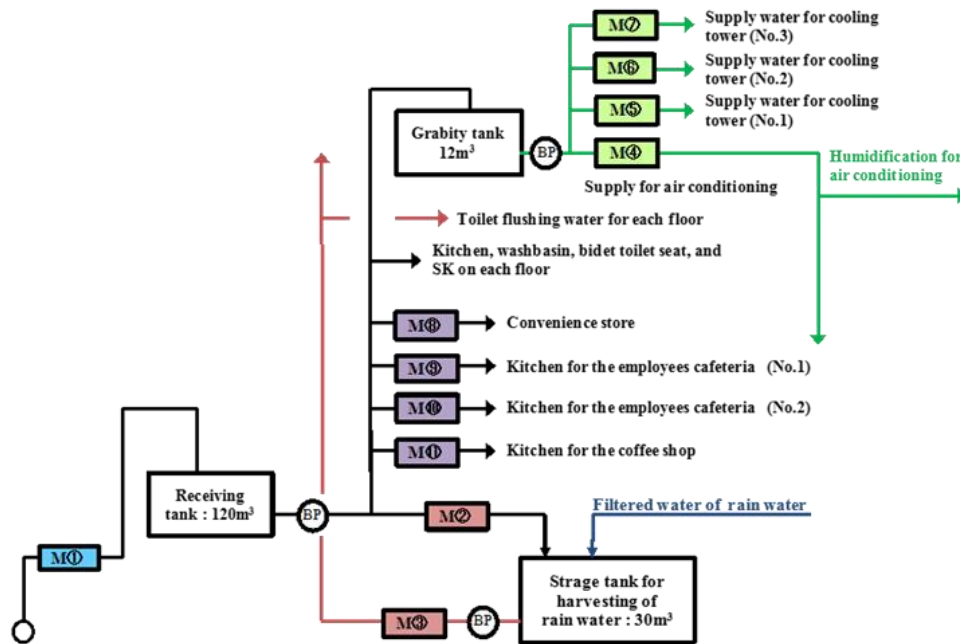
Figure 1 - Water supply systems and measurement points

2.2 Setting up calculation models based on the actual measurement data

2.2.1 Daily and hourly water consumption in the toilet flushing system
Actual measurement results in 2013 are shown for the amount of water used in the grey water system which is used for the toilet flushing water. **Figure 2** shows the daily water consumption for a week without holidays in representative months of each season. On Monday to Friday of weekdays, the water consumption shows almost stable values of 55 to 60m^3/d.
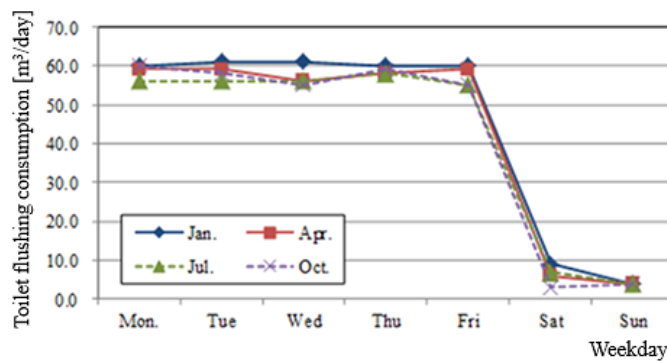
Figure 2 - Daily water consumption in the toilet flushing system

According to the accumulated data for 240 days extracted from weekdays, which are the working days of the building, the amount of water used per day per total floor area and per registered person is 3.79 $L/m^2/day$ and 59.31 L/people/day, respectively. Of the amount of water usage in the entire building, the tap water for toilet flushing accounts for 44.9%, and rain water accounts for 6.1%.

Here, **Figure 3** shows hourly changes in water consumption over a representative week, taking May as an example. Since the unit of measurement data is m^3/h, some fluctuations can be seen between adjacent time periods, but the peak value is around 5.0 to 6.0 m^3/h from 8:00 when start work to around 14:00.
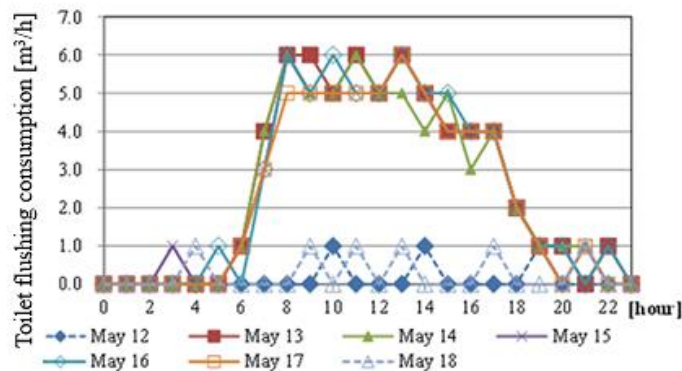
Figure 3 - Hourly water consumption in the toilet flushing system

2.2.2 Setting up calculation models
As shown in the calculation model for office buildings in previous paper [3], four standard models have been set up for changes in the attendance ratio of employees during working hours. In the case of the T-building, the start time for working is 8:30, which is earlier than the general office. In addition, since there are also long-distance commuters, the attendance ratio was revised based on the actual water consumption shown in Figure 3, assuming the use of plumbing fixtures in the early morning hours. That is, based on the "average model" out of the four standard models, males are corrected to 0.29 at 7:00 and 0.80 at 8:00, and females are corrected to 0.11 and 0.90, respectively. **Figure 4** shows the set ratio of hourly attendance model.
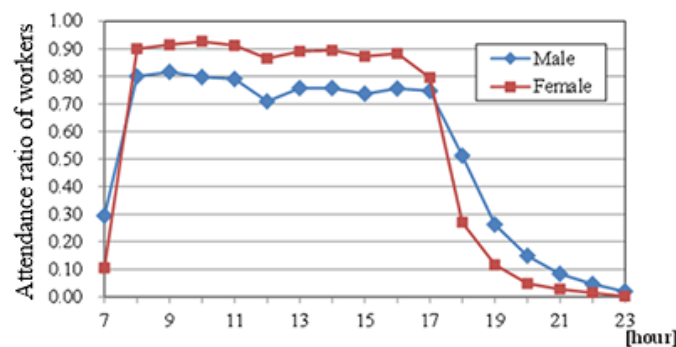
Figure 4 - Model of the attendance ratio of workers to the number of registered employees

Figure 5 shows the frequency of fixture usage per hour per person present. With reference to the actual water consumption per hour shown in Figure 3, the frequency per hour is adjusted by multiplying each value in the values of previous papers [3] by a value from 0.9 to 1.25. In the Figure 5, the usage frequency of male's toilet bowls increases after 21:00, but this is because it is shown as a value per person during the time period when the number of people present is small. The peak of the usage frequency of the plumbing fixtures appears at 12:00 time zone during the lunch break and at 18:00 time zone during the closing time.
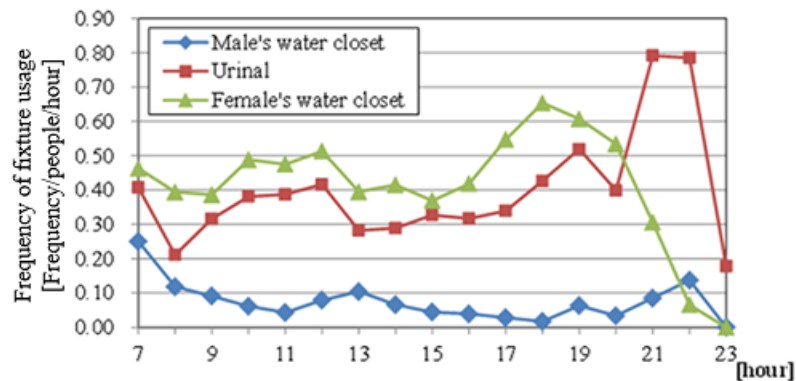
**Figure 5 - Hourly frequency of fixture usage per people present
in case of the toilet flushing system**

Table 2 shows the simulation model for the toilet flushing system. Based on the plumbing fixtures actually installed in the T-building, the toilet bowl is a 10L type and the male's urinal is a 4L type. In addition, the average number of flushes per occupancy is 1.6 times for male's toilets and 1.3 times for female's toilets, taking into consideration the fact that an imitative sound generator of water flow is installed in each booth of the female's toilets.

Table 2 - Calculation models for water supply loads in the toilet flushing system

		Male		Female
		Water closet［10L］	Urinal［4L］	Water closet［10L］
Arrival model	Arrival interval distribution	Exponential distribution, random arrival		
	Arrival ratio ［people/min］	Setting in each hourly time zone		
	Number of fixture	41	47	39
Occupancy model	Average occupancy time ［sec］	260	37	110
	Distribution; phase	Erl.3	Erl.7	Erl.3
Water volume model	Average discharge time ［sec］	6	20	6
	Distribution; phase	Exp.	Erl.10	Exp.
	Average flow rate ［L/min］	100	12	100
	Distribution; phase	Erl.6	Erl.10	Erl.6
Fixture operation model	Frequency of fixture operation per occupancy	1.60	1.00	1.30

3 Setting up unit model for the toilet flushing system

When setting up a calculation model using existing BEMS data, etc., instead of setting a detailed model based on how each sanitary fixture is used, it will be considered to set up a unit model that summarizes the fixtures for each purpose as a toilet flushing system. The model for the cafeteria in an office building already has shown the treatment as a unit model that summarizes the fixtures used for each cold and hot water [10]. Here, the applicability of the unit model will be verified by comparing the calculation results of the unit model and the calculation results of each fixture usage model.

3.1 Unit model settings

Based on the simulation models for each fixture usage of the T-building shown in Table 2, the authors set up the simulation model for the toilet flushing system as one unit. The unit model is made based on the fluctuations of instantaneous flow rates of 5-second time intervals occurred by usage of each fixture installed in the system.

In order to explain for setting of the unit model, an example of schematic instantaneous flow rates is shown in **Figure 6** [7]. From the fluctuations of flow rates in the figure, the load continued with same flow rate is regarded as one usage of water in the system. This value of flow rate is extracted as one sample of continuing water discharge flow rate in the system, and also the duration time of the same flow rate is extracted as one sample. By accumulating the values of each discharge water flow rate and duration time obtained throughout the simulation, the average values and approximate distributions are set up for the unit model.
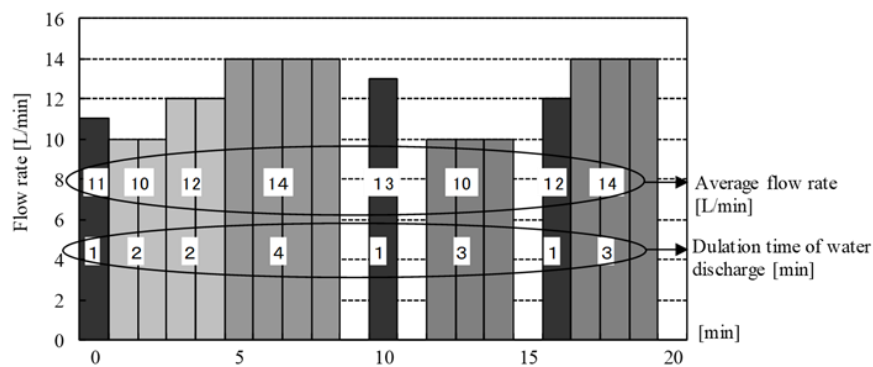
Figure 6 - Analysis to set up the unit model of flow rate and duration time of water discharge based on instantaneous flow rates in a water supply system

Based on the simulation results for each fixture usage in the toilet flushing system shown in Table 2, the authors adopted the instantaneous flow rate fluctuation values every 5-second interval at time zone of 12:00, which indicates the maximum water supply load. From this, it can be obtained the average water discharge flow rate, the average water discharge duration time, and each approximate distribution shape. **Table 3** shows the unit model of the toilet flushing system. Based on the calculated results, the average water discharge duration time was set as 5.1 seconds, the cumulative frequency distribution was set as a Hyper-exponential distribution, and phase K = 2. The average water discharge

flow rate was set to 92.4 L/min, and the cumulative frequency distribution was set as an Exponential distribution. The water usage frequency ratio required for calculation shows the same trend as the fluctuation pattern of the hourly water supply load in Figure 9, which is shown as the calculation result.

Table 3 - Unit model for water supply loads calculation of the toilet flushing system

		Unit model
Water volume model	Water discharge time distribution；phase	Hyper-exp. 2
	Average water discharge time ［sec］	5.1
	Discharge flow rate distribution	Exp.
	Average discharge flow rate ［L/min］	92.4
Frequency of water usage	Frequency per day ［times/day］	7,125

3.2 Calculation results of the toilet flushing system by unit model

As calculation results by simulation, the case of using each fixture shown in Table 2 and the case of using the unit model shown in Table 3 are compared. **Figure 7** shows a comparison of 5-second value fluctuations for the water supply load of 12:00 time zone as a sample from the simulation results of 100 trials. The 0.2% to 2% excess probability values in the Figure 7 represent the results of 100 trials with a time interval of 5- second by the unit model of the toilet flushing system. Although the fluctuation trends of the instantaneous flow rates by these two calculation models are similar, the calculated values by the unit model tend to appear larger instantaneous values.
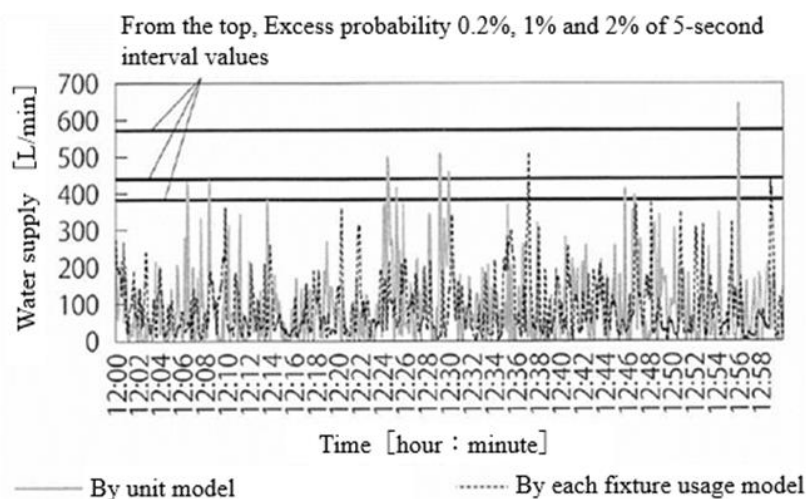
Figure 7 - Comparison of water supply loads calculation with unit model and each fixture usage model

Figures 8 and **9** show comparisons of instantaneous and hourly loads obtained by statistical processing, based on the calculation results from 100 trials of simulation. As shown in Figure 7, the instantaneous flow rates of the toilet flushing system show single high waveforms with a short duration, and the trends are particularly strong in the calculation results of the unit model. At an instantaneous value with an excess probability

of 0.2%, it is conceivable that the value calculated by the unit model predicts a high load of about once an hour. Therefore, in Figure 8, the 1.0% excess probability values for the unit model are taken and compared with the 0.2% excess probability values for each fixture usage model. As a comparison of the two models, if we look at the excess probability values in the range of 0.2 to 1%, it can be said that they show roughly similar fluctuation trends. Figures 9 shows a comparison of hourly average water supply loads. These hourly values are averages of 100 simulation trials. It can be said that the calculation results by both models are roughly similar. In the setting of the unit model, the setting of the water discharge flow rate per times of fixture operation is a major factor in the calculation of the instantaneous load, so it is necessary to set an appropriate value for the target system.
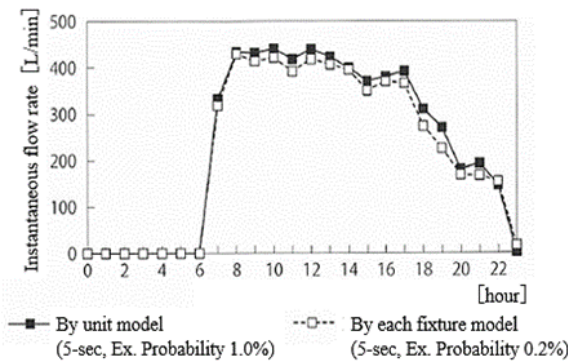
Figure 8 - Comparison of the calculation results for instantaneous flow rates
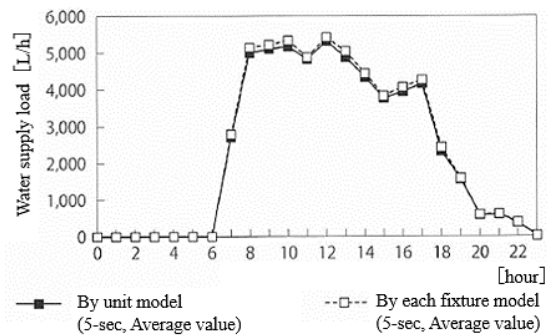
Figure 9 - Comparison of the calculation results for hourly average water supply loads

3.3 Setting of unit models by scale and calculation of water supply loads

3.3.1 Unit models by scale
As the unit models for toilet flushing system, the authors examine the average water discharge flow rate and average water discharge duration time when the number of employees and the gender composition ratio, which have a large impact on the water supply load calculation, are changed.   **Figure 10** shows the changes in average water
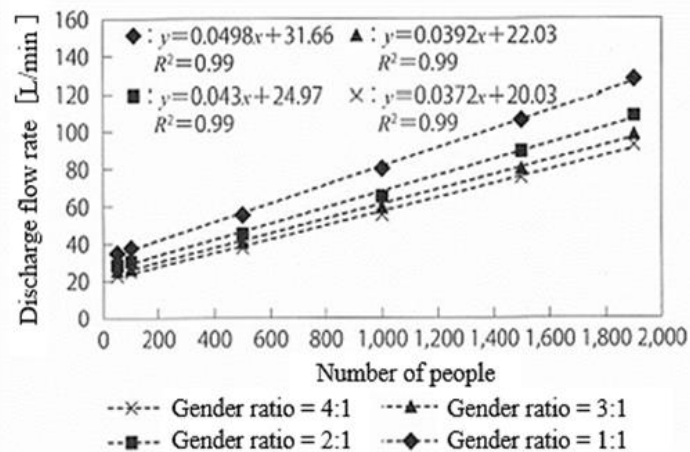
Figure 10 - Average water discharge flow rates per times by scale

discharge frow rates when the number of employees is changed to 6 levels and the gender composition ratio is changed to 4 levels based on the calculation conditions for the toilet flushing system of T-building shown in Table 2. The number of employees is based on the number of registered employees. The flow rate of discharged water increases as the proportion of women increases. Moreover, there is a high correlation between the number of employees and the water discharge flow rates.

Figure 11 shows the average duration time of water discharge by scale. Since all calculations are based on a time interval of 5-second, as the number of employees increases, the water discharge duration per times tends to converge exponentially to 5 seconds. The higher the percentage of females, the more likely they are to use flush valves, which have a shorter flushing time than men's toilet bowls and urinals, so the average flushing time tends to be shorter. However, the difference between men and women is small, and the more the number of registered people, the less the difference is seen.
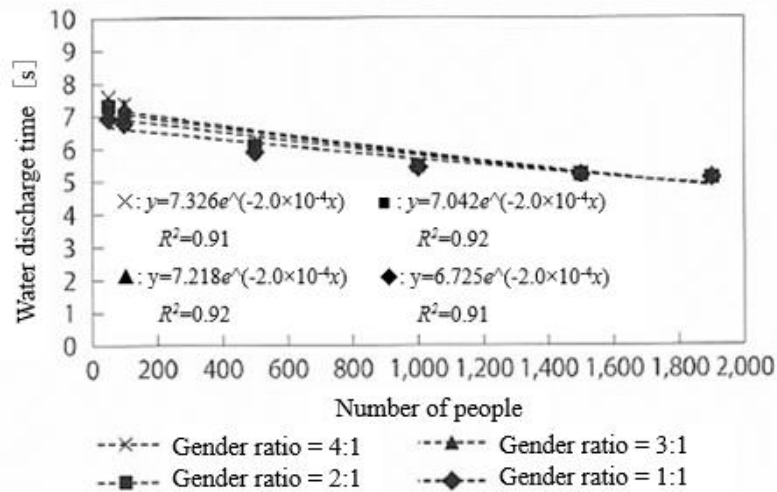
Figure 11 - Average discharge water duration per times by each scale of the number of registered employees

3.3.2 Calculation results based on the unit models by scale
Using the average water discharge flow rate and average water discharge duration time of the unit models for the toilet flushing system by each registered person as described above, the calculation results of the instantaneous water supply loads and the hourly water supply loads are shown by simulation. Each approximate distribution form is the same as Table 3.

Figure 12 shows the calculation results of the instantaneous water supply loads at the time zone of 12:00 according to the scale of the number of registered employees. The calculated values shown here are 1% values of excess probability taken over time of a 5-second interval. The instantaneous water supply load increases as the male-to-female ratio approaches the same ratio of 1:1. In addition, as the number of employees increases, it tends to increase roughly linearly.

Figure 13 shows the calculation results of water supply load per hour by number of employees. Changes in the hourly average water supply load show a similar trend

regardless of the scale of the number of employees, and the hourly water supply load increases as the number of registered employees increases in each time zone.
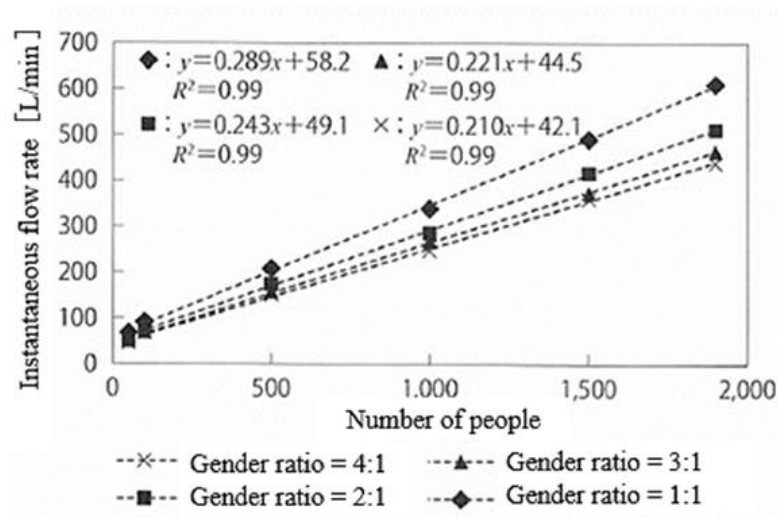
Figure 12 - Instantaneous maximum water supply loads by each scale of the number of registered employees
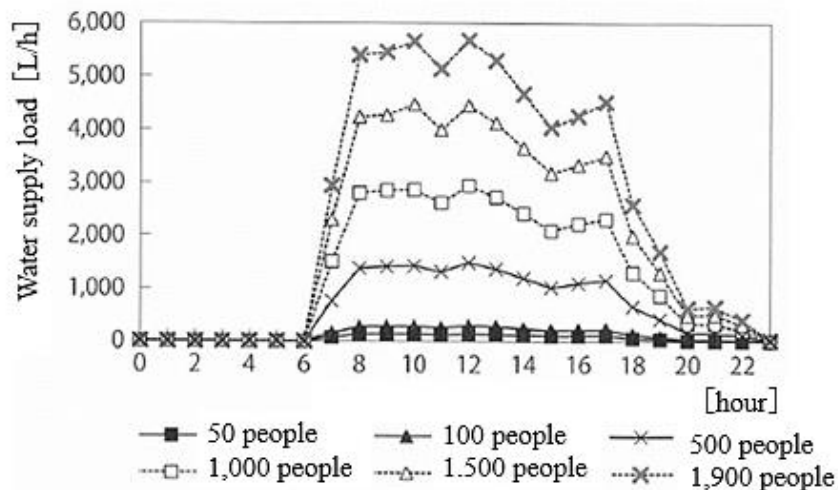
Figure 13 - Hourly average water supply loads by each scale of the number of registered employees

4 Conclusion

The authors have developed a simulation method for predicting hourly and daily load values from instantaneous values as a method for calculating cold and hot water supply loads in buildings. The development program is now widely provided free of charge to practical designers as the MSWC program. However, this method is based on detailed analysis data on people's water usage, and in order to provide more types of buildings in the future, it is desirable to construct a calculation model using a simpler method.

As one of the methods, in this paper, as the BEMS data that has been accumulated in the past, the method of utilizing the record data of water supply volume per hour was examined as an example of T-building

This is a method of treating the entire building or target system as one unit. In the model set as a unit, the setting of the water discharge flow rate and water discharge duration time per times is important. In particular, the setting of the water discharge flow rate has a large effect on the instantaneous water supply load. Based on the amount of water used per times obtained by multiplying these two values, the average frequency of water usage during the target time period can be calculated from the amount of water used per hour based on BEMS data. And, by setting the approximate distributions, a simulation can be performed.

Therefore, in this paper, the authors first clarified the validity of treating the toilet flushing system of the T-building as a unit by comparing the calculated value as a unit and the calculated value by using each fixture. Next, the set values for the water discharge flow rate and discharge duration time when the number of registered employees and their male/female composition are changed were shown.

The authors are proposing a unit model for setting a calculation model for commercial kitchens, which are equipped with many kinds of water using instruments. Including these models, the authors hope that the data of water discharge flow rate values when treated as a unit model will be accumulated, and that this calculation method will contribute to the optimization of the water supply and hot water supply systems from the perspective of energy-saving design.

5 References

1. S. Murakawa and H. Takata: Development of the Calculating Method for the Loads of Cold and Hot Water Consumption in the Apartment Houses; Proceedings of the CIB/W62 International Symposium on Water Supply and Drainage for Buildings (Ankara), pp.281-295 (2003)

2. S. Murakawa, H. Takata and K. Sakamoto: Calculation Method for the Loads of Cold and Hot Water Consumption in Office Buildings based on the Simulation Technique; Proceedings of the CIB/W62 International Symposium on Water Supply and Drainage for Buildings (Taipei), G-2, pp.1-14 (2006)

3. S. Murakawa, H. Takata and K. Sakamoto: Effect of setting up the water saving bowls in the toilets of office buildings based on the analysis of simulation technique; Proceedings of the CIB/W062 International Symposium on Water Supply and Drainage for Buildings (Sao Paulo), pp.409-424 (2014)

4. S. Murakawa, D. Ikeda, K. Sakamoto and H. Takata: Verification on the dynamic calculation method for cold and hot water supply loads, and a simple calculation method for the instantaneous maximum flow rates, Proceedings of the 46th CIB-W062

International Symposium on Water Supply and Drainage for Buildings (Online), Session A-1, pp.1-17 (2021)

5. D. Ikeda, S. Murakawa and T. Mitsunaga: Estimation of water supply loads in a general hospital by the dynamic calculation method, Proceedings of the 46th CIB-W062 International Symposium on Water Supply and Drainage for Buildings (Online), Session A-2, pp.1-12 (2021)

6. S. Murakawa, D. Ikeda, K. Sakamoto and H. Takata: New Calculation Method for Cold and Hot Water Supply Loads in Building, and Application to Plumbing Design (In Japanese), Shokokusha Co.Ltd, (2020)

7. S. Murakawa and D. Ikeda: Verification of accuracy of the dynamic calculation method for cold and hot water supply loads by each fixture usage model and unit model as the whole in an office building. Proceedings of the CIB/W062 International Symposium on Water Supply and Drainage for Buildings (Melbourne), Session C: pp.1-11 (2019)

8. K. Sakamoto, S. Murakawa, D. Ikeda and H. Takata: Design of water supply in buildings based on the estimation of instantaneous flow rates by the dynamic calculation method, Proceedings of the 46th CIB-W062 International Symposium on Water Supply and Drainage for Buildings (Online), Session A-4, pp.1-10 (2021)

9. S. Murakawa, D. Ikeda and A. Doi: Verification on the simulation technique for the estimation of water supply loads in the toilets of an office building: Proceedings of the CIB/W062 International Symposium on Water Supply and Drainage for Buildings (Kosice), pp.283-297 (2016)

10. S. Murakawa, D. Ikeda and A. Doi: Estimation of water supply loads for the company cafeteria, hot-water service rooms and restrooms in an office building, Proceedings of the CIB/W062 International Symposium on Water Supply and Drainage for Buildings (Haarlem), pp.248-263 (2017)

6 Presentation of Authors

Dr. Saburo Murakawa is the Emeritus Professor of Hiroshima University. His special fields are water environment engineering of building and city, and sanitary plumbing engineering of building services. He is now spreading the new dynamic calculation method for cold and hot water consumption in buildings, which has been called MSWC program developed with his colleagues. In addition, he is engaged in study to spread the harvesting of rainwater in buildings and urban areas.

Mr. Daisuke Ikeda had worked as a design engineer at Sogo Setsubi Consulting Co., Ltd, after completing master program at Hiroshima University. After that, he has been mainly engaged in building management work as a property manager at Tokyo Tatemono Co., Ltd. In addition to practical work, he is researching and developing a new dynamic calculation method of cold and hot water supply loads jointly with Dr. S. Murakawa et al.

Dr. Kazuhiko Sakamoto is the Professor of Okayama University of Science. His special fields are environmental and facility planning. He was engaged in building services designer at Takenaka Corporation for a long time after graduating from Kyoto University. He is studying how to reflect MSWC calculations in water supply system design. He has devised MSPS program and is researching appropriate pump capacity setting method and energy saving system.

Dr. Hiroshi Takata is an Associate Professor at the Department of Architecture and Design, Faculty of Environmental Studies, Hiroshima Institute of Technology. His special field is planning cold and hot water supply systems. Recently, he has been studying the housing environment and living behaviour, and researching building systems and environmental simulation.

Implementation of sustainability and circularity solutions in the building water cycle: The need to review sizing methods

A. Silva-Afonso (1), C. Pimentel-Rodrigues (2)

(1) asilva.afonso@outlook.pt

(2) anqip@anqip.pt

(1) ANQIP – Portuguese Association for Quality in Building Services and RISCO, Department of Civil Engineering, University of Aveiro, Portugal, and Standing Committee on Water, World Federation of Engineering Organizations, Maison de l'Unesco, Paris, France

(2) ANQIP – Portuguese Association for Quality in Building Services, and ISCIA – Instituto Superior de Ciências da Informação e da Administração, Portugal

Abstract

The need for more sustainable use of our planet's resources is currently widely recognized. Among these resources, freshwater should be highlighted, indispensable for life and economic activities, but whose scarcity is growing in several countries or regions. In this context, the development of more sustainable solutions in the urban water cycle, like use of water efficient devices, reuse of water or resort to alternative sources (rainwater, saltwater, etc.), begins to be a reality in many countries. These solutions, however, imply changes in the consumption diagrams, with implications for the sizing of pipe networks. This paper presents a reflection on the applicability of traditional methods for sizing pipe networks in buildings equipped with systems such as rainwater harvesting or greywater recovery, through a bibliographical review on the most appropriate sizing methods for networks with only one or two types of devices, as happens in these systems. A proposal for a specific probabilistic design method for these situations is also presented.

Keywords

Water supply in buildings; sizing methods; rainwater harvesting in buildings; reuse of grey water in buildings

1 Introduction

The need for more sustainable use of our planet's resources is currently widely recognized (UN, 2012; UN, 2022 EC, 2006). Among these resources, freshwater should be highlighted, indispensable for life and economic activities, but its scarcity is growing in several countries or regions of the planet (WHO, 2009; AWWA, 2006; EC, 2006). In this context, the development of more sustainable solutions in the urban water cycle, such as the application of efficient devices, the reuse of water or the use of alternative sources such as rainwater, is beginning to be a reality in many countries. These solutions, however, imply changes in the consumption diagrams or in the simultaneity coefficients normally used for sizing pipe networks, making traditional sizing methods and regulations, designed for current situations, inappropriate in these cases (Silva-Afonso, 2014).

In the case of rainwater harvesting systems, for example, where this water can be used to irrigate gardens or flushing toilets, it is necessary to duplicate the building network (drinking and non-drinking water) and the commonly used simultaneity coefficients to size a single building network are significantly changed by grouping devices with similar characteristics in each of the networks. Thus, it becomes evident that water efficiency measures in buildings make it necessary to review and validate new design bases for water supply (Pimentel-Rodrigues & Silva-Afonso, 2022).

In a communication that was previously presented at CIB W062 2014 (Pimentel-Rodrigues & Silva-Afonso, 2014), on the impacts of water efficiency measures on the sizing of water supply pipes, the need to develop further studies on this matter was already noted. In that paper, the graph reproduced in Figure 1 was presented, obtained through telemetry systems in a building with rainwater harvesting and separation of networks (potable and non-potable), showing visible differences in the hourly peaks in the two networks.
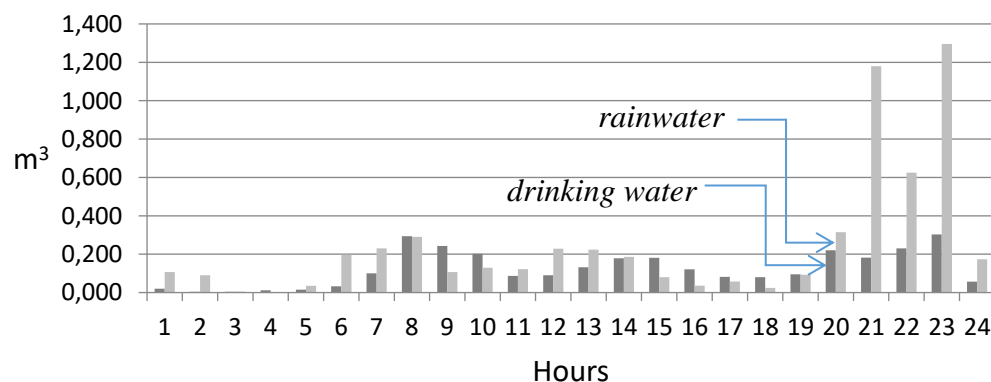
Figure 1 - Comparison of average hourly consumption in June in a building with a rainwater harvesting system (Pimentel-Rodrigues & Silva-Afonso, 2014)

This paper presents a reflection on the applicability of traditional methods for sizing pipe networks in buildings equipped with systems such as rainwater harvesting or greywater recovery, through a bibliographical review on the most appropriate sizing methods for supplying networks with only one or two types of devices (i.e. devices with similar operating parameters), as usually happens in these systems. A proposal for a specific probabilistic design method for these situations is also presented.

2 Materials and methods

Once the characteristics of the installation have been defined, the design flows and the limits and restrictions relating to velocities and pressures are usually the necessary basic elements for sizing pipe networks. The design flows are determined from the instantaneous flows in the different water using products (WuP), whose minimum values are generally fixed in regulations or standards. It should be noted, however, that the instantaneous flows and usage times can vary significantly with factors that are independent of the characteristics of the devices (such as network pressure, climatic conditions or user habits), or with the characteristics of the equipment (as is the case of washing machines or flushing toilets).

When the simultaneous operation of all devices and equipment is not foreseeable, as is usually the case, the use of the accumulated flow (i.e. the sum of all downstream flows rates) as design flow would lead, from a technical and economic perspective, to an obvious oversizing of the network. Thus, in most situations, it becomes necessary to establish criteria of simultaneities adequate to the "patterns" of device use.

Given that it is not possible to fix these standards "a priori", the determination of design flows is necessarily covered with a high degree of imprecision, which justifies the fact that numerous authors, with relatively diversified approaches, have studied and proposed different methods for its determination. In fact, references can be found in the specialized bibliography to methods based solely on probability theory or exclusively empirical methods, as well as to various "mixed" methods, weighing, in different ways, those two extreme approaches.

As previously mentioned, in situations where the simultaneous operation of all the installed WuP is not foreseeable, it becomes necessary, for the sizing of the different sections of the network, to determine a foreseeable maximum simultaneous flow, or design flow, which will naturally be lower than that which results from the sum of the instantaneous flows in the various WuP installed downstream of the section under study (or accumulated flow). The relationship between the maximum foreseeable simultaneous flow in a given section and the accumulated flow on that section can be translated into a coefficient, which is generally called the simultaneity coefficient.

In general, it's not impossible for all WuP to work simultaneously at some point, so the expression "it is not foreseeable" should be interpreted as "has a very low probability". In fact, there is always a very small probability that design flows can be exceeded in a very short period of time, which raises the question of fixing the percentage of time in which this situation is acceptable. Should be noted that some authors, such as Delebecque (1969) or Hunter (1940), associate this probability with levels of comfort in the installation.

Hunter's criterion, still accepted today, is relatively simple. Hunter considered that the system is adequately dimensioned if it is possible to supply, with a satisfactory level of comfort, the flows necessary for the operation of n devices, in a total of m existing in the building, being n fixed so that a greater number of devices will probably is not found to be operating simultaneously more than 1% of the time.

When only one type of WuP is installed, with the same characteristics and operating conditions, the probabilistic methods are particularly suitable for calculating the design flows. The next item describes two simple probabilistic methods, referred to by several authors as appropriate to determine design flows in these situations.

3 Results

3.1 Application of the method based on daily usage cycles

Several authors, such as Angelo Gallizio (1964) or Rodriguez-Avial (1971), present a formula based on the calculation of probabilities, which makes it possible to determine the number of similar devices that are likely to work simultaneously once a day at most. Designating by T the average duration of the interval between consecutive uses of a given type of device, in the period of operation of the installation P, and by t the average duration of operation of that device in each use, the proposed formula is:

$$log\left(\frac{T}{t}\right)^{n-1} - log\left(\frac{P}{T}\right) = \log\left(\begin{smallmatrix} m \\ n \end{smallmatrix}\right) \tag{1}$$

Table 1 shows the proposed range of T, P and t values for residences, hotels and offices, according to Gallizio (1964), Rodriguez-Avial (1971) and Macintyre (1982). The latter author considers office values also applicable to factories during working hours and not at shift change.

From the values in Table 1, Gallizio (1964) and Macintyre (1982) elaborated several simultaneity curves, for devices with similar times and periods of use (T, t and P), which allow us to obtain, in the function of the total number of analogous devices (m), a coefficient of simultaneity. Figure 2 shows one example of this type of simultaneousness curve (Macintyre, 1982), with the curve I applicable to bathtubs, curve II to flushing toilets, bidets and washbasins in homes, curve III to toilets with flush valves in homes,

curve IV to washbasins in offices and factories, curve V to toilets with flush valves in offices and factories and curves VI and VII are intended for comparison of results with some international standards (US and France, respectively). Figure 3 shows analogous curves, created by Gallizio (1964). It should be noted, however, that neither Macintyre nor Gallizio refer the values of *P, T* and *t* that they considered for the elaboration of the graphs, which can have different values, as indicated in Table 1.

Table 1 - Average duration of uses and intervals between uses in operating periods

WuP	*P*	*T*	*t*
Residences and Hotels:	2 hours		
- washbasins, bidets and flushing toilets		20 to 40 min	2 min
- toilets with flush valve		20 to 40 min	8 s
- bathtubs and showers		1 to 2 hours	(5 to) 10 min
Offices:	7 to 8 hours		
- washbasins		10 to 20 min	1 min
- toilets with flush valve		10 to 20 min	8 s
- flushing toilets		10 to 20 min	2 min
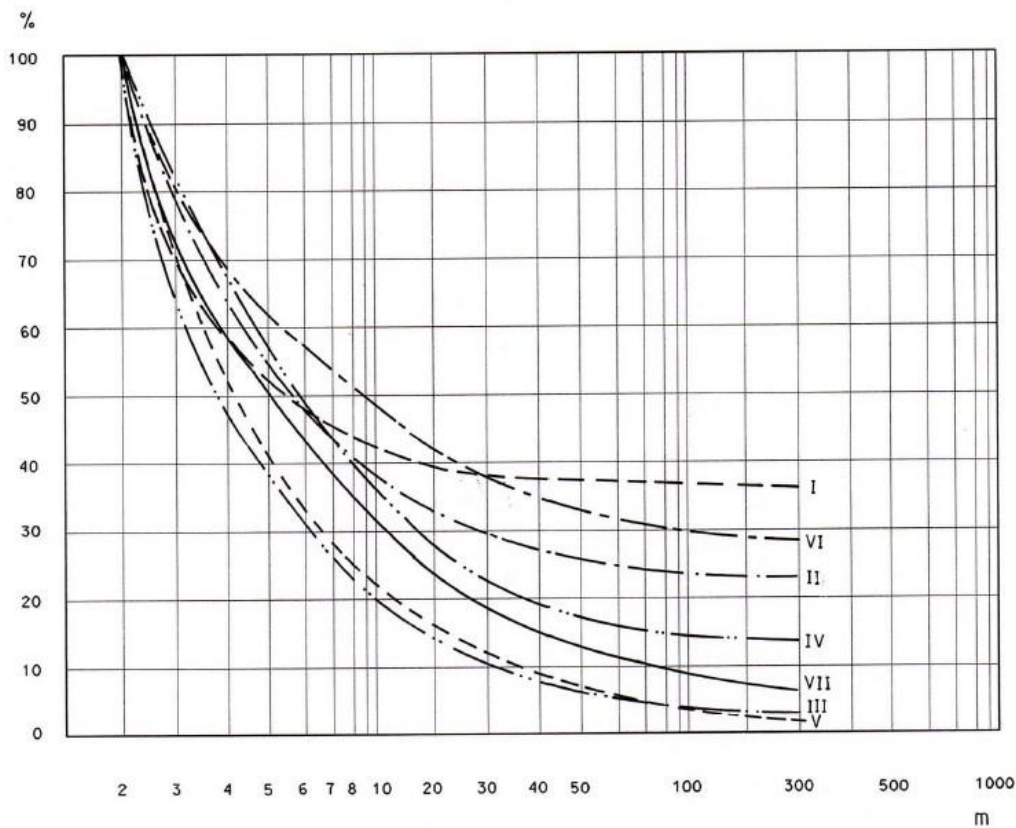
Figure 2 - Simultaneous use probability curves (Macintyre, 1982)
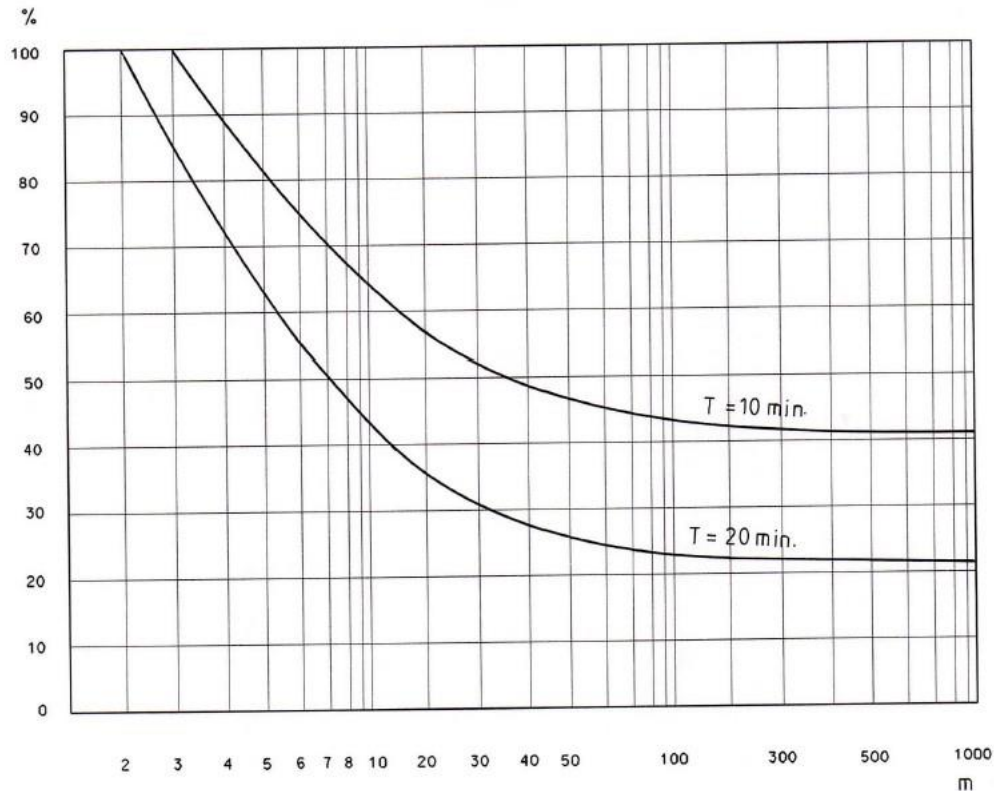
Figure 3 - Simultaneity curves for flushing toilets in offices and similar installations (Gallizio, 1964)

Consider, for example, an office building, with 40 washbasins and 20 flushing toilets, the latter being supplied from a rainwater harvesting system in the building. Based on the Macintyre and Gallizio curves, a simultaneity coefficient of 19% can be obtained for washbasins (8 in simultaneous operation) and 35% for toilets (7 in simultaneous operation) for the lower curve. Considering, according to European standards (EN 806-3:2006) a flow rate of 0.10 L/s in both devices, the design flows will then be 0.80 L/s and 0.70 L/s, respectively, at the beginning of the networks.

3.2 Analysis based on the binomial law (Bernoulli scheme)

Consider a succession of random experiments, the results of which can only be "favourable" or "unfavourable", whose hypotheses are known. In the case of identical and unrelated experiments, that is, repetition, under the same conditions, of independent experiments with the same realization hypotheses, this scheme is called "Bernoulli scheme" or repeated experiments, corresponding to a probabilistic model designated by law or binomial distribution. This model can be applied to a building system with a large

number of identical devices, assuming probabilistic independence in the use of installed devices and taking the opening or operating situation as a "favourable" event for each device.

Let p then be the probability that one utilization device is in operation and q ($q = 1 - p$) the probability of the opposite event (that is, that the device is closed). Taking into account the possible number of combinations of n devices in a total of m, $\binom{m}{n}$, the probability that, in m devices, n are in simultaneous operation and the rest are closed, will be:

$$p_n = \binom{m}{n} p^n q^{m-n} \tag{2}$$

Hunter's criterion can be translated by the expression:

$$p_{n+1} + p_{n+2} + \cdots + p_m \leq 0.01 \tag{3}$$

or, also:

$$p_0 + p_1 + \cdots + p_n \geq 0.99 \tag{4}$$

given that the adopted criterion corresponds to an accumulated probability of not less than 99%, meaning that, at least 99% of the time, the calculation flow rate must not be exceeded.

The probability of a washbasin being in operation at a given moment will be, according to Table 1 (and adopting $T = 11$ min, considering the number of employees):

$$p = \frac{t}{T} = \frac{1}{11} = 0.091 \tag{5}$$

The opposite probability will then be:

$$q = 1 - 0.091 = 0.909 \tag{6}$$

For flushing toilets, with $T = 12{,}5$ min and $t = 2$ min, it will be $p = 0.160$ and $q = 1 - 0{,}160 = 0.840$.

Two tables can then be constructed to determine the different cumulative probabilities (Tables 2 and 3). Observing the tables, it can be concluded that an accumulated probability equal to or greater than 0.99 is obtained for a number of devices equal to that determined by the method indicated in the previous item.

4 Discussion and proposal

The main difficulty in applying the probabilistic methods referred to in the previous item lies in setting "a priori" the parameters P, T and t. However, its validity is defended by several authors, always safeguarding its applicability only in networks with WuP with the

same T and t values. In addition to Macintyre, Rodriguez-Avial and Gallizio, they are also cited by Wise (1986), Swaffield and Galowin (1992), etc.

There are other methods applicable to networks with only similar devices, which will not be referred to in this paper because they are less generalized. The application of traditional methods for networks with diverse WuP (probabilistic, empirical or "mixed" methods) can also be considered in these cases, but the results will naturally suffer distortions due to the fact that these methods weight WuP with very different T and t parameters.

Table 2 - Probabilities of simultaneous operation of washbasins, for a total of 40 devices installed

n	$\binom{m}{n}$	$p_n = \binom{40}{n} 0.091^n 0.909^{40-n}$	Accumulated Probability
0	1	0.0220	0.0220
1	40	0.0881	0.1101
2	780	0.1720	0.2822
3	9,880	0.2181	0.5003
4	91,390	0.2020	0.7023
5	658,008	0.1456	0.8479
6	3838,380	0.0850	0.9329
7	18,643,560	0.0413	0.9743
_**8**_	76,904,685	0.0171	_**0.9914**_
9	2.73E+08	0.0061	0.9974
…	…	…	…

Table 3 - Probabilities of simultaneous operation of flushing toilets, for a total of 20 devices installed

n	$\binom{m}{n}$	$p_n = \binom{20}{n} 0.160^n 0.840^{20-n}$	Accumulated Probability
0	1	0.0306	0.0306
1	20	0.1165	0.1471
2	190	0.2109	0.3580
3	1,140	0,2410	0.5990
4	4,845	0.1951	0.7941
5	15,504	0.1189	0.9130
6	38,760	0.0566	0.9696
_**7**_	77,520	0.0216	_**0.9912**_
8	125,970	0.0067	0.9979
9	167,960	0.0017	0.9996
…	…	…	…

The inconvenience of Bernoulli's scheme being limited only to similar WUPs can be overcome with a new approach, presented below, which is a 2D application (for two types of devices). In theory, Bernoulli's scheme could even be generalized to more types of devices, considering applications in 3D, for example.

Consider, for example, a student residence where 60 washbasins and 20 showers are supplied with drinking water from the mains (the flushing cisterns are supplied with rainwater). It can be considered for washbasins $p = 0.100$ ($t/T = 2$ min/20 min) and for showers $p = 0.167$ ($t/T = 10$ min/60 min). For these two significantly different types of devices, it is possible to construct a matrix, with an indication of the cumulative probabilities resulting from the multiplication of the individual cumulative probabilities of the washbasins and showers.

It can already be noted that this matrix will indicate numerous combinations with joint cumulative probability equal to or greater than 0.99, with very different flows-rates, some of which without any practical logic. However, Silva-Afonso (2001) mentions that, in the tails of the distribution, a probability density (or relative frequency) of 1% is approximately equivalent to the cumulative probability of 99%. Thus, this last approach, which leads to a matrix that is easier to interpret, was adopted in this example.

In this way, Figure 4 was constructed, where it can be seen that, for the various values of joint probability density, probabilistic level "curves" are obtained, similar to topographic level curves. Situations marked in grey form the "level curve" corresponding to the probability level closest to 0.01.

Number of washbasins	Probability density	Number of showers										
		Probability density										
		0	1	2	3	4	5	6	7	8	...	20
		0,0258	0,1037	0,1976	0,2377	0,2025	0,1299	0,0651	0,0261	0,0085	...	0,0000
0	0,0018	0,0000	0,0002	0,0004	0,0004	0,0004	0,0002	0,0001	0,0000	0,0000	...	0,0000
1	0,0120	0,0003	0,0012	0,0024	0,0028	0,0024	0,0016	0,0008	0,0003	0,0001	...	0,0000
2	0,0393	0,0010	0,0041	0,0078	0,0093	0,0080	0,0051	0,0026	0,0010	0,0003	...	0,0000
3	0,0844	0,0022	0,0087	0,0167	0,0201	0,0171	0,0110	0,0055	0,0022	0,0007	...	0,0000
4	0,1336	0,0034	0,0139	0,0264	0,0317	0,0270	0,0173	0,0087	0,0035	0,0011	...	0,0000
5	0,1662	0,0043	0,0172	0,0328	0,0395	0,0337	0,0216	0,0108	0,0043	0,0014	...	0,0000
6	0,1693	0,0044	0,0176	0,0335	0,0402	0,0343	0,0220	0,0110	0,0044	0,0014	...	0,0000
7	0,1451	0,0037	0,0150	0,0287	0,0345	0,0294	0,0188	0,0094	0,0038	0,0012	...	0,0000
8	0,1068	0,0028	0,0111	0,0211	0,0254	0,0216	0,0139	0,0070	0,0028	0,0009	...	0,0000
9	0,0686	0,0018	0,0071	0,0135	0,0163	0,0139	0,0089	0,0045	0,0018	0,0006	...	0,0000
10	0,0389	0,0010	0,0040	0,0077	0,0092	0,0079	0,0050	0,0025	0,0010	0,0003	...	0,0000
11	0,0196	0,0005	0,0020	0,0039	0,0047	0,0040	0,0025	0,0013	0,0005	0,0002	...	0,0000
12	0,0089	0,0002	0,0009	0,0018	0,0021	0,0018	0,0012	0,0006	0,0002	0,0001	...	0,0000
13	0,0037	0,0000	0,0000	0,0000	0,0000	0,0000	0,0000	0,0000	0,0000	0,0000	...	0,0000
...	...	...	...	...	...	...	...	...	...	...	...	...
60	0,0000	0,0000	0,0000	0,0000	0,0000	0,0000	0,0000	0,0000	0,0000	0,0000	...	0,0000

Figure 4 - Probability densities corresponding to the simultaneous operation of devices with different characteristics

For these situations, Figure 5 was constructed, where, for the indicated situations, the probability density is replaced by the accumulated flow rate corresponding to the respective combinations of devices. It can be concluded that the most unfavourable situation corresponds to the simultaneous operation of five showers and nine washbasins (or six showers and seven washbasins), with a design flow of 1.9 L/s.

Number of washbasins	Flow rate (L/s)	Number of showers Flow rate (L/s)										
		0	1	2	3	4	5	6	7	8	...	20
		0,00	0,20	0,40	0,60	0,80	1,00	1,20	1,40	1,60	...	4,00
0	0,00											
1	0,10											
2	0,20			0,60	0,80	1,00						
3	0,30		0,50				1,30					
4	0,40											
5	0,50							1,70				
6	0,60											
7	0,70							1,90				
8	0,80		1,00									
9	0,90						1,90					
10	1,00			1,40	1,60	1,80						
11	1,10											
12	1,20											
13	1,30											
...	...											
60	6,00											

Figure 5 - Design flow rates (L/s) corresponding to the simultaneous operation of devices with different characteristics, based on the proposed criterion.

5 Conclusions

The need for a more sustainable use of our planet's resources, especially fresh water, has led to a growing development and implementation of more sustainable solutions in the urban water cycle, such as the reuse of water or rainwater harvesting in buildings. These solutions generally imply the installation of separate networks, the non-potable water networks being able to supply only one or two types of devices.

This situation implies the need to rethink pipe sizing methods, which are generally suitable for traditional networks with devices with different characteristics. When there is only one type of device, the Bernoulli scheme (or Binomial Law) is referred to by several authors as being one of the most suitable probabilistic methods for sizing. However, it has this limitation of being only applicable when there is only one type of WuP.

This work presents a generalization of Bernoulli's scheme that allows its application when the network has two different types of devices, allowing to expand the domain of application of the method. Naturally, it is just a contribution to support the sizing of conduits in these specific situations, it being important to develop or adapt other methods,

which allow a more adjusted design of the networks in this era of new solutions for the buildings water cycle, aiming a greater water efficiency.

6 References

AWWA (2006) - *Climate change and water resources: A primer for municipal water providers,* AWWA Research Foundation/University Corporation for Atmospheric Research/American Water Works Association/IWA Publishing, 1P-5C-91120-05/06-NH, Denver, 2006.

Delebecque, R. (1969) - *Les installations sanitaires,* Paris: Société de Diffusion des Techniques du Batiment et des Travaux Publiques, 1969 (in French).

European Commission, COM (2005) 718 - *Communication from the Commission to the Council and the European Parliament on Thematic Strategy on the Urban Environment*, Commission of the European Communities - SEC (2006) 16, Brussels, 2006.

European Commission (2006) - COM 718 *Communication from the Commission to the Council and the European Parliament on Thematic Strategy on the Urban Environment*; Commission of the European Communities, SEC: Brussels, Belgium, 2006.

Gallizio, A. (1964) - *Implanti sanitari*, 6ª Ed.. Milano: Edit. Ulrico Hoepli, 1964 (in Italian).

Hunter, R. (1940) - *Methods of estimating loads in plumbing systems*, Gaithersburg: US National Bureau of Standars, BMS 65, 1940.

Macintyre, A. (1982) - *Instalações hidráulicas*, Rio de Janeiro: Editora Guanabara Dois, S.A., 1982 (in Portuguese).

Pimentel-Rodrigues, C.; Silva-Afonso, A. (2014) – *The need to rethink the design criteria for water supply in buildings in light of the implementation of water efficiency measures*, Proceedings CIB W062 2014 – Water Supply and Drainage for Buildings, S. Paulo, Brazil, 2014.

Pimentel-Rodrigues, C.; Silva-Afonso, A. (2022) – *Rainwater Harvesting for Irrigation of Tennis Courts: A Case Study*. Water (2022), MDPI, ISSN: 2073-4441, 14, 752.

Rodriguez-Avial, M. (1971) - *Instalaciones en los edificios. Fontaneria y saneamiento*, 5ª Ed. Madrid: Dossat, 1971 (in Spanish).

Silva-Afonso, A. (2001) - *Contributos para o dimensionamento de redes de águas em edifícios especiais. Aplicação de modelos matemáticos,* Porto: Faculdade de Engenharia da Universidade do Porto, 2001. PhD Thesis (in Portuguese).

Silva-Afonso A. (2014) - *The bathroom of the future: its contribution to sustainability*, Proceedings of the International Symposium CIB W062 2014 – Water Supply and Drainage for Buildings, S. Paulo, Brazil, 2014.

Swaffield, J.; Galowin, L. (1992) – The engineering design of building drainage systems, Cambridge: Ashgate Publishing Limited, 1992.

United Nations (2012) - *The future we want.* New York, 2012.

United Nations (2022) - *The Sustainable Development Goals Report 2022*, Available online: https://unstats.un.org/sdgs/report/2022/ (accessed on 12 April 2023).

Wise, A. (1986) – *Water, sanitary and waste services*, 2nd Ed., London: Mitchell, 1986.
World Health Organization (2009) - *Summary and policy implications Vision 2013: The resilience of water supply and sanitation in the face of Climate Change*, WHO – Department for International Development, Geneva, 2009.

5 Presentation of Authors

Armando Silva-Afonso is a retired Full Professor at the University of Aveiro (Portugal), Department of Civil Engineering. His specializations are hydraulics and water efficiency in buildings, and he is President of the Board of ANQIP - National Association for Quality in Building Installations in Portugal and Vice-Chair of the Committee on Water of WFEO (World Federation of Engendering Organizations, UNESCO, Paris).

Carla Pimentel Rodrigues holds a PhD from the University of Aveiro (Portugal) in Civil Engineering (water efficiency). She is Executive Director at ANQIP – National Association for Quality in Building Installations and is also Visiting Professor at ISCIA - Higher Institute of Information Sciences and Administration. She has published two books in the field of water efficiency in buildings and one chapter in an international book.

Pipe sizing research in Australia; a decade on.

T. Roberts (1)
(1) Tom.Roberts@ABCB.gov.au
(1) Australian Building Codes Board, Canberra Australia

Abstract
Pipe sizing has been a focus in Australia over the last ten years. The flow determination methodologies and in turn sizing approach nominated by the National Construction Code (Australian Building Codes Board, 2022) in Australia are based on Hunter's method which is now used to assign Fixture Units for sanitary systems and Loading Units for water services (HUNTER, 1940). This method has progressively become outdated and is no longer considered appropriate for the increasing size and height of modern buildings and the increasing efficiency of water using fixtures. As such, alternative flow determination methods are commonly utilised to provide accurate hydraulic design solutions.

To support the use of performance-based solutions, Australia has focused on the quantification of performance requirements in addition to the development of more accurate and adaptable flow determination and pipe sizing methodologies.

Quantification of performance requirements has clarified existing stringency levels and maintained the ability to allow for innovation and flexibility in how these requirements are met. This has seen the introduction of metrics for maximum water service velocities, an acceptable range of water service pressures and a range for sanitary systems pressures to avoid hydraulic imbalance.

Alternative compliance methodologies for both sanitary systems and water services have been investigated to demonstrate that the required level of performance has been met, whilst allowing for variations in factors such as fixture types, quantities, flow rates and building types. This has resulted in the inclusion of an alternative sizing methodology for sanitary systems and the exploration of the effect building types have on the probability of fixture use through smart plumbing fixtures and ultrasonic water metering.

Monitoring of the water demand via ultrasonic water metering in existing buildings has also been undertaken to provide localised data inputs to support the use of the alternative flow determination equation-based methods of demonstrating compliance with the required cold water service velocities.

This wide research focus has enabled the Australian regulatory framework to provide clear compliance levels and accurate hydraulic design solutions.

Keywords
Premise plumbing; Pipe sizing; Plumbing design; Drainage design; Water demand.

1 Introduction
The Plumbing Code of Australia (Australian Building Codes Board, 2022) and referenced Australian Standards, like many other international codes and standards uses a sizing

methodology built upon the works of Dr. Roy B Hunter (HUNTER, 1940). There are several areas where influencing factors have changed since the development and introduction of the fixture unit and loading unit methodology in Australia. These changes are expected to have a significant impact on the performance of water services and sanitary systems.

Some of the areas where change has impacted the accuracy of this method includes:
- progressive changes to hydraulic design best practices through evolving best practice, plumbing codes and standards;
- increased numbers of sanitary facilities within standard designs of certain building classifications, potentially decreasing the probability of individual fixture use per building occupant;
- increased water efficiency requirements resulting in reduced demand and a reduction of pipework velocities and drainage discharges;
- changes in materials being utilised impacting the anticipated friction and pipework roughness considerations; and
- the height and complexity of the hydraulic systems being installed.

Globally, determination of flow rates for pipe sizing of water services and sanitary plumbing and drainage systems has been the focus of significant research and analysis for many years. This paper seeks to provide a high-level overview of the research undertaken over the past 10 years in Australia to highlight and share the key findings and prompt feedback on potential future developments within the Plumbing Code of Australia.

2 Overview of the Australian Plumbing Legislation

Within Australia, each State and Territory is responsible for regulating plumbing within each jurisdiction. Australia is however unified by the Plumbing code of Australia which is adopted into legislation in each jurisdiction with minor variations and additions applied by some States and Territories.

The Plumbing Code of Australia is a performance-based code which required compliance with the Performance Requirements through a Performance Solution or a Deemed-to-Satisfy Solution, which follows a prescribed method.

3 Water services

Water service sizing methodologies used by the Plumbing Code of Australia are contained in the joint Australian and New Zealand Standards AS/NZS 3500 Plumbing and Drainage, Part 1 Cold water services (AS/NZS 3500.1) (Standards Australia , 2021) and AS/NZS 3500 Plumbing and Drainage, Part 4 Heated water services (AS/NZS 3500.4) (Standards Australia , 2021) and assigns a Loading Unit value to each common plumbing fixture type for water services. This method has not adapted to significant reductions in fixture flowrates or changes to the likelihood of fixture usage through changes to the numbers of fixtures required in certain building types and modern bathroom design practices. The probability of fixture use does not take into consideration the varied usage anticipated across different building classifications.

In early 2019, research into cold and heated flow demand and water pipe sizing commenced, with the Australian Building Codes Board investigating alternative methodologies available and commenced exploration of their use within the Plumbing Code of Australia.

The Modified Wistort Method was identified as a suitable pathway for determining the 99th percentile flowrate that occurs during the peak period of usage. This method was seen to be advantageous in considering the number of fixtures, the expected flow rates from each fixture and taking into consideration the likelihood of use.

A comparison between the existing Loading Unit methodology and the Wistort Method as an alternative method of determining the probable simultaneous flow rate was undertaken (Lucid Consulting Australia, 2019). The intention of this comparison was to gain a greater understanding of the differences between these two sizing methodologies and any economic benefits which could be derived from a more accurate pipe sizing method.

The total probable simultaneous flow rates were calculated using the method outlined in Equation 1 and by using the Loading Unit methodology from AS/NZS 3500.1 and AS/NZS 3500.4. This method was compared against the method outlined in Equation 2.

$$\text{PSFR}_{\text{Total}} = \text{PSFR} + \text{Q}_{\text{Other}} + \text{PSFR}_{\text{HWPlant}} \text{ (DCW Only)} + \text{Q}_{\text{Circ}} \text{(DHW Only)} \qquad \textbf{Equation 1}$$

$$PSFR = \sum_{k=1}^{K} \frac{n_k t_k q_k}{T_k} + Z_{99} \sqrt{\sum_{k=1}^{k} \frac{n_k t_k q_{k^2}(T_k - t_k)}{T_{k^2}}} \qquad \textbf{Equation 2}$$

where -
a) K represents the total number of fixtures groups along a down-stream pipe,
b) nk represents the number of fixtures for a specific fixture group downstream of a pipework section,
c) qk represents the specific fixture flow rate,
d) tk represents the average duration of usage in seconds,
e) Tk represents the time between successive operations of an individual fixture in seconds,
f) $z99$ represents the 99th percentile of the standard normal distribution, approximated as 2.326.

To assist in the comparative analysis, a simple test calculator was developed as shown in Figure 1.

ABCB Flow Rate Calculator - Testing Draft
For the determination of Probable Simultaneus Flow Rate in accordance with the draft text of BV1.3

Result - 99th Percentile PSFR (l/s)
4.64

Input Data

Fixture type	Total number of fixtures	Average duration of flow for one use of a given fixture (s)	Time between successive operations of a given fixture (s)	Flow rate per fixture (l/s)
Basins (Apartment)	192	15	1800	0.1
Shower (Apartment)	192	480	7200	0.15
WC (Apartment)	192	30	3600	0.12
Kitchen Sink (Apartment)	136	60	7200	0.1
Dishwasher (Apartment)	136	60	14400	0.2
Washing Machine (Apartmen	136	1300	14400	0.05
Laundry Trough (Apartment)	136	120	72000	0.15
Basins (Common Area)	4	5	1200	0.1
Shower (Common Area)	1	480	1800	0.15
WC (Common Area)	4	30	1200	0.12
Kitchen Sink (Common Area)	2	20	1200	0.1
Dishwasher (Common Area)	1	60	72000	0.2
Hose Tap	2	20	21600	0.2

Figure 1 – Test Calculator

Three differing building types were evaluated through this comparison which consisted of a high-rise multi-unit residential development, a high-rise office development and a hospital which considered both the cold water services and heated water services. The results compared the use of the Wistort Method against the existing prescribed methodologies.

Cost estimates (in Australian Dollars) for the case study projects and financial outcomes for each case study was considered and are summarised in Table 1 for a high-rise multi-unit residential building, Table 2 for a high-rise office and Table 3 for a hospital.

Table 1 – High-rise Multi-unit residential

Service	AS/NZS 3500 method	Proposed alternative sizing method	Cost reduction
Cold water service	$479,508.80	$379,948.10	21%
Heated water service	$434,688.80	$421,570.90	3%
Total	$914,197.60	$801,519.00	12%

Table 2 – High-rise Office

Service	AS/NZS 3500 method	Proposed alternative sizing method	Cost reduction
Cold water service	$241,304.80	$209,683.80	13%
Heated water service	$71,798.20	$72,114.40	0%
Total	$313,103.00	$281,798.20	10%

Table 3 – Hospital

Service	AS/NZS 3500 method	Proposed alternative sizing method	Cost reduction
Cold water service	$810,377.50	$703,215.90	13%
Heated water service	$448,459.60	$417,193.80	7%
Total	$1,258,837.10	$1,120,409.70	11%

The results of this comparative analysis (Lucid Consulting Australia, 2019) demonstrated how oversized cold and heated water services are in Australia and the possible cost reductions which could be derived using alternative sizing methodologies. The report demonstrated that for the case study buildings considered in the analysis, a reduction in size of around 20% to 50% for most pipework sections and greater reductions were able to be derived from larger pipe sizes.

Across each case study, there was an estimated reduction of between 13% to 21% for the costs of the cold water services and 7% for the worked example for the hospital which took into consideration the inputs for tempered heated water and the anticipated reduction in demand associated with the use of temperature control devices. These reductions also represent embodied carbon and energy heat loss reductions derived from a reduction in pipe diameters.

During this time, the Hydraulic Consultants Association of Austrasia [HCAA] in collaboration with Deakin University commenced monitoring the flowrates of several buildings across Australia. This was the first systematic study on the actual water demand of

multi-unit residential buildings in Australia with several key findings being documented in an initial report (JOSEY, 2023).

This monitoring of water demand and observed peak flow rates was undertaken across 4 buildings. The sites monitored included the following buildings:
1. Site 1 – 143 Apartments, 1,291 Fixtures - Waterloo, New South Wales, Australia.
   a. Monitoring of this site commenced on the 13th of August 2019.
2. Site 2 – 112 Apartments, 1,223 Fixtures – Milson's Point, New South Wales, Australia.
   a. Monitoring of this site commenced on the 17th of August 2019.
3. Site 3 - 330 Apartments, 2,912 Fixtures (Manhattan) – Canberra, ACT, Australia.
   a. Monitoring on this site commenced on the 14th of December.
4. Site 4 - 115 Apartments, 859 Fixtures - Braddon, Canberra, ACT, Australia.
   a. Monitoring on this site commenced on the 17th of January 2020.

Note: Monitoring of water demand at these sites continues at the time of publication (Hydraulic Consultants Association of Australasia Ltd, 2019).

The resulting report (JOSEY, 2023) confirmed that the current flow determination methodology used in Australia is resulting in oversizing of pipes. This is also expected to extend to the oversizing of pipes, pumps, valves, and other equipment. The findings were also used to undertake a comparison between the estimations made through the Plumbing Code of Australia and tested the Wistort Method as the alternative method which was investigated in previous research (as described above) as well as other international plumbing codes and standards shown in Table 4.

Post empirical observation of different data capture frequencies, an adjustment factor of 1.2 was applied to the monitored flow rates to account for 1 minute data logging frequencies and the dilution of peak flow events. In addition to the measured and adjusted flow rates, this comparison considered the following codes and standards.

Table 4 - Water demand investigation adjusted 99th percentile and adjusted peak flow rates compared to estimated design peak flow rates determined by selected international plumbing codes (L/s)

Site	Adjusted 99th	Adjusted peak	AS/NZS 3500.1: 2021	DIN 1988-300: 2012	DIN 1988-3:1988	BS EN 806: 2006	IAPMO WDC	Wistort Method
1	2.22	2.76	9.74	2.88	4.38	5.40	2.13	6.01
2	2.45	3.72	8.74	2.84	4.31	5.25	2.10	5.96
3	4.80	5.52	18.20	3.52	5.33	8.75	5.59	12.30
4	2.32	2.82	8.33	2.62	3.95	4.20	1.76	4.35

The 99th percentile flow has been adjusted by 1.2 times the 99th percentile value for all the nonzero flow rates observed within a single hour of largest water consumption within the entire observation period. The adjusted peak value assumes 1.2 of measured peaks values.

A percentage of AS/NZS 3500.1:2021 for each of these sites is outlined in Table 5.

Table 5 - Percentage calculated using the adjusted 99th percentile flow.

Site	Percentage of AS/NZS 3500.1:2021 (%)
1	23
2	28
3	26
4	28

These percentages have been calculated using the adjusted 99th percentile flow.

In estimating the 99th percentile flow rate, the probability inputs for each specific fixture's values for tk and Tk in (JOSEY, 2021) were derived from the comparative analysis report (Lucid Consulting Australia, 2019).
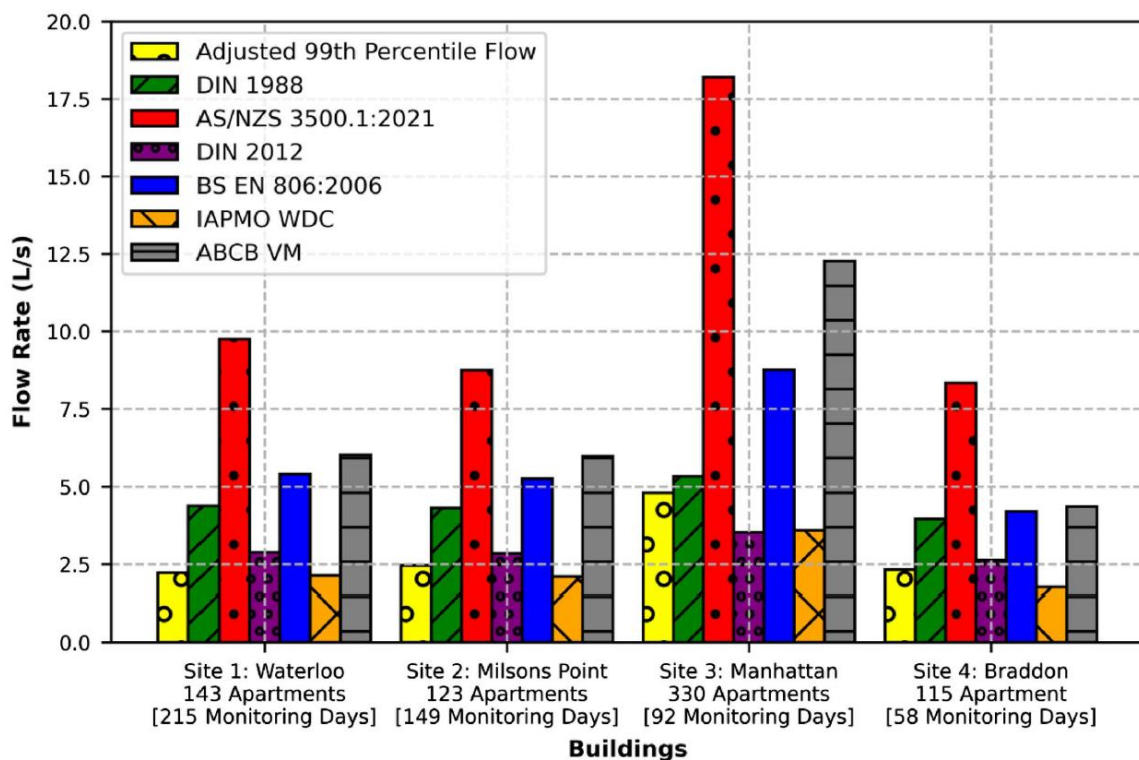
Figure 2 - Adjusted 99th percentile flows compared to selected international plumbing codes (Josey et.al. 2023).
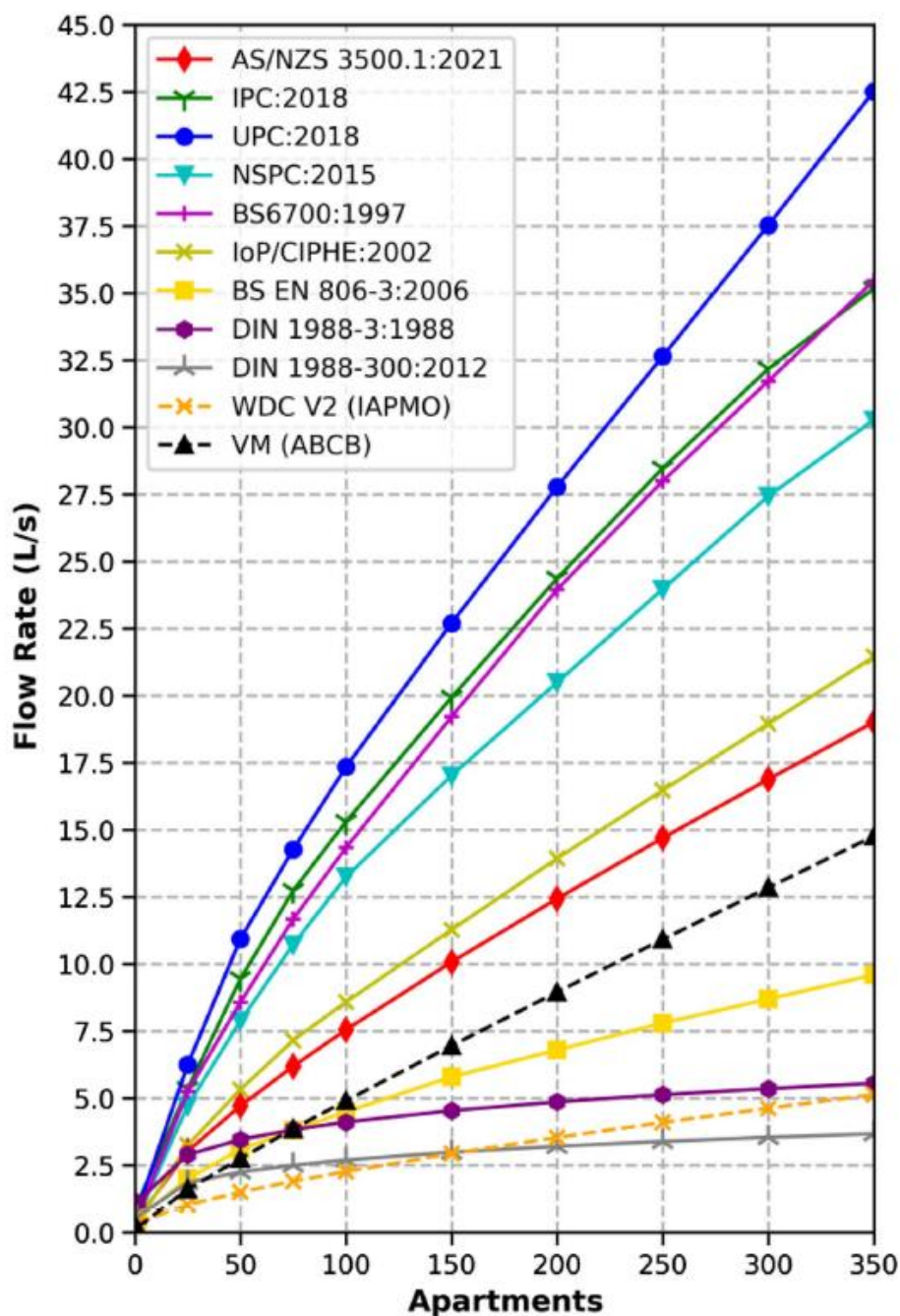
**Figure 3 - Comparison of measured peak flow against Australian
and international plumbing codes (Josey et.al. 2023)**

This comparative analysis highlighted a significant overestimation of hydraulic demand and peak flow rates within a range of 217% to 326% across the buildings observed, compared to the calculated demands using AS/NZS 3500.1:2021.

(JOSEY, 2021) conducted a numerical hydraulic modelling case study to further explore the impact of a hydraulic design based on the observed demands of the building with findings indicating that pipe sizes could be reduced from a nominal diameter of 100mm to 40mm whilst maintaining compliant operating conditions set through the Performance Requirements of the Plumbing Code of Australia.

This report also highlighted that whilst the potential use of the Wistort Method in estimating probable simultaneous peak demand did present greater accuracy over the method used in AS/NZS 3500.1, there was still a significant over estimation and further investigation into the probability of fixture usage in Australia was recommended. This investigation into these probability factors commenced in 2023 and is also proposed to be utilised primarily for the purposes of sanitary plumbing and drainage pipe sizing (see below).

2.1 Future concepts for cold water flow determination and pipe sizing

Investigations into providing the appropriate equations for meeting the Performance Requirements of the Plumbing Code of Australia in areas such as cold water service velocities are being explored. One example is outlined in Equation 3 to determine the anticipated velocity and confirm if it will be within the maximum of 3 metres per second set by the Plumbing Code of Australia. Additional equations are being considered such as the use of the Modified Wistort Method (BUCHBERGER, 2017) as outlined in Equation 4. In addition, (JOSEY, 2021) have analysed fixture usage high-level data retrieved from Australian residential end-use studies. The analysis considered both building size and expected number of building occupants to determine the probability of fixture usage for Australia residential building. The formulae to estimate probability values are outlined in Equation 5, Equation 6 and Equation 7.

It should be noted that the velocity limit defined by the Plumbing Code of Australia is an upper limit value and does not necessarily represent a suitable velocity for water service components, equipment, and pipework materials. Research is needed to ascertain suitable velocities for particular products and any specific design and installation criteria.

$$D_{min} = \sqrt{\frac{4Q_{99} \times 10^3}{\pi v}} \quad when: v = 3m/s \ D_{min} \approx \sqrt{425Q_{99}}$$

Equation 3

where:

a) D_{min} represents the minimum pipe diameter in [mm],
b) Q_{99} represents the 99th percentile [L/s],
c) v represents the maximum velocity [m/s],

It is recognised that not all water service components are selected based on the 99th percentile flowrate. The obligation would be on the hydraulic designer to ensure appropriate use of such an equation when selecting components using the 99th percentile flowrate.

$$Q_{99} = \frac{1}{1 - P_0} \left[\sum_{k=1}^{K} n_k p_k q_k + (1 + P_o) z_{99} \sqrt{\left[(1 - P_o) \sum_{k=1}^{K} n_k p_k (1 - p_k) q_k^2 \right] - P_o \left(\sum_{k=1}^{K} n_k p_k q_k \right)^2} \right]$$

Equation 4

where:

a) Q_{99} represents the 99th percentile flowrate (i.e. the designed probable simultaneous flow rate).
b) P_0 represents the probability of stagnation during peak usage (zero demand), See Equation 5.

c) K represents the total number of fixture groups.
d) k represents the index of individual fixture groups.
e) n_k is the number of fixtures for a specific fixture group downstream of a pipework section.
f) q_k is the specific fixture flow rate, See Table 6.
g) p_k is the probability of fixture use (probability that a fixture group is running water during the peak period of water consumption), See Equation 6.
h) z_{99} represents the 99th percentile of the standard normal distribution and is equal to 2.362.

Whilst the expected average fixture flow rates (q_k) can be determined based on the type selected for a particular project, explanatory information could be provided to hydraulic designers as guidance such as that presented in Table 6.

Table 6 - Recommended fixture flowrates for water efficient fixtures and appliances

Fixture	Flowrate, q_k [L/s]
Shower	0.15
Tap, Basin	0.08
Tap, Kitchen	0.12
Tap, Laundry	0.12
Toilet 3/4.5L	0.19
Washing Machine	0.22
Dishwasher	0.08
Bath	0.30

$$P_0 = \prod_{k=1}^{K}(1 - p_k)^{n_k}$$ **Equation 5**

where:

a) P_0 represents the probability of stagnation during peak usage (zero demand).
b) K represents the total number fixture groups.
c) k represents the index of individual fixture groups.
d) n_k is the number of fixtures for a specific fixture group downstream of a pipework section.
e) p_k is the probability of fixture use (probability that a fixture group is running water during the peak period of water consumption), see Equation 6.

$$p_k = p_{k,B} + F_{o,B}$$ **Equation 6**

where:

a) p_k represents the probability of fixture use.
b) $p_{k,B}$ is the baseline probability of fixture use, and assumes 1 occupant per building apartment, see Equation 7.

c) $F_{o,B}$ represents the probability adjustment factor according to occupancy, it is an increase to the baseline probability of fixture use for the total number of occupants greater than the building size.

$$p_{k,B} = p_{k,1} \text{ when: } B = 1$$
$$p_{k,B} = c_1 p_{k1} B^{-c_2} \text{ when: } 2 \leq B \leq 20$$
$$p_{k,B} = c_1 p_{k1} 20^{-c_2} \text{ when: } B > 20$$

Equation 7

where:

a) $p_{k,B}$ is the baseline probability of fixture use, this assumes 1 occupant per building apartment.
b) B represents building size, by number of apartments drawing water downstream of specific pipe section.
c) $p_{k,1}, c_1, c_2$, are coefficients.

In addition to the above calculation methods which could be used to determine the anticipated probable simultaneous flow rates and velocity based on a selected pipe diameter. Additional considerations could be given to potential probability adjustment factors. These factors allow for a suitable adjustment to the probability based on building occupancy and may allow for an increase in the probability of fixture use with an increase in building size. A method for the determination of an appropriate adjustment factor is outlined in Equation 8 with a method of determining the increased probability of fixture use per building occupant outlined in Equation 9.

$$F_{o,B} = m_{k,B}(o - B)$$

Equation 8

where:

a) $F_{o,B}$ represents the probability adjustment factor according to occupancy, it is an increase to the baseline probability of fixture use for the total number of occupants greater than the building size.
b) B represents building size, by number of apartments drawing water downstream of specific pipe section.
c) o represents the estimated total number of building occupants drawing water downstream of specific pipe section.
d) $m_{k,B}$ represents the increased probability of fixture use per additional building occupant greater than the building size, see Equation 9.

$$m_{k,B} = c_3 B^{-c_4} \text{ when: } B > 1$$

Equation 9

where:

a) $m_{k,B}$ represents the increased probability of fixture use per additional building occupant greater than the building size,
b) B represents building size, by number of apartments drawing water downstream of specific pipe section.
c) c_3, c_4, are coefficients, see Table 7.

The probability of fixture use is dependent on factors such as:

a) building size (by number of apartments, B) and
b) building occupancy (estimated number of building occupants o, drawing water downstream for a specific pipe section).

Consideration would need be given to the anticipated occupancy for each apartment building. Where building occupancy is not known, the consideration could be given to the number of bedrooms for each dwelling which could be used as an indicator of the anticipated building occupancy, (i.e. o = Number of Bedrooms). Statistics on average building occupancy rates could also be utilized to make informed assumptions.

Coefficients for each fixture are outlined in Table 7 with p-values for taps being inclusive of all installation locations with the values used having been derived from fixture use characteristics (JOSEY, 2023).

Table 7 - Coefficients to calculate probability of fixture use (residential buildings)

Fixture	p_{k1}	c_1	c_2	c_3	c_4
Shower	0.061	0.908	-0.475	0.020	-1.343
Taps	0.009	1	0	0.004	-0.880
Toilet	0.002	1	0	0.002	-0.880
Washing Machine	0.031	0.976	-0.515	0.005	-1.349
Dishwasher	0.001	1	0	0.0005	-0.880
Baths	0.006	1.460	-0.411	0.008	-1.768

The concepts being explored above demonstrate a possible methodology that could be adopted for water services. Whilst existing methods may continue to be suitable for simple and small water services, as buildings and associated water services become more complex, it is essential that flow rate determination leading to pipe sizing methods prescribed in codes and standards provide an adaptive and accurate methodology.

4 Sanitary plumbing and drainage

Sanitary plumbing and drainage systems have also been a principal consideration in the focus on pipe sizing research in Australia. An initial review, 'Fixture Unit methodology in hydraulic design', and a literature investigation into the development of the Fixture Unit method was conducted (GHD, 2015). This investigation undertook a review of available literature and provided commentary on the evolution of the fixture unit system through various codes globally.

This literature review highlighted that one of the key elements that underpins modern sanitary plumbing pipe sizing methods is consideration of the probability of fixture, and with probability theory, the larger the building the larger the sample size in the number of fixtures and the greater the accuracy of any probability-based predictions.

When considering anticipated fixture usage and the probability of simultaneous fixture use, the type of building and anticipated human behaviours within each building type are key influencing factors which is not considered within the current pipe sizing methods contained in AS/NZS 3500 Plumbing and drainage, Part 2 Sanitary plumbing and drainage (AS/NZS 3500.2).

International codes and standards were also an important consideration in investigating the origins of the Fixture Unit methodology. With the Fixture Unit being derived from the United States of America (USA), an initial comparison was conducted between the USA with Australia (GHD, 2015). Of particular interest was the work conducted by the American Water Works Association in 1975 which introduced the 'Fixture Value Method', an empirically derived approach with data inputs being obtained through data loggers in specific building categories. Whilst this approach was utilised to consider peak water demands, the approach itself was of great interest for the development of a modern and accurate pipe sizing method with the ability to utilise advancements in technology since the mid 70's to the connected fixtures and hydraulic monitoring equipment available today.

In investigating the origins of Fixture Unit methodology, consideration was given to the approaches to pipe sizing globally. Several regions were looked at such as Europe, Hong Kong, and South Africa. Most of these regions have been found to have based their pipe sizing methodologies from the original Fixture Unit method. However, these codes and standards have since evolved to adapt to local conditions, having been informed by local research and giving considerations of other analysis methods such as the Fuzzy Logic and Monte Carlo simulation.

As the Fixture Unit method focuses on a single point (99th percentile) of the peak flow of Cumulative Distribution Function, this was seen as a key metric which could be explored as a principle to quantify the Performance Requirements of the Plumbing Code of Australia.

The generalised frequency of usage factors used in Britain were of particular interest to plumbing regulatory authorities and the hydraulic industry in Australia. Using the basic principle of low, medium and high usage considerations (Chartered Institution of Building Services Engineers [CIBSE], 2014). These factors anticipate the time between fixtures and appliance uses and greatly simplify one of the key inputs into the probability of fixture use (see Equation 10).

Having regard to differing global adaptations of the Fixture Unit methodology and an international comparison in the sanitary plumbing and drainage pipe sizing methods, the next stage of the Australian Building Codes Boards investigation focused on European codes and standards, in particular those contained in British Standard (BS) European Norm (EN) 12056-2:2000 (B.S. Institute, 2000) and BS EN 752:2017 (B.S. Institute, 2017). A comparison between these methods and those used in Australia and New Zealand Standard AS/NZS 3500.2 (Standards Australia, 2018) (Lucid Consulting Australia, 2019).

A review of these standards was conducted assessing the suitability of utilising the sizing methodology. Several similarities were identified between the Australian and British standards, whilst noting that there were some minor differences in installation requirements.

The early investigations indicated that there were potential advantages over the Australian use of the Fixture Unit method. These advantages included the use of calculating the

anticipated wastewater flowrates by simply considering the total discharge (expressed as Discharge Units) and the frequency factors which consider probabilities of fixture usage across different building types. These building categories are classified as intermittent use, frequent use, congested use and special use, with some examples of building types.

This finding was a key factor which had not been considered within Australian codes and standards and was explored further (Arup, 2022). These frequency factors and their potential to be utilised in the determination of wastewater flow rates was utilised from BS EN 12056.2:2000, see Equation 10.

$$Q_{ww} = K\sqrt{\sum DU}$$ **Equation 10**

where:
  a) Q_{ww} represents the wastewater flow rate,
  b) K represents the frequency factor,
  c) $\sum$DU represents the sum of discharge units.

Frequency factors or K factors are applied to specific sanitary plumbing and drainage systems in BS EN 12056-2:2000 and outline various anticipated usage configurations from:
  a) 0.5 for intermittent use (e.g., dwelling, guest house, office),
  b) 0.7 for frequent use (e.g., hospital, school, restaurant, hotel),
  c) 1.0 for congested use (e.g., Toilets and or showers open to public use), and
  d) 1.2 for special use (e.g., laboratory).

Further investigation into the probability factors have indicated that consideration of the time intervals between fixture use constants can deliver improved outcomes via the use of this method. The research undertaken (Arup, 2023) has been able to determine the relationship between fixture usage and K-Factor values and further extrapolate these values. The potential fixture usage and k-factor relationship are outlined in Table 8.

Table 8 – Potential fixture usage and K-Factor relationship

Time between fixture use (second)	K-Factor
1200	0.5
600	0.7
300	1.0

With the assumption that there is a correlation between the intervals between fixture usage and K-Factors as outlined in Table 8. These data points have been used to develop a formula relating K-Factors to time between fixture usage, as outlined in Equation 11.

$$K = \left(\frac{300}{T}\right)^{0.5} = \sqrt{\frac{300}{T}}$$ **Equation 11**

It is noted in the report that this assumption is based on only three data points to extract a trendline and that 300 seconds of operation may not be appropriate.

$$K = \left(\frac{300}{T}\right)^{0.5} = \sqrt{\frac{300}{T}}$$

Equation 11

In the report (Arup, 2023), the variability and dependence of the K-Factor equation proposed in the 2022 report (Arup, 2022) on the time interval between fixtures was further demonstrated. Additional equations were considered to plot the relationship between the K-Factor and the duration between fixture uses with 300 seconds being retained for basins, sinks Water Closets (WC) and bidets (see Equation 12) with duration intervals given in

Table *9* and alternative frequencies being applied for showers (see Equation 13) with duration intervals given in Table 10 and baths (see Equation 14) with duration intervals given in Table 11. The report also considered low, medium and high use cases and provided a graphical representation and curve in Figure 4.

$$K = \left(\frac{300}{T}\right)^{0.5}$$

Equation 12

Table 9 – Duration between basin, sink, WC and Bidet uses.

Low use case	Medium use case	High use case
1200	600	300

$$K = \left(\frac{923.8}{T}\right)^{0.618}$$

Equation 13

Table 10 – Duration between shower uses.

Low use case	Medium use case	High use case
2700	1800	900

$$K = \left(\frac{1192}{T}\right)^{0.5}$$

Equation 14

Table 11 – Duration between bath uses.

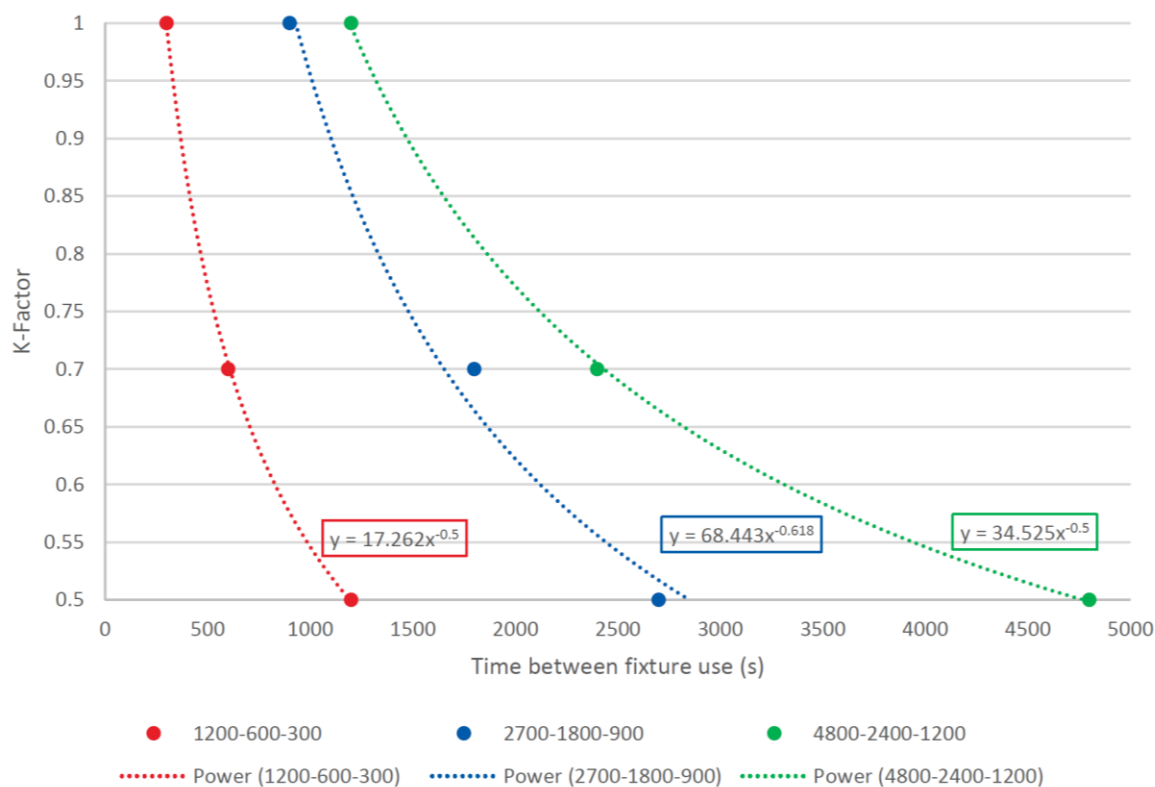| Low use case	Medium use case	High use case
4800	2400	1200

Figure 4 - Graphical representation and curve fitting
of alternative K-Factor equations *(Arup, 2023)***.**

This data was used to expand the frequency factors across different building types and is summarised in Table 12.

Table 12 – K-Factor expansion

Building type	Frequency factor (K)	Time interval between fixture use averaged over peak period(s)
Residential dwelling, duplexes or townhouses	0.5	1200
Apartment or unit	0.5 – 0.8	450 - 1200
Hotel, hostel or dormitory	0.6 – 0.8	450 - 800
Caretakers residences within storage facility	0.5	1200
Office or commercial building	0.6 – 0.8	450 – 800
Retail, shop, restaurant, cafe	0.6 – 0.8	450 – 800
Carpark, warehouse, storage building	0.6 – 0.8	450 – 800
Factory, workshop or Laboratory	0.6 – 0.8	450 – 800
Healthcare building, hospital and GP Clinics	0.6 – 0.8	450 – 800
Public event buildings, stadiums, theatres, schools, universities, and churches	1.0 – 1.2	200 - 300
Aged care facilities	0.6 – 0.8	450 – 800

It is intended that these key findings may be used to update codes and standards in Australia. Another key finding was an outline of the sum of the fixture unit rating being a simplistic method prescribed in AS/NZS 3500.1 shown in Equation 15. This may provide potential justification for the use of a fixture unit to flowrate conversion (Arup, 2023).

$$Qww = \sqrt{\frac{\sum FU}{6.75}}$$

Equation 15

where:

a) Qww = Wastewater flow rate
b) $\sum FU$ = Sum of discharge units

There are many additional complexities to consider with sanitary plumbing and drainage pipe sizing and whilst these areas being explored show potential for improvement from the Fixture Unit method, there is a large amount of additional research required to develop a modern and adaptable pipe sizing method. The risk of unintended consequences in any changes to pipe sizing measures also needs careful consideration and testing. It is acknowledged that within a sanitary drainage system, liquid flow is only one of the considerations and the effects of liquid flow on air flow, although related, do not follow the same trajectory.

5 Quantification of the Performance

The National Construction Code (NCC) is Australia's primary set of technical design and construction provisions for buildings. As a performance-based code, it sets the minimum required level for the safety, health, amenity, accessibility, and sustainability of certain buildings. It primarily applies to the design and construction of new buildings and plumbing and drainage systems in new and existing buildings.

The NCC consists of three volumes:
- NCC Volume One primarily covers the design and construction of multi-residential, commercial, industrial and public assembly buildings and some associated structures.
- NCC Volume Two primarily covers the design and construction of smaller scale buildings including houses, small sheds, carports and some associated structures.
- NCC Volume Three covers the design, construction and maintenance of plumbing and drainage systems in new and existing buildings.

In 2012, The Centre for International Economics presented a report which estimated that the introduction of performance-based building regulation has contributed to approximately $780 million in benefits to the Australian economy and notably $60 million annually to consolidation of regulation relating to building and plumbing into the NCC (The Centre for International Economics, 2012).

The report also highlighted that a lack of quantification in the performance objectives is problematic and may make it difficult to design, assess and verify compliance with the Performance Requirements of the NCC.

Since the publication of this report, there has been a strong drive in Australia to unlock these benefits which can be achieved via a performance-based codes though the increased and competent use of the performance solutions. There are four components to this initiative:
- Increased education initiatives,
- Strategic review of the NCC Performance Requirements,
- Quantification of the NCC Performance Requirements, and
- Greater collaboration between regulatory authorities and industry.

One aspect of these objectives is focussed on the quantification of the Performance Requirements of the Plumbing Code of Australia. Throughout the past publications of the Plumbing Code of Australia, a move to clarify and quantify the Performance Requirements have been progressed in parallel with the development of methods to meet these requirements through amendments to referenced standards and the addition of alternative Verification Methods. Some concepts were explored in 2019 and presented at the CIB W062 Symposium in Melbourne Australia (ZELLER, 2019).

In the 2022 edition of the Plumbing Code of Australia, several Performance Requirements were reviewed and a number were able to be quantified with a measurable metric, whilst still providing sufficient flexibility to allow for innovative solutions. These amendments were not considered to impact on the level of stringency of the requirement, but to simply provide a clear and measurable benchmark for compliance.

Areas which have been amended in the 2022 edition of the Plumbing Code of Australia include:
- Cold water velocities;
- Heated water velocities for reticulated and circulatory systems;
- Water efficiency requirements;
- Water service pressures;
- Water heater storage temperatures;
- Water heater pressure relief and temperature limitations;
- The control of legionella;
- Cross-connection control;
- Legionella control;
- Fire-fighting flow rates and pressures;
- Fire-fighting water storage; and
- Sanitary plumbing and drainage ventilation and contamination.

Some examples of amendments and quantified Performance Requirements are outlined in Table 13.

Table 13 – Quantification of Performance Requirements in the Plumbing Code of Australia.

Title	Previous requirement	Quantified requirements
Velocity	A cold water service must ensure water is provided at required flow rates and pressures for the correct	Cold water service pipework must ensure that the pipework water velocity does not exceed 3 metres per second for more than 1% of the time that water is required during the annual peak hour.

	functioning of fixtures and appliances.	

Pressures	A cold water service must ensure water is provided at required flow rates and pressures for the correct functioning of fixtures and appliances.	The points of discharge for a cold water service must—
		 (a) have—
		    i. a working pressure of not less than 50 kPa; and
		    ii. a static pressure within the building of not more than 500 kPa; or
		 (b) have water pressures suitable for the correct functioning of the fixture or appliance where water pressures outside of (a)(i) and (a)(ii) are required.

Water efficiency	A cold water service must ensure the efficient use of drinking water.	A cold water service must ensure the efficient use of drinking water by—
		 (a) limiting water usage from—
		    i. a tap or outlet for a shower, basin, kitchen sink or laundry trough, to a flow rate of not more than 9 l/m; and
		    ii. a cistern or flushing device for a urinal, to a flush volume of not more than 2.5 litres for each—
		       1. single urinal stall; or
		       2. 600 mm length of a continuous urinal wall; and
		    iii. a dual flush cistern or flushing valve that is connected to a water closet pan to a flush volume of not more than—
		       1. 6 and 3 litres; or
		       2. 4.5 and 3 litres; or
		 (b) water saving measures equivalent to or greater than those described in (a).

Ventilation	A sanitary plumbing system must ensure ventilation, to avoid hydraulic load imbalance is provided.	A sanitary drainage system must ensure that ventilation is provided to avoid hydraulic load imbalance such that— (a) there is less than a 1% likelihood during the annual peak hour that when any fixture discharges, air pressure at any trap seal exceeds ±375 Pa difference from atmospheric pressure; or

		(b) an equivalent level of safety to human health is achieved as a system complying to (a).
Legionella control		Heated water must be stored and delivered under conditions which avoid the likelihood of the growth of a Legionella bacteria count greater than or equal to 10 Legionella colony forming units (cfu) per millilitre. Explanatory information: A risk assessment should be undertaken for the control and management of Legionella in heated water systems in aged care, health-care and other similar facilities with high risk occupants.

In some areas, a metric is not able to be applied to a Performance Requirement; however a methodology for determining compliance has been developed to assist practitioners in using a Performance based design. For example, a methodology for determining compliance in relation to heated water storage systems has been developed outlining temperature-dependent minimum exposure periods. A cross-connection risk assessment process for determining the appropriate hazard levels for a water service has also been developed to determine what level of backflow protection would be required to appropriately minimise the risk of contamination to a water service.

A concept to quantify or clarify the remaining Performance Requirements within the PCA is currently being finalised for the 2025 edition and public consultation will be sought on these proposed changes in 2024. Requirements intended to be quantified or clarified include but are not limited to the following topics:
- Access to mechanical components and operational controls;
- Water service isolation;
- Uncontrolled discharge from water services and sanitary plumbing and drainage systems;
- Avoidance of damage to sanitary plumbing and drainage systems; and
- Sanitary plumbing and drainage system contamination.

6 Conclusion

There is a vast amount of research and development on flow determination for pipe sizing being undertaken internationally and all seek to solve a particular piece of a complex puzzle and modern, accurate and adaptable flow determination methods are achievable only through putting these pieces of research together. The Australian experience has demonstrated great value in the collaboration between academia, industry and codes and standards writing bodies. Where research has been conducted in collaboration with other, it has produced the greatest outcomes and is something to be encouraged. It is through the sharing of knowledge and collaborative efforts that this complex puzzle can and will be solved.

The results in Australia clearly identify some of the possibilities which could be derived from a modern and more accurate flow determination methods for pipe sizing. There is high likelihood of significant reductions in the size of water services and sanitary plumbing and

drainage systems and several hydraulic and economic benefits as a result. There are also many risks and potential unintended consequences which will need to be investigated and tested. Consideration of the regulatory framework in its entirety is considered essential to the implementation of any changes to pipe sizing.

Acknowledgement

The work described in this paper was undertaken by and with the assistance from several individuals and organisations, including but not limited to the following:

- Dr James (Jinzhe) Gong, Senior Lecturer in Water Engineering, Faculty of Science Engineering and Built Environment, Deakin University
- Mr Brendan Josey, PhD Candidate, Science Engineering and Built Environment, Deakin University
- Mr Jake Cherniayeff, Global Public Health, Hydraulic and Plumbing Research Leader - ARUP
- Mr Simon Thwaites, Director - Lucid Consulting Australia
- Mr Tom Wise, Director - Warren Smith Consulting Engineers
- Dr Brian Ashe, Director – Australian Building Codes Board

7 References

Arup, 2022. *Sanitary Plumbing and Drainage Pipe Sizing - Phase 1,* Canberra: Australian Building Codes Board.

Arup, 2023. *Sanitary Plumbing and Drainage Pipe Sizing - Phase 2,* Canberra: Australian Building Codes Board.

Australian Building Codes Board, 2022. *National Construction Code.* 2022 ed. Canberra, Australia : Australian Building Codes Board.

Australian Building Codes Board, 2022. *NCC Volume Three - The Plumbing Code of Australia.* Canberra, Australia: Australian Building Codes Board.

B.S. Institute, 2000. *BS EN 12056-2:2000 Gravity drainage systems inside buildings - Part 2: Sanitary pipework, layout and calculation.* London: sn: s.n.

B.S. Institute, 2017. *BS EN 752: 2017 Drain and Sewer Systems Outside Building - Sewer System Management..* London: s.n.

BUCHBERGER, S. O. T. W. T. H. J. &. C. D., 2017. *Peak Water Demand Study: Probability Estimates for Efficient Fixtures in Single and Multi-familiy Residential Buildings,* Ontario, CA: IAPMO.

Chartered Institution of Building Services Engineers [CIBSE], 2014. *Public health and plumbing engineering CIBSE Guide G,* London : CIBSE.

GHD, 2015. *Discussion paper - Fixture Unit Rating System ,* Canberra: Australian Building Codes Board.

HUNTER, R. B., 1940. *Report BMS 65 - Methods of Estimating Loads in Plumbing Systems,* Washington, USA: s.n.

Hydraulic Consultants Association of Australasia Ltd, 2019. *Water Demand Investigation - Our Story.* [Online]
Available at: www.waterdemand.com.au/our-story
[Accessed 30 July 2023].

JOSEY, B. B. S. &. G. J., 2023. Comparing actual and designed water demand in Australian multilevel residential buildings. *Journal of Water Resources Planning and Management,* Volume 05022013, p. 149.

JOSEY, B. M. &. G. J., 2021. *Identifying Limitations of Australian Standards for Cold-water Plumbing Design: Comparing Actual and Designed Demand in Multi-level Residential Buildings,* s.l.: Deakin University.

JOSEY, B. M. &. G. J., 2023. Determination of Fixture Use Probability for Peak Water Demand Design using High-level Water End-use Statistics and Stocastic Simulation. *Journal of Water Resources Planning and Management,* Issue in press, DOI 10.1061/WRMD%/WRENG-6146.

Lucid Consulting Australia, 2019. *ABCB Pipe Sizing Verification Method - Worked Examples,* Canberra: Australian Building Codes Board.

Lucid Consulting Australia, 2019. *Sanitary Plumbing and Drainage Pipe Sizing,* Canberra: Australian Building Codes Board.

Standards Australia , 2021. *AS/NZS 3500 Plumbing and Drainage, Part 1 Water Services.* Sydney, Australia: Standards Australia .

Standards Australia , 2021. *AS/NZS 3500 Plumbing and Drainage, Part 4 Heated water services.* Sydney, Australia : Standards Australia.

Standards Australia, 2018. *AS/NZS 3500 Plumbing and Drainage, Part 2 Sanitary Plumbing and Drainage.* Sydney: Standards Australia.

The Centre for International Economics, 2012. *Benifits of building regulation reform,* Australia: Australian Building Codes Board.

ZELLER, A. a. A. B., 2019. *Performance metrics for cold water pipework sizing in the National Construction Code. In Proc., Symp. CIB W062.* Melbourne, Australia, Australian Building Codes Board.

8 Presentation of Author

Tom Roberts a Director at the Australian Building Codes Board and has played a leadership role in the research relating to the Plumbing Code of Australia for the past 10 years. This research has contributed to several revisions to the Plumbing Code of Australia and standards used across Australian and New Zealand. Tom has driven collaboration between acidemia, government, industry, and key stakeholders to convert research findings into industry practices. Tom has also contributed to several global pipe sizing initiatives in the pursuit of accurate flowrate calculations and modern hydraulic design practices.

Towards a better understanding of hot water demand in nursing homes.

T. Delwiche (1), M. Guarini (2), C. Jacques (3), B. Poncelet (4), B. Bleys (5)

(1) thomas.delwiche@buildwise.be
(2) michel.guarini@buildwise.be
(3) colin.jacques@buildwise.be
(4) benoit.poncelet@buildwise.be
(5) bart.bleys@buildwise.be
(1), (2), (3), (4), (5) Buildwise (ex-Belgian Building Research Institute), Belgium.

Abstract

Buildwise (ex-Belgian Building Research Institute) recently developed a sizing method for domestic hot water production (DHW), applied to collective residential buildings.

Based, among others, on the analysis of the hot water demand profiles for such buildings and on simulations of the thermal loads necessary to fulfil these demands, this tool aims at providing an optimal sizing of the DHW production facility.

This tool, however, does not apply to other types of buildings, like nursing homes, which exhibit very specific demand profiles. For such buildings, a better understanding of their typical hot water demand profiles is required, prior to any further research and developments.

This paper presents the results of a measurement campaign conducted across nine nursing homes. It is shown that simple models, namely standards from neighbouring countries, fail to predict the hot water consumption characteristics of these specific buildings.

A separate study of the three departments of nursing homes, namely the kitchen, the care department and laundry is introduced as a way to further improve the predictions.

Keywords

Measurement campaign, hot water demand profile, nursing homes.

1 Introduction

Improving our understanding of domestic hot water (DHW) consumption is mandatory to design optimal hot water production systems, namely systems that allow a comfortable and safe use of DHW while using a minimum amount of energy, and, therefore, reducing the energy-related greenhouse gas emissions of buildings. The latter is now a key issue for European policies [1].

Buildwise (ex-Belgian Building Research Institute) recently developed a sizing method for domestic hot water production (DHW), applied to collective residential buildings.

Based, among others, on the analysis of the hot water demand profiles for such buildings and on simulations of the thermal loads necessary to fulfil these demands, this tool aims at providing an optimal sizing of the DHW production facility.

This tool, however, does not apply to other types of buildings, like nursing homes. For such buildings, a better understanding of their typical hot water demand profiles is required, prior to any further research and developments.

In section 2, we present a measurement campaign which has been conducted across 9 nursing homes in Belgium.

Next, in section 3, the results of this campaign are compared to DHW consumption predictions obtained by simplified models and standard from neighbouring countries. It is investigated if these models and standards are accurate enough to predict the DHW consumption.

Finally, section 4 provides the reader with conclusions and perspectives about future work.

2 Measurement campaign

A total amount of 9 nursing homes has been studied. Their main characteristics are listed in table 1 below.

Table 1 - Characteristics of the investigated nursing homes

	Beds		
	Available	Occupied	Access to a private shower
A	87	87	100%
B	103	87	0%
C	80	80	36%
D	106	106	0%
E	60	60	100%
F	79	79	100%
G	134	130	72%

H	116	99	100%
I	102	96	20%

For each of them, several parameters have been monitored, namely the temperature of the cold water, the temperature of the hot water depart, and the flow rate of consumed domestic hot water (DHW).

The flow rate has been measured using a Flexim Fluxus F60x flowmeter and the data stored on a datalogger with a sample time of 1s.

The temperatures have been measured using thermocouples and stored using the same datalogger.

The collected data (raw data) have been further processed according to the method described in [3] and [5], in order to convert the actual flow rate into standardized flow rates, corresponding to hot water at 60°C and cold water at 10°C. Parameters related to standardized DHW, will be denoted DHW_{6010}.

Finally, the flow rates have been averaged over 2s.

3 Results description and analysis

In this section, we describe and analyse the results of the measurement campaign. First, we analyse the average DHW_{6010} volume per bed. Next, we investigate the DHW_{6010} peak flow rate, and we compare this value with the peak flow rate computed using the German standard DIN 1988-300 [6] and the French standard NF DTU 60.11 P1-1 [7].

3.1 Average hot water volume per occupied bed

First, we analyse the average hot water volume consumed per bed, for a weekday. As can be seen in figure 1, for the studied facilities, it ranges from 13 to 89 l/day.person.

These values are consistent with those presented in [2], where the authors studied 65 nursing homes in France and observed a variation comprised between 10 and 95 l/day.person[1].

Furthermore, as in [2], figure 1 shows no correlation between the average hot water volume per occupied bed and the total number of occupied beds.

Considering the large range between the minimum and maximum values of DHW consumed per occupied bed, this is definitely not the single parameter to take into account if one expects to reach a good prediction of DHW consumption.

---

[1] Attention should be paid, however, to the fact that [2] expresses standardized hot water at 40°C and not at 60°C.

Figure 1 - Average hot water volume per bed, with respect to the number of occupied beds

Besides, one could wonder if the availably of a private shower impacts the consumption. From figure 2, one can see that this is not the case. This is probably because, although a shower is available, the ability of the people to effectively use this shower is quite limited. In fact, they mostly depend on the staff to assist themself during showering or bathing. This takes place in shared bathrooms, equipped with medicalized bathtubs, like the one exhibited in figure 3 below.

Although these private bathrooms do not impact water consumption, water quality should be of concern. Since a bathroom is barely used, water stagnation can be expected.

Figure 2 - Average hot water volume per bed, with respect to the availability of a private shower
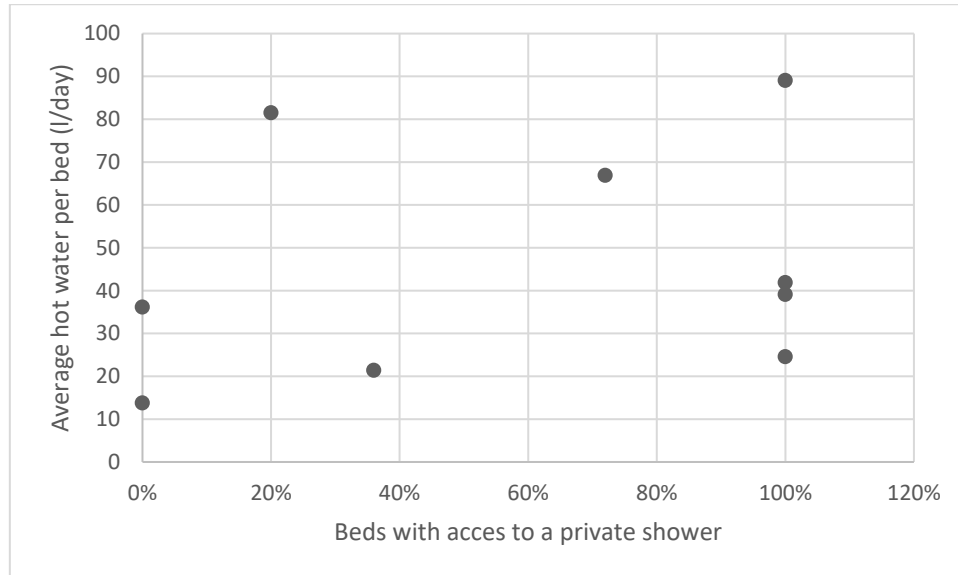

Figure 3 - Medicalized bathtub used in nursing homes.


3.2 Peak flow rate

In this sub-section, peak flow rates are compared to those predicted by using the German standard DIN 1988-300 and the French NF DTU 60.11 P1-1. The results are presented in figure 4, below.

Measured peak flow rates range from 0.5 l/s to 2,5 l/s. It can be seen that the German standard DIN 1988-300 is not able to make an accurate prediction of the peak flow rates. A study from Norway [4], investigating three nursing homes, also pointed out that that the actual flow rate was either over- or underestimated.

The same conclusion applies to the NF DTU 60.11 P1-1, although it more frequently overestimates the peak flow rates.

It is worth noticing that, in the case of apartment buildings, both standards overestimate the peak flow rates [5].

Figure 4 - Measured peak flow rates, compared to predictions obtained using the German standard DIN 1988-300 and the French standard NF DTU 60.11 P1-1
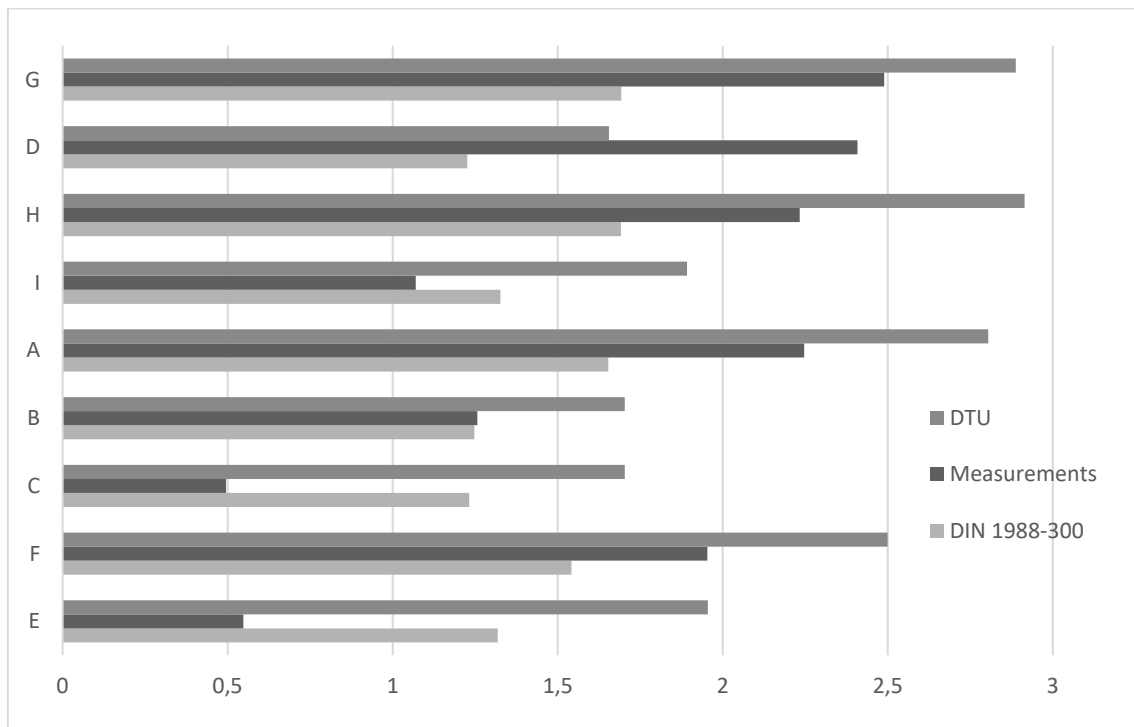
3.3 Discussion of the results

The simplified sizing methods implemented in the previous paragraphs failed to capture the use of DHW in nursing homes.

Both standards are based on a count of the taping points and apply a coefficient of simultaneity, which do not take into account the fact that certain uses (laundry, kitchen and care) are very specific and many bathrooms probably barely used.

In [2], the average volume of DHW has been found to be dependent on these uses, as shown in table 2 below.

The segmentation proposed by the authors comprises 8 different configurations.

Table 2 - Average hot water volume consumed per person, according to the specific parameters of the nursing home. DHW is considered at 40°C, reproduced from [2].

Configurations		Averaged volume used daily per person
Meals not prepared on site	Dishwashers connected to cold water, no washing machines	15 to 25 l
	Dishwashers connected to cold water, washing machines connected to warm water.	25 to 50 l
	Dishwashers connected to hot water, no washing machines	20 to 40 l
	Both dishwashers and washing machines connected to hot water.	30 to 65 l
Meals prepared on site	Dishwashers connected to cold water, no washing machines	20 to 50 l
	Dishwashers connected to cold water, washing machines connected to warm water.	30 to 75 l
	Dishwashers connected to hot water, no washing machines	30 to 70 l
	Both dishwashers and washing machines connected to hot water.	40 to 95 l

Our own interviews with facility managers have shown that further refinement is possible.

For instance, the fact that meals are prepared on site for people living on another site or the fact that baths are used instead of showers can be taken into account for more accuracy.

4 Conclusions and future works

Our measurements show that simplified methods, based on a count of the tapping points, corrected using a simultaneity factor, do not apply to nursing homes.

Both the German DIN 1988-300 and the French NF DTU 60.11 P1-1 fail to provide an accurate estimate of the peak flow rate.

Besides, it is shown that the average use of DHW per person do not depend on the availability of a private bathroom or on the number of residents. A more refined model is therefore needed.

This conclusion is in line with the work presented in [2], where a correlation has been established between the DHW consumption and the configuration of the three departments of a nursing home, namely the kitchen, the laundry and the care.

Further work includes the development of a model, which could separately capture the consumption patterns of these three departments and combine them to define a global consumption pattern for the building.

References

[1] Directive 2010/31/EU of the European Parliament and of the Council of 19 May 2010 on the energy performance of buildings

[2] Comité Scientifique et Technique des Industries Climatiques (COSTIC) – *Vers une meilleure connaissance des besoins en eau chaude sanitaire en tertiaire (in French),* Septembre 2020 (https://www.costic.com/node/17443?id=17873)

[3] O. Gerin, B. Bleys, K. De Cuyper - *Seasonal variation of hot and cold water consumption in apartment buildings* – Proceedings of the CIBW062 Symposium, 2014

[4] Karolina Stråby et al – *Pipe sizing based on domestic hot water consumption in Norwegian hotels, nursing homes, and apartment building*s, IOP Conf. Ser.: Mater. Sci Eng. 609 (2019)

[5] O. Gerin, B. Bleys, K. De Cuyper - *Domestic hot water consumption in apartment buildings* – Proceedings of the CIBW062 Symposium, 2015

[6] DIN Deutsches Institut für Normung – *Codes of practice for drinking water installations – Part 300: Pipe sizing; DVGW code of practice*, May 2012.

[7] NF Norme française – *Building works – Calculation rules for sanitary and rainwater draining off – Part 1-1: Cold and warm Sanitary networks*, August 2013

5 Presentation of the authors

Thomas Delwiche holds a Master in Mechanical Engineering and a PhD in Engineering Sciences, both from Université libre de Bruxelles. He is currently Project Leader with the Laboratory Water Technologies at Buildwise (ex-BBRI - Belgian Building Research Institute).

Michel Guarini holds a bachelor degree in Electromechanics. He is currently technician at Buildwise (ex-BBRI -Belgian Building Research Institute).
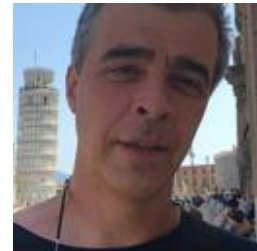
Colin Jacques holds a Master in Engineering from ECAM. He is currently Researcher with the Laboratory Water Technologies at Buildwise (ex-BBRI -Belgian Building Research Institute).

Benoît Poncelet is engineer in architecture and project leader in the Laboratory Water Technologies at Buildwise (ex-BBRI - Belgian Building Research Institute).

Bart Bleys is bioengineer and head of the Laboratory Water Technologies at Buildwise (ex-BBRI -Belgian Building Research Institute).

TECHNICAL SESSION 2 – DRAINAGE

The impact of current and future extreme rainfall events on historic buildings

D.A. Kelly (1) and J.J. Claridge (2)

(1) d.a.kelly@hw.ac.uk

(2) jjc2000@hw.ac.uk

(1-2) Heriot-Watt University, Edinburgh, Scotland, UK.

Abstract

The impact of climate change has significant implications for the built environment. Increased levels of rainfall can exceed the rainwater drainage capacity of the building, potentially causing localised flooding and damage to the building fabric.

Historic buildings pose an important challenge in relation to climate change and the risks around increased rainfall. These buildings have great importance within the built environment, providing cultural identity and providing historical context for those who live and visit a place. Extreme rainfall events that exceed the capacity of the drainage system could severely damage the fabric of the historic building due to erosion and moisture ingress. Furthermore, historic internal décor such as detailed plasterwork and timber carvings, as well as the valuable historic contents of the building are also at risk.

This paper evaluates the impact of extreme rainfall events on historic buildings by assessing the risk of gutter overtopping for a case study building: Bishop Cosin's Almshouses in the Durham World Heritage Site. The ROOFNET numerical model was used to simulate the response of the building to baseline 10 minute storms for return periods of 50 years, 100 years, and 500 years. Future rainfall was accounted for by applying uplift factors from UKCP18. Accounting for corrosion within the historic rainwater system saw a significant increase in the risk of gutter overtopping.

Keywords

Climate change, rainwater, flooding, extreme events, historic buildings, ROOFNET.

1   Introduction

The intensity and frequency of extreme rainfall has increased in recent years due to the impacts of climate change; these changes are expected to worsen further in the coming decades (Met Office, 2022). This will have major implications for the built environment and pose significant challenges on how rainwater and stormwater are managed.

Historic buildings are particularly vulnerable to the increase of extreme rainfall events due to their risk and susceptibility to water damage (Taylor, 2013). Figure 1 illustrates examples of water damage to external stonework of historic buildings.

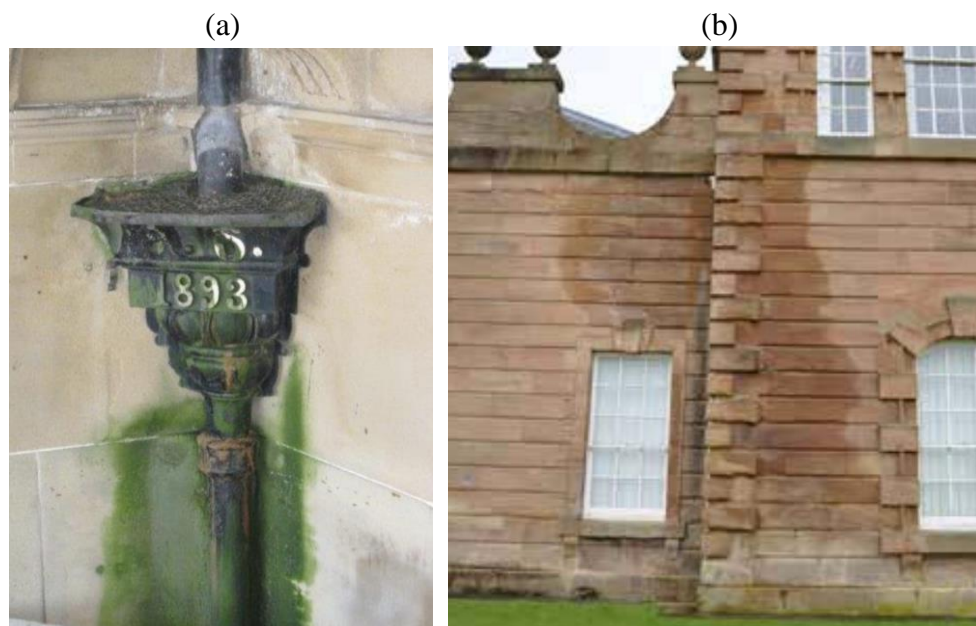(a)   (b)

Figure 1: Rainwater damage to historic buildings: (a) hopper and downpipe in poor condition causing leaking, damp and algae growth; (b) blockage in parapet gutter causing overtopping, damp and staining of stonework (adapted from Renshaw, 2015; and Curtis & Kennedy, 2016)

The further challenge is the inherent limitations around retrofitting modern drainage solutions or sustainable drainage systems to historic architecture which are often of listed status or within conservation areas – both of which limit changes or interventions to the original building.

This paper considers the impact that increased extreme rainfall events could have on historic buildings. The numerical model, ROOFNET, developed previously at Heriot-Watt University, was used to simulate the impact of a range of current and future rainfall events on a case study building, Bishop Cosin's Almhouses which sits within the Durham World Heritage site in the North East of England. Future rainfall events are based on data from the UK Climate Projections 2018 (UKCP18) developed by the Met Office which provide probabilistic projections on how the climate in the UK may change over the next century (Met Office, 2022).

2   Changing rainfall patterns

The climate is changing around the world. The latest projections indicate that further change is expected over the coming century, and extreme weather events are expected to become more frequent and intense over the coming decades (Kendon, 2022).

2.1   Observed rainfall trends

Climate change has affected rainfall patterns around the world. The "State of the UK Climate Report" by the Met Office found that the decade 2012-2021 has been, on average, 10% wetter than the 1961-1990 baseline (Kendon, 2022). Further to this, the report also found that over the same decade (2012-2021), British summers were, on average, 15% wetter than 1961-1990. This has also been observed at a global level. A study by Wasko, *et al.* (2021) looked at rainfall and flooding patterns across the world found that extreme rainfall events have become more common and have a greater intensity globally.

2.2   UK Climate Projections

The UK Climate Projections 2018 (UKCP18) provide an assessment of how the climate could change over the next century across a range of emissions scenarios (Met Office, 2022). The UKCP18 data are presented as probabilistic projections, corresponding to the 5th, 10th, 50th, 90th, and 95th percentiles of probability to account for the uncertainty related to climate projections (Met Office, 2022).

Seasonal precipitation changes between the 10th and 90th percentiles, averaged across the UK, indicate precipitation changes of between -45% to +5% in summer, and -3% to +39% in winter by 2070 under the high emission scenario. Despite summers becoming drier overall in future, localised projection data indicate future increases in the intensity of heavy summer rainfall events (Met Office, 2022), likely increasing the risk and severity of surface water flooding.

3   Historic buildings and rainfall risks

Historic buildings pose a particular challenge in relation to risks caused by increased rainfall. Most historic buildings were built at a time before the impacts of climate change, and so the design of their rainwater drainage systems may not be adequate in dealing with increased levels of rainfall and extreme weather events.

Furthermore, the rainwater drainage systems of historic buildings often form a key feature of the historic building**, see Figure 2,** and so altering or adapting these systems are often prohibited. In addition, the materials used to build historic buildings are normally local natural materials such as stone, timber, slate, etc. which may also be less resilient to rainwater damage.
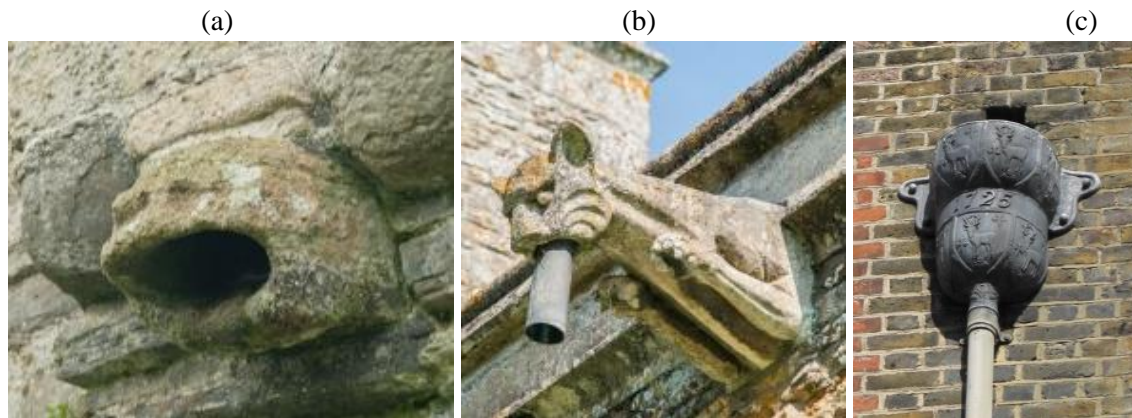
Figure 2: Decorative rainwater features: (a) stone gargoyle at Beaumaris Castle in Anglesey; (b) stone gargoyle at Lynton in Rutland; (c) cast-iron hopper at Fournier Street in Spitalfields (adapted from Britain Express, n.d.; Voller, 2010)

3.1   Potential flood risk

Historic England provides guidance on dealing with potential flooding of historic buildings (Historic England, 2015). The guidance places particular importance on preparation and mitigation and recommends first establishing the risk of flooding and then undertaking a building survey to find any areas of the building that are particularly susceptible to damage and ensuring these are well maintained.

The guidance highlights that the risk of flooding is dependent on the type of flood considered. For example, river flooding can be quite predictable, hence mitigation measures, such as flood barriers, can be put in place ahead of time to reduce the effects of river flooding (Historic England, 2015). Likewise, the risk of flooding caused by blockages in drainage systems can be reduced by ensuring regular maintenance.

However, the guidance recognises that some types of flooding are much harder to predict, such as those caused by extreme rainfall events (Historic England, 2015). Because extreme rainfall events are difficult to predict, preparing for this type of flooding is more challenging. It is important to point out that the guidance does not mention climate change as a factor in flood risk, and so the impacts of increased frequency and intensity of rainfall caused by climate change on historic buildings is not considered.

3.2   Potential rainwater damage

Moisture, typically caused by rainwater, is "*the root cause of most deterioration in historic buildings*" (Taylor, 2013). With the frequency and intensity of rainfall expected to increase, and extreme rainfall events becoming more common, the risks of damage to historic buildings caused by rainwater will increase also. The three main ways in which moisture can damage buildings are biological decay (i.e. timber rot due to moisture), physical damage (i.e. rusting of metal and weathering of stone), and chemical damage (i.e. stone degradation due to polluted rain) (Taylor, 2013), see Figure 3.
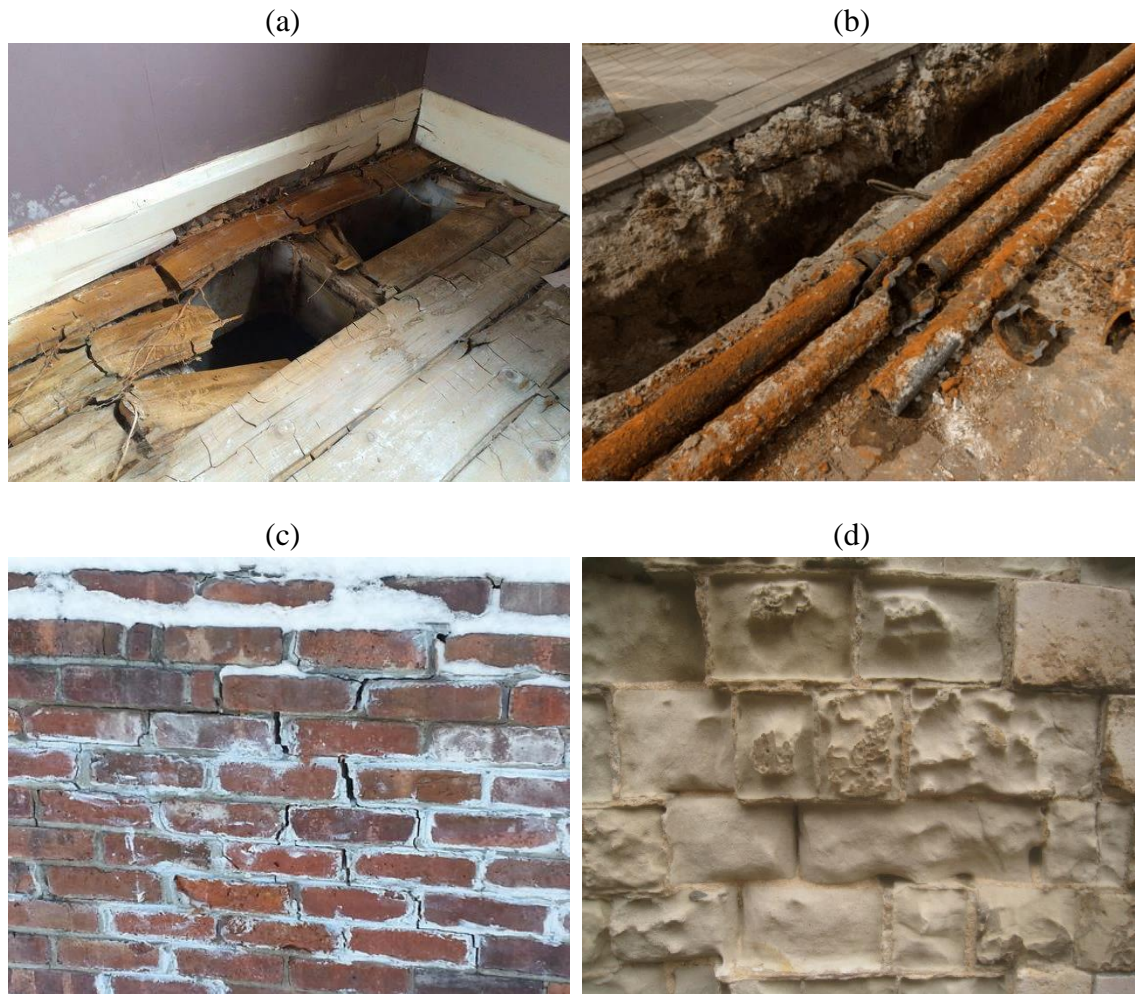
(a)   (b)

(c)   (d)

Figure 3: Examples of moisture damage to historic buildings: (a) rot in timber flooring (Allerton, 2023); rust on iron pipes (YENA Engineering, 2023; (c) freeze-thaw weathering to brick wall (SWC, 2015); (d) chemical weathering on Bell Tower of the Tower of London (Geograph, 2013)

4   The Durham World Heritage Site

The Durham World Heritage Site is located in County Durham in the North East of England, see Fugue 4. The site was added to the UNESCO World Heritage List in 1986 (Durham World Heritage, 2022).

The original boundaries of the site included only Durham Cathedral (a Norman cathedral built in 1133) and Durham Castle (an 11th century castle which now houses University College). Figure 4 shows a map of the site with the castle to the north and the cathedral to the south (both shown in orange). In 2008, the site boundaries were extended to include the Prince-Bishops complex (including almhouses, a grammar school, a courthouse, and a library) which is indicated in blue in Figure 4 (Durham World Heritage Site, 2023). The site sits on the banks of the River Wear and forms the centre of the City of Durham.
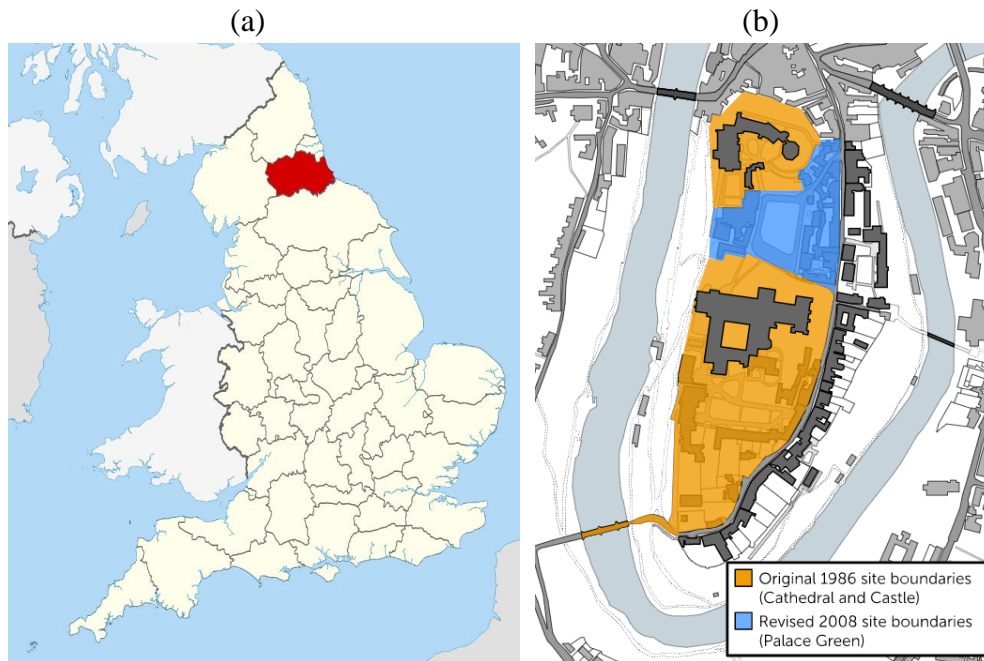
Figure 4: Maps showing: (a) the location of County Durham in the North East of England in red; (b) the Durham World Heritage Site boundaries - with the castle to the north, the cathedral to the south, and the Prince-Bishops complex and Palace Green to the centre (Durham World Heritage, 2022)

4.1 Bishop Cosin's Almhouses

Bishop Cosin's Almshouses are a Grade II listed building located on the Palace Green of the Durham World Heritage Site. The Almshouses were originally constructed by the Bishop of Durham, John Cosin, in 1666 to provide accommodation for those too poor to pay rent (Durham World Heritage, 2023). The building was used for this purpose up until 1837, when it was given to Durham University, who used the building for student accommodation until 1876 when it was converted into a museum. The building is currently used as a cafe.

Figure 5: The original 17-th century sketch of Bishop Cosin's Almhouses, together with a photograph of how it looks today (British Listed Buildings, 2023)

4.2 Risks from climate change

Whilst Historic England's guide on "Flooding and Historic Buildings" does not mention the impacts of climate change (Historic England, 2015), the Durham World Heritage Site Action Plan does recognise the risk (Durham World Heritage, 2017).

The section of the plan entitled "Climate Change and Environmental Sustainability" discusses the increased likelihood of extreme weather events and how this will impact the site. The main risk comes from the susceptibility of the stonework to erosion from wind and rain. The plan discusses the need for good maintenance of the drainage systems and remedial works to any wind or water damage (Durham World Heritage, 2017). The plan also recognises that the approach to climate change will need to be constantly reviewed against the latest climate science.

The plan sets a 6-year timescale to first conduct a risk assessment, before then developing and implementing a management plan (Durham World Heritage, 2017). While the plan recognises the need to respond to the risks of climate change and has set out a strategy to achieve this, it lacks detail on exactly how the risk assessment will be conducted and how the findings will be used.

4.2.1 Climate risks to Bishop Cosin's Almhouses

Bishop Cosin's Almhouses are constructed from sandstone and, despite being a durable material, sandstone is of particularly susceptible to water erosion due to its porosity (The Engine Shed, 2023). If water passes through the sandstone regularly, the stone cannot dry out and will begin to decay, see Figure 6 (Blamore Specialist Contracts, 2023).

Furthermore, salt contained within rainwater can build up within sandstone, which can crystallise and exert pressure on the interior of the stone causing it to break down,. Due to these factors, Bishop Cosin's Almshouses are particularly vulnerable to the expected increase in the intensity and frequency of extreme rainfall events.

Figure 6: Typical salt deterioration and crystallisation to stonework of historic buildings (adapted from Viles, 2012)

5   Numerical Modelling: ROOFNET

Research into the development of numerical models for rainwater drainage systems has been ongoing for decades. In 1999, research at Heriot-Watt University began the development of a model capable of replicating unsteady flow (Swaffield *et al.*, 1999). Until that point, the design of rainwater drainage systems relied on steady flow calculations. Numerical models can calculate the flow conditions at multiple time steps and, hence, produce data that allow for a better simulation of unsteady flow.

The initial study by Swaffield *et al.* (1999) verified the accuracy of the numerical model by comparing the findings to observed flow behaviour in a test rig; demonstrating the importance of physical models in the development of numerical modelling. The practical application of the model was also demonstrated using field data, showing the potential for numerical models to be used for rainwater system design and assessment.

Subsequent research developed the numerical model further to enable simulation of a building's rainwater drainage system as a whole: including roof, gutter, downpipe, underground drains, and local surfaces (Arthur & Swaffield, 1999; Wright *et al.*, 2006a; Wright *et al.*, 2006b).

Flow conditions on sloping roofs are simulated using a simple finite difference solution of the kinematic wave equations; full-bore pipeflow is represented by a fully dynamic approach by solving the equations of continuity and momentum of 1-D unsteady flow; and rainwater runoff from local surfaces is assessed using a simple volumetric approach based on area drained, surface type, and rainfall intensity.

The resultant numerical model, ROOFNET, is capable of predicting the performance of rainwater drainage systems under different climate conditions as demonstrated by Jack & Kelly (2012) who used ROOFNET to simulate the performance of a typical building's rainwater drainage system in response to applied climate projection data accounting for climate change impacts on future rainfall. The study made recommendations of system adaptation, in terms of larger gutter and downpipe sizes, and the application of green roofs to improve system resilience to the anticipated changes in future rainfall.

6   Methodology

The numerical model, ROOFNET, was used to investigate how the rainwater drainage system of Bishop Cosin's Almshouses performs under extreme rainfall events. The operational performance of the building's rainwater drainage system was simulated under a range of rainfall scenarios: current rainfall intensities were based on the British Standard BS EN 12056:3 2000 (British Standards, 2000); and future rainfall intensities were based on the UK Climate Projections 2018 (UKCP18) (Met Office, 2022).

6.1 Model Input

6.1.1 Bishop Cosin's Almhouses

The ROOFNET model requires input of the rainwater drainage system dimensions and characteristics, such as: roof type, dimensions and slope; gutter dimensions; downpipe diameter and lengths; and the Manning's Coefficient of the gutter and downpipes. The dimensions of the building and rainwater drainage system were found from a combination of site plans and site surveys. Figure 7 shows details of the building and system dimensions, with labelling of the roofs (R), gutters (G), outlets (O), and downpipes (P).
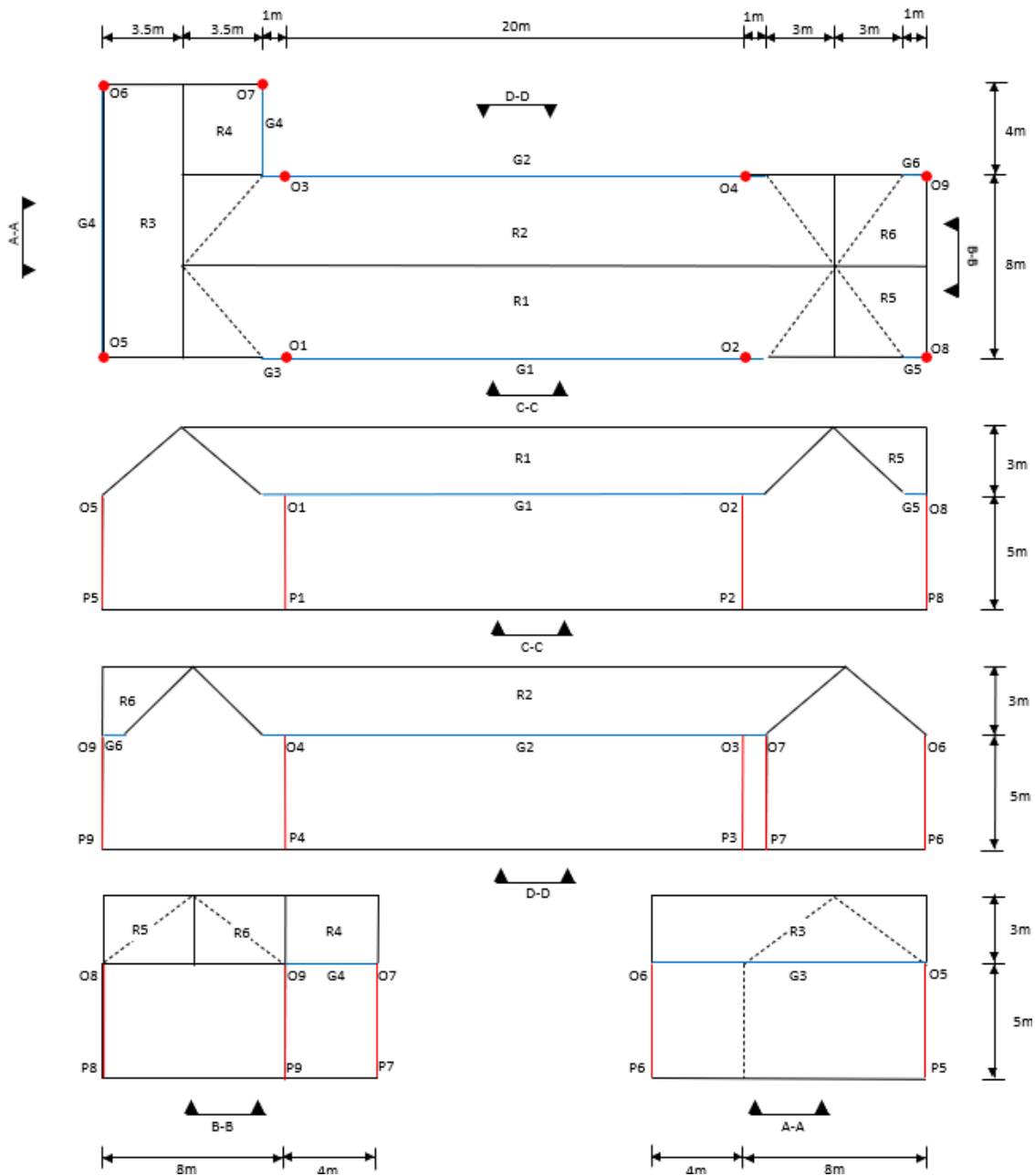

Figure 7: Drawing of Bishop Cosins Almshouses rainwater drainage systems

There are 6 systems in the network. All pipes and gutters in the system are cast iron and circular with a diameter of 125mm, apart from one box gutter. All roof surfaces are slate, with a slope of 0.75. A Manning's Coefficient of 0.015 [clean cast iron] was used for the gutter and downpipes (Engineers Edge, 2023). Figure 8 shows the rainwater system information as input to ROOFNET.

Due to limitations of the ROOFNET model, some assumptions/adjustments were made: all gutters were input as rectangular (97mm wide x 63mm deep) providing the same cross-sectional area as the circular gutter; and the short box gutter was assumed to be a 1m rectangular gutter.
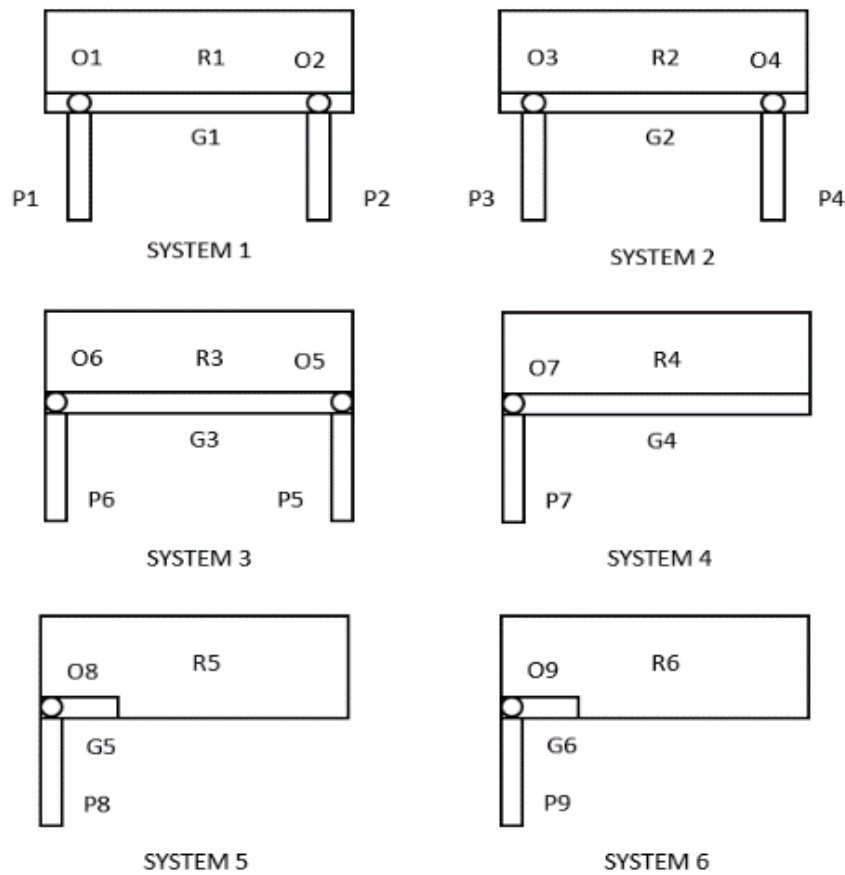
ROOF SURFACES		GUTTERS	
REF	**AREA (m^2)**	**REF**	**LENGTH (m)**
R1	176	G1	22
R2	176	G2	22
R3	42	G3	12
R4	14	G4	4
R5	16	G5	1
R6	16	G6	1

Figure 8: Diagram of rainwater drainage systems of Bishop Cosins Almhouses as input information to ROOFNET

6.1.2 Rainfall Data: Current Intensities

British Standard BS EN 12056:3 2000 provides rainfall design intensity values for rainwater drainage systems across the whole of the UK for various return periods. A 2 minute storm duration with a 5 year return period (2minM5) is used as standard with other durations and return periods calculated by applying fraction multipliers.

This study used a 10 minute storm with return periods of 50, 100, and 500 years specific to the study location of Durham in North East England. Table 1 shows the resultant rainfall design depths of the 10minM50 event (12.33 mm), the 10minM100 event (14.4 mm), and the 10minM500 event (18.5 mm).

Table 1: Design Rainfall Intensities derived from BS EN 12056:3 2000

M = 50 YEARS		
2minM5	3	mm
10 min fraction of 2minM5	2.74	
10minM5	8.22	mm
M50 rainfall intensity ratio	1.5	
10minM50	12.3	mm
M = 100 YEARS		
2minM5	3	mm
10 min fraction of 2minM5	2.74	
10minM5	8.22	mm
M100 rainfall intensity ratio	1.75	
10minM100	14.4	mm
M = 500 YEARS		
2minM5	3	mm
10 min fraction of 2minM5	2.74	
10minM5	8.22	mm
M500 rainfall intensity ratio	2.25	
10minM500	18.5	mm

6.1.3 Rainfall Data: Future Intensities

The UK Climate Projections 2018 (UKCP18) provides information on projected future climates for different regions of the UK under varying emission scenarios and time periods over the current century.

The emission scenarios represent low (RCP2.6), medium (RCP4.5, RCP6.0), and high (RCP8.5) emissions relative to the 1981-2000 baseline. The projections also include an update on the UKCP09 medium emissions scenario (SRES A1B).

The time periods cover 2020-2039, 2030-2049, 2040-2059, 2050-2069, 2060-2079, 2070-2089, and 2080-2099; and the data is presented corresponding to the 5th, 10th, 50th, 90th, and 95th percentiles of probability (Met Office, 2022).

The projected changes in future rainfall is presented as a percentage change relative to the 1981-2000 baseline. Hence, values of projected rainfall for a particular emission scenario and time period is determined by applying the percentage change as an uplift factor to the mean rainfall value for the baseline period for the particular location. For the purposes of this study, the uplift factor was applied to the design rainfall intensities derived from BS EN 12056:3 2000, as detailed in the previous section.

The SRES A1B emissions scenario, for the 2040-2059 time period was selected as this showed the greatest percentage change relative the 1981-2000 baseline. The 50th, 90th, and 95th percentiles of probability were used, with rainfall uplift factors of 17%, 38%, and 45%, respectively. Figure 9 shows the resultant rainfall profiles for each return period (50 years, 100 years, and 500 years), and for each percentile of probability. The rainfall profile was assumed to be the typical symmetrical, single-peak profile with uniform time steps of 60 seconds (The Wallingford Procedure, 1981).
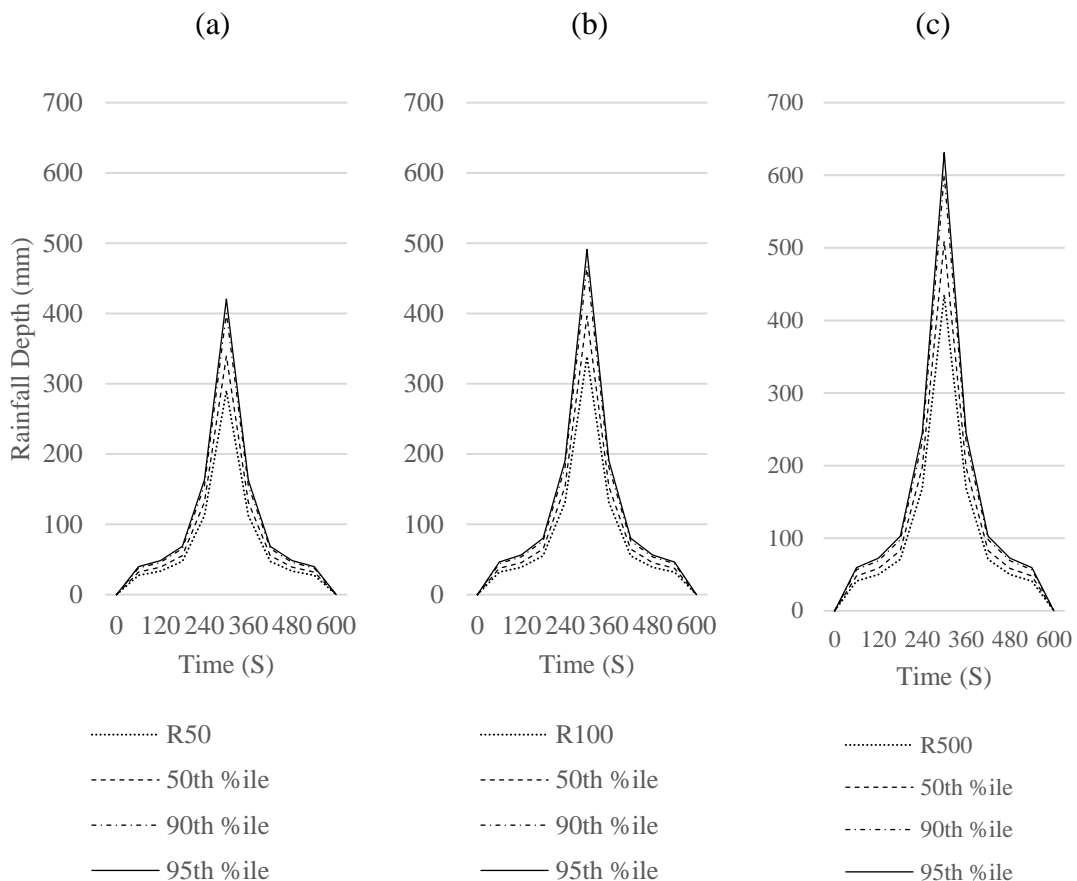

Figure 9: Rainfall profiles for a 10 minute event with 50th, 90th, and 95th percentiles for return periods of: (a) 50 years; (b) 100 years and; (c) 500 years

Table 2 summarises the resultant rainfall depths for all simulated events, including the baseline and future rainfall scenarios with applied uplift factors.

Table 2: Resultant rainfall depths for the 10 minute baseline event with return periods of 50 years, 100 years, and 500 years, and applied uplift factors representing possible future rainfall

	Event			
	Baseline	50th %ile	90th %ile	95th %ile
	Uplift (%)			
	0%	17%	38%	45%
	Depth (mm)			
10minM50	12.3	14.4	17.0	17.9
10minM100	14.4	16.9	19.9	20.9
10minM500	18.5	21.7	25.5	26.8

6.2   Effects of Corrosion

Due to the age of Bishop Cosin's Almhouses, like many historic buildings, the cast iron rainwater goods are vulnerable to corrosion. The process of corrosion can cause layers of rust to build up, changing the surface roughness and internal dimensions of the pipes and gutters. The effect of corrosion can reduce the capacity of the rainwater system, making it more likely for gutter overtopping to occur.

A set of simulations were carried out to take account of the likely effects of corrosion. The Manning's Coefficient for the gutter and downpipes was changed from 0.015 [clean cast iron] to 0.035 [dirty, tuberculed cast iron] (Engineers Edge, 2023).

In addition, as the rate of corrosion for cast iron is approximately 0.1 mm/year (Sarna, 2016), it was assumed that the internal dimension of the gutter was reduced by 5 mm on all sides (conservatively assuming the corrosion effects of a 50 year old system). The internal dimensions of the gutter were, therefore, reduced by 10 mm to both the depth and width, see Figure 10.
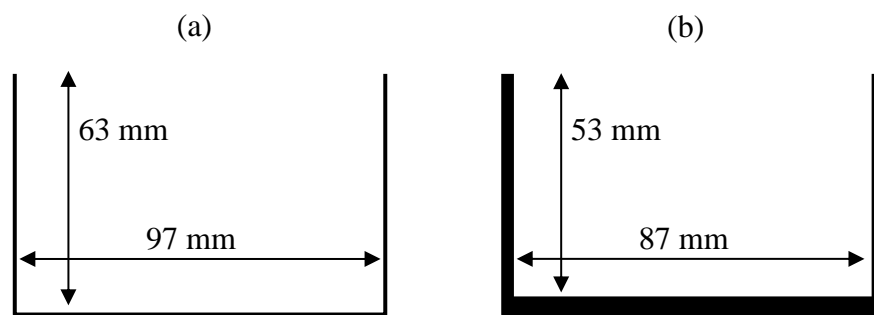
(a)   (b)

Figure 10: Cross-section of gutter showing dimensions: (a) without corrosion; and (b) with corrosion

7 Results

7.1 Baseline storms and future rainfall

The ROOFNET model was initially run using the baseline rainfall depths for a 10-minute storm with return periods of 50, 100, and 500 years (the 10minM50, 10minM100, and 10minM500, respectively), before then being run for each of the storms with the uplift factors applied to represent potential future rainfall. Figure 11 depicts the gutter flow depths for each simulated storm, and for each roof/gutter on the building. The peak flow depth occurs in gutters G1 and G2, which collect the rainwater from roofs R1 and R2, respectively, as detailed previously in Figure 7.

For the 10minM50 storm, the gutter flow depth peaks at 35.3 mm, with no apparent risk of overtopping as the depth of the gutter is 63 mm. With uplift factors for the SRES A1B emission scenario for the 2040-2059 time period applied, the gutter flow depth increased to 38.9 mm for the 50th percentile, 43.1 mm for the 90th percentile, and 44.4 mm for the 95th percentile. Again, there is no apparent risk to gutter overtopping for these storms.

For the baseline 10minM100 storm, the gutter flow depth peaks at 38.8 mm, increasing to 42.7 mm, 47.3 mm, and 48.8 mm for the 50th, 90th, and 95th percentiles, respectively. Finally, the baseline 10minM500 storm produces a peak gutter flow depth of 45.3 mm, and then peaks of 50.1 mm, 55.5 mm, and 57.3 mm for the 50th, 90th, and 95th percentiles, respectively. Whilst no gutter overtopping is simulated to occur for this range of applied storms, the 10minM500 storm with an uplift factor representing the 95th percentile, and having a peak gutter depth of 57.3 mm, is less than just 6 mm lower that the 63 mm gutter depth. In that storm simulation, a rainfall depth of 26.8 mm occurs during the 10 minute storm. If full capacity of the system were to be compromised due to debris in the gutter or downpipe, for example, there would be a risk of gutter overtopping.

7.2 Determining system failure point

To determine the point at which the system would fail and gutter overtopping would occur, the rainfall depth was increased sequentially, firstly for the system without corrosion, and secondly for the system with corrosion assumed in the gutter and downpipes. Once the failure point was established, the rainwater depth was increased a further three times to provide examples of extreme gutter overtopping.

7.2.1 System without corrosion

Assuming clean cast iron for the gutter and downpipes, the failure point occurred when the rainfall depth reached 32 mm for a 10 minute storm. This resulted in an overtopping volume of 0.9 litres of rainwater from gutters G1 and G2. By further increasing the rainwater depth to 35 mm, 40 mm, and 50 mm, the resultant overtopping volumes increased to 11.8 litres, 51.7 litres, and 154.8 litres, respectively. Figure 12 shows the gutter flow depths and Figure 13 shows the resultant gutter overtopping rate.
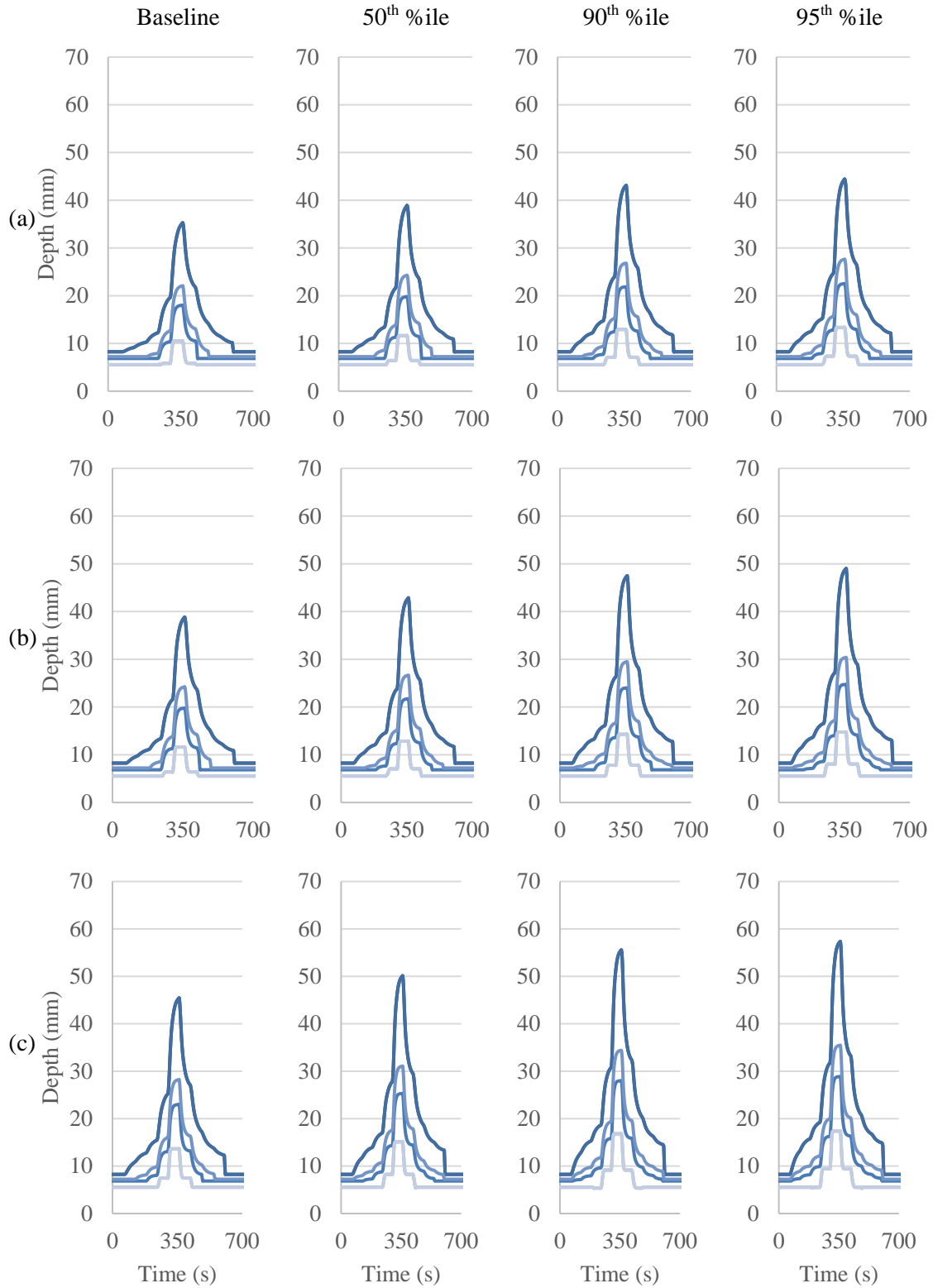
Figure 11: Simulated maximum gutter flow depths for baseline 10-minute storms with return periods of 50, 100, and 500 years: (a) 10minM50; (b) 10minM100; and 10minM500. With future rainfall represented by the SRES A1B emissions scenario for the 2040-2059 time period for the 50th, 90th, and 95th percentiles
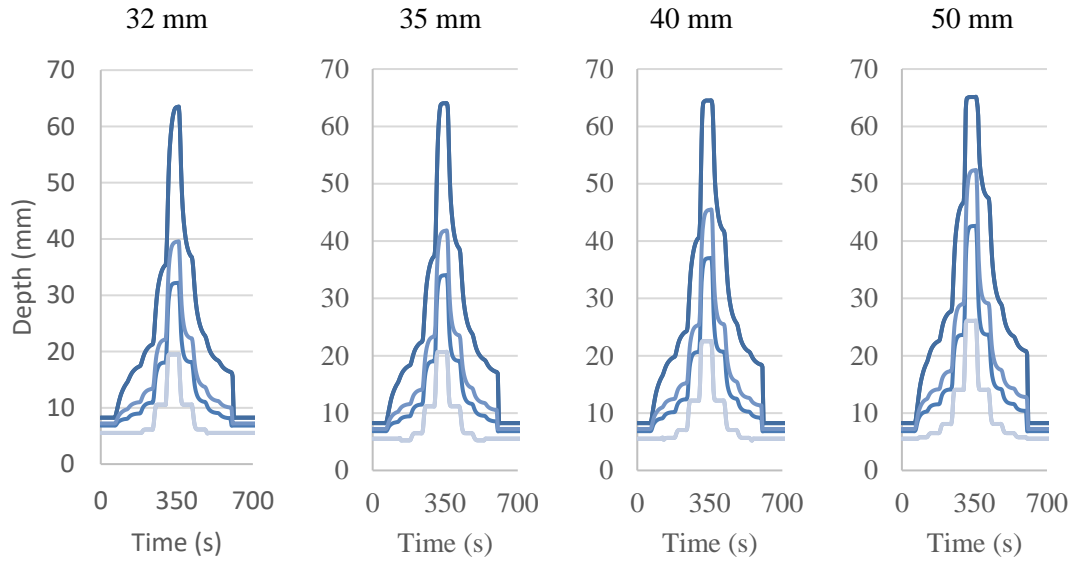
Figure 12: Simulated maximum gutter flow depths when determining system failure point and extreme gutter overtopping for the system without corrosion. System failure occurred at a rainwater depth of 32 mm for a 10 minute storm
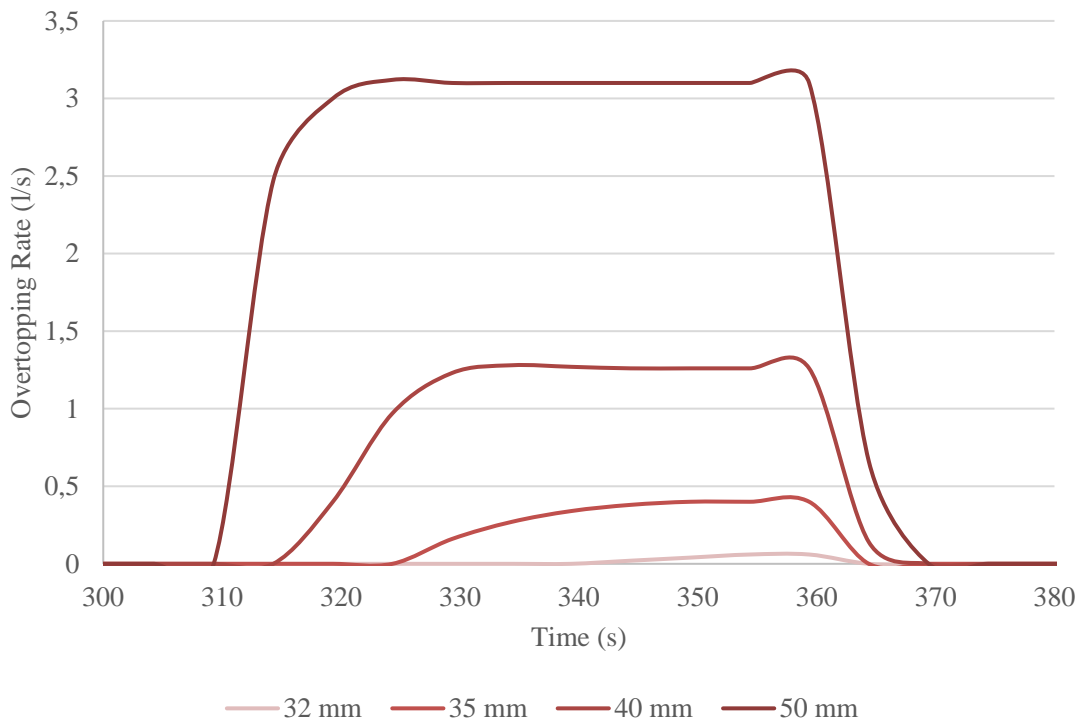

Figure 13: Simulated gutter overtopping rates for the system with corrosion for rainwater depths at and above the system failure point of 32 mm for a 10 minute storm

7.2.2 *System with corrosion*

When corrosion of the gutter and downpipes was taken into account, the failure point of the system was found to reduce significantly. As described in Section 6.2, the Manning's Coefficient of the gutter and downpipes was increased to 0.035 to represent dirty, tuberculed cast iron. The internal dimensions of the gutter were also reduced from 63 mm deep x 97 mm wide, to 53 mm deep x 87 mm wide, representing a reduction of 10 mm to both the depth and width to mimic the effects of corrosion.

The failure point of the system reduced and occurred when the rainfall depth reached just 15 mm for a 10 minute storm. This produced an increased overtopping volume of 1.9 litres of rainwater from gutters G1 and G2. With the representation of system corrosion, the failure point occurs at a rainwater depth less than half that of when corrosion is not taken into account (i.e. dropping from 32 mm to 15 mm of rainwater during a 10 minute storm). Furthermore, the overtopping volume at the failure point is more than doubled, increasing from 0.9 litres to 1.9 litres.

Tables 3 reproduces the rainfall depth information for the baseline and future rainfall events, as previously depicted in Table 2, and highlights the events where system failure would occur when corrosion is taken into account. Failure would be expected to occur for events where the rainfall depth is equal to or greater than 15 mm for a 10 minute storm. It can be seen that all but three of the events would result in system failure and gutter overtopping to some extent.

Table 3: Failure potential for baseline and future rainfall events when system corrosion is taken into account. Failure would be possible for events with rainfall depths of 15 mm or above for a 10 minute storm, as highlighted

	Event			
	Baseline	50th %ile	90th %ile	95th %ile
	Uplift (%)			
	0%	17%	38%	45%
	Depth (mm)			
10minM50	12.3	14.4	17.0	17.9
10minM100	14.4	16.9	19.9	20.9
10minM500	18.5	21.7	25.5	26.8

Further increasing the rainwater depth for the corroded system to 20 mm, 25 mm, and 30 mm, resulted in overtopping volumes of 38.7 litres, 90.1 litres, and 149.2 litres, respectively. Figure 14 shows the gutter flow depths and Figure 15 shows the resultant gutter overtopping rate.
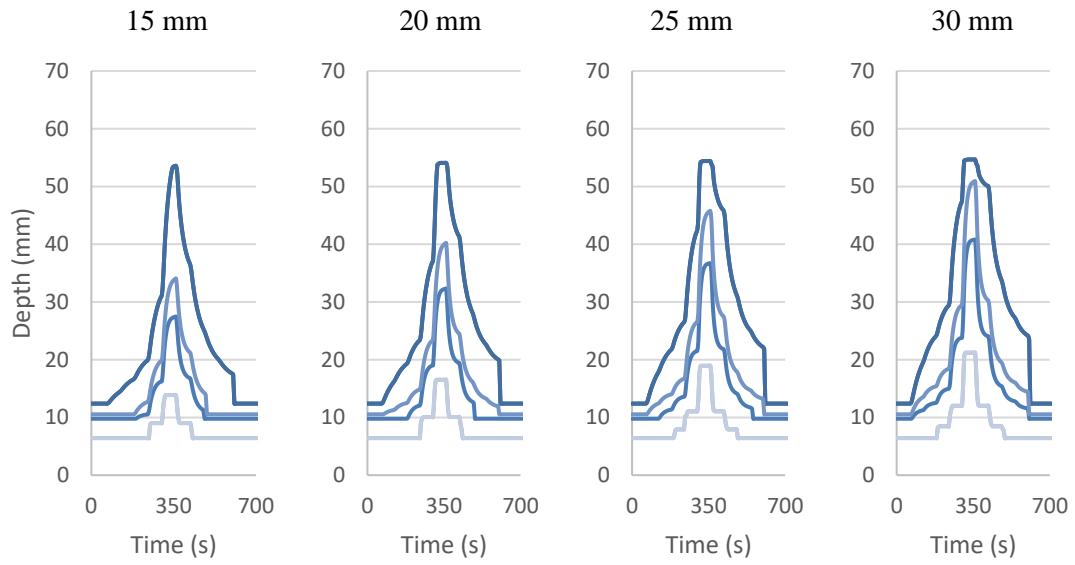
Figure 14: Simulated maximum gutter flow depths when determining system failure point and extreme gutter overtopping for the system with corrosion. System failure occurred at a rainwater depth of 15 mm for a 10 minute storm
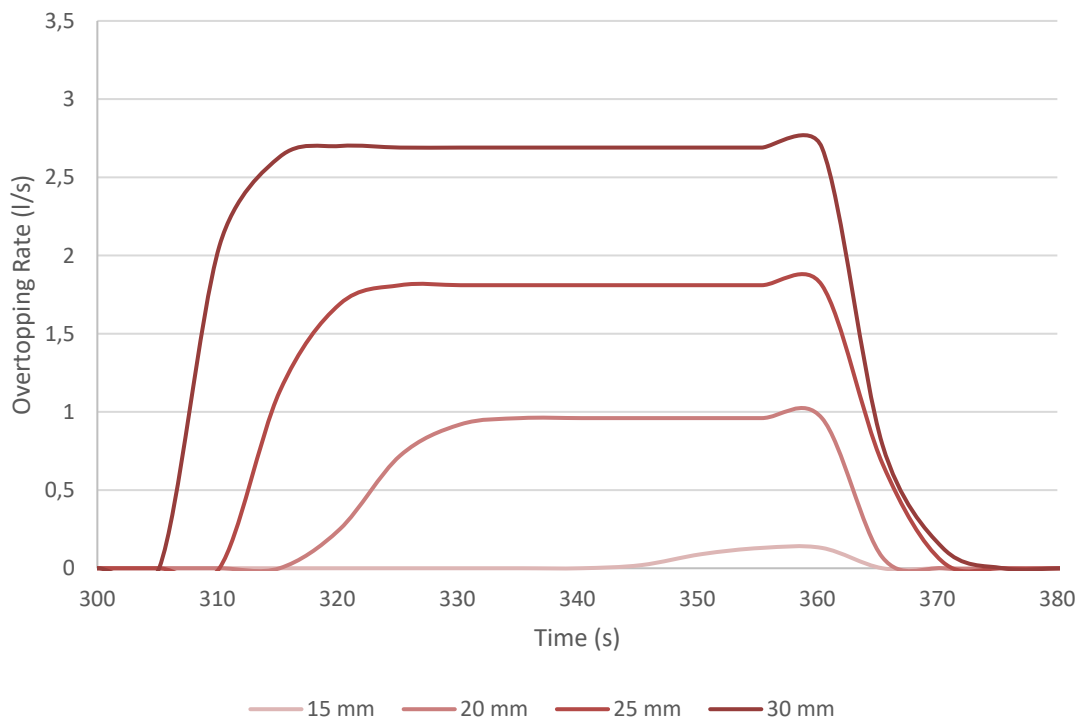

Figure 15: Simulated gutter overtopping rates for the system with corrosion for rainwater depths at and above the system failure point of 15 mm for a 10 minute storm

8   Discussion

The results of the ROOFNET simulations show that, when subject to the baseline and future rainfall events, no overtopping occurred at Bishop Cosin's Almshouses when a new and clean rainwater drainage system was assumed. The largest of the applied rainfall events was the 10 minute storm with a 500 year return period (10minM500) with an uplift factor of 45% to represent the 95th percentile of the future rainfall event. The rainfall depth of that event was 26.8 mm, which resulted in a peak gutter depth of 57.3 mm (just 5.7 mm lower than the 63 mm gutter depth). The failure point of the system occurred when the rainfall depth reached 32 mm for a 10 minute storm. This would require an uplift of 73% be applied to the 10minM500 storm before gutter overtopping would occur.

Those initial results, however, assumed that the cast iron gutters and downpipes were new and clean when, in reality, the system could be affected by corrosion (and possible debris). When the model was run with system data that assumed levels of corrosion in the gutter and downpipes, the failure point reduced significantly, reducing from 32 mm to 15 mm for a 10 minute storm. When comparing this reduced failure point to the baseline rainfall events, the 10minM50 storm, with a rainfall depth of 12.3 mm, would require an uplift of 22% for gutter overtopping to occur, whilst the 10minM100 storm, with a rainfall depth of 14.4 mm, would require an uplift of just 4% for gutter overtopping to occur. The rainfall depth for the 10minM500 storm already exceeds the 15 mm failure point, with a depth of 18.5 mm.

Of the 120 projected uplift factors for rainfall under the UKCP09 medium emissions scenario (SRES A1B), covering the full 2020 to 2099 time period, 24 scenarios show an uplift of 22% or greater (across the 50th, 90th, and 95th percentiles of probability) (Met Office, 2022). This increases to 89 scenarios for an uplift of 4% or greater. This indicates that, in reality, when system corrosion and debris are taken into account, historic buildings could therefore be susceptible to gutter overtopping to a wide range of current and future rainfall events. More research on the extent of corrosion and the condition of roof drainage systems of historic buildings is needed, however, this assessment of gutter overtopping risk highlights the importance of system maintenance and repair to ensure optimum performance.

It should also be noted that due to the uncertainty related to climate change projections and the limitations around climate modelling for specific building or system operation, the outputs of any such modelling, particularly those that apply rainfall data (which is inherently difficult to predict) should be used tentatively. However, the use of such data for building/system modelling does, at least, allow some assessment of climate change impacts and future building/system performance to be made that would otherwise not be possible. Such modelling and risk assessment helps to provide insight and enables future planning. In regard to historic building preservation, this level of climate modelling and assessment allows for more informed adaptation planning for future resilience.

9   Conclusion

This paper has evaluated the impact of extreme rainfall events on historic buildings, by assessing the risk of gutter overtopping for a case study building, Bishop Cosin's Almhouses in the Durham World Heritage Site, in response to baseline 10 minute storms with return periods of 50 years, 100, years, and 500 years, simulated using the ROOFNET numerical model. Future changes to rainfall were taken into account by applying uplift factors based on the UKCP09 medium emissions scenario (SRES A1B), for the 2040-2059 time period and for the 50th, 90th, and 95th percentiles of probability.

The initial simulations assumed a new and clear rainwater drainage system (which is unlikely for a historic building) and in that scenario, no gutter overtopping was found to occur. The largest simulated storm (the 10minM500 with 45% uplift) with a rainfall depth of 26.8 mm produced a maximum gutter depth of 57.3 mm, just 5.7 mm lower than the 63 mm gutter depth. The failure point of the system occurred for a 10 minute storm with rainfall depth of 32 mm.

When corrosion was taken into account (by setting the Manning's Coefficient for the gutter and downpipe for dirty, tuberculed cast iron, and reducing the internal gutter dimension) the failure point of the system reduced significantly by dropping to 15 mm. This depth was exceeded for the baseline 10minM500 storm, plus most of the future rainfall scenarios once uplift factors were applied. In some cases, the resultant volume of rainwater overtopping the gutter was significant and would pose a flooding and damage risk to the historic building. Even small volumes of gutter overtopping could cause significant damage to the building fabric over the medium to long term.

Whilst climate modelling for specific building or system operation is currently limited due, primarily, to climate change projection uncertainty and modelling accuracy, it does provide an insight into the potential risks and enables more informed adaptation planning. This study has highlighted the importance of system maintenance and repair to ensure optimum performance of rainwater drainage systems belonging to historic buildings.

10 References

Allerton (2023). Dry rot. [Online] Available at: https://alldamp.co.uk/dry-rot [Accessed 31/05/2023].

Arthur, S. & Swaffield, J. A. (1999). Numerical modelling of the priming of a siphonic rainwater drainage system. Building Serv. Eng. Res. Tech., 20(2), pp. 83-91.

Blamore Specialist Contracts (2023). Sandstone Decay. [Online] Available at: https://www.balmore-ltd.co.uk/sandstone-decay/ [Accessed 18/02/2023].

Britain Express (n.d.). Gargoyles in English Architecture. [Online] Available at: https://www.britainexpress.com/architecture/gargoyles.htm [Accessed 31/05/2023]

British Listed Buildings (2023). Bishop Cosin's Almhouses. [Online] Available at: https://britishlistedbuildings.co.uk/101322865-bishop-cosins-almhouses-city-of-durham#.Y_DYinbP1PY [Accessed 18/02/2023].

British Standards, 2000. BS EN 12056:3 2000. Gravity drainage systems inside buildings - Part 3: Roof drainage, layout and calculation, London: BSI.

Curtis, R. and Kennedy, A. (2016). INFORM, Damp: Causes and Solutions. Historic Environment Scotland. [Online] Available at: https://www.historicenvironment.scot/archives-and-research/publications/publication/?publicationId=bd396452-624b-4b87-9ae4-a59500b4dff4 [Accessed 31/05/2023].

Durham World Heritage (2017). Durham World Heritage Site Management Plan, Durham: Durham County Council.

Durham World Heritage (2022). Durham World Heritage Site. [Online] Available at: https://www.durhamworldheritagesite.com/about [Accessed 19/04/2023].

Durham World Heritage (2023). Bishop Cosin's Almshouses. [Online] Available at: https://www.durhamworldheritagesite.com/learn/architecture/palace-green/cosins-almshouses [Accessed 18/02/2023].

Engineers Edge (2023). Manning's Roughness Coefficient Chart Table. [Online] Available at: https://www.engineersedge.com/fluid_flow/manning-constant.htm [Accessed 08/06/2023].

Geograph (2013). Chemical weathering - close up. [Online] Available at: https://www.geograph.org.uk/photo/3291153 [Accessed 26/02/2023].

Historic England (2015). Flooding and Historic Buildings, London: Historic England.

Jack, L. & Kelly, D. (2012). Property-based rainwater drainage design and the impacts. Building Serv. Eng. Res. Technol., 33(1), pp. 19-33.

Kendon, M. (2022). State of the UK Climate 2021. International Journal of Climatology, 42 (S1), pp. 1-80.

Met Office (2022). UK and Global extreme events – Heavy rainfall and floods. [Online] Available at: https://www.metoffice.gov.uk/research/climate/understanding-climate/uk-and-global-extreme-events-heavy-rainfall-and-floods [Accessed 31/05/2023].

Renshaw, J. (2019). Guide to Building Maintenance in a Changing Climate. Edinburgh World Heritage. [Online] Available at:

https://www.adaptationscotland.org.uk/application/files/7115/8393/7645/The_Guide_to_Building_Maintenance_in_a_Changing_Climate_-_full_publication.pdf [Accessed 31/05/2023].

Swaffield, J. A., Escarameia, M. & Campbell, D. P. (1999). Unsteady roof gutter flow: Development and application of simulation. Building Serv Eng Res Technol , 20(2), pp. 83-91.

SWC (2015). How the Freeze-Thaw Cycle Can Cause Devastating Damage To Your Building. [Online] Available at: https://southwestcoinc.com/news-updates-2/2015/3/9/what-the-freeze-thaw-cycle-does-to-buildings [Accessed 26/02/2023].

Taylor, J. (2013). Rainwater. [Online] Available at: https://www.buildingconservation.com/articles/rainwater/rainwater.htm [Accessed 31/05/2023].

The Engine Shed (2023). Sandstone. [Online] Available at: https://www.engineshed.scot/building-advice/building-materials/sandstone/#erosion [Accessed 18/02/2023].

The Wallingford Procedure (1981). Design & analysis of urban storm drainage: The Wallingford Procedure Volume I. Principles, methods & practice. National Water Council, Standing Technical Report No. 28, 1981

Voller, D. (2010). Old rainwater hopper-head, Fournier Street, Spitalfields. [Online] Available at: https://www.geograph.org.uk/photo/2403559 [Accessed 31/05/2023]

Viles, H. (2012). Salt Crystallisation in Masonry. [Online]. Available at: https://www.buildingconservation.com/articles/salt-crystallisation/salt-crystallisation.htm [Accessed 02/06/2023]

Wasko, C., Nathan, R., Stein, L. & O'Shea, D. (2021). Evidence of shorter more extreme rainfalls and increased flood variability under climate change. Journal of Hydrology, 603, Volume B, p. 126994.

Wright, G., Arthur, S. & Swaffield, J. (2006a). Numerical simulation of the dynamic operation of multi-outlet siphonic roof drainage systems. Building and Environment, 41(1), pp. 1279-1290.

Wright, G., Jack, L. & Swaffield, J. (2006b). Investigation and numerical modelling of roof drainage systems. Building and Environment, 41(1), pp. 126-135.

YENA Engineering (2023). Why Does a Metal Pipe Rust. [Online] Available at: https://yenaengineering.nl/why-does-a-metal-pipe-rust [Accessed 25/02/2023].

11 Presentation of authors

Dr David Kelly is Associate Professor of Architectural Engineering at Heriot-Watt University. His research interests include water supply system design together with the analysis of end-user water conservation actions. His work also includes the evaluation and minimisation of disease transmission from building drainage systems, the impact assessment of climate change on rainwater systems, and the use of nature-based solutions of stormwater management.

James Claridge is a Senior Planner at TWO PLUS TWO. With a background in Civil Engineering, he has worked as a consulting engineer and as a planner for a Civil Engineering contractor. In his current role, James has developed an interest in forensic planning and delay analysis.   He has recently completed his MSc in Building Services Engineering at Heriot-Watt University.

Modification of the Building Drainage System airflow and pressure regime due to airflow from the sewer network.

K.S.Sharif (1), M.Gormley(2),

1. kss32@hw.ac.uk
2. m.gormley@hw.ac.uk

(1) & (2)   School of Energy, Geoscience, Infrastructure and Society, Heriot-Watt University, Edinburgh, Scotland, UK.

Abstract

Urbanisation, particularly the proliferation of high-rise buildings, and the effects of climate change significantly affect wastewater management systems. Given this wider global challenge, it is crucial to consider the impact of the sewer network on individual building drainage system (BDS) airflow and pressure regimes. It has been established that this aspect of system performance is currently absent from any drainage system code or standard – above and below ground codes alike. In order to quantify the impact of air from the sewer on BDS air pressure and air flow regimes, a laboratory investigation was conducted to explore the interaction between building height and the influence of sewer air on the airflow and air pressure within the system. The study aimed to analyse the impact of sewer air on the pressure regime in a dry stack drainage system and to investigate the drainage system's behaviour when exposed to sewer air, with particular attention paid to the pressure changes observed in buildings of varying heights. The results indicate that there is a direct correlation between pressure changes within the system and building height when exposed to sewer air. The findings of the study contribute to improving our understanding of the relationship between building structures and sewer systems, as well as identifying potential design considerations to optimise building drainage performance.

Key words:

Sewer System, Building Drainage System, Network Integration, Air Movement, Pressure Regime

Abbreviations

$\Delta P_{updraft\ air}$ Pressure change along the dry system, Qas sewer air flow rate

1. Introduction

The expansion of urban areas and the effects of climate change have created a risk of urban flooding and placed strain on the wastewater infrastructure in the UK (Miller and Hutchins, 2017). In regions that are already vulnerable to severe weather conditions, the combined sewer system is particularly at risk of increased flooding, resulting in a potential loss of ability to manage the increasing flows. This could lead to flows moving backward, causing surge problems and airflow propagation throughout the network (Hamam, 1982).

Due to network integration between the above and below ground drainage system, in some cases, the building drainage system serves a secondary purpose as a vent for the main sewer network (Sharif and Gormley, 2021). Excessive water or airflow rates and the generation of air pressure transients must be avoided to prevent compromising the water-trap seal (Gormley *et al.*, 2021).

Hence, it is essential to investigate and comprehend the air movement within the network to understand its effects on the pressure regime inside the building drainage system. Although codes and standards do not explicitly state this, guidelines often imply the need for a source of air at the top of the drainage stack when connecting multiple houses to the sewer network (*Building Regulation 2010 Approved Document H Drainage and waste disposal*, 2015).

To replicate the airflow from the sewer an extractor fan can be connected to a horizontal loop pipe to induce airflow through the pipe. As the fluid moves through the pipe, it experiences a reduction in pressure, known as separation loss, in addition to frictional losses. The magnitude of these losses is dependent on the fluid velocity and a dimensionless loss coefficient, K, that is determined by the system's flow conditions and geometry. The total energy losses incurred by the fluid in the pipe can be classified into two categories, major losses and minor losses.

The total pressure loss in a pipe can be obtained using the Darcy equation to sum the major and minor losses; this equation is useful for low airflow conditions.

$$\Delta P = (f_d \frac{L}{D_h} + \sum K) \frac{\rho V^2}{2}$$

The K factor is a dimensionless coefficient that depends on the geometry of the transition, V is the mean air velocity, f is the pipe friction factor, ρ is the fluid density. The hydraulic diameter D_h is a parameter that relates the cross sectional area of a pipe to its wetted perimeter. In the case of circular pipes, the hydraulic diameter is equal to the diameter of the pipe itself. It is worthy of mention that the test was evaluated in terms of losses due to friction, joints and fittings. A comparison was made based on Darcy equations to assess the accuracy and validity of the measurements. Within the illustrated Figure (1), an essential parameter has been incorporated into the system, namely the pressure drop resulting from the sewer connection. This pressure drop is denoted as $\Delta P_{updraft\ air}$, reflecting its influence on the overall airflow dynamics within the system.
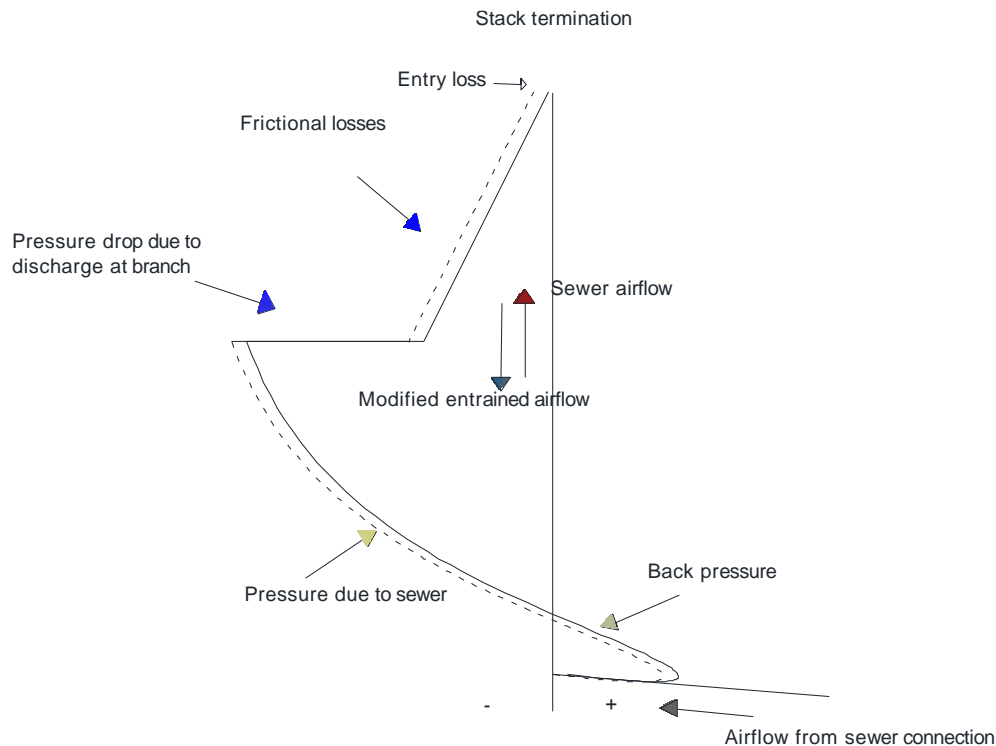
Figure 1Modification of the pressure losses due to sewer connection.

This parameter should then be added to previous developed pressure losses along the drainage pipe (Gormley and Campbell, 2005), which are induced by motive force of the work down on the air by water.

$$\Delta P_{total} = \Delta P_{entry} + \Delta P_{dry\ pipe\ friction} + \Delta P_{branch\ junction} + \Delta P_{back\ pressure} - \Delta P_{updraft\ air}$$

2. Methods
2.1 General
This study aimed to explore the relationship between the physical characteristics of a building, such as its height, and the impact of sewer air on the pressure within its drainage system. A comprehensive set of laboratory experiments were conducted to collect system response data and develop a model capable of being applied to buildings of varying heights. A new testing apparatus was constructed at the HWU laboratory for this purpose. The investigation involved setup of an extractor fan connected to horizontal loop 100mm diameter pipes of varying lengths, with the objective of (i) measuring the induced continuous airflow within the system, (ii) measuring pressure fluctuations along different pipe lengths, and (iii) analysing the system's response to these changes in pipe length.

2.2 Data collection
Measurements were conducted using a fan connected to pipes of varying lengths, Figures (3 and 4), with pressure transducers installed at three locations to measure the

pressure differential across the entire system. The pressure differential was measured at p1 across the fan, p2 at the inlet side near the fan, and then at p3, p4 and p5 at the end of the pipe system, with all measurements taken separately for the different pipe lengths of 9, 30, and 40 meters. Data were collected at a frequency of 1KHZ per second, with each recording lasting for a minimum of two minutes. In order to measure air velocity within the system created by the fan, hot wire anemometers were used, which were positioned at least 1 meter away from any bends or joints in the system.

The experiment involved recording data with the fan turned off, and then turning it on to high speed, followed by gradually reducing the fan speed using an inline controller, with separate measurements taken for at least two minutes at each speed. The experiment was concluded by turning the fan off. To verify the accuracy and reliability of the acquired data, a series of four distinct tests were conducted. These tests consisted of running the fan at varying speeds, including high, medium, and low settings. Furthermore, to control the speed of the fan, the outlet area of the pipe was sealed and gradually opened until it reached its fully open state. This process allowed for precise control over the speed of the fan during the experiments. The purpose of these tests was to ensure that the data collected were consistent across a range of operating conditions and to obtain a more complete understanding of the behaviour of the system under various conditions. The sensor and hot wire had been calibrated before use.

The second graph illustrates a specific instance of data measurements depicting the relationship between air velocity and the corresponding pressure change along the 40 m pipe length over time.
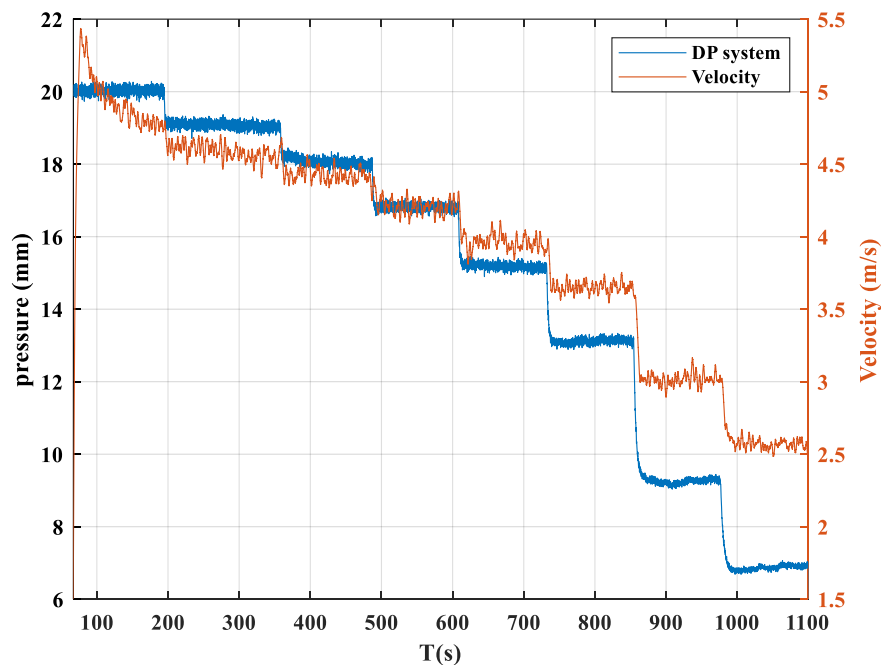

Figure 2 One example of measuring the air velocity and pressure changes along the pipe
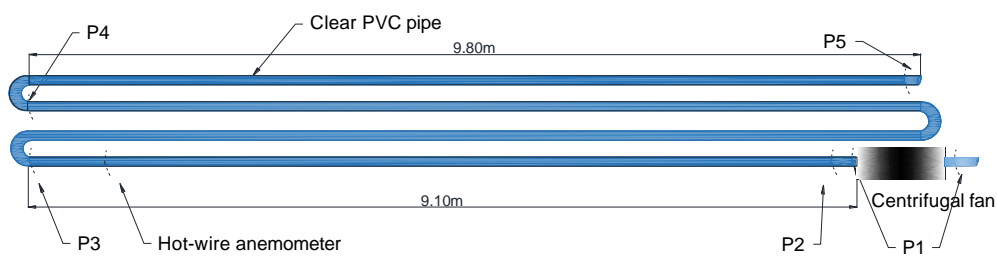
Figure 3 Laboratory test rig

Figure 4 Sketch of laboratory test rig to show the pressure sensors and anemometer location.

3.Results

Prior to conducting the tests, the collected data for each pipe length were compared with theoretical calculations based on the Darcy equation. This step was taken to evaluate

the accuracy and validity of the data in accordance with the established theoretical framework.
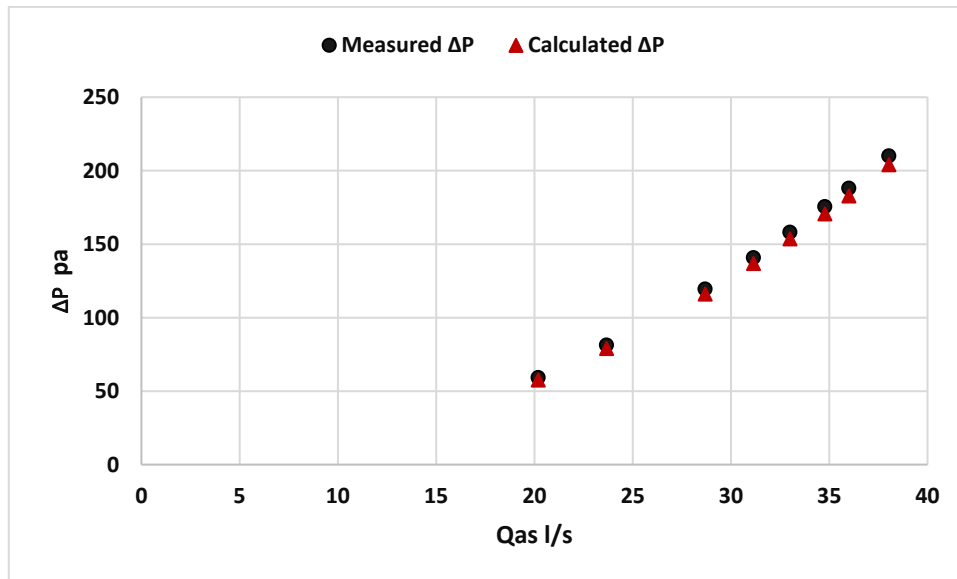

Figure 5 Measured and calculated pressure change for 40m pipe length

Figure (5), comparing measured and calculated data, can provide valuable information for understanding the behaviour of fluid flow in the system under steady state and can help to validate the use of the Darcy equation as a predictive model. This is just one example in which the length of pipe is 40m, and taking into consideration the Renold number, Friction and Minor and Major Coefficients.

In the experiment, the relationship between simulated sewer airflow and pressure differential across the drainage system was investigated. The results were displayed in a graph where the x-axis represented air flow from the sewer, while the y-axis represented the pressure drop across the entire system.

The graph, Figure (6) displays various lengths of the pipe system that were tested, and the pressure drop measurements at different points along the system.
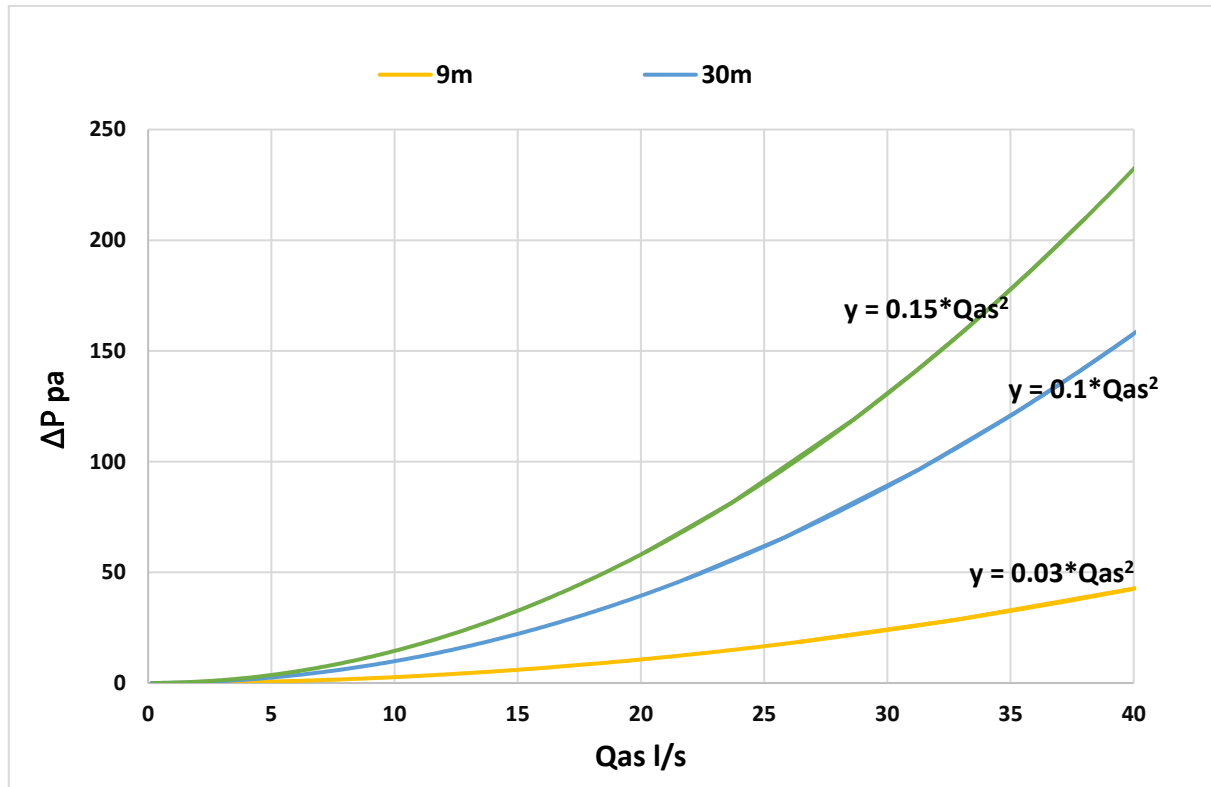
Figure 6 Pressure changes across the system for various lengths.

This graph indicates that the pressure difference between different points in the drainage system increased as the air flow from the sewer increased. This could be attributed to the fact that with increasing air flow, there is a greater amount of air moving through the pipes, which in turn creates a greater pressure differential between different points in the system. Additionally, the figure shows that the pressure differential increased with increasing length of the pipe system.

Examining the data for buildings up to 30 storeys in height and various airflow rates confirms that pressure changes occur along the system under different conditions, Figure (7).
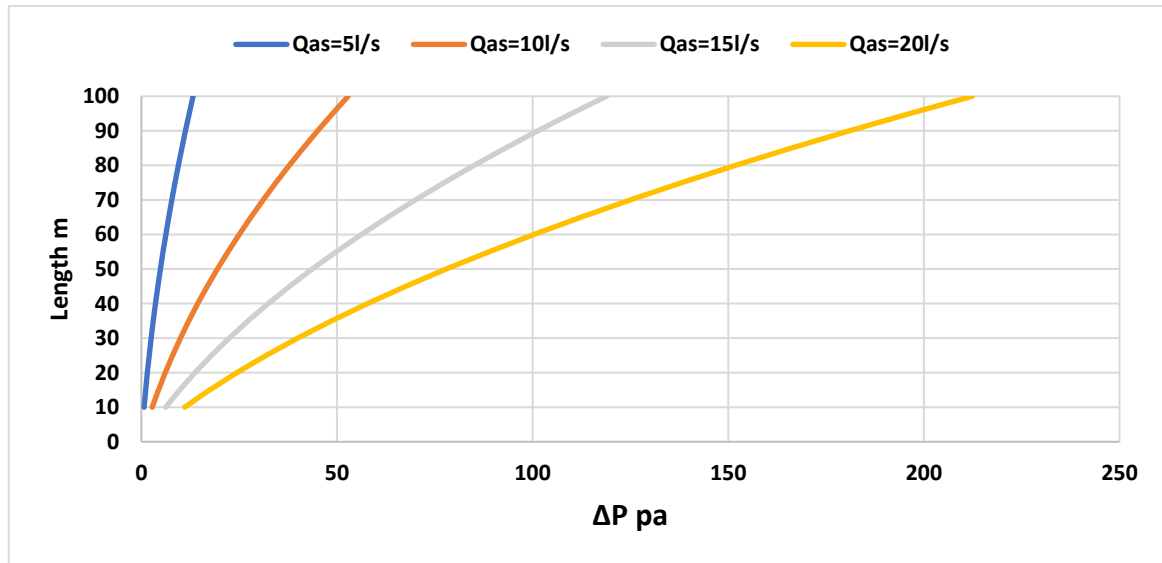
Figure 7 Pressure changes across the system vs lengths for various airflow rates

Following the exploration of various correlations, a model was developed after the experimental test to improve the system's performance by expressing the pressure changes as a function of airflow rate and system length, ΔP=f {Qas, L}. The following equation was then used to determine pressure changes at different lengths and airflow rates:

$$\Delta P_{updraft\ air}/_L = \Delta P_{min} + L\Delta P_C$$

where L is a pipe length, ΔP_L is the change of pressure in the system, ΔP_{min} is a pressure changes for min pipe length, assuming 10m as preliminary result, and ΔP_C is the rate of pressure changes due to increasing the pipe length. They can be calculated from the following equations:

$$\Delta P_{min} = K_1 (Q_{as})^2$$
$$\Delta P_C = K_2 (Q_{as})^2$$

Where Qas is continuous airflow rate, K1 and K2 are constant.

These equations can be applied after taking measurements between various air flow measurements up to 20 l/s and find correlations corresponding to pressure change across a specific length of the system. The result shows that with 100m pipe length and 20 l/s airflow rate, the pressure change is around 200 pa, which is equivalent to 20mm w gauge.

4. Conclusion
In conclusion, this paper has focused on the modification of the building drainage system's airflow and pressure regime due to airflow from the sewer network. The study highlights the importance of considering the impact of sewer air on individual building drainage systems. The research conducted laboratory investigations to explore the

interaction between building height and the influence of sewer air on airflow and air pressure within the system.

The results of the study indicate a direct correlation between pressure changes within the system and building height when exposed to sewer air. It was observed that as the airflow from the sewer increased, there was a greater pressure differential between different points in the drainage system. Additionally, the length of the pipe system had an impact on the pressure differential, with increasing length leading to higher pressure changes.

The findings of this research contribute to improving our understanding of the relationship between building structures and sewer systems. They also identify potential design considerations to optimise building drainage performance. By quantifying the impact of sewer air on the pressure regime in a dry stack drainage system, this study provides valuable insights for developing guidelines and standards in the field of wastewater management and building design.

Overall, this research highlights the importance of considering the airflow from the sewer network in building drainage system design and provides a basis for further investigations and advancements in this area. It emphasises the need to integrate the design of tall buildings and their drainage systems with the public sewer network to ensure efficient and effective wastewater management.

5. References

Building Regulation 2010 Approved Document H Drainage and waste disposal (2015). Available at: https://assets.publishing.service.gov.uk/government/uploads/system/uploads/attachment_data/file/442889/BR_PDF_AD_H_2015.pdf on 11/06/2020.

Gormley, M. *et al.* (2021) 'Building drainage system design for tall buildings: Current limitations and public health implications', *Buildings*, 11(2), pp. 1–17. doi: 10.3390/buildings11020070.

Hamam, M. (1982) *Transition of Gravity to Surcharged Flow in the Sewers. Ph.D. dissertation*. Windso, Ontario, Canada. Available at: Ph.D. dissertation.

Miller, J. D. and Hutchins, M. (2017) 'The impacts of urbanisation and climate change on urban flooding and urban water quality: A review of the evidence concerning the United Kingdom', *Journal of Hydrology: Regional Studies*. Elsevier, 12(July), pp. 345–362. doi: 10.1016/j.ejrh.2017.06.006.

Sharif, K. and Gormley, M. (2021) 'Integrating the design of tall building, wastewater drainage systems into the public sewer network: A review of the current state of the art', *Water (Switzerland)*, 13(22). doi: 10.3390/w13223242.

6. Authors

Khanda S Sharif is a PhD student at the School of Energy, Geoscience, Infrastructure and Society, Heriot-Watt University, Edinburgh, UK. She is working with the municipality of Sulaymaniyah/ Iraq as a senior engineer and responsible for delivering drainage design on multi- disciplinary civil engineering and construction projects. Her research interests include design integration of the BDS into the public sewer network, the use of sustainable drainage systems (SuDS) & Natural flood management.

Michael Gormley is Professor of Public Health and Environmental Engineering at the School of Energy, Geoscience, Infrastructure and Society at Heriot-Watt University. His research specialisms are: mathematical modelling of air and water flows in building drainage systems, infection spread via bioaerosols and product development.

A hybrid particle-polygon technique for the simulation of solid transport in a building drainage system

M.C.B. Teixeira (1), L. S. Pereira (2), R.A. Amaro Jr (3), L.Y. Cheng (4) L.H. Oliveira (5)

(1) matband@usp.br
(2) lucas_pereira@usp.br
(3) rubens.amaro@usp.br
(4) cheng.yee@usp.br
(5) lucia.helena@usp.br
(1, 2, 4, 5) Polytechnic School, University of São Paulo, Brazil
(3) Instituto de Ciências Matemáticas e de Computação, University of São Paulo, Brazil

Abstract

The steady reduction of water consumption due to sustainable provisions leads to concerns about the self-cleaning performance of building drainage networks. Moreover, the accurate prediction of complex free surface flows inside drainage pipes is particularly challenging. In a previous work, the hydrodynamics in the vicinity of a wye of a building drainage system and their influences on the solid conveyance performance were investigated through a fully particle-based modeling. Since the particle-based wall modeling of the pipe leads to more dissipative non-smooth surfaces, as a step forward on the study, a wall modeling based on unstructured triangulated surfaces associated to a polygon-to-particle contact model is adopted herein to improve the accuracy of the numerical results. The flow inside a simplified bathroom drainage system, which is represented by two drains connected by a wye to a vertical stack, is simulated considering a steady flow from a trap connected to a shower and a wash basin, and a transient flow from water closet discharge. Following the previous study, water closet discharge volumes of 4.8 and 6.0 liters (L), main drain diameters of 75 and 100 mm, and piping slopes of 0%, 1% and 2 % are considered. The computed results showed that the discharge of 4.8 L provides a better solid conveyance performance than 6.0 L, then mitigating potential issues due to clogging. In addition, the results confirm the reduction in unphysical frictional loss by using polygon-based wall modeling.

Keywords

Building Drainage System, Computational Fluid Dynamics, Particle-based Method, Moving Particle Semi-implicit, Polygon Wall Boundary.

1 Introduction

Low flush volume water closet (w.c.) has been adopted as one of the water-saving measures to alleviate the ever-growing demand on limited urban area water resources. In order to investigate the influence of the low flush volume w.c. on the self-cleaning performance of the building drainage network, numerical modeling and simulations of complex hydrodynamics inside the drains and main drains that directly receive the w.c. effluents have been conducted by using a particle-based method [1–3]. Focusing on discrete solid conveyance performance, configurations such as straight pipe and the influences of the local singularities have also been investigated [4–6].

In the author's previous work [6], the solid conveyance under the confluence flows near a wye of a drain have been studied numerically. As a result, the flow confluence at a 45° wye might deteriorate the performance and the solid might stop at the wye, showing potential for clogging, mainly in the cases featuring large diameter and zero slope. Nevertheless, as pointed by [7] unphysical frictional losses occur in the simulations of the free surface flow inside the horizontal pipes when conventional particle-based modeling of the pipe wall is adopted. As a result, flow velocity and water levels are affected by numerical model resolution. This issue resembles the additional friction due to non-smooth wall surface modeling using discrete particles.

Within this context, in the present work, following [7], the pipe wall boundaries were represented by an unstructured triangulated surface for more accurate modeling of the smoother pipes surface. In addition to this, the effects of the confluence flow on solid conveyance performance are investigated again by using a solid modeled by particles together with a polygon-to-particle contact model. Finally, the results obtained by the new numerical modeling are analyzed and the differences in relation to those obtained in the previous work [6], which is owing to smoothness of the wall modeling by particles and by polygon mesh, are also discussed.

2 Numerical model

In the present study, the fully Lagrangian meshfree moving particle semi-implicit (MPS) method, as described in [1–3], was adopted, using the free surface and solid contact models detailed in the previous works [9, 10]. However, instead of the distance of contact proposed in [10], the distance between the solid particle and the closest triangle is considered for the solid collisions. Considering a pipe flow with relatively low water level, the modeling of the air pressure oscillation due its entrapment was neglected.

Rigid pipe wall boundary

Contrary to the conventional particle wall modeling [6], the explicitly represented polygon (ERP) wall boundary technique [11], in which fixed solid walls are modeled by

a mesh of triangles, was adopted herein. In what follows, only essential formulations are presented. The reader can find more details in [8, 9].

The compact support of fluid particles near the polygon walls is not fully filled with particles. Hence, the numerical operators of these particles are divided into the contribution due fluid particles $\langle\rangle^{particle}$ and polygon walls $\langle\rangle^{wall}$, see Figure 1.
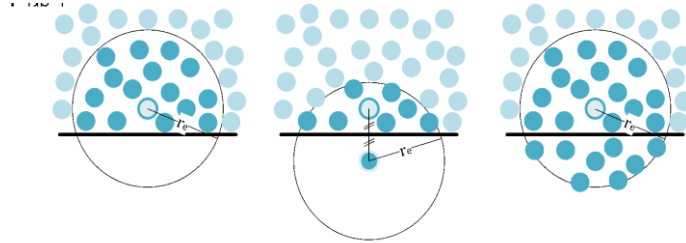

Figure 1 – Polygon wall modeling. Calculation of numerical operators with ERP model.

First, the position of the mirror particle i' corresponding to particle i is computed by:

$$r_{i'} = 2r_i^{wall} - r_i ,$$

(1)

where r_i^{wall} is the closest point on the polygon to particle i.

Afterwards, the pressure gradient and Laplacian of the velocity, no-slip boundary condition, of the mirror particle i' are computed considering its neighbors $\Omega_{i'}$, and are multiplied by R_i^{ref} and the identity matrix I [11], respectively:

$$\langle\nabla P\rangle_i^{wall} = R_i^{ref} \frac{d}{pnd^0} \sum_{j\in\Omega_{i'}} \left(P_j + P_i - 2\hat{P}_i\right)\frac{(r_j - r_{i'})}{\|r_j - r_{i'}\|^2}\omega_{i'j} ,$$

(2)

$$\langle\nabla^2 u\rangle_i^{wall} = -I\frac{2d}{\lambda^0 pnd^0} \sum_{j\in\Omega_{i'}} \left(u_j - u_{i'}\right)\omega_{i'j} .$$

(3)

Finally, the operators are added to the numerical operators $\langle\rangle^{particle}$ of particle i:

$$\langle\nabla P\rangle_i = \langle\nabla P\rangle_i^{particle} + \langle\nabla P\rangle_i^{wall} ,$$

(4)

$$\langle\nabla^2 u\rangle_i = \langle\nabla^2 u\rangle_i^{particle} + \langle\nabla^2 u\rangle_i^{wall} .$$

(5)

The transformation matrix for reflection across the plane R_i^{ref} is expressed as:

$$R_i^{ref} = I - 2n_i^{wall}\otimes n_i^{wall} ,$$

(6)

where n_i^{wall} represents the unit normal vector at the position of particle i.

The Eq. (3) represents the Laplacian of velocity for the no-slip boundary condition on a wall, here with velocity $u_i^{wall} = 0$, whose velocity of the mirror particle i' is:

$$u_{i\prime} = -I\{u_i - 2[u_i^{wall} - (n_i^{wall} \cdot u_i^{wall})n_i^{wall}]\}, \tag{7}$$

A repulsive force f_i^{rep} based on Lennard-Jones potential [12] is added to Eq. (15) to prevent penetrations of the fluid particles at curved edges of the mesh:

$$f_i^{rep} = \left\{-\frac{D_{rep}}{\|r_{iw}\|}\left[\left(\frac{0.5l_0}{\|r_{iw}\|}\right)^{n1} - \left(\frac{0.5l_0}{\|r_{iw}\|}\right)^{n2}\right]n_i^{wall} \; \|r_{iw}\| \le 0.5l_0 \; 0 \; otherwise \right., \tag{8}$$

where $r_{iw} = r_i^{wall} - r_i$, $(n_1, n_2) = (4,2)$, $D_{rep} = \rho C_{rep}|V_{MAX}|^2$, with V_{MAX} the maximum fluid's velocity, and the repulsive coefficient $C_{rep} = 1$ are used for all simulations.

It is worth noticing that in the ERP the Neumann boundary condition for pressure is satisfied and the free-slip/no-slip condition for velocity on the walls can be applied.

3 Simplified bathroom drainage system

Following [2] and [6], the simulated model consists of two drains. Pipe 1 receives the discharge of a w.c. and the Pipe 2 connects to a trap that receives the effluent of a shower and a wash basin. Both drains are connected through a wye to a stack. Figure 2 shows the main dimensions of the simulated model along with the curves representing the flow rate over time. For Pipe 1, two diameters (75 mm and 100 mm), three pipe declivities (0%, 1% and 2%) and two discharge volumes of water (4.8L and 6.0L) were considered. The diameter of the Pipe 2 is 50 mm for all simulations. The heights of the water surface level at the sections S1 to S6, see Figure 2, were measured along the simulation.
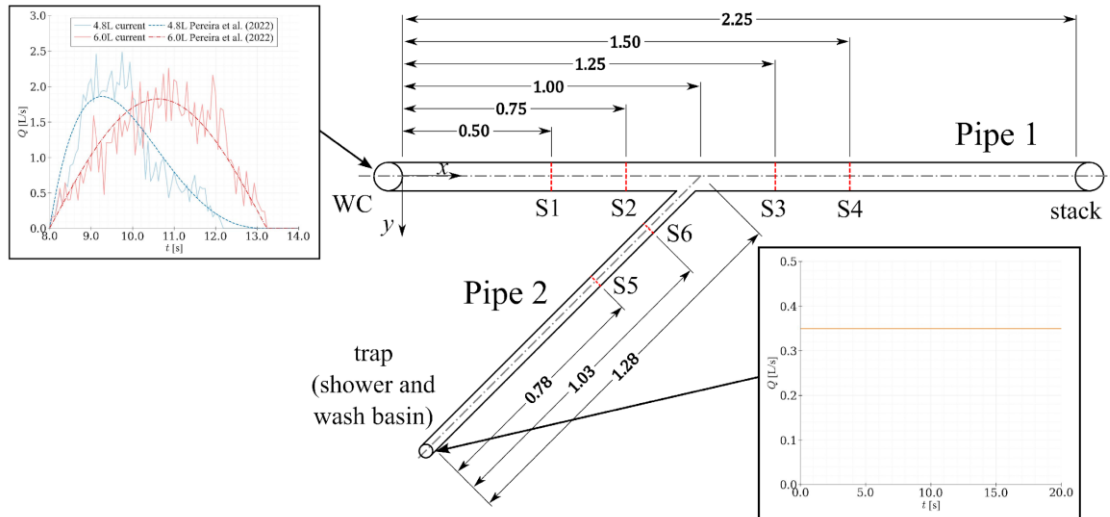

Figure 2 - Main dimensions, positions of the sensors of the simulated model (in meters). Time series of the flow rate of shower and wash basin and the w.c. flushes of the current work and of [6].

It is worth to mention that the flow rate over time of the 4.8L and 6.0L discharges, experimentally measured (solid lines), were used in the present study, while the smooth fittings (dashed lines) were used in the previous study [6].

Considering the different time scales of the flows originating from Pipe 1 and Pipe 2 (several minutes and a few seconds, respectively), the study focuses on the effects of the transient w.c. flush, while the constant flow rate from the shower of 0.35 L/s (0.2 L/s from the shower and 0.15 L/s from the wash basin) is applied as the upstream boundary condition for Pipe 2. Once the flow reaches steady state (after 8 seconds in simulations using polygon wall, and after 10 seconds using particle wall modeling [6]), the w.c. flush is discharged upstream in Pipe 1. The total duration of the simulations was 20 seconds.

The solid transport performance was evaluated by using a cylindrical-shape rigid body, six degrees of freedom (6DOF), positioned upstream of the Pipe 1 at beginning of the simulation. The material and dimensions of the solid, a cylinder of 30mm diameter and 80mm length, is based on the waste substitute of an experimental study [13]. Table 1 shows the mechanical and numerical parameters used herein.

Table 1 – Material properties and numerical parameters.

Material	Density ρ [kg/m³]	Mass m [kg]	Collision coef. ξ_n	Static friction coef. μ
Solid	1010	0.06	0.05	–
Pipe	∞	∞	–	0.22

The simulations were performed using the distance between particles of 2.0 mm and time step of $2 \cdot 10^{-4}$ s. The pressure smooth coefficient (γ) and the artificial compressibility coefficient (α) adopted were 0.01 and 10-8, respectively. For the chosen resolution, the models have approximately 600 thousand particles at their peak. Each case took approximately 16 hours to process on Intel® Xeon® Processor E5-2680 v2 2.80GHz, 10 Cores (20 Threads).

The nomenclature of the 12 simulated cases also follows that adopted in [6]), i.e., VaaDbbbAc. where "aa" is 48 or 60 and stands for the discharge volume of 4.8L and 6.0L, respectively; "bbb" is 075 or 100 denoting the pipe diameter, in mm; and "c" is 0, 1 or 2, the value of the pipe slope in %. For example, the case V48D075A0 means 4.8L discharge in 75 mm pipe at 0% slope.

4 Flow confluence at wye

Figure 3 depicts the time series of water level for all sensors (S1 to S6) for two cases V60D100A2 and V48D075A0. The position of the sensors (S1 to S6) is also shown in detail in Fig. 3b.
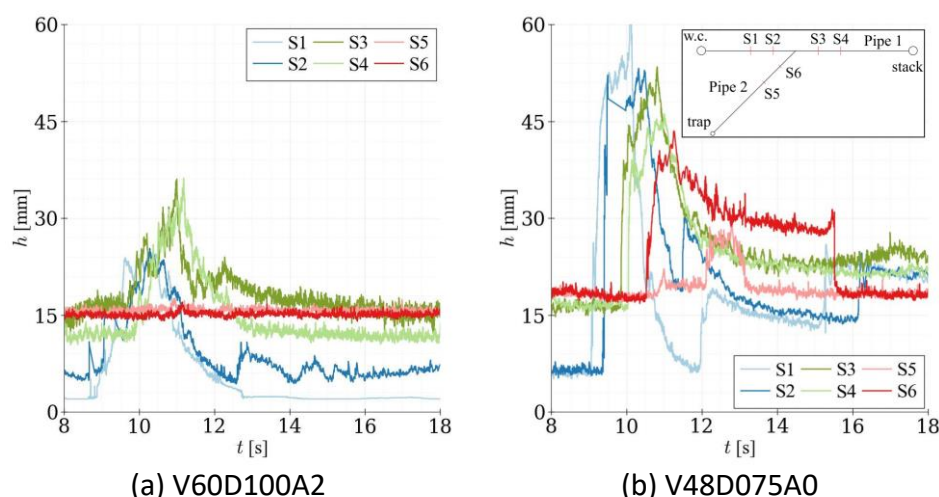

(a) V60D100A2	(b) V48D075A0

Figure 3 – Water level in the sections S1 to S6 for the cases (a) V60D100A2 and (b) V48D075A0 - without solid.

The flow from the trap which consists of the discharge of the shower and the wash basin reaches steady state at $t = 8$ s when the water level measured in the sensors located in the Pipe 2 (S5 and S6) remains constant. The water level height in both sensors S5 and S6 before the w.c. flush is approximately 15mm in V60D100A2. As expected, it is slightly lower than in V48D075A0, about 18 mm, due to larger pipe diameter and slope. After the w.c. flush discharge at $t = 8$ s, the water level in Pipe 1, S1-S4, increases.

The water level at sensor S1 in case V60D100A2 displays a single peak of about 25 mm at t=10 s, as illustrated by Fig. 3a. After the peak w.c. flush in the section, the water level inside the Pipe 1 decreases steadily to the initial condition.

From Fig. 3b, the sudden increase of water level is steeper for the case V48D075A0, and at $t = 10$ s, a peak of approximately 60 mm at the sensor S2 was computed. After a decrease in the height until near $t = 12.5$ s, the water level at the sensors S1 and S2, upstream the wye, rises again around $t = 12.5$ s and $t = 16$ s. The second and third peaks are associated with the encounter of discharged flows in the wye, leading to a backwater wave in Pipe 1 upstream to the wye. This phenomenon is more evident for the cases where Pipe 1 has smaller diameter and lower slope.

Regarding the Pipe 2, the cases V48D075A0 and V60D100A2 showed some distinct characteristics. In case V60D100A2 the water level of Pipe 2 remains unchanged during the w.c. discharge (Fig. 3a). On the other hand, from Fig. 3b, there is an increase in the water level in section S6 at $t =$10.6 s and in S5 at $t =$12 s, in V48D075A0. This is owing

to the backward wave propagation from the wye to upstream caused by the encounter of the peak w.c. flush with the steady flow at the wye. At $t = 11$ s, the sensor S6 presents a peak water level height of 43 mm. The current results in upstream sections of Pipe 2, S5 and S6, exhibit a water level peak magnitude, with shorter duration due to the w.c. flush discharge, smaller than those obtained by [6]. After $t = 16$ s, the water level in the upstream sections return to the initial level prior to the w.c. discharge.

Figure 4 presents the maximum pipe filling (dimensionless water level) in section S6 of the Pipe 2 as a function of the slope for all simulated cases. The scenarios with Pipe 1 diameter of 75 mm exhibit pipe filling higher than those with the diameter of 100 mm, in special for the null pipe slope, in which the maximum pipe filling exceeds 0.85. An increase in pipe slope leads to a decrease in the maximum pipe filling value, more evident for the cases with Pipe 1 diameter of 75 mm (V48D075 and V60D075). Furthermore, very close water levels were obtained for all cases with 1% and 2% slope.
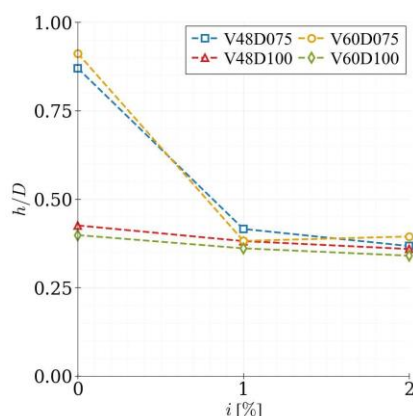
Figure 4 – Maximum pipe filling (dimensionless water level) in section S6 as a function of slope – without solid.

5 Solid conveyance near the wye

To evaluate the solid conveyance performance in the simplified bathroom drainage model, a rigid body 6DOF was initially positioned close to the upstream end of Pipe 1.

Figure 5 shows snapshots from the cases V60D075A0 and V48D100A0 with the solid. The color scale of the fluid particles represents their velocity magnitude, and the body is represented by black color. At $t = 8$ s, the w.c. flush is discharged generating a wave that propagates inside the Pipe 1.

Figure 5 – Snapshots of the simulations of the cases (a) V60D075A0 and (b) V48D100A0 - with solid.

In case V60D075A0, the wavefront of the w.c. discharge hits the solid, which is abruptly accelerated and slides in contact with the p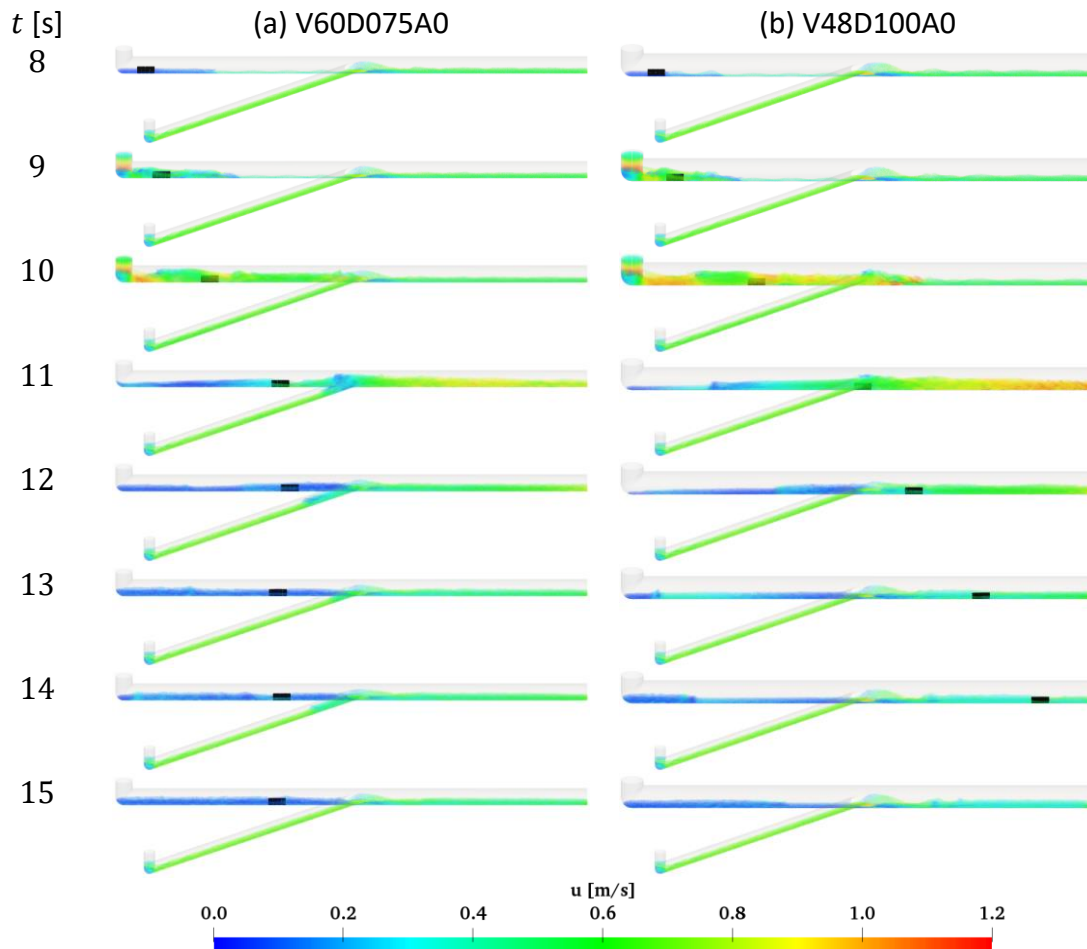ipe invert (Fig. 5a). As the solid approaches the wye, its velocity decreases due to the influence of the flow from Pipe 2. Afterwards, the solid stops at $t = 12$ s and remains deposited until the simulation's end.

In case V48D100A0 (Fig. 5b), the flow confluence near the wye decelerates the solid but is not enough to stop it, which passes through the wye at $t = 11$ s. After that, the velocity of the solid increases once again, reaching the stack before $t = 15$ s.

Despite the lower w.c. flush volume, the solid reaches the stack in case V48D100A0, while it stops before the wye in case V60A075A0. This is because the discharge of the 4.8L w.c. flush has a steeper increase of flow rate and consequently higher flow velocity that provides larger momentum transfer to the solid through the impact even when the Pipe 1 diameter is larger, as shown in Figure 5 at $t = 10$ s.

Figure 6 provides the time series for the x position of the solid within Pipe 1 across all simulated scenarios. The origin of the coordinate system of the x-axis is at the upstream (left) end of Pipe 1, as depicted in Figure 1. Before the w.c. flush discharge, the solid

slides slowly along the pipe invert for the scenarios with 1% or 2% of pipe slope. As a result, the position of the solid at $t = 8$ s varies slightly for each case.
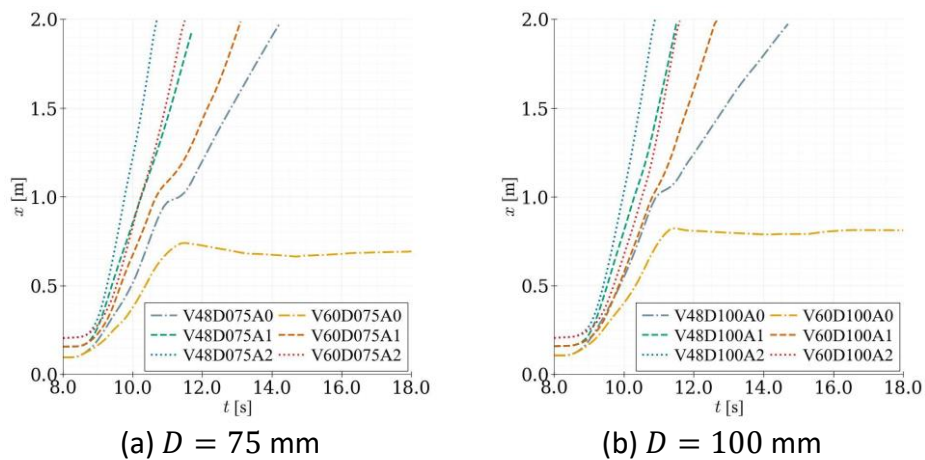

(a) $D = 75$ mm   (b) $D = 100$ mm

Figure 6 – Time series of the solid position in x-axis, Pipe 1 diameter of (a) 75 mm and (b) 100 mm.

The times series exhibit a sudden increase of solid velocity due to the impact of the wavefront of the w.c. flush discharge on the solid. After that, an inflection occurs in most cases when the solid reaches the wye. Out of the 12 simulated cases, in the two (V60D075A0 and V60D100A0) with 6.0 L w.c. flush volume and null pipe slope, the solid do not reach the stack during the simulation (Fig. 6a and Fig. 6b) and remains deposited near the position $x = 0.7$ m until the simulation's end.

On the other hand, it is interesting to point out that in the other two cases with null pipe slope and flush volume of 4.8 L (V48D075A0 and V48D100A0), the solid is able to pass through the wye, although its motion is decelerated near the wye. In the other words, in the worst situation of null pipe slope, the cases with flush volume of 4.8 L, which presents steeper increase of flow rate, provide better solid conveyance performances than the cases with 6.0 L.

Figure 7 presents the comparison between the time series of solid position in x-axis of cases with null pipe slope obtained by the current study and those performed previously by [6]. From the numerical results by using the polygon-based wall modeling, the steeper increase of flush rate in 4.8 L discharge is critical for the solid conveyance through the wye. On the other hand, the results from the previous study using particle-based wall modeling, a numerical technique that induces unphysical frictional loss, the diameter of Pipe 1 is a critical factor that leads to the clogging.
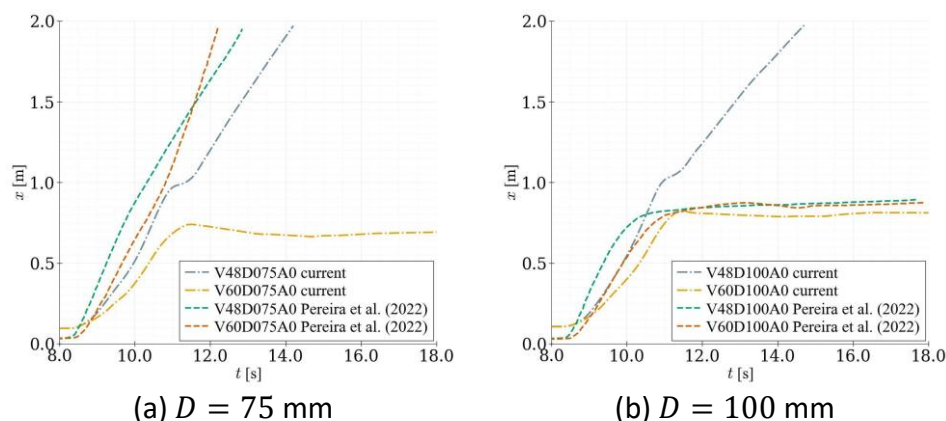
(a) $D = 75$ mm   (b) $D = 100$ mm

Figure 7 – Time series of the solid position in x-axis, Pipe 1 diameter of (a) 75 mm and (b) 100 mm for the current simulations and performed by [6].

6 Final considerations

This work focused on the investigation of hydrodynamics and solid transport in a simplified bathroom drainage model considering 2 pipes: Pipe 1 receives the discharge of a w.c. and Pipe 2 connects to a trap that receives the effluent of a shower and a wash basin. 12 scenarios considering different w.c. flush volumes, Pipe 1 diameters and slopes, were evaluated. An improved modeling of wall boundary based on an unstructured triangulated mesh was adopted to represent smoother pipe surfaces.

Concerning the flow confluence on the wye, a backwater wave is generated by the convergence of the discharges in the wye and propagates upstream in Pipe 1 in the cases with smaller Pipe 1 diameter and lower pipe slope. Compared to the computed results of the former study carried out using conventional particle-based modeling of the pipe wall, the water level heights in the upstream sections of Pipe 2 exhibits a smaller peak magnitude with shorter duration due to the w.c. flush discharge flowing through the wye. These differences can be explained by the present smoother representation of the pipe wall boundary using polygons, with reduced unphysical frictional loss.

Regarding the solid conveyance, the confluence at the wye might negatively impact the solid transport performance when the pipe slope is null and the 6.0 L w.c. flush volume is adopted. On the other hand, despite the lower flush volume, the 4.8 L discharge provides better conveyance performance due to the steeper increase of flow rate. In two cases with 6.0L and 0% pipe slope, V60D075A0 and V60D100A0, the solid stopped before the wye. Reductions in solid velocity were also observed in cases with 1% pipe slope.

As future works, it is recommended to validate the numerical model through experimental results. In addition, considering the relatively high-water levels in cases with lower pipe slope, the modeling of the effect of entrapped air is recommended for further studies.

Acknowledgments

7 References

[1]   L.-Y. Cheng, L. H. Oliveira, and E. H. Favero, "Particle-based Numerical Analysis of Drainage Flow inside Building System.," *International Symposium Cib W062 on Water Supply and Drainage for Buildings*, no. 1, pp. 227–238, 2012.

[2]   L.-Y. Cheng, L. H. Oliveira, E. H. Favero, I. B. Oliveira, and O. M. Gonçalves, "Simulation of drainage system in building using particle-based numerical method.," in *International Symposium Cib W062 on Water Supply and Drainage for Buildings*, 2013, pp. 77–91.

[3]   L. Y. Cheng, L. H. Oliveira, D. A. Ferracini, and O. M. Gonçalves, "A numerical study on waste transport in main drain," in *International Symposium Cib W062 on Water Supply and Drainage for Buildings*, 2014, pp. 1–12.

[4]   L.-Y. Cheng, L. H. Oliveira, P. H. S. Osello, and Rubens Augusto Amaro Jr., "A numerical modeling of solid waste transport in main drain," in *International Symposium Cib W062 on Water Supply and Drainage for Buildings*, 2016, pp. 1–10.

[5]   L.-Y. Cheng, L. H. Oliveira, P. H. S. Osello, and A. Jr. Rubens Augusto, "A numerical investigation on the hydrodynamic impact loads of the solid waste transport inside main drains," *International Symposium Cib W062 on Water Supply and Drainage for Buildings*, no. 1, pp. 463–474, 2017.

[6]   L. S. Pereira, M. C. B. Teixeira, R. A. Amaro, L. Y. Cheng, and L. H. Oliveira, "Particle-based Numerical Investigation on the Hydrodynamics in the Vicinity of a Wye in a Building Drainage System," in *International Symposium Cib W062 on Water Supply and Drainage for Buildings*, 2022, pp. 433–446.

[7]   L. S. Pereira, R. Amaro Junior, and L.-Y. Cheng, "The Influence of Wall Boundary Modeling on the Unphysical Frictional Loss Inside Horizontal Main Drain," 2021, pp. 1262–1275. doi: 10.1007/978-3-030-51295-8_89.

[8]   S. Koshizuka and Y. Oka, "Moving particle semi implicit method for fragmentation of incompressible fluid," *Nuclear Science and Engineering*, vol. 123, no. 3, pp. 421–434, 1996.

[9]   M. M. Tsukamoto, L. Y. Cheng, and F. K. Motezuki, "Fluid interface detection technique based on neighborhood particles centroid deviation (NPCD) for particle methods," *Int J Numer Methods Fluids*, vol. 82, no. 3, pp. 148–168, 2016, doi: 10.1002/fld.4213.

[10]   R. A. Amaro Jr., L.-Y. Cheng, and P. H. S. Osello, "An improvement of rigid bodies contact for particle - based non - smooth walls modeling," *Comput Part Mech*, vol. 6, no. 4, pp. 561–580, 2019, doi: 10.1007/s40571-019-00233-4.

[11]   N. Mitsume, S. Yoshimura, K. Murotani, and T. Yamada, "Explicitly represented polygon wall boundary model for the explicit MPS method," *Comput Part Mech*, vol. 2, no. 1, pp. 73–89, 2015, doi: 10.1007/s40571-015-0037-8.

[12]   R. A. Amaro Junior, A. Gay Neto, and L. Cheng, "Three-dimensional weakly compressible moving particle simulation coupled with geometrically nonlinear shell for hydro-elastic free-surface flows," *Int J Numer Methods Fluids*, vol. 94, no. 8, pp. 1048–1081, Aug. 2022, doi: 10.1002/fld.5083.

[13]   K. Akiyama, M. Otsuka, and H. Shigefuji, "Basic Study on a Method for Predicting the Waste-Carrying Performance in the Horizontal Drain Pipe of a Water-Saving Toilet," in *CIB W062*, 2014, p. 12. Accessed: Nov. 23, 2018. [Online]. Available: https://www.irbnet.de/daten/iconda/CIB_DC27571.pdf

8 Presentation of Authors

Matheus Carlos Bandeira Teixeira is an undergraduate student in the civil engineering at Escola Politécnica of University of São Paulo, where he is performing his undergraduate research focusing on particle-based numerical simulations.

Lucas Soares Pereira is a doctor degree student in the Graduating Program in Civil Engineering, Polytechnique School of the University of São Paulo, where he is performing research on particle-based numerical simulations.

Rubens Augusto Amaro Junior is a postdoctoral fellow at the Institute of Mathematics and Computer Sciences from the University of São Paulo (ICMC-USP), Brazil. His research is related to the development of particle-based methods, including coupled solution strategies (particle-mesh), and their application to environmental fluid mechanics problems.
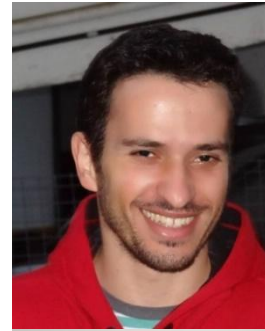
Liang-Yee Cheng is an assistant professor at Department of Construction Engineering of Escola Politécnica of University of São Paulo, where he teaches and conducts research on CFD modeling and simulation of fluid-structure interactions and graphic geometry for engineering and architecture.

Lúcia Helena is an associate professor at the Department of Construction Engineering of Escola Politécnica of University of São Paulo, where she teaches and conducts research work on building services.

Studies on High-pressure Washing of Drainage Pipe in Apartment Building

Part1: Cleaning Performance in Actual Piping and Piping with Pseudo-Dirt

Yoshifusa Nishimura (1), Koji Sakai (2), Kyosuke Sakaue (3), Takehiko Mitsunaga(4)

(1) Yoshifusa_Nishimura@haseko.co.jp

(2) sakaik@meiji.ac.jp

(3) sakaue@carrot.ocn.ne.jp

(4) mitsunaga@meiji.ac.jp

(1) Technical Research Institute, HASEKO Corporation, Japan

(2) Professor, Dep. Of Architecture, School of Science & Technology, Meiji University, Japan

(3) Emeritus professor, Meiji University, Japan

(4) Dep. Of Architecture , School of Science & Technology , Meiji University , Japan

Abstract

Accidents of backflow of drain from the drainage stacks of apartment building are often reported. In Japan, the drainage stacks are often installed in the exclusive area of a dwelling unit, and high-pressure washing methods are often used to clean them by spraying water at high pressure using special fixture to break up and remove adhering dirt. On the other hand, The inner wall surface of drainage stack is not uniform even if it is the same stack due to dirt, which is oil and rust due to corrosion of piping that could not be removed by cleaning. Therefore, it is important to select nozzles, hoses, set water pressure, etc. used for high-pressure washing according to state of drainnage stack.

  In this study, The cleaning performance of high-pressure washing method is experimentally investigated using actual piping, which is used in the actual apartment building, and piping with pseudo-dirt for the purpose of maintaining drainage performance and extending life of drainage stack. As a result, the following is clarified.

A nozzle with connection screw diameter of 1/4" (inner diameter of about 6.3 mm) used for the stack insert method has a higher detergency than a nozzle with connection screw diameter of 1/8" (inner diameter of about 4.0 mm) used for the fixture insert method.

As the number of washings increases, Adhesion dirts are easier to remove and washing performance is excellent, so it is effective to wash while checking removal status with a camera.

Keywords

High-Pressure Washing Methods; Washing Nozzle; Detergency; Apartment building; Drainage Pipe

1 Introduction

In Japan apartment building, drainage stack is often installed in the exclusive area of dwelling unit, and high-pressure washing methods are often used to clean them by spraying water at high pressure using special fixture to break up and remove adhering dirt. On the other hand, The inner wall surface of drainage stack is not uniform even if it is the same stack due to dirt, which is oil and rust due to corrosion of piping that could not be removed by cleaning. Therefore, it is important to select nozzles, hoses, set water pressure, etc. used for high-pressure washing according to state of drainage stack. In this study, The cleaning performance of high-pressure cleaning method is experimentally investigated using actual piping and piping with pseudo-dirt for the purpose of maintaining drainage performance and extending life of drainage stack.

2 Types of high-pressure washing method

There are two high-pressure washing methods in Japan. One is the fixture insert method, which inserts special fixture from exclusive area of dwelling unit and wash up to drainage stack. The other is the stack insert method, which inserts from rooftop stack vent and wash up to drainage stack. (See Figure1)

2.1 Fixture insert method

The fixture insert method is to wash down to dwelling units 1-floor below via fixture drain and horizontal drainage pipes installed in exclusive area of dwelling unit. The drainage stack is washed to use the nozzle with the connection screw diameter of 1/8" (inner diameter of about 4.0mm).

2.2 Stack insert method

The stack insert method is to wash fixture drain and horizontal drainage pipes inside the dwelling unit are washed from inside the dwelling unit, and the drainage stack are washed from the rooftop stack vent or from the top floor dwelling unit to the underfloor building drain on the first floor. The horizontal drainage pipe is washed to use the nozzle with the connection screw diameter of 1/8" (inner diameter of about 4.0 mm), and the drainage stack is washed to use the nozzle with the connection screw diameter of 1/4" (inner diameter of about 6.3 mm) or 3/8" (inner diameter of about 9.5 mm).
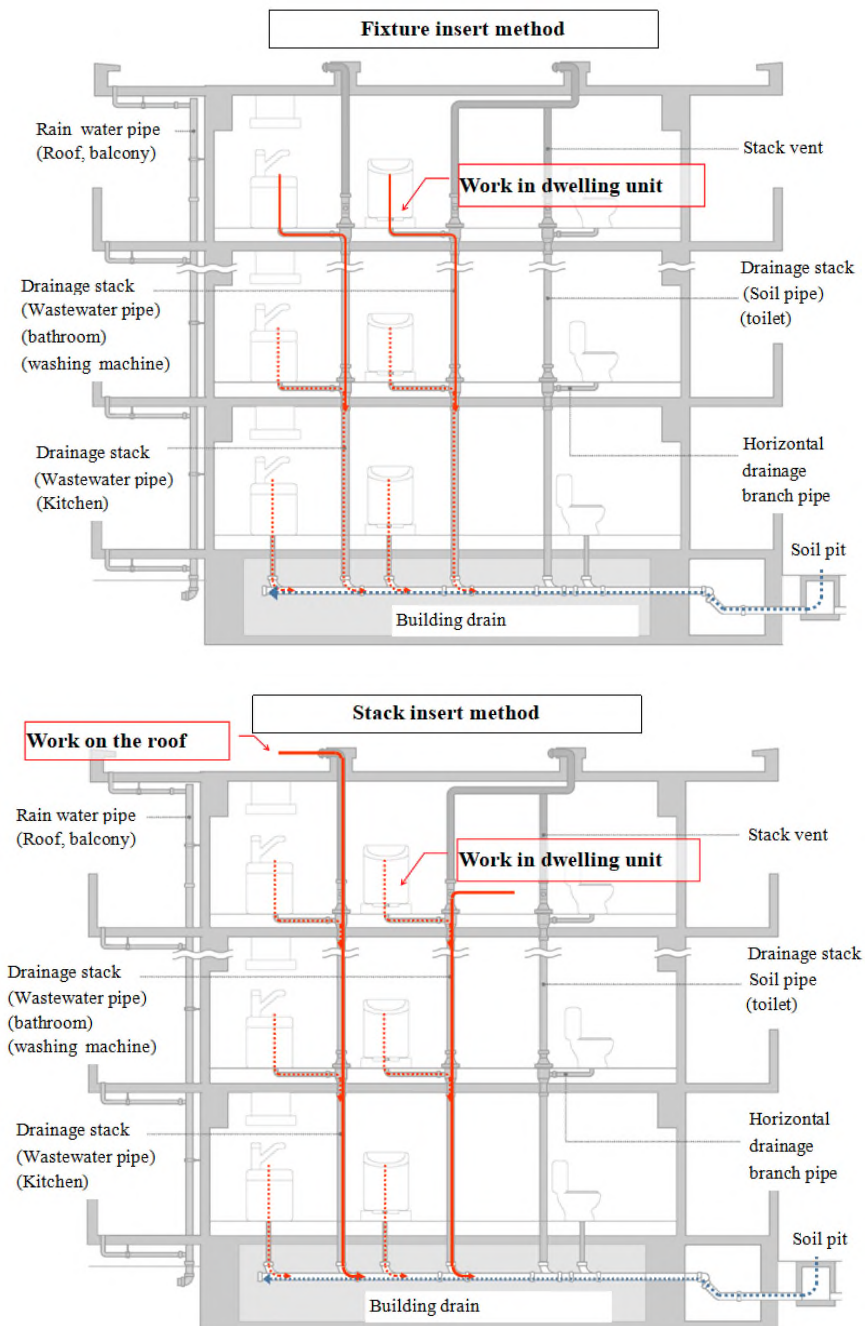
Figure 1 – Types of high-pressure washing method

3 Test piping

3.1 Actual piping

3.1.1 Actual piping outline

100φ test pipings are sampled from each floor drainage stack of 3 systems in a 50-year-old 8-floors apartment building (See Photo 1, Table 1). The piping of system A and system B received drainage from toilet, bath and kitchen, but the piping of system C received drainage from toilet and bath piping on the 1-floor to 6-floors, and toilet, bath and kitchen piping on the 7-floors to 8-floors. The test piping has a length of about 300 mm (285 mm to 370 mm), and the average adhesion volume is 490 cm^3 (150 cm^3 to 1240 cm^3). The adhesion volume is calculated from volume of water injected into test piping, assuming no erosion.

3.1.2 Clogging rate of adhesion

Figure 2 shows the clogging rate of the test piping calculated from the adhesion volume.The clogging rate on 5-floors of system A is the highest at about 44%. Comparing each system, the average for system A is 26.3%, the average for system B is 8.6%, and the average for system C is 15.8%. Even with the same piping, the clogging rate differs depending on the system and the number of floors.

3.1.3 Remaining piping thickness

Figure 3 shows the results of piping thickness measured using an ultrasonic thickness gauge. Five measurement points are equally divided in the longitudinal direction, and four measurement points are set every 90° from the reference axis, for total of 20 points. The measurement is performed before and after washing, and after washing, the inner surface is wiped off after removing dirt. Since the outer diameter of test piping is 111 mm, it is assumed that the thickness of new piping is 6 mm. Even the same test piping, the remaining piping thickness is different, and the piping thickness on the 7-floors of the system B is 5.00mm at maximum and 3.81mm at minimum, and the 6-floors of system B is 5.19mm at maximum and 2.52mm at minimum.

Photo 1 – Sampling of actual piping

Table 1 – Outline of actual piping

|		7-Floors	6-Floors	5-Floors	4-Floors	3-Floors	2-Floors	1-Floor	Average
System A	Pipe length(mm)	285	296	297	300	298	298	294	295
	Adhesion volume(cm^3)	210	620	1240	1080	830	400	850	747
System B	Pipe length(mm)	360	360	365	360	355	360	370	361
	Adhesion volume(cm3)	390	360	150	290	210	290	200	270
System C	Pipe length(mm)	300	302	300	297	300	298	300	300
	Adhesion volume(cm3)	160	420	310	650	440	690	410	440
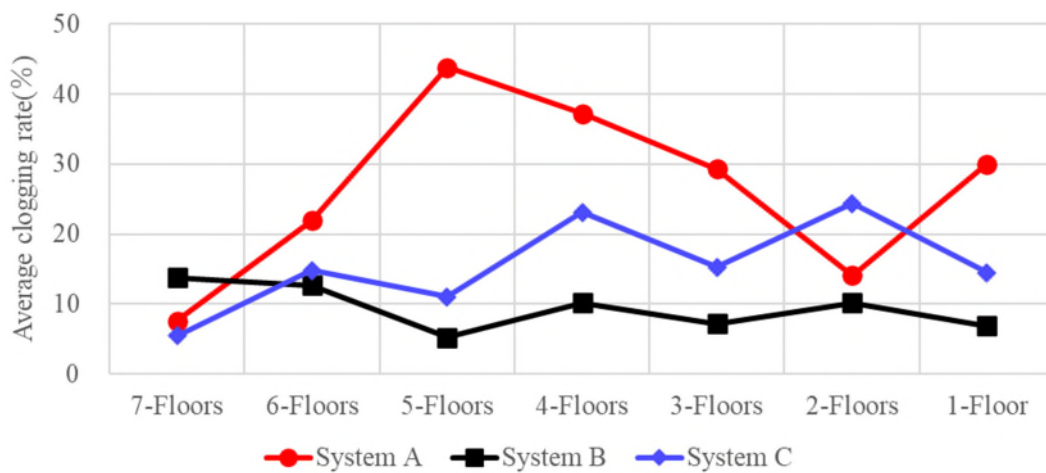
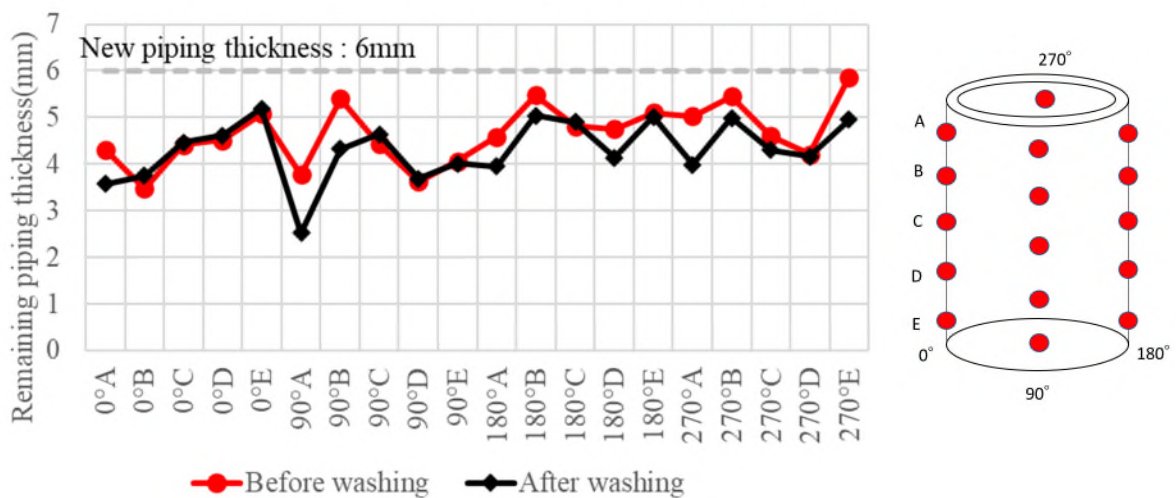**Figure 2 – Clogging rate of actual piping**

Figure 3 – Remaining thickness of actual piping

5/12

3.2 Piping with pseudo-dirt

The piping with pseudo-dirt is made in following three steps. First, water-based paint and silica sand for casting are mixed in a ratio of 1:1. Next, add about 1/3 of the weight of the water-based paint to the water and stir. Finally, split a 1m transparent rigid polyvinyl chloride pipe in half and apply it with a brush (See Photo 2). The pseudo-dirt is adjusted so that it is dry to the touch. It is not solidify to the inside, and is not sticking to the fingure even if the surface lightly touched. In order to dry to the touch, the piping with pseudo-dirt is cured in a high-temperature and high-humidity room (28°C, 50%) for about 2 hours after the application. The application is done by brushing once, and the application volume is about 90g in wet state and about 45g in dry state.

Piping with pseudo-dirt
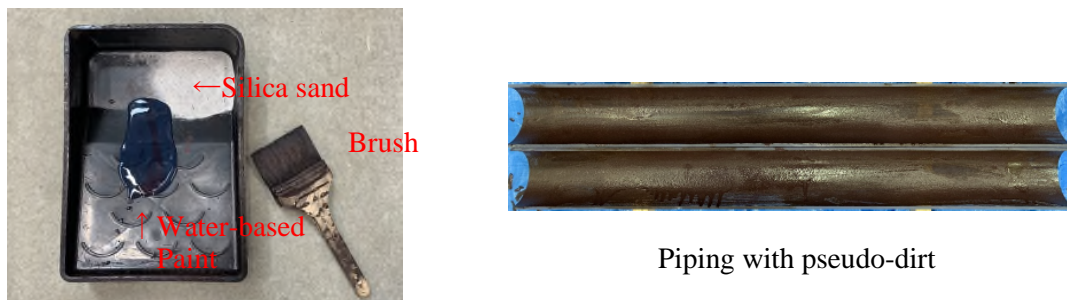
Photo 2 – Piping with pseudo-dirt

4 Experiment outline

Figure 4 shows the test piping, Table 2 shows the nozzle used, and Table 3 shows the experimental case. For the test piping, after assembling the drainage stack and the horizontal drainage pipe with rigid polyvinyl chloride pipes of 100φ, each part of the drainage stack and horizontal drainage pipe is cut so that the test piping could be attached. There are two types of connection screw diameters for the nozzle: 1/8" used for the fixture insert method and 1/4" used for the stack insert method, and two types of nozzle shapes: the rotating nozzle and the fixed nozzle (See Tables 2 and 3). The hose is made of polyurethane resin and had the hose length of 100 m.

Figure 4 – Experiment piping

Table 2 – Types of the nozzle

Nozzle	NozzleA	NozzleB	NozzleC	NozzleD
Fixing/Rotating	Fixed nozzle	Rotating nozzle	Fixing nozzle	Rotating nozzle
Connection screw diameter	1/4"	1/4"	1/8"	1/8"
Injection direction	Backward 6 hole 30 degrees 180 degrees guide	Side・Backward 4 hole 30 degrees, 80 degrees	Backward 5 hole 45 degrees 360 degrees guide	Backward 4 hole 30 degrees, 80 degrees
Form				

Table 3 – Experiment case

Experiment case	Case1	Case2	Case3	Case4	Case5
Nozzle	NozzleA	NozzleB	NozzleC	NozzleD	NozzleD
Connection screw diameter	1/4"	1/4"	1/8"	1/8"	1/8"
Water temperature	Normal temperature	Normal temperature	Normal temperature	Normal temperature	hot water about 40℃

4.1 Actual piping experiment method

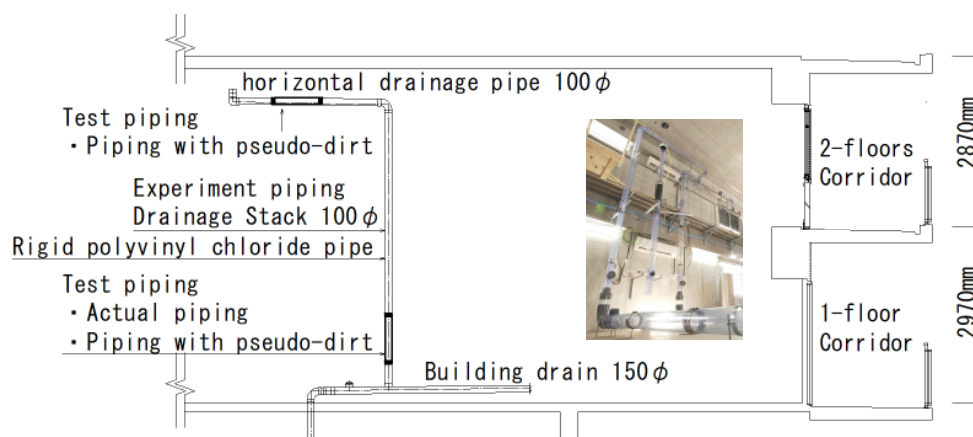Five cases of Case 1 to Case 5 in Table 3 are performed in the experiment. The actual piping experiment method is performed by washing in one direction from the upper floor to the lower floor 5 times, followed by washing in reciprocating motion from top to bottom for 3 minutes. If there is no change in the removal volume during the 5 times, it is performed by washing in reciprocating motion from top to bottom for 3 minutes without performing the remaining times. Since there are variations in the clogging rate of test piping, three test piping are tested for each case, and the average value is evaluated. The washing speed is adjusted to about 5m/min. The washing water pressure is adjusted to 12 MPa at the hand pressure of the washing hose by adjusting the water supply pressure of high-pressure washing vehicle. In principle, the washing water is normal temperature, excpect that only Case 5 is tested with hot water (about 40°C). The adhesion volume is calculated from the difference in the water volume injected after removing the test piping from the experiment piping for each washing.

4.2 Piping with pseudo-dirt experiment method

Four cases of Case 1 to Case 4 in Table 3 are performed in the experiment. The washing of test piping with pseudo-dirt is experimented in two places: the drainage stack and the horizontal drainage pipe assuming the ceiling pipe in a common area such as an entrance. The piping with pseudo-dirt experiment method is performed by washing the test piping of drainage stack and horizontal drainage pipe consistenly and in one direction from the upper floor to the lower floor 1 time. One test piping is tested for each case, and the value is evaluated. The washing speed is about 5m/min, and the washing water pressure is 12MPa, which is the same as the actual piping. The test piping is prepared in a high-temperature and high-humidity room, and is attached to the

test piping without leaving any time while it is dry to the touch. The adhesion volume is calculated by measuring the weight of the test piping before the experiment when it is dry to the touch containing water, and the weight of the test piping after the experiment when it is in a dry state (measured after drying so as not to include washing water). Therefore, a dry to the touch pipe made under the same conditions as the test piping is dried separately, and assumed from the weight difference.

5 Experiment result

5.1 Actual piping result

Table 4 shows the a dhesion change by washing, and Figure 5 shows the removal rate of adhesion. Looking at Case 1 and Case 2 (connection screw diameter 1/4"), adhesion is removed as the number of washings increases, and the removal rate decreases after 4 time washing. After that, washing for 3 minutes continuously increased the removal rate again, reaching a removal rate of 40% to 60%. There is no significant difference in the removal rate between the fixed nozzle and the rotating nozzle. For this reason, it is suggested that it is effective to reciprocate the nozzle several times in the pipe in order to effectively remove adhesion in actual cleaning. Looking at Case 3 and Case 4 (connection screw diameter 1/8"), even if the number of washings is increased, the removal rate hardly increases. Considering that the removal rate is 5% to 10% even after continuous washing for 3 minutes, it is speculated that the removal rate may be low with the connection screw diameter 1/8" used for the fixture insert method. Looking at Case 4 and Case 5 (normal temperature water and hot water), there is no significant difference in the removal rate. It is thought to be due to the low oil content in the test piping. However, since the comparison is made with the connection screw diameter of 1/8", it is necessary to verify with the connection screw diameter of 1/4" in the future. In all Cases, when the inner surface of the piping is wiped with a waste cloth after washing, it is adhered the dirt. For this reason, it is thought that some dirt adheres to the surface of the pipe even after washing.

Table 4 – Adhesion change by washing（Actual piping）

	Experiment case	Case1	Case2	Case3	Case4	Case5
	Nozzle	NozzleA	NozzleB	NozzleC	NozzleD	NozzleD
	Connection screw diameter	1/4"	1/4"	1/8"	1/8"	1/8"
	Water temperature	Normal temperature	Normal temperature	Normal temperature	Normal temperature	hot water about 40℃
Adhesion volume	Before washing(cm^3)	1169	839	476	616	777
	After 1 time washing(cm^3)	966	702	492	572	787
	After 2 times washing(cm^3)	812	619	469	589	777
	After 3 times washing(cm^3)	729	596	476	582	767
	After 4 times washing(cm^3)	679	662	452		772
	After 5 times washing(cm^3)	656	662	442		
	3 minutes consecutive washing(cm^3)	449	562	446	559	737
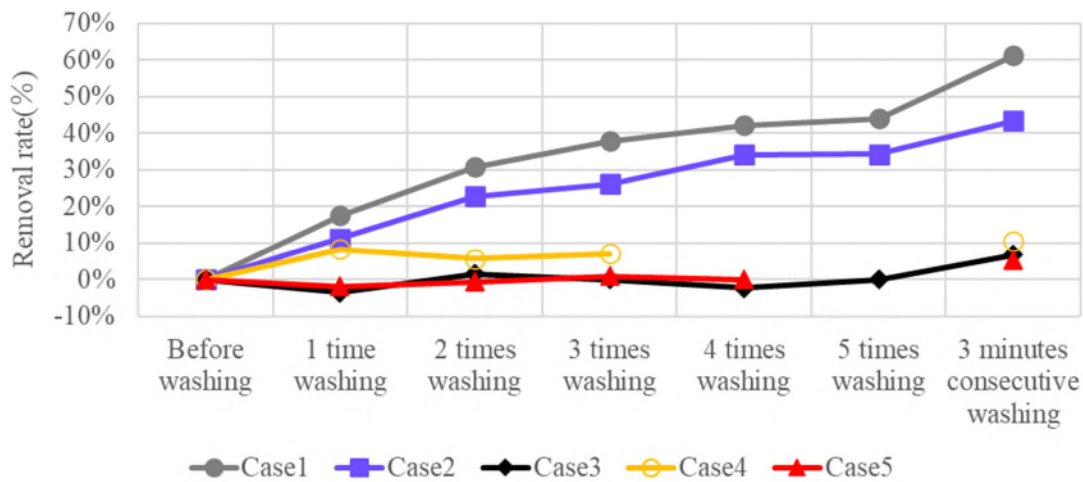
Figure 5 – Removal rate of adhesion（Actual piping）

5.2 Piping with pseudo-dirt result

Table 5 shows the dhesion change by washing, Photo3 shows the removal situation after washing and Figure 6 shows the removal rate of adhesion. Looking at the adhesion volume, in Case 1 and Case 2 with the connection screw diameter of 1/4", the washing effect of 15% to 30% on the drainage stack and 3% to 24% on the horizontal drainage pipe is confirmed in Case 1, similar to the actual piping. Comparing the drainage stack and the horizontal drainage pipe, the removal rate of the stack is higher. It is thought to be due to the fact that the washing of horizontal drainage pipes tends to concentrate on the lower part of the pipe because the nozzle is inserted along the lower part of the piping. In actual horizontal drainage pipes, drain often flows at half-full flow, and it is assumed that the degree of dirtiness is uneven, so it is necessary to verify with the method of creating a piping with pseudo-dirt in the future. Looking at the connection screw diameter of 1/8" in Case3 and Case4, we could not confirm the washing effect as in Case1 and Case2. Since this is the same tendency as the actual piping, it is suggested that it is possible to evaluate even the piping with pseudo-dirt. On the other hand, when comparing Case 1 and Case 2, the washing effect of Case 1 is higher for the actual piping, but the washing effect of Case 2 is higher for the piping with pseudo-dirt. It is thought to be due to surface unevenness and the unevenness of the aggregates because the pseudo-dirt is applied with a brush. Therefore, it is necessary to verify with the application method and drying condition of the pseudo-dirt in the future. From the above, it is suggested that it is effective to wash piping using the connecting screw diameter of 1/4".

Table 5 – Adhesion change by washing（Piping with pseudo-dirt）

		Case	Case1	Case2	Case3	Case4
		Nozzle	NozzleA	NozzleB	NozzleC	NozzleD
		Connection screw diameter	1/4"	1/4"	1/8"	1/8"
		Water temperature	Normal temperature	Normal temperature	Normal temperature	Normal temperature
adhesion volume (Dry state)	Before washing(g)	Drainage Stack	44.4	46.0	47.2	45.7
		Horizontal drainage pipe	45.5	45.1	46.3	45.7
	After washing(g)	Drainage Stack	37.9	32.1	46.6	44.5
		Horizontal drainage pipe	43.9	34.1	46.9	48.7

Drainage stack	Drainage stack
Horizontal drainage pipe	Horizontal drainage pipe
Case1	Case2
Drainage stack	Drainage stack
Horizontal drainage pipe	Horizontal drainage pipe
Case3	Case4
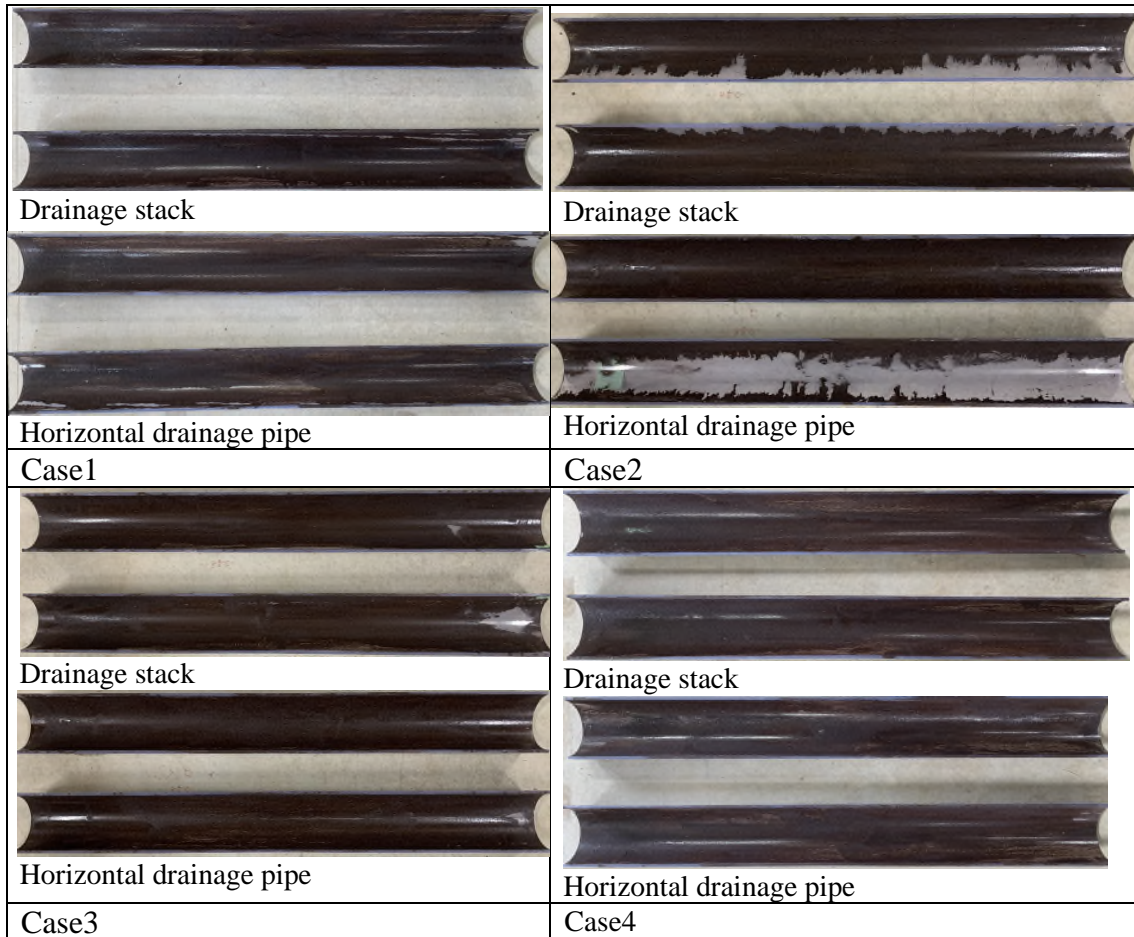
Photo 3 –Removal situation after washing（Piping with pseudo-dirt）
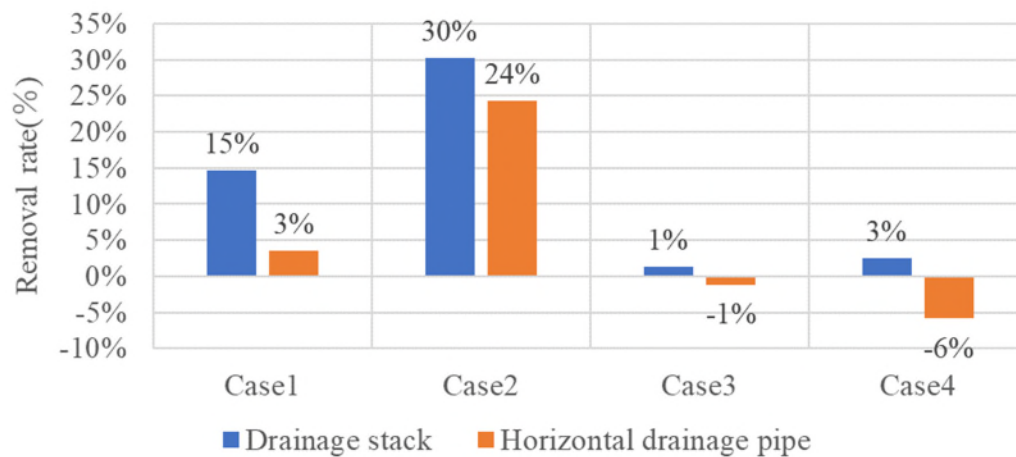
Figure 6 – Removal rate of adhesion（Piping with pseudo-dirt）

6 Conclusion

In this study, Cleaning performance of high-pressure cleaning method is experimentally investigated using actual piping and piping with pseudo-dirt for the purpose of maintaining drainage performance and extending life of drainage stack. As a result, the following is clarified.

A nozzle with connection screw diameter of 1/4" used for stack insert method has a higher detergency than a nozzle with connection screw diameter of 1/8" used for fixture insert method.

As the number of washings increases, Adhesion dirts are easier to remove and Washing performance is excellent, so it is effective to wash while checking removal status with a camera.

7 References

[1] Y. Nishimura et al: Studies on Drainage Pipe Cleaning by High-Pressure for Apartment Houses Part2 Cleaning Performance in Actual Piping, Technical Papers of annual meeting AIJ, pp1757-1758, Sep, 2022

[2] M. Murakami: An abstract of revision for JIS G5525 Cast-iron drainage pipes and fittings, Technical paper of annual meeting SHASE, pp537-540, Sep, 1999

[3] T.Aoki et al: Establishment of evaluation method of drainage pipe cleaning by hige-pressure washing system (Part 1) Evaluation result by a pressure-sensitive sheet, Technical paper of annual meeting SHASE, pp21-24, Sep, 2016

[4] H.Yamaga et al: Establishment of evaluation method of drainage pipe cleaning by hige-pressure washing system (Part 2) Evaluation result by pseudo-dirt, Technical paper of annual meeting SHASE, pp25-28, Sep, 2016

[5] The Society of Heating, Air-Conditionning and Sanitary Engineers of Japan:SHASE-G 2007, Drainage Pipe cleaning method guidelines, 2015

8 Presentation of Authors

Yoshifusa Nishimura belongs to Haseko Corporation. His fields of specialization include building construction , building services engineering.

Koji Sakai (Dr.Eng) is a professor at Department of Architecture, School of Sciience & Technology, Meiji University. His fields of specialization include heat, air environment and air conditioning equipment.

Kyosuke Sakaue (Dr.Eng.) is a professor emeritus at Meiji University. His fields of specialization include water environment, building services engineering and plumbing system.

Takehiko Mitsunaga (Ph.D) is a senior associate professor at Department of Architecture, School of Sciience & Technology, Meiji University. His fields of specialization include water environment, building services engineering and plumbing system

Study on simulation of building drainage systems by CFD
Part 1 Verification based on existing experimental results

Shizuo Iwamoto (1), Ryo Fujimoto (2), Kyosuke Sakaue (3), Takehiko Mitsunaga (4)

(1) iwamotos@jindai.jp
(2) ryo-fujimoto@kanagawa-u.ac.jp
(3) sakaue@carrot.ocn.ne.jp
(4) mitsunaga@meiji.ac.jp
(1) Professor, Dept. of Architecture and Building Engineering, Faculty of Architecture and Building Engineering, Kanagawa University, Japan
(2) Research Associate, Dept. of Architecture and Building Engineering, Faculty of Architecture and Building Engineering, Kanagawa University, Japan
(3) Emeritus Professor, Meiji University, Japan
(4) Senior Assistant Professor, Dep. of Architecture, School of Science & Technology, Meiji University, Japan

Abstract

The flow of water and air in sanitary fixtures and drainage pipes has been analyzed mostly by full-scale experiments because model rules are difficult to apply. Further knowledge is required for optimizing the design of drainage systems, and, in addition to analyses by experiments, analyses by computational fluid dynamics (CFD) simulations are expected to play an important role. Thus far, such CFD simulations have been carried out using the particle-based method and the volume of fluid (VOF) method; however, further studies are necessary to attain the optimal design. In this study, we examine the feasibility of analysis by the VOF method. Although the use of free software is desirable, the analysis in the present study is conducted using the commercial software scFLOW. The calculation method is outlined, the calculation of simple drainage systems is performed, and the mesh arrangement, calculation results, and calculation time are reported.

Keywords

Building drainage system (BDS); computational fluid dynamics (CFD); volume of fluid (VOF) method

1 Introduction

Computational fluid dynamics (CFD) is currently an important and widely used tool for evaluating the indoor and outdoor environments of buildings and for planning and designing building services. However, it is not widely used in the field of plumbing and sanitation.

The flow of water and air in sanitary fixtures and drainage pipes has usually been analyzed by full-scale experiments because model rules are difficult to apply. Further knowledge is required to optimize the design of drainage systems, and, in addition to analyses by experiments, analyses by CFD simulation are expected to play an important role. CFD simulations using the particle-based method and the volume of fluid (VOF) method have been conducted thus far; however, further studies are necessary to attain the optimal design.

Cheng et al. [1] have described the application of particle methods to building drainage systems (BDSs) and have discussed their future potential. The VOF method proposed by Hirt and Nichols [2] was the first method used to study two-phase flow, and it enables the analysis of both gas and liquid. In a BDS, the flow of air in the pipe accompanying drainage is important; the VOF method appears to be an effective approach to investigating it.

In a previous study, Sakai et al. [3] conducted an oscillation analysis of trap water. They carried out calculations using commercial software, thereby providing a useful example of an attempt to apply the VOF method. Their calculation results agreed well with experimental results. In general, calculations for BDSs are transient and the calculation time might be long; however, with improvements in computer speed and the enhancement of parallel calculations by commercial software, transient calculations can be conducted within a short time.

The present study is basic research on the application of the VOF method to BDSs. This paper includes an outline of the calculation method and a calculation example based on previously reported experimental and calculation results.

2 Outline of the calculation method

The basic equations for incompressible fluids of the VOF method of Hirt and Nichols [2] are as follows. The symbols follow the standard convention.

$$\frac{\partial \rho u_i}{\partial t} + \frac{\partial \rho u_i u_j}{\partial x_j} = -\frac{\partial P}{\partial x_i} + \frac{\partial}{\partial x_j}\left\{\rho \nu \left(\frac{\partial u_j}{\partial x_i} + \frac{\partial u_i}{\partial x_j}\right)\right\} - \delta_{ij}\rho g \tag{1}$$

$$\frac{\partial \rho u_j}{\partial x_j} = 0 \tag{2}$$

$$\rho = \rho_{\mathrm{w}}F + \rho_{\mathrm{a}}(1 - F) \tag{3}$$

$$\frac{\partial F}{\partial t} + u_j \frac{\partial F}{\partial x_j} = 0 \tag{4}$$

where δ_{ij} is the Kronecker delta, ρ_w is the density of water, ρ_a is the density of air, and F is the volume of fluid ($F = 0$ corresponds to air, $F = 1$ corresponds to water, and $0 < F < 1$ corresponds to the air–water interface).

When the turbulence model is used, the advection–diffusion equation is constructed similarly for the turbulent flow. Values of variables such as the air velocity, static pressure, and the VOF can be obtained by solving these equations numerically one by one.

Another proposed method is the fine interface reconstruction method (FIRM) first suggested by Youngs [4]; it is similar to the VOF method but does not solve the VOF advection equation (equation (4)). It determines the VOF from the inflow and outflow rates of the two-phase flow in the mesh, which is suitable for handling droplets and bubbles.

In this paper, we show trial calculation results obtained by the FIRM based on the VOF method.

3 Oscillation of P-trap

A supplementary test of the calculation by Sakai et al. [3] was performed to confirm the effectiveness of the VOF method and the FIRM. The calculation target was the P-trap shown in Figure 1, which was also the calculation target of Sakai et al. [3]. The oscillation of the sealing water was calculated using the water level in Figure 1(a) as the initial condition.

(a) Initial condition (mm)   (b) Mesh layout 1   (c) Mesh layout 2
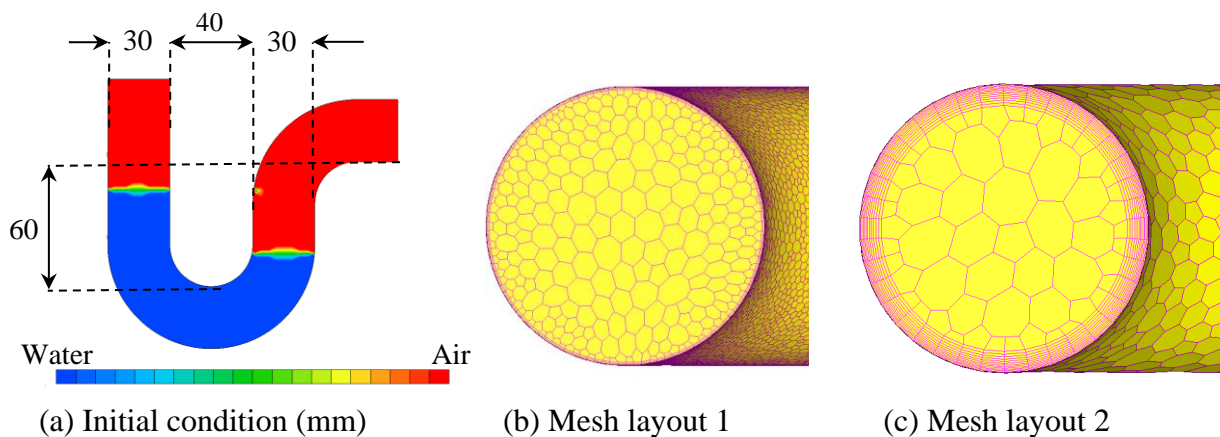
Figure 1 - Analysis of the same P-trap model used by Sakai et al. [3].

The software used was scFLOW (Software Cradle) [5], which uses polyhedral meshes. The two mesh types shown in Figure 1(b) and (c) were used. Sakai et al. [3] used a mesh of 0.25 mm attached to the pipe wall surface; however, the scFLOW mesher prepares multiple meshes with a thickness that is 1.1 times (geometric progression) the thickness of the first mesh attached to the pipe wall surface. Figure 1(b) shows the default two layers, and Figure 1(c) shows the 12 layers equivalent to Sakai et al. [3].

The inlet leg and outlet leg exits of the trap are free boundaries; the total pressure is equal to 0 Pa in the case of inflow, and the static pressure is equal to 0 Pa in the case of

outflow. Because directly checking the water level from the calculation results is difficult, the average water level in the trap was obtained based on the amount of air flow from the free boundary.

The calculation method was the FIRM for two-phase flow with air and water (fixed at 20°C). As in the study of Sakai et al. [3], the contact angle was set to 90° in consideration of the surface tension set at 0.0727 N/m (the scFLOW default value). The calculation time interval was 0.1 ms (10,000Hz), and the transient calculation was performed for 4 s. The Reynolds number obtained from the analytical maximum velocity was ~5000; the flow was therefore assumed to be in the zone between laminar flow and turbulent flow. A low-Reynolds-number turbulence model should be adopted. In this work, the SST k-omega turbulence model recommended in scFLOW was used. Laminar flow calculations were also performed in the same manner as those performed by Sakai et al. [3]. scFLOW uses a combination of first order and second order upwind schemes in laminar flow calculations.

Figure 2 shows the calculation results by the VOF method. The natural frequency was ~1.94 Hz, which is approximately the same as in the study of Sakai et al. [3]. Attenuation of the amplitude was slightly smaller in mesh layout 1 and was the same as that of Sakai et al. [3] in mesh layout 2. The difference between laminar and turbulent model calculation results was not significant for any mesh layout. Although not shown in the figure, no significant difference was observed in the calculation results between the VOF method and the FIRM.

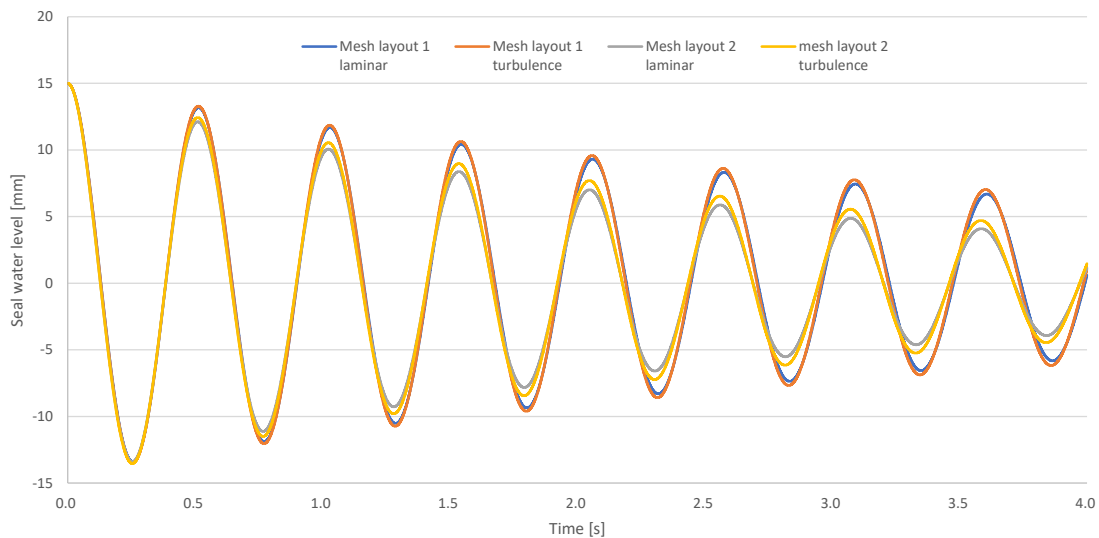Figure 2 - Fluctuation of the P-trap water seal level

A high-performance computer (HPC) with an Intel(R) Core i9-9900K CPU operating at 3.60 GHz (8 cores) and 64.0 GB of RAM was used for the calculations, and the calculation time was 6 h 58 min for laminar flow with mesh layout 1 (~160,000 mesh) and 9 h 22 min in turbulence, 1 h 28 min in laminar flow, and 1 h 50 min in turbulence with mesh layout 2 (~35,000 mesh).

The aforementioned results verify the calculation using scFLOW. However, the boundary layer should be fine meshes at the wall boundary and the default setting of the scFLOW mesh layout is insufficient.

4 Storage water washing in a simple basin, drainage pipe, and S-trap

We next performed calculations for a basin and a drainage pipe with an S-trap. Figure 3 shows the initial state, including 4 L of washing water, and the calculation geometry. The basin shown in Figure 3 is a 340 mm-diameter virtual washbasin made of a rotating 2D polyline. The trap is a 25A trap with a diameter of 28.6 mm. Therefore, the water was set at the initial VOF value, the top surface of the basin was set as a free inflow surface for air only, the total pressure was set to 0 Pa, and the outlet surface on the outlet leg side of the trap was set as an outflow surface.

A virtual washbasin with a diameter of 340 mm and made of a rotating 2D polyline

4 L storage water

50 65

28.6 mm-diameter straight pipes and S-trap

Water   Air
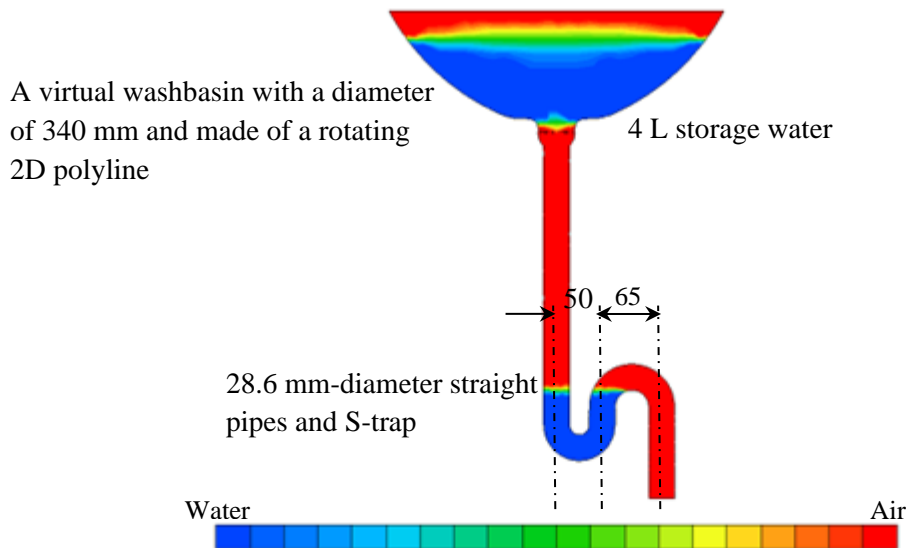
Figure 3 - Analysis model of a basin and S-trap, along with the initial conditions

The SST k-omega turbulence model, which is a low-Reynolds-number turbulence model, was used for transient calculation. The time difference interval adopted for use in scFLOW could freely set the time interval such that the Courant number was less than 0.9. The contact angle was not set considering that the surface tension was set at 0.0727 N/m.

For the mesh layout, the thickness of the first mesh attached to the pipe wall surface was 1.2 mm and seven boundary layers were prepared; the total number of meshes was 57,809. The calculation was performed for 10 s, and the calculation time was approximately 2 h 9 min.

Figure 4 shows the cross-sectional distribution of the VOF 0.2, 0.4, 0.6, 2.0, 4.0, and 5.0 s after the flow started. After 5 s, the flow stopped; the sealed water was less than its initial value, but the seal was not broken.

(a) After 0.2 s   (b) After 0.4 s   (c) After 0.6 s

(d) After 2.0 s   (e) After 4.0 s   (f) After 5.0 s
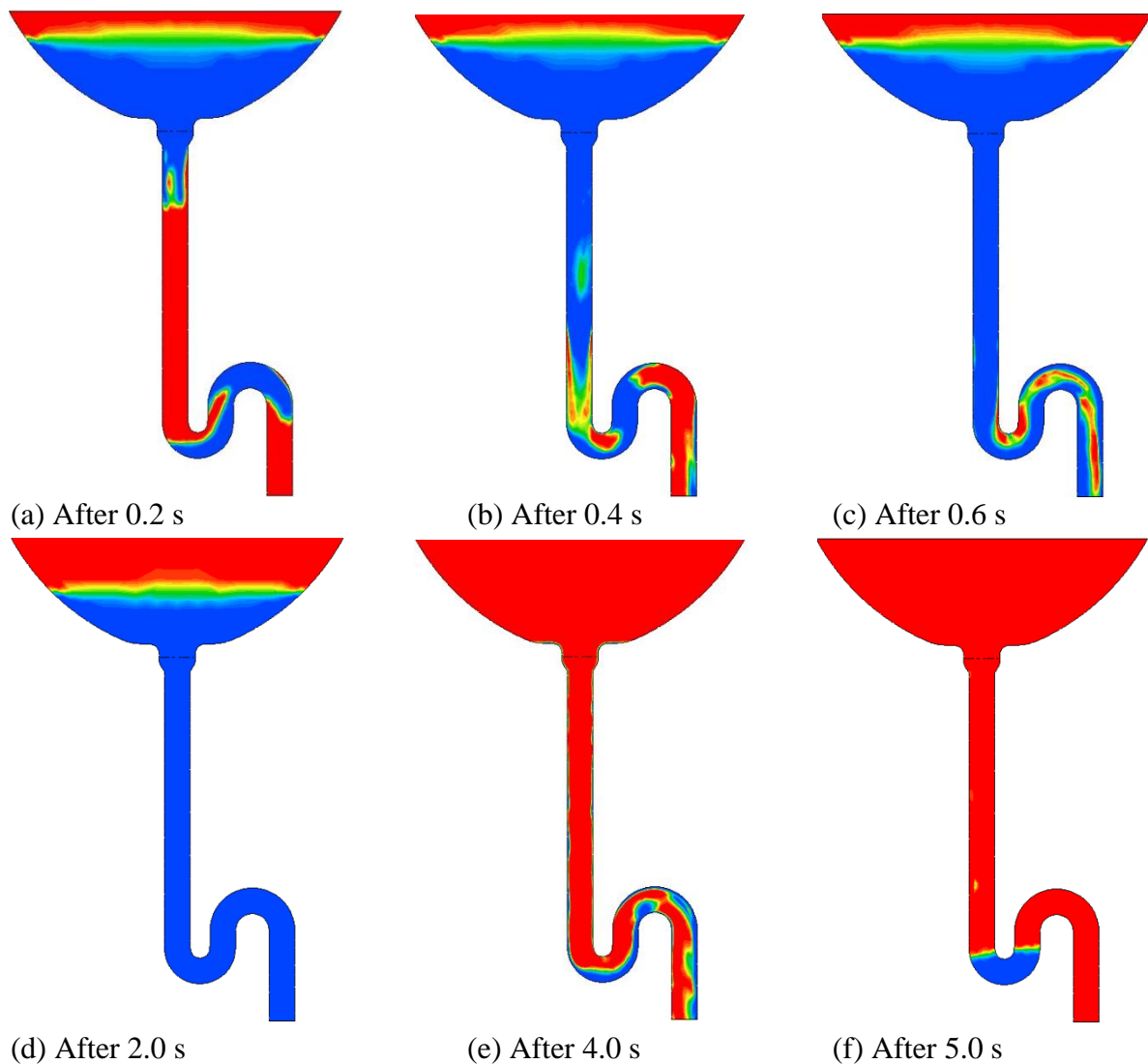
Figure 4 - Calculation results of the VOF distribution

Figure 5 shows the temporal changes in the flow rate of air and water discharged from the outlet leg surface of the trap. Such calculation results can be easily obtained, which is one of the advantages of CFD. The total amount of water before and after the calculation was 4.0956 and 0.0724 L, respectively; the total amount of discharged water was 4.0106 L. The difference was 0.0126 L, which is estimated to have flowed out from the top of the basin.

When we used the VOF method of Hirt and Nichols [2] without the FIRM under the same conditions, almost no sealing water remained, and the entire area became air (results not shown). Although this calculation result has not been verified, future verification by experimental results is planned. We would like to focus on the fluctuation of the pressure inside the pipe.
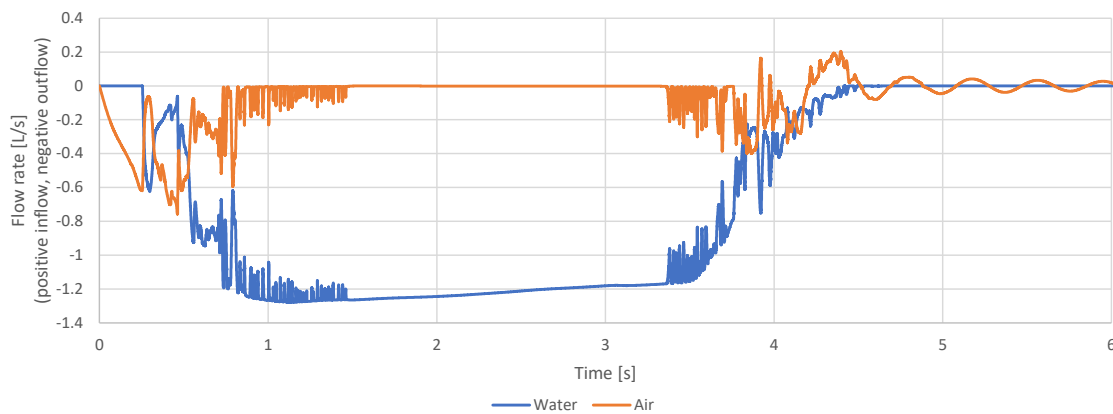
Figure 5 - Calculation results of the flow rate of water and air

5 Conclusion

The results of this study are summarized as follows:
(1) The FIRM based on the VOF method was used, and a follow-up test of the previous research was performed; the results showed that an equivalent solution could be obtained.
(2) The feasibility of the FIRM was demonstrated by calculating storage water washing around a simple basin and a simple drainage pipe with an S-trap.

Verification based on experimental results is left as a future task.

Acknowledgments

6 References

1) Cheng LY, Amaro Jr RA, Pereira LS, Gomes DSM, Motezuki FK – Particle-based simulation of building drainage systems, Proceedings of CIB-W062 Symposium, Oct. 2022.
2) Hirt CW, Nichols BD – Volume of fluid (VOF) method for the dynamics of free boundaries, Journal of Computational Physics 99, 201–225, 1981.
3) Sakai K, Mitsunaga T, Sakaue K, Tomonari H – CFD simulation of seal water oscillation in drain trap, Proceedings of CIB-W062 Symposium, Sep. 2008.
4) Youngs D – Time-dependent multi-material flow with large fluid distortion, Numerical Methods in Fluid Dynamics, Academic Press, Editors: Morton KW and Baines MJ, 1982.
5) Cradle CFD | Smart Multiphysics Focused CFD simulation | Hexagon https://www.cradle-cfd.com/, viewed June 30, 2023

7 Presentation of Authors

Shizuo Iwamoto (Dr. Eng.) is the presenter of this study and a professor at Department of Architecture and Building Engineering, faculty of Architecture and Building Engineering, Kanagawa University. He is interested in built environment and building services such as air conditioning and hot water supply system.
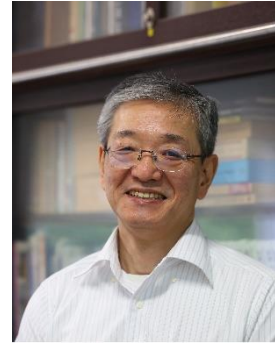
Ryo Fujimoto (M. Eng.) is a research associate at Department of Architecture and Building Engineering, Faculty of Architecture and Building Engineering, Kanagawa University. He is interested in built environment and building services such as air conditioning.

Kyosuke Sakaue (Dr. Eng.) is a professor emeritus at Meiji University. His fields of specialization include water environment, building services engineering and plumbing system.

Takehiko Mitsunaga (Ph.D.) is a senior associate professor at Department of Architecture, School of Science & Technology, Meiji University. His fields of specialization include water environment, building services engineering and plumbing system.

Study on suitability of hybrid feed-forward-PSO ANN Model for predicting pressure profile data in the building drainage system.

I. Mahapatra (1), M. Gormley (2)

1.) im95@hw.ac.uk

2.) m.gormley@hw.ac.uk

1.) and 2.) School of Energy, Geoscience, Infrastructure and Society, Heriot Watt University, Scotland, UK

Abstract

Pressure profile data for Building drainage systems (BDS) represent a temporal snapshot of the pressure regime within the system and therefore an indicator of system security against water trap seal failure. A model was developed based on pressure and flow data from a 32-storeyed building in Northampton, UK (NLT). Pressure sensors and air-flowmeter gave real-time data throughout the experimentation for both open and closed ventilation systems. The data thus obtained was used to examine the suitability of a hybrid Feed Forward (FF)-Particle Swarm Optimization (PSO)-Artificial Neural Network Model. The developed Feed Forward multilayer neural network scheme was used to predict the pressure profile for given flow conditions with its assumed weight vector and bias. This has been compared with the experimentally obtained target data. A PSO algorithm has been employed to reduce the intrinsic error in the Feed Forward model by refining the weights and biases. The convergence of PSO was controlled through the adapted values of the inertia weights, population size, damping factor, and acceleration coefficients. The performance of FF-PSO found to be dependent on the population size and iteration. The model is found to be reliable for its application in predicting pressure profile data inside a building drainage system.

Keywords: ANN modelling, Pressure Profile, Feed Forward, Particle Swarm Optimization.

1 Introduction

Fluid flow inside the vertical stack is unsteady in nature. Any fluid-carrying system will inevitably experience variations in flow conditions, which will result in local pressure spikes in the form of transient pressures or surges. Since all flows are the consequence of erratic discharges of unsteady flows from sanitary devices like toilets, sinks, baths and showers, pressure rise in building drainage systems (BDS) occurs more frequently. Another important aspect of BDS is that although it is intended to remove wastewater from a building, the system's vulnerability depends on its capacity to handle the significant airflows that are caused by the shear force created by the interaction of the water falling in the main stack with an entrained central air core as per Gormley and Kelly (2019). Destructive pressure transient propagation that results in system failure or, at the very least, calls for surge prevention in system design is typically linked to forces in massive, intricate fluid systems. The unsteady nature of the fluid flow can lead to the failure inside the building drainage system. The fluid flow is two-phase inside the vertical stack, where the air is propelled by the water's discharge flow rate and these flow waves are subject to shear forces as they travel through the vertical stack, according to Swaffield (2010). Air pressure transients in building drainage and vent systems (DVS) can have detrimental effects since they jeopardize the integrity of the appliance trap seal. a building's livable space's against potentially dangerous sewage and drainage network odours. Rapid variations in flow conditions in fluid systems are the root cause of pressure transients. The definition of the air pressure transient generation and propagation process as well as its nature and impact on the Building drainage system air pressure regime have been extensively studied in the past as Gromley(2007). The Early in 2003, there was an outbreak of SARS a virus whose spread was aided by the drainage and ventilation system of the Amoy Gardens complex in Kowloon, Hong Kong. 42 fatalities and 329 documented cases in Amoy Gardens led to an immediate review of the procedures used to ensure acceptable design as Jack et al(2006).The SARS virus resulted due to the pressure transients occurred inside the building drainage system. Therefore, the application of hybrid FF-PSO-ANN model will be prioritize on detecting the air pressure profile inside the vertical stack.

2 Two-Phase Flow

There are very few research works available on two-phase flow with certain boundary condition in a vertical stack using ANN model. Determination of the pressure distribution for air movement in the vertical stack from experimental investigation though very costly but reliable. As described previously the computational method, for designing an optimum strategy for the prediction of the pressure in the two-phase flow in bottom-hole vertical pipe, an ANN model was opted by Jahanandish et al(2011). Beigzadeh and Rahimi (2012) reported that prediction of the friction factor and Nusselt number in a helical tube by using an ANN model is better in comparison to the other existing model. Alizadehdakhel et al (2009) reported the pressure drop in pipe experimentally, numerically using commercial CFD code and using ANN

model. Three parameters such as gas and liquid velocity and tube slope were taken as an input parameter whereas the pressure drop is taken as an output parameter. While comparing the results, the numerical calculation using CFD code results accurately than the ANN model. But when ANN model trained with large number of data the level of accuracy is more and model is easy to handle. Osman and Aggour(2002) formulated an ANN model for predicting pressure drop in the horizontal pipe for the multiphase flow. Not only Osman and Aggour(2002) designed ANN model for multiphase flow but also Sablani and Shayya(2003) designed an ANN model calculation of the friction factor on the closed pipe with taking the input parameter as the Reynolds number and flow behavioural index in the tube.

3 FF-PSO-ANN Algorithm

In this section, the application of an ANN model (i.e. FF-PSO ANN model) based on the hybrid concept of the Feed Forward ANN model and PSO ANN model has been outlined in a detailed manner. Its suitability for establishing a pressure profile in the vertical stack of a BDS has been explained. This hybrid FF-PSO ANN model has two components i.e. 1. unsupervised learning using Feed Forward ANN 2. training of data using the concept of supervised learning by PSO. The input variables are processed using the FF-ANN model and outputs are predicted. By comparison with target data, the error is computed, which gets back propagated for the training of data through refinement of weight vector and bias values. The backpropagation algorithm is carried by PSO evolutionary algorithm.

3.1 ANN Algorithm

Artificial Neural Network are analytical tools which behaves in the similar way as human brain. An ANN model is more preferred over other model as the model is adaptive in characteristics and can also determine the complex pattern with limited information available as suggested by Osman and Aggour(2002). These models are not only adaptive but also develop some bonding between the object and the data. According to Bar et al (2010), An ANN model consists of multi-layered network of neuron and each neuron is connected to the other neurons. Each neuron in the ANN has input layer, one or more hidden layer and output layer. The input is passed among the neurons and each neuron is transferred by adjusting weights. After the weights adjustment they are sent to the hidden layer. The hidden layer consists of an activation function where the activation function uses two sigmoid functions. According to Bar et al (2010), tan-sigmoid function is more advantageous than the log-sigmoid function as the tan-sigmoid has the greater slope than the log-sigmoid. Secondly, tan-sigmoid has positive and negative response but log-sigmoid has always positive response only. The learning rate can be adjusted by inter-connected to the neurons.
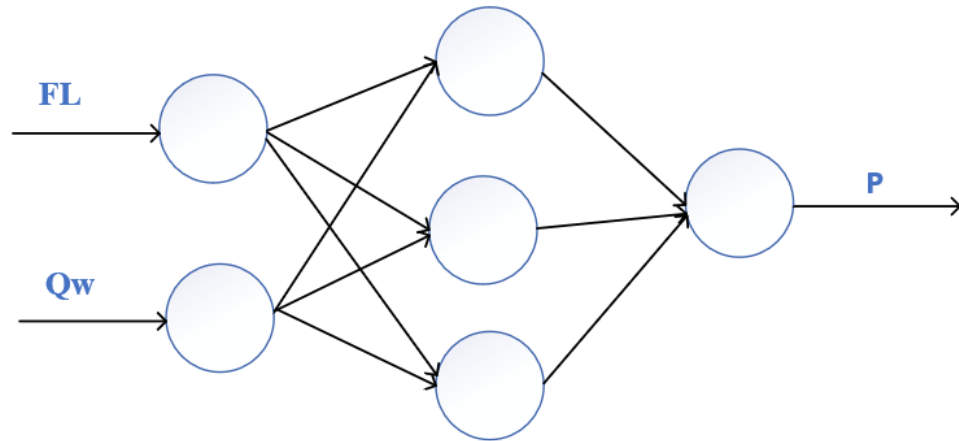
Figure 1:Topology of FF-ANN Model

Topology of the model shown in figure(1), shows the arrangement of neurons in the input layer (I), hidden layer(H), and output layer(O) that are interconnected through weight vectors and transfer functions. Number of neurons in the input layer(I), hidden layer (H), and output layer(O) are M, N and P respectively. The indices i,j,k represent the position of the neuron present in the input layer i.e. i=1,2….M), hidden layer (i.e. j=1,2,….N) and output layer (i.e. k=1,2…P) respectively. The linear transfer function, tan-Sigmoid transfer function and log-Sigmoid transfer function are considered to be the activation functions at input layer, hidden layer and output layer respectively. The input and output from a neuron is depicted by 'I' and 'O' respectively through 1st subscript.

The output from ith neuron at the input layer (I) considering linear transfer function is represented as

$$I_{Oi} = I_{Ii} \tag{1}$$

The inputs to the hidden neurons (H_{Ij}) that are connected by the weights, can be represented as

$$H_{Ij} = W_{1j}I_{O1} + \cdots + W_{ij}I_{Oi} + \cdots + W_{Mj}I_{OM} \tag{2}$$

where W_{1j}….W_{Mj} denote connecting weights of the neurons (ith=1,2…M) at the input layer to the hidden neuron(j).

The use of the log-sigmoid function with a_1 coefficient for hidden neurons, yields output from the hidden neuron (H_{Oj}) as

$$H_{Oj} = \frac{1}{1 + e^{-a_1 H_{Ij}}} \tag{3}$$

similarly a_2 indicates about the coefficient of the tan-sigmoid function.

The input to the output neuron (O_{Ik}) can be determined using V(V_{1k}….V_{Nk}) weight vector as

$$O_{Ik} = V_{1k}H_{O1} + \cdots + V_{jk}H_{Oj} + \cdots + V_{Nk}I_{ON} \tag{4}$$

The output from the output neuron uses the tan-sigmoid function with a_2 coefficient and is denoted as O_{Ok} , which can be represented as

$$O_{Ok} = \frac{e^{a_2 O_{Ik}} - e^{-a_2 O_{Ik}}}{e^{a_1 O_{Ik}} + e^{-a_1 O_{Ik}}} \tag{5}$$

As per Bar et al(2010), use of the tan-sigmoid activation function at the hidden inlayer and the log-sigmoid function at the output layer is preferred.

Pratihar(2013) mathematically defined error (E_k) as the representation of difference between the target data and predicted data from the output layer as

$$E_k = \frac{(T_{Ok} - O_{Ok})^{\wedge(2)}}{2} \tag{6}$$

where T_{Ok} is the target data and O_{Ok} is the predicted data from the output layer. The steps followed through equations 1 to 6, outlines the mathematical representation of Feed Forward Artificial Neural Network (FFANN) algorithm with given weight vectors, bias and activation functions. The training and testing with FFANN is successful when the error resulted is negligible. The predicted data matches with targeted data only when correct guess of weight vectors, appropriate activation functions and correct bias are chosen, which very rarely occurs. In order to make the ANN model a successful one, Pratihar (2013) proposed FFBP-ANN model. The error obtained is used to rectify the guessed weight vectors and direction is reversed for finding out the corrections.

3.2 PSO Algorithm

PSO-Algorithm is an incredible approach for optimizing variety of functions. Particle swarm optimization has clear connections with evolutionary computation. It is a population-based approach that imitates the movement patterns of animals like fish and birds that travel in herds. Conceptually, it resembles both evolutionary programming and genetic algorithms as per Kennedy and Eberhart (1995). The PSO has several advantages over conventional optimization methods, including faster learning and less memory usage as per Other evolutionary computation models directly manipulate potential solutions that are represented as hyperspace locations. This algorithm's first stage is to create a "swarm" of the initial population. The population of potential solutions known as "particles" that make up the swarm each assumes a random position is known as a candidate solution. Based on the particles' objective function, the placements are determined. The movement of the particles is altered by considering both the location of the elite particle and the ideal location for the entire swarm as per Bahiraei et al(2021).

Each particle in the network, while searching in the multi-dimensional space, must modify itself according to the position and position of other particle in the swarm. The population algorithms are assigned with the random velocity and are allowed to move into different problem space. The particle has been assigned with the best position which has greatest fitness which is known as the global best position of the swarm. Each particle is assigned with some random velocity while moving in the problem space. The particle of the i-th position in the problem space is represented as:

$$X_i = (x_{i1} + x_{i2} + \cdots \ldots \ldots \ldots x_{id}) \tag{7}$$

where d is the dimension in the problem space. Similarly, the velocity of i-th position of the particle is denoted by

$$V_i = (V_{i1} + V_{i2} + \cdots \ldots \ldots \ldots \ldots V_{id}) \tag{8}$$

The best position of the i-th particle can be denoted as

$$P_i = (p_{i1} + p_{i2} + \cdots \ldots \ldots \ldots \ldots p_{id}) \tag{9}$$

Also, the global best position can be represented as

$$P_g = (p_{g1} + p_{g2} + \cdots \ldots \ldots \ldots \ldots p_{gd}) \tag{10}$$

The velocity and position of the particle are updated and represented as

$$V_{id}(t+1) = wV_{id}(t) + C_1 r_1 (P_{i1} - X_{id}(t)) + C_2 r_2 (P_{gd} - X_{id}(t)) \tag{11}$$

$$X_{id}(t+1) = X_{id}(t) + V_{id}(t+1) \tag{12}$$
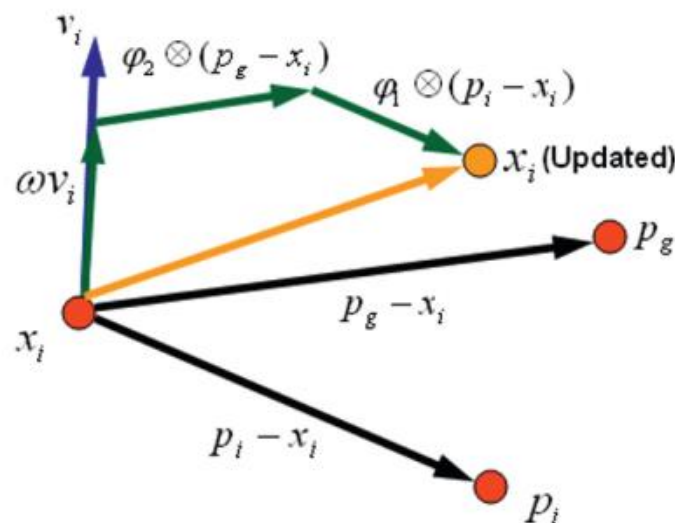
Figure2: Component vectors in the PSO problem space as per Blum and Li (2008)

4 Results and Discussion

In the hybrid FF-PSO ANN model, Feed Forward multilayer neural network scheme has been employed to predict the pressure profile data for a given flow condition with its assumed weight vector and bias. This has been compared with the experimentally obtained target data which quantifies the error. As discussed in the previous section, PSO algorithm has been employed to reduce the error by refining the weights and biases. The convergence of PSO was controlled through the adapted values of the inertia weights, population size, damping factor, and acceleration coefficients. The simulations are conducted for the discharge from the 9th floor

with a flow rate of 2l/s.The performance of the FF-PSO-ANN model has been discussed in the following section from the obtained results.

4.1 Effect of Hidden Neurons
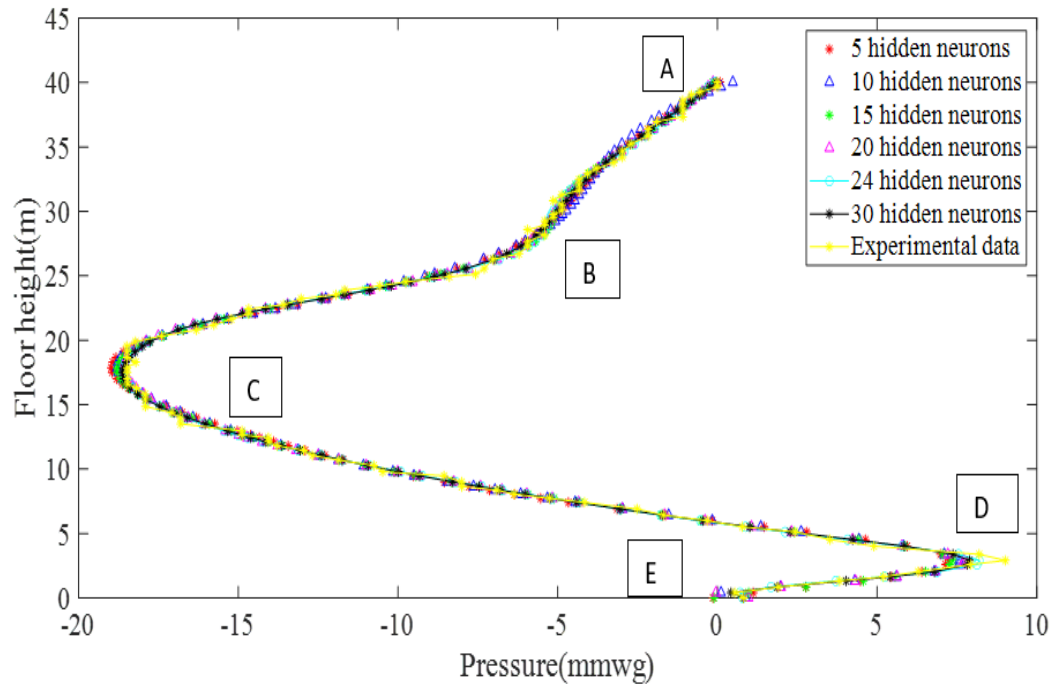
Figure 3: Distribution of the pressure profile by changing the hidden neurons.

Figure 3 shows a good agreement of the experimental data with that of FF-PSO ANN predicted results. It is observed that the predicted results match perfectly well with the experimental results for both the dry-stack region (A-B) and wet stack region (C-D -E). A small deviation is observed at peak points C and point D. The Table represent the optimal performance of the network is obtained at 24 hidden neurons as the MSE value and RD value are the lowest, whereas R^2 value is the highest. The performance of FF-PSO-ANN model signifies excellent agreement from Table (1) as shown below.

Table 1: Performance Table of FF-PSO-ANN Model with different hidden neurons

Number of hidden neurons	MSE	R^2	MRD (%)
5	0.0047	0.9953	10.36
10	0.0039	0.9961	9.43
15	0.0035	0.9965	8.56
20	0.0027	0.9973	6.85
24	0.0022	0.9976	1.08
30	0.0025	0.9975	4.29

4.2 Effect of Population Size

As it is understood that there is no deterministic rule for fixing up of the network parameters for optimal performance of the ANN model, the population size has been varied to examine its performance. In addition, convergence criterion and computational time are controlled using population size. For investigation purpose, the population size of 10, 30, 50, 80, and 100 are used, keeping hidden neuron as 24. The Table-2 below represent about the performance of FF-PSO-ANN model with different population size such as 10,30,50,80 and 100. The performance with 50 population size performs better than the rest population size as the MSE value is optimum and correlation coefficient is maximum for 50 population size.
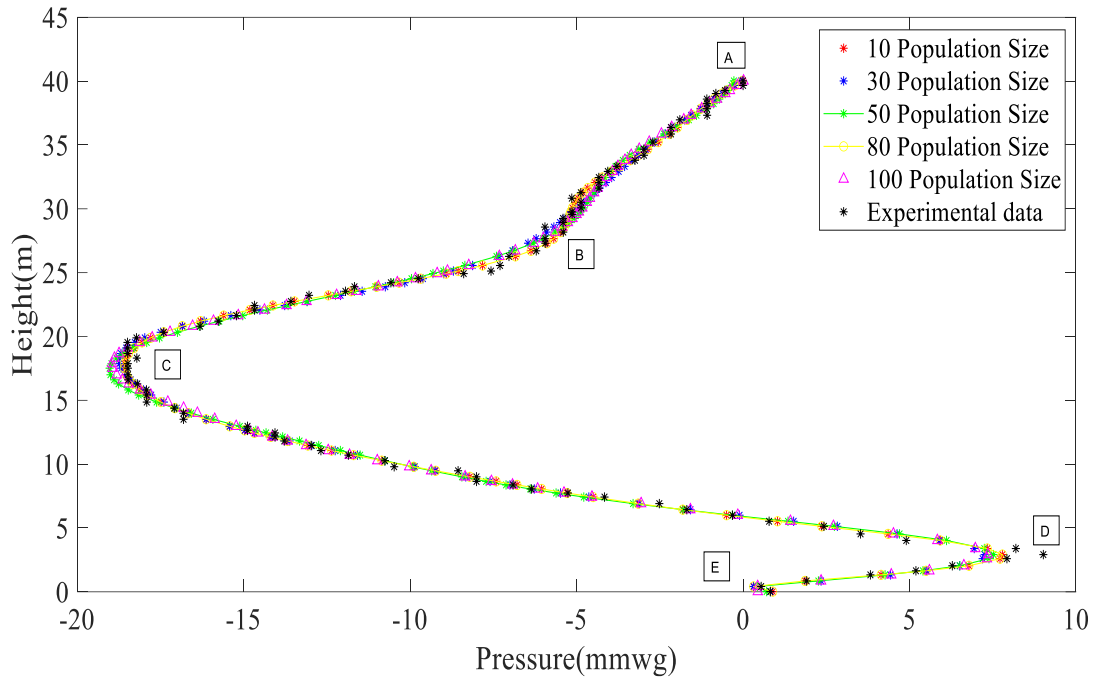
Figure 4: Pressure variation with height for different population size.

Table 2: Performance Table of FF-PSO-ANN Model with different population size

Population size	MSE	R^2	MRD (%)
10	0.0025	0.9975	6.30
30	0.0041	0.9959	1.15
50	0.0022	0.9976	1.08
80	0.0025	0.9975	5.65
100	0.0051	0.9949	5.06

The simulation with the FF-PSO model has been performed by changing the discharge flow rate from a fixed floor height. The convergence controlling parameters such as; the inertia weight is taken as 1, the damping factor of the inertia weight is set as 0.99, and the acceleration coefficients are set as 1.5 and 2.0 respectively. The discharge flow takes place from different flow rate such as 1L/s, 2L/s, 3L/s and 4L/s. The relative deviation lies within 10-15% when trained using FF-PSO-ANN model. The table 3 below represent the performance of the model is better when the discharge takes place at 2L/s.
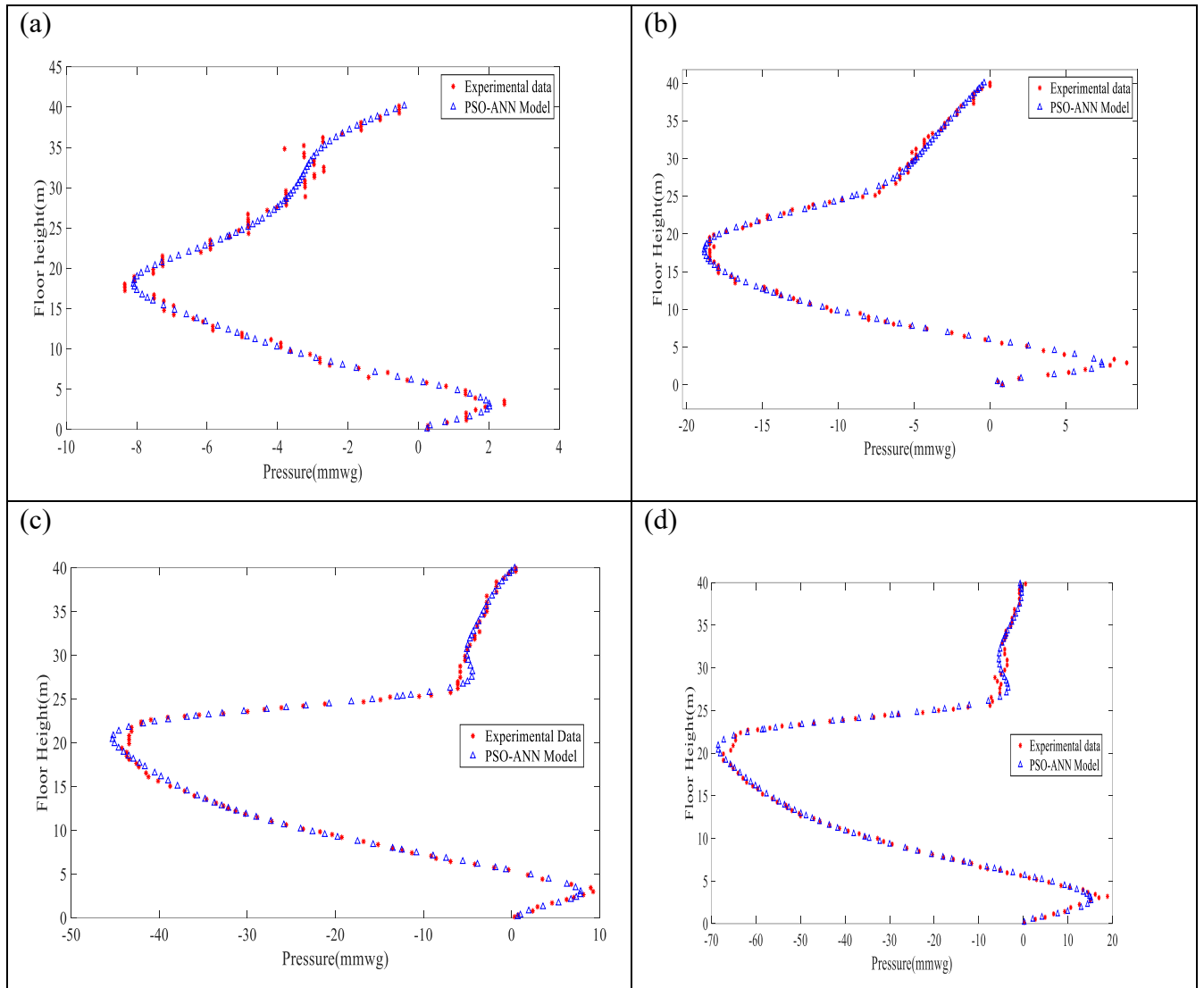
Table 4: Performance Table of FF-PSO-ANN Model by changing the discharge flow rate

Discharge flow rate	MSE	R^2	MRD(%)
1 L/s	0.0107	0.9951	10.28
2 L/s	0.0021	0.9981	1.53
3 L/s	0.0024	0.9976	3.46
4 L/s	0.0026	0.9974	6.43

5 Conclusion

In the present scenario, the optimal simulation performance of the FF-PSO-ANN model is for 24 hidden neurons which performs best among other hidden neurons. Even the simulation performance of FF-PSO-ANN model is better when the simulation takes for 50 population size with 24 hidden neurons. The performance of FF-PSO-ANN model is best when the discharge flow rate takes place at 2L/s and the discharge takes place from 9th floor. Overall, FF-PSO-ANN model works very well for the different flow conditions.

6 Acknowledgement

7 References

1. Alizadehdakhel, A., Rahimi, M., Sanjari, J. and Alsairafi, A.A., 2009. CFD and artificial neural network modeling of two-phase flow pressure drop. *International Communications in Heat and Mass Transfer*, *36*(8), pp.850-856.
2. Bahiraei, M., Nazari, S. and Safarzadeh, H., 2021. Modeling of energy efficiency for a solar still fitted with thermoelectric modules by ANFIS and PSO-enhanced neural network: A nanofluid application. *Powder Technology*, *385*, pp.185-198.
3. Bar, N., Das, S.K. and Biswas, M.N., 2013. Prediction of frictional pressure drop using artificial neural network for air-water flow through U-bends. *Procedia Technology*, *10*, pp.813-821.
4. Blum, C. and Li, X., 2008. Swarm intelligence in optimization. *Swarm intelligence: introduction and applications*, pp.43-85.
5. Gormley, M. and Kelly, D.A., 2019. Pressure transient suppression in drainage systems of tall buildings. *Building Research & Information*, *47*(4), pp.421-436.
6. Gormley, M., 2007. Air pressure transient generation as a result of falling solids in building drainage stacks: definition, mechanisms and modelling. *Building Services Engineering Research and Technology*, *28*(1), pp.55-70.
7. Jack, L.B., Cheng, C. and Lu, W.H., 2006. Numerical simulation of pressure and airflow response of building drainage ventilation systems. *Building Services Engineering Research and Technology*, *27*(2), pp.141-152.
8. Jahanandish, I.E., Salimifard, B. and Jalalifar, H., 2011. Predicting bottomhole pressure in vertical multiphase flowing wells using artificial neural networks. *Journal of Petroleum science and engineering*, *75*(3-4), pp.336-342.
9. Kennedy, J. and Eberhart, R., 1995, November. Particle swarm optimization. In *Proceedings of ICNN'95-international conference on neural networks* (Vol. 4, pp. 1942-1948). IEEE.

10. Osman, E.S.A. and Aggour, M.A., 2002. Artificial neural network model for accurate prediction of pressure drop in horizontal and near-horizontal-multiphase flow. *Petroleum Science and Technology*, *20*(1-2), pp.1-15.
11. Pratihar, D.K., 2013. *Soft computing: fundamentals and applications*. Alpha Science International, Ltd.
12. Safikhani, H., Abbassi, A., Khalkhali, A. and Kalteh, M., 2014. Multi-objective optimization of nanofluid flow in flat tubes using CFD, Artificial Neural Networks and genetic algorithms. *Advanced Powder Technology*, *25*(5), pp.1608-1617.
13. Swaffield, J., 2010. *Transient airflow in building drainage systems*. Routledge.

8 Presentation of Authors

Ishanee Mahapatra is a PhD student in the School of Energy, Geoscience, Infrastructure and Society at Heriot Watt university joined in the year January 2020. She is currently working on ANN model with an application to building drainage and vent system. She graduated from University of Manchester with a MSc. degree in the year 2019 in Thermal Power and Fluid Engineering.

Michael Gormley is Professor of Public Health and Environmental Engineering at the School of Energy, Geoscience, Infrastructure and Society at Heriot-Watt University. His research specialisms are; mathematical modelling of air and water flows in building drainage systems, infection spread via bioaerosols and product development.

TECHNICAL SESSION 3 - MISCELLANEOUS

Experimental study of the heat transfer coefficient between human skin and the flowing water during showering

L.T. Wong (1), C.W. Poon (2), K.W. Mui (3), D.D. Zhang (4)

(1) beltw@polyu.edu.hk

(2) wayne.poon@connect.polyu.hk

(3) behorace@polyu.edu.hk

(4) beee-dadi.zhang@polyu.edu.hk

(1), (2), (3), (4) Department of Building Environment and Energy Engineering, The Hong Kong Polytechnic University, Hong Kong.

Abstract

Showering, as an indispensable part of modern people's daily routine, is closely related to people's comfort and energy consumption. To get an insight into these relationships and further improve people's comfort and energy efficiency, it is crucial to understand the heat transfer coefficient between human skin and the flowing water during showering. Although it was investigated by several studies before, the value varied significantly (from 43.2 to 588 W/(m^2·°C)) among these studies, and no consistent conclusion can be identified. Therefore, this study conducted a series of experiments to deeply understand the heat transfer coefficient under different showering conditions. This experiment used a skin model made of an insulated Styrofoam board and a thin aluminium sheet to simulate human skin exposure to the flowing water. Four showerheads with different patterns, three water temperatures (35, 38, and 41 °C), and three water flow rates (5, 6, and 7 L·min^{-1}) were investigated. Results indicated that the heat transfer coefficient increased significantly with the water flow rate. Moreover, this value also differed with various water patterns. For the same showerhead, the higher the pattern's nozzle area ratio, the higher the heat transfer coefficient. These findings could help to identify the most effective showering condition with the highest heat transfer coefficient between human

skin and flowing water and contribute to people's thermal comfort and energy saving during showering.

Keywords

Showering; heat transfer coefficient; water pattern; water temperature; water flow rate.

1 Introduction

Showering is an indispensable daily activity in modern life, which could significantly impact people's hygiene and comfort. People usually experience significant heat exchange during showering because the whole body is exposed to the water and the heat transfer coefficient between water and skin is higher than between air and skin. Consequently, people's skin temperature, which is stable in normal conditions, also varies significantly during showering (Munir et al., 2010). This directly influences peoples' thermal comfort and health. Moreover, the process, especially the efficiency, of heat exchange between the shower water and human skin is also closely related to energy and water consumption. Therefore, to take a healthy, comfortable, and energy-efficient shower, it is crucial to understand the heat transfer process between the shower water and human skin, and the core of the investigation of the heat transfer process between water and skin lies in the determination of the convective heat transfer coefficient between them.

The investigation of the convective heat transfer coefficient between water and human skin is a topic that has been discussed previously. Some researchers have studied it since half-century ago, using various methods, such as theoretical derivation, model simulation, copper manikin experiment, and human subject experiment (Boutelier et al., 1977; Rnadel et al., 1974). However, because of the different methods and physical conditions (such as various water temperatures, water flow rates, etc.), the results obtained in the previous studies are inconsistent and varied a lot: from 43.2 to 588 W/(m²·°C). Among the earlier studies on heat transfer coefficients, the method proposed by Munir (named "replicated skin model") was the relatively new and simple one. Besides, unlike other studies that considered water immersion or swimming, this study was, as far as we know, the only one that thought of the showering scenario. However, Munir et al. (2010) only tested one condition with one specific, yet unknown, water temperature and flow rate. They concluded that the heat transfer coefficient for showering between skin and water was 104 W/m²·K. More conditions should be considered since the heat transfer coefficient varied with the water's thermophysical properties and flow velocity (Laloui et al., 2020).

Therefore, the current study conducted experiments to determine the heat transfer coefficient for showering under different conditions. Like Munir's study, a replicated skin model was applied to simulate the heat exchange process between skin and water during showering. Based on the experiment's results, the heat transfer coefficient can be calculated, which could help determine the most efficient showering condition.

2 Methodology

2.1 Experiment setup

Figure 1 illustrates the experimental setup in the current study. A shower head was mounted on a tripod stand, and a skin model was fixed on the ground using two stand clamp clips. Similar to the model developed by Mumir (2010), this skin model also consists of a Styrofoam board (20cm*50cm) and a thin aluminium board (20cm*40cm) which represents human skin. A high-speed camera was installed in front of the direct shower zone (see Figure 1) to capture and investigate the water flow pattern generated by different showerheads.
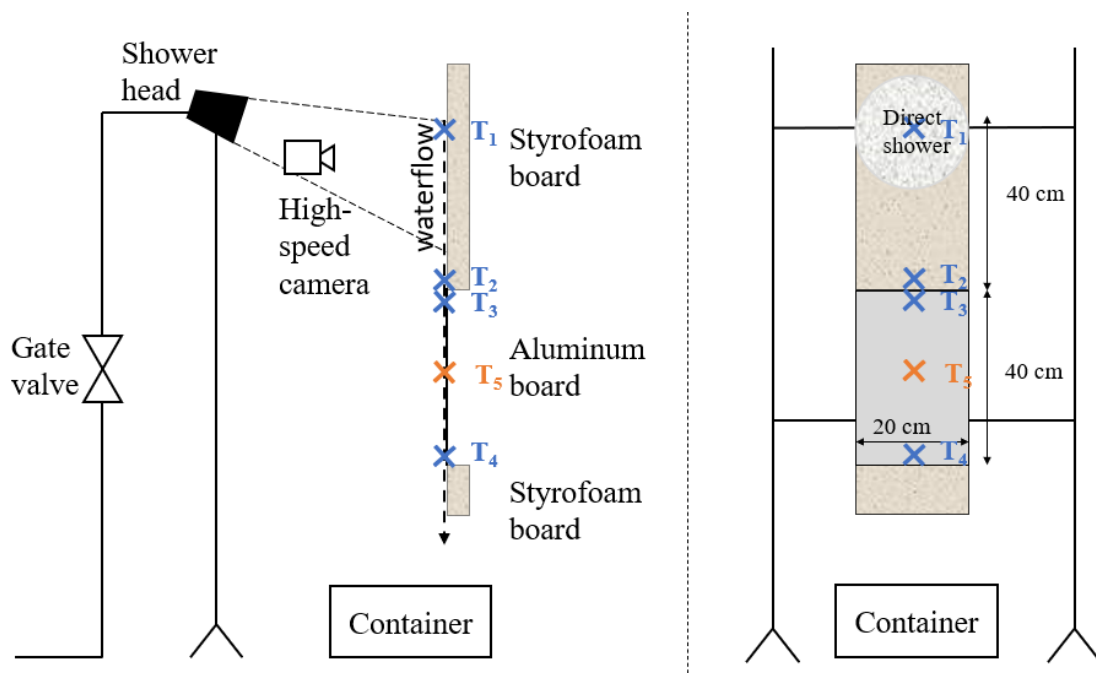
Figure 1 - Experiment setup (side view; right: front view)

Five Pt1000 sensors (1000 ohm temperature sensors) were applied to measure the temperatures at five locations during the experiment. As shown in Figure 1, T1 was the temperature of the water when it first touched the Styrofoam board; T2 was the temperature of the water before it flowed past the Styrofoam board; T3 was the

temperature of the water when it first touched the aluminium board; T4 was the temperature of the water before it flowed past the aluminium board; T5 was the temperature of the aluminium board. All the Pt 1000 sensors were attached on the front side of the boards and in the middle of the water flow, except the fifth one. Since T5 was the temperature of the aluminium board, the fifth Pt 1000 was attached at the back of the aluminium board to avoid water interference. Considering that aluminium is a high thermal conductivity material and the board is very thin, the temperatures of both sides of the aluminium board were assumed to be the sawm. The Pt1000 sensors were connected to a data acquisition solution (DA200) to convert the resistance to temperature and record the results. Besides, the water flow rate was measured manually by measuring the water volume collected in the container (see Figure 1) after one minute of continuous "showering".

2.2 Testing scenarios

Four different water flow rates and three water temperatures were selected in the current study to investigate the heat transfer coefficient under different conditions. Based on the Voluntary Water Efficiency Labelling Scheme on Showers recommended by the Hong Kong Water Supplies Department (2018), the water flow rates tested in the experiment were set as 5, 6, and 7L/min. Considering the occupant's thermal comfort during showering identified by Wong et al. (2022), the water temperature was set as 35, 38, and 41 °C. In addition, four showerheads with several different spray patterns (see Table 1) were applied to investigate the impact of the water flow pattern. The nozzle area ratio, as equation (1), was used to qualify the spray distribution of different showerhead patterns.

$$\emptyset_A = \frac{A_s}{A_f} \qquad\qquad (1)$$

Where A_s is the total area of the working nozzles (m^2), A_f is the area of the whole faceplate of the showerhead (m^2). Therefore, in total 126 (3 water flow rates × 3 water temperatures × 14 water flow patterns) scenarios were tested in this study.

Table 1 - Information on the selected showerhead patterns

	Description of different patterns	Diameter(mm)	Number of 1/2/3mm Nozzles, n1/n2/n3	Nozzle area ratio
A				
	1 The outermost (blue) circle	70	60/0/0	0.0122
	2 The outermost & second outermost	70	60/12/0	0.0220
	3 The outermost & middle point	70	60/0/1	0.0141
	4 The outermost & third outermost	70	60/6/0	0.0171
	5 The second outermost	70	0/12/0	0.0098
B				
	1 The innermost circle	100	0/0/9*	0.0036
	2 The outermost & the innermost	100	47/0/9*	0.0083
	3 The outermost	100	47/0/0*	0.0047
	4 The outermost & middle	100	47/10/0*	0.00695
	5 The middle	100	0/10/0*	0.00225
C				
	1 One circle	90-50	15/0/0	0.00625
D				
	1 The outermost (blue) circle	70	60/0/0	0.0122
	2 The outermost & middle	70	60/15/0	0.0245
	3 The outermost & the innermost	70	60/0/6	0.0233

* For showerhead B, the diameters of the three types of nozzles are 1/1.5/2mm.

2.3 Experiment procedure

The experiment was conducted in an indoor lab. During the investigation, the temperature

in the lab was around 23°C and the relative humidity was around 50%, which was controlled and maintained by an HVAC (heating, ventilation, and air-conditioning) system. The experiment procedure was straightforward. After the setup was completed and the parameters were adjusted to the specific levels, the researcher turned the showerhead on and counted for one minute. The camera was also on and recording the water movements on the board continuously. The Pt1000 measured all the temperatures and automatically recorded them per second in the DA200. After one minute, the researcher turned off the showerhead and measured the water amount in the container with the measuring cup.

2.4 Data processing

In this experiment, the heat exchange between the hot water and the skin model can be divided into two parts. For the Styrofoam board part, the heat was only transferred from the water to the air since the Styrofoam is adiabatic. The heat was transferred from the hot water to the air and the aluminium board (i.e., the skin) for the aluminium board part. Regarding the heat loss of the water flowing through the Styrofoam board (Q_{w_s}), it can be calculated based on the water temperature difference using equation (2).

$$Q_{w\_s} = mc_p(\overline{T_1} - \overline{T_2}) \tag{2}$$

Where m is the water flow rate (kg/s); c_p is the heat capacity of water, which is 4184 J/(kg·°C); $\overline{T_1}$ and $\overline{T_2}$ are the average temperatures measured at the corresponding positions marked in Figure 1. This amount of heat was all transferred to the air. Similarly, the heat loss of water during its flowing through the aluminium board (Q_{w_a}) can be calculated using equation (3).

$$Q_{w\_a} = mc_p(\overline{T_3} - \overline{T_4}) \tag{3}$$

This amount of heat can be divided into two parts. One part was transferred to the air, which was assumed to be equal to the Q_{w_s} since the area of the Styrofoam between T1 and T2 was the same as the area of the aluminium board between T3 and T4. The other part was transferred to the aluminium board, which can be calculated using equation (4).

$$Q_{skin} = \alpha A \left(\overline{T_4} + \frac{\overline{T_3} - \overline{T_4}}{2} - \overline{T_5} \right) = mc_p(\overline{T_3} - \overline{T_4}) - mc_p(\overline{T_1} - \overline{T_2}) \tag{4}$$

Where, A is the area of the aluminium board (m²). Therefore, the heat transfer coefficient between water and skin (α) can be calculated as follows:

$$\alpha = \frac{mc_p(\overline{T_3}-\overline{T_4})-mc_p(\overline{T_1}-\overline{T_2})}{A\left(\overline{T_4}+\frac{\overline{T_3}-\overline{T_4}}{2}-\overline{T_5}\right)}$$ (5)

After calculations, the collected temperatures, water flow rate, and the calculated heat transfer coefficient, together with the experiment conditions (i.e., water temperature, showerhead no. and pattern), were imported and analysed in three steps using SPSS version 27.0 (SPSS Inc. Chicago, IL, USA). First, the z-scores of the heat transfer coefficients were calculated and the cases where the absolute values of the z-scores were larger than 3 were considered outliers and excluded. Second, descriptive analyses were conducted to get a basic understanding of the collected data. Third, the impacts of water temperature, water flow rate, and showerhead patterns were investigated using one-way ANOVA.

3 Results and discussion

3.1 Descriptive results of the collected data and the heat transfer coefficients

In total, 126 conditions were tested in the current study. Figure 2 illustrates the average temperatures measured under these conditions and their changes with time. As can be seen, T1-T4 remained relatively steady after 15 seconds, while T5 continuously increased during the experiment. Besides, since the locations of T2 and T3 are very close, their water temperatures measured at these positions are similar.
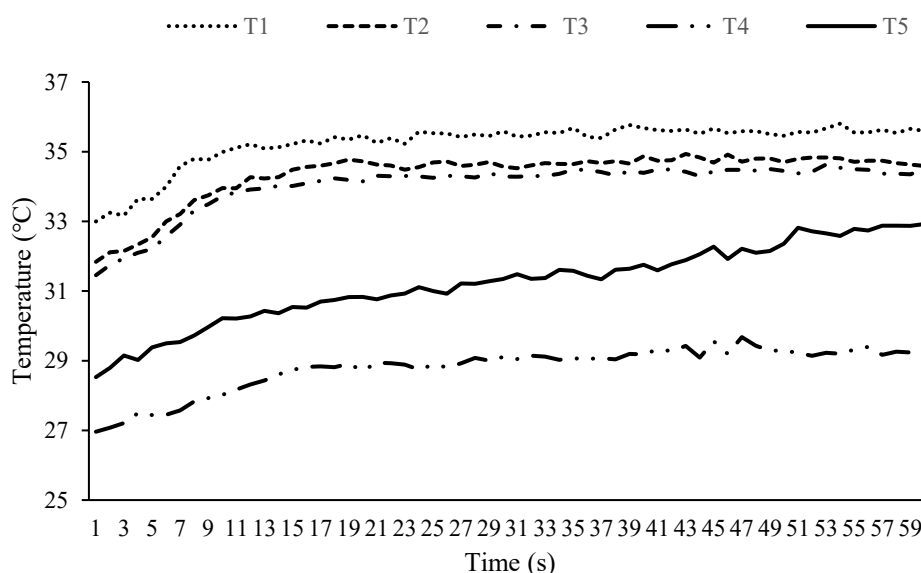
Figure 2 - Average temperatures of different conditions.

Based on equation (5), the corresponding heat transfer coefficients between the water and

2023 Symposium CIB W062 – Leuven, Belgium

the skin model were calculated. The results varied a lot between different experimental conditions. The average value was 96 W/(m^2·°C), and most of the results were between 74 and 117 W/(m^2·°C) (representing the first and third quartile of the results respectively). The result obtained by Munir et al. (2010), which was 104 W/(m^2·°C), also falls in this range.

3.2 Impact of water temperature and water flow rate on the heat transfer coefficient

According to the one-way ANOVA test results, there was no significant difference in the heat transfer coefficient between the conditions with different water temperatures ($F_{(2,125)}=0.166$, $p=0.847$). Figure 3 a) shows that the average heat transfer coefficient between the water and the aluminium board was always around 96 W/(m^2·°C). This does not consist with the results found by previous studies that the convection heat transfer coefficient was positively correlated with the temperature difference between the surface and the liquid (Kurazumi et al., 2008). The limitation of the experiment conditions might cause this inconsistency. More temperature settings with more extensive ranges should be tested in the future.

a) impact of water temperature   b) impact of water flow rate
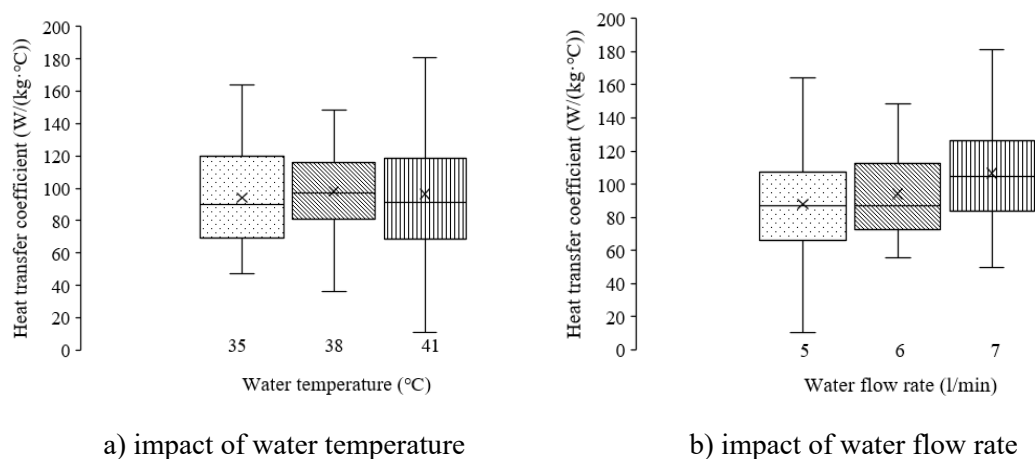
Figure 3. Heat transfer coefficients in conditions with different water temperatures (a) and water flow rates (b).

A significant difference was identified in the heat transfer coefficients between the experimental conditions with different water flow rates ($F_{(2,125)}=4.093$, $p=0.019$). As shown in Figure 3 b), the higher the water flow temperature, the higher the heat transfer coefficient, which agrees with the statement mentioned by Laloui et al. (2020). Moreover, a Tukey post hoc test revealed that the statistically significant difference in the heat transfer coefficient was only found between the conditions when the water flow rate was

5 l/min and 7 l/min (p = 0.016). At the same time, there was no statistically significant difference between other pairwise comparisons.

3.3 Impact of water flow patterns on the heat transfer coefficient

Regarding the showerhead type's impact, no significant difference was identified in the heat transfer coefficients between the conditions with different showerheads ($F_{(3, 122)}=1.661$, p=0.179). However, if comparing the results between different showerhead patterns, significant differences were identified, as shown in Figure 4a ($F_{(13, 112)}=3.215$, p<0.001). Based on the Tukey post hoc test results, the significant differences in the pairwise comparisons were only identified between the two highest results (B-2 and D-2) and the three lowest (A-1, A-5, and D-1).

Additionally, regarding the nozzle ratio's impact, no significant correlation was found between it and the heat transfer coefficients (r=0.118, p=0.188), either. Nevertheless, if comparing the results among the same showerhead, significant moderate correlations were observed (0.4<r<0.5, p<0.05). As shown in Figure 4b-d, the higher the nozzle ratios for the same showerhead, the higher the heat transfer coefficient. These findings demonstrate the importance of the wise choice of the showerhead pattern. Considering that different showerheads could significantly impact energy and water saving (Wong et al., 2016), more profound research on the influence of the showerhead pattern should be conducted in the future.
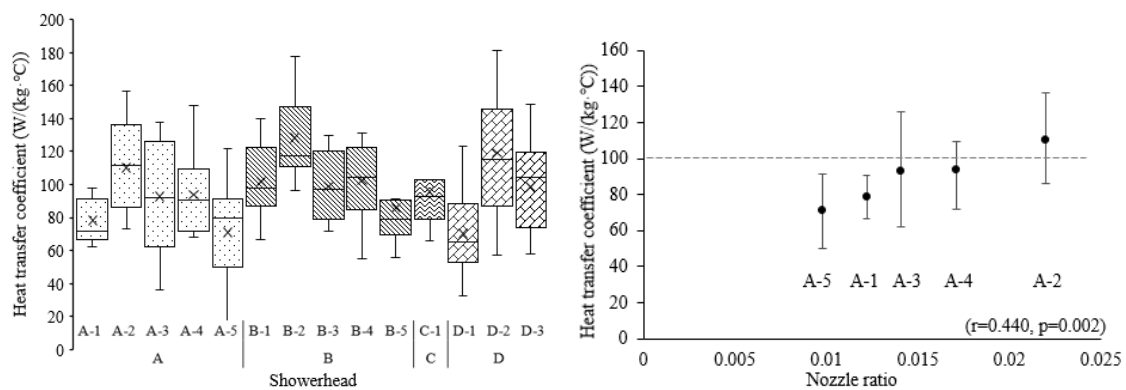
a) Impacts of showerhead type   b) Impact of nozzle ratio of showerhead A
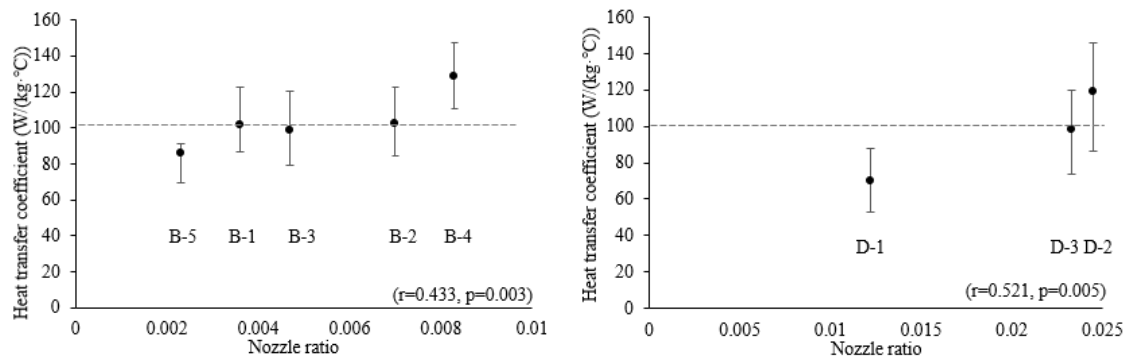
c) Impact of nozzle ratio of showerhead B   d) Impact of nozzle ratio of showerhead D

Note: the dush line in figures b-d represents the result obtained by Munir et al. (2010).

Figure 4. Heat transfer coefficients in conditions with different showerhead patterns.

4 Conclusion

This study conducted a series of experiments to measure the convection heat transfer coefficient between hot water and a skin model to understand the heat transfer between water and human skin during showering. A skin model, namely a thin aluminium board, was adopted by a previous study. Three water temperatures (35, 38, and 41 °C), three water flow rates (5, 6, and 7 L/min), and four showerheads with several different patterns were tested. Results indicated that the heat transfer coefficient varied significantly with other experiment conditions, and the average result was about 96 W /(m^2·°C), which was compatible with the result identified by previous studies. Moreover, it was found that both the water flow rate and showerhead pattern (nozzle area ratio) had significant impacts on heat transfer coefficients. The higher the water flow rate and the nozzle area ratios, the higher the heat transfer coefficient between the water and skin was observed. However, the small amount and randomly selected showerhead samples might lead to misreading the results obtained in the current study. Considering the remarkable impacts of these factors on energy and water saving, more profound studies on these impacts should be conducted in the future.

5 Acknowledgments

6 Reference

Boutelier, C., Bougues, L., Timbal, J., & Boutelier, F. (1977). Experimental study of convective heat transfer coefficient for the human body in water. *Journal of Applied Physiology*, *42*(1), 93–100.

Hong Kong water supplies department. (2018). *Voluntary Water Efficiency Labelling Scheme on Showers for Bathing*. Hong Kong Water Supplies Department. https://www.wsd.gov.hk/en/plumbing-engineering/water-efficiency-labelling-scheme/wels-on-showers-for-bathing/voluntary-water-efficiency-labelling-scheme-on-sho/index.html

Kurazumi, Y., Tsuchikawa, T., Ishii, J., Fukagawa, K., Yamato, Y., & Matsubara, N. (2008). Radiative and convective heat transfer coefficients of the human body in natural convection. *Building and Environment*, *43*(12), 2142–2153. https://doi.org/10.1016/j.buildenv.2007.12.012

Laloui, L., Loria, R., & Chapter, A. F. (2020). Heat and mass transfers in the context of energy geostructures. In *Analysis and Design of Energy Geostructure* (pp. 69–135).

Munir, A., Takada, S., Matsushita, T., & Kubo, H. (2010). Prediction of human thermophysiological responses during shower bathing. *International Journal of Biometeorology*, *54*(2), 165–178. https://doi.org/10.1007/s00484-009-0265-9

Rnadel, E., HOLMkR, I., J St, J. A., Holmer, I., Bergh, U., Astrand, P., & J Stolwijk, J. A. (1974). Energy exchanges of swimming man. *Journal of Applied Physiology*, *36*(4), 465–471.

Wong, L.-T., Mui, K.-W., & Chan, Y.-W. (2022). Showering Thermal Sensation in Residential Bathrooms. *Water (Switzerland)*, *14*(19). https://doi.org/10.3390/w14192940

Wong, L.-T., Mui, K.-W., & Zhou, Y. (2016). Impact evaluation of low flow showerheads for Hong Kong residents. *Water (Switzerland)*, *8*(7). https://doi.org/10.3390/W8070305

7 Presentation of author(s)

Dr. L.T. Wong is an associate professor at the Department of Building Environment and Energy Engineering, The Hong Kong Polytechnic University.

C.W. Poon is a Department of Building Environment and Energy Engineering graduate from The Hong Kong Polytechnic University.

Prof K.W. Mui is a professor at the Department of Building Environment and Energy Engineering, The Hong Kong Polytechnic University.

Dr. D. Zhang is a postdoc fellow at the Department of Building Environment and Energy Engineering, The Hong Kong Polytechnic University.

Current Circumstances and Issues Surrounding Disposable Underwear Crushing/Disposal Systems to be Installed at Care and Nursing Homes

Yuto Ino(1), Masayuki Otsuka(2), Ayaka Kimura(3), Michitaro Maki(4)

(1) m22j3003@kanto-gakuin.ac.jp
(2) dmotsuka@kanto-gakuin.ac.jp
(3) aya.98pc@outlook.jp
(4) michitarou.maki@lixil.com

(1) Graduate Student, Graduate School of Engineering, Kanto Gakuin University, Japan

(2) Prof. Dr. Eng. Department of Architecture and Environmental Design, College of
  Architecture and Environmental Design, Kanto Gakuin University, Japan

(3) Former Graduate school of Engineering, Kanto Gakuin Univ., M. Eng.

(4) LIXIL Corporation, Japan

Abstract

The world's population is aging with the proportion of those aged 65 and over that is expected to reach 17.8% by 2060. With old age, people have trouble urinating and defecating, and often use disposable underwear to help excretion. The production volume of disposable underwear is on the increase. This trend imposes burdens on carers of the elderly and care and nursing home staff as to how to properly store, transport and treat used disposable underwear that needs disposal.

Under these circumstances, in Japan, the Ministry of Land, Infrastructure, Transport and Tourism launched a project in 2018, and has been promoting ever since, the development of rational underwear wastewater treatment systems for used disposable underwear, and various types of systems have been proposed.

This study focuses on how disposable adult underwear has been becoming more widely available in line with the aging population of Japan, and indicates problems surrounding the disposal of such disposable underwear. The study also presents a brief introduction of the disposable underwear crushing/disposal system which has been developed and achieved, as a result of hard work by the authors, on the basis of the results of performance evaluation.

Keywords

1. Background and purpose of study

The global population reached around 7.8 billion in 2020, and it is expected to grow to 10.1 billion by 2060. In 2020, 9.3% of the global population was aged 65 and over (the population aging rate), and this ratio is expected to increase to 17.8% by 2060[1)2)]. With this, the market for disposable adult underwear has been expanding; the market value was 9.2 billion US dollars in 2015 and it grew by 1.5 times to around 14 billion US dollars in 2012. As the population aging continues, the market for disposable adult underwear is also predicted to expand further in the future[3)] (Fig. 1).
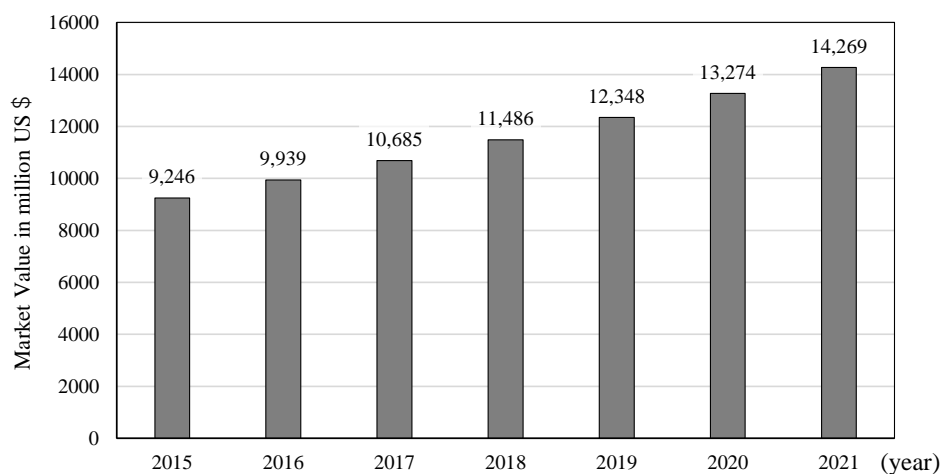
Fig. 1 Market size of disposable adult underwear[3)]

In view of these backgrounds, in Japan, the Ministry of Land, Infrastructure, Transport and Tourism has been conducting a project on proposals of disposable underwear crushing/disposal systems in three categories and promoting research on their practical applicability with the aim of reducing burdens on carers, as to how to properly handle used disposable underwear, by efficient disposal solutions[4)] (Fig. 2).

These three categories are Type A, Type B and Type C. In Type A, used disposable underwear is separated from urine and faeces by a disposable underwear separator, and the separated underwear is collected on site and only the urine and the faeces are discharged through existing pipework into the sewer. In Type B, used disposable underwear is crushed by a disposable underwear crusher, and the crushed underwear is then discharged through dedicated pipework and out of a building to be collected at the other end, while the separated urine and faeces are discharged into the sewer. In Type C, used disposable underwear is crushed by a disposable underwear crusher, and then discharged, while still containing urine and faeces, through dedicated pipework into the sewer. Type A and Type C are expected to be introduced in ordinary houses and low-rise

buildings, while Type B is expected to be introduced in mid-to-high-rise care and nursing homes.

For Type B which is suitable for care and nursing homes where disposable underwear is most frequently used, this study aims to propose a system-specific horizontal fixture branch, the research and development of which has been conducted since 2018, and a planning and designing method for a drainage stack system to which the horizontal fixture is connected.
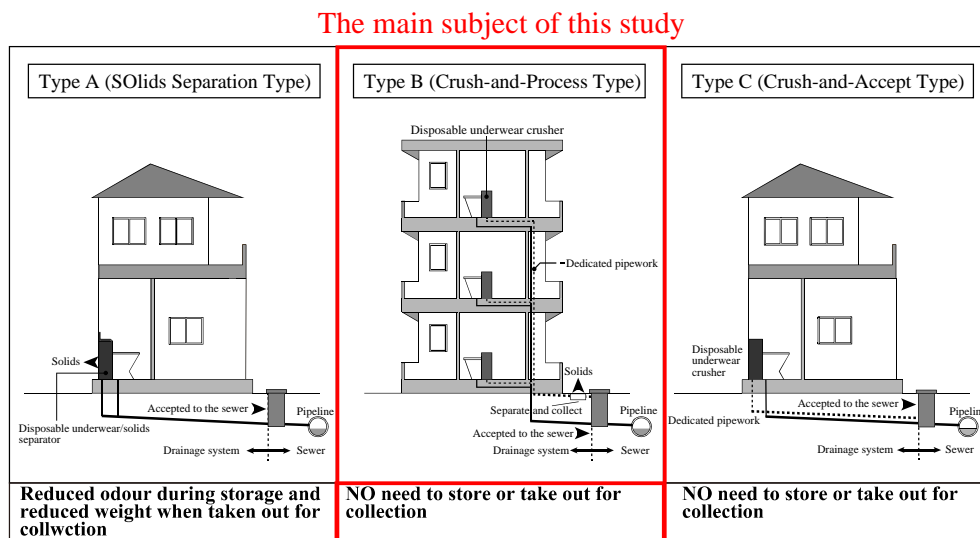
Fig. 2 Classification of disposable underwear crushing/disposal systems [4]

Fig. 3 shows the schematic and process flow of Type B which is the main subject of this study. Type B is designed such that a disposable underwear crushing/disposal machine is provided on each floor of the building; used disposable underwear is fed into the machine to be crushed and stirred, and discharged through the dedicated pipework, which is separate from the other drainage pipework, into the dehydrate-and-separate section provided outside the building; solid matters are then collected and the urine-containing wastewater is discharged into the sewer. This study discusses Type B with the focus on a particular part of the process sequence which is from the stirring of used disposable underwear in the stirring section of the disposable underwear crushing/disposal machine to the discharging of the same through the dedicated pipework.
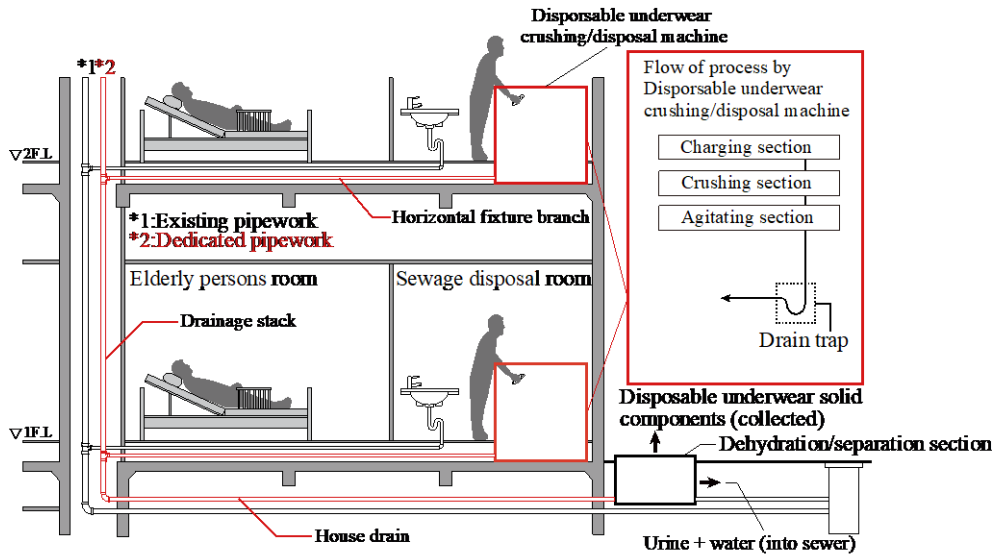
Fig. 3 System diagram of Type B

3. Planning and designing overview

The Type B system is planned and designed by following the steps shown in Fig. 4. These steps are: 3.1 determine the size of a facility for design; 3.2 determine a discharge volume for design; 3.3 plan and design the horizontal fixture branch; and 3.4 plan and design the drainage stack system.

The basis for these determination criteria are explained below in connection with the experiment results.

3.1 Determine the size of a facility for design

3.2 Determine a discharge volume for design

3.3 Plan and design the horizontal fixture branch

3.4 Plan and design the drainage stack system
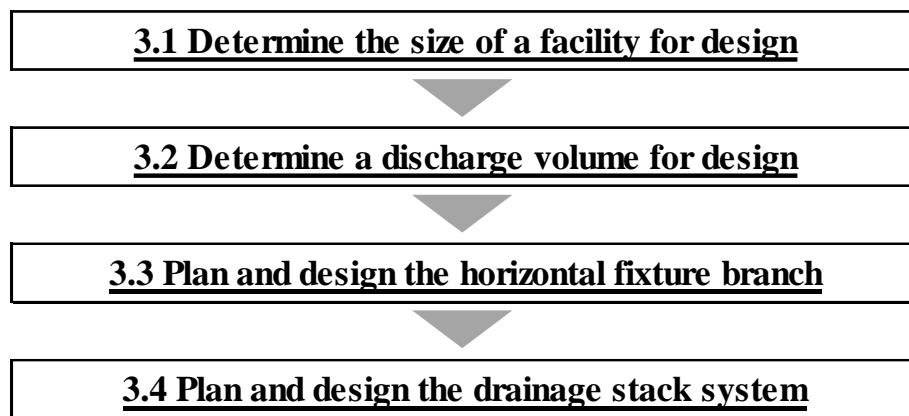
Fig. 4 Planning and designing process

3.1 Determining the size of a facility for design

In order to ascertain the number of storeys of a building in which the system is introduced, a storey survey was carried out on the care and nursing homes in two major

urban areas in Japan; Osaka City, and Tokyo consisting of 23 wards[5) 6)] (Fig. 5). Fig. 5 shows that the buildings of most care and nursing homes have three storeys, accounting for around 30% of the total number. Moreover, the buildings having up to eight storeys account for a cumulative percentage of around 90% or more. Accordingly, in consideration of marketability, it is conceivable to introduce the Type B system in buildings of eight storeys. Incidentally, as for the drainage stack system for design, an independent drainage system is adopted with a disposable underwear crushing/disposal machine solely installed on each floor.
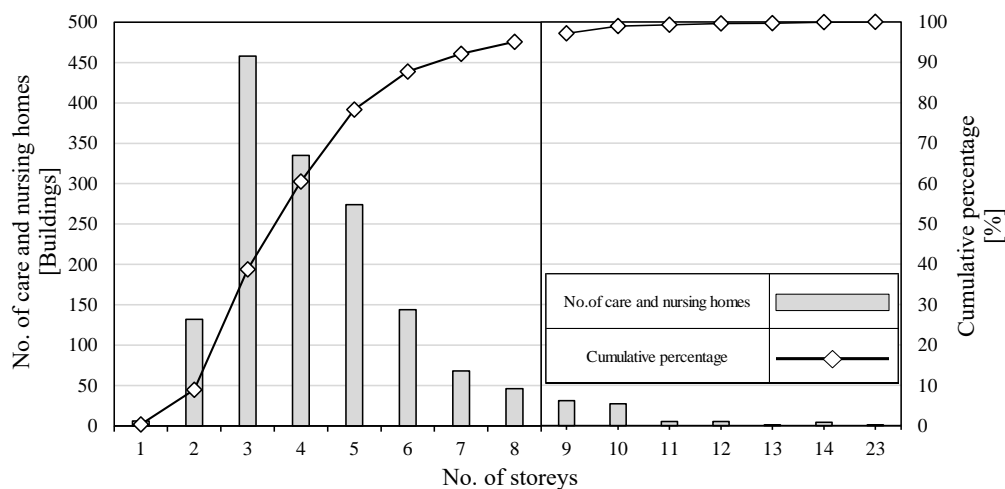
Fig. 5 Storey survey on care and nursing homes created by the authors based on 5) and 6)
(Total between Osaka City and Tokyo's 23 wards)

3.2 Experimental disposable underwear and determining a discharge volume

Two types of disposable underwear are used: a typical combined use of taped underwear and an incontinence pad (①[large]) by care and nursing homes; and sole use of an incontinence pad (②[small]). In addition, the discharge volume required for draining the experimental underwear from an experimental stirrer is set to 20L for [large] and 10L for [small], which are both conceivable drainage load conditions and design volumes of water for the drainage stack system (Table 1). Under these drainage load conditions, the verification of drainage performance is conducted in 3.3 and 3.4.

Table 1 Experimental disposable underwear and design discharge volumes

Usage	Experimental disposable underwear	Drainage amount
①Tape type + urine pad	Large (approx. 520g)	20L
②Urine pad only	Small (approx. 120g)	10L
Photos of disposable underwear [large]		Photos of disposable underwear [small]	
Before crushing	After crushing	Before crushing	After crushing

Note*1: Types of disposable underwear for adults include tape type and pants type, and these types may be used together with flat type and urine pads.

3.3 Planning and designing the horizontal fixture branch

The consideration of the horizontal fixture branch to be designed involves three types of horizontal fixture branch systems which have diameters of 50A and 75A and are connected to the experimental stirrer. The stirrer mimics the stirring section of a disposable underwear crushing/disposal machine. The drainage performance and carrying performance of these systems were evaluated. Fig. 6 shows the three types of horizontal fixture branch systems used for the evaluation which are: (a) straight pipe model; (b) model with equally-spaced bends; and (c) actual pipe model which would be used in a real building. Moreover, the items for evaluating the horizontal fixture branch of each system are shown in Table 2, where (2) the residue level represents the stagnant state of crushed disposable underwear which is determined with reference to Table 3.
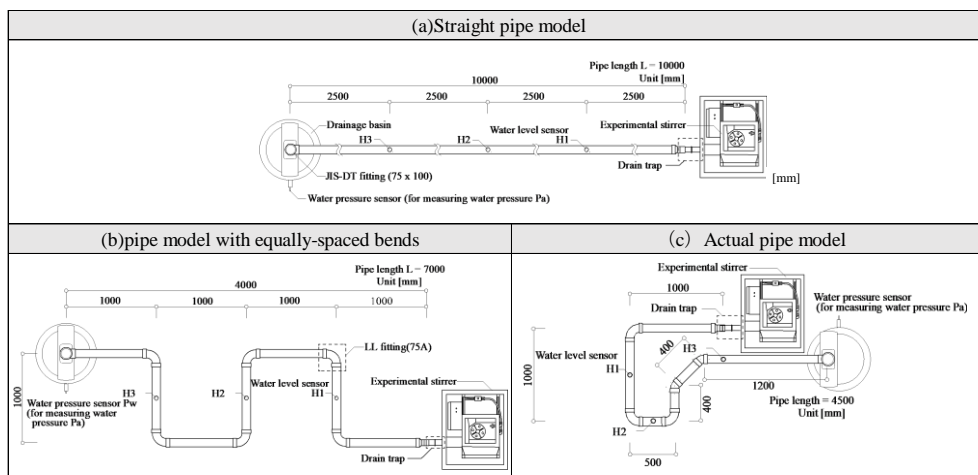
Fig. 6 Experimental horizontal fixture branch systems

Table 2 Drainage performance evaluation during horizontal fixture branch experiment

Evaluation item	(1) Stagnation range	(2) Residue level	(3)Discharge rate*
	[m]	[Ⅰ ,Ⅱ ,Ⅲ,Ⅳ]	[%]
Evaluation criteria	· Below ½ the pipe length	Levels Ⅲ or Ⅳ	Avg. is 90% or more
			Stagnation is cleared by draining 5 L additional water once
Evaluation item	(4)Fixture discharge characteristics*	(5)Internal water level	(6)Leading velocity*
	[L/s]	[mm]	[m/s]
Evaluation criteria	qd' [L/s] at the end	Max. water level is less than ½ of inner diam.	0.6 m/s or more (SHASE-S206)
	Discharge volume 20 L: 0.9 or more		
	Discharge volume 10 L: 0.3 or more	The drainage pipe is half full	

Note*: 5 attempts are made and average, min. and max. values are obtained. Evaluation items (1), (2) and (3) are determined, as appropriate, after each attempt.

Table 3 Residue level classification

Level	Ⅰ	Ⅱ	Ⅲ	Ⅳ
Length direction	Drainage water Main component :Plastic	Main component:Plastic+Pulp	Polymer	
Cross-section				
Photo				

Based on an overall understanding of the results of the experiment, Table 4 shows the results of the evaluation conducted for each of the evaluation items in Table 2. As shown in Table 4, in all of the pipe models, crushed disposable underwear did not become stagnant over any range exceeding the prescribed range which is half the length of the fixture discharge pipe. Moreover, the residue levels all met either level III or level IV which are defined in Table 3. Furthermore, the average crushed underwear discharge rate was approximately 90% or more, ensuring the carrying performance to be satisfactory, and even after the crushed underwear became stagnant, one flush using clean water (5L stored water) was enough to drain away the crushed underwear completely. As for the water levels in the pipes, the discharge volume of 20L completely filled the pipes with a 50A pipe diameter and caused blockage. In contrast, the discharge volume of 20L filled the pipes with a 75A pipe diameter only half or so, and maintained a half-filled flowing state, without resulting in blockage, ensuring smoother drainage than when applying the 50A pipe diameter. In addition, regardless of piping configuration, when the pipe diameter was 75A and the pipe gradient was 1/50, all the measurement items satisfied all the corresponding evaluation criteria.

Table 4 Verification results of drainage performance in horizontal fixture branches (horizontal fixture branch experiment)[7]

type	Diameter	Gradient	(1)Stagnation range	(2)Residue level	(3)Discharge rate	(4)Fixture discharge characteristics	(5)Internal water level	(6)Leading velocity
(a)	50A	1/50	○	○	○	○	×	○
		1/100	○	○	○	×	×	○
	75A	1/50	○	○	○	○	○	○
		1/100	○	○	○	○	○	○
(b)	50A	1/50	○	○	○	○	×	○
		1/100	○	○	○	×	×	○
	75A	1/50	○	○	○	○	○	○
		1/100	○	○	○	×	○	○
(c)	50A	1/50	○	○	○	×	×	○
		1/100	○	○	○	×	×	○
	75A	1/50	○	○	○	○	○	○
		1/100	○	○	○	○	○	○

※○ : The criteria in Tabel2 are met ※× : The criteria in Tabel2 are not met ※Overall determination based on the results using the 20L discharge volume

As a result of overall determination made on the basis of the results obtained above, the horizontal fixture branch to be planned and designed will have the following conditions: pipe diameter 75A; maximum total pipe length 7m; maximum no. of elbows 6; and pipe gradient not more than 1/1000 (recommended gradient 1/50).

3.4 Overview of drainage stack system experiment

(1) Determining pipe diameters for the drainage stack system

Fig. 7(1) shows the 8-storey experimental drainage stack system which is of a conceivable size. This experimental drainage stack system used for this study has been designed by applying the drainage load calculation using the fixture-unit rating, which is one of the drainage calculation methods suggested by SHASE-S 206[8], Japan. The design flow is shown in Table 5. The system adopts a loop vent system. The pipe diameter of the drainage stack is 100A, the pipe diameter of the house drain is 125A (with a minimum gradient of 1/50), and the pipe diameter of the loop vent pipe is 50A.

(2) Drainage performance verification of the design system

The 8-storey experimental drainage stack system was installed to the experimental tower shown in Fig. 7(2). The actual drainage loads shown in Table 1 were applied to carry out performance verification.

1) Drainage load conditions and measurement items

During this experiment, wastewater from the experimental stirrers was discharged from: the 8th and 7th floors; the 8th and 6th floors; the 6th and 5th floors; and the 4th and 3rd floors. Moreover, the drainage load conditions included combined drainage from two experimental stirrers, i.e., crushed disposable underwear-containing drainage loads, and clean-water-only drainage loads. As for the measurements made during the experiment,

2023 Symposium CIB W062 – Leuven, Belgium

the internal pipe pressure [Pa] of the horizontal fixture branch connected to the drainage stack at each floor, the seal loss [mm] of the trap disposed on the floor immediately below the floor where a drainage load was applied, and the inner water level fluctuation [mm] among different water level sensor points along the house drain were obtained. Thereafter, the distance [m] between internal water level points was divided by the difference in rising time [s] between waveforms when wastewater passed the water level points to obtain the leading velocity [m/s]. In addition, the discharge rate [%] of crushed disposable underwear at the end point of the house drain was obtained, and the residue level was also measured when the crushed disposable underwear became stagnant in the house drain. These measurement items are referred to as drainage performance evaluation items.

(2)Experimental drainage stack system

(1)Experimental tower
(Kanto Gakuin University)
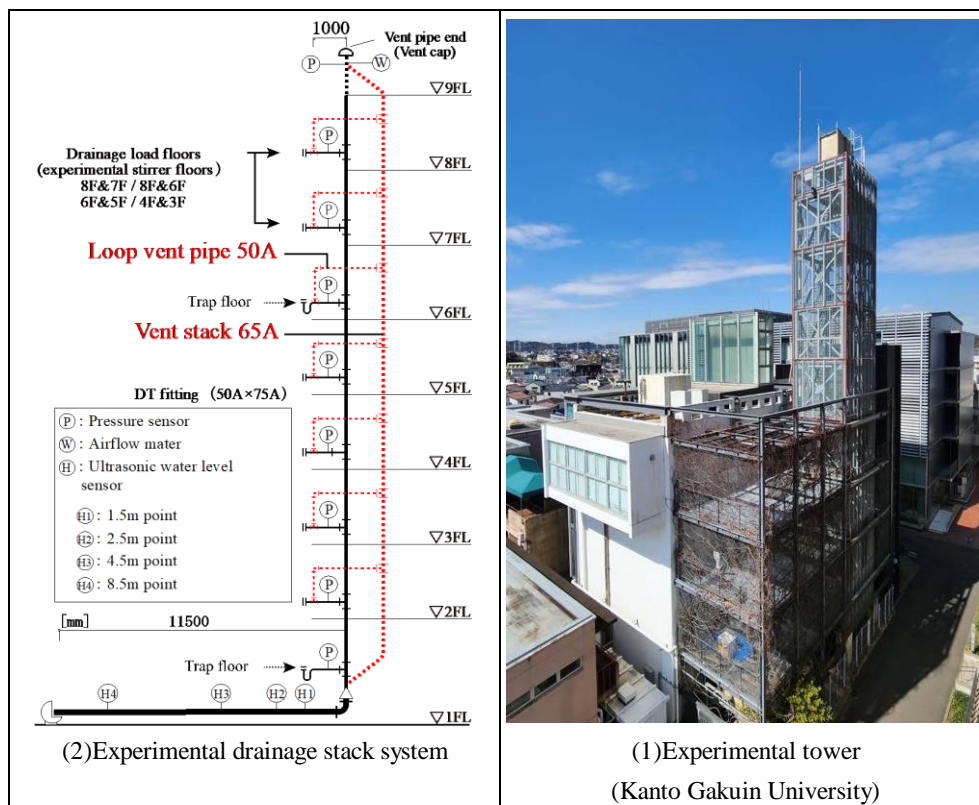
Fig. 7 Experimental drainage stack system

Table 5   Steps of determining drainage vent pipe[8]

1. Calculate the number of experimental stirrer fixture-unit values as load factors	

Max.fixture discharge flow rate of the 20L discharge volume $qmax = 2.51[\text{L/s}]$

is applied to $\dfrac{2.51}{0.48^{*1}}$ <6

2. Determine pipe diameters using the drainage load calculation using the fixture-unit rating

(1) Drainage stack total	$6 \times 8^{*2}= 48$	$<$	60(75A)	$=$	<u>100A</u> [*3]
(2) House drain					<u>125A</u>
(3) Vent stack(total length 27m)	48	$<$	100(65A)	$=$	<u>65A</u>
(4) Loop vent pipe	6	$<$	10(40A)	$=$	<u>50A</u> [*4]

*1 The fixture-unit values were calculated by applying the maximum discharge flow rate 0.48[L/s] for washbasins, which is defined as fixture unit 1.

*2 Coefficient 8 corresponds to 8-storey building to which the system is applicable.

*3 A calculations using the steady flow rate method was made at the same time, resulting in 100A, which was applied in the experiment.

*4 One size larger 50A was adopted for providing surplus ventilation capacity.

2) Drainage performance evaluation items

Table 6 shows the evaluation items, for which the experiment was conducted using the drainage stack system, and the experiment results[9]. The internal pipe pressure was measured and its minimum value (Psmin) was approximately -350Pa which is within the reference range of ±400Pa[10] for internal pipe pressures in drainage stack systems in accordance with SHASE-S 218 in Japan. The seal loss of the trap disposed on the floor immediately below the floor where a drainage load was applied was also measured, and its maximum value was measured as 13mm, satisfying the SHASE-S 218 requirement of less than half the seal depth. Meanwhile in the house drain, the leading velocity of 0.6m/s specified by SHASE-S 206[8], which is the minimum value required for carrying sewage, was exceeded under all the applied conditions. The average discharge rate was approximately 96%, significantly surpassing the criterion, with no sign of crushed disposable underwear stagnating in the house drain. As for the crushed disposable underwear that adhered to the insides of the stirrer and the pipe, one flush with stored water completely carried the crushed disposable underwear out of the pipework. In evaluating this designed experimental drainage stack system, the experiment results satisfied the criteria for all the evaluation items.

Table 6 Verification results of drainage performance of drainage stack system (drainage stack experiment)[9]

Evaluation item	(1) Internal pipe pressure [Pa]	(2) Seal loss [mm]	(3) Internal water level [mm]
Evaluation criteria	・Within ±400Pa (SHASE-S 218 standard)	・Not more than 25 mm (SHASE-S 218 standard)	-
Experiment result[*1]	Psmin : -350Pa Psmax : 50Pa	Seal loss : 13mm	-
Evaluation result	○	○	-
Evaluation item	(4) Leading velocity [m/s]	(5) Discharge rate [%]	(6) Residue level [I , II ,III,IV,]
Evaluation criteria	・0.6 m/s or more (SHASE-S 206 standard)	・Average value: 90% or more ・Complete draining of stagnant matters by 1 flush using 5L stored water (clean water)	・Level III or IV
Experiment result[*1]	Minimum flow rate: 1.26m/s	Average value: 96%	Level III or IV
Evaluation result	○	○	○

[*1] ○: The evaluation criteria are met. ×: The evaluation criteria are not met.

As a result of overall determination made on the basis of the results obtained above, the design conditions were set as follows: loop vent system to be adopted; drainage stack diameter 100A; loop vent pipe diameter 50A; house drain diameter 125A (minimum gradient 1/150); and house drain length not more than 10m from the drainage stack, where provided with a disposable underwear collection point (the dehydrate-and-separate section).

On the basis of the foregoing results, Fig. 8 shows the result of adding the design conditions to the evaluation items in the design flow shown in Fig. 4. The steps of designing the disposable underwear crushing/disposal system and the design conditions are summarised below.

3.1 Determine the size of a facility for design
・Conceivable no. of storeys: max. of 8
・Independent drainage system using dedicated pipework

▼

3.2 Determine a discharge volume for design
【Design discharge volume】
・Underwear [large]: 20L
・Underwear [small]: 10L

▼

3.3 Plan and design the horizontal fixture branch
・Pipe diam. 75A
・Total length not more than 7m in
・No. of elbows not more than 6
・Min. gradient not more than 1/100

▼

3.4 Plan and design the drainage stack system
・Drainage stack diam. 100A (horizontal fixture branch diam. 75A)
・Loop vent pipe diam. 65A
・House drain diam. 125A
・The dehydrate-and-separate section is provided along the house drain not more than 10m away from the drainage stack.

Fig. 8 Design flow and key factors

5. Conclusion

This report describes the process of planning and designing a disposable underwear crushing/disposal system which has been developed for the elderly and which is to be introduced to care and nursing homes having mid-rise (8-storey) buildings with high marketability. The process also specifies design conditions including equipment specifications and conditions for the horizontal fixture branch, the drainage stack, the house drain, and the vent stack, which have been determined on the basis of the experiment results.

The next step will be to, on the basis of the acquired knowledge, introduce the disposable underwear crushing/disposal system to an actual care and nursing home and conduct verification on the system.

6.References

1) UN, World Population Prospects：The 2019 Revision

2) Statistics Bureau, Ministry of Internal Affairs and Communications, Japan: Population Estimates, 2020.9

3) Price Hanna Consultants Announces Release of New Report, Adult Diapers Market Value 2016-2021 in million USD

4) Sewerage and Wastewater Management Department, Water and Disaster Management Bureau, Ministry of Land, Infrastructure, Transport and Tourism, Japan: Study Roadmap toward Acceptance of Paper Diapers in Sewerage Systems, 2018.9

5) Bureau of Social Welfare and Public Health, Tokyo Metropolitan Government: Bureau of Social Welfare and Public Health, Lists of Institutions and Facilities for the Elderly

6) Facilities for the Elderly Group, Facilities for the Elderly Section, Policies and Measures for the Elderly Department, Health and Welfare Bureau, City of Osaka: A List of Long-term Care Health Facilities under the Jurisdiction of City of Osaka

7) Ayaka Kimura, Masyayuki Otsuka, Michitaro Maki, Yusuke Kubota: Development and Drainage performance Evaluation of Disposable Underwear Shredder System Applicable Caring Facilities. The 46th International Symposium CIB W062 2021

8) The Society of Heating, Air-Conditioning and Sanitary Engineers of Japan(SHASE): SHASE-S206-2019 "Plumbing Code"

9) Yuto Ino, Masyayuki Otsuka, Ayaka Kimura, Michitaro Maki: Drainage performance evaluation and design considerations of drainage stack system with disposable underwear crushing/disposal system installed thereto. The 47th International Symposium CIB W062 2022

10) The Society of Heating, Air-Conditioning and Sanitary Engineers of Japan(SHASE): SHASE-S218-2021 "Testing Methods of Flow Capacity for Drainage Stack System"

7.Presentations of authors

Yuto Ino is a graduate student at the Otsuka Laboratory of Kanto Gakuin University, Japan. He has been mainly involved in research on developing crushing/disposal systems for used disposable underwear. Ino is a member of AIJ (Architecture Institute of Japan) and a member of SHASE (The Society of Heating, Air-Conditioning and Sanitary Engineers of Japan).

Masayuki Otsuka is a professor at the Faculty of Architecture and Environment, Kanto Gakuin University, Japan. He has been conducting a wide range of research on water supply, drainage and sanitary equipment. Otsuka is a member of AIJ (Architecture Institute of Japan). He also fulfilled his role as the Chairperson of SHASE (The Society of Heating, Air-Conditioning and Sanitary Engineers of Japan).

When Ayaka Kimura was a graduate student at the Otsuka Laboratory of Kanto Gakuin University, Japan, she was mainly involved in research on living space hygiene contributory to preventive measures against COVID-19. Kimura currently works for TEPCO Energy Partner, Inc., and is engaged in work in relation to power demand and energy conservation.

Michitaro Maki works for LIXIL Corporation and is engaged in developing a crushing/disposal system for used disposable underwear.
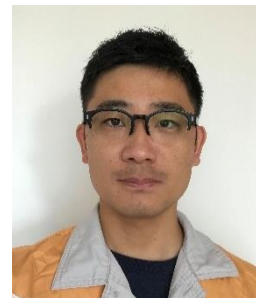
Aqua Container House for natural disasters

Part 2 Suitability evaluation by water use experiment

Masaaki Hashimoto (1), Hiroshi Iizuka (2),

Kyosuke Sakaue (3), Takehiko Mitsunaga (4)

(1) masaaki@hat.co.jp

(2) iizukah@nikken.jp

(3) sakaue@carrot.ocn.ne.jp

(4) mitsunaga@meiji.ac.jp

(1) Hashimoto Sogyo Holdings Co. Ltd., Japan

(2) Nikken Sekkei Construction Management, Inc., Japan

(3) (4) Meiji University, Japan

Abstract

In Japan, natural disasters such as torrential rains as well as earthquakes frequently occur. Water supply and sewerage systems stop functioning in large-scale natural disasters, making it impossible to use sanitary water. On the other hand, in countries where water supply and sewerage systems are not developed, unsanitary toilets and water usage are seen as problems. To address these situations, we have developed a mobile hygienic Aqua Container House. ACH consists of Water-use Container House and Infrastructure Container House. In the first report, we introduced the concept and components of ACH, including residential container houses, and described the results of our study on the characteristics and capacity of each component. After that, we used the main equipment of the Water Use CH and the Infrastructure CH, measured the amount of water before and after water purification and wastewater treatment, and tested the

water quality. The second report describes the details and the results of the study.

Keywords

Natural disasters；unsanitary areas；movement；water use containers；measurement of water quantity and quality；water use questionnaires

1 Introduction

Large-scale natural disasters in Japan include earthquakes, tsunamis, and floods. A tsunami occurs after an earthquake. Floods are caused by typhoons and torrential downpours (local downpours). There are also landslide disasters in which houses near mountains collapse due to landslides caused by heavy rain. Torrential rain occurs every year. There are four plates around the Japanese archipelago, and earthquakes have occurred frequently. In 2016, the Cabinet Office announced the probability of occurrence within 30 years [1]. These overviews are shown in Figure 1 and Table 1. Regarding the Nankai Trough earthquake, the Earthquake Research Committee has raised the probability of a large-scale magnitude 8-9 earthquake occurring within 40 years to 90% in 2022. There is an urgent need for countermeasures against earthquake disasters. Japan has many large-scale disasters and can be called a country of disasters. In these disasters, the water supply and sewage systems often stop functioning due to the damage. Under such circumstances, not only damaged houses but also normal houses and evacuation facilities will not be able to use water, which will hinder their lives. Water supply after a disaster has been handled by water trucks and disaster toilets, but there are many inadequacies and unsanitary conditions have arisen.

On the other hand, in developing countries, there are many areas without water supply and sewerage, leading to unsanitary living. In order to improve this situation, there is a demand for an independent means of water usage that does not depend on water supply and sewerage.

In response to the above requests, we have developed an Aqua Container House (ACH) that can be transported and is compatible with natural disasters and unsanitary areas. ACH has two basic configurations, Water-use CH and Infrastructure CH, but Residential CH can also be added. Water-use CH is equipped with a washbasin, a sink, and a shower. A water tank, a water purifier, and a storage battery are installed in the infrastructure container. Besides, a waste water treatment device is installed. An ordinary EV is used to supply power to the storage battery. These are collectively called

2023 Symposium CIB W062 – Leuven, Belgium

the ACH system. Water-use CH is already completed. Then, we connected the main equipment of the Infrastructure CH and conducted a water usage experiment. In the first report, we introduced the concept and components of ACH, including residential container houses, and discussed the results of our study on the characteristics and capacity of each component [2].

After that, we conducted a subject experiment on the feeling of water use using the main equipment of the Water-use CH and the Infrastructure CH, measured the water quality and volume in water supply purification and wastewater treatment, and conducted a questionnaire survey on water use. The second report describes the details and the results of the study.
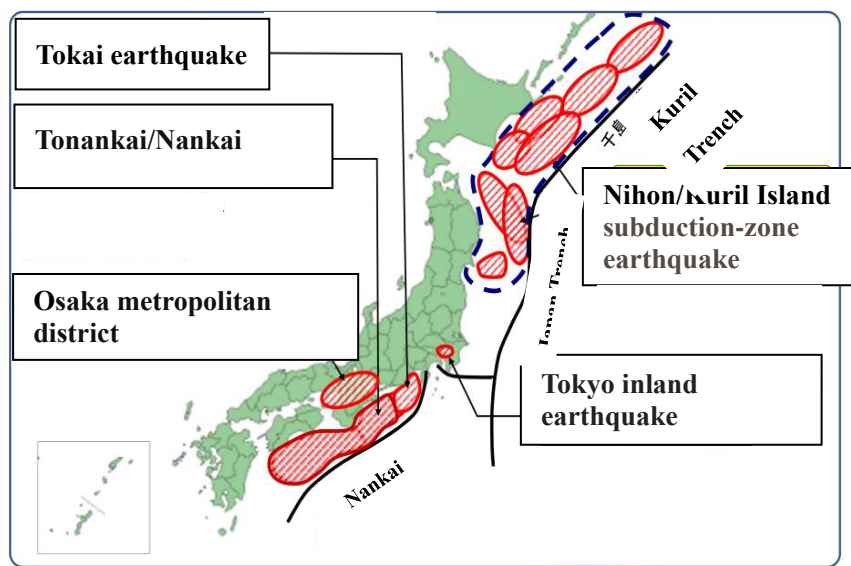
Figure 1-Expected large-scale earthquakes [1]

Table 1-Probability of earthquake occurrence within 30 years [1]

Expected large-scale earthquakes	Probability of earthquake
Tokai earthquake	87%
Tonankai earthquake	70%
Nankai earthquake	About 60%
Middle District/Osaka metropolitan district inland earthquake	-
Nihon/ Kuril Island subduction-zone earthquake	99%
Tokyo inland earthquake	About 70%

2 ACH

2.1 Water use in water-use containers

The ACH consists of the Water-use CH and the Infrastructure CH. The Water-use CH is equipped with a washbasin, a sink, a shower room, a WC (with pressure pump), a solar panel, tatami beds, a table and chairs. Floor plan and inside elevation of the Water-use CH are shown in Figure 2, and Interior view is shown in Figure 3. The Infrastructure CH is equipped with a water storage tank, a water purification system, and a water supply pump for water supply, a wastewater treatment system (septic tank) and a drainage pump for wastewater, and a solar panel and storage battery for power supply. Floor plan and inside elevation of Infrastructure CH are shown in Figure 4.
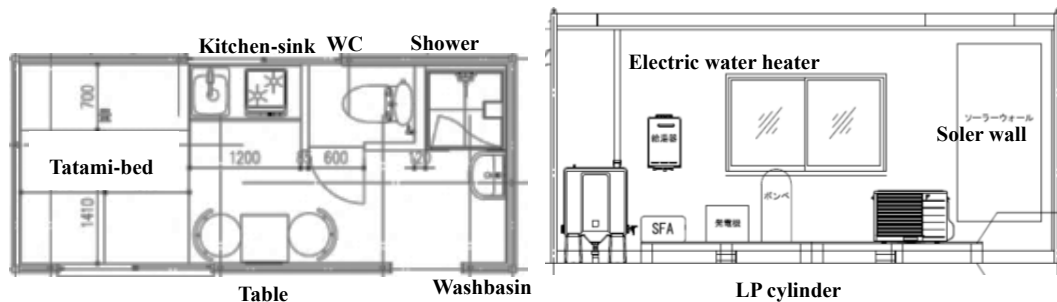
Figure 2-Floor plan and inside elevation of water-use CH

Washbasin Shower-room Toilet Kitchen-sink Tatami-bed

Figure 3-Interior view of water-use CH

(a) Floor plan (b) Elevation
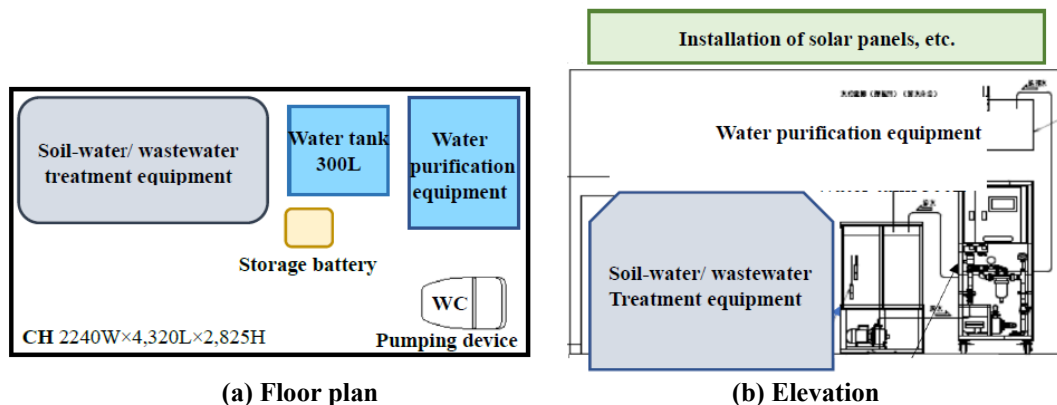
Figure 4-Floor plan and inside elevation of Infrastructure CH

2023 Symposium CIB W062 – Leuven, Belgium

3 Water use experiment

Subjects were asked to wash their hands, wash dishes, and use the toilet in the water-use CH, and a questionnaire survey was conducted on the usability and analyzed the water quality.

3.1 Experimental method

Water-use experiment was conducted by connecting a raw water tank, a filtration device/water purification device, a purified water storage tank, a pressurized water supply pump, a drainage pump, and a septic tank (combined treatment) to be installed in Infrastructure CH to Water-use CH. Rainwater is used as raw water, and after storing in a rainwater storage tank, it is supplied to a filtration device by membrane filters and a water purification device by UV sterilization at a constant frequency. Figure 5 shows the raw water tank, filtration system and water purification system. Figure 6 shows a septic tank that treats wastewater after water use. Figure 7 shows the system diagram of the ACH system and the flow rate measurement points and water quality test sampling points.

Figure 6-Septic tank

Figure 5-Raw water tank, filtration device / water purification device
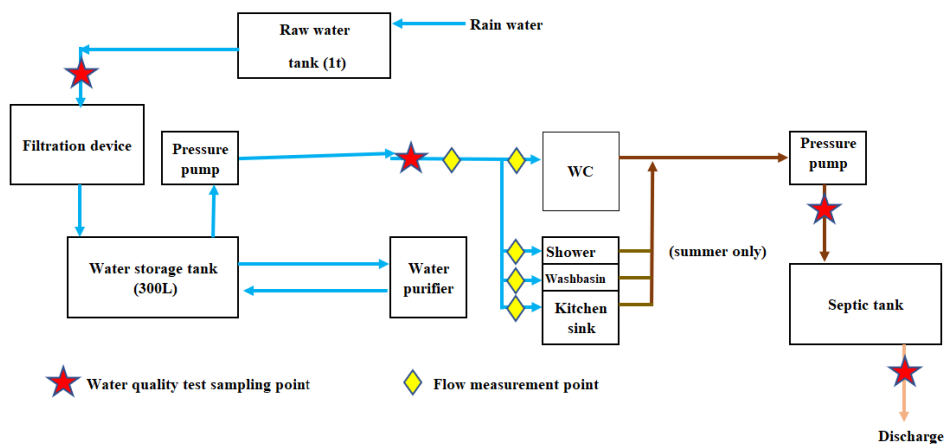
Figure 7-System diagram and measurement points of ACH system

3.2 Questionnaire method

We asked the subjects to wash their hands, wash the dishes, and use the toilet bowl in Water-use CH, and conducted a questionnaire about the feeling of use. The subjects

Table 2-Questionnaire items

Wash basin	Kitchen
1. Sticky feeling when using water in hand washing 2. Sticky feeling when using soap in hand washing 3. Feeling sticky when using water in facial cleaning 4. Sticky feeling when using soap for face washing 5. Odor in face wash 6. Sensation of taste in gulls	1.Dirt removal in dishwashing (Using detergent)
	Toilet
	1. Type of filth 2. Odor

were 9 males) and 3 females. Table 2 shows the contents of the questionnaire.

3.2 Experiment results

3.2.1 Amount of water used and water quality

(1) amount of water used

Concerning usage conditions, the washbowl was mainly used for hand washing and gargling, the kitchen sink was used for cleaning bento containers, and the toilet was used for urination. The amount of water used was generally about 3-4 L/use in the toilet, about 15 L/use in the shower, about 0-4 L/use in the washbasin and about 1-6 L/use in the kitchen sink.

(2) Water quality

Water was collected from rainwater tanks, water purifier feed pipes, and septic tank drain pipes. There are 51 items in the water quality standards for tap water. Of these, 16 major items such as general bacteria, E. coli, pH, turbidity, iron, copper, zinc, and lead were selected as inspection items. For septic tank effluent, two inspection items, pH and BOD, which are water quality control standard survey items, were used.

Table 3 shows the turbidity being 0.3 lower than the standard values, the standard values were cleared. Table 4 shows the inspection results for the water purifier feed pipe. Almost all items were improved compared to the rainwater tank (Table 3). Other than the pH being 0.2 lower and the turbidity being 0.3 lower than the standard values, the

standard values were cleared. Only the pH value was 0.1 lower than the reference value. It was clear that the water quality was suitable for drinking. The test results of the effluent from the septic tank were 8.0 for pH against the standard value of 5.8-86, and 10 mg/L for BOD against the standard value of 20 mg/L or less. Since only urine was processed, the BOD was extremely small. The septic tank is judged to be functioning properly.

Table 3-Inspection results in rainwater tank

Inspection item	Inspection results	Standard value	unit
general bacteria	Not detected	under 100	Quantity/mL
Escherichia coli	Not detected	Not detected	-
nitrite nitrogen	less than 0.004	less than 0.004	mg/L
Nitrate nitrogen / nitrite nitrogen	0.48	less than 10	mg/L
Chloride ion	2.8	less than200	mg/L
Organic matter (TOC amount)	0.6	less than 3	mg/L
pH value	<u>5.6</u>	5.8 to 8.6	-
taste	Unanalyzable	No abnormality	-
odor	No abnormality	No abnormality	-
Chromaticity	1.5	less than 5	degrees
Turbidity	<u>2.3</u>	less than 2	degrees
iron and its compounds	less than 0.03	less than 0.3	mg/L
copper and its compounds	less than 0.1	less than 1.0	mg/L
zinc and its compounds	less than 0.1	less than 1.0	mg/L
lead and its compounds	Not detected	less than 0.01	mg/L
Evaporation residue	less than 5	less than 500	mg/L

Table 4-Inspection results in water supply pipe of water purifier

Inspection item	Inspection results	Standard value	unit
general bacteria	Not detected	under 100	Quantity/mL
Escherichia coli	Not detected	Not detected	-
nitrite nitrogen	less than 0.004	less than 0.004	mg/L
Nitrate nitrogen / nitrite nitrogen	0.39	less than 10	mg/L
Chloride ion	1.1	less than200	mg/L
Organic matter (TOC amount)	0.6	less than 3	mg/L
pH value	<u>5.7</u>	5.8 to 8.6	-
taste	Unanalyzable	No abnormality	-
odor	No abnormality	No abnormality	-
Chromaticity	less than 0.5	less than 5	degrees
Turbidity	less than 0.2	less than 2	degrees
iron and its compounds	less than 0.03	less than 0.3	mg/L
copper and its compounds	0.8	less than 1.0	mg/L
zinc and its compounds	0.2	less than 1.0	mg/L
lead and its compounds	0.099	less than 0.01	mg/L
Evaporation residue	less than 5	less than 500	mg/L

3.2.2 Feeling of using water

Figure 8 shows the feeling (taste) of gargling in the washbasin. Figure 9 shows the results of a questionnaire on water usage and soap usage for hand washing and face

washing. As for the stickiness in hand-washing, the majority of respondents gave positive evaluations for both using water and using soap. The taste of gargling was the majority, and it was pointed out that it tasted like lactic acid. It is evaluated that there is no problem in washing the body other than gargling and drinking. Figure 10 shows the results of a questionnaire survey on the state of foaming and dirt removal when cleaning lunch box containers (using detergent) in the kitchen sink. Somewhat bad, but accounted for the majority. The type of detergent may have had an effect.

(1) gargling   **(2) After gargling**

Figure8-Taste in gargling

(1) Stickiness after hand washing (water)   **(2) Foaming in hand washing (soap)**

(3) Stickiness after hand washing (soap)   **(4) Stickiness after face wash (water)**

Figure9-Usability in hand washing and face washing

(1) bubbling (2) dirt removal
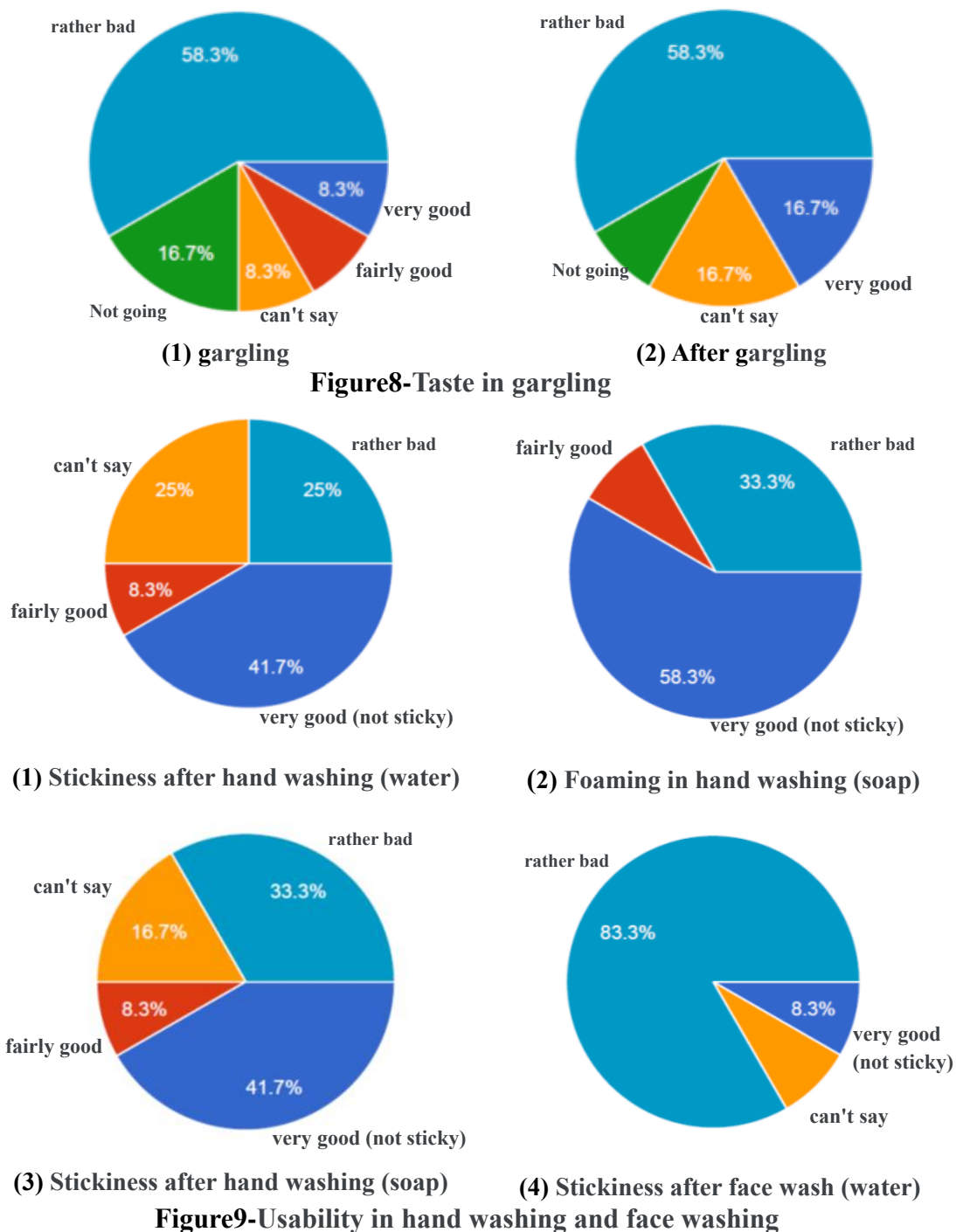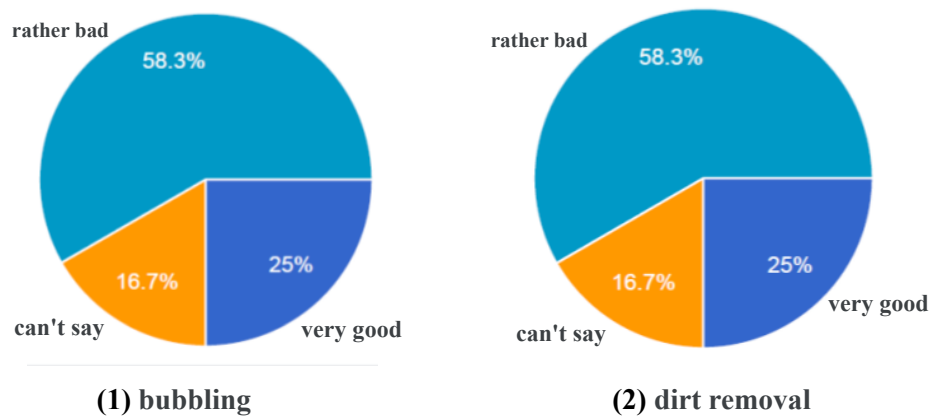
Figure10-Usability in washing lunch box containers

5 Conclusion

Japan is a country prone to natural disasters such as earthquakes, and there are many cases where water supply and sewerage systems cannot be used. On the other hand, in developing countries, there are many areas where water supply and sewage systems are not developed. To address this, we developed his mobile ACH system. Since it does not rely on water and sewage, it is positioned as part of LCP (Life Continuity Planning) and SDGs (Sustainable Development Goals). It is also compatible with UN water sanitation activities as it helps improve unsanitary conditions. Water-use CH has already been produced. By connecting the main equipment of Infrastructure CH to this, we conducted a misuse water use experiment, measured the amount of water and tested the water quality (mainly 16 items), and conducted a questionnaire survey on usability.

As a result, although the taste was strange, it was drinkable, suitable for cleansing the body, and there were no particular problems with the feeling of use. In addition, the water quality after wastewater treatment also met the wastewater management standard.

In the future, we plan to complete the Infrastructure CH and move a long distance to conduct a demonstration experiment of water use.

6 Reference

[1] Headquarters for Earthquake Research Promotion: Derivation probability of assumed large-scale earthquake。 (2017)

[2] Masaki Hashimoto, Hiroshi Iizuka, Kyosuke Sakaue: Concept and Configuration of Aqua Container House for Disaster Response, Proceedings of CIB W 62, (2022)

7 Presentation of Authors

Masaaki Hashimoto serves as the chairman of Hashimoto Sogyo Holdings Co. Ltd., a general trading company with a building service, and is a doctoral student at Faculty of Science and Technology, Keio University. His fields of specialization include the management and the technology development of building services and plumbing systems. In recent years, he has devoted himself to human resource development and international cooperation.

Hiroshi Iizuka belongs to Nikken Sekkei Construction Management, Inc.. His fields of specialization include the design of building services. Recently, he has been active in the technical development and international cooperation of plumbing systems.

Kyosuke Sakaue (Dr. Eng.) is a professor emeritus at Meiji University. His fields of specialization include water environment, building services engineering and plumbing system. In recent years, he has been working on the development and dissemination of extended drainage systems and the performance regulation of Plumbing Standards.

Takehiko Mitsunaga (Ph. D) is a senior assistant professor at Department of Architecture, School of Science & Technology, Meiji University. His fields of specialization include water environment, building services engineering and plumbing system.

Role of Discharge Water Temperature Upon Hydraulic Performance of High-Rise Wastewater Drainage Stacks

Colin Stewart

School of Energy, Geoscience, Infrastructure and Society (EGIS), Heriot Watt University, Edinburgh EH14 4AS, UK;
colin.stewart@hw.ac.uk

High-rise building wastewater stacks are normally designed in accordance with building standards agency design codes. These codes recommend stack and vent lines are sized to encourage co-current air-water annular flow. This flow regulates system pressures and reduce risk of siphonage of water trap seals. However, design codes make no explicit statements regarding effect of discharge water temperature upon this system performance. To investigate impact of water temperature, a series of experimental tests has thus been performed in a 100mm ID, 6m tall laboratory rig. The results show that such that the air and water flowing in a stack rapidly reach thermal equilibrium, suggesting that the air-water interface in the annular flow has a large heat transfer coefficient. The mass flowrate of air drawn into the stack is also sensitive to temperature differences between feed streams. However, temperature differences in streams appear also to effect air density, such that there is minimal impact upon in-situ air flowrates and upon hydraulic pressure profiles. density changes, such that discharge water temperature has a minimal impact upon the in-situ air-to-water flowrate and a minimal impact on the hydraulic pressure profile.

1. Introduction

Vertical wastewater stacks admit and dispose of the water streams which produced by domestic appliances. These systems also admit air, in order that these streams drain in an efficient and orderly fashion. The stack and the parallel air vents component are normally sized according to building standards agency design codes ([e.g., [1], [2], [3], [4]). When sized according to this guidance, these components admit sufficient air to promote downwards air-water annular flow. A strong intake of air promotes system operation at low pressure, and it enable stacks to be constructed from relatively inexpensive materials.

Generally, the transport of air and water in an annular flow geometry creates a significant pressure gradient, and generates substantial wall fraction. Within a vertical pipe, this flow geometry ensures that potential energy held in the wastewater stream is largely dissipated, and consequently, that the stack operating pressure is regulated. The integrity of a wastewater system can therefore normally be maintained by installing shall water trap seals at appliance outlets (operating water depth in the 25mm – 50mm range). These seals are normally sufficiently deep to resist siphonage (provided stack pressure excursions do not exceed ±50 mm H_2O) and thus, prevent release of potentially contaminated droplets and air as evidence suggests to have occurred during recent COVID-19 outbreaks ([5], [6]). However, the development of design codes is based primarily on tests which were performed in the 1940-1970's era, and many limitations in these test programs have been highlighted ([7]). There is particular concern that core tests have been performed with test rigs which are of limited height; that the underlying physics of the annular flow mixture which tends to be generated in stacks is incompletely understood, and that ability to regulate system pressure becomes increasingly as stack height and water discharge flowrate are increased.

Another potentially significant factor in system performance standards is the *temperature* of the discharge water stream (or more specifically, the *difference in temperature* between the feed water and feed air streams). There is, notably, no discussion of this potential performance factors within design

codes ([1] – [4]). This absence of discussion has motivated the construction of a test rig and the carrying out of exploratory tests to investigate potential impact of water temperature on the system performance. In the sections that follow the experimental test rig and an experimental test sequence are described, background theory is presented, experimental results are presented, and experimental results are interpreted based on background theory and sample calculations. The results suggest that while the water temperature influences air intake to the stack, water temperature does *not* affect volumetric flowrates of air flowing in stacks under in-situ conditions, and also does *not* strongly influence hydraulic pressure profiles.

2. Test Apparatus and Procedure

A series of experimental tests have been performed using a flow loop constructed in the EGIS water laboratory (Heriot-Watt University), illustrated in Figures 1a and 1b. In this loop water is pumped from a sump tank to the upper end of a 5.4 m long, 100 mm ID vertical test section, then discharged through a 45° angled tee shown. The water is commingled with an air supply which is drawn in freely from atmosphere through an extended intake vent. The water and air form an annular flow within the test section which then passes through a 87° angled bend into a 3-metre drain section. At the exit from this drain section water is returned to the sump while the air is ejected to atmosphere. The system is instrumented with sensors detailed in Table 1, allowing monitoring of discharge flowrate (Q_w), inlet air velocity ($U_{a(i)}$), fluid temperatures at inlets and outlets ($T_{a(i)}, T_{w(i)}, (T_{a(o)}$ and $T_{w(o)})$ and wall pressures in the wet stack (P_o to P_6). Note that while the measurements of water flowrates, air velocities and temperatures are very accurate, the measurement wall pressures in the two-phase flow region of the test section is considerably less precise (the flow is subject to swirl and to surges, and sensor output is sensitive to *mounting location* and to thermal stresses induced in pipework, and pressure excursions arising from water discharge are generally *very small*). Nevertheless the data is sufficiently reliable, for purpose of this study, to allow meaningful conclusions to be drawn.

(2.1 Test Procedure)

The sump tank was filled with warm water taken from a nearby tap at a 45°C and, over a period of 24 hours, allowed to cool slowly to ambient temperature. This cooling water was used to perform four sets of experimental tests detailed in Table 2. Each test commences with water being circulated through the test section at a 'peak rate' of approximately $Q_w = 5$ l s^{-1} while air is drawn in freely from atmosphere through the intake line. Once steady flow establishes, fluid temperatures at inlets and outlets are recorded ($T_{a(i)}, T_{w(i)}, T_{a(o)}$ and $T_{w(o)}$). The water flowrate is then stepped down a reduced rate $Q_w \sim$ 2 l s^{-1} though a series of steps undertaken at intervals of approximately 30 seconds, whilst water flowrate, inlet air velocity and pressure data are collected from sensors. On the first day of testing three such test were performed: a 'hot water' set of tests ($n_i = 5$ water flowrates), a 'warm water' set of tests ($n_i = 5$ water flowrates) and a 'cool water' set of tests ($n_i = 5$ water flowrates). The water in the sump was then left overnight to cool fully to ambient temperature. On the following day, a "cold water" set of tests was performed ($n_i = 10$ water flowrates). The ambient air temperature and feed water temperatures for each set of tests is are summarized Table 2. Note that the difference in the feed stream temperatures $T_{w(i)} - T_{a(i)}$ is positive for the first three tests, but negative for the final test, i.e. water eventually cools to below the ambient air temperature.

Figure 1 : Experimental Test Facility: Schematic Drawing and Image
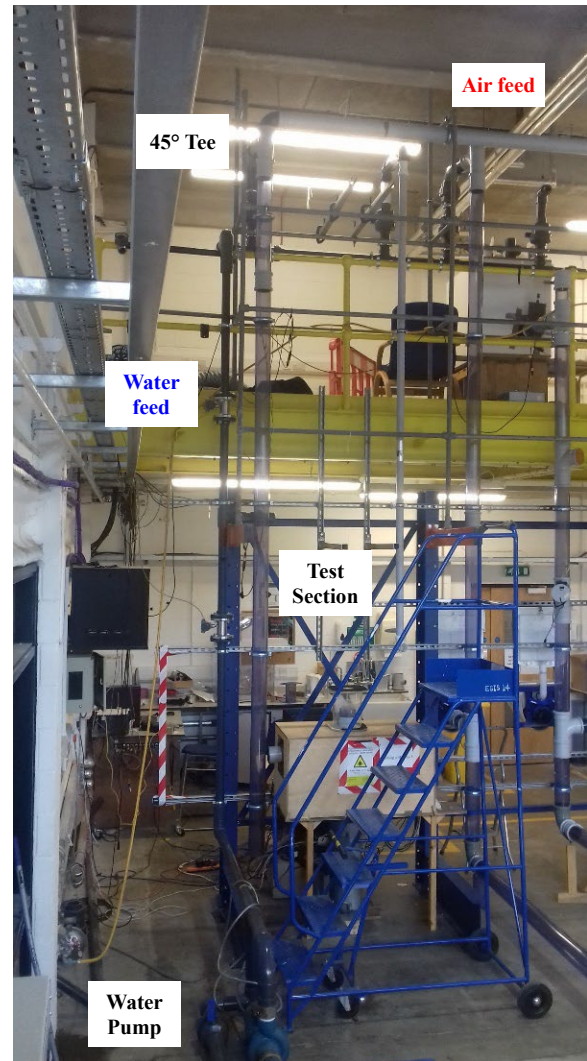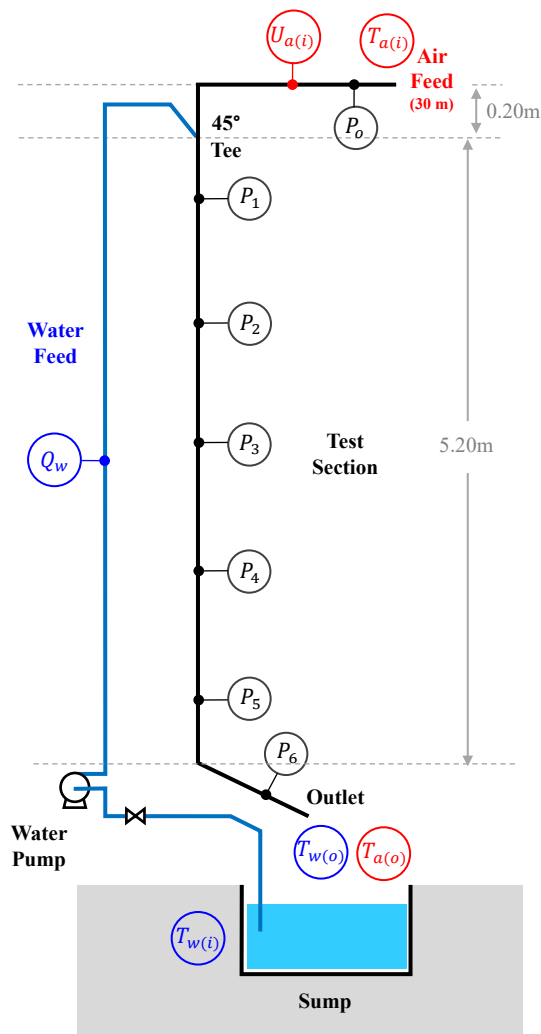
Table 1: Instrumentation Details

Measurement		Sensor Type	Notes
Water Flowrate	Q_w	BLFT-50 (Bell Flowmeters)	$4 – 40$ m^3 range, with 1% accuracy.
Inlet Air Velocity	$U_{a(i)}$	AV-D Hot Wire Anemometer (Sontay)	$0 – 4$ m s^{-1} range with 1% accuracy. Device installed 10m upstream of the 45° tee
Wall Pressures	P_o	HDIM-100D (First Sensor)	P_o is installed in the dry piping above the 45° tee.
	P_1 to P_6	CTE7000-10 (First Sensor)	P_1 to P_5 are flush-mounted to stack vertical test section at evenly-spaced intervals (distances z = 0.52, 1.56, 2.60, 3.64, 4.68 m from tee)*. P_6 is flush-mounted to the upper wall of drain section (0.50m downstream of the base elbow)
Fluid Temperatures	$T_{a(i)}$, $T_{w(i)}$ $T_{a(o)}$, $T_{w(o)}$	Techpel 870 Thermocouple	Hand-held thermocouple with 1°C accuracy. Temperatures are recorded for the for maximum water discharge cases, at start of each test, only.

*Note: The equivalent vertical elevations of P_1 to P_5 sensors are h = 4.68, 3.64, 2.60, 1.56, 0.52 m.

Table 2: Experimental Tests: Key Data

Series		'Hot Water' Tests	'Warm Water' Tests	'Cool Water' Tests	'Cold Water' Tests [1,2]
Max/min water flowrates (no of flowrate steps)		$5.2 \rightarrow$ $2.2\,\mathrm{l\,s^{-1}}$ $(n_i = 5)$	$5.3 \rightarrow$ $2.5\,\mathrm{l\,s^{-1}}$ $(n_i = 5)$	$5.4 \rightarrow$ $2.9\,\mathrm{l\,s^{-1}}$ $(n_i = 5)$	$5.1 \rightarrow$ $1.4\,\mathrm{l\,s^{-1}}$ $(n_i = 10)$
Water feed temperature	$T_{w(i)}$	42°C	35°C	29°C	16°C
Air feed Temperature	$T_{a(i)}$	18°C	18°C	18°C	21°C

Note 1: 'Cold Water' tests performed on the following day.

Note 2: As part of 'cold water' tests, the feed of air was to the test section disrupted to assess system response. This disruption is clearly visible in Figure 2(d) but is not relevant to analysis of results.

3. Theoretical Background

The experimental tests generate sets of samples of steady-state flow within the test section. The feed mass flowrates, feed superficial velocities, and feed volumetric flowrates for each steady-state flow sample are related by the expressions:

$$\dot{m}_w = \rho_w U_w = \rho_w Q_w / A$$

$$\dot{m}_a = \rho_a U_a = \rho_a Q_a / A$$

(1)

The water phase is incompressible, and its density has relatively weak dependency on temperature, such that water density ρ_w can be considered constant. The air phase is, however, compressible, and its density has significant dependency on temperature and pressure (in accordance with the its equation of state $P = \rho_a RT$). Thus, while the water flowrate Q_w is uniform throughout the test section during each test ($dQ_w/dz = 0$), the air flowrate Q_a may vary as a function of distance according to local fluid temperature and pressure ($dQ_a/dz \neq 0$). However, a reference air flowrate can be defined for each test, occurring under conditions of ambient temperature and pressure ($T = T^R$ and $P = P^R$). This reference air flowrate shall be denoted as $Q_{a(i)}$.

The discharge of water through the tee and intake of air at steady rates cause a hydraulic pressure profile to develop in the test section. Following [8], the pressure gradient function $\Phi(z)$ may be defined in terms of 'junction' and 'developed flow' components as:

$$\frac{dP}{dz} = \left(\frac{\partial P}{\partial z}\right)_j + \left(\frac{\partial P}{\partial z}\right)_d$$

(2)

where the junction component is negative-valued only for a 'region of influence' close to the junction (and zero elsewhere) while the developed flow component is constant (independent of distance z). Equation (2) can be written in shorthand form as:

$$\Phi = \Phi_j + \Phi_d$$

(3)

The experimental test rig shown in Figure 1 is approximately two storeys in height (height-to-pipe diameter ratio $h/D = 54D$). This ratio is very low compared to a typical high-rise wastewater system,

but it is just sufficient to ensure the annular flow film can accelerate to a terminal velocity ([9], [10]) and to ensure that 'hydraulic development' of flow is completed ([8]). Thus by the time fluids reach the bend at the test section base, a uniform annular flow is expected to for characterised by a constant pressure gradient, and a constant, and uniform cross-section void fraction.

Since the air pressure is defined by the equation $P = \rho_a RT$, pressure gradient is a function of air density and air temperature. Thus, the pressure gradient divided into "thermal" (constant density) and "density" (constant temperature) components defined as:

$$\frac{dP}{dz} = \rho_a^r R \left(\frac{\partial T}{\partial z}\right)_\rho + RT_a^r \left(\frac{\partial \rho_a}{\partial z}\right)_T \tag{4}$$

Or in shorthand form:

$$\Phi = \Phi|_\rho + \Phi|_T \tag{5}$$

Thus it follows from equation (2) and (3) that Φ can be divided into junction "thermal" and "density" components and 'developed flow' "thermal" and "density" components, according to:

$$\Phi = \left\{\Phi_j\big|_\rho + \Phi_j\big|_T\right\} + \left\{\Phi_d|_\rho + \Phi_d|_T\right\} \tag{6}$$

Or equivalently, that any measured pressure change occurring over a finite distance Δz can be divided into four components:

$$\Delta P = \left\{\Delta P_j\big|_\rho + \Delta P_j\big|_T\right\} + \left\{\Delta P_d|_\rho + \Delta P_d|_T\right\} \tag{7}$$

Pressure gradients for steady-state, fully-developed annular flows may be estimated using empirical correlations taken from academic literature. A widely-known and easy-to-use correlation which has been developed by from Chisholm [11] takes the form:

$$\Phi_d = \left\{1 + \frac{\dot{m}_a}{\dot{m}} \frac{\rho_w}{\rho_a}\right\} \left(\frac{dP}{dz}\right)_w \tag{8}$$

where $\dot{m}_a/\dot{m}$ is fraction of the total mass flow in the gas phase $(dP/dz)_w$ is the 'water-phase only' pressure gradient (i.e. an equivalent gradient achieved water flows alone within the pipe section) and ρ_a is the *mean density* of the air within the section of pipe of interest. For the conditions tested in this study, $(\dot{m}_a/\dot{m})(\rho_w/\rho_a) > 1$, such that:

$$\Phi_d \cong \frac{\dot{m}_a}{\dot{m}_w} \frac{\rho_w}{\rho_a} \left(\frac{dP}{dz}\right)_w \tag{9}$$

This expression makes no explicit reference to a fluid temperature, T. However, temperature dependency will exist if, for a given liquid phase flowrate, the air mass flowrate $\dot{m}_a$ and the mean air density ρ_a vary with temperature.

Various energy streams are important, for purposes of analysis of experimental test data, which are defined within in Table 3. These streams are, respectively, the thermal mass carried by the water feed stream upon entry to the system $\dot{E}_w^i$, the thermal mass flow carried by the air feed stream upon entry to the system $\dot{E}_a^i$, and the rate of heat transfer to the environment through the feed lines and the test section pipe walls, $\dot{Q}$. The heat transfer term $\dot{Q}$. arising due to temperature difference between flowing water and the ambient air. The overall heat transfer coefficient ("U-value") which defines $\dot{Q}$ is dependent upon the thermal conductivity for the plastic material k_w and the material wall thickness t_w according

to the definition $U = 1/(k_w/t_w)$ [1]. The test apparatus is made from PVC-type plastic, as shown in Figure 1; this plastic is a good thermal insulator and thus it prevents large rates of heat transfer to the surroundings.

Table 3: Energy Streams: Expressions

| Stream	Energy Flow (J s⁻¹)
Water Thermal Mass Flow	$\dot{E}_w^i = Q_w \rho_w C_v^w T_w$
Air Thermal Mass Flow	$\dot{E}_a^i = Q_a \rho_a C_v^a T_a$
External Heat Loss	$\dot{Q} = U\, A\, \Delta T_x$

4. Test Results

Figure 2 displays, in entirely, the data gathered from four experimental tests. The graphs illustrate water flowrate data $Q_w(t)$, air flowrate data $U_a(t)$, and pressure transmitter output data $P_0(t)$ - $P_6(t)$ (filtered at 1 Hz to remove broadband noise) while the tables to the left summarize the inlet and outlet fluid temperatures recorded at the start of each test. A series of downward steps in the water flowrate and the air velocity occurs is observable as each test proceeds. The test section is evidently subject to a suction pressure profile which becomes less extreme as the water flowrate is reduced. Inspecting Figures 2(a) and 2(b), it is clear that many of the flush-mounted pressure transducer readings are subject to large fluctuations, attributed to changing properties of flow, and to 'sensor drift'. This drift is attributed to thermal strain on sensors, and it implies that sensor data have low accuracy. In Figure 2(d), a series of sudden spikes in pressures are evident: these spikes occur as the air supply has been deliberately interrupted as part of test procedure. While this effect is significant, it is not of interest within this currelt study.

The temperature data shown in the tables indicate that, firstly, that the difference in feed stream temperatures is much smaller at the outlet of the test section than at inlets ($\left|T_{w(o)} - T_{a(o)}\right| \ll \left|T_{w(i)} - T_{a(i)}\right|$), and secondly, that water stream temperature does not change between the sump and the outlet ($T_{w(o)} - T_{w(i)} = 0$K). Consequently, the difference $T_{a(o)} - T_{a(i)}$ is large, and the air temperature moves towards the water temperature as fluids mix in the test section. The fluids thus move closely towards a thermal equilibrium as they pass through the test section and the mixture undergoes a process of *thermal development* analogous to the process of *hydraulic development* described above as it transitions into a fully-developed annular flow.

---

[1] This expression neglects any insulating 'skin' effects occurring fluid-wall boundaries and it provides a conservatively large estimate of the pipe U-value.

Figure 2: Experimental Test Results. Pressure, Flowrate, and Air Velocity Data (lowpass filtered at 1Hz), and inlet and outlet feed stream temperatures for the 'peak steady-state water flowrates' which are discharged at start of each test.
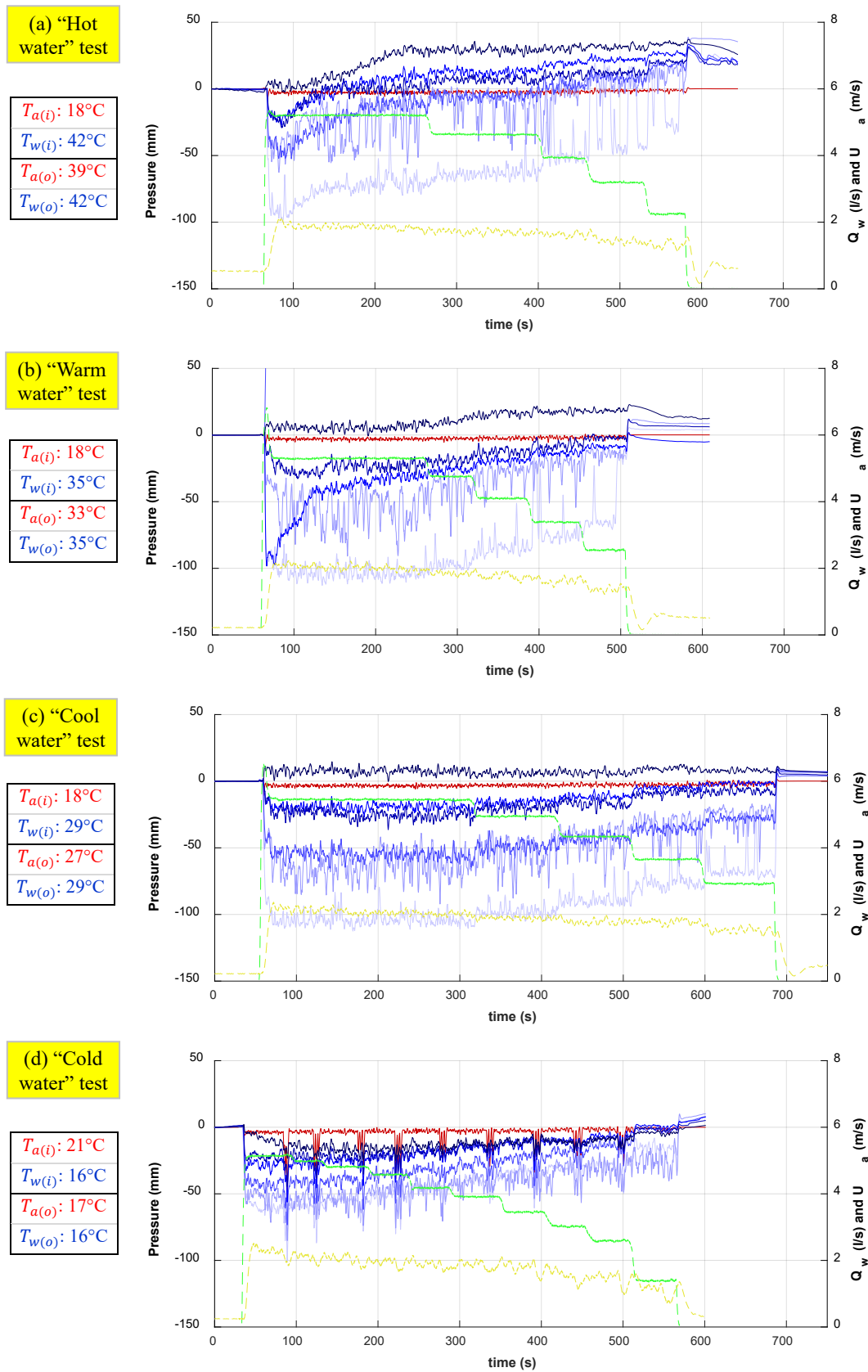
5. Analysis

Figures 3 illustrates a set of steady-state pressure profiles which are by averaging the data collected from the P_o to P_6 sensors (for 'warm water' series of tests, $T_{w(i)} = 35°C$). These profiles demonstrate that a representative suction pressure profile forms in the test section, in accordance with theory outline in Section 3, which can be separated into 'junction' and 'developed flow' regions. In the junction region there is rapid pressure loss while in the developed flow region the pressure gradient remains relatively constant. Estimates for 'net junction loss' and a net 'developed flow' pressure gradient parameters can be extracted from these pressure profiles according to the expressions:

$$\Delta P_j \cong \overline{P_1} - \overline{P_0} \qquad\qquad \Phi_d \cong \frac{\overline{P_5} - \overline{P_2}}{z_5 - z_2} \qquad\qquad (10)$$

where, for the data shown, the net junction loss ΔP_j is of the order of $50 - 100$ mm H₂O and increases with the superficial water velocity U_w, in accordance with [8]. The pressure gradient Φ_d also increases with water velocity U_w ($\partial\Phi_d/\partial U_w > 0$) in accordance with [8].

Discussion presented in [8] also suggest that the 'developed flow' pressure gradient component Φ_d should be a of the water velocity U_w *and* air velocity U_a, [8]. To test this hypothesis, Figure 4 displays the Φ_d dataset obtained from all experimental tests s functions of velocities U_a and U_w (U_a is the x-axis variable and U_w is indicated by the colour scheme shown). Data from the current study are bounded by the dotted red line and alternative data collected from similar test rigs [12], [13] and [14] are superimposed for comparison. Pressure gradient data collected from the current system are broadly consistent with data collected from the alternative sources. Furthermore, while the air velocity U_a has not been controlled in current tests, a tendency for Φ_d to decrease with also U_a is discernible ($\partial\Phi_d/\partial U_a < 0$, in accordance with [12], [13], [14]).

Neither Figure 3 nor Figure 4 illustrate the impact of feed stream temperatures. However, Figure 5 illustrates a group of steady-state profiles obtained for similar flow velocities $U_{w(i)} \sim 0.6$ ms⁻¹ and $U_{a(i)} \sim 2$ m s⁻¹, but having a varying feed stream temperature difference T^* (where T^* is defined as $T_{w(i)} - T_{a(i)}$). These profiles display 'junction' and 'developed flow' components as per Figure 3. However, to within the level of measurement accuracy which is provided by the pressure sensors, *no* distinct trends in the parameters ΔP_j and Φ_d are discernible.

Finally, Figure 5 shows mean steady-state inlet air velocity $U_{a(i)}$ plotted as a function the of the water velocity U_w and the temperature difference parameter T^*. The data suggest that, for a given velocity U_w, there is a weak tendency for air velocity to decrease with difference T^* (i.e. $\partial U_{a(i)}/\partial T^* < 0$). The variation in $U_{a(i)}$ is approximately about 10% over the entire range of T^* that is tested. Note that the x-axis and y-axis variables shown in this plot are proportional to the fluid mass flowrates $\dot{m}_w$ and $\dot{m}_a$. Thus, the data also suggest that for a given water mass flowrate $\dot{m}_w$, that the air mass flowrate decreases weakly with difference T^* ($\partial\dot{m}_a/\partial T^*|_{\dot{m}_w} < 0$).

Figure 3: Typical Steady-State Flow Pressure Profiles (1).
($T_{w(i)}$ = 35°C; 'Warm Water' Tests).
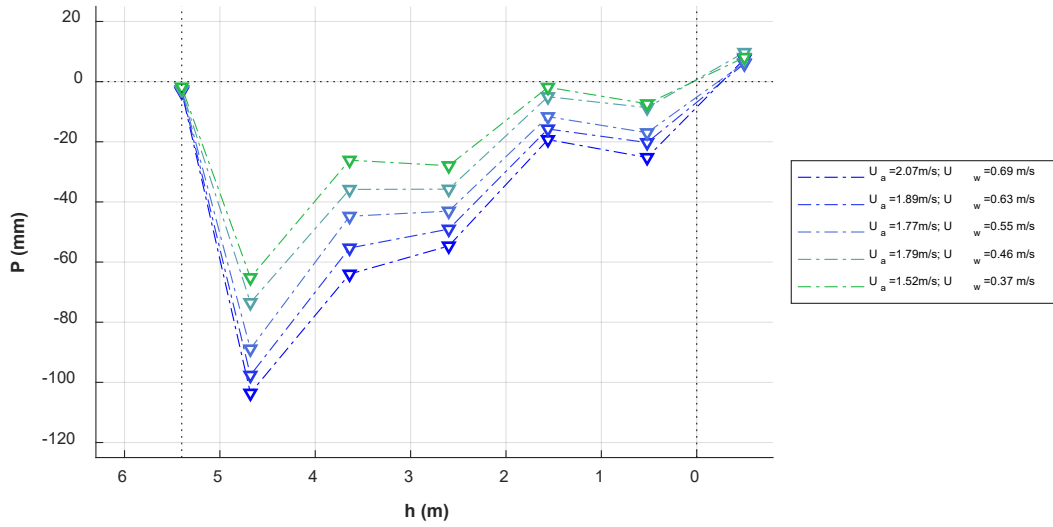
Figure 4: Developed flow pressure gradient component, Φ_d (all tests).
Data from Refs. [12], [13] and [14] shown for comparison.
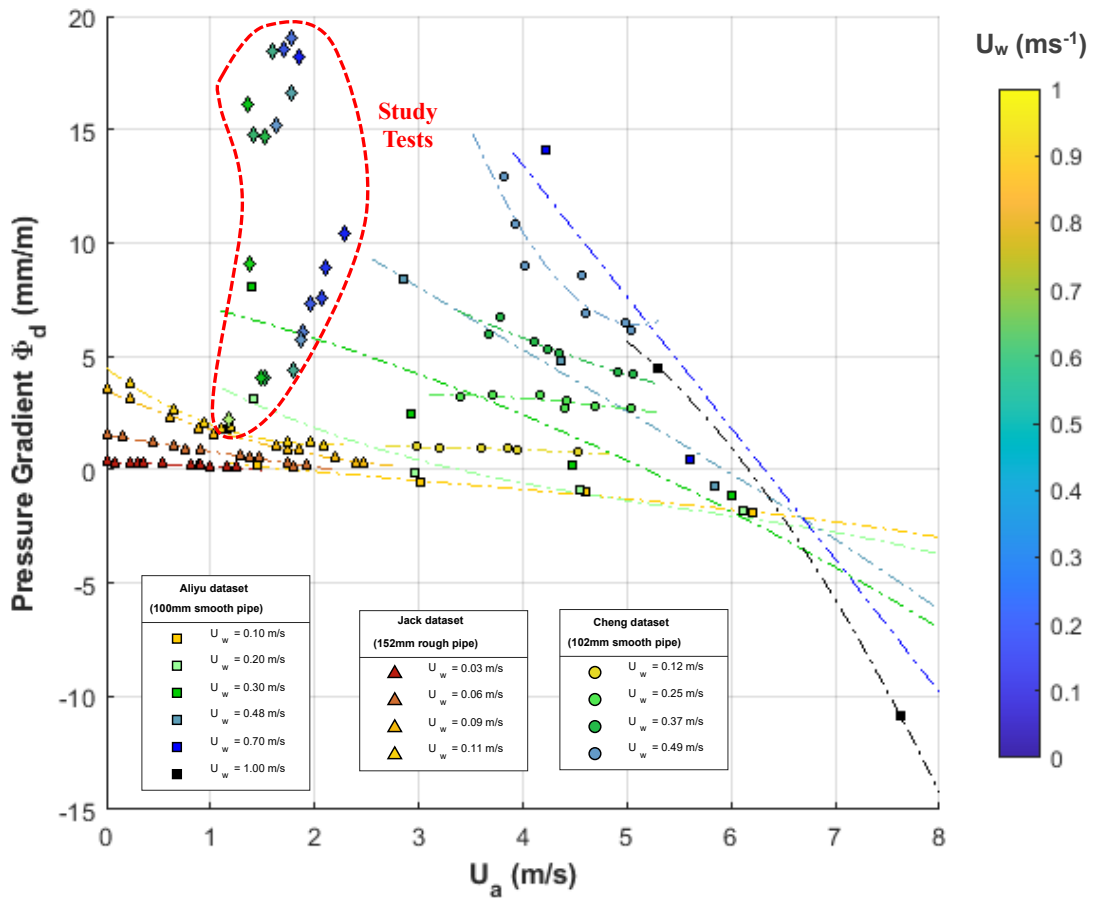
Figure 5: Typical Steady-State Flow Pressure Profiles (2).
$(U_w \cong 0.6 \text{ m s}^{-1} \ (Q_w \cong 5 \text{ l s}^{-1}) \text{ and } U_a \cong 2 \text{ m s}^{-1})$
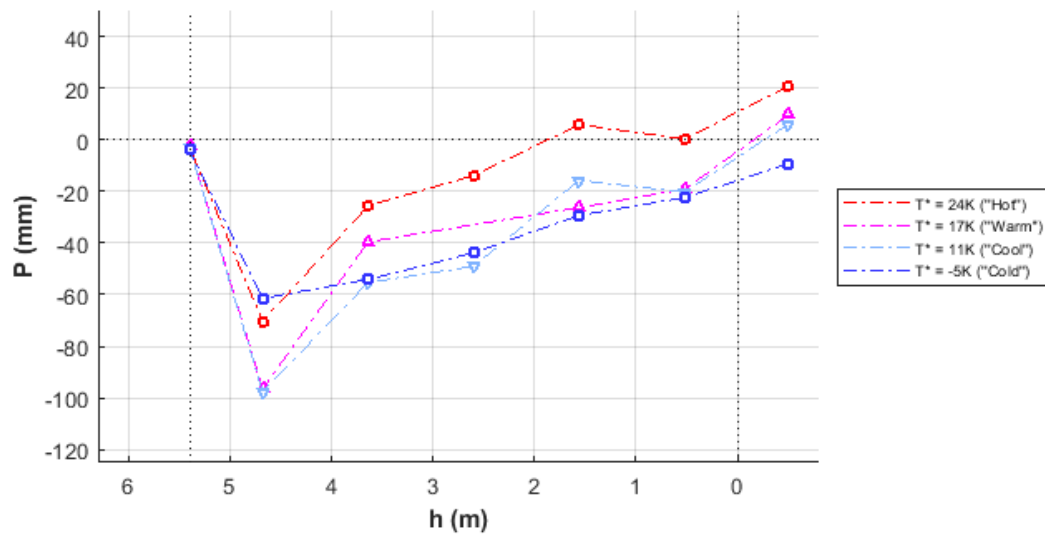
Figure 6: Inlet Air Velocity $U_{a(i)}$ vs. Water Velocity U_w
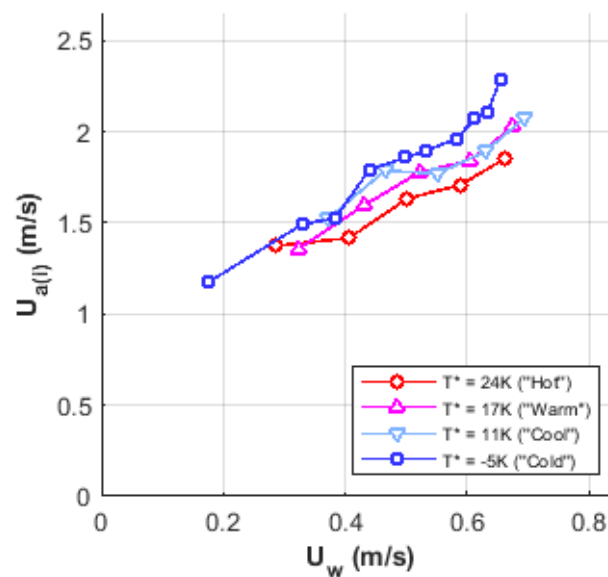
6. Thermal Calculations

Table 4 displays representative values for the energy stream quantities $\dot{E}_w^i$, $\dot{E}_a^i$ and $\dot{Q}$. (These values are based on test data and make assumptions that are conservative for the argument that now follows). The ratios of the water stream thermal mass $\dot{E}_w^i$ to the air stream thermal mass $\dot{E}_a^i$ and to the external heat transfer $\dot{Q}$ are evidently very large ($\dot{E}_w^i/\dot{Q} = 380$ and $\dot{E}_w^i/\dot{E}_a^i = 2380$). These ratios indicate that the water stream acts as a substantial thermal reservoir for heat transfer processes occurring between the feed inlets and the outlet.

The parameters $\dot{E}_w^i$, $\dot{E}_a^i$ and $\dot{Q}$ values define a change in water temperature required to achieve a thermal equilibrium of the air and water fluids, $(\Delta T_w)^e$:

$$(\Delta T_w)^e \quad = \quad T_{w(i)} \; - \; \frac{\dot{E}_w^i \quad + \quad \dot{E}_a^i}{\left(\dot{E}_w^i/T_{w(i)}\right) + \left(\dot{E}_a^i/T_{a(i)}\right)} \tag{11}$$

and a change in water temperature arising due to heat transfer with the surrounding environment $(\Delta T_w)^x$:

$$(\Delta T_w)^x \quad = \quad - \; \frac{\dot{Q}}{\dot{E}_w^i} \, T_w \tag{12}$$

For conditions defined in Table 4, these temperature differences are respectively $(\Delta T_w)^e$ = -0.07 K and $(\Delta T_w)^x$ = -0.4 K. Thus the combined effect of both processes is, theoretically, to cause minimal change in the water temperature. This prediction is exact agreement with experimental data within the measurement accuracy of the temperature sensor ($\Delta T_w \equiv T_{w(o)} - T_{w(i)}$ = 0 K as shown by tables to the left of Figure 2).

The calculation of the parameter $(\Delta T_w)^e$ assumes that the annular flow air-water interface has an infinitely large heat transfer coefficient (such that a perfect thermal equilibrium achieved at the system outlet). The test data suggest that thermal equilibrium is *substantially* but not perfectly achieved at the outlet; it can therefore be concluded that while this assumption is incorrect, the annular flow interface heat transfer coefficient must still be very large. This outcome is consistent with findings reported in academic literature. Efficient heat transfer is reported with general discussions presented in [15] and is predicted using CFD methods described in [16].

Table 4: Representative Values of Energy Streams

Stream	Representative Value	Basis
Water Thermal Mass Flow $\dot{E}_w^i$	1669 kJ s^{-1}	Conservatively small value based on a minimum Q_w value (1.4 l s^{-1})
Air Thermal Mass Flow $\dot{E}_a^i$	4.4 kJ s^{-1}	Conservatively large value based on a maximum $U_{a(i)}$ value (2.3 m s^{1})
External Heat Transfer $\dot{Q}$ [1]	0.7 J s^{-1}	Conservatively large value based on a maximum T^* value ($T_{w(i)} - T_{a(i)}$ = 24K)

Note 1: The pipe U-value is calculated based upon a pipe wall thickness t_w = 2mm and a pipe wall thermal conductivity k_w = 0.15 W m^{-1} K^{-1}, leading to U = 30 W m^{-2} K^{-1}. A conservatively large thermal interface area $A = 2\pi h D$ is assumed in the stream calculation (i.e. a surface area which is twice the test section surface area, accounting for water supply and water downflow).

(6.1 Calculations based on 'Rapid Thermal Development' of Flow)

A series of calculations is now undertaken on the basis that there is a *rapid hydraulic and thermal development* of annular flow within the test section. If it is assumed that these processes complete within the junction region of the system (assumption "*J*"), then:

$$\Phi_j\big|_T \to 0 \quad (z \geq z_d)$$
$$\Phi_j\big|_\rho \to 0 \quad (z \geq z_d) \tag{13}$$

where distance z_d is of the order of 1.0 m based on data shown in Figure 3 and 5 (i.e. the distance between the tee and a location midway between sensors P_1 and P_2). There is consequently, according to assumption "J", no change to fluid temperatures within the region $z \geq z_d$.

According to equation (7), junction pressure loss is the sum of two components:

$$\Delta P_j \quad = \quad \Delta P_j\big|_\rho \quad + \quad \Delta P_j\big|_T \tag{14}$$

Under assumption "J" the 'thermal' component $\Delta P_j\big|_\rho$ of ΔP_j must be defined as:

$$\Delta P_j\big|_\rho \quad = \quad \rho_a^R\, R\, T^* \tag{15}$$

where ρ_a^R is the reference air density (1.20 kg m^{-3}) and T^* is the feed temperature difference defined in Section 4 above. It follows that a relative change in air density must occur across the junction region defined as:

$$\frac{\Delta \rho_{a(j)}}{\rho_a^R} = \Delta P_j\big|_T / P^R \tag{16}$$

Figures 7(a) displays the ratio of 'density' pressure loss component $|\Delta P_j|_T$ to the observed pressure loss $|\Delta P_j|$, as functions of water velocity U_w and the temperature difference T^*. Provided assumption "J" is valid, this figure indicates that component $\Delta P_j|_T$ is significantly larger that the measured pressure loss $\Delta P_j|$ in magnitude. Thus, it is inferred that junction pressure drops shown in Figure 3 and Figure 5 are small and these measured values mask two much larger *components* of pressure drop. Considering a scenario where $T^* > 0$, these components are (a) a large pressure gain arising from the heating of the air phase ($\Delta P_j|_\rho > 0$) and (b) a large, opposing, pressure loss arising from a reduction in the air phase density ($\Delta P_j|_T < 0$). Figure 7(b) illustrates this relative change in the air phase density $\Delta \rho_{a(j)}/\rho_a^R$ as a function of the water velocity U_w and the temperature difference T^*. The data suggest that, at the location $z = z_d$, air density reduces by 10% when T^* is large.

Mass continuity dictates that $d\dot{m}_a/dz = 0$ under conditions of steady-state flow, with $\dot{m}_a = \rho_a Q_a/A$ according to equation (1). Thus changes in air density, air flowrate and air superficial velocity within the test section must be related by the expressions:

$$\frac{\Delta \rho_a}{\rho_a^R} = -\frac{\Delta Q_a}{Q_{a(i)}} = -\frac{\Delta U_a}{U_{a(i)}} \tag{17}$$

Thus, within the region $z \geq z_d$ where flow is fully-developed, ratios of air velocities and flowrates to inlet values are defined as:

$$\frac{U_{a(d)}}{U_{a(i)}} = \frac{Q_{a(d)}}{Q_{a(i)}} = \left(\frac{P_a^R}{P_a^R + \Delta P_j\big|_T} \right) = \left(\frac{\rho_a^R}{\rho_a^R + \Delta \rho_a} \right) \tag{18}$$

Figure 8 displays calculated values for $U_{a(d)}$ at the location $z = z_d$, as a function of the parameters U_w and T^*. The four sets of data shown in this plot are in notably better agreement that the equivalent data which are plotted in Figure 4. This agreement lends support to assumption "J" , and suggested that while

air velocity is measurably sensitivity to the temperature difference T^* at the mixing junction ($\partial U_{a(i)}/\partial T^* \neq 0, z = 0$), air velocity is *insensitive* to temperature difference T^* once the annular flow is fully developed ($\partial U_{a(d)}/\partial T^* = 0 \; \forall \; z \geq z_d$). Identical arguments apply to the air flowrate ($\partial Q_{a(i)}/\partial T^* \neq 0, z = 0$ and $\partial Q_{a(d)}/\partial T^* = 0 \; \forall \; z \geq z_d$). Furthermore, for any point in the region $z \geq z_d$ where flow is 'fully-developed':

$$\frac{1}{\dot{m}_a} \frac{d\dot{m}_a}{dT^*}\bigg|_{\dot{m}_w} \cong \frac{1}{\rho_a} \frac{d\rho_a}{dT^*}\bigg|_{\dot{m}_w} \tag{19}$$

A verbal summary of this outcome, for a scenario where $T^* > 0$, is as follows. Firstly, the hot discharge water raises the temperature of cold air, causing an observable reduction in the mass flowrate of air drawn into the system. However, premise "*J*" indicates that this heating must causes a reduction in the air density. The net result is a minimal effect upon the air flowrate within the fully-developed flow region of the system.

(6.3 Implications)

If isothermal flow occurs within the fully-developed flow region of the system ($\partial T_a/\partial z = \partial T_w/\partial z = 0, \forall \; z \geq z_d$), then according to equation (6), pressure gradient is attributed solely to changes in fluid density:

$$\Phi_d = R \, T_a^r \, \frac{d\rho_a}{dz} \tag{20}$$

This outcome can also be derived by inspection of the Chisholm pressure gradient correlation ([11]), which from Section 3, this correlation is:

$$\Phi_d \cong \frac{\dot{m}_a}{\rho_a} \left\{ \frac{\rho_w}{\dot{m}_w} \left(\frac{dP}{dz} \right)_w \right\} \tag{21}$$

For a constant water discharge flowrate $\dot{m}_w$, the terms in the bracket are constant. Moreover, the ratio $\dot{m}_a/\rho_a$ is insensitive to the temperature difference T^* in accordance with equation (19), and thus equation (21) also indicates that pressure gradient Φ_d should be insensitive to the temperature difference T^*.

Figure 7: Data analysis. (a) Ratio of junction pressure loss components $|\Delta P_j|_T/ |\Delta P_j|$ versus discharge water velocity U_w; (b) Relative density change $\Delta\rho_a/\rho_a^R$ versus discharge water velocity U_w
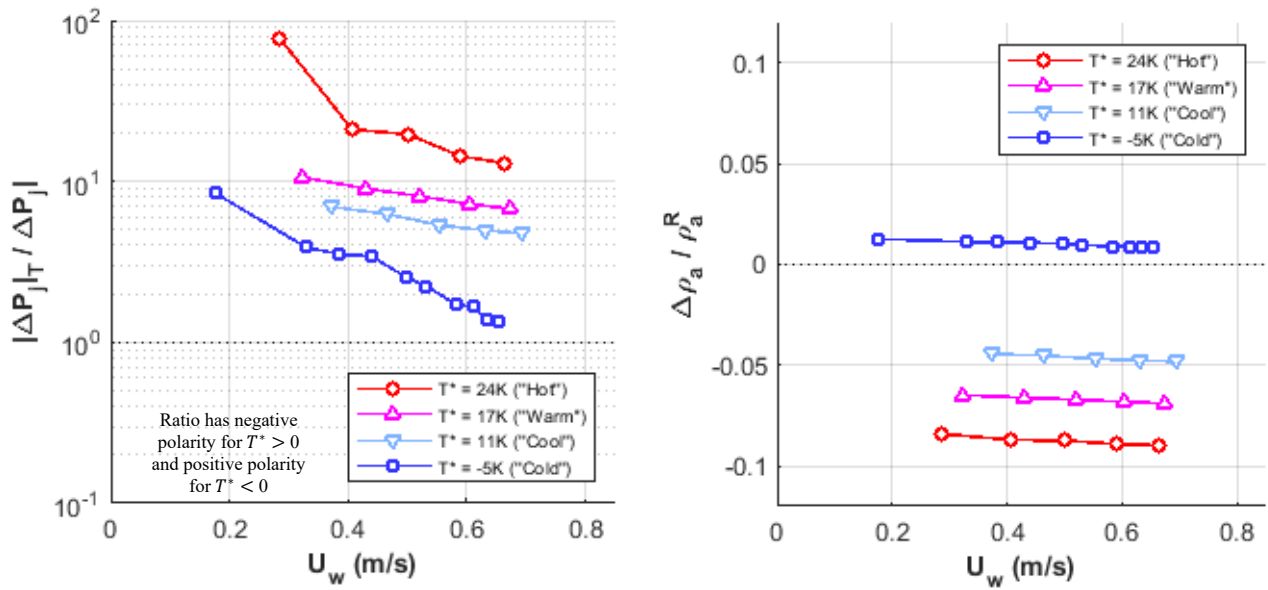

Figure 8: Calculated air velocity $U_{a(d)}$ at location $z = z_d$, versus water discharge velocity U_w.
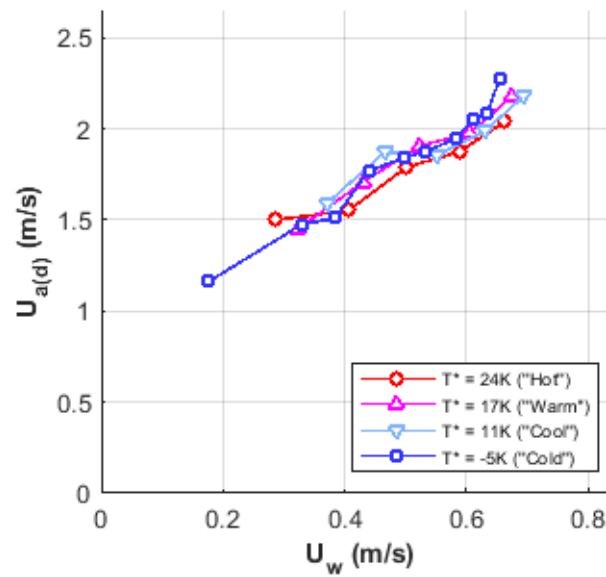
7. Summary and Conclusions

An experimental study has been conducted to investigate the impact of water temperature upon the thermal and hydraulic performance of wastewater stacks. Steady-state flow tests have been performed using a laboratory rig. The results have been presented and the results have been analysed by applying theoretical arguments and assumptions.

The conclusions of this study are as follows:

1. Annular flow promotes rapid heat transfer between the air and water feed streams, causing the air stream to rapidly adopt the water stream temperature.

2. The mass flowrate of air drawn into the system is sensitive to feed stream temperature difference T^* (decreasing when the discharge water temperature exceeds the ambient air temperature).

3. Once fully developed annular flow conditions are achieved, volumetric flowrate of air is *not* sensitive to feed stream temperature difference T^* (the air density adjusts as its temperature changes). There is therefore, no observable change in the air-to-water flowrate ratio.

4. The steady-state hydraulic pressure profile is *not* strongly sensitive to feed stream temperature difference T^*.

The net outcome of this study, is therefore, that discharge water temperature does *not* have a significant impact on high-rise wastewater stack performance. While this is a 'null result' it is an important outcome as no explicit statement on the role of water temperature has been provided within building services agency design codes.

References

1. BSI. Gravity Drainage System inside Buildings—Part 2: Sanity Pipework, Layout and Calculation; British Standard BS-EN-1206-2:2000; BSI: London, UK, 2002.

2. Standards Australia International. Australian/New Zealand Standard AS/NZS 3500.2:2003. Plumbing and Drainage, Part 2: Sanitary Plumbing and Drainage; Standards Australia International: Sydney, Australia, 2003; ISBN 0 7337 5496 1.

3. IAMPO. US Uniform Plumbing UPC 1-2003-1. An American Standard; IAPMO: Ontario, CA, USA, 2003.

4. International Code Council. US. International Plumbing Code; International Code Council: Country Club Hills, IL, USA, 2003.

5. Gormley, M., Swaffield, J.A., Sleigh, P.A. and Noakes, C.J., 2012. An assessment of, and response to, potential cross-contamination routes due to defective appliance water trap seals in building drainage systems. Building Services Engineering Research and Technology, 33(2), pp.203-222.

6. Gormley, M., Aspray, T.J., Kelly, D.A. and Rodriguez-Gil, C., 2017. Pathogen cross-transmission via building sanitary plumbing systems in a full scale pilot test-rig. PLoS One, 12(2), p.e0171556.

7. Gormley, M. and Stewart, C., 2023. Design Methodologies for Sizing of Drainage Stacks and Vent Lines in High-Rise Buildings. Buildings, 13(6), p.1458.

8. Stewart, C., Gormley, M., Xue, Y., Kelly, D. and Campbell, D., 2021. Steady-state hydraulic analysis of high-rise building wastewater drainage networks: modelling basis. Buildings, 11(8), p.344.

9. Wise, A.F.E.; Swaffield, J. Water, Sanitary and Waste Services for Buildings; Routledge: Abingdon, UK, 2012..

10. Cheng, C.L., Liao, W.J., He, K.C. and Lin, J.L., 2011. Empirical study on drainage stack terminal water velocity. Building Services Engineering Research and Technology, 32(2), pp.171-181.

11. Chisholm, D., 1967. A theoretical basis for the Lockhart-Martinelli correlation for two-phase flow. International Journal of Heat and Mass Transfer, 10(12), pp.1767-1778.

12. Cheng, C.L.; Lu, W.H.; Shen, M.D. An empirical approach: Prediction method of air pressure distribution on building vertical drainage stack. J. Chin. Inst. Eng. 2005, 28, 205–217.

13. Aliyu, A.M.; Lao, L.; Almabrok, A.A.; Yeung, H. Interfacial shear in adiabatic downward gas/liquid co-current annular flow in pipes. Exp. Therm. Fluid Sci. 2016, 72, 75–87.

14. Jack, L.B. An Investigation and Analysis of the Air Pressure Regime within Building Drainage Vent Systems. Ph.D. Thesis, Heriot-Watt University, Edinburgh, UK, 1997.

15. Jayanti, S. and Hewitt, G.F., 1997. Hydrodynamics and heat transfer in wavy annular gas-liquid flow: a computational fluid dynamics study. International Journal of Heat and Mass Transfer, 40(10), pp.2445-2460.

16. Talens-Alesson, F.I., 1999. The modelling of falling film chemical reactors. Chemical engineering science, 54(12), pp.1871-1881.

Study on the performance and quality evaluation of unit bathrooms in Taiwan

Cheng-Li Cheng (1), Chen-Yuan Lo (2)

(1) CCL@mail.ntust.edu.tw

(2) M11013021@mail.ntust.edu.tw

(1) (2) National Taiwan University of Science and Technology, Department of Architecture, Taiwan, R.O.C.

Abstract

The bathroom is a crucial space in people's daily lives, and in Taiwan, traditional construction methods are still prevalent in bathroom design. This study collected relevant literature and conduct surveys on unit bathroom designs in Taiwan, analyze its composition system, and use the Fuzzy Delphi method to set the primary evaluation factors, propose an evaluation framework for unit bathroom quality indicators, and introduce Failure Mode and Effects Analysis to establish an evaluation model, providing a reference for domestic unit bathroom product quality evaluation and serving as a basis for future architectural design decision-making. We analyzed the composition of the unit bathroom system, proposes a unit bathroom quality evaluation framework, and establishes indicator score formulas by setting factor weights and performance ratings. Finally, these scores were transformed into a percentage-based Unit Bathroom Indicators Total Score (UIT), completing the establishment of the unit bathroom quality evaluation model. With the evaluation model, designers and consumers can quickly assess and review the unit bathroom system and its quality as a basis for design or purchasing considerations.

Keywords:

Unit Bathroom; Evaluation Model; Fuzzy Delphi Method; FMEA.

1. Introduction

In recent years, Taiwan has been facing challenges such as labor and material shortages, leading to the growing trend of prefabricated construction methods. Prefabrication in unit bathroom construction involves using precast materials and adopting dry construction techniques instead of the traditional wet construction methods, significantly reducing construction waiting time. The modular nature and materials of unit bathroom construction also result in a lighter weight of the bathroom space, allowing for lightweight buildings. Additionally, the production of construction waste generated during construction and repairs is reduced compared to traditional methods, contributing to a decrease in the carbon footprint of buildings.

In 2020, the global spread of the COVID-19 virus increased the emphasis on epidemic prevention in building design. Currently, Taiwan is actively promoting the legalization of same-level drainage systems. The characteristics of unit bathroom construction, combined with same-level drainage, further reduce the potential for mosquito-borne disease transmission.

2. Material and Methods

2.1 Literature Review

In the 1960s, the Japanese company TOTO developed a unit bathroom system using reinforced fiberglass (FRP). This innovative approach, which saves time and labor, quickly gained popularity in Japan. Over time, the technology and materials used in unit bathrooms continued to evolve. Nowadays, unit bathrooms are widely used in residential complexes, hotels, and other buildings in Japan, Europe, and America, becoming the mainstream for bathroom system planning and design.

According to data from the Architecture and Building Research Institute under Taiwan's Ministry of the Interior, the current supply structure of unit bathrooms in Taiwan consists of approximately 80% domestic manufacturers and 20% imports. Over the past decade, the annual production capacity has been around 15,000 sets, with the current annual capacity at 3,700 sets. Unit bathrooms are primarily applied in hospitals and residential buildings, with a higher prevalence in new construction projects [6].

When considering factors such as initial cost, maintenance and renovation costs, and the net present value of life cycle costs, traditional bathrooms are generally more cost-effective and better meet the expectations of designers and users [1]. However, if we evaluate the architectural life cycle of sixty years and the durability of unit bathrooms of thirty years, Unit bathrooms are expected to have lower costs and provide the benefits of

a circular economy [7]. By combining the use of lowered floor slab drainage methods, although it may increase the initial construction cost, it can enhance the bathroom environment and the lifespan of the building.

2.2 Expert Questionnaire

This research aims to explore the application of unit bathroom design in Taiwan. Through the collection and compilation of literature, a quality indicator framework for unit bathrooms will be proposed, and an evaluation model will be established to provide reference for assessing the quality of domestic unit bathroom products. To ensure the objectivity and practicality of the research, an expert questionnaire was conducted using the fuzzy Delphi method to analyze the feasibility of the unit bathroom quality factor framework. The survey participants included experts from various fields related to the research, including the industry, government departments, and academia. In total, 18 valid questionnaires were collected.

3. Unit Bathroom Quality Indicators

3.1 Indicator Framework

This study synthesizes the "Unit Bathroom Performance and Application Research" based on a literature review and practical application analysis. Four major dimensional indicators are identified, and relevant assessment factors are collected within these indicators. The selection of assessment factors and framework is guided by the principles of objectivity, scientific rigor, measurability, and comparability, resulting in a total of sixteen relevant assessment factors being summarized.

Table 1-Fromwork of Unit Bathroom Quality Indicators

Tire 1	Unit Bathroom Quality Indicators			
Tire 2	Safety & Sturdy (SS)	Rational & Comprehensive (RS)	Health & Sanitary (HS)	Comfort & Sustainability (CS)
Tire 3	1.Structure (SSs)	1.Space (RSs)	1.Sound Environment (HSs)	1.Water Supply (CSs)
	2.Construction (SSc)	2.Drainage (RSd)	2.Light Environment (HSl)	2.Colour Type (CSc)
	3.Material (SSm)	3.Maintenance (RSm)	3.Thermal Environment (HSt)	3.Human Factors (CSh)
	4.Equipment (Sse)	4.Cost (RSc)	4.Ventilation Environment (HSv)	4.Accessory (CSa)

(1) Safety and Sturdy Indicator: Safety and Sturdy are the fundamental requirements of an unit bathroom, ensuring the basic performance of the bathroom and related to the reliability and usability of the products. It includes factors such as structure, construction, materials, and equipment.

(2) Rational and Comprehensive Indicator: Rational and comprehensive refers to the rationality and completeness of the unit bathroom system, examining the system from a design and planning perspective, considering factors such as design, cost, and maintenance and updates. It includes spatial layout, drainage system, maintenance and updates, cost and pricing, and other aspects.

(3) Health and Sanitary Indicator: Health and Sanitary are related to the condition of the usage environment of the unit bathroom system, examining the impact of the spatial environment internally and externally, ensuring hygiene and comfort. It includes factors such as sound, lighting, thermal environment, and ventilation.

(4) Comfort and Sustainability Indicator: Comfort and sustainability primarily concern the comfort and sustainable principles of the unit bathroom system, considering the system from a user's perspective, ensuring comfort in usage. It includes features such as hot water supply, color and patterns, ergonomics, storage and hanging functions.

3.2 The Result of Expert Questionnaire

After analyzing the expert questionnaire using the fuzzy Delphi method, this study set the arithmetic mean of 80% as the threshold consensus value among the experts, and retained all the factors.

Table 2- Analysis of Expert Questionnaire Results

Assessment Dimention	Assessment Factors	Optimistic Cognitive Value		Conservative Cognitive Value		Arithmetic mean			Test Value	Expert Consensus Value
		min (C_L^i)	max (C_U^i)	min (O_L^i)	max (O_U^i)	C_M^i	O_M^i	Single Value	$M^i - Z^i$	G^i
Safety & Sturdy	1.Structure	3	8	7	10	5.20	8.71	7.02	2.52	7.38
	2.Construction	4	7	6	10	5.59	8.98	7.17	2.39	6.68
	3.Material	4	7	6	10	5.62	8.88	7.22	2.26	6.68
	4.Equipment	3	7	8	10	5.52	8.91	7.11	4.39	7.22
Rational & Comprehensive	1.Space	4	7	8	10	5.44	9.02	7.34	4.58	7.23
	2.Drainage	4	8	8	10	5.82	9.25	7.56	3.44	7.54
	3.Maintenance	4	7	8	10	5.89	8.97	7.32	4.08	7.43
	4.Cost	3	7	7	10	4.51	8.35	6.22	3.84	6.43
Health & Sanitary	1.Sound Environment	2	6	7	10	3.94	7.95	5.78	5.00	5.94
	2.Light Environment	3	6	6	9	4.09	7.34	5.99	3.25	5.71
	3.Thermal Environment	3	6	7	10	4.55	8.36	6.43	4.81	6.46
	4.Ventilation Environment	5	8	9	10	6.32	9.34	7.85	4.02	7.83
Comfort & Sustainability	1.Water Supply	4	8	8	10	5.86	9.15	7.55	3.29	7.50
	2.Colour Type	3	7	6	9	4.04	7.35	5.64	2.31	6.31
	3.Human Factors	4	7	8	10	5.55	8.81	7.10	4.26	7.18
	4.Accessory	3	7	5	9	4.12	6.96	5.68	0.84	5.81
						Average of G^i	6.833	Threshold Value 80%		5.467

4. Evaluation Model

4.1 Evaluation values and grading

The grading criteria definition for the sixteen factors in the unit bathroom indicator framework refers to the Failure Mode Theory, ensuring the reliability and safety of the unit bathroom system. The factors are divided into four levels. When the system lacks the most basic performance, it is defined as the "Failure" criterion, assigned a weighting value of "0.0". When the system meets the basic performance specifications and quality, it is defined as the "Basic" criterion, assigned a weighting value of "0.9". When the system has moderate performance or quality, it is defined as the "Medium" criterion, assigned a weighting value of "1.0". When the system has higher performance or quality, it is defined as the " Superior " criterion, assigned a weighting value of "1.2".

Table 3- Factors Grading

Grades	Superior	Medium	Basic	Failure
Value	1.2	1.0	0.9	0.0

4.2 Evaluation Indicator Formula

After the classification and definition of values mentioned above, this study attempts to propose a simple formula to assess the rationality and quality of the unit bathroom system. Formulas (1) to (4) represent the scores of quality indicators for four dimensions. The weighted values of sub-factors within each dimension are multiplied together. If there are more medium factors, the indicator scores will approach 1, whereas if there are more superior factors, the indicator scores will approach 2 (with a maximum value of 2). This indicates a system with good quality and performance. However, if any of the factors experience a performance failure, regardless of the performance ratings of the remaining factors, the product will be 0, indicating system failure.

$$SS = SSs \times SSc \times SSm \times SSe \quad (2.0 \geqq SS \geqq 0)\ldots\ldots\ldots\ldots\ldots\ldots\ldots\ldots(1)$$

SS：Safety and Sturdy Indicator Scores
SSs、SSc、SSm、SSe：Values of Factors for the Safety and Sturdy Indicator

$$RC = RCs \times RCd \times RCm \times RCc \quad (2.0 \geqq RC \geqq 0)\ldots\ldots\ldots\ldots\ldots\ldots\ldots(2)$$

RC：Rational and Comprehensive Indicator Scores
RCs、RCd、RCm、RCc：Values of Factors for the Rational and Comprehensive Indicator

$$HS = HSs \times HSl \times HSt \times HSv \quad (\, 2.0 \geqq HS \geqq 0 \,)\ldots\ldots\ldots\ldots\ldots\ldots\text{(3)}$$

HS：Health and Sanitary Indicator Scores

HSs、HSl、HSt、HSv：Values of Factors for the Health and Sanitary Indicator

$$CS = CSs \times CSc \times CSh \times CSa \quad (\, 2.0 \geqq CS \geqq 0 \,)\ldots\ldots\ldots\ldots\ldots\ldots\text{(4)}$$

CS：Comfort and Sustainability Indicator Scores

CSs、CSc、CSh、CSa：Values of Factors for the Comfort and Sustainability Indicator

Formula (5) represents the calculation method for the Unit Bathroom Indicators Integrated Score (UI). UI is obtained by multiplying the scores of each indicator. If any of the sub-factors within the indicators have a performance failure, UI will be 0, indicating that the product's performance or quality does not meet the basic standards. Finally, this study proposes a percentage-based Unit Bathroom Indicators Total Score (UIT). Formulas (6) and (7) are used to convert UI into UIT. If UI is greater than 1, Formula (6) is applied, resulting in a score range of 60 to 100. This indicates that the product has at least a moderate or higher level of quality. If UI is less than or equal to 1, Formula (7) is applied, resulting in a score range of 0 to 60, indicating that the product only possesses basic quality performance or even fails to meet the required standards.

$$UI = (\, SS \times RC \times HS \times CS \,) \quad (\, 0 \leqq UI \leqq 16 \,)\ldots\ldots\ldots\ldots\ldots\ldots\text{(5)}$$

UI：Unit Bathroom Indicators Integrated Score

When UI > 1.0

$$UIT = UI * 2.5 + 60 \quad (\, 60\sim100 \,)\ldots\ldots\ldots\ldots\ldots\ldots\ldots\ldots\ldots\ldots\ldots\ldots\ldots\text{(6)}$$

When UI $\leqq$ 1.0

$$UIT = UI \times 60 \quad (\, 0\sim60 \,)\ldots\ldots\ldots\ldots\ldots\ldots\ldots\ldots\ldots\ldots\ldots\ldots\ldots\ldots\ldots\ldots\text{(7)}$$

UIT：Unit Bathroom Indicators Total Score

The evaluation model uses the Unit Bathroom Indicators Total Score (UIT) of 60 points as the threshold to differentiate between qualified and unqualified products. Products scoring below 60 points are likely to have multiple factors that only meet basic or even fail to meet the required standards, indicating unqualified products. Through a series of unit bathroom quality assessment formulas, it is possible to identify areas where system

performance or quality is lacking and make improvements to those areas that do not meet the standards, thus enhancing the unit bathroom quality.

5. Conclusion

This study analyzes the composition of the unit bathroom system, proposes a unit bathroom quality evaluation framework, and establishes indicator score formulas by setting factor weights and performance ratings. Analytic Hierarchy Process (AHP) was adopted to determine the relative importance between dimensions and factors, introducing these weights into the evaluation model to optimize and rationalize the evaluation formulas. Finally, these scores were transformed into a percentage-based Unit Bathroom Indicators Total Score (UIT), completing the establishment of the unit bathroom quality evaluation model. With the evaluation model, designers and consumers can quickly assess and review the unit bathroom system and its quality as a basis for design or purchasing considerations. On the manufacturing side, it enables the evaluation of areas where quality and performance could be improved.

References

[1] Kung-Jen Tu et al. Survey and analysis of maintenance performance of residential bathroom systems. Architecture and Building Research Institute, Ministry of the Interior, TW,2004

[2] Kuen-chi He. Research in Drainage System Decision-Making and Performance Evaluation of High-Rise Buildings. Unpublished master's thesis, NTUST, TW,2005

[3] Hsiu-Chung Huang. Study on the Performance and Application of Integrated Unit Trap in Bathroom. Unpublished master's thesis, NTUST, TW,2016

[4] CHEN CHIUNG JUI. Study on the Application and Feasibility of Same Floor Drain System in Residential Buildings. Unpublished master's thesis, NTUST, TW,2019

[5] Cheng-Li Cheng et al. Study on the Standardization and Technical Specification Revision of Same Floor Drainage Method in Collective Housing. Architecture and Building Research Institute, Ministry of the Interior, TW,2020

[6] Shih-Meng Huang et al. Survey and research on key technologies and methods for integrating overall bathroom systems in collective housing. Architecture and Building Research Institute, Ministry of the Interior, TW,2022

[7] Cheng-Chen Chen et al. Cost-Benefit Analysis of Circular Economy In Social Housing: Unit Bathroom Decoration Design. Journal of Property Management, (13)1, 54-64, TW,2022

Presentation of Authors

Cheng, Cheng-Li is the Professor at National Taiwan University of Science and Technology, Department of Architecture. He is a research scholar for water supply and drainage in building. He has published extensively on a range of sustainable issues, including the water and energy conservation for green building.

Lo, Chen-Yuan is the master student at National Taiwan University of Science and Technology, Department of Architecture. His research is focus on building environment and equipment.

TECHNICAL SESSION 4 – HEALTH & HYGIENE I

Analysis of the possibility of dispersion of SARS-CoV-2 in bathrooms using computational fluid dynamics (CFD)

L.S. Vieira (1), L.H. Oliveira (2), F.A. Kurokawa (3), A.S. Oizuni (4)

(1) ludmila.vieira@usp.br

(2) lucia.helena@usp.br

(3) fernando.kurokawa@usp.br

(4) amandasayuri@usp.br

(1, 2, 3, 4) Department of Construction Engineering, Polytechnic School, University of São Paulo, Brazil

Abstract

The epidemiological crisis generated by the SARS-CoV-2 virus, which caused the COVID-19 pandemic, caused profound changes around the world, challenging science and social relations. Although the first studies on the mode of transmission of the disease indicated that it occurs through droplets and respiratory secretions, researchers has raised the hypothesis that the infection could also occur through the oral-fecal route. When considering this other possibility of transmission, public restrooms and those in health units whose users have been have been diagnosed with COVID-19 become critical places due to the greater potential for spreading the disease. Considering the dynamics of flushing in the toilets, the force of water turmoil would be able to cause the suspension of aerosol particles and water droplets that could contain the infectious agent that could be inhaled by other users. In this context, this article analyzes the possibility of SARS-CoV-2 dispersion in toilets, using the concepts of computational fluid dynamics (CFD), through the OpenFOAM software to perform computational simulations. A toilet model traditionally marketed in Brazil was adopted as a geometric reference for the computational model. The behavior of the multiphase system was observed for a laminar flow, in order validate the simulation, in a preliminary way. The results obtained do not identify the potential for dispersion of aerosols and droplets contaminated by SARS-CoV-2 when a turbulence model is not applied.

Keywords

Computational fluid dynamics; SARS-CoV-2; toilet.

1 Introduction

The World Health Organization (2020) has recognised the possibility of transmission of SARS-CoV-2 through aerosols, which can come from body secretions and excretions, spread through activities such as talking, coughing, sneezing, especially in closed environments.

In atmospheric air, its transmission capacity can also be affected by meteorological and climatic factors, such as temperature, humidity and certain pollutants, such as particulate matter, carbon monoxide and nitrogen oxides (Barcelo, 2020).

Although the first studies on the mode of transmission of COVID-19 indicated that it occurs through droplets and respiratory secretions, researchers began to hypothesize that the infection could also occur through fecal-oral route. Suspicion about this new means of contamination began in early 2020, after a person in the USA presented to an urgent care clinic with a history of nausea and vomiting for two days, besides the common complaint of persistent dry cough, demonstrating that the virus could also be present in the patient's gastrointestinal system (Holshue, 2020).

A study developed by Bourouiba (2021) captured an image at 2,000 frames per second of the trajectories of droplets generated due to the flushing of a toilet in a hospital. Data analysis revealed that a large number of the generated droplets are not visible to the naked eye. These emissions represent more than 6 mL and can remain suspended in the air for a long time compared to the larger visible droplets (up to 6 mm in diameter) that settle on surfaces.

Weidhaas (2021) reported the presence of SARS-CoV-2 in a sewage samples collected from areas whose users were diagnosed with COVID-19, corroborating the reflection that the virus would be present in sanitary appliances. Thus, the bathrooms, especially those of public use and health care facilities, such as hospitals and outpatient clinics, would be critical sites because of the enormous potential for disease dissemination. The concern becomes even greater due to the dynamics of flushing the toilet, since the force of swirling water is capable of causing the suspension of aerosol particles that could contain the infectious agent.

Johnson et al. (2013) analysed three models of toilets with similar flush volumes and found that all of them were capable of generating bioaerosols with the actuation of the flush, their production being proportional to the increase of the flush energy. Analyzing the dynamics of bioaerosol production, Liu et al. (2020) performed a simulation using computational fluid dynamics (CFD) as methodology and demonstrated that, during toilet flushing, massive upward transport of aerosol particles, presumably infected with SARS-CoV-2, can occur.

In this context, the aim of this paper is to analyse the possibility of dispersion of SARS-CoV-2 by means of aerosols from Brazilian toilets, after flushing, employing the concepts of computational fluid dynamics (CFD).

2 Computational Fluids Dynamics Approach

It is possible to simulate any flow through channels, pipes and around a body, whether rigid or mobile, by processing the equations that govern fluid dynamics quickly, providing highly accurate results, with a minimised margin of error and, still simulating scenarios that are faithful to reality (Kurokawa, 2019).

Despite the great advantages of the CFD technique, Kurokawa (2019) also points out that there are complex situations to be modeled such as, for example, the turbulence phenomenon. McDonough (2007), reiterates that most fluid flows encountered in engineering practice are turbulent and states that their understanding is "one of the most intriguing, frustrating and important problems in classical physics". Thus, in this article, a simplification of the model was adopted, considering that it is a laminar flow.

Assuming the flow to be incompressible, the equations necessary to solve problems of flow of Newtonian and isothermal fluids are the equations of conservation of mass and momentum, given respectively by Equations 1 and 2.

$$\nabla \cdot \mathbf{u} = 0 \qquad\qquad\qquad\qquad\qquad \text{Eq. 1}$$
$$\frac{\partial \mathbf{u}}{\partial t} + \nabla(\mathbf{uu}) = \frac{1}{\rho}\nabla p + \nu\nabla^2\mathbf{u} + F \qquad\qquad\qquad \text{Eq. 2}$$

where, $\mathbf{u}$ is the velocity vector, t is time, ρ is the fluid density, p is the pressure, ν is the viscosity coefficient and, F represents the external forces.

The differential equations, together with the boundary conditions, are solved numerically in the OpenFOAM environment using the finite volume method (FVM), in which the domain of interest is subdivided into a finite number of smaller parts, called control volumes, and the quantities of interest are calculated approximately in each of these volumes. The resulting solution satisfies the conservation of quantities as mass, quantity of movement, energy in any finite control volume.

The method of calculation of the numerical solution employed by the tool is the PISO - Pressure-Implicit with Splitting of Operators (Issa, 1986). However, a modification was performed in the solver of the tool, pisoFoam, for the calculation of the numerical solution. The objective was to change the time step on-the-fly from stability and convergence constraints, i.e., reduce the number of iterations with the automatic adjustment of the time step during processing conditioned by the analysis of the number of Courant (Courant et al., 1967).

The interpolation scheme adopted for the discretization of the $1^{\underline{st}}$ order temporal derivatives was Implicit Euler, and for the discretization of the diffusive and advective terms the central differences scheme was adopted. In the case of the solution of the pressure variable algebraic system, it was used the Geometric-algebraic multi-grid (GAMG) iterative method with Gauss-Seidel buffer

3 Methodology

The field of analysis of this research are restrooms, having as key element a toilet. Figure 1 shows a restroom and Figure 2 shows an elevation of the toilets.
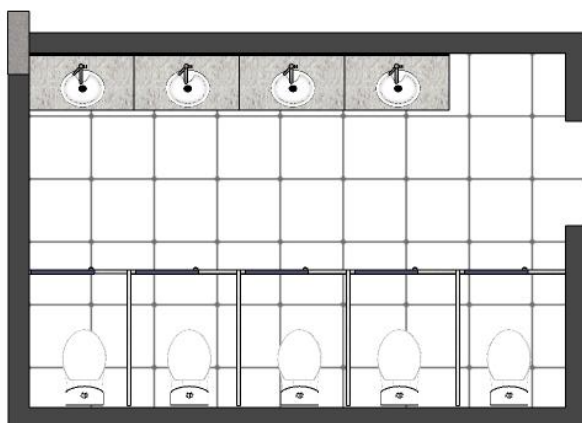

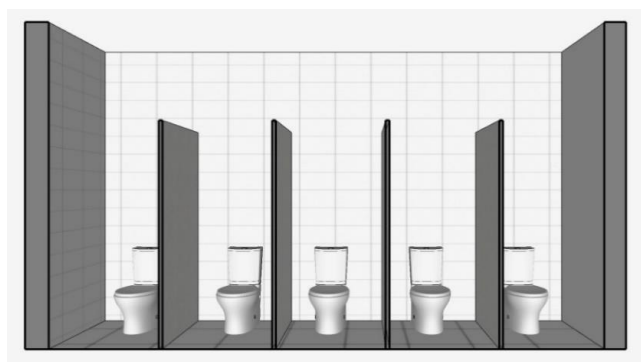**Figure 1 - Schematic plan of restroom**
Fonte: Vieira (2022)

Figure 2 - View of the toilets boxes
Fonte: Vieira (2022)

This restroom is located in the city of São Paulo, where gravitational acceleration is 9.81 m/s² and air temperature is assumed to be 27 degrees Celsius.

The toilet reference model adopted has a nominal flush volume of 6 litres. The water enters the basin laterally, producing a vortex-like flow, enhancing the discharge of solid waste. It is a consolidated brand in the Brazilian market, being widely used in public establishments. Figures 3 and 4 show the cross-sectional and longitudinal views and sections, respectively.

Figure 3 - Views of the toilet
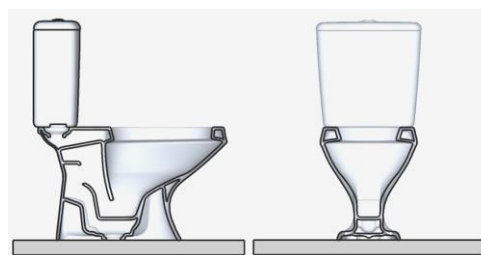Fonte: Vieira (2022)

Figure 4 – Toilet sections
Fonte: Vieira (2022)

From this reference of a toilet, Figure 5 (a), to validate the parameters and conditions of the computer simulation, a simplified geometric model of a toilet was adopted Figure 5 (b) and, for the mesh generation, the tool *SnappyHexMesh* from OpenFOAM was used.
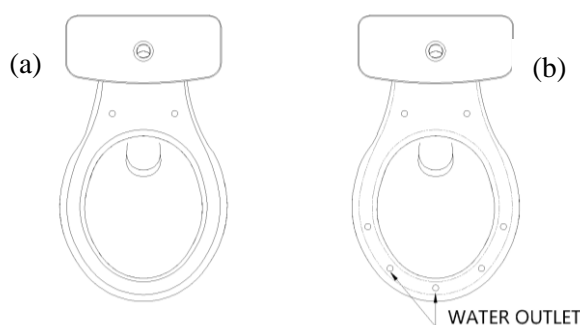

Figure 5 – Original toilet (a) and simplified toilet (b)

Fonte: Vieira (2023)

Regarding computational resources, they were used, in a first moment, for model validation:

- notebook with Intel Core i5-7200U processor and Turbo Boost function, NVIDIA GeForce 940MX graphics card with 2GB of dedicated RAM and 8GB DDR4 memory;

- software version OpenFOAM-v2106, June 2021, installed in a virtual machine with Linux operating system (Ubuntu); and

- for the post-processing stage, we used the software Paraview (embedded in the OpenFOAM package), version 5.4.1, which allows interactive visualization of the results.

It is considered, for this computer simulation, the analysis of a multiphase system, since the presence of two phases is verified: water in liquid state and air. The model does not

consider the presence of solids. Simulating multiphase flows is not an easy task either. The complex nature of multiphase flows is due to the transient nature of the flows; the existence of dynamically changing interfaces; discontinuities; the interactions of small-scale structures such as bubbles and particles; particle-particle interactions; mass transfer and phase change; turbulence; among other factors (Berlemont, 1995).

4 Results and discussions

In this study, the Volume of Fluid (VOF) method, developed by Hirt and Nichols (1981), is used to evaluate the interface between the two phases. In this method, the phases of a multiphase system are mathematically treated as continuous and interpenetrating, in which the volume of each phase cannot occupy the volume of another phase. Thus, introducing the concept of volume fraction of phases, using a scalar indicator function, which varies from zero (without material) to one (completely filled with material), as follows:

$$\alpha q = 0: \text{no fluid};$$

$$0 > \alpha q > 1 \text{ interface; e}$$

$$\alpha q = 1 \text{ with fluid.}$$

The solution of the system of equations composed of the equations of the volume fraction of each phase combined to a single equation of the quantity of motion, are all integrated in each cell of the model mesh. Using conventional computational resources, the mesh of this model was generated with 302.031 cells. Figure 6 illustrates the visualized fluid behavior for each of the identified simulation times, and visualization of the generated mesh.

t= 0.1

t= 0.1

t= 1

t= 1
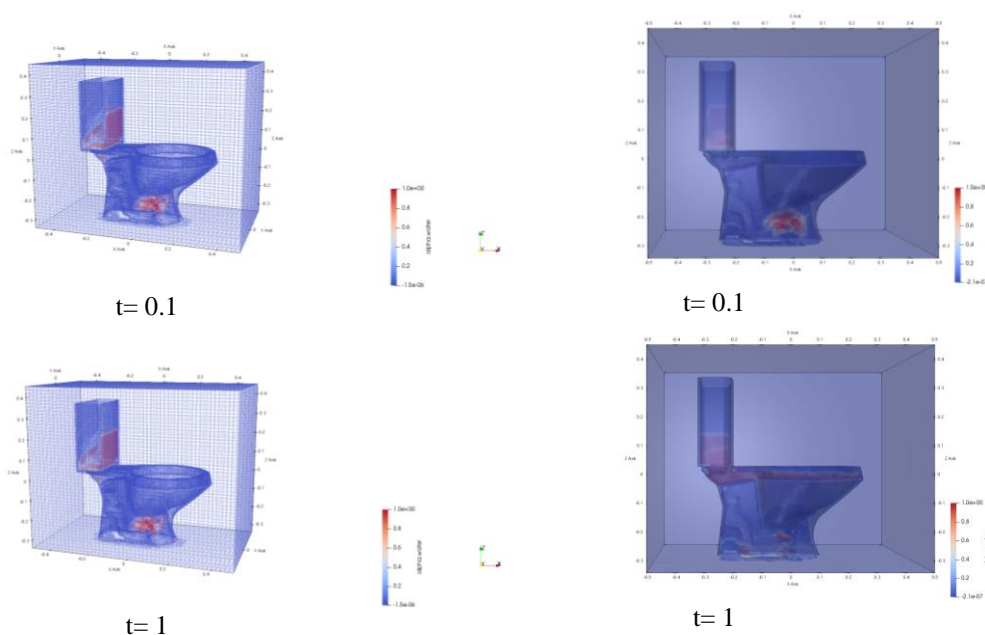
Figure 6 – Results viewed on Paraview
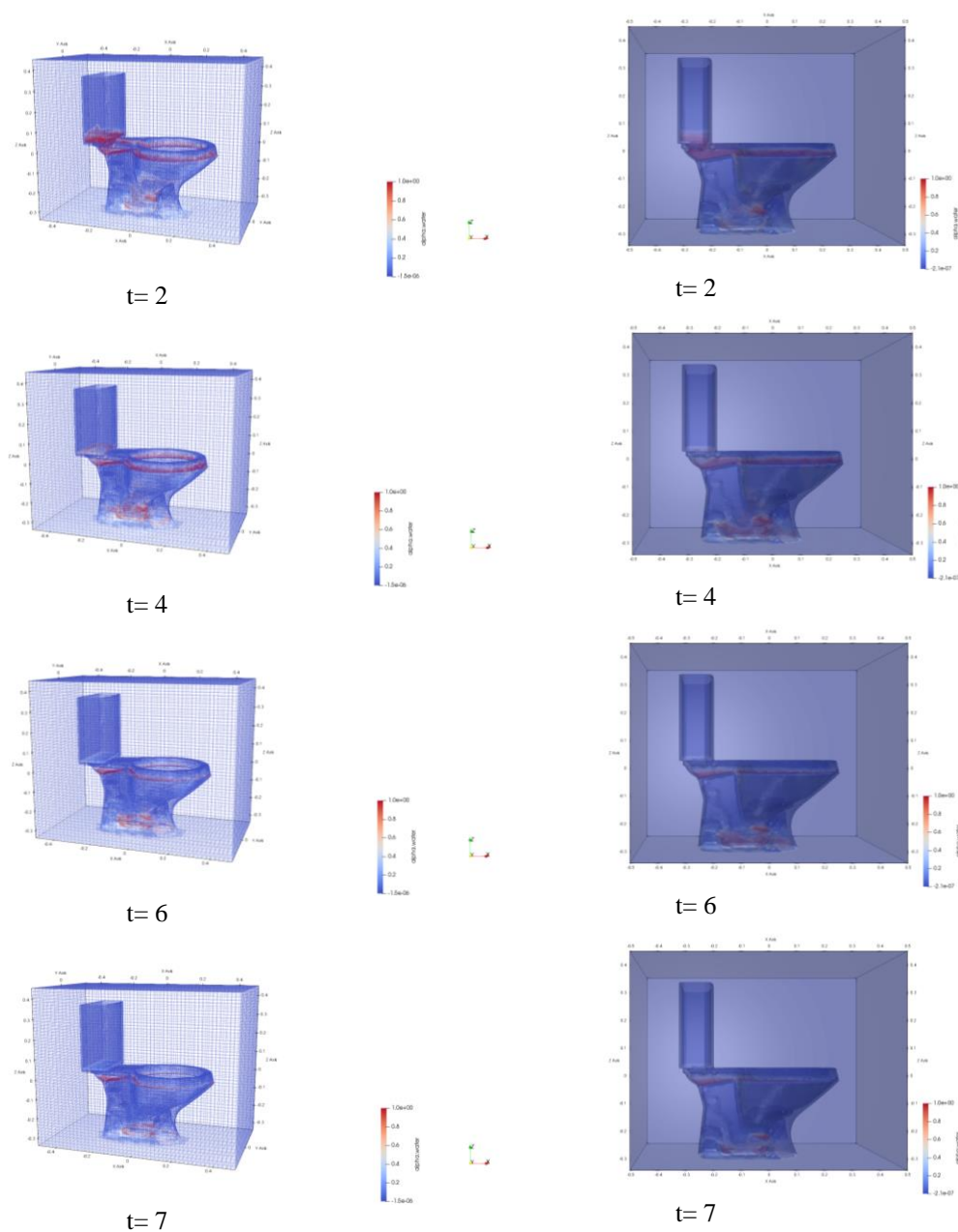
Analyzing the simulation results, although a simplified were adopted considering the computational resources available, it can't be observed that, after the flushing of the toilet, there is the possibility of aerosol suspension beyond the limits of the toilet seat; therefore, the hypothesis of the spread of diseases through aerossol needs validation using more robust experiments.

5 Final considerations

The continuation of this study intends to evaluate the behavior of the system by inserting a turbulence model. In the OpenFOAM tool, several turbulence models of the RANS (*Reynolds Average Navier Stokes*) and LES (*Large Eddy Simulation*) type are available. These models cover a relatively large set of flow problems that include time-dependent variables, fluid-structure interaction and heat transfer.

Thus, the the Standard $k - \varepsilon$ (Launder; Spalding, 1974) turbulence model will be used in the next phase of the research. This model is semi-empirical based on the modeling of the transport equations of the turbulent kinetic energy (k) and the energy dissipation rate (ε) given respectively, by Equations 3 and 4.

$$\frac{\partial \kappa}{\partial t} + \nabla \cdot (\kappa \mathbf{u}) = \nabla \left(\left(\mu + \frac{\nu_t}{\sigma_\kappa} \right) \nabla \kappa \right) + P - \varepsilon \qquad \text{Eq. 3}$$

$$\frac{\partial \varepsilon}{\partial t} + \nabla \cdot (\varepsilon \mathbf{u}) = \nabla \left(\left(\mu + \frac{\nu_t}{\sigma_\varepsilon} \right) \nabla \varepsilon \right) + C_{1\varepsilon} \frac{\varepsilon}{\kappa} P - C_{2\varepsilon} \frac{\varepsilon^2}{\kappa} \qquad \text{Eq. 4}$$

where P is the mean turbulent kinetic energy production term, σ_κ and σ_ε are the turbulent diffusion coefficients, and $C_{1\varepsilon}$ and $C_{2\varepsilon}$ are empirical constants. The turbulent viscosity, ν_t is calculated by Equation 5.

$$\nu_t = C_\mu \frac{k^2}{\epsilon} \qquad \text{Eq. 5}$$

where C_μ is also an empirical constant. The other constants are obtained from the correlation of experimental data from various turbulent flows, and are given by: $C_\mu = 0.09$, $C_{1\varepsilon} = 1.44$, $C_{2\varepsilon} = 1.92$, $\sigma_\kappa = 1.0$ e $\sigma_\varepsilon = 1.3$.

After inserting the turbulence parameters in the computational model, it is estimated that it will be possible to visualize the possibility of aerosol suspension beyond the limits of the toilet seat, a situation that may represent a new potential for disease dissemination through aerosols.

6 References

Barcelo, D. (2020). An environmental and health perspective for COVID-19 outbreak: meteorology and air quality influence, sewage epidemiology indicator, hospitals disinfection, drug therapies and recommendations, *Journal of Environmental Chemical Engineering*, 8 (4): 104006.

Berlemont, A., Grancher, M.S., Gouesbet, G. (1995). Heat and mass transfer coupling between vaporizing droplets and turbulence using a Lagrangian approach, *International journal of heat and mass transfer*, 38(16), 3023-3034.

Bourouiba, L. (2021). The fluid dynamics of disease transmission. *Annual Review of Fluid Mechanics*, 53, 473-508.

Courant, R., Friedrichs, K., Lewy, H. (1967).On the partial differential equations of mathematical physics. *IBM Journal Research and Development*, 11, 215-234.

Hirt, C.W., Nichols, B. D. (1981). Volume of fluid (VOF) method for the dynamics of free boundarie. *Journal of computational physics*, 39 (1), 201-225.

Holshue, M.L. et al. (2020). First case of 2019 novel coronavirus in the United States. *New England Journal of Medicine*.

Issa, R.I. (1986). Solution of the implicitly discretised fluid flow equations by operator-splitting, *J. Comput. Phys.*, 62, 40–65**.**

Johnson, D. et al. (2013). Aerosol generation by modern flush toilets. *Aerosol Science and Technology*, 47 (9), 1047-1057.

Kurokawa, F.A. (2019). *Contribuições das investigações de técnicas numéricas para o desenvolvimento de modelagens em CFD para problemas de engenharia civil*. [Tese de Livre-docência, Universidade de São Paulo].

Launder, B.E., Spalding, D. B. (1974). The numerical computation of turbulent flows. *Computer methods in applied mechanics and engineering*. 3 (2), 269–289.
Liu, Y. et al. (2020). Aerodynamic analysis of SARS-CoV-2 in two Wuhan hospitals. *Nature*, 582 (7813), 557-560.

Mcdonough, J.M. (2007) *Introductory lectures on turbulence: physics, mathematics and modeling*.

Weidhaas, Jet al. (2021). Correlation of SARS-CoV-2 RNA in wastewater with COVID-19 disease burden in sewersheds, *Science of The Total Environment*, 775:145790.

World Health Organization (2020). *Novel coronavirus (2019-nCoV). Situation report – 1.* <https://www.who.int/docs/default-source/coronaviruse/situationreports/20200121-sitrep-1-2019ncov.pdf?sfvrsn=20a99c10_4>.

7   Presentation of Authors

Ludmila Souza Vieira holds a Master's of Civil Engineering from *Escola Politécnica* of the University of São Paulo, Department of Construction Engineering. Her thesis analyzes the dispersion of SARS-CoV-2 by means of aerosols from sanitary basins using CFD.

Lúcia Helena de Oliveira is Associate Professor at the Department of Construction Engineering of *Escola Politécnica* of the University of São Paulo, where she teaches and conducts research work on building services.	
Fernando Akira Kurokawa is Assistant Professor at Department of Construction Engineering of *Escola Politécnica* of University of São Paulo, where he teaches and conducts researches on CFD simulations and graphical geometry for engineering.	
Amanda Sayuri Oizuni is an undergraduate student at Department of Construction Engineering of *Escola Politécnica* of University of São Paulo with scholarship granted by PUB-USP for the undergraduating research on Computational Modeling and Prototyping in Civil Engineering.	

Designing a lead measuring protocol in de domestic drinking water installation

E.J.M. Blokker (1), A. Dash (2)

(1) Mirjam.blokker@kwrwater.nl

(2) Amitosh.dash@kwrwater.nl

(1) KWR Water Research Institute, The Netherlands. TU Delft, The Netherlands.

(2)) KWR Water Research Institute, The Netherlands.

Abstract

Lead intake is unsafe, particularly for young children. The norm for the maximum lead concentration in drinking water will be lowered to 5 μg/L. This norm is related to the weekly average intake of lead through drinking water from the tap. If the intake is too high, there is a need to take measures to remove the lead source. In the Netherlands, the source of lead in drinking water can be lead pipes (in the domestic drinking water installation, or in the connection between the drinking water distribution system and the domestic system), lead solder in copper pipes, or brass fittings. Both the weekly intake and the concentrations in individual samples are a consequence of the lead leaching into the drinking water from the pipe (or fitting) and is affected by contact time, and thus by drinking water demand patterns on all taps in the system. There is a need for a measurement protocol that can be used to a) assess the weekly average intake and b) in case of norm exceedance finding the location of lead, so it can be removed from the system. The approach we followed was building a hydraulic (network) model of the domestic drinking water installation with stochastic demand patterns (from SIMDEUM) on all taps. We used EPANET as a hydraulic solver and water quality solver. We did a sensitivity analysis for a variety of pipe lengths, pipe diameters, family size, and water using efficiency to determine the effect on weekly average intake and concentrations that would be found in samples. Results were used to assess the effectiveness of various measurement protocols on giving information on weekly intake and determining lead locations in the system.

Keywords

Domestic drinking water installation, lead intake, lead detection, measurement protocol.

1 Introduction

Lead intake is unsafe, particularly for young children. The norm for the maximum lead concentration in drinking water will be lowered from 10 to 5 μg/L. This norm is related to the weekly average intake of lead through drinking water from the tap. If the intake is too high, there is a need to take measures to remove the lead source. In the Netherlands, the source of lead in drinking water can be lead pipes (in the domestic drinking water installation (DDWI), or in the connection between the drinking water distribution system and the domestic system), lead solder in copper pipes, or brass fittings.

Numerous sampling protocols have been devised over the course of history. It is acknowledged that there is no universal protocol that answers all questions (for example, exposure at communal/household scale, presence/location of lead releasing component) and that each protocols answers a specific question (Triantafyllidou et al. 2021). There is a need for a measurement protocol that can be used to a) assess the weekly average intake and b) in case of norm exceedance to find the location of lead, so it can be removed from the system. For this reason we have assessed two protocols, viz. proportional sampling and profile sampling, using a modelling approach.

2 Methods and materials

Both the weekly intake and the concentrations in individual samples are a consequence of the lead leaching into the drinking water from the pipe (or fitting) and is affected by contact time, and thus by drinking water demand patterns on all taps in the system.

The approach we followed was building a hydraulic (network) model of the domestic drinking waterinstallation with stochastic demand patterns (from SIMDEUM) on all taps. We used EPANET as a hydraulic solver and water quality solver. We did a sensitivity analysis for a variety of lead sources in the DDWI (lead pipes, lead solder in copper pipes, and brass fittings in water meters and faucets), pipe lengths, pipe diameters, family size, and water using efficiency to determine the effect on weekly average intake and concentrations that would be found in samples.

The starting point of the simulations is the definition of an indoor premise plumbing system with pipe lengths and diameters and points-of-use. We consider a typical Dutch household with water usage spread out over three stories (Moerman et al. 2014). The water enters the ground floor via a service line (Dash et al. 2022) and continues into the indoor plumbing via the water meter. A toilet and kitchen is located on the ground floor, a toilet and shower on the first floor and a washing machine on the second floor. Moreover, on the second floor the boiler serves to supply hot water. Information about

the points-of-use, together with the composition of the household (number of adults and children, attitude towards water consumption) are fed to SIMDEUM (Blokker et al. 2017), a stochastic drinking water demand model. This program generates realistic water consumption patterns at each usage point. These generated demand patterns are then added to the EPANET model.

The final aspect of the modelling involves the selection of lead releasing piping/components in the installation. These components are deemed to release dissolved lead into the water according to a lead dissolution model. In EPANET, we make use of a first order saturation growth model for the bulk reaction (Dash et al. 2022). The lead dissolution model is described by:

$$\frac{dC}{dt} = \frac{4M}{DE}(E - C) \tag{1}$$

Here, the increase in dissolved lead concentration (C) in time (t) is governed by the pipe diameter (D), the dissolution rate (M), and equilibrium lead concentration or plumbosolvency (E). In our simulations, $E = 110$ µg/l and $M = 0.115$ µg/(m^{2}s).

The transport of lead is only governed by advection in our simulations. We limit ourselves to the analysis of dissolved lead so particulate lead is currently not being concerned. Dash et al. (2022) give some more information on specific simulation settings.
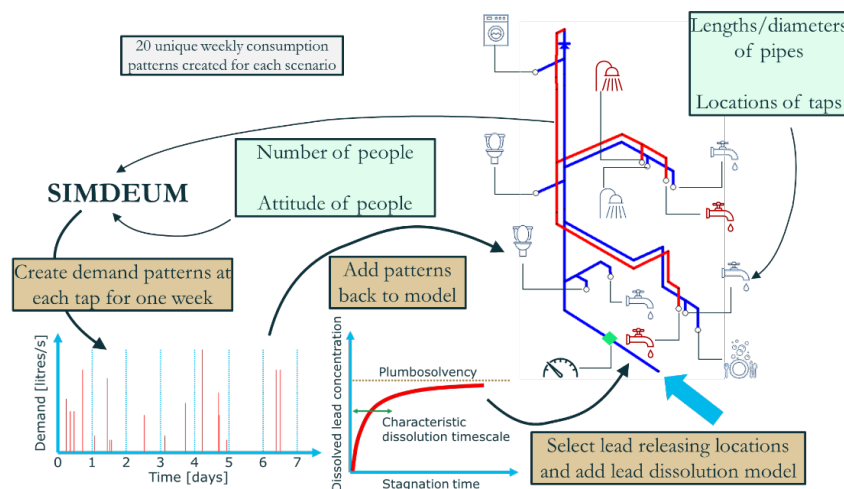
Figure 1: Framework and components of the numerical simulations.
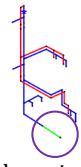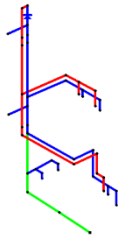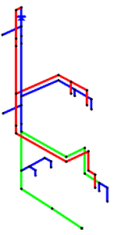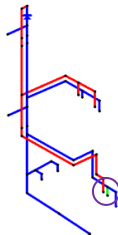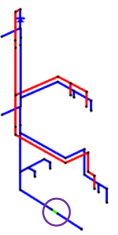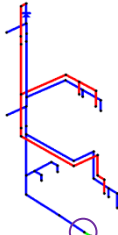
In order to determine the value of the sampling methods, various scenarios were simulated, see Table 1. A benchmark scenario was established, on which variations in the location of the lead releasing components are made. Dash et al. (2022) describe a more rigorous sensitivity analysis.

1. Benchmark case: The geometry as defined above is considered. The water consumption patterns are generated using SIMDEUM with the assumption that it is inhabited by two adults with average water usage characteristics (by Dutch

standards). The service line is the sole lead releasing component. For this case, 20 weeks with different consumption patterns were simulated.

2. Six variations in location of lead releasing components: First, the system of pipes responsible for lead dissolution is exaggerated. In one case, all pipes from the shutoff valve to the kitchen are responsible for lead dissolution. In another case, all pipes from the shutoff valve to the kitchen tap (excluding the kitchen tap itself) release lead. Then, the length of the lead releasing pipe is reduced to a piece of 20 cm, which is used for three cases - the kitchen tap itself, immediately upstream of the water meter and immediately downstream of the shutoff valve. In the final case, the service line is modified to have a diameter of 25 mm and a length of 3 m. The most upstream, the most downstream, and the central 20 cm of the service line release lead (an exaggerated form of lead soldering).

Table 1: Schematic description of scenarios. Lead releasing locations are shown in green and are encircled.

Benchmark	(Pipes of certain lengths and diameters)	(Two adults with average Dutch consumption characteristics)	(Lead service line)
Variations in lead releasing part(s)	(Shutoff valve to kitchen)		(Shutoff valve to kitchen tap)
	(Kitchen tap only)		(Piece at water meter)
	(Piece at shutoff valve)		(Lead solder in service line)

On top of the generated water demand patterns, sampling protocols were added on. For each scenario, the following protocols were simulated:

1. Proportional Sampling: no additions/modifications were made to the water consumption patterns. Every moment of water usage at the kitchen tap is treated as a potential sample and no distinction is made whether the water is consumed or not (for example, drinking versus washing hands).

2. Profile sampling: Following a prolonged stagnation of six hours (between 0100-0700), twenty samples of 300 ml are collected consecutively at 07:00 on each day of the simulation. These samples are appended as demand (300 mL in 10 seconds). During the prolonged stagnation, any water usage generated in the house by SIMDEUM is annulled. In our simulations, the measurement protocol is implemented as follows. A prolonged standstill is imposed on each of the 140 days of the simulation between 01:00-07:00. This means that any water consumption created by SIMDEUM, everywhere in the household, in this timeframe is removed. Immediately following the prolonged standstill, twenty consecutive samples with a volume of 300 ml are collected at the kitchen tap.

3   Results

3.1   Proportional Sampling

One of the parameters that needs to be assessed is the weekly lead consumption via drinking water. In this section, we present typical weekly lead consumption trends and how these are affected by the scenarios illustrated in Table 1. To clarify, the simulations considered here do not have any sampling protocol added onto the consumption patterns generated by SIMDEUM.

The weekly lead consumption via drinking water is especially of interest to the Dutch water utilities who wish to know whether copper mains with lead soldering can lead to norm exceedance. The scenarios wherein extensive lead plumbing is present unsurprisingly leads to norm exceedance. The presence of a small lead component (length 20 cm) can lead to breaches depending on its location relative to the point-of-use. When located at the kitchen tap itself, the norm is breached since the lead cannot be transported elsewhere. However, when these pieces are located further away (for example, in the service line), the lead discharge gets spread out. Our results suggest that the presence of copper service lines with lead solder might not lead to norm exceedance and need not be prioritized by the water utilities.

Scenario ↓ / Week nr →	1	2	3	4	5	6	7	8	9	10	11	12	13	14	15	16	17	18	19	20	Mean	Min	Max
Benchmark	5.8	8.8	5.1	4.6	8.7	6.8	5.4	4.9	4.1	5.3	5.2	6.6	5.9	6.9	6.6	7.8	4.0	6.2	6.1	5.6	5.8	4.0	8.8
Shutoff valve to kitchen	25.1	43.1	27.5	32.4	36.6	29.3	27.9	23.1	25.2	24.9	35.6	38.7	25.6	39.6	29.6	32.1	24.7	25.3	24.4	31.8	29.1	23.1	43.1
Shutoff valve to kitchen tap	41.2	60.0	45.3	50.9	59.3	46.4	43.2	37.4	41.1	36.3	50.4	56.4	46.6	59.7	46.5	55.6	40.0	35.8	39.4	48.4	45.5	35.8	60.0
Kitchen tap only	10.4	16.4	10.3	14.1	15.6	13.4	10.0	11.2	10.6	9.8	14.6	15.6	11.9	21.0	14.8	17.8	11.3	10.1	13.8	12.1	12.6	9.8	21.0
Piece at water meter	1.7	1.4	1.0	0.8	2.1	2.4	1.0	1.1	0.7	1.9	0.6	0.9	1.1	1.7	1.7	2.0	0.5	0.7	1.4	1.8	1.3	0.5	2.4
Piece at shutoff valve	0.6	1.5	0.7	2.4	3.1	1.7	1.3	0.4	0.8	0.6	1.2	0.5	2.1	2.1	1.3	1.0	1.4	1.2	1.3	1.1	1.2	0.4	3.1
Lead solder	2.4	3.4	2.3	2.1	5.3	4.5	2.6	1.7	2.6	1.7	4.3	2.0	2.4	2.9	2.6	2.0	1.7	2.1	3.3	2.8	2.7	1.7	5.3

Figure 2: Weekly variations and statistics thereof for dissolved lead concentrations at the kitchen tap. In green values < 5 µg/L (below new norm) and in red values > 10 µg/L (above old norm).

Proportional sampling is rightly perceived as the gold standard as far as measurement of lead consumption at household scales is concerned. However, the sample is typically collected over a week. In Figure 2, we present how week-to-week variations in water consumption affects the dissolved lead concentrations at the kitchen tap across the scenarios. Note that demand patterns in all scenarios are the same. Thus, for a certain week, consumption pattern across the scenarios are correlated – for example, from week 4 to week 5, increased lead exposure is seen across all scenarios. In the final three columns, the average, minimum, and maximum values across the twenty weeks are shown. In brief, it is irrefutable that week-to-week variations in water consumption patterns trigger variations in dissolved lead concentrations which, in turn, can affect the plan-of-action. This means, that in some weeks the weekly intake is below the norm – and now action would be needed. While in another week the norm may be exceeded and further action is required. Thus, it is recommended to implement proportional sampling over a longer timeframe – for example, five non-consecutive weeks spread out over a year.

3.2 Profile sampling

In this section, we consider sampling of individual homes, in order to establish if lead releasing components are present. The current sampling protocol of the water utilities is the so called Random Daytime (RDT) approach, which entails collecting a sample of water at a random time (during working hours) on a random day (working day). The current protocol that is recommended by the Dutch National Institute for Public Health and the Environment (RIVM), involves collecting a one Liter sample following a six hours stagnation period. Based on previous modelling exercises (Blokker 2021) we have suggested a profile sampling approach after stagnation (6 hours of stagnation, then twenty consecutive samples of 300 ml are collected at the kitchen tap). An example of this collection strategy is shown in Figure 3(a). Please note that the addition of a sampling protocol is intrusive and will affect the numerical values reported in Figure 2.

The corresponding lead concentrations computed at the kitchen tap are shown in Figure 3(b). The pink line shows what would have been measured by a hypothetical lead concentration sensor inside the tap. From the lead concentrations corresponding to normal usage, it can be seen that there are instances wherein the lead concentration at the tap exceeds the (future) norm of 5 µg/L. This clearly illustrates that the RDT approach may be susceptible to these outliers and planning actions on basis thereof is

unreliable. Blokker (2021) showed that the probability of exceeding the lead norm with an RDT sample in the modelled home (with lead pipes) is less than 5%. In the inset of Figure 3(b), it can also be seen that three of the twenty samples yield strikingly high lead concentrations (close to imposed plumbosolvency).
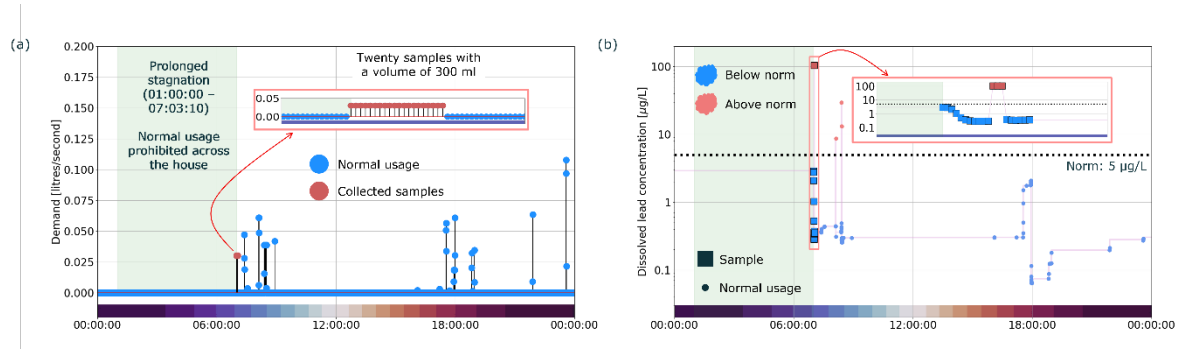
Figure 3: Example of a typical input/output in the simulations over one day at the kitchen tap for (a) water usage and samples for profile sampling (b) dissolved lead concentrations. The gradient colorbar at the bottom is a visual representation of the time of the day.

To investigate the statistics behind the performance of profile sampling, Figure 4 is considered. Basically, in Figure 4(a), for each sample under each scenario, the probability that the lead concentration exceeds 5 µg/L is shown. The last column shows the sum of samples 1-3 is, which roughly corresponds to the results the RIVM protocol would have (0.9 Liter instead of 1.0).

In the benchmark case the RIVM protocol has a chance of ~12% to have concentrations above 5 µg/L. However, samples 12-14 have a 100% chance of meeting the criterion. From a practical perspective, this is attractive. This means that irrespective of the day/week/month on which this sampling protocol is performed, samples 12-14 are guaranteed to have lead concentration above 5 µg/L. Also, in all scenarios where lead is present, at least one of the twenty samples is guaranteed to show lead concentrations above 5 µg/L. Even the small components of 20 cm long are picked up by this protocol. This partly demonstrates the robustness of profile sampling under realistic water consumption patterns. It is important to realize that the choice of 20 samples of 300 ml is instrumental. Had sampling been coarser (for example, 10 samples of 600 ml or 5 samples of 1200 ml), samples with high lead concentrations could have gotten diluted, diminishing the robustness of this sampling protocol.

To firmly establish the robustness of profile sampling, Figure 4(b) is considered. Here, the numbers are conditionally averaged lead concentrations over the samples in which the concentration exceeds 5 µg/L. For the benchmark case, samples 12-14 have average concentrations above 100 µg/L, while for the other samples, it varies between 20-40 µg/L. In fact, for every sample/scenario combination in Figure 4(a) with 100%, the corresponding conditionally averaged lead concentration is in the vicinity of the plumbosolvency of 110 µg/L. This means that the lead from the lead releasing

components will not only invariably end up in the same sample but will also end up in a high concentration, facilitating easy and unambiguous detection.

(a)

Scenario ↓ / Sample nr →	1	2	3	4	5	6	7	8	9	10	11	12	13	14	15	16	17	18	19	20	RIVM
Benchmark	11%	12%	12%	0%	2%	2%	3%	1%	1%	0%	2%	100%	100%	100%	0%	0%	0%	0%	0%	0%	12%
Shutoff valve to kitchen	57%	57%	61%	100%	100%	100%	100%	100%	100%	100%	100%	100%	100%	100%	0%	0%	0%	0%	0%	0%	58%
Shutoff valve to kitchen tap	83%	100%	100%	100%	100%	100%	100%	100%	100%	100%	100%	100%	100%	100%	0%	0%	0%	0%	0%	0%	94%
Kitchen tap only	100%	0%	0%	0%	0%	0%	0%	0%	0%	0%	0%	0%	0%	0%	0%	0%	0%	0%	0%	0%	33%
Piece at water meter	2%	4%	4%	0%	1%	0%	1%	0%	0%	0%	1%	100%	0%	0%	0%	0%	0%	0%	0%	0%	3%
Piece at shutoff valve	1%	2%	2%	2%	0%	0%	1%	0%	1%	0%	0%	0%	1%	100%	0%	0%	0%	0%	0%	0%	2%
Lead solder	7%	6%	11%	0%	1%	0%	1%	0%	1%	0%	0%	0%	1%	100%	1%	3%	0%	0%	0%	0%	8%

(b)

Scenario ↓ / Sample nr →	1	2	3	4	5	6	7	8	9	10	11	12	13	14	15	16	17	18	19	20	RIVM
Benchmark	35.0	36.0	40.0		18.0	18.0	19.0	20.0			18.0	104.0	104.0	104.0							37.0
Shutoff valve to kitchen	44.0	40.0	40.0	107.0	107.0	107.0	107.0	106.0	106.0	106.0	106.0	106.0	106.0	106.0							41.3
Shutoff valve to kitchen tap	66.0	110.0	109.0	108.0	107.0	107.0	107.0	106.0	106.0	106.0	106.0	106.0	106.0	106.0							95.0
Kitchen tap only	110.0																				36.7
Piece at water meter	41.0	41.0	25.0		18.0		19.0				12.0	103.0									35.7
Piece at shutoff valve	19.0	43.0	23.0				18.0		12.0				19.0	103.0							28.3
Lead solder	28.0	40.0	23.0		21.0		28.0		15.0				21.0	106.0	15.0	25.0					30.3

Figure 4: (a) Probability (%) that a sample in a certain scenario contains dissolved lead with concentration > 5 μg/L. (b) Conditionally averaged lead concentrations in all samples in which the dissolved lead concentration > 5 μg/L.

Figure 5 summarizes the principle behind profile sampling. The plumbing between the distribution network and a single faucet is shown. The water meter is preceded by a service line. The plumbing is partitioned into equal volumes representing the volume of each sample that is to be collected following a prolonged standstill. Based on sample collection over two days, a lot of information can be extracted from the profiles. The first day of measurements returns predictions for potential locations of the lead releasing components. The second day of measurements help classify the true and false positives. For example, in the schematic, sample 5 from day 1 is a false positive since it does not possess high concentrations on day 2. However, samples 12, 13 are true positives and correspond to the lead releasing component. We refer to samples 12, 13 as the peak. Following the peak, the lead is flushed away and there is no chance that a sample will contain any dissolved lead. Based on this peak, the following information can be gathered and can be useful in prioritizing which households need to be investigated first.

1. Location of the peak: If a drawing of the premise plumbing is available, based on the location of the peak and the volume of the individual samples, it should be theoretically possible to estimate where in the plumbing system the lead originates from. The location can be relevant in determining whether it is the responsibility of the premise owner or the water utility. The further away the lead releasing component is from the tap, the better it is for the safety of the inhabitants, since the dissolved lead gets spread out.
2. Breadth of the peak: The total volume of the peak indicates the severity of the problem. Naturally, the narrower the peak, the better it is for the inhabitants.
3. Height of the peak: This contains information about the local level of plumbosolvency which will likely be related to the water chemistry and

temperature, specific to the distribution area. The lower the peak, the better it is for the inhabitants.
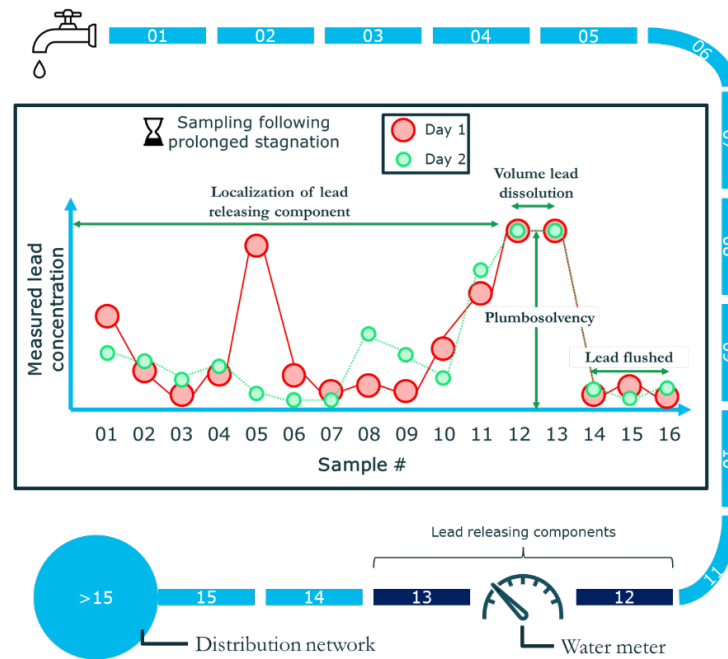
Figure 5: Schematic of the functionality of profile sampling and the information that can be derived therefrom.

4   Discussion

In judging the results presented here, it is important to realize that the absolute values of lead concentration are valid for the assumptions made by us about the values for plumbosolvency and lead dissolution rate. For example, there are numerous factors, such as pH levels and temperature, that will lead to variations in lead leaching rates. Moreover, the results are specific to this household. Nevertheless, the results show the value of such simulations in assessing lead consumption at household scales. The preliminary results show that any lead piping leads to exceedance of the norm for the weekly intake, but lead solder and brass fittings in water meters are far less contributing to the weekly intake.

The profile sampling performs better than RDT and the RIVM protocol in determining if there is a lead releasing component in the house. Next to that it also provides information on where this component is located. So, the profile sampling is very robust and could be made even more robust by fully flushing the plumbing prior to stagnation, thus eliminating any false positives. This means, eliminate the positives that do show there is a lead releasing component, but do no reliably show its location or inform us on plumbosolvency. In order to establish whether the robustness of profile sampling as demonstrated with the model can withstand real conditions a measurement campaign is planned.

Each sampling protocol has its own objective. The objective of the proportional sampling is to determine the weekly intake. The objective of profile sampling is to detect and localize the lead releasing components. The model shows that week-to-week variations in water consumption patterns lead to variations in the weekly intake. Thus, it is recommended to implement proportional sampling over a longer timeframe – for example, five non-consecutive weeks spread out over a year. However, this sampling protocol has various practical difficulties, and it would be interesting to see whether an empirical correlation can be established between the weekly lead consumption and the parameters that are measured with profile sampling: location, height of the peak and breadth of the peak.

In this paper we have applied the premise plumbing modelling approach to determine the effect of lead releasing components on the weekly intake of lead and the chance of finding lead in water quality samples at the kitchen tap. A sensitivity analysis was performed to show the effect of variations in consumption, pipe diameters and pipe lengths (Dash et al. 2022). The same approach will also be applied for nurseries. The model can also be used to determine what the effect is of future scenarios such as decreasing demand and manganese dosing (Hatam et al. 2023).

The model's added value is found in modelling concentrations of substances that are entering the system close to the point of use, e.g. at the service line, water meter or within the premise plumbing. The concentration of such a substance is highly influenced by the (variation) in drinking water demand patterns and the layout of the drinking water installation. Next to metals, a substance of interest could be volatile components such as benzene that can permeate from contaminated soil through a PE service line into the drinking water system.

5   References

Blokker, E. J. M. (2021). "When is the lead norm in a home exceede>? Facts and figures. Modelling lead exposure at the kitchen tap." (in Dutch) *KWR 2021.004*, KWR, Nieuwegein.

Blokker, E. J. M., Agudelo-Vera, C., Moerman, A., van Thienen, P. and Pieterse-Quirijns, E. J. (2017). "Review of applications for SIMDEUM, a stochastic drinking water demand model with a small temporal and spatial scale." *Drinking Water Engineering and Science*, 10(1), 1-12. http://www.drink-water-eng-sci.net/10/1/2017/dwes-10-1-2017.pdf

Dash, A., van Steen, J. E. and Blokker, E. J. M. (2022). "Robustness of profile sampling in detecting dissolved lead in household drinking water." *WDSA CCWI*, Valencia, Spain.

Hatam, F., Blokker, M., Doré, E. and Prévost, M. (2023). "Reduction in water consumption in premise plumbing systems: Impacts on lead concentration under different water qualities." *Science of The Total Environment*, 162975, doi:https://doi.org/10.1016/j.scitotenv.2023.162975.

Moerman, A., Blokker, E. J. M., Vreeburg, J. and van der Hoek, J. P. (2014). "Drinking water temperature modelling in domestic systems." *16th Conference on Water Distribution System Analysis, WDSA*.

Triantafyllidou, S., Burkhardt, J., Tully, J., Cahalan, K., DeSantis, M., Lytle, D. and Schock, M. (2021). "Variability and sampling of lead (Pb) in drinking water: Assessing potential human exposure depends on the sampling protocol." *Environment international*, 146, 106259.

Study on Hand Washing for Preventing COVID-19 in Various Countries, Regulatory Trends, and Issues

Megumi Itabashi (1),   Masayuki Otsuka (2)

(1) m22J3002@kanto-gakuin.ac.jp

(2) dmotsuka@kanto-gakuin.ac.jp

(1) Graduate Student, Graduate School of Engineering Kanto Gakuin University, Japan

(2) Prof. Dr. Eng, Department of Architecture and Environmental Design, College of Architecture and Environmental Design, Kanto Gakuin University, Japan

Abstracts

Since January 2020, the pandemic of the new coronavirus infection (COVID-19) has overwhelmed the world. However, as of 2023, mandatory mask-wearing, both indoors and outdoors, has been shifted and COVID-19 countermeasures are gradually becoming relaxed in many countries. As for hand washing, it is recognised by CDC and WHO as an effective preventive measure against contact infections, not only by COVID-19 but also by infectious bacteria. Therefore, hand washing should continue to be regarded as an important preventive measure against many types of viral infections.

Accordingly, this report investigates and describes trends in research on hand washing practised in a wide range of fields, including the water supply/drainage and sanitary equipment field, the medical field and the public health field, in Japan, as well as mentioning research trends in other countries. In addition, the report presents a hand-washing experiment, conducted by the authors, in which participating students were asked to wash their hands the way they normally would, and the report suggests, on the basis of the experiment results and through a comparison between the students' hand-washing actions and a recommended hand-washing method, issues that need to be addressed by researchers in future studies.

Keywords
COVID-19,   Hand washing,   Measures against contact infections,
Hand-washing actions

1 Background and purpose of study

1.1 Background of study

Since January 2020, the pandemic of the new coronavirus infection (COVID-19) has been confirmed worldwide. However, as of 2023, restrictions introduced as COVID-19 countermeasures are gradually becoming relaxed in many countries. On the 5th of May, 2023, the World Health Organization (WHO) declared the end of the 'Public Health Emergency of International Concern' (PHEIC) regarding COVID-19. Also in Japan, since the 8th of May, 2023, the classification of COVID-19 has been lowered to Category V under the infectious disease law, and the Japanese government has lifted more or less all the requirements including mandatory mask-wearing. Nonetheless, the WHO continues to warn that COVID-19 is still a very serious health threat. Therefore, bearing in mind that new COVID-19 cases are still being reported in Japan, it is important that people take precautions based upon their own judgement especially when interacting with the vulnerable including the sick and elderly. In addition, hand washing is considered as an important measure for preventing and controlling the spread of common colds and seasonal flu.

Moreover, well before the COVID-19 pandemic, hand washing-related documents were produced in many different fields to promote infection prevention and control, including documents with the main focus on 'hand washing at the time of surgery and by medical workers' and 'daily hand washing and eradication rates' in the medical and public health fields, and only a few but still important documents relating to 'amounts of water used for sanitary fixtures' in the building construction field. After the outbreaks of COVID-19 in 2020, the medical field has seen some increases in the number of documents relating to 'hand washing by medical workers and disinfection and prevention effects', 'infectious disease countermeasures for patients with certain diseases' and 'awareness surveys on infection preventive measures including hand washing'. Meanwhile, little research has been done, in the light of building facilities, regarding types of faucets and water flow rates for hand washing.

1.2 Purpose of study

The previous report[1] presented an examination, which was conducted through experiments, on changes in water usage amounts and disinfection effects due to flow rate setting for an automatic faucet when hand washing was performed by applying the hand-washing method and rinsing time recommended by the Ministry of Health, Labour and Welfare (MHLW) of Japan. The report also consequently indicated that when the flow rate of the automatic faucet was set to 2.0[L/min] and approximately 0.6-0.8L of water was used for washing hands, the disinfection effect of hand washing was approximately 85% or more.

However, the fact is that the experiment participants most likely use manual faucets for daily hand washing, and less likely to practise the MHLW-recommended hand-washing method.

Accordingly, this study aims to examine a water-saving, hygienic hand-washing method, which

could be useful in future cases of infectious disease outbreaks and disasters, by analysing hand washing-related documents that were published both domestically in Japan and globally, and the infection measures that were issued by various countries during the COVID-19 pandemic.

2 Overview of hand washing-related guidelines by academic organizations of various countries

This chapter examines hand washing-related guidelines and web sites, which were launched, subsequent to the spread of COVID-19, by organizations expert in hygiene and infectious diseases, and building facilities, and aims to discuss hand-washing methods as infection preventive measures, and differences among the methods.

2.1 Hand washing-related guidelines

Since before the COVID-19 pandemic, medical and hygiene-related organizations have been presenting guidelines for medical personnel as to how and when to wash hands. Among such organizations, the CDC[2)-4)] and theWHO[5)-6)] are the two major organizations, and the guidelines presented by them have often been referenced by many governments and other organizations. Table 1 shows a summary of the hand washing-related information that was provided, following the COVID-19 pandemic, in the forms of guidelines, posters and web sites, by four authorities and organizations; the internationally influential CDC and WHO, and the MHLW and the SHASE in Japan.

The examination of the guidelines by these four authorities and organizations found no significant difference among them in terms of which parts of hands should be washed and how they should be washed. However, as indicated in bold letters in Table 1, there are some differences in terms of 'water for washing hands', 'materials for drying hands' and 'time lengths' for rinsing hands. With regard to the 'water for washing hands', it is considered that these authorities and organizations, except the WHO, recommend washing hands under running water. As for the 'materials for drying hands', it is inferred that these authorities and organizations all recommend using disposable and/or clean materials for drying hands.

Moreover, the time length required for washing hands suggested by these authorities and organizations are divided into 'soap-scrubbing time' mainly spent on scrubbing hands with soap, and 'rinsing time' spent on rinsing suds off the hands. The CDC specifies the soap-scrubbing time to be 20 seconds, and indicates that the scrubbing process could be completed by the time the happy birthday song was sung twice. However, there is no mention of rinsing time by the CDC. Meanwhile, the WHO specifies the entire hand-washing process to be 40-60 seconds, i.e., the WHO does not clearly state recommended time lengths for soap scrubbing and rinsing separately. The MHLW of Japan made posters based on a document[7)] recommending the soap-scrubbing time be 10 seconds and the rinsing time be 15 seconds, once or twice for each activity. Therefore, it is presumed that the recommended

values for soap scrubbing and rinsing set by the MHLW are 10 seconds and 15 seconds respectively. Furthermore, the SHASE also recommends the soap-scrubbing time be at least 10 seconds and the rinsing time be approximately 15 seconds with reference to the abovementioned document.

Consequently, the examination of the guidelines by these four authorities and organizations found specific soap-scrubbing time lengths indicated by all of them, but found no clear suggestions on the rinsing time by the CDC and WHO with global reach.

Table 1 - Hand washing-related guidelines, posters and websites launched by authorities and organizations[2]-[17]

Purpose	Ref. no.	Conclusion	Rinsing		Drying	
			Rinsing time [s]	Water flow rate [L/min]	Method	No. of towels
Disinfection effect	10)	• The virus removal effect is increased by washing hands more thoroughly and more frequently. • The virus removal effect is increased by scrubbing hands longer and more times. • Washing hands under running water reduces the virus count to 1/1000 from before washing hands	15	—	Paper towel	—
Soap-scrubbing time	11)	• When the rinsing time is 15 sec., the appropriate soap-scrubbing time is 8-15 sec. • Resident bacteria are thought to be lifted from deep under the skin to the skin surface when the soap-scrubbing time is 15 sec. or longer, in which case the rinsing time needs to be longer than the soap-scrubbing time.	15	6.0	Washed towel	1
	12)	• The number of bacteria increases as the soap-scrubbing time increases. • The longer the soap-scrubbing time, the longer the rinsing time needed to sufficiently remove bacteria.	15	6.0	None	—
Rinsing time	11)	• The disinfection effect increases as the rinsing time increases.	15,30,60	6.0	Washed towel	1
	12)	• Bacteria on fingertips are hard to remove by rinsing. • The disinfection effect did not improve even by rubbing fingertips together when rinsing under running water.	4~15, 3,60,120	6.0	None	—
Drying	11)	• At least 2 paper towels are required to sufficiently remove moisture when drying hands.	15	6.0	Paper towel	1,2,3
	12)	• Hand drying is effective in reducing the number of bacteria.	15	6.0	Paper towel	1
Water amount	13)	• The minimum amount of water required for hand washing is 0.33L which is run for 10 sec. at a flow rate of 2.0[L/min].	Arbitrary	2.0~8.0	Arbitrary	—

3 Examination of hand washing-related documents published in Japan and other countries

3.1 Japan

Since before the COVID-19 pandemic, hand washing has always been regarded as important in taking measures against infectious diseases, and a lot of effort has been made to encourage hand washing in the medical and public health fields. When breaking down into different aspects of hand washing, 'disinfection effects'[10], 'hand drying'[11-12], 'rinsing time'[11-12] and 'awareness surveys' are the main aspects which are discussed in many documents, while a very few documents[13] discuss amounts and flow rates of water for hand washing, both of which are required when using water supply and drainage equipment.

This section examines documents published in Japan concerning 'disinfection effects', 'hand drying' and 'rinsing time' which are key factors in hand washing, as well as documents concerning 'amounts of water' which is the focal point of this report. This section then presents the acquired knowledge, as listed below and as shown in Table 2.

(1) The longer time spent on scrubbing hands with soap, the more resident bacteria lifted from deep under the skin to the skin surface due to the cleansing effect of soap, i.e., the longer time spent on scrubbing hands with soap, the longer time needed for rinsing hands in order to sufficiently remove lifted resident bacteria from the skin surface.

(2) Many bacteria remain on fingertips, when compared to the other parts of hands, after rinsing hands and drying them with a paper towel.

(3) The minimum amount of water required for hand washing is 0.33L which is run for 10 seconds at a flow rate of 2.0[L/min]. With an automatic faucet, in consideration of hygiene and water conservation, it is possible to wash hands effectively using 1.0L or less water at the flow rate of 2.0[L/min].

Table 2 – Hand washing-related documents published in Japan

Purpose	Ref. no.	Conclusion	Rinsing		Drying	
			Rinsing time [s]	Water flow rate [L/min]	Method	No. of towels
Disinfection effect	10)	· The virus removal effect is increased by washing hands more thoroughly and more frequently. · The virus removal effect is increased by scrubbing hands longer and more times. · Washing hands under running water reduces the virus count to 1/1000 from before washing hands	15	—	Paper towel	—
Soap-scrubbing time	11)	· When the rinsing time is 15 sec., the appropriate soap-scrubbing time is 8-15 sec. · Resident bacteria are thought to be lifted from deep under the skin to the skin surface when the soap-scrubbing time is 15 sec. or longer, in which case the rinsing time needs to be longer than the soap-scrubbing time.	15	6.0	Washed towel	1
	12)	· The number of bacteria increases as the soap-scrubbing time increases. · The longer the soap-scrubbing time, the longer the rinsing time needed to sufficiently remove bacteria.	15	6.0	None	—
Rinsing time	11)	· The disinfection effect increases as the rinsing time increases.	15,30,60	6.0	Washed towel	1
	12)	· Bacteria on fingertips are hard to remove by rinsing. · The disinfection effect did not improve even by rubbing fingertips together when rinsing under running water.	4~15, 3,60,120	6.0	None	—
Drying	11)	· At least 2 paper towels are required to sufficiently remove moisture when drying hands.	15	6.0	Paper towel	1,2,3
	12)	· Hand drying is effective in reducing the number of bacteria.	15	6.0	Paper towel	1
Water amount	13)	· The minimum amount of water required for hand washing is 0.33L which is run for 10 sec. at a flow rate of 2.0[L/min].	Arbitrary	2.0~8.0	—	—
			Arbitrary	6.0		

3.2 Other countries

Outside Japan, there are also many hand washing-related documents which were published well before the COVID-19 pandemic, and these documents, similarly to the aforementioned Japanese documents, relate to 'disinfection effects'[14], 'hand drying' and 'awareness surveys' which are the crucial measures against infectious diseases from the medical and public health point of view. Meanwhile, there are documents about 'hand washing in developing countries'[15], presenting studies that focus on hand washing using water taps for everyday use and with not as much disinfection effect as hand washing for surgery provides. More precisely, these documents describe washing fingertips, using Tippy Taps which are made of used containers, such as bottles, and which work by tipping water out of the containers to enable hand washing under running water. (Photo 1)

In the same manner as the examination of the Japanese documents, this section examines documents relating to a globally distinctive concept of 'hand washing in developing countries', in addition to documents concerning 'disinfection effects' which is an important factor of the process of hand washing, as well as documents concerning 'amounts of water' [16]-[17] which is the focal point of this report. This section then presents the acquired knowledge, as listed below and as shown in Table 3.

(1) Knowledge about the importance of hand hygiene leads to understanding of time lengths for hand washing and reduction of pathogens that adhere to hands.

(2) In public places, alcohol-based disinfectants, which can be easily provided, are more effective for hand hygiene than hand washing with soap and water.

(3) With regard to hand washing in developing countries, simple hand washing points, such as Tippy Taps, can be set up instead of plumbed faucets so as to enable hand washing under running water.

(4) The removal of bacteria from hands is largely dependent on the length of soap scrubbing time and the amount of water used for hand washing.

(5) Between the pre-and post-COVID-19 pandemic periods, the amount of water used for hand washing at a time has increased by 2.5-2.7 times.

Photo 1 - Tippy Tap example [from 18]

Table 3 - Hand washing-related documents published in other countries

Ref. no.	Purpose	Conclusion	Rinsing		Drying	
			Rinsing time [s]	Water flow rate [L/min]	Method	No. of towels
14)	· Elucidation of hand contamination among food handlers · Impact of hand washing instructions on reduction of hand contamination	· Among 150 food handlers, 2/3 had transient bacteria, but this was reduced to 1/3, i.e., the number of transient bacteria carriers was halved, by providing hand washing instructions.	—	—	—	—
15)	· Comparison between Cool Form and Tippy Tap	· 5L of water enables hand washing approx. 14-15 times (better than Tippy Tap by approx. 1.4-3.75 times.) · 1 dollar worth of soap lasts up to 15000 washes, better than Tippy Tap by 9.4-30 times.	—	—	—	—
16)	· Soap scrubbing and water amounts during hand washing	· A difference was found in the average water consumption between a high-disinfection effect participant group and a low-disinfection effect participant group. · The degree of hand disinfection effect is closely related to the amount of water used for hand washing.	—	—	—	—
17)	· Amounts of water used for hand washing between the pre-and post-COVID-19 pandemic periods	· Water consumption/person/hand washing increased by approx. 2.5-2.7 times through and after the COVID-19 pandemic.	—	—	—	—

4. Experiment using manually operated faucet

On the basis of the aforementioned research trends in and outside Japan, this report, like the previous report[1], focuses on flow rates and amounts of water used for hand washing, and evaluates effective hand washing methods, from both water-saving and hygienic points of view, by comparing the automatic faucet experiment results obtained in the previous report[1] and experiment participants' arbitrary ways of washing their hands using a manually operated faucet which is found in many households and shelters.

4.1 Experiment overview

4.1.1 Experimental system

The experimental water supply system used for this experiment includes a manually operated faucet and the same automatic soap dispenser as in the previous report[1], which are mounted on an experimental pedestal washbasin. (Fig. 5) The height of the experimental washbasin is approximately 80 mm which conforms to the height specified by the Center of Better Living, Japan. (Fig. 3) Using this system, washing flow rates [L/min] during hand washing were measured with a propagation time difference flow rate sensor disposed in the water supply section (pipe diameter approximately 12 mm) of the faucet, and the integrated flow rate of the supplied water was used to calculate water consumption [L]. In addition, the hand washing actions of the experiment participants were filmed from above the pedestal washbasin in order to check the manner in which each participant washes their hands (Fig. 4)

4.1.2 Experiment method

The participants include 35 students of Kanto Gakuin University (27 males in their 20s and 8 females in their 20s). The experiment was conducted to 'discuss cleansing effects by arbitrary hand washing methods', in which the participants were allowed to wash their hands as they normally would in terms of time spent on washing their hands with soap, hand washing routine, time spent on rinsing their hands, and washing flow rate used for rinsing. The conditions set for the experiment are shown in Table 1. As in the previous report[1], two paper towels were used for drying the participants' hands in order to measure disinfection effects by hand washing.
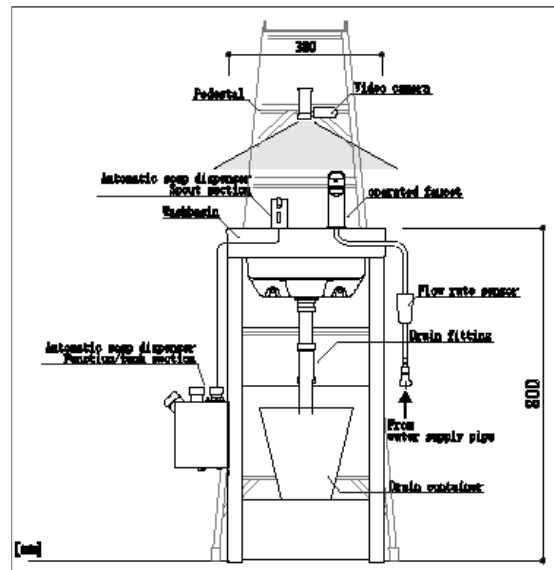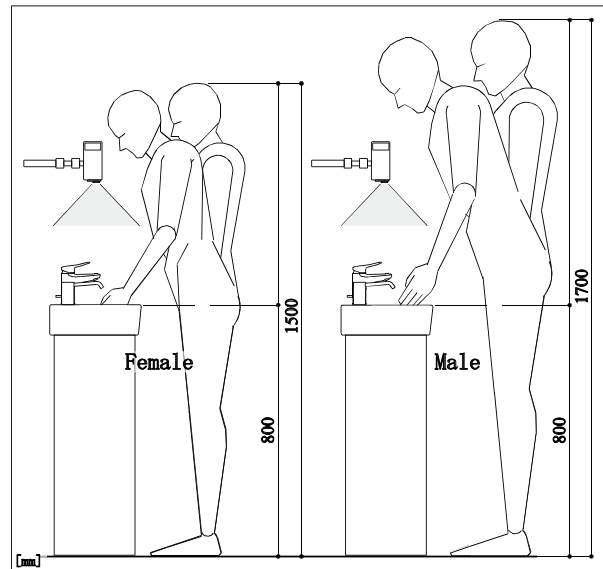
Fig. 2 - Experimental water supply system

Fig. 3 - Experimental water supply system in use - example
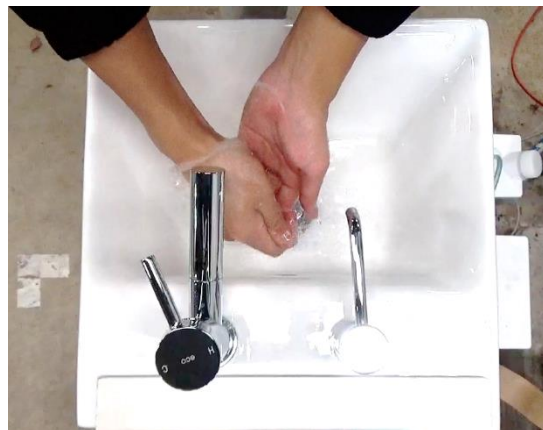
Fig. 4 - Photography point

4.2 Experiment results and discussion

4.2.1 Turning on and off of faucet

Fig. 5 shows an example of how washing flow rates and water consumption vary depending on how the faucet is turned on and off by the participants during hand washing. As the graph shows, the participants' hand washing routines are sorted into three types mainly by how they turn on and off the faucet during hand washing. These three types are: 'on and off' in which the faucet is turned on for wetting hands before applying the hand soap, the faucet is then turned off during soap scrubbing and is turned on again for rinsing; 'leave on' in which the faucet is turned on for wetting hands and is left on during hand washing; and 'rinse only' in which the hand soap is applied to dry hands, and the faucet is turned on only for rinsing.

The experiment found that 60%, i.e., more than half, of the 35 participants used the 'on and off' routine in which they turned off the faucet while scrubbing their hands with the soap, in the same manner as when they used the automatic faucet. The experiment also found that although only a few, approximately 10-15% of the participants used the 'leave on' and 'rinse only' routines. (Fig. 6)
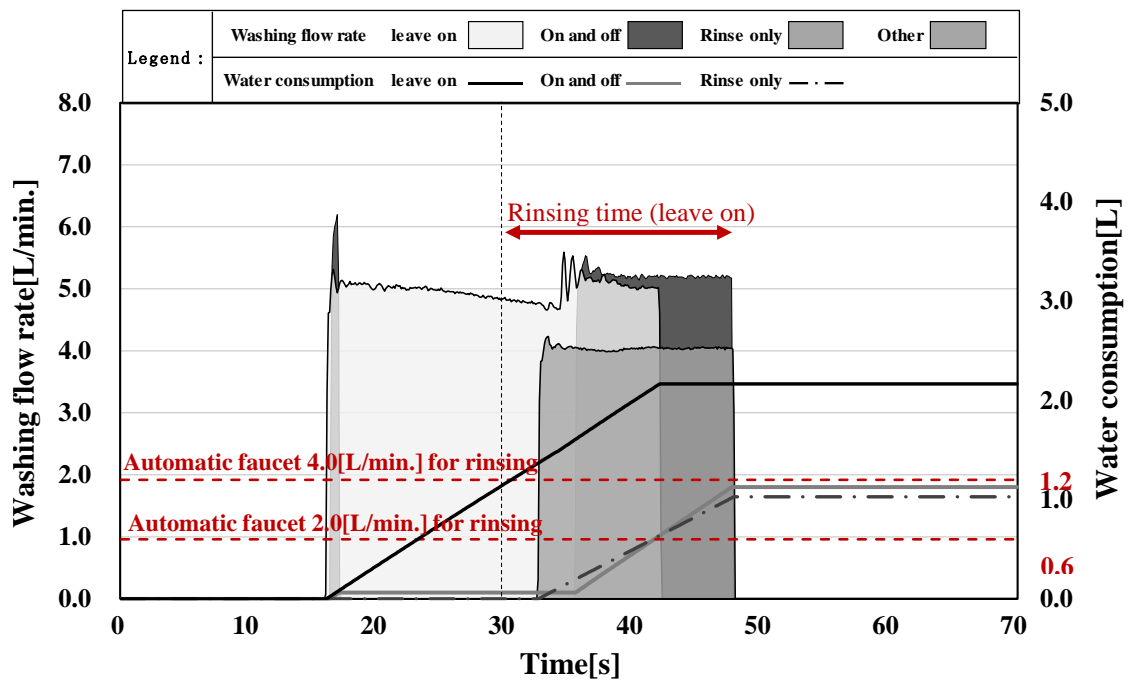
Fig. 5 - Turning on/off of faucet by participants during hand washing
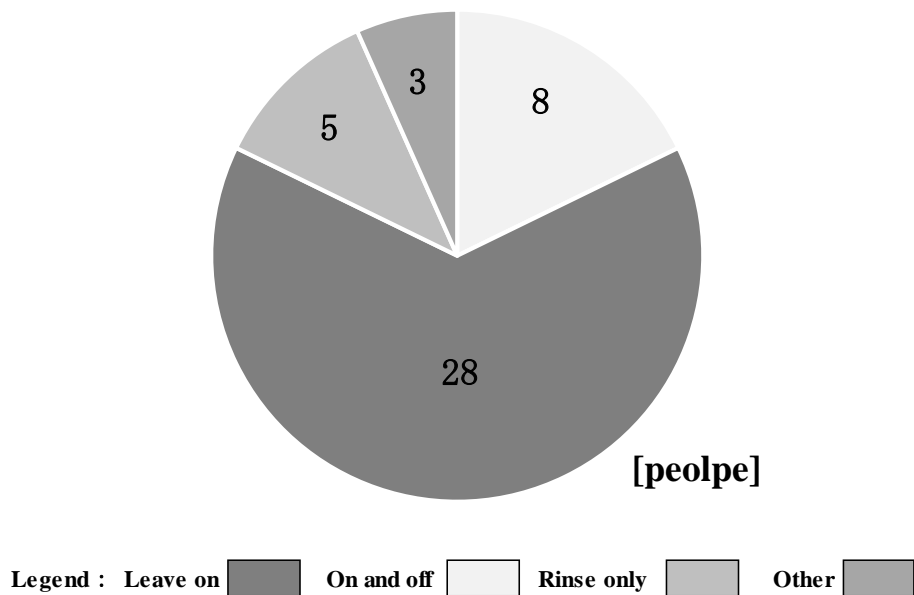
Fig. 6 - Different ways of turning on/off faucet by participants

4.2.2 Rinsing time

Fig. 7 shows the lengths of rinsing time in relation to the faucet on/off operations, respectively. As shown in the graph, the time lengths of rinsing (average values) included in the entire hand washing routines are: 'on and off' approximately 13 seconds; 'leave on' 27 seconds; 'rinse only' 18 seconds; and 'other' approximately 14 seconds. Meanwhile, the average values of rinse-only time using the 'on and off', 'leave on' and 'other' routines all fall short of the MHLW-recommended rinsing time of 15 seconds by 10 seconds, 12 seconds and 10 seconds, respectively, and this clearly indicates that many of the participants do not rinse their hands adequately. Furthermore, comparing the rinsing time included in each hand washing routine and the rinse-only time, the difference therebetween is approximately 16 seconds with the 'leave on' routine in which the faucet is left on during soap scrubbing, and it is only 3 seconds with the 'on and off' and 'other' routines. With the 'leave on' routine, the rinse-only time is approximately 12 seconds while the rinsing time included in the entire hand washing process is approximately 16 seconds, and this confirms that a shorter time is spent on the washing than on the rinsing.
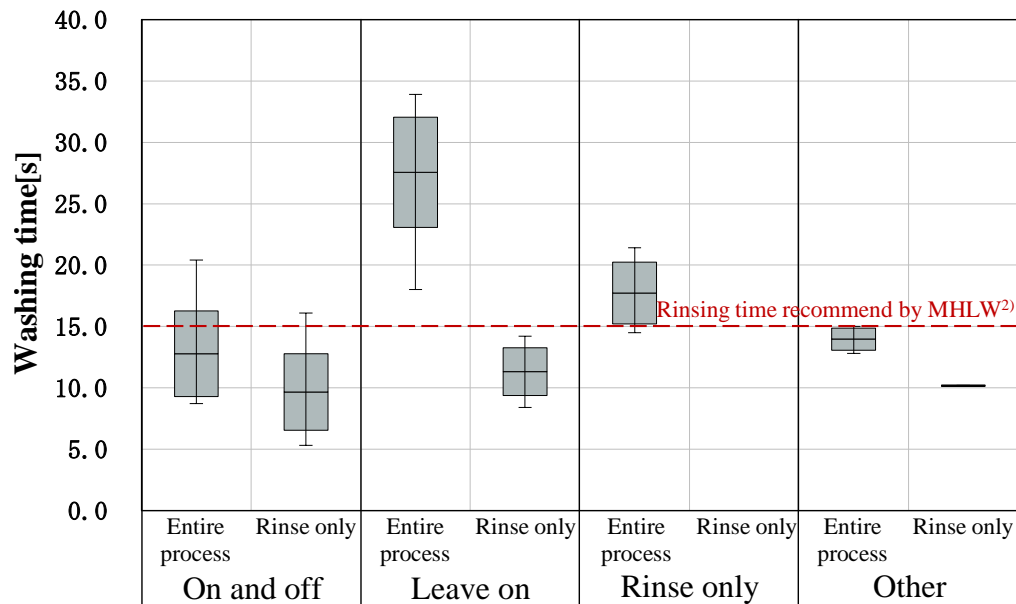
Fig. 7 - Washing time lengths and faucet on/off operations

4.2.3 Washing flow rates and water consumption

Fig. 8 shows the washing flow rates in relation to the faucet on/off operations, respectively. As shown in the graph, the washing flow rates (average values) used during the 'on and off', 'leave on' and 'rinse only' routines are, approximately, 5.0[L/min], 5.5[L/min] and 4.0[L/min] for both the entire hand washing process and the rinsing process. The maximum flow rates used during these routines are approximately 6.0[L/min] which is the same as the maximum flow rate set for the faucet and is more than twice as high as that for the automatic faucet.

Fig. 9 shows the actual water consumption (the actual amount of water used) which was measured during each faucet on/off operation performed by the participants. As shown in the graph, during the 'on and off' and 'other' routines, the average water consumption for both the entire hand washing process and the rinsing process stayed within the water consumption range for the automatic faucet which was described in the previous report[1]. Moreover, during the 'leave on' routine, the same washing flow rate was used for both the entire hand washing process and the rinsing process, yet the water consumption for the rinsing process stayed within the water consumption range for the automatic faucet.

In addition, during the 'other' routine, the washing flow rate (average value) used for both the entire hand washing process and the rinsing process was approximately 4.0[L/min], but because the washing flow rate was changed during the rinsing process, the actual water consumption during the rinsing process was 0.6L, resulting in 0.3L less than the water consumption for the entire hand washing process.

Fig. 8 - Washing flow rates and faucet on/off operations

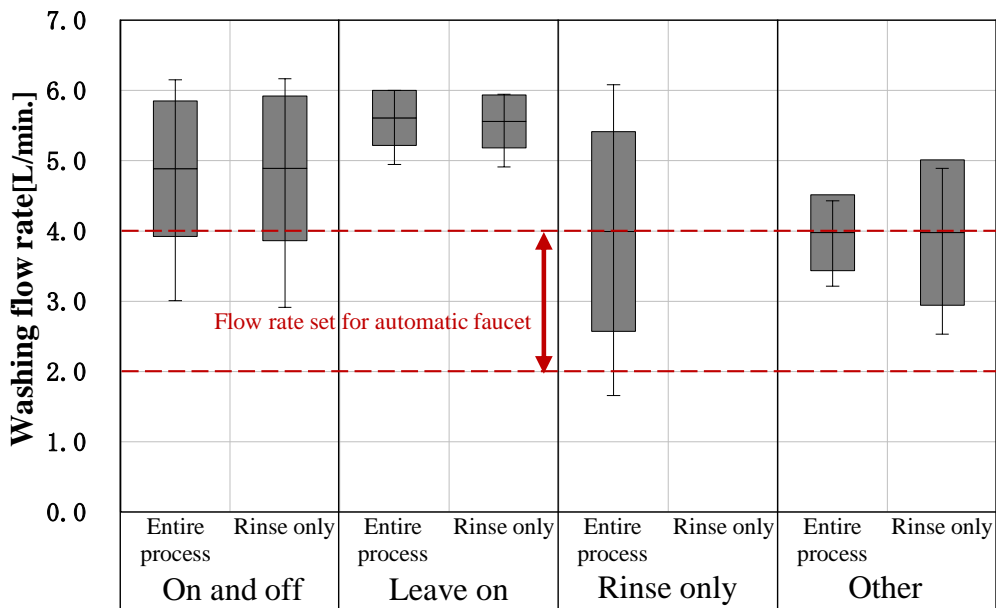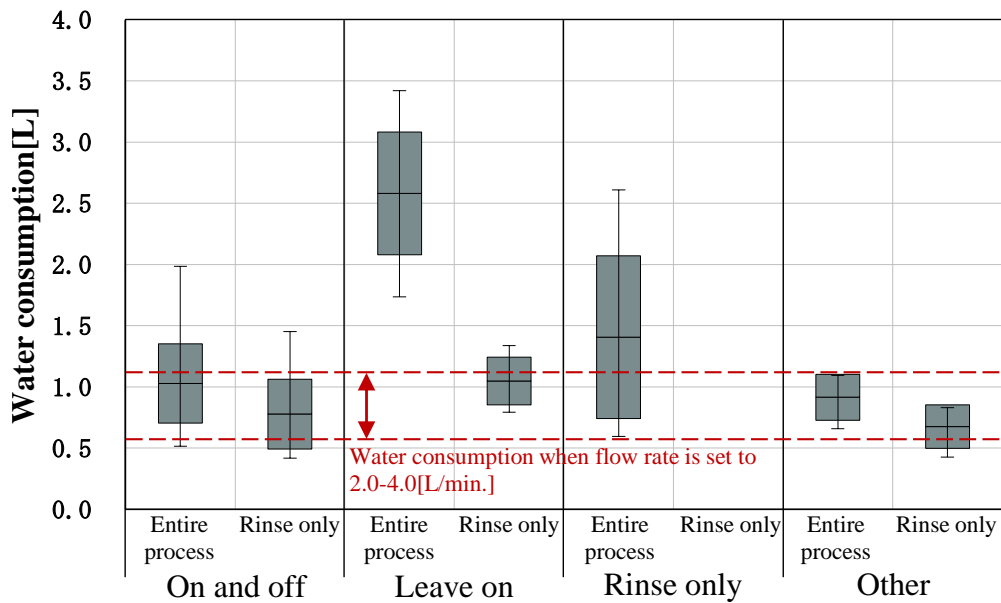**Fig. 9 - Water consumption for each faucet on/off**

5 Conclusion

This report examined documents relating to hand washing which every person in the world has been encouraged to practise thoroughly due to the COVID-19 pandemic. With regard to hand washing using a faucet, the following two points are considered equally important:

(1) Scrubbing hands with soap for longer helps lift resident bacteria from deep under the skin to the skin surface.

(2) The longer time spent on scrubbing with soap, the longer time needed for rinsing off the resident bacteria lifted to the skin surface.

However, the document examination has revealed that different documents describe different methods for ensuring high disinfection effects, by 'hand washing with soap and water' and by 'alcohol disinfection'. This suggests that it is important to conduct further examination on hand washing-related documents, and hand washing conditions and subsequent outcomes.

Moreover, the examination conducted by the authors, involving a manually operated faucet and participants, has confirmed that the manner in which the faucet is turned on and off greatly affects the water consumption by approximately 0.5-3.5L. In addition, with the exception of the 'other' routine, the average washing flow rates used during all of the hand washing routines were between 5.0[L/min] and 4.0[L/min], which are higher than the washing flow rate of the automatic faucet by 1.5-3 times. Furthermore, as for the rinsing time, the examination could not confirm adequate rinsing; many of the participants spent less time on rinsing their hands during all of the hand washing routines, falling short of the MHLW-recommended rinsing time of 15 seconds.

In consideration of foregoing, it is vital, from the perspective of SDGs, to ensure hygiene in places like developing countries which are not fully equipped with water and sewerage systems and faucets, even under normal circumstances as well as under circumstances which might arise though not as serious as the worldwide spread of COVID-19. Furthermore, not only inside Japan but also outside Japan, hand washing that ensures water conservation and hygiene is required at places like shelters in cases of natural disasters. Therefore, it is considered important to continue to discuss hand washing methods in consideration of hygiene and water conservation.

6 Acknowledgement

7 References

1）Megumi Itabashi: Proposal of infectious disease prevention I consideration of hygiene and water conservation by hand washing using automatic faucet, 2022Symposium CIB W062-Taichung, Taiwan, pp. 296-309, (2022 October 23-26)

2）CDC: Guideline for Hand Hygiene in Health-Care Settings, Morbidity and Mortality Weekly Report, 25 October 2002, Vol. 51, No. RR-16

3）CDC: Handwashing at Home, at Play, and Out and About, CDC, https://www.cdc.gov/handwashing/fact-sheets.html, (Date viewed 2023,06,07)

4）CDC: Stop Germs! Wash Your Hands, CDC, https://www.cdc.gov/handwashing/fact-sheets.html, (Date viewed 2023,06,07)

5）WHO: WHO Guidelines on Hand Hygiene in Health Care First Global Patient Safety Challenge Clean Care is Safer Care, WHO, 15 January 2009, pp. 155-156

6）WHO: SAVE LIVES: Clean Your Hands - in the context of COVID-19, WHO, 5 April 2020, https://www.who.int/publications/m/item/save-lives-clean-your-hands-in-the-context-of-covid-19 , (Date viewed 2023,06,07)

7）MHLW: About handwashing, MHLW, https://www.mhlw.go.jp/stf/seisakunitsuite/bunya/0000121431_00094.html, (Date viewed 2023,06,07)

8）MHLW: Keep your surroundings clean, https://www.mhlw.go.jp/stf/seisakunitsuite/bunya/0000121431_00094.html, (Date viewed 2023,06,07)

9）SHASE: Operation of air-conditioning and sanitary equipment for SARS-CoV-2 infectious disease control, SHASE, 5 July 2021, http://www.shasej.org/recommendation/covid-19/covid-19.html, (Date viewed 2023,06,07)

10）Kohji Mori: Effects of Handwashing on Feline Calicivirus Removal as Norovirus surrogate, The Journal of the Japanese Association for Infectious Diseases, 26 April 2006, Vol. 80, No. 5, pp. 496-500

11）Ugai Kazuhiro: Effective hand-washing with Non-medicated Soap for Removing Bacteria, 5 May 2003, Vol. 26, No. 4, pp. 59-66

12）Yukiko Yamamoto: Effective Handwashing with Nonmedicated Soap from the View Point of the Changes in the Number of Bacteria on the Hands in Handwashing Process, JSEI Journal, 26

November 2002, Vol. 17 No. 4, pp. 329-334

13）Fumitoshi Kiya: Bacteriological Study on the Effect of Washing Hands - Experimental Study on the Minimum Demand for Water -, Transactions of the Society of Heating, Air-conditioning and Sanitary Engineers of Japan, 25 February 1990, Vol. 15 No. 42, pp. 29-36

14）Hasan Shojaei: Efficacy of simple hand-washing in reduction of microbial hand contamination of Iranian food handlers, Food Research International, 17 October 2005, Vol. 39 Issue. 5, pp. 525-529

15）Jaynie Whinnery: Handwashing with a Water-Efficient Tap and Low-Cost Foaming Soap: The Povu Poa "Cool Foam" System in Kenya, Global Health: Science and Practice, 27 Jun 2016, Vol. 4 No. 2, pp. 336-341

16）Girum Gebremeskel Kanno: Effective Handwashing Practice in Dilla University Referral Hospital; Duration of Hand Rubbing and the Amount of Water as Key Enablers, Environ Health Insights, 19 April 2022, pp. 1-9

17）Barry Michaels: Water temperature as a factor in handwashing efficacy, Food Service Technology, 1 October 2002, Vol. 2 Issue. 3, pp.139-149

18）Biran, Adam, Enabling Technologies for Handwashing with Soap: A Case Study on the Tippy-Tap in Uganda, wsp WATER AND SANITATION PROGRAM: WORKING PAPER, February 2011, Vol. 16, pp. 1-9

8 Presentations of authors

Megumi Itabashi is a graduate student at the Otsuka Laboratory of Kanto Gakuin University, Japan. She has been mainly involved in research on wash flow rate and water volume and bacterial removal effects during handwashing. Itabashi is a member of AIJ (Architecture Institute of Japan) and a member of SHASE (The Society of Heating, Air-Conditioning and Sanitary Engineers of Japan).

Masayuki Otsuka is a professor at the Faculty of Architecture and Environment, Kanto Gakuin University, Japan. He has been conducting a wide range of research on water supply, drainage, and sanitary equipment. Otsuka is a member of AIJ (Architecture Institute of Japan). He is also the former president of SHASE(The Society of Heating, Air-Conditioning and Sanitary Engineers of Japan).

Climate Change – underestimated risk factor for domestic water hygiene

Frank Schmidt (1),

frank.schmidt@kemper-group.com

Gebr. Kemper GmbH + Co. KG

Abstract

The year 2022 was the warmest year since records began in Germany in 1881. Nine of the ten warmest years in Germany even fall in the 21st century. What is rarely considered: Climate change also affects drinking water hygiene in buildings. This is because increased outdoor air and ground temperatures influence drinking water temperatures.

The growth of pathogenic germs, such as Legionella spec., is particularly possible in temperature ranges between 25 °C and 45 °C. For cold water, increasing heat loads pose new challenges to the compliance with drinking water hygiene. Until now, unacceptable temperature increases could be permanently prevented by temperature-controlled flushing. A Big Data analysis of 8.6 million measured values from 2126 flush valves in operation confirms that temperature-controlled flushing measures are ecologically and economically limited.

Especially in the summer months the flushing volumes for temperature maintenance increase. Flushing measures for maintaining the temperature of domestic cold water in the summer months have their ecologic and economic limits. The installation of a cold water circulation with cooling can be used to maintain required cold water temperatures in a sustainable, ecological and economic way and flushing is only required anymore to limit the water age and avoid stagnation in the domestic water installation.

Keywords

climate change, domestic water hygiene, cold water circulation,

1 Introduction

The quality of water for human consumption is specified in the German Infection Protection Act (IfSG). The consumption shall not be likely to cause damage to human health, especially by pathogens.

To meet this requirement, plumbing installations shall be designed and operated in a way that:

- the velocity of the water is in the right range (turbulent flow),
- the water content of the installation is exchanged frequently,
- the used material does not emit nutrition to bacteria,
- the temperatures are not within the bacteria growth range.

This document focus are measures for temperature maintenance of domestic cold water and their evaluation.

2 Influence factors for domestic cold water temperature

According to German DIN 1988 – 200 standard, the temperature for domestic cold water should not exceed 25°C. The Health Technical Memorandum 04-01, Part A from the UK even recommends a maximum temperature of 20°C and refers to the Water Supply (Water Fittings) Regulations, which also recommend a maximum temperature of 20°C where reasonably practical.

2.1 Internal heat loads of buildings

Due to better insulation of buildings and a more compact installation of the MEP-systems, the energy density in the installation areas is high. Domestic cold water pipes pick up this energy and the cold water temperature increases.

2.2 External heat loads of buildings

The mean annual temperature of 2022 in Germany was 10,5 °C which is higher as the before hottest years 2020, 2019, 2018 and 2014.
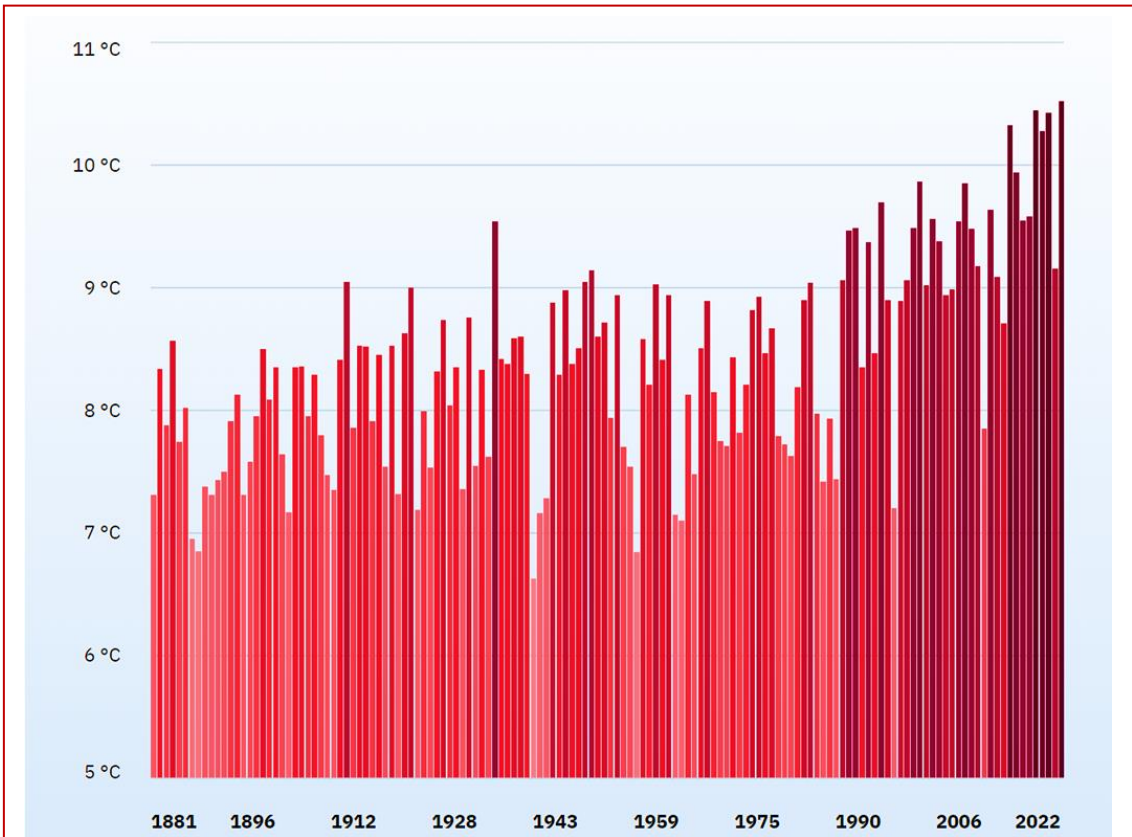
Figure 1: mean annal temperature in Germany since 1881 (source: DWD)

The increased air and ground temperatures have an impact on the temperature of the water supply coming into the buildings and are challenging the water hygiene.
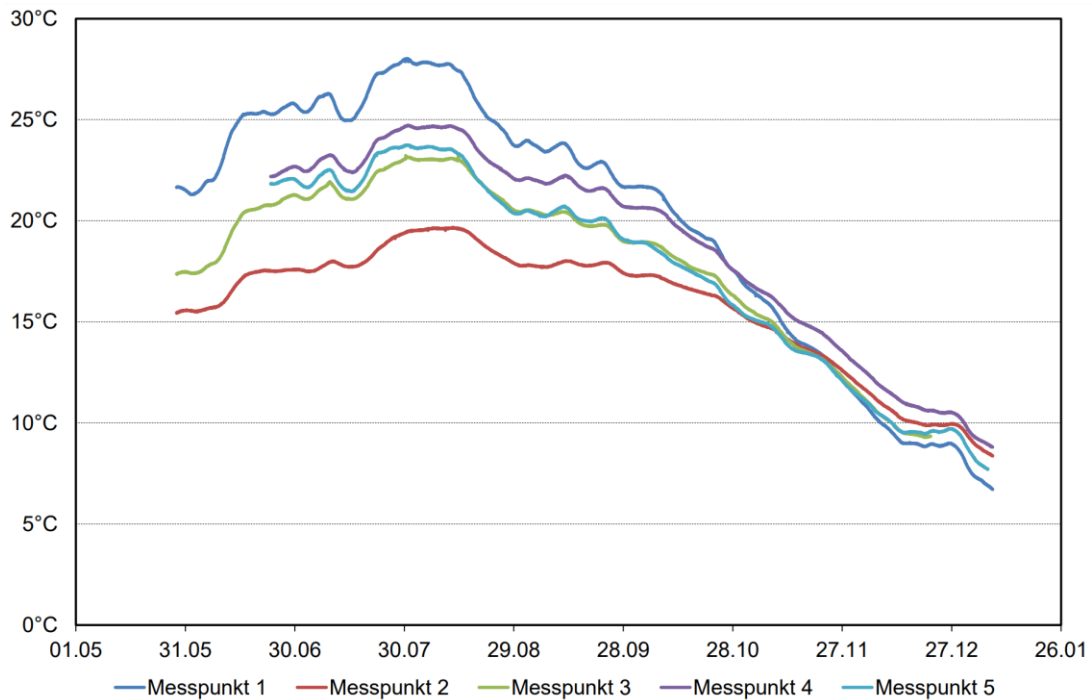
Figure 2: Cold water supply temperatures from 5 measuring points in 1,4 m depth in ground, rural area in south Germany (source: DVGW – Dr. Korth)

3   Data analysis of flushing measures considering environmental conditions

To minimize the risk of bacteria growth, many domestic water installations in Germany, but also abroad, are equipped with technology that avoids stagnation and maintains temperature. Both goals are realized by flushing measures. For avoiding stagnation, the flushing events are executed on a timed basis, either a weekly schedule or a timer. To keep a cold water temperature under a certain limit, a temperature sensor is installed at every end of a branch that triggers a flush when the temperature limit is reached.

Data of 153 buildings in Germany with such technology has been collected over eight years and was analyzed in a bachelor thesis. The data was collected from the following building types:

- 41,3 % hospitals & nursing homes
- 25,8 % administration
- 12,5 % schools
- 10,7 % hotels
- 7 % residential
- 2 % sports facilities
- 1,6 % unspecified

The data comprises 8,6 million flush events from 2126 flush points and showed that a temperature-controlled flush was executed every 2 h 50 minutes in average. The median of this intervals was 1 h 44 minutes.
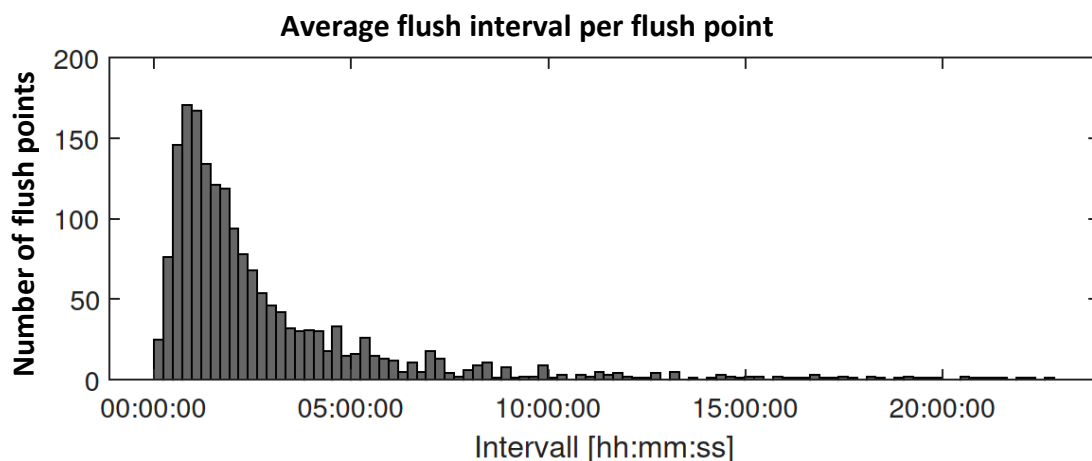
Figure 3: Average interval for temperature-controlled flush events per flush points (Source: Tobias Krause 2021)

4 Data analysis of flushing measures for temperature maintenance in a hospital

The collected data from a domestic cold water installation in a hospital showed the impact of outdoor- and ground temperature on the temperature controlled flush events for maintenance of cold water temperature below a certain limit. This data was collected from 2015 to 2020 in a hospital that was partially equipped with air conditioning. During summer, the amount of flushed water for temperature maintenance reached a peak of more than 16 m³/day.
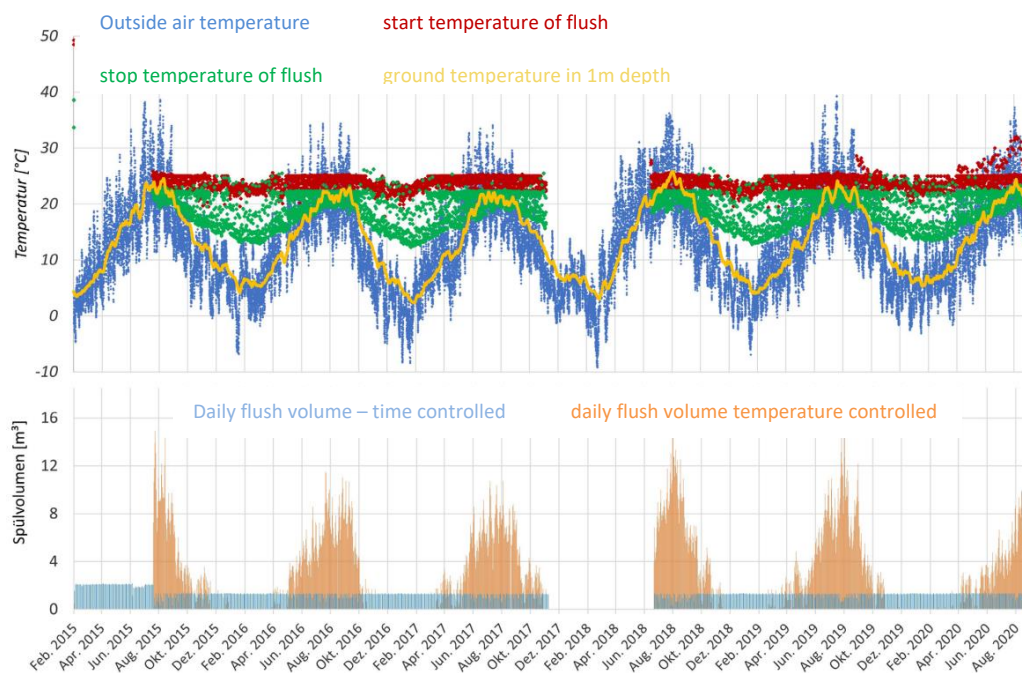
Figure 4 : Impact of outside air and ground temperature on flushed water volume of a hospital (source: Tobias Krause 2021)

5 Conclusions for ecologic and economic domestic cold water temperature maintenance

Maintaining domestic cold water temperature below the critical growth range of pathogens by flushing measures only can become uneconomic and unecological. Especially in summer or in areas with hot climate and under the aspect of the increasing value of the water resources, it is important to find the best solution for temperature maintenance of domestic cold water.

These measures start with passive measures during the design of the building and contain:

- enough space for MEP installation
- separate shafts / pipe traces for hot and cold pipework
- thermal separation between distribution pipework and pipework in drywalls
- thermal separation inside drywalls (cold at bottom, hot at top)
- thermal separation at fixtures / outlets

The passive measures shall be considered in the first place, as they increase the efficiency of active measures. The two options for active measures for domestic cold water temperature maintenance are:

- flushing water on temperature basis
- cold water circulation with cooling

6   Cold water circulation with cooling

A cold water circulation with cooling can be the most ecologic and economic solution for large installations. The setup is similar to a common known hot water circulation system. A constant cold water temperature in the domestic cold water pipework between 15 and 20°C is possible. Based on experience, small installations only need a cooling capacity of 1 kW and large installations usually require 3 to 6 kW cooling capacity.
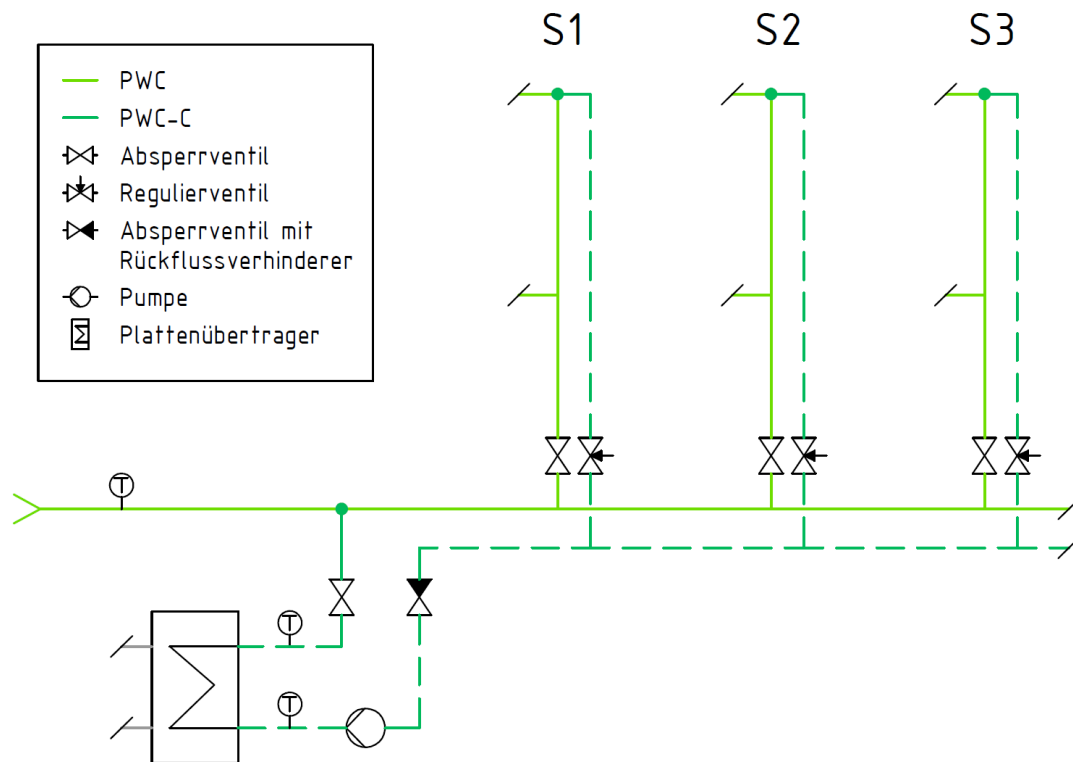
Figure 5 : Example schematic of a domestic cold water installation with circulation and cooling (source: BTGA)

7 References

https://www.umweltbundesamt.de/sites/default/files/medien/479/publikationen/uba_rund_um_das_trinkwasser_ratgeber_web_0.pdf

https://www.sanitaerjournal.de/oekonomische-temperaturhaltung-durch-kaltwasser-zirkulation_14942

https://www.dwd.de Open Data Server DWD

https://www.gat-wat.de/wp-content/uploads/2017/12/Korth_Vortrag.pdf

https://www.kemper-group.com/de-de/gebaeudetechnik/wissen/trinkwasserhygiene/

https://www.dwd.de/DE/klimaumwelt/aktuelle_meldungen/230123/artikel_jahresrueckblick-2022.html

https://www.dvgw.de/themen/forschung-und-innovation/forschungsprojekte/dvgw-forschungsprojekt-wasserdargebot

Bachelor thesis Tobias Krause 2021, Big Data Analysis for domestic cold water flushing measures considering environmental conditions.

https://www.btga.de/

https://www.kemper-group.com/de-de/gebaeudetechnik/wissen/kaltwasser-zirkulation/

8 Presentation of Author

Dipl. -Ing. Frank Schmidt M. eng. is international market developer at Gebr. Kemper GmbH + Co. KG. He is a trained plumber and graduated as Dipl-Ing for Building Technology and M.Eng for Technical Management. In the past 13 years with Gebr. Kemper, Frank supported many plumbing installation projects worldwide and gave seminars in more than 15 countries.

TECHNICAL SESSION 5 – ENERGY AND GHG EMISSIONS REDUCTION

Advanced building facilities embodying the transition to carbon neutrality

Kosuke Osako(1), Uwais Roslan(2), Katsuhiko Shibata(3), Naoki Aizawa(4), Masayuki Otsuka(5)

(1) kosuke_osako@tte-net.com

(2) uwais_roslan@tte-net.com

(3) katsuhiko_shibata@tte-net.com

(4) naoki_aizawa@tte-net.com

(5) dmotsuka@kanto-gakuin.ac.jp

(1), (2), (3), (4) Takasago Thermal Engineering Co., Ltd., Japan

(5) Prof. Dr. Eng, Department of Architecture and Environmental Design, College of Architecture and Environmental Design, Kanto Gakuin University, Japan

Abstracts

To achieve carbon neutrality by 2050, Japan's Basic Energy Plan positions renewable energy sources, such as solar power, woody biomass, and geothermal energy, as important domestic energy sources. Although energy and resource self-sufficiency has been touted as part of this transition, concrete examples are lacking. The Takasago Thermal Engineering Innovation Center, which was completed in January 2020, has achieved an energy-self-sufficient system by combining renewable energy sources such as woody biomass gasification power generation, solar power generation, and geothermal water utilization with storage batteries. This report presents an overview of the equipment, water use, electricity, and thermal energy performances of the facility throughout the year. In addition, owing to the increasing interest in water resource conservation and reuse, this report proposes evaluation methods for zero-water building (ZWB) in relation to geothermal water and water utilization.

Keywords

Groundwater use; Reclaimed water use; Net zero-water building (ZWB); Renewable energy sources

1 Introduction

The importance of building facilities to achieve carbon neutrality by 2050 is increasing, as buildings must be environmentally friendly with a focus on energy conservation and use of renewable energy while maintaining a comfortable environment inside the building. In the areas of water supply, drainage, and sanitary facilities, zero-water buildings (ZWBs) are attracting attention as buildings that not only save water and recycle water, but also recycle water resources to reduce the burden on the water supply and sewerage infrastructure.

Under these circumstances, the Takasago Thermal Engineering Innovation Center (Figure 1) was constructed in conjunction with the relocation of the former Technical Research Institute, based on the design concept of "a sustainable building that both reduces global environmental impact and improves intellectual productivity," and was completed in January 2020. This report provides an overview of the facilities and achievements of the groundwater heat utilization systems. The ZWB of the facility was estimated based on the definition provided by the U.S. Department of Energy. In addition, interpretations of the use of groundwater heat are discussed.

Location	Tsukubamirai City, Ibaraki Prefecture, Japan
Site area	Research Facilities
Building area	22,746.18㎡
Extended bed area	7,129.74 ㎡
Total floor area	11,763.97 ㎡
Number of stairs	2 above ground, 1 in tower
Building Height	15.455 m
Structure	steel construction, RC construction in part
Construction period	February 2019 - January 2020

Figure 1 - Takasago Thermal Engineering Innovation Center

2 Building Overview

2.1 Building and Facilities Overview

The facility consists of two main buildings: an office building (area of approximately 4,750 m^2) with an exhibition area, café/restaurant, office space, and a laboratory building (area of approximately 6,050 m^2) for experiments and analysis. The office building was arranged around a four-axis layout, and the façade was designed to match the heat and light environment in each direction to effectively take in the prevailing wind from the northeast and create a façade that is in line with the environment. Changing rooms, toilets,

conference rooms, etc., which do not require natural ventilation or views, are located in corner areas, and high windows are used to reduce the solar load to the maximum extent possible. The interior and exterior surfaces of the roof slab were insulated to reduce the heat load.

Figure 2 presents an overview of the facilities installed to achieve ZEB. The building has achieved a significant reduction in energy consumption through the use of natural energy to reduce the air-conditioning load in the building plan and the introduction of advanced facilities, such as latent-sensible air conditioning. Photovoltaic power generation, combined biomass heat and power generation, and storage batteries have been introduced as renewable energy sources, while groundwater heat and water have been effectively used to reduce CO_2 emissions.
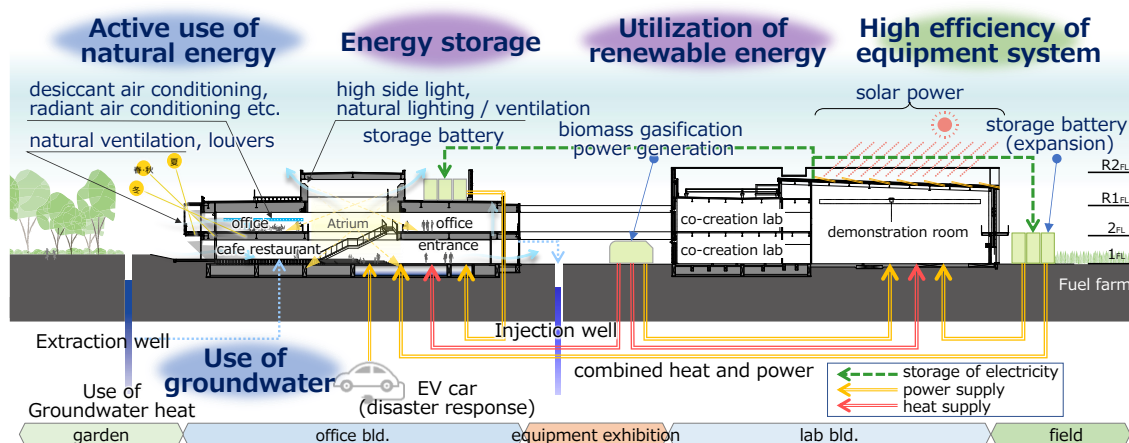
Figure 2 - Overview of equipment installed for ZEB

2.2 Certification

In acquiring certification under various evaluation systems, the company achieved a BEI of 0.09 and a BELS rating of *5 Nearly-ZEB (BEI = 0.33 if energy creation is excluded). In the CASBEE-Wellness Office (WO) evaluation, the building received an S-rank certification with an overall rating of 86.6 points, and in LEED v4, the building's comprehensive environmental performance evaluation received a gold certification of 72 points.

2.3 Evaluation of Energy and CO_2 Emissions

Simulations of the office building based on ASHRAE90.1_2010 for the former R&D center yielded a design value of -130 MJ/sqm/year compared to the baseline value of 421 MJ/sqm/year, with 131% energy savings. The actual 2021 records show a further 14.3%

reduction in the proposed value through continuous operational improvements. Furthermore, the power generated by the PV panels and biomass CHP units would reduce the primary energy consumption to -263 MJ/sqm/year, or 162% savings compared to the baseline, achieving the status of net ZEB (Figure 3).
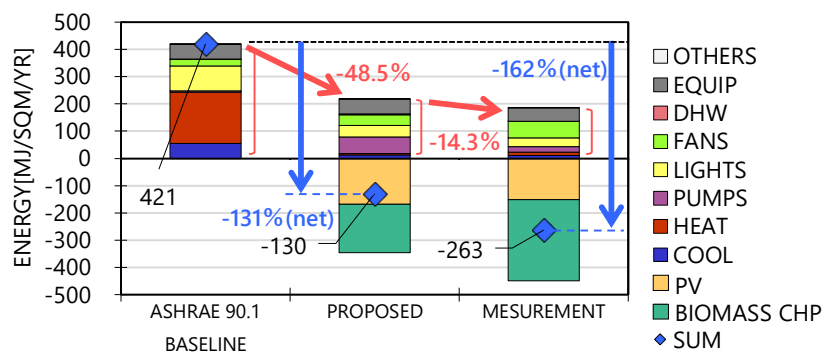
Figure 3 - Primary energy consumption

An aggressive use of renewable energy sources and a highly efficient system set-up and operation yielded an operational carbon emission of -159 t - CO_2/year (-33.4 kg - CO_2/sqm/year), definitely conferring the status of "Zero Emission" to this building (Figure 4). (The CO_2 emission baseline unit is 0.457 kg - CO_2/kWh according to the Tokyo Electric Power Co.).
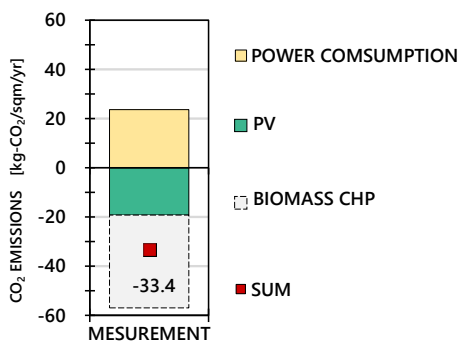
Figure 4 - Operational CO_2 emissions.

As a result of the above operational achievements, the center has been recognized as the leading facility for a carbon-neutral society in Japan and has received the Academic Award from the Society of Heating, Air-Conditioning, and Sanitary Engineers of Japan (SHASE) and the Carbon Neutrality Award from the Japanese Association of Building Mechanical and Electrical Engineers (JABMEE).

3 Groundwater Heat Utilization System

This section discusses the groundwater heat utilization system of the installed facilities. This system effectively utilizes groundwater heat and water, which contributes to energy and water conservation and carbon neutrality.

3.1 Overview of the groundwater heat utilization system

This facility uses groundwater heat and water effectively. Figure 5 shows a schematic of the groundwater utilization. The system has two wells–a pumping well and a return well–both of which are approximately 150 m deep. The pumping and return wells are almost identical; however, the return well has a backwash pump to prevent blockage. Figure 6 shows a schematic of the water-return process. Groundwater pumped from the pumping well is used for floor radiation at the entrance, daytime outdoor air conditioning, radiant air conditioning, etc., and is subsequently used as the heat source water for the water-source heat pump unit in a three-stage heat cascade. A portion of the heat-utilized groundwater is used for miscellaneous purposes, and the remainder is returned to the ground through a water return well.
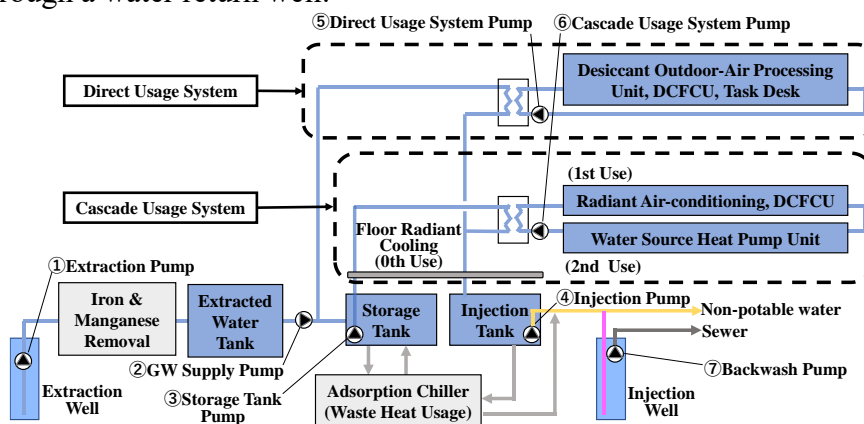
Figure 5 - Overview of the groundwater heat utilization system
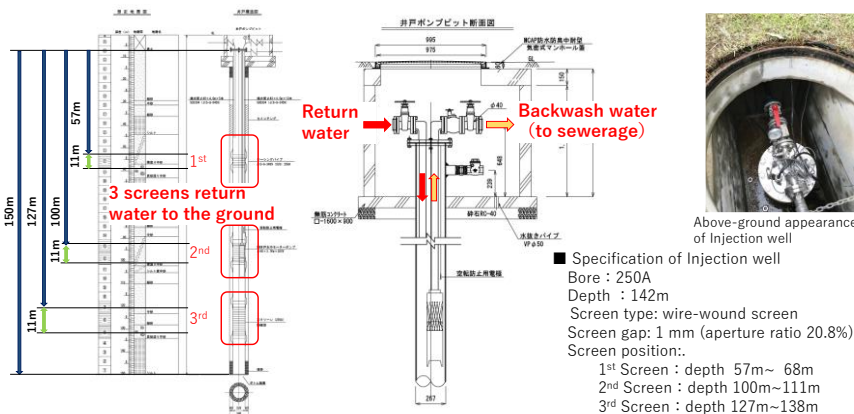
Figure 6 - Overview of injection well

Figure 7 shows the actual groundwater heat use in FY2022. The amount of cold heat is the sum of cold heat from the direct groundwater heat utilization system, cascade utilization system, and cold heat from heat pumps. "Groundwater Heat" in Figure 7 is the amount of cold heat used by exterior air conditioners, radiant panels, personal air conditioners, and individual air conditioners with water heat sources. "Heat pump" is the amount of cold heat produced by air-source heat pumps. Groundwater heat accounts for approximately 65% of the total annual cold heat. Groundwater heat was used for cooling from April to October, and the system COP during this period was 7.5 for the groundwater heat and 3.9 for the heat pump, confirming the energy efficiency of the groundwater heat use (Figure 8).
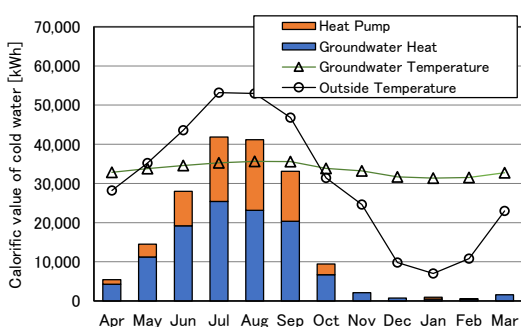
Figure 7 - Quantity of cold heat
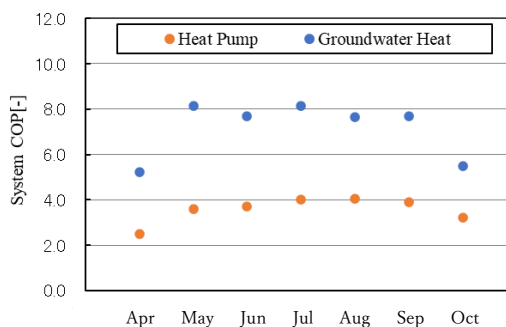
Figure 8 - SCOP value

3.2 Groundwater Use and Water Balance

In this building, tap water is stored in a receiving tank and supplied to the building; groundwater is pumped and used as heat for air conditioning; and a portion of the groundwater is used for miscellaneous purposes, such as toilet flushing water.
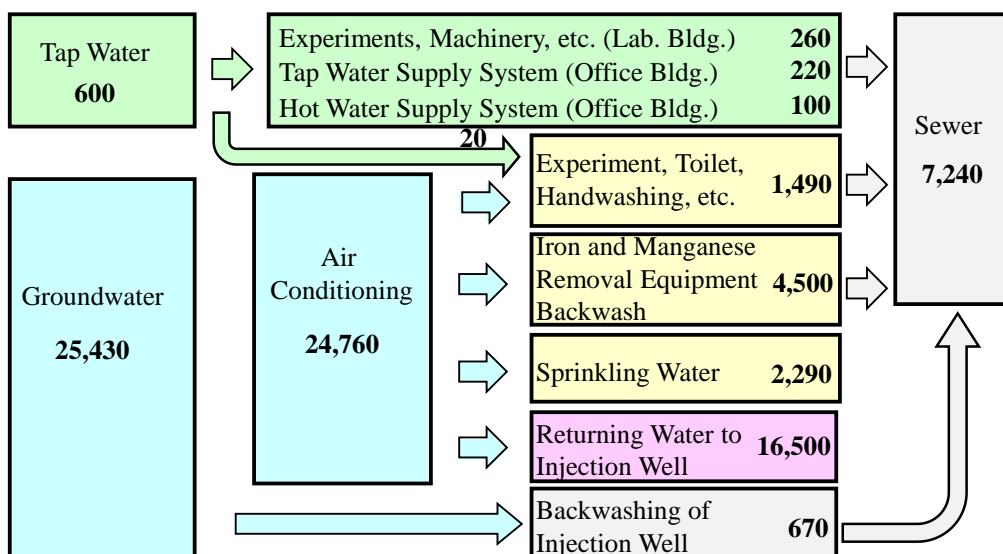
Figure 9 - Diagram of the Flow of Water Usage in the Facility ［m³/year］

As shown in Figure 9, the volume of drinking water was 600 m^3/year. The percentage of essential drinking and kitchen water was 53% (320/600), and the remainder could be reclaimed from groundwater. The well backup contained 20 m^3/year of tap water. The groundwater used for air conditioning was reused along with water for the experiments, hand washing and flushing of toilets, backwashing of iron and manganese removal equipment, and irrigation, among other uses. The well water used for the experiments, hand washing, toilet flushing, etc. amounts to 1,490 m^3/year, which implies an increase over the previous year. This was because of the increase in the number of experiments conducted in the laboratory building. The volumes of tap water, groundwater, and sewage were approximately 600 m^3/year, 25,430 m^3/year, and 7,240 m^3/year, respectively, making the discharge rate to sewage to approximately 28 %, with the remainder 72 % recycled. The amount of water used for backwashing the iron and manganese removal equipment accounted for approximately 60% of the total sewage volume, which could be reduced by changing the backwashing conditions.

3.3 Relationship between Groundwater Pumping and Water Use

Figure 10 shows the amount of tap water and groundwater used each month. From April to October, when the cooling demand is high, the amount of pumped groundwater ranges from approximately 1,200 m^3/month to 4,600 m^3/month (an average of approximately 3,100 m^3/month). However, from November to March, when the cooling demand is low, groundwater is pumped for miscellaneous water usage, averaging approximately 640 m^3/month.
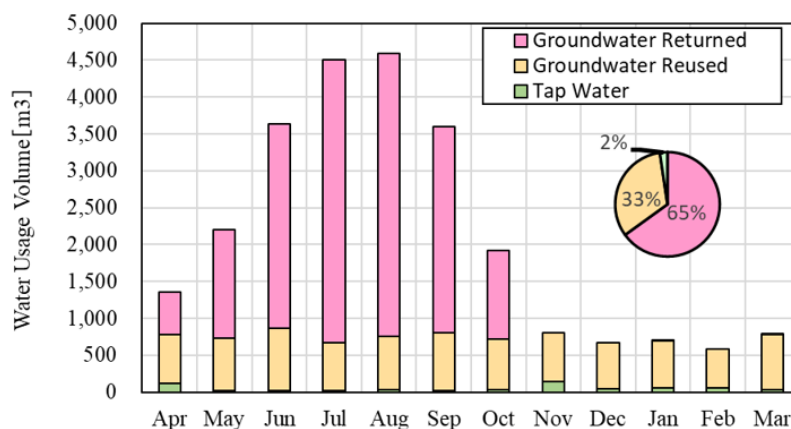
Figure 10 - Monthly quantity of tap water and groundwater

From the above, the groundwater heat utilization system at this facility was shown to not only utilize groundwater heat, which is renewable, but also to effectively use groundwater by reusing part of it after heat utilization for miscellaneous water usage.

4 ZWB Evaluation

While various ZWB evaluation formulas have been reported, this study focuses on analyzing and discussing them in accordance with the ZEB evaluation method proposed by the U.S. Department of Energy (USDE).

4.1 Method for Evaluating ZWB

The definition of ZWB as stated on the U.S. Department of Energy's website is shown in Table 1. ZWB is defined as a building where the sum of the alternative water use (AW) and return to groundwater (WR) equals the total water use (WU). The ZWB attainment percentage calculation is simple: WU is divided by the sum of AW and WR. The ZWB attainment rate is calculated by dividing WU by the sum of AW and WR. If the ZWB formula in Table 1 yields a value greater than 100%, then ZWB is achieved.

In this study, underground stormwater infiltration was not considered given that no facilities contributing to stormwater infiltration were installed. In addition, some water uses could not be clearly sorted based on the ZWB definition. Some interpretations of the various uses of groundwater are difficult and should be examined in the future.

Table 1 - Definition of ZWB by the U.S. Department of Energy

TERM		DEFINITION
AW	Alternative water use	A sustainable water source not derived from fresh-, surface-, or groundwater sources. Alternative water includes: ・Harvested rainwater, stormwater, sump-pump (foundation) water ・Graywater ・Air-cooling condensate ・Rejected water from water purification systems ・Reclaimed wastewater ・Water derived from other water reuse strategies. A net zero water building (or campus) uses alternative water sources to offset the use of freshwater.
WR	Water returned	The amount of water collected from the building systems, such as green infrastructure and on-site treated wastewater, and returned back to the original water source over the course of a year.
WU	Total water use	Total water use is the amount of water consumed within the boundaries of a building from all sources (potable and non-potable including freshwater[※] and alternative water) over the course of a year.
ZWB	Zero Water Building	$\text{ZWB} = (\text{AW}+\text{WR})/\text{WU} \times 100$

※：Freshwater is water sourced from surface or groundwater such as lakes and rivers.

4.2 Results and Discussion of ZWB Evaluation

Each water volume in Figure 9 is shown in Figure 11, and Table 2 lists the calculated results of the ZWB evaluation (Case-1).
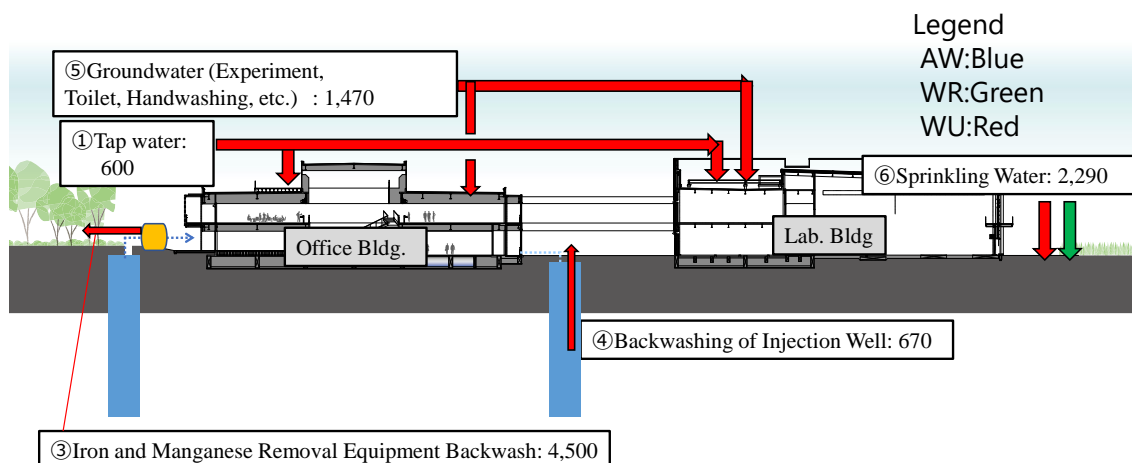
Figure 11 - Water and Groundwater Consumption in FY2022 (Case-1)

Table 2 - Calculated results of ZWB based on USDE (Case-1)

Term	Unit	Value	Remarks
AW	m^3/year	0	
WR	m^3/year	2,290	⑥
WU	m^3/year	9,530	①+③+④+⑤+⑥
ZWB	%	24	

None of the alternative waters defined in Table 1 are applicable for water use at the facility. Groundwater plant irrigation and stormwater groundwater infiltration were considered applicable to the amount of water returned. Total water use was the sum of the groundwater used for miscellaneous purposes, including drinking water, backwash water from the iron and manganese removal equipment and injection wells, and sprinkling water. This resulted in a ZWB rating of 24%.

Given that no examples of ZWB evaluations for facilities that use groundwater for heat and water, such as the facility considered in this study, have been reported, and the definitions in Table 1 are not applicable, groundwater heat use was not included in water consumption in this ZWB evaluation estimation. However, it is incongruous that groundwater pumped up from underground and returned to the ground after heat use is

not included in water usage. It is expected that an increasing number of facilities, such as the aforementioned facility, will have diverse water use methods, such as heat use of water. Therefore, it is necessary to discuss how to define ZWB for diverse water use methods as soon as possible.

Consider the case in which groundwater used as heat in this facility is included in the calculation of water consumption (Case-2). Figure 12 shows the respective water volumes. Under the present conditions, the groundwater used for backwashing of the iron and manganese removal equipment, and the groundwater used for miscellaneous purposes were considered as alternative water volume, given that the water after air conditioning used as groundwater heat is considered to be reused water. In addition, the amount of groundwater returned to the ground through the injection wells after heat utilization is added to the amount of water to be returned to the ground. The total water consumption is defined as the sum of drinking water, groundwater used for heat utilization, and groundwater used for miscellaneous purposes, including sprinkling water after heat utilization. As a result, the ZWB evaluation value was 72%, as shown in Table 3.
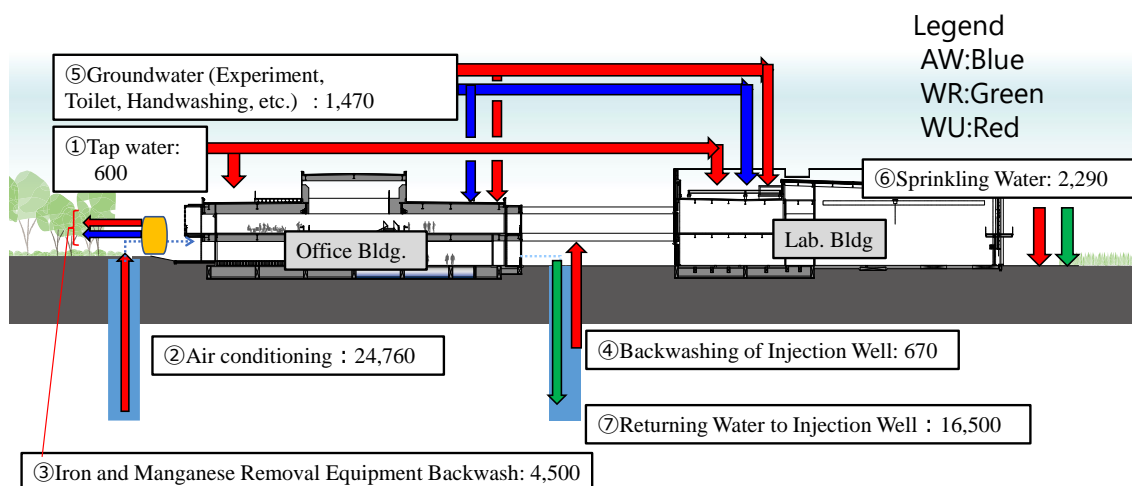
Figure 12 - Water and Groundwater Consumption in FY2022 (Case-2)

Table 3 - Calculated results of ZWB using heat-utilized water as AW (Case-2)

Term	Unit	Value	Remarks
AW	m³/year	5,970	③+⑤
WR	m³/year	18,790	⑥+⑦
WU	m³/year	34,290	①+②+③+④+⑤+⑥
ZWB※	%	72	

※: ZWB reaches 120% if underground infiltration water from rainfall on the site is included in the WR.

In Case-2, both groundwater pumping and return water are taken into account, resulting in a 48% improvement in the ZWB value compared to Case-1. This is considered to be a calculation in line with actual water use. With the increasing focus on efficient water resource utilization in the pursuit of carbon neutrality, there is a growing consensus that evaluations should encompass not only water usage but also heat usage, and should be more accurate for diverse water resources.

In addition, because this facility does not currently have rainwater infiltration facilities, this study estimates the rainwater infiltration water as WR as zero. However, we believe that incorporating the underground infiltration of rainwater and rainwater utilization will bring us closer to achieving a ZWB. In the estimation, including the underground infiltration water of rainfall at the site as WR, the ZWB was estimated to be 120%, which is expected to achieve the ZWB.

5 Conclusions

This study introduces a research facility in Japan constructed as a sustainable building considering the global environment. We propose a new ZWB that can be applied to various systems, including factors such as water heat utilization, rather than simply evaluating the ZWB from the viewpoint of water consumption alone. We propose a new ZWB that can be applied to various systems.

6 References

1) Kosuke Osako, Naoki Aizawa, Takeshi Aoyama, Akihiro Shimizu, Daisuke Hatori, and Yuka Mutoh, Planning and Evaluation of the Energy Self-Sufficient Innovation Center (Part 20) Operational Results in the Use of Groundwater and Waste Heat, pp193–196, 2022.
2) U.S. Office of Energy Efficiency & Renewable Energy, Federal Energy Management Program "Net-zero Water Building Strategies",
URL:https://www.energy.gov/femp/net-zero-water-building-strategies,
(accessed June 23, 2023)

7 Presentation of authors

Kosuke Osako is chief research engineer at the HVAC Environment office in the R&D center of Takasago Thermal Engineering Co., Ltd., Japan. He is involved in research on zero water building and the effective use of water. He is a member of SHASE (The Society of Heating, Air-Conditioning and Sanitary Engineers of Japan).

Uwais Roslan is an engineer at the HVAC Environment office in the R&D center of Takasago Thermal Engineering Co., Ltd., Japan. He is involved with research regarding groundwater heat utilization system and zero water building research. He is a member of SHASE (The Society of Heating, Air-Conditioning and Sanitary Engineers of Japan).

Katsuhiko Shibata is fellow at the R&D center of Takasago Thermal Engineering Co., Ltd., Japan. He is involved in research on facility management systems and improving QOL in polar habitats. He is a member of AIJ (Architectural Institute of Japan) and technical fellow of SHASE (The Society of Heating, Air-Conditioning, and Sanitary Engineers of Japan).

Naoki Aizawa is manager at the HVAC Environment office in the R&D center of Takasago Thermal Engineering Co., Ltd., Japan. He is involved in research IAQ Control and energy management of building. He is a member of SHASE (The Society of Heating, Air-Conditioning and Sanitary Engineers of Japan).
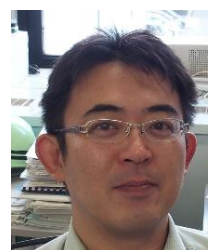
Masayuki Otsuka is a professor at the Faculty of Architecture and Environment, Kanto Gakuin University, Japan. He has conducted a wide range of research on water supply, drainage, and sanitary equipment. Otsuka is a member of AIJ (Architectural Institute of Japan). He is also the former president of SHASE (The Society of Heating, Air-Conditioning, and Sanitary Engineers of Japan).

Impact of domestic hot water safety advices on energy consumption and the energy transition in The Netherlands

Andreas Moerman (1), Frank Oesterholt (2)
(1) andreas.moerman@kwrwater.nl
(2) frank.oesterholt@kwrwater.nl
(1, 2) KWR Water Research Institute, Nieuwegein, The Netherlands

Abstract

In the energy transition, increasing attention is being paid to low-temperature (LT) district heating systems (< 55 °C). These systems are more sustainable because of lower heat losses during transport of heat compared to conventional district heating. A recent study shows that 60% of existing homes in The Netherlands are suitable for LT-heat solutions with only minor modifications (Pothof *et al.*, 2022). However, the production of domestic hot water (DHW) can be a bottleneck for LT-heat systems, since DHW demands temperatures above LT for reason of public health (*Legionella* safety). Recently the *Legionella* prevention regulations for drinking water in NL was thoroughly evaluated (Berenschot & KWR, 2021). Based on this evaluation it is recommended among others to maintain DHW temperatures at the domestic water heater at a minimum of 60 °C as a primary and essential barrier against *Legionella*. This advice is introduced to cover the ineffectiveness of periodic heat-shock measures in a situation where lower temperatures are maintained, as was shown by an extensive literature review (Berenschot & KWR, 2021, see also the CIB 2023 paper Van der Wielen and Oesterholt). This advice has significant impact on energy use for sustainable DHW-systems, in particular heat pumps and solar water heaters. The results of this study and the discussions about domestic hot water energy efficiency and public health in The Netherlands also show a discrepancy between scientific facts and practical realities. This discrepancy needs to be bridged to be able to implement new hot water safety advices in existing regulation in The Netherlands.

Keywords
Domestic hot water, public health, energy use, energy transition

1 Context and timeline

In the energy transition, increasing attention is being paid to low-temperature (LT) district heating systems (< 55 °C). These systems are more sustainable because of lower heat losses during transport of heat compared to conventional district heating. A recent study shows that 60% of existing homes in The Netherlands are suitable for LT-

heat solutions with only minor modifications (Pothof *et al.*, 2022). Domestic hot water (DHW) can be a bottleneck for LT-heat systems, since DHW demands temperatures above LT for reason of public health (*Legionella* safety). This leads to a societal debate in The Netherlands about the actual necessity of DHW temperatures. Below a timeline about the development of this debate is shown:

1. In 2018, a motion (from representative Van der Lee) was passed in the House of Representatives. This motion relates to the 55-degree requirement for DHW in the Dutch Drinking Water Decree. In this motion the government was asked to *"investigate the possibilities of lowering this requirement without posing public health hazards"*.

2. Following the Van der Lee motion, a report commissioned by the Ministry of Infrastructure and Water Management (I&W) was written by a consultant (Van Wolferen, 2019) in which was concluded that the 55-degree requirement is a functional requirement and, strictly speaking, according to current laws and regulations, it does not relate to *Legionella* prevention.

3. Following the publication of the Van Wolferen report, a letter was sent by RIVM (National Institute for Public Health and the Environment) and KWR to the Ministry of I&W, pointing out scientific insights indicating that the requirement to keep DHW at 55 °C cannot be lowered without posing public health hazards.

4. On behalf of the Ministry of I&W, the consultancy company Berenschot together with KWR carried out an evaluation of the existing regulations for *Legionella* prevention in tap water installations based on an extensive scientific and legal analysis (Berenschot/ KWR, 2021; see also CIB 2023 paper Van der Wielen and Oesterholt). This so-called Berenschot/ KWR report was presented to the House of Representatives by the Minister of I&W in late 2021, also on behalf of the Minister of the Interior and Kingdom Relations (BZK). In this report it is recommended among others to maintain DHW temperatures at the water heater at a minimum of 60 degrees Celsius.

5. There are questions from the practical context to what extent advices from the Berenschot/ KWR report can lead to increased energy use and impact on opportunities for application of (new) technology for DHW use in practice. TKI Urban Energy and RVO (Netherlands Enterprise Agency) therefore asked KWR to determine the impact of the Berenschot/ KWR advices on residential heat transition (Moerman and Oesterholt, 2023).

2   General principles

For this impact study, the assumption is that all the advices from the Berenschot/ KWR report will be followed by the Dutch government, which need not be the case. This includes the advice to maintain a minimum hot water temperature of 60 °C everywhere in the water heater. Determining the actual impact of regulatory changes can only take place when the minister makes additional decisions based on follow-up research (see point 4 in Paragraph 1).

One general principle is that systems are constructed and set up in accordance with the applicable standards (including the Dutch norm NEN 1006). This means that a water heater is capable of supplying instantaneous DHW at a temperature of 58 °C to meet the requirement of 55 °C at the tap, assuming a temperature loss of 3 °C between water heater and point of use (Scheffer, 2000).

3   Scenario's

3.1   Energy demand for DHW

3.1.1   Residents and behaviour
Energy demand for DHW is mainly determined by behaviour of the buildings residents. In the study, therefore two types of households were considered:
- a two-person household (adults);
- a four-person household (parents with two children).

These two resident categories correspond to the categories 'A' and 'D' from ISSO Publication 30 (ISSO Publication 30, 2007). A further specification of these categories can be found in Moerman, Slingerland *et al* (2015).

3.1.2   Installation properties
A second factor that determines hot water energy demand are the characteristics of the DHW system. This includes:
- the number and type of DHW taps and related volume flows, etc.;
- the plumbing specifications, such as pipe length and diameters.

The installation is based on the 'Standard plus' (also called '0+') type from ISSO Publication 30 (ISSO Publication 30, 2007), without hot water circulation. A further specification of this type of installation and the assumptions for pipe lengths and diameters is described in Moerman, Slingerland et al. (2015).

3.1.3   Gross heat demand for DHW
The assumptions described in Paragraphs 3.1.1 and 3.1.2 lead to two different scenarios for hot water consumption. Calculations for these scenarios were made by Moerman, Slingerland et al. (2015), reported during a former CIB-Symposium (Blokker *et al.*, 2017) using the stochastic model Simdeum® (Blokker, Pieterse-Quirijns *et al.*) to simulate the total gross heat demand per day per scenario for a large number of households. By using Monte Carlo simulation, variation in demand by different type of residents within the same category is incorporated. Table 1 shows the gross heat demand based on this calculation.

**Table 1 – Summary gross heat demand hot water for two demand scenarios.
The values represent the variability between the 10-90 percentile with the middle value (bold) being the median.**

	Scenario A0+	Scenario D0+
	kWh_{th}	kWh_{th}
Total gross heat demand/ day*	1,6 – **4,4** – 8,3	5,0 – **9,8** – 15,7
Total gross heat demand/ year**	567 – **1596** – 3035	1843 – **3559** – 5714
Comparison with EU tap pattern (class)	S – **S** – M	S – **M** – L

3.2 Water heaters
Water heaters considered in this study are described in the following sub-paragraphs. The technical assumptions for all scenarios are summarised in Annex I.

3.2.1 Scenario 0 – Electrical boiler (reference)
As a reference for sustainable hot water preparation, this study considers an (somewhat older) alternative for hot water heating; an electric night boiler (scenario 0). Scenario 0a concerns a combi system for both space heating and DHW preparation. Scenario 0b involves hot water preparation only. For the night-time boiler, a vessel with a capacity of 120 litres is assumed.

3.2.2 Scenario's 1a-1d – Heat pump
These scenario's involve (i) air-to-water heat pumps with outside air as the heat source (1a-1b) and water-to-water heat pumps with a closed loop soil energy system as the heat source (1c-1d). For hot water storage two sub-scenario's were defined; 150 l (1a-1c) and 300 l (1b-1d).

3.2.3 Scenario's 2a-2b – Solar water heater
This scenario involves a solar water heater system using the principle of pre-heating by solar energy. In pre-heated solar water heaters, the storage vessel of the solar water heater itself does not contain a post-heating element to raise the hot water temperature to the required temperature to serve 55 °C at the tap. This post-heating is provided, if necessary (especially in the winter season), by a downstream heating device. In this study post-heating is assumed to be realized by electrical resistance heating (COP=1). For hot water storage two sub scenarios were defined; 150 l (2a) and 300 l (2b).

4 Method

4.1.1 Calculation of final heat demand
The final energy demand, including energy losses was calculated using the following categories (conform Dutch building norm NTA 8800):
1. heater efficiency;
2. electrical auxiliary energy use;
3. storage losses;
4. solar energy system contribution *(optional)*.

Based on the gross heat demand (Table 1, in kWh_{th}) storage losses (in kWh_{th}) and (optional) contribution of the solar system (%), the total heat demand (in kWh_{th}) was calculated. While using the heater efficiency and the auxiliary electrical energy use the final energy demand (in kWh_e) was calculated.

4.1.2 Additional assumptions and boundary conditions
The following general assumptions and boundary conditions were applied:
- The ambient temperature as assumed to be equal to 20 °C.
- For heat pumps a annual efficiency (sCOP) of 50% of the theoretical maximum Carnot-efficiency was assumed, based on expert judgement.
- For air-to-water heat pumps an annual average outside air temperature of 10 °C was assumed.

- For water-to-water heat pumps an annual average ground source temperature of 15 °C was assumed.
- Heat loss between water heater and tap during hot water use was assumed to be equal to 3 °C (Scheffer, 2000). Hence in the current situation, a water heater should be able to deliver a hot water temperature of minimal 55 + 3 = 58 °C.
- Heat pumps are not always able to deliver hot water at a temperature of 58 °C, so that a temperature of 55 °C can be delivered to the tap point. This shortcoming was taken into account by not using the heat pump reported efficiency for the whole temperature range for water heating. Therefore the efficiency of electrical resistance heating (100%, COP=1) was used for hot water temperatures above 55 °C.

A summary of all technical assumptions per heater type can be found in Annex I.

5 Results

5.1 Qualitative considerations

In the Berenschot/ KWR report it is advised to consistently maintain 60 °C everywhere in the DHW heater. For storage systems – when applied literally – this is by definition problematic because the vessel temperature is not constant over time and place, due to stratification and hot water use. When hot tap water is taken from the storage vessel, new (cold) drinking water flows into the vessel, causing the temperature in the vessel to drop temporarily. The extent to which this happens depends on the vertical position in the storage vessel; due to stratification it is always warmer at the top than at the bottom. To maintain a temperature of minimal 60 °C in a storage vessel, the temperature at the vessels top should therefore be > 60 °C, assumed in this study to be 65 °C.

The impact on solar water heating systems of this measure is severe. In solar water heating systems without integrated reheating (also known as 'pre-heater solar water heating'), the storage vessel is used to conserve pre-heated water supplied by the solar collector. When there is a hot water demand, the pre-heated water is reheated, if necessary (i.e. under low-sun conditions), by a downstream device, usually a gas-driven heater. Solar thermal systems without integrated post-heating can no longer be used if this advice is implemented consistently, because this type of solar thermal system does not have the ability to regulate the temperature in the storage vessel. Strict implementation of the Berenschot/ KWR advices would therefore require technical modification of these systems.
In general it can be stated for solar water heaters that the effectiveness decreases when a higher water temperature in the storage vessel is required because fewer days a year heat from the solar collector can be used effectively. As a result, it is expected that there is no longer a good business case for residential solar heating systems when a requirement of 60 °C is consistently applied everywhere in the water heater.

5.2 Quantitative analysis

Based on the scenario's for hot water energy use, scenario's for domestic water heating, both described in Paragraph 3 and the boundary conditions and method described in Paragraph 4, the hot water energy use was calculated for the actual situation and the situation after implementation of the '60-degree-advise' (Figure 1).
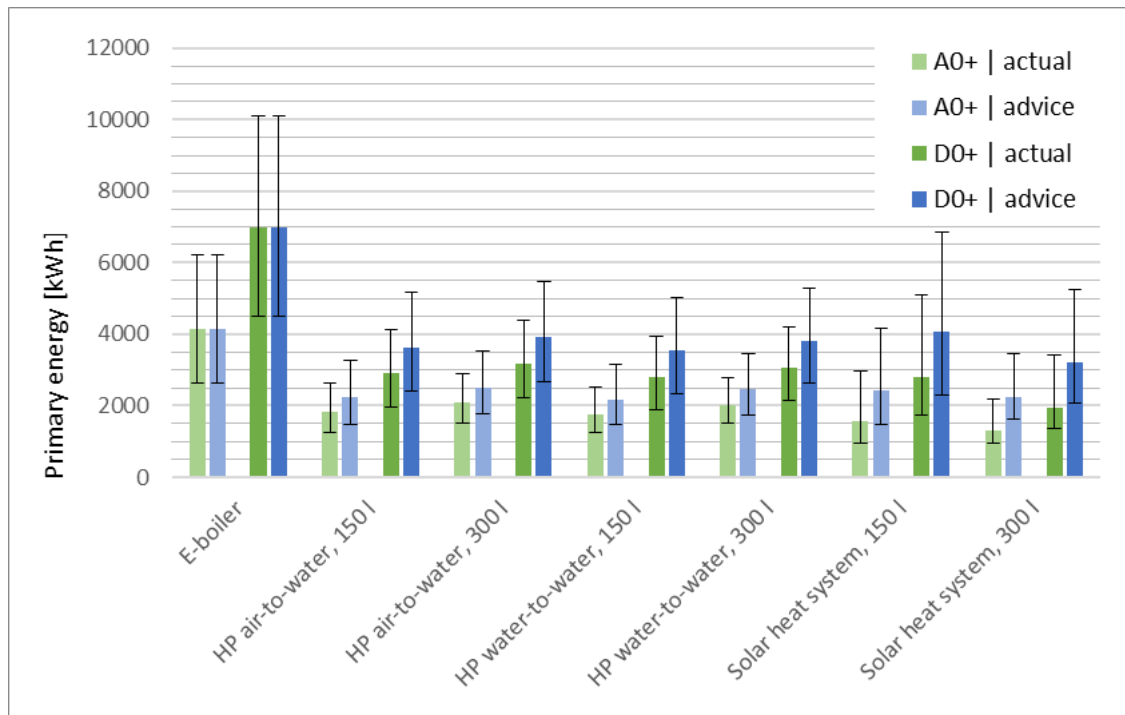
Figure 1 – Primary energy for hot water use in the current situation and after implementation of the '60-degree-advise'. Values refer to the median. The error bars represent the 10-90 percentile based on Simdeum® calculations.

The quantitative impact of the implementation of the '60-degree-advise' can be derived from the results shown in Figure 1 and are summarized in Table 2.

Table 2 – Summary impact of 60-degree-advice on the energy demand of the water heater for a single dwelling (above) and impact on the annual electrical energy use (below, on page 7).

		Storage	Scenario A0+	Scenario D0+
	Gross heat demand/ year [kWh$_{th}$]		567 – **1596** – 3035	1843 – **3559** – 5714
	European Tap pattern (class)		S – **S** – M	S – **M** – L
Increase final energy use [%]	Heat pump (average scen. 1a en 1c)	150 l	19% – **22%** – 26%	22% – **25%** – <u>28%</u>
	Heat pump (average scen. 1b en 1d)	300 l	<u>16%</u> – **20%** – 24%	20% – **24%** – 26%
	Solar heater (scenario 2a)	150 l	55% – **54%** – 39%	<u>33%</u> – **47%** – 35%
	Solar heater (scenario 2b)	300 l	67% – <u>**72%**</u> – 57%	50% – **68%** – 53%

		Storage	**Scenario A0+**	**Scenario D0+**
	Gross heat demand/ year [kWh$_{th}$]		567 – **1596** – 3035	1843 – **3559** – 5714
	European Tap pattern (class)		S – **S** – M	S – **M** – L
Increase annual energy use (SJV) [%]	Heat pump (average scen. 1a en 1c)	150 l	<u>3%</u> – **5%** – 8%	5% – **8%** – 12%
	Heat pump (average scen. 1b en 1d)	300 l	3% – **5%** – 8%	5% – **8%** – <u>13%</u>
	Solar heater (scenario 2a)	150 l	13% – **22%** – 30%	<u>8%</u> – **18%** – 25%
	Solar heater (scenario 2b)	300 l	17% – **24%** – <u>32%</u>	10% – **18%** – 25%

The variation depends on the type of user (economical, inefficient). The values represent the variability between the 10-90 percentile with the middle value (in bold) being the median. The lowest and highest values for all heat pump scenarios and solar boiler scenarios are underlined. These values represent the ranges also mentioned in the summary for heat pumps and solar water heaters as entire groups.

5.3 National projection of results

5.3.1 Projection in 2023

Based on data of the Dutch Statistical Bureau (CBS, 2023), a housing stock of 7.7 million occupied dwellings in the Netherlands is assumed. Until recently natural gas was a cheap heat source, with The Netherlands as a considerable net exporter of natural gas. Therefore > 80% of the residential buildings in The Netherlands still have a gas-driven combi-heater for both space heating and hot water production (CBS, 2021). Based on the current share of all-electric homes (see elaboration in Moerman and Oesterholt, 2023) it is assumed that 304,000 homes will have a sustainable water heater containing a storage vessel. This is 3.9% of the current stock of inhabited residential buildings.

The total electricity use of homes in the Netherlands is estimated by multiplying the number of homes with the average Standard Annual Energy Demand (SJV) for electricity, equal to 2,500 kWh$_e$ (MilieuCentraal, 2023) which results in 19.25 TWh$_e$ for the entire housing stock.

Based on the above assumptions, a national projection can be made from the results of this study. The additional annual final energy due to a higher temperature at the water heater is 275 – 514 kWh$_e$ per dwelling with a heat pump, depending on the demand scenario (median values of A0+ and D0+) and the scenario for a storage appliance (1a to 1d). For solar water heaters, the median variety is 594 – 898 kWh$_e$ (median values of A0+ and D0+ and scenarios 2a and 2b). These value ranges, multiplied by the estimated numbers of houses for full heat pumps and solar boilers respectively, leads to a national additional final energy demand of 0.13 – 0.21 TWh$_e$ in the current situation. This is 0.7 – 1.1% compared to the current electricity use of the total current housing stock (19.25 TWh$_e$).

5.3.2   Projection in 2030

Relative to 2030, the same analysis can be carried out as in Paragraph 5.3.1, subject to modification of some parameters such as the projected housing stock and the number of sustainable stock heaters for hot water preparation. Hot water demand has been fairly constant in recent years. It is therefore assumed that in terms of hot water demand, no major changes will take place until 2030. The number of inhabited residential buildings in 2030 is estimated as 8.45 million, see Moerman and Oesterholt (2023) for elaboration. The average Standard Annual Consumption (SJV) in 2030 for all homes combined is estimated at 2,350 kWh$_e$ (Luteijn, Bik *et al.*, 2021). This implies a total electricity use of 19.86 TWh$_e$ in 2030. It is estimated that by 2030 a number of 1.2 million homes will be equipped with a sustainable water heater containing storage (see Moerman and Oesterholt (2023) for elaboration). This is 14.2% of the estimated stock of estimated inhabited dwellings in 2030.

Based on the above assumptions, a national projection for 2030 can be estimated from the outcomes of this study. The variety of additional final energy mentioned in Paragraph 5.3.1, multiplied by the estimated number of dwellings with a sustainable storage hot water appliance in 2030 (1.2 million), leads to a national additional final energy demand of 0.58 – 1.05 TWh$_e$ in 2030. This is 2.9 – 5.3% compared to the estimated final electricity use of the total housing stock in 2030 (19.86 TWh$_e$).

5.3.3   Further projection

How the contribution of additional final energy will develop further between 2030 and 2050 is difficult to estimate because all the variables used in the above estimate become very uncertain on such a time scale. Based on the Start Analysis of the Netherlands Environmental Assessment Agency (PBL), it can be estimated that in 2050 roughly 25% of homes will have a storage appliance for sustainable hot water heating. The above estimate for 2030 is therefore expected to increase further towards 2050.

6   Discussion

The question can be raised to which extent maintaining 60 °C *everywhere in the water heater* is actually necessary, since there are already several systems on the market that aim to deliver safe hot water (at 58-60 °C) with a LT hot water storage, through hydraulic separation (heat exchanger) with downstream reheating to supply hot tap water not directly from a the LT storage tank.

European tap patterns (also known as tap classes) are generally used to determine gross heat demand for hot water. These standard patterns are important as reference when assessing water heaters on energy efficiency. However, these tap patterns do not incorporate the large variation in hot water demand in practice, which is strongly dependent on the type of user (economical, inefficient) and the composition of a particular dwelling. To make a realistic estimate of the impact of the '60-degree-advice' on the Standard Annual Energy Use (SJV), it was therefore consciously chosen not to use the European standardized tap patterns but statistics of hot water demand, calculated by Simdeum® according to Blokker *et al.* (2017).

The values for gross heat consumption for hot tap water used in this study are based on the Dutch situation. This means, among other things, that the energy use for hot water in washing machines and dishwashers is not included in the net/gross heat demand for

DHW. After all, the hot water for these applications is prepared in the respective appliances themselves by means of an electrical resistor. In some other countries (such as the US), it is common for these applications to also be supplied with hot water from the water heater.

Due to climate change, average temperatures (and especially minimum temperatures during colder seasons) are increasing. This has an effect on determining the energy required for DHW in e.g. 2050. This effect was not included in this study.

7   Conclusion

Application in practice of the advice to maintain a hot water temperature of 60 °C everywhere in the domestic water heater has substantial impact on the energy use of individual homes which are equipped with a sustainable system for domestic hot water production containing hot water storage (heat pumps, solar water heaters). For homes with a heat pump, an increase in annual final electricity use has been calculated at 16 – 28%. For solar water heaters, this increase has been calculated at 33 – 72%, assuming electric post-heating for solar water heaters. Plotted against the average standard annual electricity use (SJV) of individual homes, this means an increase of 3 – 13% for heat pumps and 8 – 32% for solar boilers. The variability in reported outcomes depends on hot water consumption due to household composition and occupant behaviour.

For now, the impact of increasing the temperature in the domestic water heater has a limited impact on a national scale of 0.7 – 1.1% compared to the current electricity use of the total housing stock in The Netherlands. However, this impact will increase with further electrification of residential heat demand where the share of homes with a sustainable system for water heating increases. For 2030, this increase is therefore estimated at 2.9 – 5.3% compared to the estimated final electricity use of the total housing stock in The Netherlands in 2030. It is likely that this value will increase further towards 2050 when the Netherlands aims to be climate neutral.

8   Future work

This study shows that the impact of consistently implementing the advices of Berenschot/ KWR is substantial. The message here is that in general a safe application of sustainable domestic hot water systems should be sought. To this end, further interpretation of some of the advices from the Berenschot/ KWR report is desirable. The outcome of this study also underlines the usefulness and necessity of further studies announced by the Dutch Minister of Infrastructure & Watermanagement to help determine the actual *Legionella* risk in residential systems in general and in residential systems with a sustainable system for water heating. Thus, this study, together with the Berenschot/ KWR report and the announced follow-up studies, form the building blocks to realise a more effective policy for *Legionella* prevention. These building blocks are also necessary to bridge the gap between science (advising 60 °C everywhere in the water heater) and practice, where this '60-degree-advise' is meeting resistance from parties who rightly see societal challenges in implementing this advice, but who are not always immune from financial interests.

9   References

Berenschot en KWR (2021), Met recht naar een doeltreffender legionellapreventie, Berenschot & KWR, Utrecht, https://www.rijksoverheid.nl/documenten/rapporten/2021/11/16/bijlage-1-rapport-met-recht-naar-een-doeltreffende-legionellapreventie.

Blokker, E. J. M., *et al.*, Simdeum, Grip op watervraag voor verduurzaming drinkwaterinstallaties en drinkwaternetten, https://www.kwrwater.nl/tools-producten/simdeum/, Assessed on: 8 February, 2023.

Blokker, E.J.M. et. al. (2017), Using a stochastic demand model to design cold and hot water installations inside buildings, CIBW062 Symposium 2017, Haarlem.

CBS (2021), Woningen; hoofdverwarmingsinstallaties, wijken en buurten, 2021, https://www.cbs.nl/nl-nl/cijfers/detail/85337NED?q=hoofdverwarmingsinstallaties, Assessed on: 12 February, 2023.

CBS (2023), Aantal bewoonde woningen, https://www.cbs.nl/nl-nl/cijfers/detail/85058NED?q=aantal%20bewoonde%20woningen, Assessed on: 12 February, 2023.

ISSO Publicatie 30 (2007), Leidingwaterinstallaties in woningen, ISSO, Rotterdam.

Luteijn, G., *et al.* (2021), Ontwikkelingen in de energierekening tot en met 2030, PBL-4731, PBL, Den Haag, https://www.pbl.nl/publicaties/ontwikkelingen-in-de-energierekening-tot-en-met-2030.

MilieuCentraal (2023), Gemiddeld energieverbruik, https://www.milieucentraal.nl/energie-besparen/inzicht-in-je-energierekening/gemiddeld-energieverbruik/, Assessed on: 12 February, 2023.

Moerman, A., *et al.* (2015), Efficiënte bereiding warm tapwater in woningen, BTO 2015.006, KWR, Nieuwegein, https://library.kwrwater.nl/publication/53699348/.

Moerman, A. and Oesterholt, F.I.H.M. (2023), Impactanalyse adviezen legionella-regelgeving op de warmtetransitie van woningen, KWR 2023.014, KWR, Nieuwegein, Rapport_Impactanalyse_adviezen_legionella-regelgeving_op_de_warmtetransitie_va_CL5zAh1.pdf (topsectorenergie.nl)

NEN 1006 (2018), Algemene voorschriften voor leidingwaterinstallaties, NEN, Delft,

NTA 8800 (2022), Energieprestatie van gebouwen - Bepalingsmethode, NEN, Delft, https://www.nen.nl/nta-8800-2022-nl-290717.

Pothof, I., *et al.* (2022), Field measurements on lower radiator temperatures in existing buildings, Manuscript for Energy and Buildings, WarmingUP, Utrecht, https://www.warmingup.info/documenten/11205149-hye-001_field-measurements-on-lower-radiator-temperatures-in-existing-buildings_def.pdf.

Rijksoverheid (2021), Woningbouwkaart toont bouwlocaties tot 2030, https://www.rijksoverheid.nl/actueel/nieuws/2021/06/09/woningbouwkaart-toont-bouwlocaties-tot-2030, Assessed on: 15 June, 2023.

Scheffer, W. (2000). Oog voor realiteit bij legionellapreventie; Watertemperatuur als criterium. Intech. November 2000**:** 50-53.

Van der Wielen and Oesterholt (2023), Legionella legislation for drinking water in the Netherlands revisited, CIBW062 Symposium 2023, Leuven.

Van Wolferen, J. (2019), Mogelijkheden voor het verlagen van de vereiste temperatuur van warm tapwater, Rapport 2019-006, Van Wolferen Research, Apeldoorn, https://www.tweedekamer.nl/kamerstukken/detail?id=2019D52581&did=2019D52581.

10 Presentation of Authors

Andreas Moerman M.Sc. is a scientific researcher and project manager at KWR working in the energy-water-nexus. His expertise is modelling and analysis in several domains in the energy-water-nexus, like aquathermal energy, (domestic) hot water systems and impact of the energy transition on (drinking) water systems.
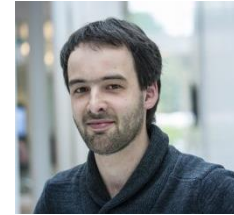
Frank Oesterholt M.Sc. is a senior scientific researcher and project manager, working in the field of the energy-water-nexus and resource recovery and is also specialized in *Legionella* prevention in man-made water systems.

Annex I – Technical assumptions

Below the technical assumptions are summarized in Tables I.1 and I.2.

Table I.1 Technical assumptions actual situation

Heater scenario	Heater efficiency	Electrical auxiliary energy	Storage losses**	Solar system contribution ***	Other conditions
Electrical boiler 120 l	100%	-	2,5 W/K (class G)	-	$T_{set,hw} = 80\ °C$
HP air/ water 150 l	295% $\eta_{carnot} = 50\%$	*	2,0 W/K (class C)	-	$T_{set,hw} = 58\ °C$ $T_{evaporator} = 10\ °C$
HP air/ water 300 l	295% $\eta_{carnot} = 50\%$	*	2,5 W/K (class C)	-	$T_{set,hw} = 58\ °C$ $T_{evaporator} = 10\ °C$
HP water/ water 150 l	320% $\eta_{carnot} = 50\%$	*	2,0, W/K (class C)	-	$T_{set,hw} = 58\ °C$ $T_{evaporator} = 15\ °C$
HP water/ water 300 l	320% $\eta_{carnot} = 50\%$	*	2,5 W/K (class C)	-	$T_{set,hw} = 58\ °C$ $T_{evaporator} = 15\ °C$
Solar heater 150 l	100%	25 kWh$_e$/ jaar ***	2,0 W/K (class C)	46-58% | A0+ 31-55% | D0+	$T_{set,ww} = 58\ °C$ $T_{vessel,annualy} = 45\ °C**$
Solar heater 300 l	100%	48 kWh$_e$/ jaar ***	2,5 W/K (class C)	68-78% | A0+ 54-76% | D0+	$T_{set,hw} = 58\ °C$ $T_{vessel,annualy} = 45\ °C**$

ΔT_{vessel} = difference between lower and upper storage vessel temperatures, equal to 5 K.

η_{carnot} = maximum practical efficiency (sCOP) based on source and delivery temperature and theoretical maximum COP (Carnot).

$T_{set,hw}$ = setpoint temperature for DHW supplied by the generator either directly to the system of outlet pipes (flow-through system) or via a storage vessel (storage system).

$T_{evaporator}$ = source temperature (year-round average) on evaporator side of heat pump.

*) For electrical auxiliary energy use, according to the Dutch building norm NTA 8800:2022, these energy quantities are not allocated to DHW preparation when there is a combi appliance for both space heating and DHW preparation.

**) Source: NTA 8800:2022, Table 13.9. For scenarios with a solar water heater, an annual average tank temperature of 45 °C is assumed, based on an average between 20-30 °C in winter and 60-70 °C in summer.

***) These are average values based on quality assessments of solar boiler systems after 2020 from various manufacturers as registered by the Dutch Council for Control and Registration of equivalency (BCRG).

Table I.2 Technical assumptions situation maintaining 60 °C everywhere in the water heater

Heater scenario	Heater efficiency	Electrical auxiliary energy	Storage losses**	Solar system contribution ***	Other conditions
Electrical boiler 120 l	100%	-	2,5 W/K (class G)	-	$T_{set,ww} = 80$ °C
HP air/ water 150 l	270% $\eta_{carnot} = 50\%$	*	2,0 W/K (class C)	-	$T_{set,hw} = 65$ °C $T_{evaporator} = 10$ °C
HP air/ water 300 l	270% $\eta_{carnot} = 50\%$	*	2,5 W/K (class C)	-	$T_{set,ww} = 65$ °C $T_{evaporator} = 10$ °C
HP water/ water 150 l	290% $\eta_{carnot} = 50\%$	*	2,0, W/K (class C)	-	$T_{set,hw} = 65$ °C $T_{evaporator} = 15$ °C
HP water/ water 300 l	290% $\eta_{carnot} = 50\%$	*	2,5 W/K (class C)	-	$T_{set,hw} = 65$ °C $T_{evaporator} = 15$ °C
Solar heater 150 l	100%	25 kWh$_e$/ jaar ***	2,0 W/K (class C)	46-58% | A0+ 31-55% | D0+	$T_{set,hw} = 65$ °C $T_{vessel,annualy} = 60$ °C
Solar heater 300 l	100%	48 kWh$_e$/ jaar ***	2,5 W/K (class C)	68-78% | A0+ 54-76% | D0+	$T_{set,hw} = 65$ °C $T_{vessel,annualy} = 60$ °C

Study on Energy Efficiency Evaluation Indicators for Building Hot Water Systems in Taiwan

Hsuan-Mao Huang(1), Cheng-Li Cheng (2)

(1) M11113032@mail.ntust.edu.tw

(2) CCL@mail.ntust.edu.tw

(1) (2) National Taiwan University of Science and Technology, Department of Architecture, Taiwan, R.O.C.

Abstract

During the operational phase of the building life cycle, over 60% of energy consumption and carbon emissions occur, with hot water energy consumption being a significant factor. This study aims to investigate the energy consumption characteristics of fixed hot water equipment in residential buildings in Taiwan, as well as update and confirm the standards for hot water system equipment and domestic hot water usage in Taiwan. The results of the hot water energy consumption in Taiwanese residential buildings indicate that hot water usage is a critical factor influencing the energy efficiency of the hot water systems. Additionally, the choice of heating equipment is crucial as well. In the calculations, we found that natural gas consumes 10.3% less energy than electricity for the same heating time. If electric heating is used, it is recommended to use high-efficiency heat pumps, which can reduce energy consumption by up to four times. Finally, based on the investigation of hot water energy consumption and the proportion of heating equipment, the average annual total hot water energy consumption rate for Taiwanese residential buildings was determined to be 1.15 classified as existing buildings.

Keywords: Hot water system, Hot water energy consumption, Residential building

1. Introduction

The energy consumption of Taiwan's construction industry accounts for 30% of the national total, highlighting the importance of energy-saving and carbon reduction in buildings. During the lifecycle of a building, over 60% of energy loss and carbon emissions occur during the daily use phase, with residential buildings having the highest proportion of fixed equipment energy consumption. To align with Taiwan's 2050 Net Zero Emission policy, the domestic construction sector has implemented legislative measures for building energy efficiency assessment and labeling systems, along with setting carbon benchmarks for major fixed equipment in residential buildings. However, these parameters require clear updates in evaluation criteria, including current hot water usage in buildings, the utilization and energy efficiency benchmarks of various types of water heating devices, as well as carbon emission coefficients and potential benefits of carbon reduction. Therefore, the main objective of this study is to estimate the carbon emission intensity of residential hot water systems in Taiwan through energy efficiency formulas for building hot water systems, and to analyze the usage patterns and energy efficiency benchmarks of water heating devices in residential buildings. This will provide a clear assessment of the proportion of energy loss in buildings and contribute to the goal of reducing carbon emissions.

2. Methodology

2.1 Survey

This study integrates existing literature and statistical data, taking into account factors such as hot water usage, heat loss, and equipment efficiency. Additionally, we included a sample of 30 randomly selected residential buildings certified with green building labels as the research subjects. Through Monte Carlo simulation, we obtained relevant coefficients for residential buildings in Taiwan, including average occupancy per household, hot water design length, and bathtub utilization rate. Finally, using these coefficients, we estimated the energy consumption and carbon emissions of hot water in Taiwan.

2.2 Energy consumption assessment methods

Currently, the assessment methods used abroad widely rely on the Building Energy Efficiency Index (BEI) standard established by the Japan Housing Performance Evaluation and Labeling Association (2017) to estimate the energy consumption level of

buildings' hot water systems. This standard takes into account factors such as building structure, envelope, hot water, and equipment. It categorizes buildings into five levels, allowing for comparisons of hot water energy consumption levels among different buildings. Furthermore, by estimating the hot water energy consumption score of residential buildings, it is also possible to reference the subsequent Green Building Evaluation Index for Residential Buildings (EEWH-RS) scoring method to obtain a more comprehensive assessment of building energy efficiency.

Table 1-Distribution of BEI grades in Japanese residential buildings

grades	★★★★★	★★★★	★★★ reference criteria	★★ Energy-saving Criteria	★ Existing Building Criteria
BEI	0.8and above	0.85	0.9	1	Below 1.1

2.3 Monte Carlo simulation method

By utilizing the Monte Carlo simulation method, the sampled green building cases can be simulated to obtain data that can be used in future formula coefficients. The basic principle of the Monte Carlo method is to simulate outcomes by repeatedly generating random numbers. In practice, the probability of all possible outcomes is defined as a probability density function, and this function is then accumulated to create a cumulative probability function. The maximum value of the cumulative probability function is adjusted to 1, establishing a simulation of normalized standard distribution values. The standardized normal distribution represents the probability characteristics of all events occurring with a total probability of 1, and it establishes a connection with the actual problem simulation through random sampling.

3. Hot Water Energy Consumption Assessment

3.1 Energy Consumption Formula

This study refers to the Japan Building Energy Efficiency Standards and Calculation Manual, 3rd Edition (1996) to establish the annual overall hot water energy consumption rate for residential buildings in Taiwan. Through this formula, the hot water energy consumption level of Taiwanese residential buildings is calculated. The formula considers four energy consumption factors: usage energy, transmission energy, storage energy, and heating energy. These factors collectively influence the overall hot water energy consumption in residential buildings.

$$AH_R = \frac{\sum_{M=1}^{12} \left[\frac{H_u + H_p + H_S}{H_i \times ei}\right]}{\sum_{M=1}^{12} EH} \ldots\ldots\ldots\ldots\ldots..\ldots\ldots\ldots\ldots\ldots\ldots\ldots\ldots\ldots eq(1)$$

式中,			
AH_R		Annual Overall Hot Water Energy Consumption Rate	[kcal]
EH	:	Monthly Reference Hot Water Energy Consumption	[kcal]
H_u		Monthly Design Hot Water Energy Consumption	[kcal]
H_P	:	Monthly Hot Water Transmission Energy Consumption	[kcal]
H_S		Monthly Stored Hot Water Energy Consumption	[kcal]
H_i	:	Energy Value	-
e_i		Heater Efficiency	-

*Heat value (H_i): natural gas=8900 Kcal/m^3, electricity=860 Kcal/kWh

3.2 Hot water energy consumption

The energy consumption of hot water usage in each household can be considered from two aspects: usage time and usage volume. This study investigated the average number of occupants per household in Taiwan, which is currently 2.65 people, and combined it with the residential hot water usage data compiled by Wang Yiting (2022). Based on this information, it is found that the average hot water usage in Taiwan households during the summer is 218.6 liters and during the winter is 224.2 liters. Finally, using the above data, the average annual hot water energy consumption in Taiwan households is calculated to be 1,208,981 kcal.

Table 2- Daily Per-Household Hot Water Usage Volume Statistics

Season (Month)	Summer (5、6、7、8、9、10)	Winter (1、2、3、4、11、12)
Hot Water Usage (Q_u)	218.6(ℓ)	224.2(ℓ)
Average Time (t)	1.17(h)	1.40 (h)

$$H_u = Q_u \times (TH - 0.93 \times TA_M + 1.78) \ldots\ldots\ldots\ldots\ldots\ldots\ldots\ldots\ldots\ldots eq(2)$$

式中,			
H_u		Design Hot Water Energy Consumption	[kcal]
Q_u	:	Hot Water Usage	[ℓ]
TH		Hot water temperature(39.9 ˚C)	˚C
TA_M	:	Ambient Temperature	˚C

* Temperature: (Lee et al.,2014)

3.3 **Energy Loss in Transmission**

Based on the previously mentioned water usage and duration, it is possible to estimate the amount of heat lost during the transmission of hot water. During the pipeline transport process, the temperature of the hot water can be affected by factors such as the length of the pipelines, the materials used, and the outdoor ambient temperature, resulting in heat loss. Through a case study of residential properties in Taiwan, it was found that approximately 80.9% of residential hot water pipes are insulated, and the average length of the pipelines is 10.62 meters. Finally, based on the research by Li Mengjie (2006), a simplified calculation formula was utilized to estimate the energy loss in the transmission section of the residential hot water systems in Taiwan, which amounted to 17,285 kcal.

3.4 **Thermal Energy Storage Consumption**

The heat losses generated during the storage process can be calculated based on the energy efficiency rating standards for storage-type electric water heaters announced by the Ministry of Economic Affairs in Taiwan (2014). Furthermore, according to the survey conducted by Wang Yiting (2022), it was found that approximately 28.7% of households in Taiwan use storage-type electric water heaters, and 73% of these households have the habit of turning off the water heater after use, which can reduce electricity consumption by 60%. Based on the number of households, a storage tank capacity of 60 liters was chosen.

Table 3-Storage Energy Consumption Classification

60(L)	24 (h) 27%	4 (h) 73%	Total(kWh)
Lv 1	0.54	0.09	0.2115
Lv 2	0.64	0.11	0.2531
Lv 3	0.74	0.12	0.2874
Lv 4	0.84	0.14	0.329
Lv 5	0.93	0.16	0.3679

3.5 Heating Energy Consumption

This study selected representative heating equipment for residential purposes, including instant gas water heaters, instant electric water heaters, storage electric water heaters, heat pump water heaters, and solar water heaters for evaluation. Subsequently, referring to the equipment energy consumption allowance standards announced by the Energy Bureau of the Ministry of Economic Affairs (2012), the following table summarizes the energy consumption impact of each heating equipment on the overall residential hot water system.

Table 4 - Annual energy consumption statistics for hot water equipment

Hot Water Equipment	Energy Consumption (m3/flat/year)* (kWh/flat/year)	Transmission Loss (m3/flat/year)* (kWh/flat/year)	Storage Loss (m3/flat/year)* (kWh/flat/year)
(IGH1)Instantaneous Gas Water Heater Lv 1	175.75*	2.51*	-
(IGH2)Instantaneous Gas Water Heater Lv2	180.89*	2.59*	-
(IGH3)Instantaneous Gas Water Heater Lv 3	190.94*	2.73*	-
(IGH4)Instantaneous Gas Water Heater Lv4	199.57*	2.85*	-
(IGH5)Instantaneous Gas Water Heater Lv5	206.22*	2.95*	-
(ESH1)Electric storage water heater Lv 1	1,562.26	22.34	85.78
(ESH2)Electric storage water heater Lv 2	1,562.26	22.34	102.65
(ESH3)Electric storage water heater Lv 3	1,562.26	22.34	116.56
(ESH4)Electric storage water heater Lv4	1,562.26	22.34	133.43
(ESH5)Electric storage water heater Lv 5	1,562.26	22.34	149.20
(EH)Electric Water Heater	1,562.26	22.34	-
Heat Pump Water Heate	366.792	5.244	27.592
Solar water heater	137,572.520	10,653.113	8,518.231

4. Estimate of carbon dioxide emission

By combining the energy consumption of the aforementioned hot water systems with the results of a survey conducted by Wang Yiting (2022), the adoption rate of different hot water devices in Taiwan can be determined. Additionally, data from the Water Resources Agency and the Ministry of Economic Affairs (2021) provide information on the carbon emissions associated with water and heating energy sources. It is estimated that 1 cubic meter of water results in 0.152 kg of CO_2 emissions, while natural gas emits 0.502 kg of CO_2 per cubic meter, and electricity emits 0.502 kg of CO_2 per 1 kWh. Furthermore, based on data from the Directorate-General of Budget, Accounting and Statistics (2023), the total number of households in Taiwan is 8,086,905, with an average residential area of 148.76 square meters per household. Using this information, the carbon dioxide emissions from the residential sector in Taiwan can be calculated.The findings indicate that the storage-type electric water heater has the highest energy consumption ratio, followed by the instantaneous gas water heater.

Table 5-Percentage of carbon dioxide emissions from the residential sector in Taiwan.

	Residential Proportion	Users	Carbon Emissions (thousand tons/year)	Carbon Percentage
(IGH)Instantaneous Gas Water Heater	48.70%	3,938,323	143.12	**33.98%**
(ESH)Storage Electric Water Heater	28.70%	2,320,942	198.32	**47.09%**
(EH)Instant Electric Water Heater	10.40%	841,038	66.90	**15.88%**
Heat Pump Water Heate	2.00%	161,738	3.24	**0.77%**
Solar water heater	10.20%	824,864	9.59	**2.28%**
Total:	**100.00%**	**8,086,905**	**421.17**	**100.00%**
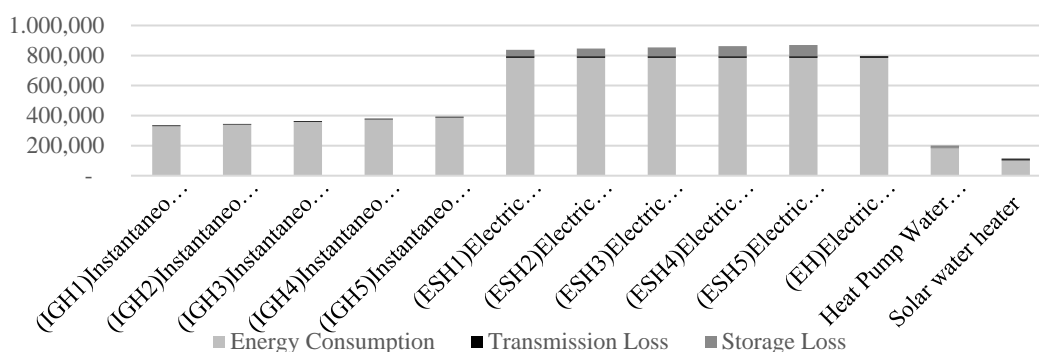
Figure 1 - Total carbon dioxide emissions from each hot water equipment (kgCO2/flat/year)

5. Conclusion

The main objective of this study is to investigate the overall energy consumption of the hot water systems in residential buildings in Taiwan, in order to understand the current proportion of carbon emissions from the residential sector and the annual total hot water energy consumption rate in Taiwanese residential buildings. The results of the hot water energy consumption in Taiwanese residential buildings indicate that hot water usage is a critical factor influencing the energy efficiency of the hot water systems. Additionally, the choice of heating equipment is crucial as well. In the calculations, we found that natural gas consumes 10.3% less energy than electricity for the same heating time. If electric heating is used, it is recommended to use high-efficiency heat pumps, which can reduce energy consumption by up to four times. Finally, based on the investigation of hot water energy consumption and the proportion of heating equipment, the average annual total

hot water energy consumption rate for Taiwanese residential buildings was determined to be 1.15 classified as existing buildings. Through this study, we aim to improve the energy efficiency of hot water equipment in Taiwanese residential buildings, reduce carbon emissions, and provide strategies for energy conservation and carbon reduction.

6. References

Building Energy Standards and Calculation Manual, 3rd Edition, Japan: Building Energy Efficiency Center , 1996

Lin, Y.-H, Study on Energy Consumption of Hot Water Distribution in Residential Buildings, Unpublished master's thesis,NTUST , 2005

Lee, M.-C, Study on Energy Consumption Evaluation and Energy Saving Methods of Domestic Hot Water in Residential Buildings, PhD dissertation, NTUST, 2006

Wang, R.-J, Guo, B.-Y, Study on Energy Calculation Standards and Labeling for Residential Green Buildings, Taiwan: Institute of Architecture, Ministry of the Interior , 2020

Global Status Report for Buildings and Construction, IEA, pp 13-15, 2021

Wang, Y.-T, Study on Hot Water Usage and Equipment Energy Consumption in Buildings, Unpublished master's thesis, NTUST, 2022

Edition, Taiwan: Institute of Architecture, Ministry of the Interior , 2022

Lin, H.-T et al, Green Building Assessment Manual - Accommodation Category, 2023

Presentation of Authors

Huang, Hsuan-Mao is the Master at National Taiwan University of Science and Technology, Department of Architecture. He research is focus on water resource and green building.

Cheng, Cheng-Li is the Professor at National Taiwan University of Science and Technology, Department of Architecture. He is a research scholar for water supply and drainage in building. He has published extensively on a range of sustainable issues, including the water and energy conservation for green building.

The energy-saving efficiency of hot water transmission pipeline between PU-insulated and uninsulated stainless pipes.

M. C. Jeffrey Lee (1)

(1) MCJL@nutc.edu.tw

Department of Interior Design, National Taichung University of Science and Technology, Taichung 40401, Taiwan

Abstract

After the hot water is used, the residual hot water within the pipeline is subjected to the influence of the low ambient temperature. To ensure a sufficient hot water supply temperature, it is usually necessary to reheat the water and flow out the cooled water in the pipes, which wastes water and consumes energy. To effectively address this problem, a low U-value PU insulation material technology was developed to wrap stainless steel pipes directly. Experiments were conducted on 13mm and 20mm diameter stainless steel pipes with different lengths (1m, 2m, 4m, 8m, 16m) to compare the temperature drop time and wasted water between insulated and uninsulated pipes under ambient temperature environments. According to the experimental results, the hot water drop time from 55℃ to 35℃ inner the insulated pipes was about 1.90 to 1.94 times longer than that in uninsulated lines (depending on pipe length and diameter, which affects heat capacity). The energy-saving efficiency of insulated pipes over uninsulated pipes was approximately 1.1-1.6 times (varying depending on conditions). This confirms that wrapping stainless steel pipes with PU insulation provides energy-saving benefits.

Keywords

energy saving efficiency, hot water transmission pipeline, PU-insulated stainless pipes, uninsulated stainless pipes

1 Introduction

The traditional approach to hot water piping has been buried installation in Taiwan, this lack of insulated pipe results in the need to drain off uncomfortable-temperature water (under 35℃) before using hot water. Lee [1] pointed out approximately 82.5 million liters (11 liters per household) of water are wasted daily when draining off the uncomfortable temperature water during showers in 7.5 million households with an average of four members, amounting to a staggering annual waste of up to 30.1 billion liters (approximately 30.1 million metric tons) in Taiwan.

Hot water supply in general buildings is generated through water heaters, and the supply methods can be classified into direct heating system and indirect storage heating system. Direct heating system was used for low-demand applications such as households and offices. Indirect storage heating system was suitable for high-demand hot water usage in hotels, dormitories, and hospitals. However, transmission pipes without insulators act as significant heat dissipators, causing a gradual decrease in water temperature via ambient temperature. Cheng and Lee [2] have shown that by regressing the tangent slope of the temperature loss curve, known as the temperature drop gradient (T_D), as shown in Figure 1, the rate of temperature decrease can be determined, as shown in Figure 2.

Generally, shorter pipelines drop temperature faster due to lower heat capacity, as shown in Figure 3. The water temperature inner pipes decreases from 60℃ to indoor temperature (25℃) just 10 to 15 minutes in a 1 meter long pipe, but the water temperature drops within half hour at the same conditions in a 8 meter long pipe [3]. This rapid temperature drop in transmission pipelines means that if hot water is not used within 15 minutes, the cooled water in the pipes will be drained off and replaced by subsequently heated water exceeding 40℃.
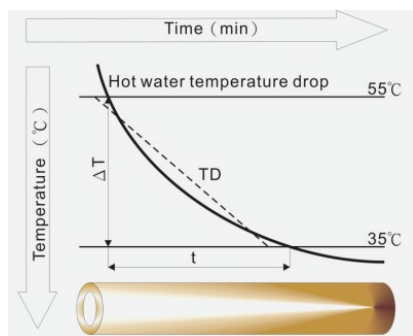

Figure 1 Temperature gradient conceptual diagram [2]

$$q = \frac{(T_i - T_o) \times L_p}{\dfrac{1}{2\pi}\left(\dfrac{2}{D_i h_i} + \dfrac{1}{k_p}\ln\dfrac{D_o}{D_i} + \dfrac{2}{D_o h_o}\right)}$$

$$T_D = \frac{\Delta T}{t} \quad (\text{℃/min})$$

Figure 2 Simplified temperature gradient equation [2]
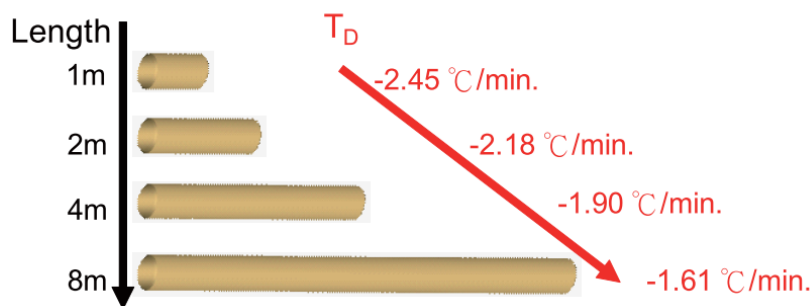
Figure 3 Relationship between manager and temperature [3]

Covering the insulation materials to delay the temperature drop, reducing the wastage of uncomfortable temperature water and mitigating carbon emissions from heating energy consumption is possible. This study evaluates the energy consumption difference between insulated and non-insulated pipes by experimenting on commonly used pipe diameters and lengths in residential buildings. The study investigates the differences between energy consumption and water usage, and further analyzes the relative carbon emission equivalent.

2 Methods

Most residential water supply piping in buildings adopts stainless steel press-fit pipes and the joints that comply with CNS 13392 and CNS 14645. These differ in pipe thickness from standard heavy-gauge pipes conforming to CNS 6331. This study aims to evaluate the energy-saving benefits through experimental tests on stainless steel non-insulated pipes and joints and BNX insulation pipes (coated with PU foam and stainless-steel press-fit pipes complying with CNS 13392). The study analyzes the thermal losses to assess energy efficiency.

The experiments were conducted in a location without direct sunlight to minimize external interference and avoid influencing the piping temperature and water temperature measurements. The flow meters were installed at the inlet and return ends of the test pipe, the pressure and temperature sensors installed according to the existing experimental field and distance requirements by previous study [1]. Two types of pipe assemblies were used for testing: one consisting of BNX insulation pipes with internal pipe diameters referred to as 20SU (stainless steel pipe with external diameter 22.2mm, inner diameter 20.2mm) and 13SU (stainless steel pipe with external diameter 15.9mm, inner diameter 14.3mm),

both with a 6mm foam insulation layer; and another assembly using non-insulated pipes of the specification and diameter as the control for comparison.

The experimental concept adopted a 24L gas water heater and used BNX insulation pipes with 13SU and 20SU diameters and non-insulated stainless-steel pipes. To explore their insulation performance, the experiments were conducted with different pipe lengths of 1m, 2m, 4m, 8m, and 16m. Various parameters were measured to analyze the temperature drop under the similar ambient temperature for different pipe diameters and lengths, thus evaluating the insulation benefits.

Due to the differences in assembly methods between the previous experiments using stainless steel pipes with threaded and quick-connect joints [1], this study using BNX stainless steel pipes with press-fit joints, adjustments were made to the total length of the pipes from the original 20m to 16m due to variations in bending lengths. Additionally, the installation of measuring instruments differed, requiring adjustments to the measurement equipment. Initially, three devices were used: fluid temperature meters, fluid pressure gauges, and flow meters. They were replaced with a combined flow meter and temperature meter for simplicity, and the pressure gauge was installed only at the inlet, as previous experiments demonstrated its functionality in monitoring water flow. The final experimental configuration was determined after three rounds of discussion and drawing, as shown in Figure 4. Three versions were considered: the initial design for a 20m length with instruments installed at 10m and 20m (Figure 4, top); the second version adjusted based on the instrument installation positions from the referenced literature (Figure 4, middle); and the third version with a total length of 16m (Figure 4, bottom) due to space constraints.

Based on this concept, the overall piping and measurement instrument configurations were redesigned for the experiments, and relevant pipes were installed, as shown in Figure 5. The assessment of temperature decrease time for insulated and non-insulated pipes was conducted to compare the heat loss conditions, analyze carbon emissions.

T	溫度傳送器
P	壓力傳送器
F	水龍頭
V	流量計/溫度
B	球塞閥
C	逆止閥

T6	20M
T5	16M
T4	8M
T3	4M
T2	2M
T1	1M
T0	0點
T7	回水
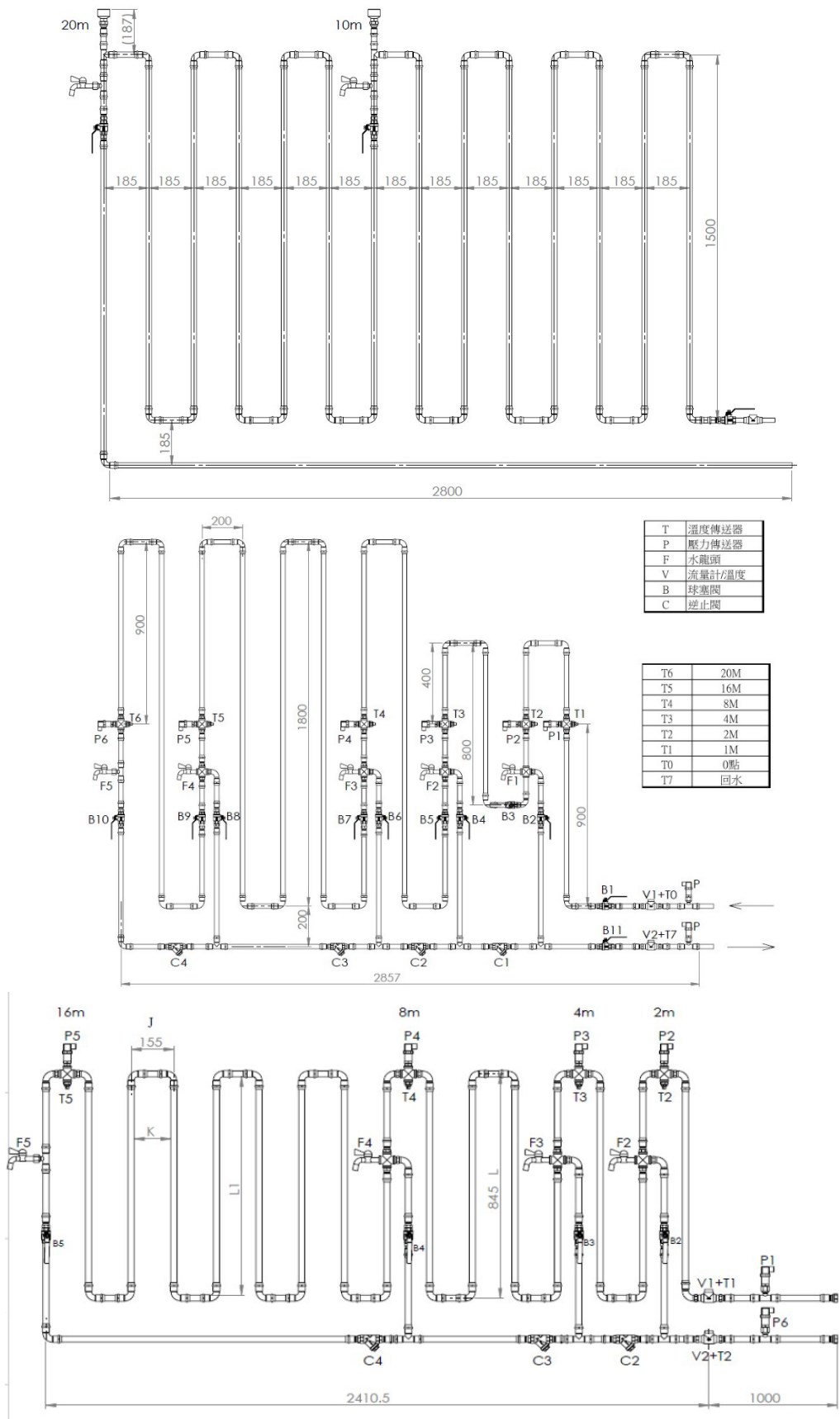
Figure 4 Modified version of the piping method

Figure 5 Assembly and water testing of insulated and non-insulated pipes of the same diameter and different pipe lengths

The experimental setting conditions are as follows:

1. The water temperature setting was 60°C by gas heater, and the temperature setting for closing the outlet was slightly higher than 54°C (approximately 55°C).
2. The pipe diameters used were 13SU and 20SU.
3. The pipe lengths tested were 1m, 2m, 4m, 8m, and 16m.
4. The pipe numbering scheme is as follows:

   No.0 measurement point for inletting water from the urban water piping.

   No.1 and No.7 describe the inlet points of the non-insulated (B) and insulated (I) pipes. No.1 is start inlet point, No.2 to No.6 represent the non-insulated (B) pipes with lengths of 1m, 2m, 4m, 8m, and 16m. No.8 to No.12 represent the insulated (I) pipes with lengths of 1m, 2m, 4m, 8m, and 16m, where water temperature, flow rate, and pressure measurements were taken.
5. The Campbell CR3000 Micrologger® was utilized for long-term monitoring of water temperature (°C), water flow rate (l/min), pressure (Bar), and ambient temperature (°C) at a sampling rate of every 2 seconds. The thermocouples (Type J) were sensing for ambient temperature.
6. During the heating phase, the infrared thermal imager captured consecutive images at a rate of one shot every 2 seconds. In the cooling phase, images were captured at intervals of 5 minutes until the surface temperature reached a stable state, at which point the imaging process was halted (continuous imaging lasted approximately 2-3 hours).

The experiment was conducted with three researchers: Researcher A, Researcher B, and Researcher C. At the beginning of the investigation, Researcher A opened the faucet to

initiate water flow and let the water heater start heating and supplying hot water. It was necessary to open the inlet faucet for the direct heating experiment. Once the experiment started, Researcher B verified the normal operation of the automated monitoring system and began recording data, including the internal temperatures, flow rates, and pressures at the inlet and outlet of the water pipe. When the outlet water temperature reached the predetermined maximum temperature, Researcher A closed the inlet faucet, stopping the water supply and causing the water heater to cease operation. Researcher A then returned to the site from the inlet faucet location to record the consumption of gas (measured by weight) and the water heater's energy consumption. The water level in the tank was also recorded to assess the water usage.

Meanwhile, Researcher C utilized an infrared thermal imager to continuously capture the variation of water temperatures inside the pipe, with an image taken approximately every 2 seconds during the heating phase. Once the data from the fluid temperature meter indicated that the pipe was uniformly heated to approximately 55°C, the imaging process was stopped, and images capturing the temperature decrease were taken at intervals of approximately 5 minutes. This allowed the analysis of temperature variations over time. After completing the experiments for various lengths of 20SU pipes for direct heating (including both insulated and non-insulated pipes), the entire experimental piping system was replaced, and the same procedure was repeated for 13SU pipes (including both insulated and non-insulated pipes), as depicted in Figure 6.
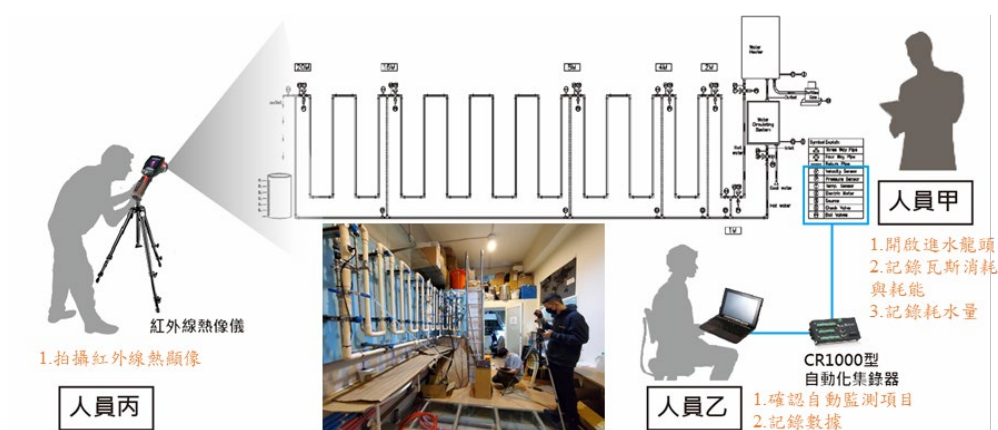

Figure 6 Configuration diagram of the experimental personnel for the system

3. Experiment and Results

The direct heating time of the supplied water, the natural cooling time, and the ambient

temperature were measured and recorded during the experiment period. The insulated stainless-steel pipes of 20SU and 13SU were initially adopted to assess the heat dissipation through the pipes and simulate the temperature reduction experienced in typical households with insulated pipes. A comparison was made with non-insulated pipe materials to verify the effectiveness of insulation. Experimental setups were arranged for five different pipe lengths: 1m, 2m, 4m, 8m, and 16m. Relevant equipment, measuring instruments, and data recorders were installed accordingly.

Additionally, an infrared thermal camara was used to capture surface temperature changes of pipes and record the various of natural cooling process. Due to the extensive duration of the natural cooling process and the substantial amount of data involved, only the infrared thermal images depicting the temperature decrease for 16m pipes of different diameters were provided (as shown in Table 1 and Table 2). Analyzing the natural cooling time of the insulated pipes facilitates the examination of the influence of ambient temperature on the water temperature inner pipes. This analysis is essential for exploring the differences in waiting time between successive users and the energy consumption associated with supplying hot water at the desired temperature or discarding water that doesn't meet the desired temperature. It also allows for an evaluation of the carbon reduction value attributed to the insulation of the pipes.

Based on the experimental results, it is evident that the surface temperature of pipes reaches the same temperature within a similar timeframe in each pipe condition (insulated and non-insulated pipes) when influenced by water temperature. Figure 7 illustrates the temperature decrease trend in 20SU pipes, while Figure 8 represents the trend in 13SU pipes. Notably, the time required for the water temperature to decrease inside the insulated pipes is approximately twice that of non-insulated pipes.
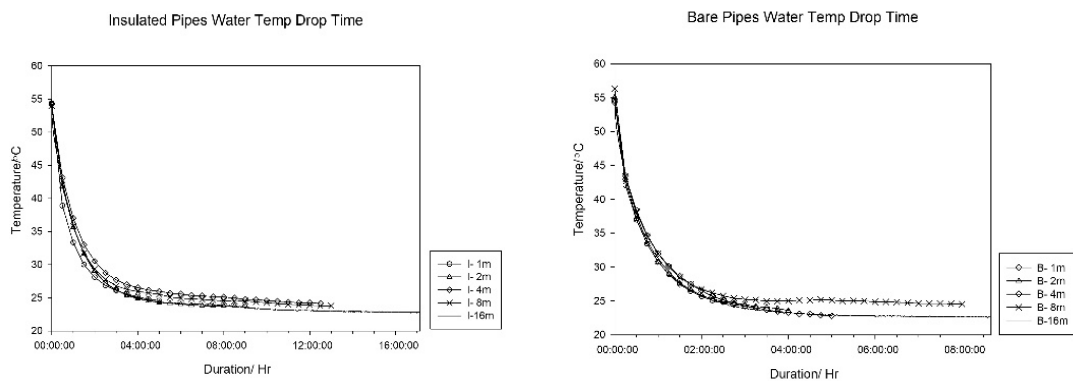
The trend of temperature drops in insulated pipes   The trend of temperature drops in non-insulated pipes

Figure 7 Water temperature drops trend in 20SU Insulated and Non-insulated pipes
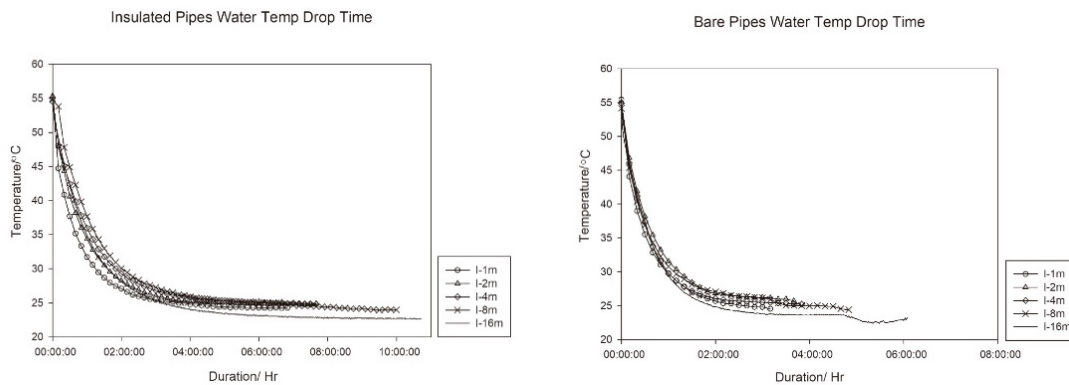
The trend of temperature drops in insulated pipes   The trend of temperature drops in non-insulated pipes

Figure 8 Water temperature drops trend in 13SU Insulated and Non-insulated pipes

Table 1   20SU insulated tube 16m infrared thermal image recording

20SU Insulation Pipe 16m (I-16m)
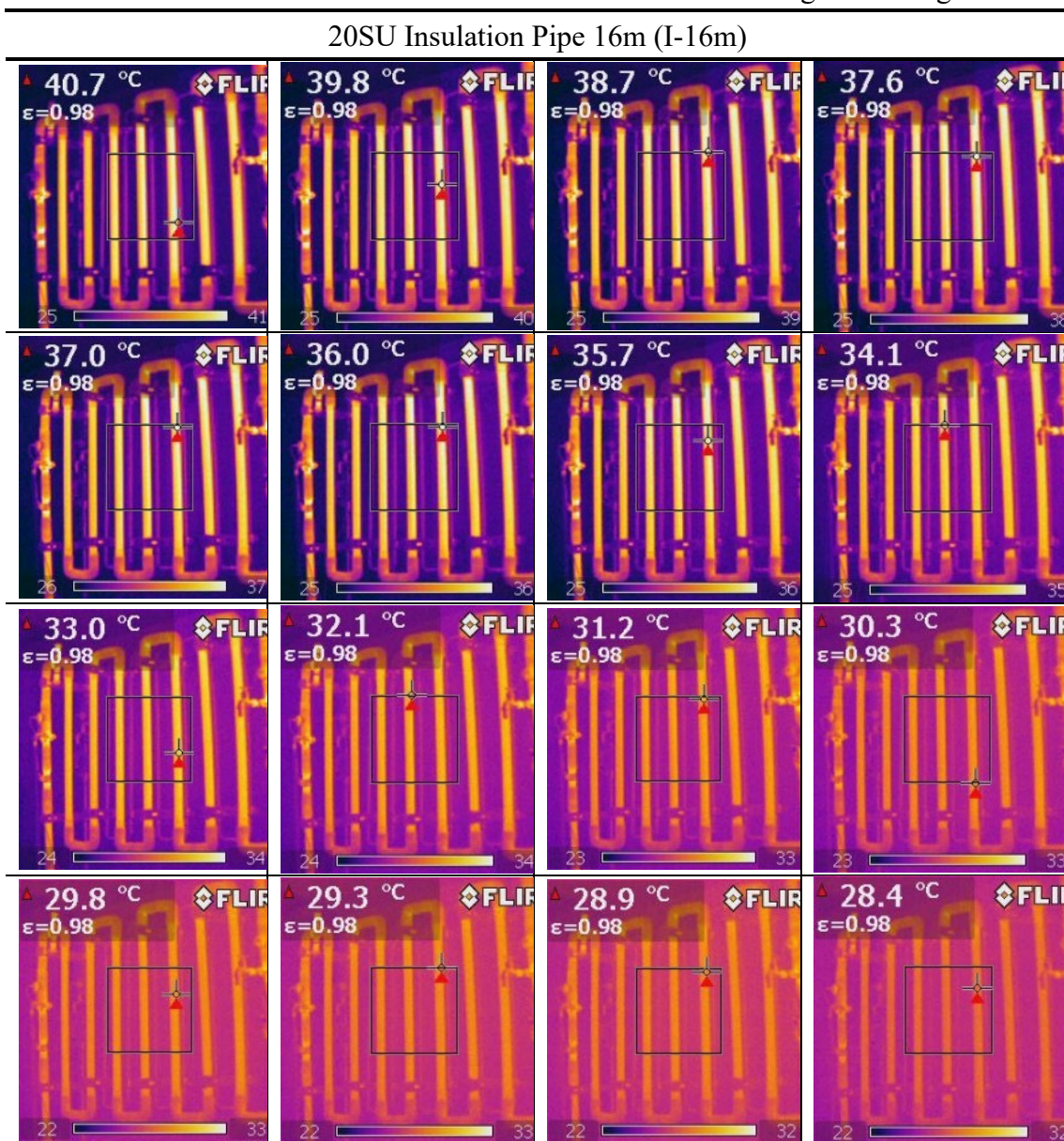
17hr 8min 26sec cooling results

Table 2   13SU insulated tube 16m infrared thermal image recording

13SU Insulation Pipe 16m (I-16m)

10hr 42min 48sec cooling results
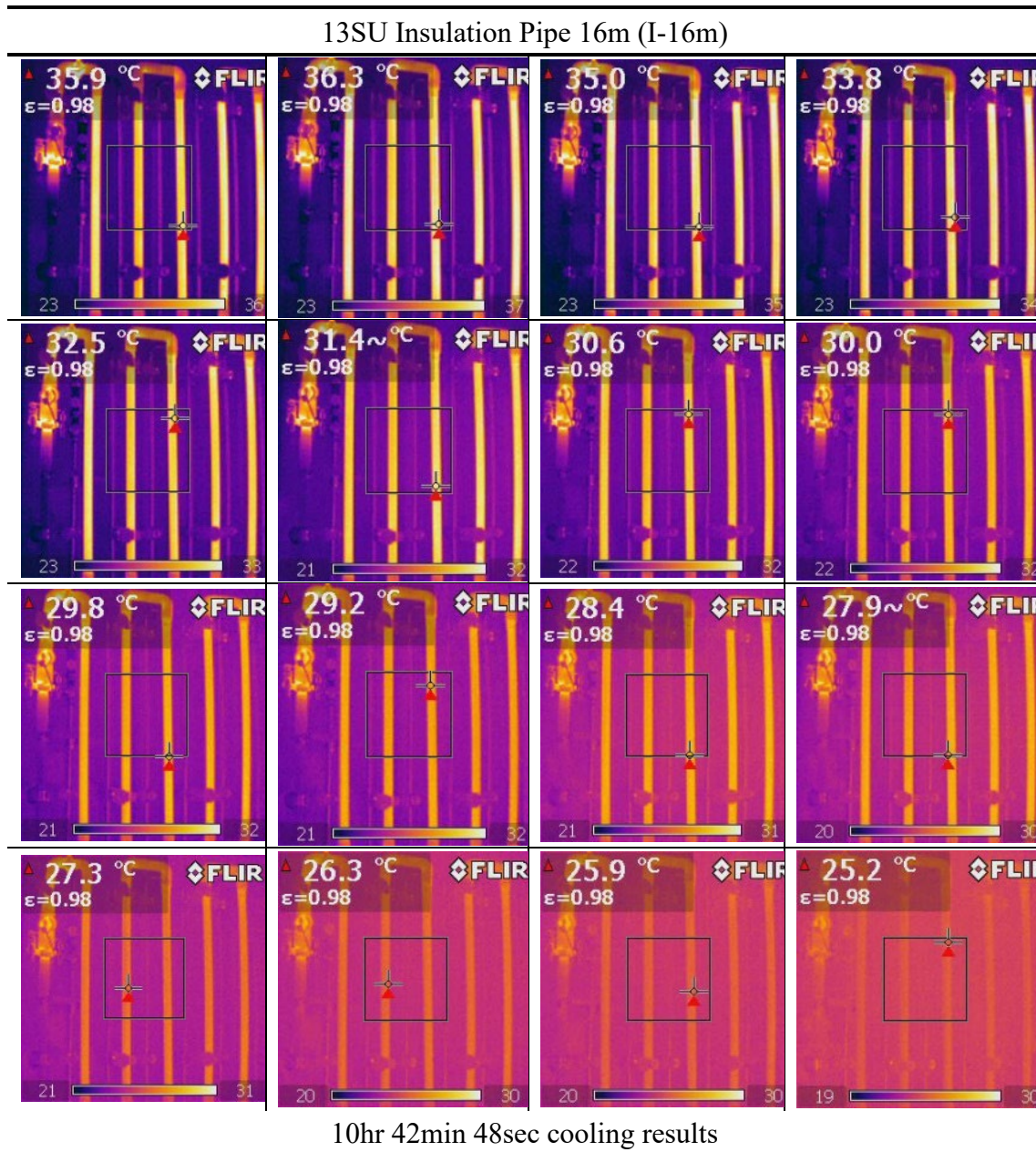
The natural cooling time is crucial for assessing the insulation efficiency of the pipes. The natural cooling time for each pipe condition was used to calculate the temperature decrease rate. Various temperature decrease intervals were examined, such as T_{10min} (temperature decrease in 10 minutes), T_{20min} (temperature decrease in 20 minutes), T_{30min} (temperature decrease in 30 minutes), T_{40min} (temperature decrease in 40 minutes), and T_{50min} (temperature drop in 50 minutes). These intervals were used to determine the time required for the water temperature to decrease from the outlet temperature of

approximately 55°C (as supplied by the water heater) to the perceived hot (warm) water temperature of 35°C.

Regarding to the temperature decrease criteria, the trends of pipe conditions (insulated pipe [I], non-insulated pipe [B]), pipe diameters (13SU, 20SU), pipe length (L_p), ambient temperature (T_a), cold water temperature (T_c), and water heater outlet temperature (T_h) were organized and presented in Figure 9. It is evident that despite the influence of varying ambient temperatures, the time required for water decreasing to 35°C in both insulated and non-insulated pipes to differs at least 10 minutes (represented by the dashed line for non-insulated pipe [B] and the solid line for insulated pipe [I]). Moreover, the larger diameter pipes (20SU) exhibit longer temperature decrease times due to their higher thermal capacity. Subsequently, these temperature decrease results will be utilized for energy consumption analysis.
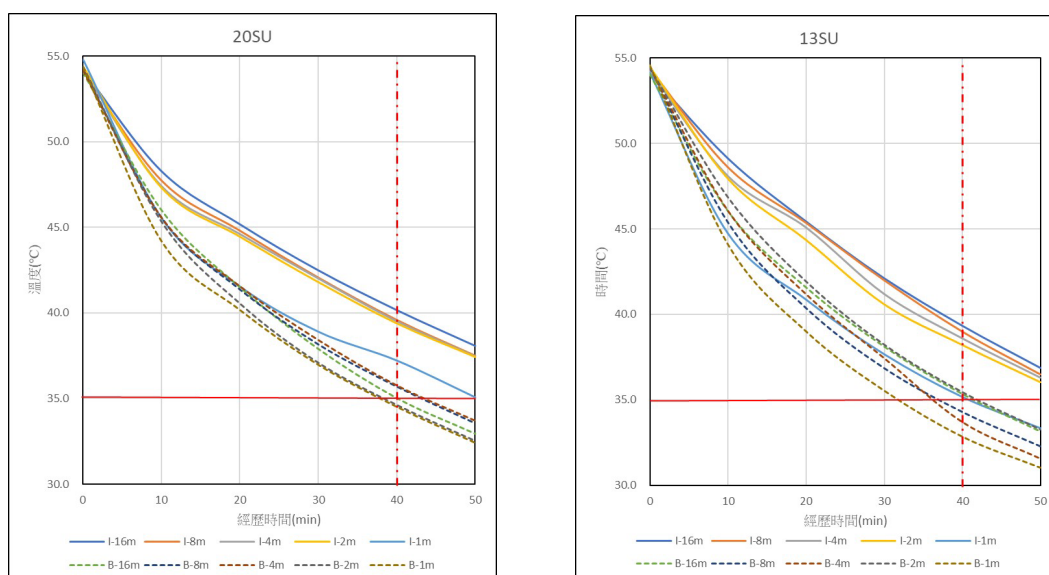
Figure 9 The trend of temperature drop from 10 min to 50 min for different piping.

4. Discussion

Based on the water temperature drops trends in relevant pipe conditions by natural cooling in Figure 7 and Figure 8. The regression analysis was performed for statistical correction, as presented in Table 3. It shows that the cooling time for 20SU insulated pipes is approximately 1.94 times longer than that of 20SU non-insulated pipes, while the cooling time for 13SU insulated pipes is approximately 1.90 times longer than that of 13SU non-insulated pipes. This indicates that the insulation efficiency of the insulated pipes is

approximately two times of non-insulated pipes in the same diameter. Due to the larger thermal capacity of the 20SU pipes, their insulation efficiency is slightly higher by 0.04 times in 13SU. The insulation effect of the insulated pipes is significantly demonstrated, as they can effectively increase the waiting time by approximately two times. Thereby avoiding the water temperature decreases too quickly, necessitating the disposal of unsuitable temperature water and subsequently wasting energy.

Table 3 Ratio of temperature drop time between insulated and non-insulated pipes

Pipe Diameter	Regression for Time Correction of Temperature Drop for 20SU (s)			Regression for Time Correction of Temperature Drop for 13SU (s)		
Pipe Length (m)	Insulated Pipe	Non-insulated Pipe	Ratio	Insulated Pipe	Non-insulated Pipe	Ratio
16	61,270	31,501	1.95	38,605	20,622	1.87
8	51,115	26,304	1.94	34,312	18,216	1.88
4	40,960	21,106	1.94	30,020	15,811	1.90
2	30,804	15,909	1.94	25,727	13,405	1.92
1	20,649	10,712	1.93	21,435	11,000	1.95
Average	**1.94**			**1.90**		

When hot water flows through the pipes, considering the hot (warm) water condition perceptible to the human body (35°C), the insulation effect (R_i) of the insulated pipes during the first 50 minutes (from 10 to 50 minutes) ($R_i = 1/ Q_i$ (heat loss), $i = 10, 20, 30, 40, 50$ min) is approximately 1.1-1.6 times that of non-insulated pipes (slight variations occur due to the influence of pipe length, diameter, and thermal capacity). Therefore, the insulated pipes delay temperature reduction time by approximately 60% compared to non-insulated pipes, as shown in Table 4.

This indicates that the insulated pipes can prolong the time required for subsequent hot water, resulting in energy-saving benefits. However, suppose the time is extended until the water temperature cools back to the original cold-water temperature, as demonstrated in Table 3. In that case, the difference between insulated and non-insulated pipes is approximately 1.9 times, signifying that as the temperature approaches ambient temperature, the heat dissipation from insulated pipes decreases, leading to an increased time delay effect. Considering the heat exchange significant variations in dynamic water flow , the heat loss results in Table 4 were obtained through experimental data and

theoretical formula calculations. It indicates that when the water temperature decreases from 55°C to around 35°C, non-insulated pipes consume approximately 1.3-1.4 times more energy than insulated pipes.

Table 4 Insulation efficiency ratio (I/B) between insulated and non-insulated pipes at different cooling period

Pipe Diameter	Pipe Length (m)	R_{10min}	R_{20min}	R_{30min}	R_{40min}	R_{50min}	Average
20SU	16m	1.6	1.4	1.3	1.3	1.2	1.4
	8m	1.6	1.6	1.4	1.3	1.2	1.4
	4m	1.4	1.4	1.3	1.3	1.3	1.3
	2m	1.2	1.2	1.2	1.2	1.1	1.2
	1m	1.1	1.2	1.2	1.1	1.1	1.1
13SU	16m	1.4	1.4	1.4	1.4	1.3	1.4
	8m	1.4	1.4	1.3	1.3	1.2	1.3
	4m	1.3	1.3	1.3	1.3	1.2	1.3
	2m	1.3	1.4	1.4	1.3	1.3	1.3
	1m	1.1	1.1	1.1	1.1	1.1	1.1

I=Insulated pipe、B=Non-Insulated pipe

Based on the experimental results, the heat loss for various pipe lengths under different pipe conditions was calculated to evaluate the energy-saving potential in kilocalories (kcal). Subsequently, the carbon emissions equivalent (kgCO2eq) from heating by bottled gas (propane) were evaluated. According to the calculations, the BNX insulation pipe did not save much energy compared to non-insulated pipes in one household. However, based on approximately 7.5 million households with 4 residents, if each person takes one shower per day, requiring one heating operation for the pipes, and considering four operations per household per day, the total number of heating operations would reach approximately 10.8 billion annually in Taiwan.

The carbon reduction from insulated and non-insulated pipes can be estimated in ton (T). Assuming that the water temperature decreases from around 55°C to 35°C, the process would take approximately 40 minutes for non-insulated pipes, and 50 minutes for insulated pipes. Consequently, the carbon reduction after 50 minutes was evaluated, showcasing significant benefits among the 7.5 million households in Taiwan, as shown in Table 5.

Table 5 Carbon reduction of 50 minutes with Insulated pipes and Non-insulated pipes

Pipe Diameter	Pipe Length (m)	Insulated Pipe Heat Loss (kcal)	Non-insulated Pipe Heat Loss (kcal)	Energy Savings per Instance (kcal)	Carbon Reduction per Instance (kgCO$_2$eq)	Annual Household Water Usage Frequency in Taiwan	Carbon Reduction (T)
20SU	16m	689.3	945.8	256.5	0.00040	10.8b	43,460
	8m	496.8	644.2	147.4	0.00023	10.8b	24970
	4m	391.7	496.8	105.1	0.00016	10.8b	17,810
	2m	343.6	457.7	114.1	0.00018	10.8b	19,330
	1m	367.7	420.9	53.2	0.00008	10.8b	9,010
13SU	16m	544.8	776.1	231.3	0.00036	10.8b	39,190
	8m	423.7	596.8	173.1	0.00027	10.8b	29,320
	4m	352.6	496.3	143.6	0.00023	10.8b	24,340
	2m	327.1	406.6	79.5	0.00012	10.8b	13,470
	1m	347.4	421.6	74.1	0.00012	10.8b	12,560

In addition to the energy consumption from heating hot water, the disposal of unsuitable temperature water after heating leads to another carbon emission factor. Cheng [4] have indicated that the carbon emission of one ton of water is approximately 0.1002 kg. The estimated carbon emission resulting from the disposal of unsuitable temperature water between non-insulated and insulated pipes were compared and summarized in Table 6.

Table 6 Total carbon emission for the difference between non-insulated and insulated pipes.

Pipe Diameter	Pipe Length (m)	Insulated Pipe Water Leakage (l)	Non-insulated Pipe Water Leakage (l)	Difference in Water Consumption (l)	Carbon Emissions per Instance kgCO$_2$eq	Annual Household Water Usage Frequency in Taiwan	Carbon Emissions (T)
20SU	16	38.4	40.3	1.98	0.000198	10.8b	21,370
	8	27.7	28.9	1.23	0.000122	10.8b	13,270
	4	22.3	23.2	0.85	0.000085	10.8b	9,220
	2	19.7	20.3	0.67	0.000067	10.8b	7,200
	1	18.3	18.9	0.57	0.000057	10.8b	6,190
13SU	16	27.1	32.7	5.53	0.000553	10.8b	59,750
	8	21.4	24.6	3.22	0.000322	10.8b	34,790
	4	18.5	20.6	2.06	0.000207	10.8b	22,300
	2	17.1	18.6	1.49	0.000149	10.8b	16,060
	1	16.4	17.6	1.20	0.000120	10.8b	12,940

Based on Table 6, the carbon emission between the multiples of 13SU and 20SU is calculated for the difference in water wasted between non-insulated pipes and insulated pipes. It is found that the pipe diameter of 13SU is smaller than 20SU, the heat capacity in 13SU is smaller and cooling faster, so the flow out unsuitable temperature water is

much more than it in 20SU. Therefore, the estimated carbon emission in 13SU is higher than it in 20SU.

5. Conclusion

This study has determined the energy consumption associated with various pipe conditions, with the key factors being the disposal of unsuitable mixed-flow temperature water during direct heating of the water supply and the energy consumption of hot water that cannot be reused due to temperature reduction caused by ambient conditions. Based on the experiment results conducted on direct heating of the water supply, the energy-saving benefits of insulated pipes compared to non-insulated pipes were found to be approximately 1.1-1.6 times (varying depending on factors such as pipe length and diameter). Therefore, from the results of natural cooling period, it can be concluded that the insulation efficiency of the insulated pipes is approximately 1.90 times (13SU) to 1.94 times (20SU) that of non-insulated pipes, confirming their performance benefits.

6.Acknowledgments

7 References

[1] M.C. Lee, Reducing CO2 emission in the individual hot water circulation piping system, Energy and buildings, 84, 2014, 475-482.

[2] C.L. Cheng, M.C. Lee, Y.H. Lin, Empirical prediction method of transmission heat loss in hot water plumbing, Energy and Buildings 38, 2006, 1220-1229.

[3] M.C. Lee, C.L. Cheng, Y.H. Lin, Empirical approach to transmit energy for hot water plumbing system, CIB-W62 2005, 31st International Symposium (2005.9.14-16, Brussels, Belgian)

[4] C.L. Cheng, Study of the inter-relationship between water use and energy conservation for a building, Energy and Buildings 34 (2002) 261–266.

8 Presentation of Author(s)

Meng-Chieh, Jeffrey Lee is a PhD in Architecture. He is also the Professor at department of interior design and the Deputy dean of school of design in National Taichung University of Science and Technology. His major is water plumbing system, sanitary equipment safety and new technology development, interior environmental control, and energy saving.

Climate resilience design of potable water installations in buildings – hygienic safe temperature reduction of potable water hot (PWH)

C. Schauer (1)

(1) christian.schauer@viega.de

(1) Viega GmbH & Co. KG, Germany

Abstract

The demands placed on climate-resilient potable water installations will continue to increase in the future. In addition to sustainability and resource conservation issues, above all climatic effects create a need for action – from the basic availability of potable water to the provision of cold potable water by the utility company at a temperature level that ideally does not require any subsequent cooling.
For this reason, planners (and operators) already take a holistic view of all potable water installations, from the building entrance to the last draw-off point, with regard to potable water hygiene and energy efficiency as well as with regard to reducing the required water volumes as much as possible. In the future, a whole package of measures will be needed to ensure that potable water installations are not only perfectly hygienic but also climate-resilient. Today, these measures include in particular

- reducing the system volume of a potable water installation to keep the water volume that has to be permanently hygienically controlled as low as possible,
- reducing ambient temperatures as much as possible to protect PWC against external heating,
- reducing the PWH volume kept at a temperature to avoid external heating of PWC within the building,

and, for the future, in the context of energy-efficient buildings

- using innovative technologies such as the presented systemic UFC technology to reduce the increasing share of potable water heating in the primary energy

requirement, because PWH no longer has to be heated to 60 °C for hygienic reasons.

Keywords

Potable water hot; distribution concept; PWH; PWH-C; energy efficiency; sustainability; hygienic stability; ultrafiltration; circulation bypass.

1 Introduction

As a result of climate changes and their effects, housing technology is faced with challenges that have probably never existed before in this dimension – and with these types of consequences: To curb global warming, for example, it is necessary to drastically reduce the consumption of fossil fuels in order to cut CO_2 emissions. At the same time, however, weather changes associated with rising average temperatures and local conditions are causing an increasingly threatening long-term shortage of water resources and are having a critical impact on water hygiene for the water supply in Central Europe as well (see also Figure 1).

Ongoing revision of the EPBD and other EU directives are dealing with energy efficiency and sustainability of buildings and are part of the Renovation wave and the Fit for 55 package. This demands the importance to look at how the changing regulatory environment can contribute to making our built environment healthy and sustainable at the same time.

In Europe 40 % of the energy consumption and 36 % of the CO_2-emissions results from the building sector.
35 % of the buildings in the EU-member states are more than 50 years old.
75 % of the existing buildings are classified as inefficient.
85 % of the actual buildings will also be used in 2050.

Conventional (and technologically well proven) models of heat generation, potable water consumption and supply, as well as potable water heating must therefore be thoroughly scrutinized. With focus on climate protection heat generation and potable water heating will have to change from

- systems with high operating temperatures, as are typical for oil or gas boilers, among others,
- to low-temperature systems based on regenerative heat generators, such as heat pumps or "cold" local heating networks with usual supply temperatures of 30 to 40 °C in constant operation.

This in turn has direct consequences for potable water heating because the temperature level of 60/55 °C, which is (still) required due to hygienic reasons, counteracts these efforts. In addition, the power requirement for potable water heating becomes a considerably higher proportion of the heat requirement of a building – in relative terms - when the primary energy requirement of new buildings, including passive houses, also continues to decrease.

The task of technical building services planners is to recognize these developments and to combine them – in this case in the form of climate-resilient potable water installations – so that they not only reduce the primary energy use but also take into account the additional demand to use as little potable water as possible.

The key question derived from this is therefore: What requirements must a potable water installation fulfil in order to be climate-resilient in regard to the (environmental) effects of tomorrow and the associated demands? It must therefore not only fulfil the primacy of primary energy savings, which are currently prioritized in public discourse - in correlation with potable water heating – but it must also take into account climate-related consequences such as impermissible external heating (with corresponding cooling requirements) or the lowest possible use of potable water (among other things, for the water exchange necessary for hygienic reasons to protect against stagnation risks).

The World Health Organization (WHO) describes the requirements for preventing contamination that water is safe to drink at the point of use:

- constructing systems with materials that will not leach hazardous chemicals into the potable water
- maintaining integrity to prevent the entry of external contaminants
- maintaining the supply of potable water to consumers; and
- maintaining conditions to minimize the growth of microbial pathogens (e.g. *legionella*) and biofilms, scaling and accumulation of sediments.

2 Potentials for the energy efficiency of buildings

2.1 Distribution concept for potable water hot (PWH)

The building and the building services engineering must be planned, built and operated in a way that is economical and sustainable and conserves resources. This also applies to the potable water installation, the potable water heating system and the routing concepts for the hot potable water pipes. For example, hot potable water pipes release between 7 and 11 W/m of energy into the environment, even if they are well insulated.

For this reason, right from the planning stage, it is necessary to account for the fact that a consistent reduction in the volume of the piping system for hot potable water should be the consequence. This objective can be achieved partly by using the actual zeta values to calculate the piping system and create lean pipe routing, and partly by examining critically the piping sections that should be integrated into the circulation system. It would not be productive to integrate a utilisation unit with a water volume of < 3 l in the circulation system. As well as an associated and undesirable application of thermal energy to the pre-wall – which causes the cold potable water to heat up and produces huge amounts of thermal losses in each utilisation unit - a series installation results in fewer metres of piping, a reduced water volume in the system, reduced insulation requirements and lower heat losses. An installation of this type therefore conserves resources and energy. For this reason, the circulation system should be designed only in central areas (in the leg for vertical distribution or in the corridor for horizontal distribution). Circulating storey connection pipes can be implemented in installations with central potable water heating wherever no decentralised consumption measurement is anticipated for the storey concerned. Classic examples of this are the distribution and circulation pipe systems in the suspended ceilings in hospital corridors. Storey and single supply lines in service units with a volume of < 3 litres must not be integrated into the circulation system.

Compliance with the generally recognised rules of technology for the planning, construction and operation of potable water installations that are needed to meet the legal requirements does not call for a highly complex potable water installation. The less complex the potable water installation is, the less effort the planners, installers and operators of the potable water installation require to achieve the protection goal of the German Potable Water Ordinance. Hydraulically simple systems, therefore, are also more manageable systems. Complicated, meshed networks not only present an increased hygiene risk for planning, construction and operation. The fact that these networks allow a greater volume of hot potable water – and hence energy captured in the water – to circulate also increases the energy losses occurring throughout the piping network due to the much longer pipe lengths. These systems neither conserve resources nor ensure energy efficiency. They are also questionable from a hygiene perspective as the flow paths of the circulating potable water cannot be determined with certainty.

For hygienic reasons, the planning of potable water installations should therefore fulfil the following criteria:

1. Based on demand with correspondingly adjusted minimum system volumes.
2. Clearly structured hydraulics to avoid energy losses and heat transfer to potable water cold (PWC)

3. Avoidance of small, nested circulation pipes, which, for example, are routed into each utilisation unit up to the last draw-off point. (energy losses)
4. Regular water exchanges (intended operation)

2.2 Energy efficiency in buildings

In well-insulated new buildings to energy standard, hot potable water heating now accounts for a disproportionately high amount of the total energy requirement. Depending on the insulation standard, it can be as much as 40% of the primary energy requirement. Keeping hot potable water at the temperature of 60/55°C required by the standards, however, is prohibitive to the use of renewable heating systems. The optimum operating point of an energy-efficient heating pump, for example, is around 45°C. Such temperatures are ideal for heat generation with the heat distributed through surface heating, but not for heating hot potable water to a high temperature. To reach the 60/55°C required, therefore, hot water tanks are often reheated by an expensive process using power from fossil energies through an electric heating cartridge. Ecologically and economically, this makes little sense.
The conflict between improved energy efficiency and meeting the protection objective of "maintaining potable water quality" cannot be resolved through the conventional approach.
The latest research results and pilot studies suggest that a gradual reduction of the supply temperature of hot potable water to 47/45°C, for example, can be achieved if the framework conditions required for this are met. This calls for

- hygiene-conscious planning of the potable water installation with reliable hydraulic balancing,
- guaranteed operation as intended and
- a reduction of the total cell count by **u**ltra**f**iltration in the **c**irculation bypass (UFC-Technology) (Figure 2).

In this way, the possible growth potential for legionella and other pathogens can be sustainably minimised beyond the temperature limits. The aim is neither operating temperatures nor energy efficiency, but that of achieving the required potable water quality. The German Environment Agency (UBA) has already described the energy-efficient optimisation of operating temperatures in hot water without any compromise on potable water hygiene. Ultrafiltration technology (UFC) in combination with potable water heating zoned in case of need can play a key role here.

The ultrafiltration module in the bypass of the circulation return (PWH-C) is used in a system-specific way in conjunction with a continuous-flow potable water heater and electronic circulation regulation valves (Figure 3). Scalable and networked controllers record and log all operating data and use such information to proactively control the hygiene-relevant system parameters. The tests show a hygienic stabilization via a

significant reduction in the total cell count (TCC) as well as the elimination of value scattering (Figure 4) even when this ultrafiltration-technology is used. The addition of automatic rinsing fittings to the use of draw-off points can additionally support the cleaning process of the ultrafiltration technology; the low values (TCC) remain even after the rinsing fittings have been removed. A project in Berlin, Germany additionally shows a reducing and stabilizing effect on the bacteria concentration after 6 weeks in the potable water installation (Figure 5).

3 Figures
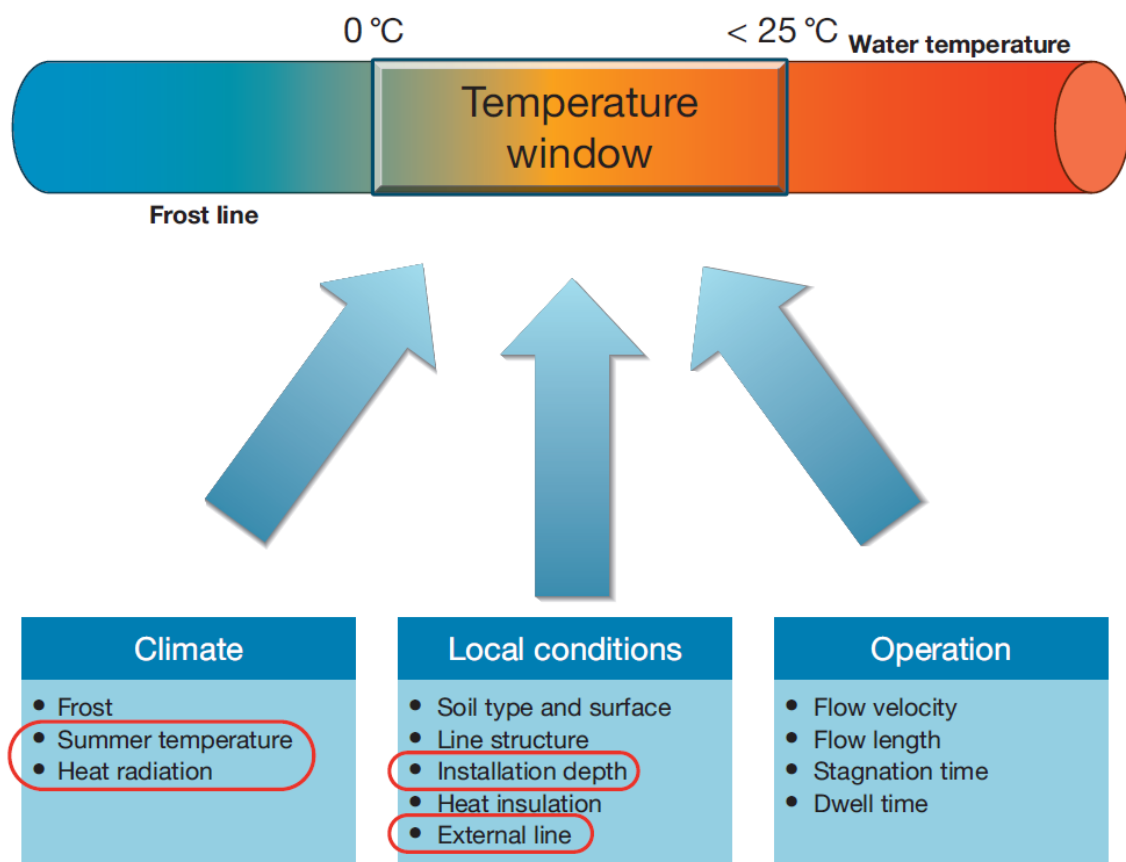
Figure 1 – Influence factors for the temperature window of potable water cold for the water supply
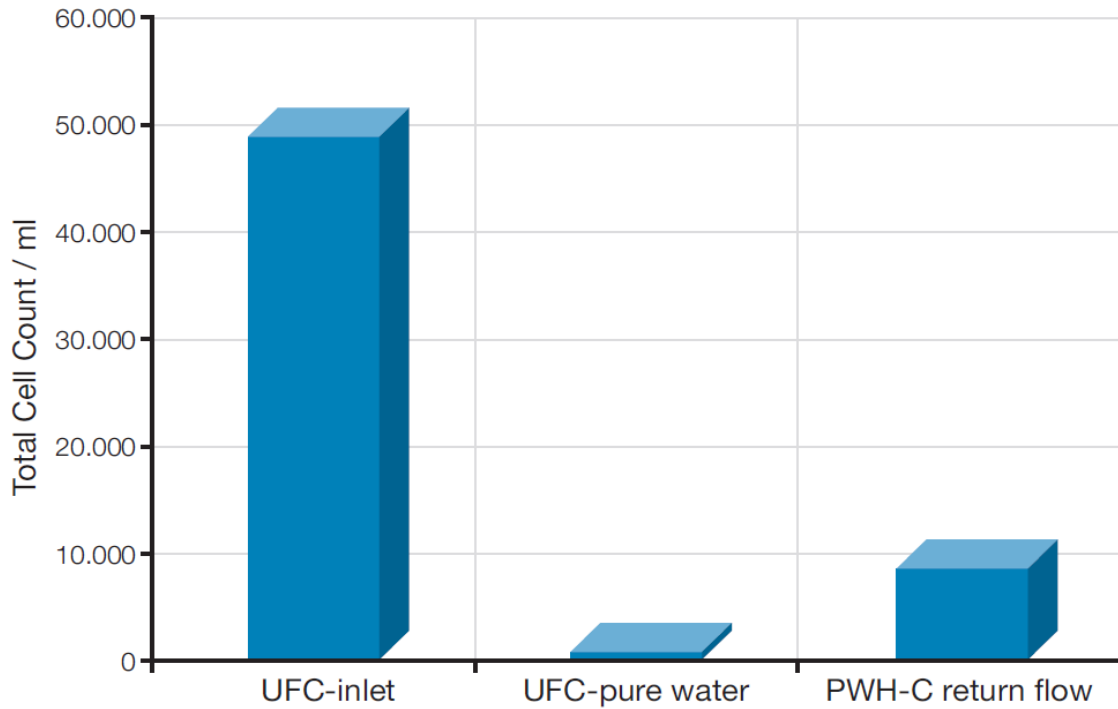
Figure 2 - Dedusting of the total cell count (TCC) in systemic samples (n = 123, 49 weeks) in the ultrafiltration unit (Hippelein et al. 2018)
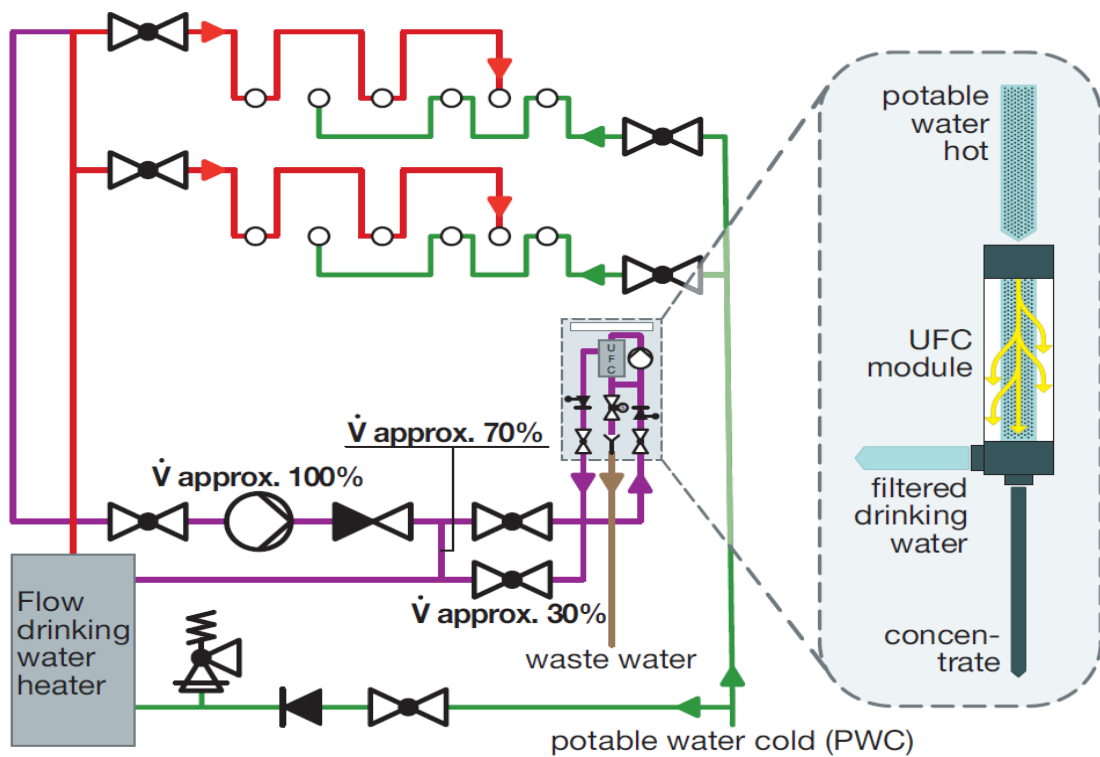
Figure 3 - Function principle of the UFC module (simplified illustration) in the bypass of the circulation return flow of the PWH-C system
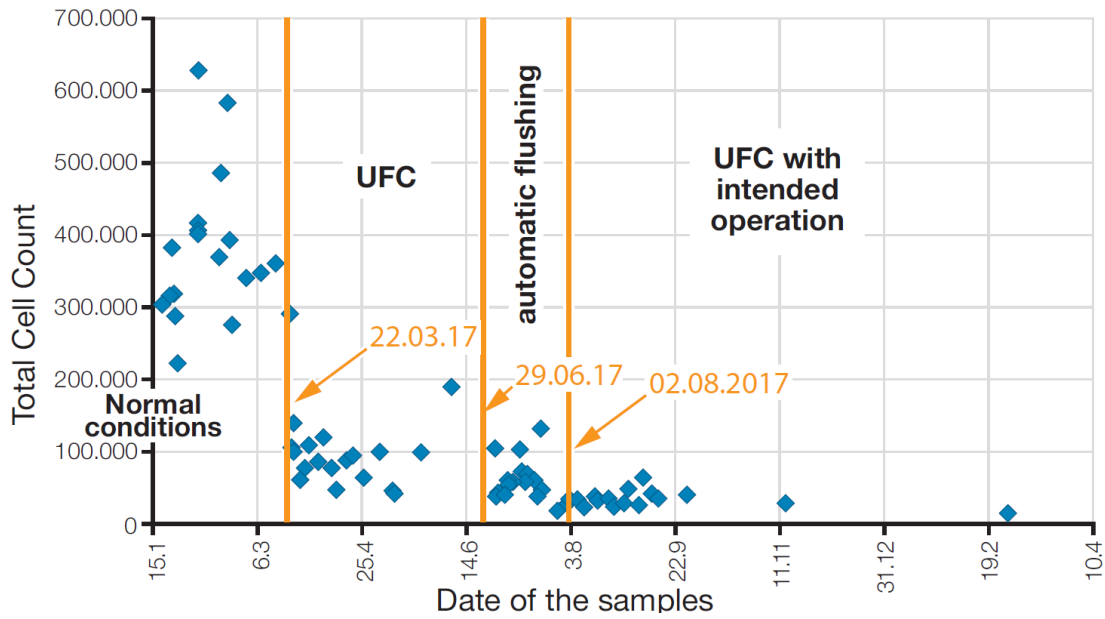
Figure 4 - Total cell count in a pilot project dependent on the deployed technology (Hippelein et al. 2018)
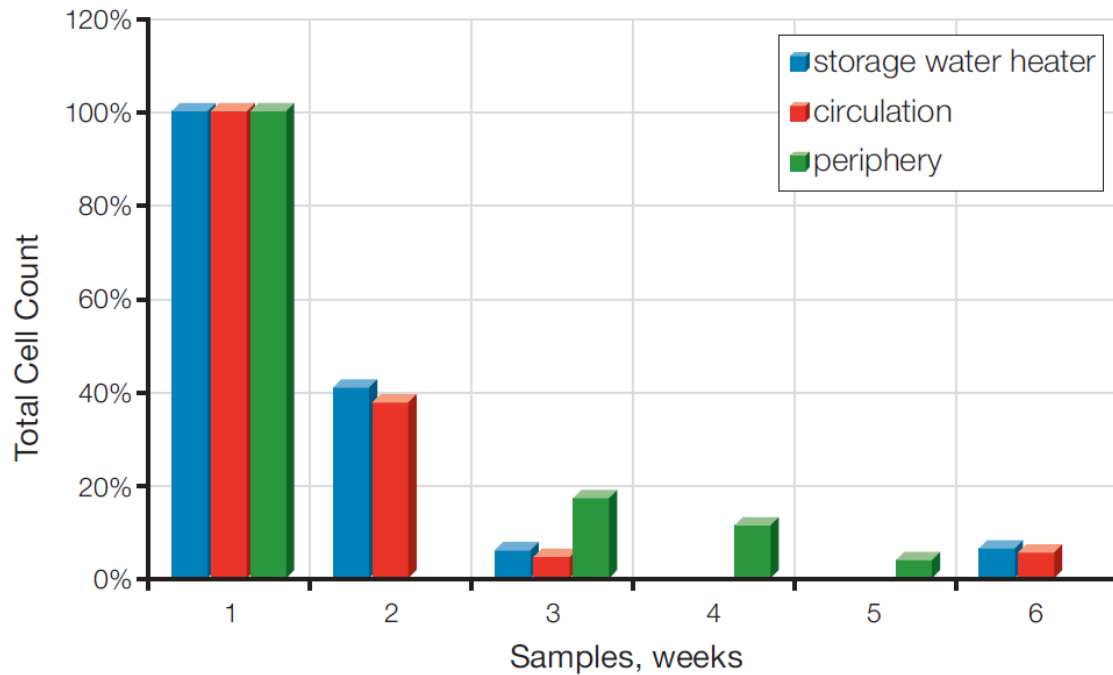
Figure 5 - Pilot project Berlin, residential building, effect of UFC-technology (Hippelein et al. 2018)

References

C. Schauer, K. Dinne, W. van der Schee, J. Mampaey, I. Gatto, J. Perackova, D. Petras, B. Bleys, T. Juhna, D. Ljubas, M. Cerroni, I. Aho, Hygiene in Potable Water Installations in Buildings, REHVA, Brussels, 2019.

DVGW W 551, Drinking water heating and drinking water piping systems – Technical measures to reduce Legionella growth - Design, construction, operation and rehabilitation of drinking water installations, 04/2004.

C. Schauer et al.: Planung und Betrieb 4.0. In: C. van Treeck, T. Kistemann, C. Schauer, S. Herkel, R. Elixmann (Hrsg.): Gebäudetechnik als Strukturgeber für Bau- und Betriebsprozesse, Springer Verlag Berlin, 2018, p. 167–275.

M. Hippelein, N. Puls, H. Fickenscher, B. Christiansen, Einsatz der Zytometrie zur Überwachung der Substitution energieintensiver Hygienisierung häuslicher Trinkwasser-Installationen (TCC-Analytics for the monitoring of the energy efficiency), Central Facility Medical Investigation Office and Hygiene, University Medical Center Schleswig-Holstein, Kiel, project report, december 2018.

M.D. Genuardi, M. Wiegand, O. Opel, Installation of an ultrafiltration plant in a multi-family house to reduce the hot water temperature and energy demand: A case study in Germany, Journal of Building Engineering, 66 (2023), 105898.

5 Presentation of the Author

Dr. Christian Schauer received the degree in chemistry in 2004 at the Institute of Water Chemistry at the Technical University Munich. He has 18 years of experience in environmental analysis, water treatment and drinking water hygiene. His current role is the head of the center of excellence of drinking water at Viega.

TECHNICAL SESSION 6 - LOW WATER CONSUMPTION BUILDINGS I

Rainwater practices in urban areas in Košice, Slovakia

D. Káposztásová (1), D. Košičanová(2) and Z. Vranayová (3)

(1) daniela.kaposztasova@tuke.sk

(2) danica.kosicanova@tuke.sk

(3) zuzana.vranayova@tuke.sk

(1) Department of Building Services, Institute of Architectural Engineering, Faculty of Civil Engineering, Technical University of Kosice, Slovakia

(2) Department of Building Services, Institute of Architectural Engineering, Faculty of Civil Engineering, Technical University of Kosice, Slovakia

(3) Department of Building Services, Institute of Architectural Engineering, Faculty of Civil Engineering, Technical University of Kosice, Slovakia

Abstract

Massive construction of residential buildings in Slovakia was accompanied by draining of rainwater into the sewerage system. This practice has been used for many decades, but the growth of cities and the densification of construction had to change in recent years. Innovative solutions are in green infrastructure designed to protect the quality and quantity of water by reducing rainwater runoff, solutions for storing and treating rainwater before it reaches surface waters, systems for artificial retention of rainwater in city structures and their alternative solutions. The aim of the article is to present the application of rain gardens and rainwater harvesting urban areas. Based on previous practice and control of residential buildings in Košice city many them are suitable for new green solutions with added value of water saving.

Keywords

Rain garden; environment; green infrastructure, rainwater

1 Introduction

Rainwater management in urban areas can be based on the principle of retaining rainwater in the environment where it falls.

Current practice is oriented towards the fastest possible removal of rainwater from the territory of inner-city areas. Innovative solutions based on the artificial retention of rainwater in the city's structures during periods without rain allow this water to be used to improve the microclimate of the city, irrigate parks, or through recycling for other city needs. In the world, rainwater harvesting and rain gardens are parts of hybrid infrastructure (Figure 1).

Figure 1 – Example of Rain Garden and RWH system

Here are some examples of cities in Europe and United States of America (USA) that have implemented rain gardens and rainwater harvesting systems:

- Gdynia, Poland: Gdynia has implemented sustainable water management practices, including rain gardens, to manage stormwater runoff and reduce the impact of urbanization on the environment [1] [2].
- Paris, France: Asnièrs, a city close to Paris, has implemented sustainable water management practices, including rain gardens, to manage stormwater runoff and reduce the impact of urbanization on the environment [1].
- Germany: More than 1.8 million German households and companies collect rain in concrete or plastic tanks, in order to water the garden, flush the toilet or wash their cars. Cities and municipalities in Germany are increasingly relying on water from the sky, too. Many new development areas are built with a requirement of implementing rainwater tanks in gardens or adding rain collection systems under streets, parking lots, etc [3].
- District of Columbia, USA: The Riversmart Homes program offers incentives for homeowners to install rain barrels, rain gardens, and other green infrastructure practices to manage stormwater runoff [4].
- Los Angeles, USA: The city's RainWater Harvesting Program provides rebates for residents who install rain barrels, cisterns, and other rainwater harvesting systems to reduce the amount of stormwater runoff that enters the sewer system [5].
- Contra Costa County, California, USA: The Contra Costa Water District offers resources and incentives for residents to install rain gardens and rainwater harvesting systems to reduce water use and manage stormwater runoff [1].

These are just a few examples of cities in Europe and USA that have implemented rain gardens and rainwater harvesting systems.

Many other cities around the world have also implemented these practices to manage stormwater runoff and reduce the impact of urbanization on the environment.

2 Rainwater harvesting and rain gardens

Rainwater harvesting (RWH) and rain gardens (RG) are two green infrastructure practices that can be used in urban areas to manage stormwater runoff and reduce the impact of urbanization on the environment.

Rainwater harvesting faces several challenges, including ensuring water quality and safety, designing an efficient system with an optimal tank size, addressing water quality issues, selecting appropriate disinfection technologies, complying with water-related legislation, securing adequate financial support, and coordinating efforts at the national level. Despite these challenges, RWH is an effective way to conserve water in urban areas. Apartment dwellers can maximize the benefits of this method by assessing their building's potential for rainwater harvesting, collaborating with building management, designing an efficient system, and ensuring regular maintenance. By doing so, they can make a positive impact on the environment [6].

Rain gardens help to maintain the balance of the environment by creating new biocenters in urban areas, affecting the microclimate, and enhancing the aesthetics of the environment during the blooming period through the positive influence of plants [7]. Rain gardens are a simple and cost-effective solution that can be easily incorporated into landscape architecture or revitalization plans. They serve as an element of water management by safely draining rainwater, reducing runoff from your property, and helping to control pollution. Additionally, rain gardens can protect against flooding, create habitat for wildlife such as butterflies and songbirds, and conserve water [8] [9]. By filtering out pollutants in runoff and reducing stormwater runoff, rain gardens can also reduce contamination of surface water with pesticides, sediment, metals, and fertilizers. Rain gardens are very important for building system recovery in an urban circular economy [10] (Figure 2).
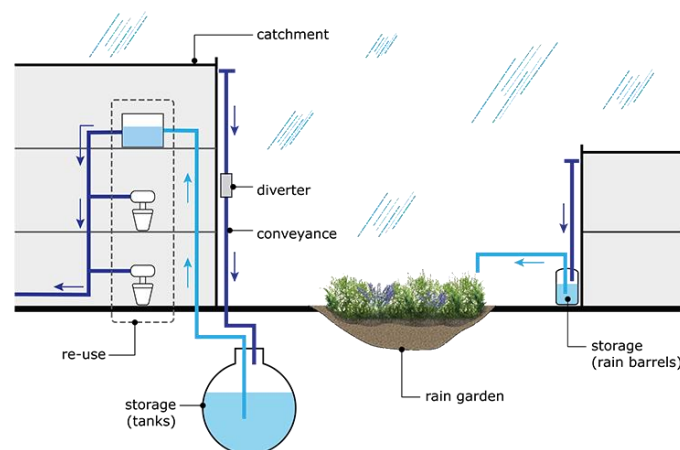

Figure 2 - Combination of Rain garden and RWH system [11]

3 Aims and methods

In Slovakia, there is not much experience in designing rain gardens, although in the world such "wetland" gardens are designed on a much larger scale. In the article we describe the design of a rain garden for a school building in Košice.

The project was based on the creation of a pond or ponds for the green toad in the area of the city of Košice, specifically in Zuzkin Park, Košice Západ – Terrace (Luník I), where the water in the body of the fountain occurs depending on atmospheric precipitation. Frogs stay in the fountain throughout the year. They use pipes and cracks in curbs as shelters. The planned reconstruction of the fountain will have a significant impact on the green toad population on the site, therefore it was necessary to create a substitute habitat for the reproduction of the green toad. The replacement biotope consists of a water area and shelters for amphibians. The space that will suit is in the nearby grassy area between the school buildings.

The design of the water area fully respects the instructions of the Regional Center for Nature Protection given for the design, which are as follows:
- water area should be at least 10 m ^{2}.
- depth 0-60 cm.
- shape and dimensions according to spatial possibilities, ideal is the so-called "kidney" shape. Location in a semi-shady place, not completely under trees.

Suggested pond parameters
- the expected volume of the lake is 11.65 m ^{3}.
- circuit with slopes - Level 1 - height 100,
- second lowered platform- Level 2, height 200 mm
- third lowered platform - Level 3, height 600

Perpendicular walls according to the detail drawing should be inclined to a 45% slope, which will make it easier to apply a 10 cm layer of sand. And at the same time there will be no slippage.
The volume of the pond up to the top edge is approx. 7m ^{3}.

3.1 Design of rain gardens

The idea of directly connecting rainwater to the ponds is unrealistic, if there is to be animal life in the pond, the pond would be washed out with its contents onto the surrounding terrain. That is why a system of technical equipment is designed in combination with rain gardens so that rainwater is used aesthetically and efficiently and disposed of safely at the same time.

The meaning of the garden is as follows: it retains rainwater where it falls on the ground, beautifies the environment around the school, reduces the load on the public sewage system by rainwater that remains on the property (Figure 3).

At the same time, this space with the pond will be an excellent educational tool in the school premises, and at the same time it will improve and build the students' relationship with nature. Soaking after rain takes place at a depth of 30 cm for about 2 days. By increasing the volume of the rain garden by 50%, we will extend the soaking by 1 day and at the same time catch the excess water. Multiple systems may have alternative solutions.
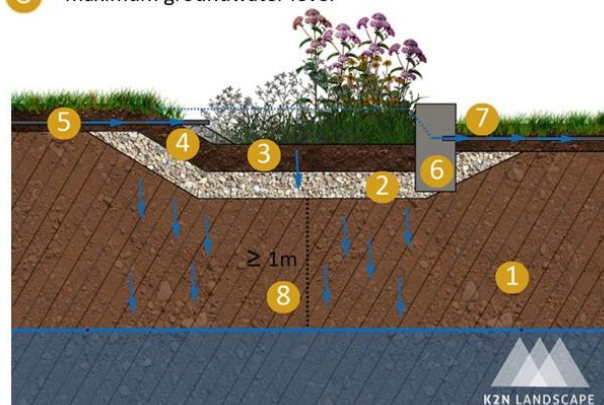
Figure 3 - Basic information about the rain garden [12]

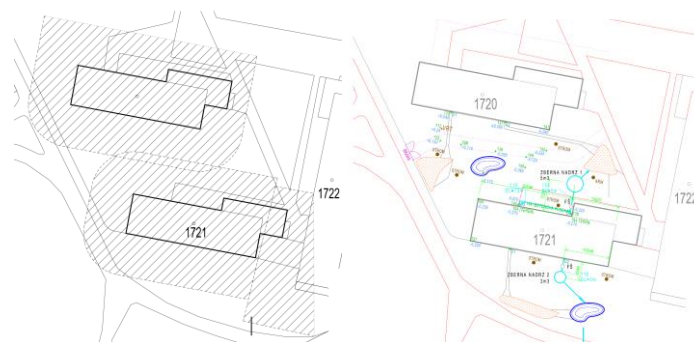**Figure 4 - Composition of building services facilities with rain gardens and ponds**

Areas for rain gardens were designated in the space between the buildings in a zone suitable for placing a rain garden. The hatched part represents a 10 m zone where the rain garden cannot be placed in order not to waterlog the buildings. 3 rain gardens with different shapes are designed for the free space (Figure 4).

The overall situation (Figure 4) shows the location of ponds, rain gardens, collection containers and sewers. Main function of rainwater disposal is rain gardens, and part of it is taken over by collection containers, with a relatively small volume. These will serve as rainwater storage for ponds in case of excessive evaporation or as watering for rain gardens in times of extremely long drought.

Rain gardens are designed so that the area of the garden can drain all the water from the roofs into the wetland. In the case of torrential water, discharge points are proposed, where the water is poured onto the surrounding land, where it soaks in. The garden will hold water for 2-3 days, depending on the depth of the excavation, then it will slowly dry out. That is why it is important to correctly design suitable plants that can withstand this water cycle. If it has been dry for a very long time, it is advisable to water the garden. Thanks to the short retention time of the water, mosquitoes do not have time to hatch in the garden, because they need a much longer time to do so.

Proposal for building no. 1720 – roof area 150 m^2: rain should be 50 m^2
Rain garden 1 – 30 m^2
Rain garden 2 – 28 m^2
Total: 58 m^2 - the area is satisfactory with a reserve.

Proposal for building no. 1721 – area approx. 300 m^2
Rain garden 3 – 27 m^2
Collection tank   5 m^3
Collecting tank   2 m^3

The collection tank will be installed in the ground with a pump, to be used for refilling the pond, or for watering the rain garden in times of drought.

The pipe between the collection tank and the waste will be PVC destined for the ground, dimension 110 or 150 according to PD. The depth of the pipe from the roof runoff trap is approx. 0,7 m, sloping towards the collection tank. Filter shafts with a collection basket will be installed on the route.

3.2 Bringing water to the rain garden

There are several options for bringing rainwater from roofs and paved surfaces into a rain garden. It is possible simply disconnect the rain gutter pipes from the storm drain and redirect the water to the rain garden through the surface sloped ditch. Alternatively, an underground PVC pipe can be installed below the surface to bring rainwater from the roof to the rain garden. To protect against strong flow of water and erosion from the pipe to the rain garden, it is advisable to cover the outlet of the pipe with geotextile and stones [14].

flowers	height	flowering time	description
Siberian iris (Iris Siberia)	60-80 cm	May ,June	long narrow leaves, varieties of different colors, also grows in a regular flower bed
Lily of the valley (Hemerocallis)	30 - 100 cm	June, July	grass-like leaves, many varieties with different colors, heights and flowering periods, edible flowers
Juncus (Juncus effusus)	60 cm	July -August	grass-like domestic perennial, small green-brown inflorescences, the 'Spiralis' variety has twisted leaves
Spiny millet (Panicum virgatum)	80-120 cm	July - September	ornamental grass with dense tufts, red in autumn, airy flower panicles, height according to the variety
Smooth flycatcher (Amelanchier laevis)	up to 4 m	April	shrub with white flower clusters, edible fruits, nice autumn coloration
Royal Osmunda (Osmunda regalia)	up to 180 cm	June - August	stout fern for partial shade, instead of flowers it forms spore leaves
Swamp forget-me-not (Myosotis palustris)	30-70 cm	April - June	blue flowering perennial, small flowers with a yellow center

Figure 7 - Examples of plants suitable for a rain garden (according to botanist M. Pizňak [13])

3.3 Depth and slopes of rain garden slopes

The size of the rain garden will affect the depth and slope of the slopes. The ideal depth of a rain garden is between 15-30 cm. At a depth of 15 cm, the rain garden will need to be quite large to have enough capacity to accumulate the collected volume of rain. On the other hand, a rain garden deeper than 30 cm may retain rainwater for too long depending on the soil substrate. In general, rain garden slopes of more than 12% are not suitable. It is recommended to install a rain garden in the lowest areas of the flat part of property.

The supply of rainwater to the rain garden is by gravity directly from the gutter pipe on the surface or under the surface. The discharge of the inflow into the garden must be secured against the torrential inflow of rainwater, so that there is no erosion of the bottom and deformation of the flora in the garden [14].

A simple calculation - an estimate - for an apartment building with a roof area of approx. 200 m^2, the payback is approx. 3 years, if we count the purchase of material (a layer of gravel, humus), flowers and self-help excavation of a shallow area of the garden.

4 Conclusion

Rain bioclimatic gardens can be integrated into already built plots and areas. A certain concern for rain gardens is their long-term protection and maintenance, especially if they are located in several residential areas where maintenance is provided by individual owners. In such situations, it is important to establish a certain management that will ensure their long-term functioning. The application of ecological approaches such as rain gardens is a crucial step to improve the negative impact of climate changes in urban areas. In Košice, there are a lot of apartment buildings that have sufficient grassy space, where the rain garden could be beautifully integrated into the environment. Improvement of the surroundings of apartment buildings is only the added value, since the primary goal is to keep rainwater where it falls, reduce the flow in the sewer and save on rainwater drainage.

Acknowledgments

5 References

[1] Trojanowska (Monika), Health-Promoting Places: Rain Gardens and Sustainable Water Management. IOP Conference Series: Materials Science and Engineering. (2020) 960. 022025. 10.1088/1757-899X/960/2/022025.

[2] Kasprzyk,(Magda) et al - *Technical solutions and benefits of introducing rain gardens – Gdańsk case study*, Science of The Total Environment, Volume 835,2022, 155487, ISSN 0048-9697, (https://doi.org/10.1016/j.scitotenv.2022.155487)

[3] Ziegler (Helmut) 2023. Raindrops falling in my reservoir - Harvesting Rain in Germany and the EU | Smart Cities Dive

[4] EPA 2023. https://www.epa.gov/green-infrastructure/what-green-infrastructure

[5] Water Capture, Diversion, and Recycling 2023. https://greenportal.wca.ca.gov/strategies/water-capture

[6] RMS. Rainwater Harvesting at an Apartment Complex in Blacksburg Virginia. https://rainwatermanagement.com/blogs/news/rainwater-harvesting-at-apartment-complex-in-blacksburg-virginia. (last accessed on 2023/12/05)

[7] Environmental Protection Agency US 2020. https://www.epa.gov/soakuptherain/soak-rain-rain-gardens

[8] Online.https://groundwater.org/rain-gardens/

[9] Online. https://www.tenthacrefarm.com/build-rain-garden/

[10]   Energy.gov. Online:https://www.energy.gov/femp/water-efficient-technology-opportunity-rainwater-harvesting-systems (accessed 22/2/20203)

[11]   https://byjus.com/biology/rainwater-harvesting/ (accessed 22/3/20203)

[12]   K2N LANDSCAPE: http://k2n-landscape.com/en/home-2/ (accessed 27/05/2023)

[13]   Pizňak (Martin). ZahradART: https://zahradart.sk/projekt-z%C3%A1hrady

[14]   Kravčík (Michal)2010: https://blog.sme.sk/kravcik/nezaradene/dazdove-zahrady-pre-zdravu-klimu-miest-iii (accessed 27/05/2023)

5 Presentation of Author(s)

Zuzana Vranayova has been involved in scientific research and teaching activities at the TUKE for a long time. Her professional interest is oriented toward the sustainable and safe water supply in buildings. She belongs to significant scientific experts in the field of green buildings and their water management and actively participates in international conferences.

Daniela Kaposztasova has been involved in scientific research and teaching activities at the TUKE for more than 10 years. Her professional interest is oriented toward the sustainable and safe water supply in buildings.
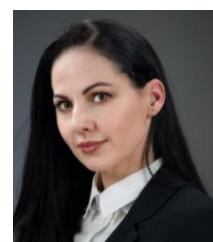
Danica Košičanová is assoc. prof. at TUKE and she is working in the field of heating systems.

Research of water saving design and near zero water consumption feasibility for office buildings

Wei-Che Chang (1), Cheng-Li Cheng (2), Kawamura Sadahico(3)

(1) peko7799@gmail.com
(2) CCL@mail.ntust.edu.tw
(3) sadahico@gmail.com
(1) (2) (3)National Taiwan University of Science and Technology, Department of Architecture, Taiwan, R.O.C.

Abstract

The world is moving towards zero energy and zero or near-zero water consumption in buildings to achieve sustainable development goals and net-zero emissions by 2050 in Taiwan. A self-contained water cycle within the building system is the ultimate goal. This study focused on office buildings, which have simple water usage characteristics and can be used as a reference for other types of buildings. A water estimation model was established through literature review and data collection from existing green office building cases in Taiwan. The median water usage per unit floor area per year was calculated, and the current water-saving design status and water-saving rate were explored. It was found that the median water-saving rate was 53%, far from the goal of near-zero water consumption building, mainly due to infrequent use of compensatory water usage in designs. Recent green office buildings have reduced basic equipment water usage by using water-saving equipment in their designs. Based on current water-saving equipment development, the remaining equipment water usage and additional water usage can be compensated for by increasing water reuse. Looking at it from the perspective of future inclusion of a regenerated drinking water filtration system and a shared water treatment plant for buildings in the same area, additional water usage can be reduced or

compensatory water usage can be increased by increasing rainwater harvesting area, using non-water-cooled central air conditioning or water-saving air conditioning, reducing water-consuming lawns, or using smart irrigation, thereby achieving the goal of zero water consumption building.

Keywords

Green building；Office building；Sustainable buildings；Near zero water building；Water resource

1 Introduction

Based on the global issue of environmental resource shortage, the United Nations Sustainable Development Summit adopted the 2030 Sustainable Development Agenda in September 2015, which includes 17 Sustainable Development Goals (SDGs). The establishment of these global sustainable development goals aims to enable humanity to survive on Earth in the long run. In 2021, the International Energy Agency (IEA), a globally influential energy policy organization, released a prediction report titled "Net Zero by 2050: A Roadmap for the Global Energy Sector," hoping to assist countries in formulating related energy policies. In response to the global net zero trend, Taiwan officially announced the "Taiwan's 2050 Net Zero Emissions Pathway and Strategy Summary" in March 2022, referring to the direction of net zero development in the United States, European Union, Japan, and other countries. This plan provides a trajectory and action path towards net zero emissions by 2050, as well as development goals for each time period and promotion strategies for different fields, aiming to promote technology, research, and innovation in various fields to build a sustainable home.

As an important part of Earth's resources, water resources are also closely related to global sustainable development. Although Taiwan's rainfall is about 2.5 times the world average, the uneven distribution in space and time results in each person having access to only 20% of the world's average rainfall. In recent years, the problem of water shortage in Taiwan has become increasingly prominent and severe. If the dry season continues to lengthen and the frequency of typhoons decreases, the amount of rainfall that each person can access will be further reduced. The ultimate goal in building design should be to achieve a self-contained water cycle within the building system, balancing water

2023 Symposium CIB W062 – Leuven, Belgium

consumption and regeneration, and becoming a near-zero water consumption building (nZWB). This study aims to summarize the water-saving assessment of green buildings in Taiwan's office buildings and feasible strategies for near-zero water consumption planning in green buildings.

2 Research basis and literature review

2.1 Classification of water use and water-saving in office buildings

This study classifies water use and water-saving in office buildings into three categories based on current office building design: equipment water use, additional water use, and compensatory water use, as shown in Table 1 below. Subsequently, the evaluation formulas and calculations for water use and water-saving in office buildings will be established and conducted based on this classification.

Table 1-Classification of water use and water-saving in office buildings

Office buildings					
equipment water usage		additional water usage		water-saving	
a.	toilet	a.	irrigate	a.	rainwater recycle
b.	urinal	b.	pool	b.	graywater recycle
c.	faucet	c.	cooling tower	c.	condensed water
d.	water dispenser			d.	reverse osmosis water

2.2 Annual water consumption intensity per unit area of the building (WUI)

In terms of existing literature research and practical application, because the scale of a building is related to the number of people, most of the estimation of building water consumption is based on the floor area of the building to convert the number of users, and then design and calculate water use equipment based on the number of people. This study aims to unify, the annual water consumption intensity per unit area of the building ($m^3/m^2 \cdot year$) will be used as the unit benchmark for water use. According to calculations based on "Research on Water Standards and Water Saving Potentials of Green Buildings" (Chen, S. J., 2016), the annual water consumption intensity per unit area of the building of standardized office buildings is 2.63 ($m^3/m^2 \cdot year$).

2.3 Green Building Evaluation Manual – Water Resource Indicator

" Water Resource Indicator " is one of the two threshold indicators of the Green Building Evaluation Manual. The evaluation items of the water resource index include toilets, urinals, water cocks for public use, bathtubs or shower facilities, rainwater facilities or water-saving irrigation systems, air conditioning water conditioning and smart water meters and other projects. In recent years, it has been difficult to obtain actual water consumption due to the personal information law. This study will use the case of office buildings that have obtained the green building label as the research object to estimate and review the water consumption of buildings.

2.4 Monte Carlo simulation method

The basic principle of the Monte Carlo method is to repeatedly obtain random numbers to simulate the results. In operation, the probability of all possible results is defined as a probability density function, and the probability density function is accumulated into a cumulative probability function, and its value is adjusted. The maximum value is 1, and the numerical simulation of normal standardized distribution is established. The normalized normal distribution reproduces in the simulation a probability characteristic that reflects the sum of all events occurring with a probability of 1, and establishes a link with the actual problem simulation with random number sampling.

3 Methodology

This study uses the calculation methods of existing literature and regulations and the reasonable frequency of water use in office buildings to establish an estimation method for water consumption and water saving for office building equipment and additional water use, as well as a calculation method for making up water, so as to explore green buildings. Case water consumption and water saving benefits. Using formula 1, calculate the total annual water consumption per unit area of each office green building case design, so as to facilitate the follow-up discussion on the design water distribution of the current office green building, and use the calculated data into formula 5 to calculate the building design water saving rate.

$$W_{total} = WE_{use} + WA_{use} - WS_{use} \tag{1}$$

$$WE_{use} = W_t + W_u + W_f + W_d \tag{2}$$

$$WA_{use} = W_i + W_p + W_c \tag{3}$$

$$WS_{use} = WS_r + WS_g + WS_c + WS_o \tag{4}$$

W_{total}: Total annual water consumption intensity per unit area of the building (m³/m²·year)

WE_{use}: Annual water consumption intensity per unit area of the building -Equipment (m³/m²·year)

WA_{use}: Annual water consumption intensity per unit area of the building -Additional (m³/m²·year)

WS_{use}: Annual water consumption intensity per unit area of the building- Water-saving (m³/m²·year)

W_t: Annual water consumption intensity per unit area of Toilet use (m³/m²·year)

W_u: Annual water consumption intensity per unit area of Urinal use (m³/m²·year)

W_f: Annual water consumption intensity per unit area of Faucet use (m³/m²·year)

W_d: Annual water consumption intensity per unit area of Water dispenser use (m³/m²·year)

W_i: Annual water consumption intensity per unit area of Irrigate use (m³/m²·year)

W_p: Annual water consumption intensity per unit area of Pool use (m³/m²·year)

W_c: Annual water consumption intensity per unit area of Cooling tower use (m³/m²·year)

WS_r: Annual water consumption intensity per unit area of Rainwater recycle save (m³/m²·year)

WS_g: Annual water consumption intensity per unit area of Graywater recycle save (m³/m²·year)

WS_c: Annual water consumption intensity per unit area of Condensed water save (m³/m²·year)

WS_o: Annual water consumption intensity per unit area of Reverse osmosis water save (m³/m²·year)

The total water-saving rate calculated by formula 5 includes the amount of water used for equipment, additional water, and supplementary water. Compared with the previous discussion of the water-saving rate for equipment alone, the water-saving design of the building can be discussed in depth, because although it is an office building, it may be due to Some factors, such as the owner and the environment, must set up additional water consumption. The maximum water consumption of each case will be different due to reasons such as the site area and design strategy. The utilization rate of making up for water will also affect the total water consumption of the building. Incorporating it into the calculation of the water-saving rate can more accurately understand the distribution of the total water-saving rate of office green buildings, so as to explore whether there is room for a near-zero water consumption building.

$$S_{rc} = \left(1 - \frac{W_{total}}{WE_{max} + WA_{max}}\right) \times 100\% \tag{5}$$

S_{rc}: Total water saving rate

WE_{max}: Maximum annual water consumption intensity per unit area of the building -Equipment (m³/m²·year)

WA_{max}: Maximum annual water consumption intensity per unit area of the building -Additional (m³/m²·year)

4 Cases evaluation and analysis

In this study, a total of 73 cases of office buildings that have obtained green building labels were randomly selected. Firstly, the water consumption of equipment, additional water consumption and supplementary water consumption of the cases were calculated separately, and 10,000 data were simulated by Monte Carlo simulation method to explore the ratio of water use, and then use the data to calculate the water-saving rate, and analyze the current design of the water-saving rate distribution of office green buildings.

4.1 Distribution of water consumption

4.1.1 Distribution of basic equipment's water consumption

The basic equipment is the daily necessary water equipment, including toilets, urinals, water cocks, drinking fountains, etc. According to Figure 1 below, the designed maximum and minimum building unit area per capita annual water consumption of basic equipment WUI is between 0.72 (m^3/ m^2·year) to 1.79 (m^3/m^2·year), while the median of actual water consumption is 0.86 (m^3/ m^2·year), and the median of simulated water consumption is 0.88 (m^3/ m^2·year). The digits are very close, and they are biased towards the design minimum water consumption. It can be seen that the adoption rate of water-saving equipment in office green buildings is very high. In many cases, as long as a little effort is made, the water consumption of the equipment can be very close to the design minimum. On the contrary, if the water consumption of the equipment designed by the future architect is greater than the median Although water-saving equipment is used, it can be seen that it is relatively insufficient, and its design should be re-examined.
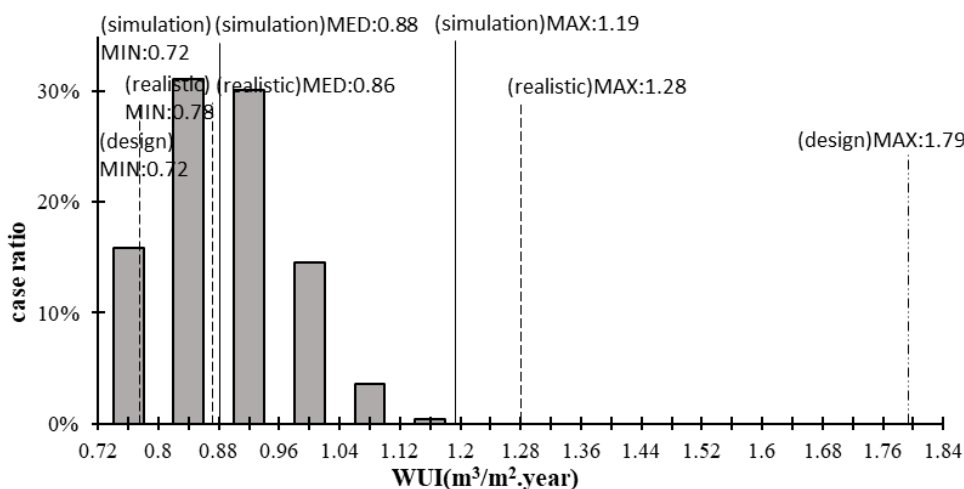
Figure 1- Distribution of basic equipment's water consumption

4.1.2 Distribution of additional water consumption

The additional water consumption is roughly designed for non-essential water use, and its factor is more complicated than that of equipment water use, which is roughly related to the selection of irrigation, landscape pools, and cooling water towers. Following Figure 3, as the boundary basis, when the design is greater than 0.5 (m^3/m^2·year), a water-saving irrigation system or a water-saving cooling tower should be used in the design. According to the investigation of existing literature, when the cooling water tower adopts humidity control, The average water saving can reach 62.6%, and the use of smart water-saving irrigation system can save about 50% of irrigation water and reduce the total additional water consumption. However, based on the goal of becoming a near-zero water-consumption building, additional water-consuming designs should be eliminated as fundamentally as possible, such as reducing the design area of water-consuming turf, canceling the setting of pools, or replacing them with air-cooled and inverter-type air conditioners for water-cooled air conditioners, etc., the water consumption is designed to be 0, so as to achieve the goal of nearly zero water consumption.
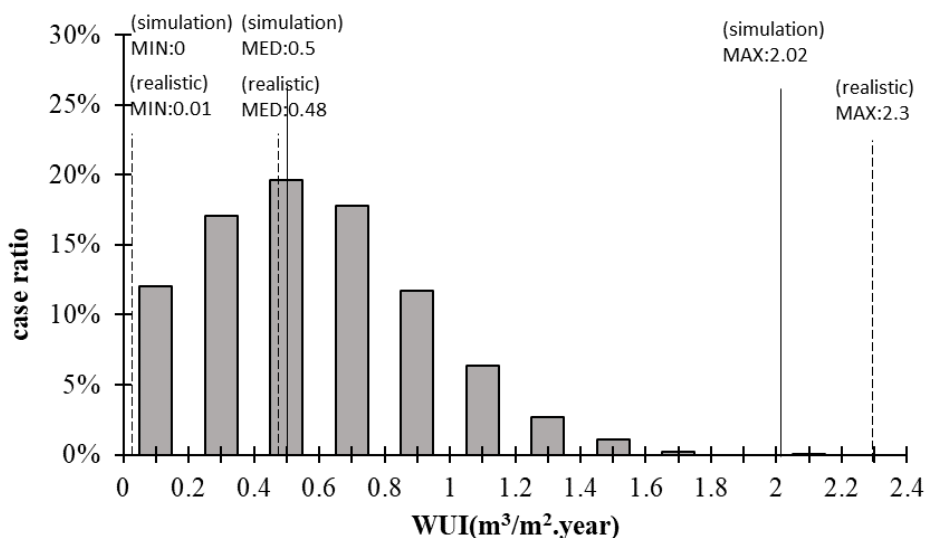
Figure 2- Distribution of additional water consumption

4.1.3 Distribution of water-saving

Among the 73 office-type green building cases collected in this study, a total of 58 cases have the design to use make-up water, because there will be a gap between the original design use of make-up water and the estimated actual make-up water, and not necessarily use all available water in the design To make up the amount of water, this study calculates the three items of water to be made up respectively, and draws the following Figure 3.

From this figure, it can be seen that there is still a lot of room for making up for the use of water in most cases. Judging from the average water consumption, the average available make-up water is 1.32 (m³/ m²·year), the original design make-up water is 0.32 (m³/ m²·year), and the estimated actual make-up water is 0.28 (m³/ m²·year), the amount of available make-up water is about 5 times of the actual amount of make-up water, and the amount of rainwater recovery that can be used to make up water is calculated based on the rainwater collection on the roof. should increase by about 3 times.
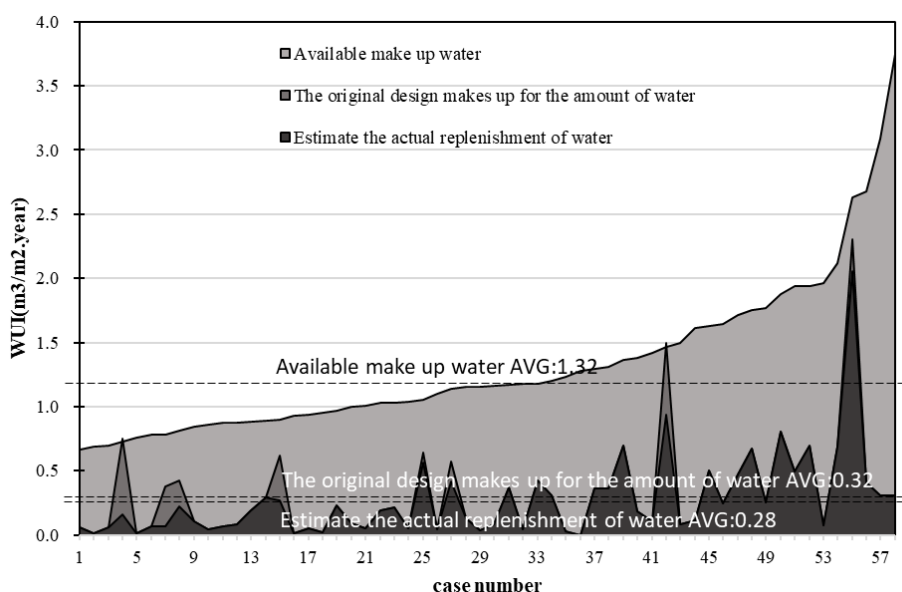
Figure 3- Distribution of water-saving

4.2 Water saving status

This study first calculates the equipment water consumption, additional water consumption and supplementary water consumption of the case, respectively discusses the proportion of the water used, and then uses the data to calculate the water saving rate, and analyzes the current situation of the water saving rate distribution design of office green buildings. As shown in the distribution of water saving rate in Figure 4 below, the water saving rate ranges from 26% to 76%, the median is 53%, and the average is 52%. After Monte Carlo simulation of 10,000 pieces of data, the water saving rate range falls between 18% and 88%, and the median is 52%. This shows that the promotion of water saving in green buildings has achieved certain results in recent years. In most cases, about half of the water consumption can be saved, but the ultimate goal of water saving is "nearly zero consumption." There is still a considerable gap between 90% and 100% of the water saving rate of water buildings.
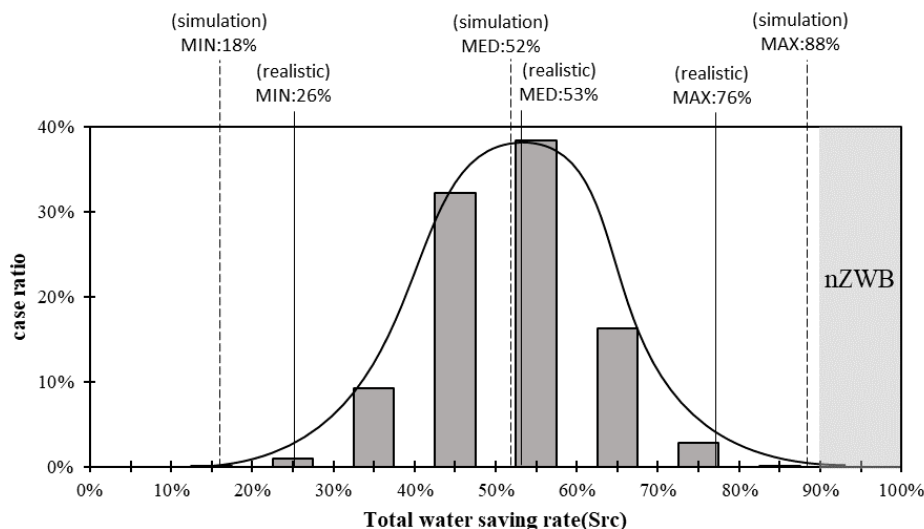
Figure 4- Distribution map of water saving rate

4.3 Feasibility review of near-zero water consumption

In the design without additional water usage, using only the basic equipment water, such as toilets, urinals, faucets, and water dispensers, the water consumption is approximately 0.72 ($m^3/m^2 \cdot$year). However, due to the restrictions imposed by Taiwanese regulations, recycled and reclaimed water cannot be used as a substitute for water in contact with human bodies. This study defines the criteria based on whether "recycled and reclaimed water can be used as a substitute (compensatory water)" and organizes the data in Table 1. It can be observed that within the minimum equipment water consumption, 0.24 ($m^3/m^2 \cdot$year) can be replaced with recycled and reclaimed water. According to the median value of 1.23 ($m^3/m^2 \cdot$year) for available make-up water, it is possible to fully compensate for the water usage and even have a significant surplus of compensatory water for other purposes. However, the remaining 0.48 ($m^3/m^2 \cdot$year) cannot be replaced under the current regulatory restrictions.

Table 2- Minimum equipment water consumption comparison table

Equipment items	Minimum water consumption ($m^3/m^2 \cdot$year)	Whether recycled water can be used as a substitute for compensatory water	
		can	can not
Toilet	0.24	V	
Urinal	0	V	
Faucet	0.45		V
water dispenser	0.03		V

5 Conclusion

According to the existing literature related to office building water use, the annual water consumption benchmark value of the unit floor area of office buildings is 2.63 ($m^3/m^2 \cdot$year) based on per capita building area density, per capita annual water consumption benchmark, and building facility utilization rate. In this study, the water consumption of office buildings is calculated using the established water estimation method for office buildings to calculate the water consumption of each water use item in the case of office green buildings. It is known that in recent years, office green buildings have been designed to use water-saving equipment, and the median water consumption of basic equipment is 0.88 ($m^3/m^2 \cdot$year), when all additional water consumption items are designed and used, the median value of additional water consumption is 0.8($m^3/m^2 \cdot$year), which shows that a lot of water is saved compared with the baseline value. In addition, according to the in-depth discussion of this study, based on the development of existing water-saving equipment, under the condition of rational water use in office buildings, the water consumption of basic equipment should be reduced to 0.72 ($m^3/m^2 \cdot$year) through water-saving equipment, which cannot be used due to the current regulations in Taiwan When reclaimed water makes up for the water in contact with the human body, except for the 0.48 ($m^3/m^2 \cdot$year) water used by office buildings that cannot be made up for the water used by the human body, the rest of the water used by equipment and additional water can be made up by increasing the reusable water make-up rate. Become a nearly zero water consumption building.

From the point of view that the recycled drinking water filtration system may be included in the future, buildings in the same area share a water purification plant, and only design the building that uses equipment water or equipment water plus the median additional water used by current office buildings Water, in view of the available make-up water in the current design, is enough to make up it. If the water consumption of office buildings is taken as the median of the water consumption of equipment plus the additional water used by office buildings, it is necessary to increase the rainwater collection area, use non-water-cooled central air conditioners or water-saving air conditioners, and reduce water consumption. Design or use smart watering and other methods to reduce additional water consumption or increase available water to make up water, so as to achieve the goal of zero water consumption buildings.

6 References

Lin, X. D,& Lin, T. P,& Tsai, Y. H. -Green Building Evaluation Manual -Basic Version. Report of Architecture and Building Research Institute, Ministry of the Interior. New Taipei City: Architecture and Building Research Institute, Ministry of the Interior,2019.

Regulations for Management of Water Efficiency Label- Annex I：product item and specification standard of the Water Efficiency Labeling, Taipei: Ministry of Economic Affairs,2020.

Cheng, C. L. -Research on Water Resource Efficiency and Water Saving Evaluation of Green Buildings. Report of Architecture and Building Research Institute, Ministry of the Interior. New Taipei City: Architecture and Building Research Institute, Ministry of the Interior,2022.

Chen, S. J.- Green Building Water Benchmark and Efficiency Study. Unpublished master's thesis. Department of Architecture, National Taiwan University of Science and Technology, Taipei,2016.

7 Presentation of Authors

Chang, Wei-Che is the Master at National Taiwan University of Science and Technology, Department of Architecture. His research is focus on water resource and green building.

Cheng, Cheng-Li is the Professor at National Taiwan University of Science and Technology, Department of Architecture. He is a research scholar for water supply and drainage in building. He has published extensively on a range of sustainable issues, including the water and energy conservation for green building.

Sadahico Kawamura is the Ph.D student at National Taiwan University of Science and Technology, Department of Architecture. His research is focus on energy conservation for green building.

Study on water balance and environmental performance evaluation in buildings

(Part3)Water Balance and CO_2 Emissions by Precipitation Characteristics of Rainwater Utilization Buildings

J. Oyagi (1), T. Nshikawa (2)

(1) dm22020@g.kogakuin.jp

(2) t-nskw@cc.kogakuin.ac.jp

(1) Graduate student , Kogakuin University, Japan

(2) Prof., School of Architecture, Kogakuin Univ., Dr.Eng., Japan

Abstract

In a previous study[1], the relationship between building water balance and environmental impacts was evaluated quantitatively by calculating the zero-water achievement rate and CO_2 emissions for a building in Tokyo that uses reclaimed water and adding rainwater use conditions. As regards rainwater use in buildings, precipitation characteristics affect the water supply replacement rate and rainwater runoff control. Therefore, rainwater storage equipment must be optimized according to such precipitation characteristics. In this study, we modeled rainwater utilization equipment in a building, calculated the zero-water building (ZWB) achievement rate and CO_2 emissions related to water supply and wastewater treatment. The capacity of the rainwater storage tank was used as a parameter, and the optimal rainwater storage tank capacity was determined according to the rainfall characteristics. In months with high rainfall, the ZWB achievement rate increased after 100 m^3 of rainwater storage tank capacity; however, in months with low rainfall, the ZWB achievement rate tended to reach a maximum at a capacity of 100 m^3. In addition, in all rainfall characteristics, CO_2 emissions related to water supply and wastewater treatment showed a decreasing trend as the number of rainwater utilization tanks increased, with the decreasing trend slowing down for rainwater storage tanks with a capacity of 100 m^3 or more. Based on these results, considering the maintenance and operational aspects of the rainwater storage tank, a rainwater volume of about 100 m^3 is considered appropriate for the building C (the investigated building).

Keywords

Net zero water, Rainwater utilization, Precipitation characteristic, Water balance, ZWB achievement rate, CO_2 emission,

1 Introduction

In a previous study[1] , the zero-water building (ZWB) achievement rate and CO_2 emissions related to water supply and wastewater treatment were calculated for a university building that uses reclaimed water through a wide-area circulation system, with a case study of rainwater use added. The relationship between the ZWB achievement rate and CO_2 emissions related to water supply and wastewater treatment differs between reclaimed water use and rainwater use. From the perspective of environmental impact, the aim should be for optimal water use depending on the area where the building is located. In this study, we modeled the rainwater storage equipment of a previous study[2] for Evaluation Building C (rainwater harresting building), inputting the rainfall data and CO_2 intensity of the water supply and sewerage facilities in the four regions into the model. Subsequently, we calculated the water balance and CO_2 emissions related to the water supply and wastewater treatment for the capacity of each rainwater storage tank, and we considered the optimization of the rainwater storage tank capacity.

2 Overview of evaluation

2.1 Overview of evaluation building

Evaluation Building C, which was completed in 2013, is a 20-story, 1-basement office complex, with a total floor area of approximately 36,000 m^2. The building comprises retail stores and a hall on the lower floors (B1-8) and offices and restaurants on the upper floors (9-20). The size of the building area is approximately 3,000 m^2 and that of the site area approximately 6,100 m^2, with the land-use classification comprising buildings, paved surfaces, and plantings[*1)]. Rainwater collected from the roof surface is used for miscellaneous purposes, and rainwater storage plays the role of replacing tap water and suppressing rainwater runoff.

2.2 Calculation boundaries for the water balance

Figure 1 shows the water balance in Evaluation Building C. Part of the rainfall on the premises is collected from the roof surface and stored in a rainwater storage tank. Uncollected rainwater flows down the site and is discharged through sewage pipes, with the remaining rainwater returned to the ground and atmosphere through infiltration and evapotranspiration. A pressurized water supply system[*2)], is used in the building and the amount of water supplied is measured in accordance with the

hourly water demand. Tap water is drawn into a water tank (effective capacity 100 m³) and supplied to each floor and the cooling tower using a water-supply pump. In addition, part of the tap water is supplied to the miscellaneous water tank (effective capacity 70 m³), and the collected rainwater is used as a miscellaneous water source. The rainwater storage tank, that temporarily stores the collected rainwater has an effective capacity of 300 m³ and is preferentially replenished from the miscellaneous water tank. When precipitation exceeds the effective capacity of the rainwater storage tank, the excess water is discharged into the public sewage system via a seepage water tank (rainwater runoff control tank). The site boundary was set as the boundary for calculating the water balance, and the rainwater utilization model for Evaluation Building C was used to calculate the water balance according to the precipitation
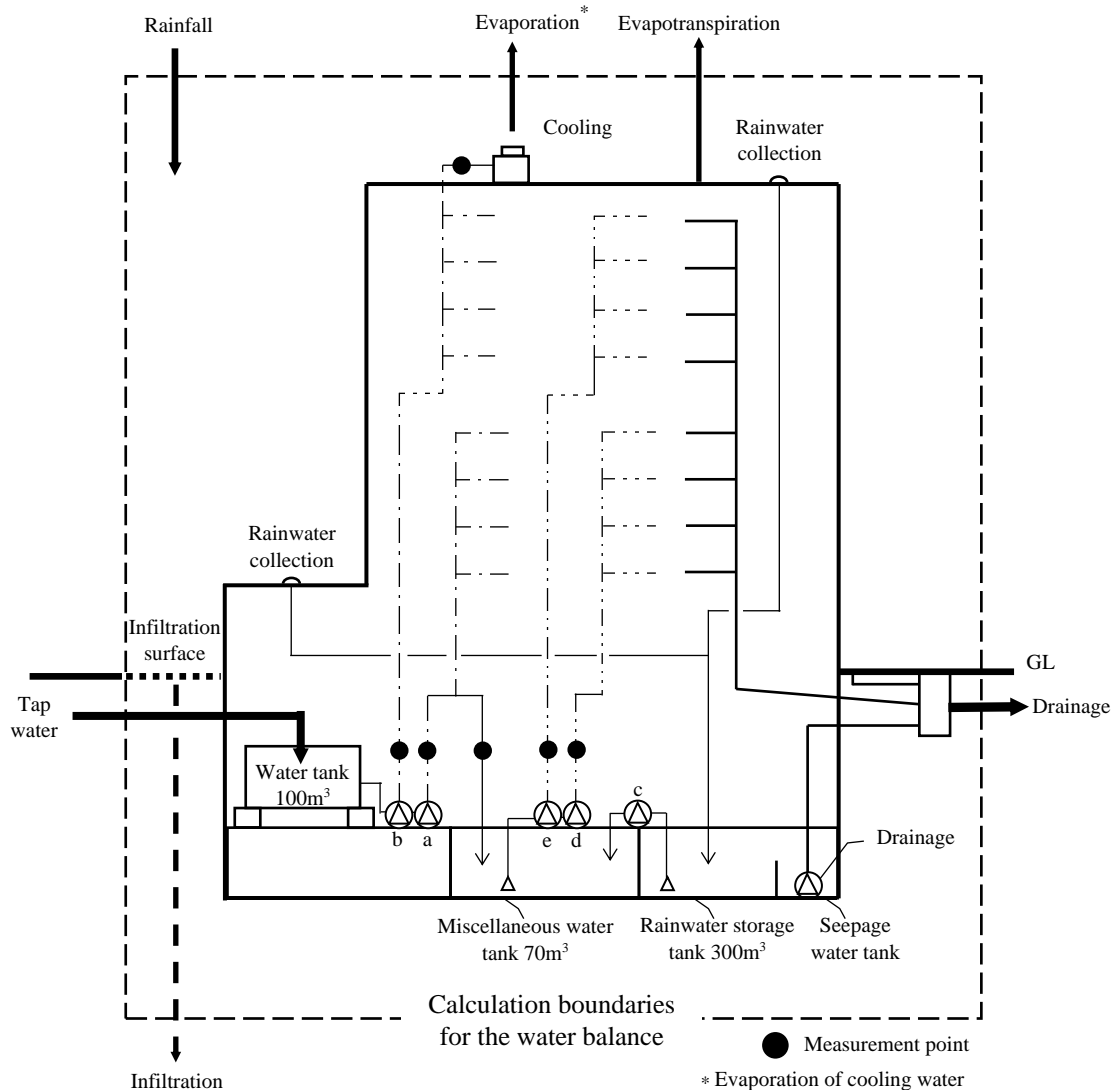
Pump Usage
    a ： Water supply for low-rise drinking water, replenishment to miscellaneous water tank
    b ： High-rise drinking water supply, cooling water supply
    c ： Rainwater filtration and rainwater replenishment to miscellaneous water tank
    d ： Water supply for low-rise miscellaneous water
    e ： Water supply for high-rise miscellaneous water

Figure 1   Water balance in evaluation building C

data[*3)]. Figure 2 shows a model of the rainwater utilization equipment[*4)]. The initial conditions for the rainwater utilization facilities were as follows: the water holding capacity of the miscellaneous water tank was 70 m^3 and the storage capacity of the rainwater storage tank was 0 m^3.

Evaluation model for rainwater utilization equipment

Miscellaneous water use
$WU_m(t)$

Rainwater collection
$RC(t)$

Replenishment water from rainwater storage tank
$RW_r(t)$

（To the public sewer）

Drainage

Drainage

Replenishment water from receiving tank
$RW_d(t)$

Overflow

$V_{m\,start}$ (40m^3)

$V_{r\,cw}$ (50m^3)

Miscellaneous water tank (70m^3) $V_m(t)$

Rainwater storage tank (300m^3) $V_r(t)$

Seepage water tank （Buffer tank）

Overview of water level control for miscellaneous water tanks [*3)]

1   Low water level in miscellaneous water tank due to use of miscellaneous water
2   When the water volume $V_m(t) < V_{m\,start}$(40m^3) in the miscellaneous water tank, Replenish water ($RW(t)$) at the effective capacity $V_{m\,max}$ (70m^3) of the miscellaneous water tank
3-1 When the rainwater storage tank capacity $V_r(t) > V_{r\,cw}$(50m^3), rainwater in the rainwater storage tank is replenished to the miscellaneous water tank ($RW(t) = RW_r(t)$)
3-2 When the capacity of the rainwater storage tank $V_r(t) < V_{r\,cw}$(50m^3), tap water in the water tank is replenished to the miscellaneous water tank($RW(t) =RW_d(t)$)
4   Replenishment ends when the water volume $V_m(t)$ in the miscellaneous water tank reaches $V_{m\,max}$ (70m^3)

**Figure 2   Evaluation model and control conditions
for rainwater utilization equipment**

2.3 Evaluation area of CO_2 emissions related to water supply and wastewater treatment

Figure 3 shows the evaluation area for CO_2 emissions related to the water supply and wastewater treatment. After the water supply facility obtains raw water from the water intake river, the water is treated and distributed to Evaluation Building C. Sewage from the building is discharged to the sewerage system through the same sewage pipe as that for rainwater flowing down the site. After sewage treatment, the water is discharged to the discharge river. Sludge generated during sewage treatment is incinerated at sewerage facilities, and the generated incinerated ash is transported to a final disposal site. We calculated CO_2 emissions from the series of tap water supplies

for the operation of the water supply pumps of Evaluation Building C and the sewage treatment [*5~9)].
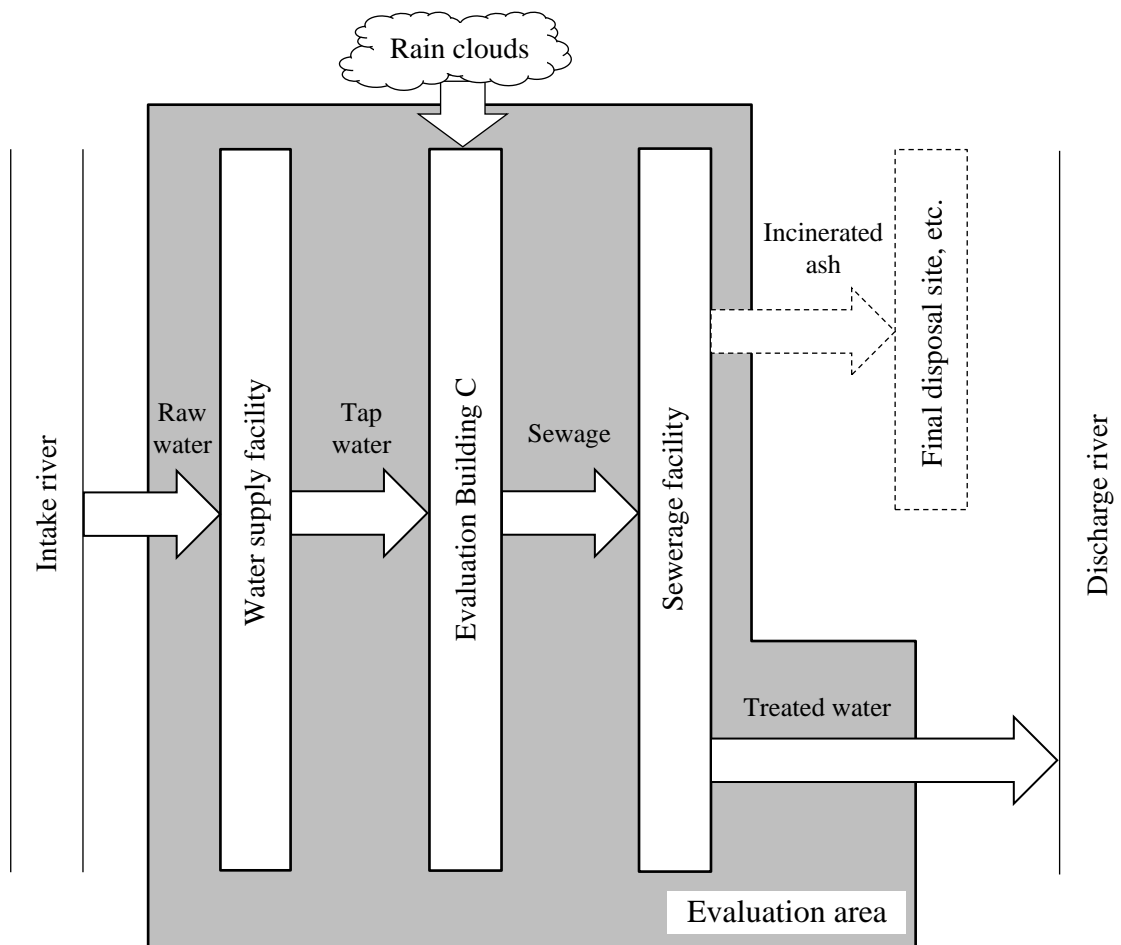
Figure 3   Evaluation area of CO$_2$ emission related to water supply and wastewater treatment

2.4 Overview of precipitation data used for evaluation

Using precipitation data and CO$_2$ emissions intensity of water supply and sewerage facilities in Tokyo, Matsuyama, Fukuoka, and Naha cities, which are regions in Japan with high drought frequency[3], we calculated the water balance and CO$_2$ emissions related to water supply and wastewater treatment. By using precipitation data for precipitation characteristics in areas with high drought frequency, we attempted to consider the optimal rainwater storage tank capacity, taking into account the seasonal maldistribution of precipitation.Figure 4 shows the hourly precipitation data for fiscal year (FY)2014 for each study region. In FY2014, precipitation exceeding the climatological standard normal occurred in these regions, namely 1,761 mm/yr in Tokyo City, 1,489 mm/yr in Matsuyama City, 1,743 mm/yr in Fukuoka City, and 2,271 mm/yr in Naha City [4]. The maximum rainfall intensity was 55 mm/h in Tokyo City, 23 mm/h in Matsuyama City, 30 mm/h in Fukuoka City, and 77 mm/h in Naha City. Tokyo and Naha Cities experienced heavy rainfall with intensities of 50 mm/h or even higher.
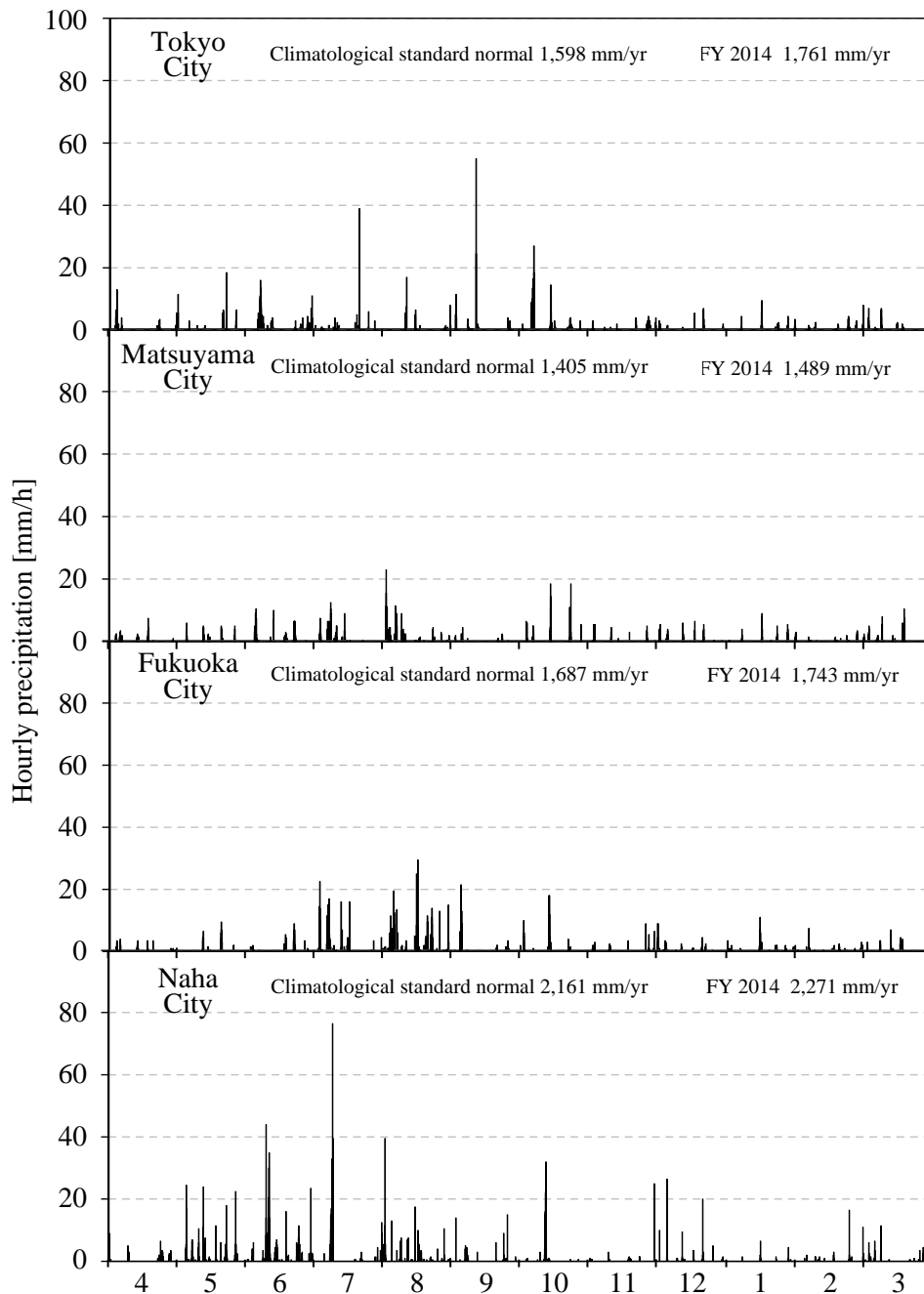
Figure 4   Hourly precipitation data for the evaluation region

3. Effects of precipitation characteristics on water balance and CO₂ emissions related to water supply and wastewater treatment

Figure 5 shows the breakdown of precipitation and CO_2 emissions related to water supply and wastewater treatment in FY2014, calculated for a rainwater utilization epuipment model (Figure 2: Evaluation Building C) with a rainwater storage tank capacity of 300 m³. Rainwater use was 3,500 m³/yr in Tokyo City, 3,400 m³/yr in Matsuyama City, 3,600 m³/yr in Fukuoka City, and 4,000 m³/yr in Naha City. More annual precipitation means more rainwater use, and in terms of overflow, Tokyo City

has more annual overflow even though it has less annual precipitation than Fukuoka City. The volume of CO_2 emissions related to the water supply and wastewater treatment was not dependent on the amount of rainfall. Although the amount of rainfall in Tokyo City was less than that in Naha City, the annual volume of CO_2 emissions related to the water supply and wastewater treatment was higher than that in Naha City. The average annual CO_2 emissions related to water supply and wastewater treatment across the four regions, indicated that 31% derived from building pumps, 31% from water supply facilities, and 38% from sewerage facilities, i.e., sewerage facilities accounted for the largest portion of emissions.
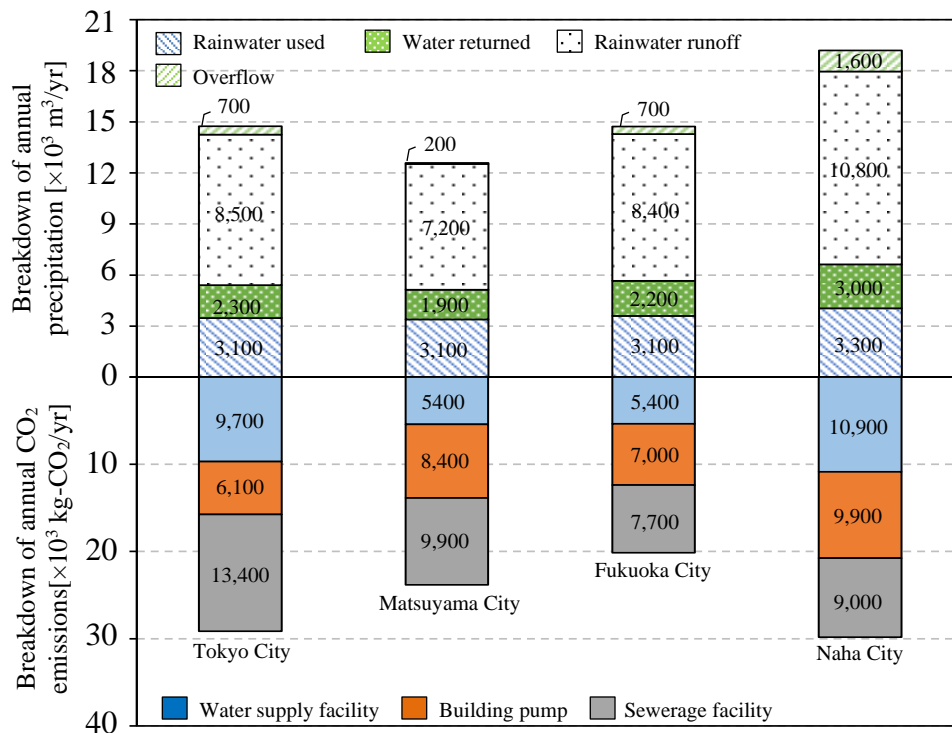
Figure 5   Breakdown of annual precipitation and annual CO_2 emissions during the operation phase of water supply and sewage systems

4. Analysis of optimization of rainwater storage tank capacity

4.1 Relationship between rainwater storage tank capacity and ZWB achievement rate

Figure 6 shows the monthly and annual ZWB achievement rates[*10)] for each rainwater storage capacity in each region. In Tokyo City, the annual ZWB achievement rate was 9% when the rainwater storage tank capacity was 50 m^3, 13% for 100 m^3, 14% for 150 m^3, 15% for 200 m^3, and 16% for 300 m^3. The largest increase in annual ZWB achievement rate was achieved in Tokyo City, with an increase in rainwater storage tank capacity from 50 m^3 to 100 m^3. In months with high precipitation, such as June and October in Tokyo City, the ZWB achievement rate increased along with an increase in rainwater storage tank capacity after 100 m^3. However, in months with low precipitation, such as December and January, the ZWB achievement rate was the

highest when the rainwater storage tank capacity was 100 m^3. A similar trend was observed in other areas, and the required capacity of rainwater storage tanks varied depending on the intensity of rainfall and the amount of rainfall used to estimate rainwater.
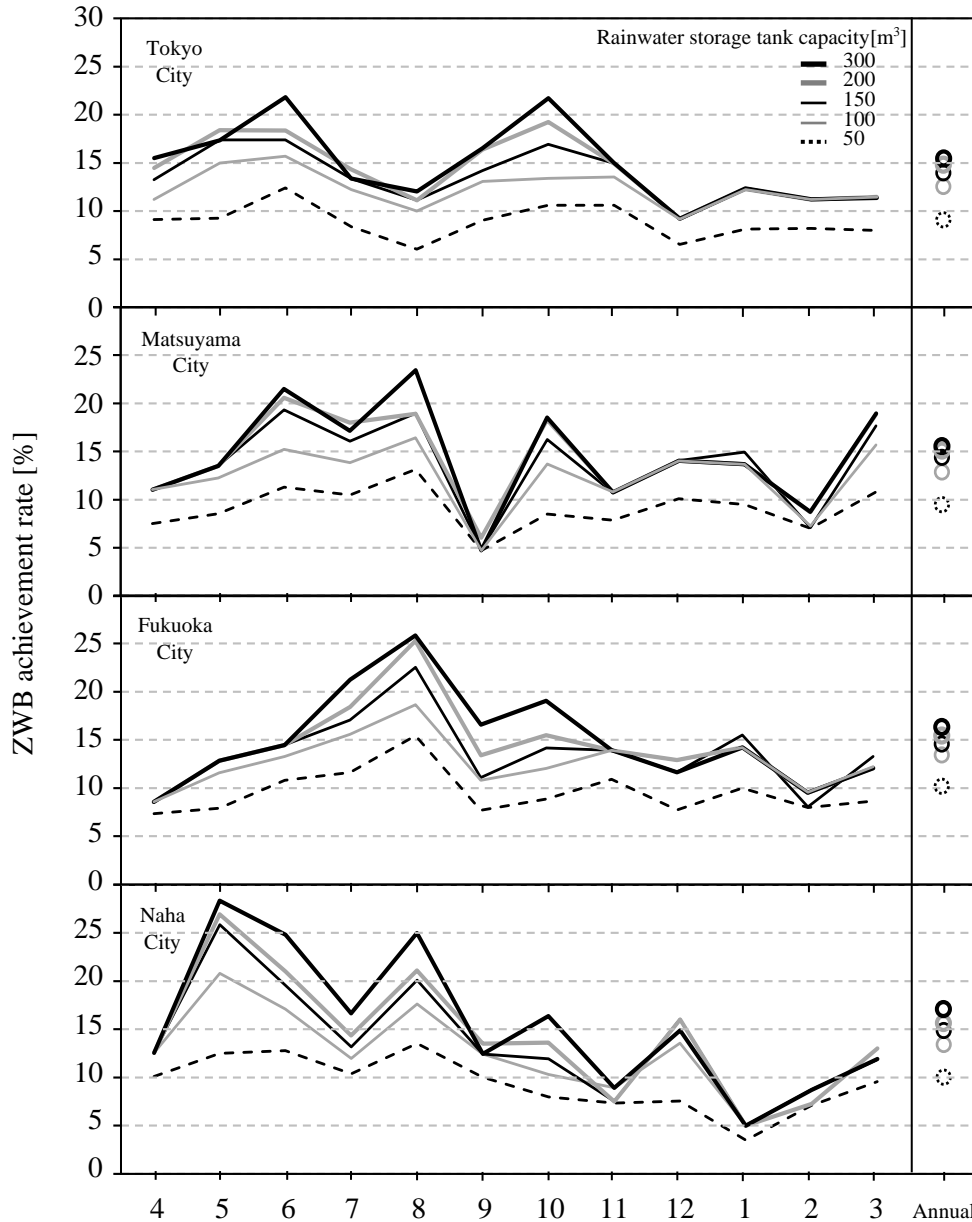
Figure6   Monthly ZWB achievement rate by rainwater storage tank capacity

4.2 Relationship between rainwater storage tank capacity and CO$_2$ emissions related to water supply and wastewater treatment

Figure 7 shows changes in CO$_2$ emissions related to water supply and wastewater treatment associated with changes in rainwater storage tank capacity. CO$_2$ emissions from water supply and wastewater treatment decreased by 3.8% in Matsuyama City, 4.0% in Fukuoka City, 4.6% in Naha City, and 5.7% in Tokyo City when the rainwater storage tank capacity was 100 m^3 compared to when the rainwater storage tank

capacity was 0 m^3 (no rainwater utilization). In all regions, CO_2 emissions related to water supply and wastewater treatment showed a decreasing trend as the number of rainwater storage tanks increased, with the decreasing trend slowing down for rainwater storage tanks with a capacity of 100 m^3 or more.
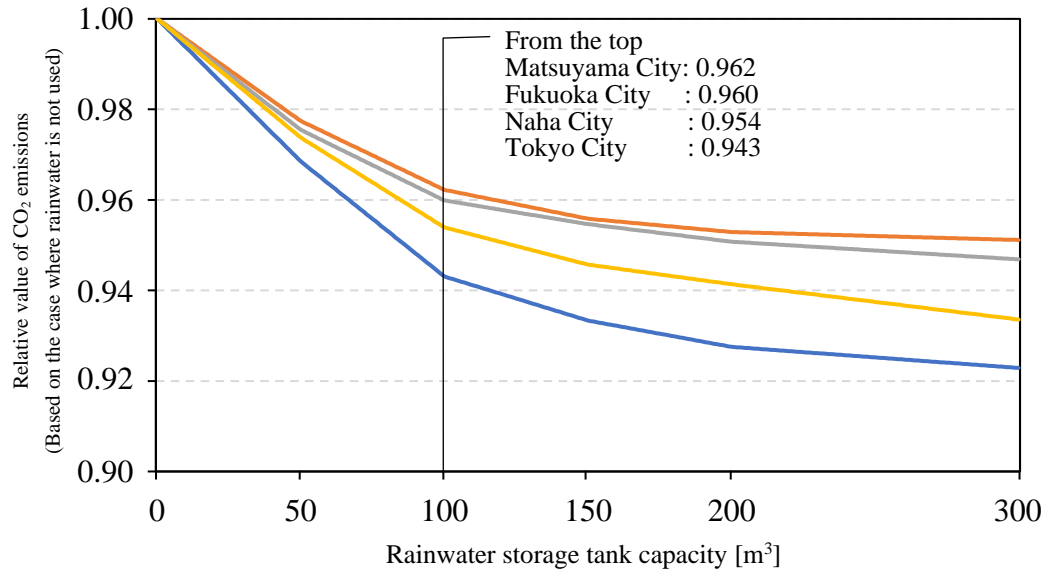
Figure7 Change in CO_2 emissions related to water supply and wastewater treatment with respect to change in rainwater storage tank capacity

5. Conclusion

In this study, we calculated the ZWB achievement rate and CO_2 emissions related to the water supply and wastewater treatment for each rainwater storage tank capacity. In months with high precipitation, such as June and October in Tokyo City, the ZWB achievement rate increased along with an increase in rainwater storage tank capacity after 100 m^3. However, in months with low precipitation, such as December and January, the ZWB achievement rate was the highest when the rainwater storage tank capacity was 100 m^3. In all regions, CO_2 emissions related to water supply and wastewater treatment showed a decreasing trend as the number of rainwater storage tanks increased, with the decreasing trend slowing down for rainwater storage tanks with a capacity of 100 m^3 or more. Based on these results, considering the maintenance and operational aspects of the rainwater storage tank, a rainwater volume of about 100 m^3 is considered appropriate for Evaluation Building C

Notes

*1) Appendix 1 shows the ground surface area and runoff coefficient of Evaluation Building C.

Appendix 1 Runoff coefficient by surface type [5]

| Ground surface type			i : Symbol	A : Area [m²]	C : Runoff coefficient [-]
Roof	Main building	Catchment surface	-	2,300	0.9
		Non-catchment surface	1	700	0.9
	Parking		2	1,400	0.9
Pavement concrete			3	1,300	0.9
Planting			4	400	0.2

*2) Appendix 2 shows the outline of the pumps for Evaluation Building C.

Appendix 2 Overview of the water supply and replenishment pumps for Evaluation Building C

Pump	Symbol	Operation method	System	Discharge amount [L/min]	Output [kW]
Pressurized water pump	b	Estimated constant end pressure (2/3 Units parallel)	Water supply for low-rise drinking water, replenishment to miscellaneous water tank	1,050	30 (2 Unit)
	c		High-rise drinking water supply, cooling water supply	900	37 (2 Unit)
	d		Water supply for low-rise miscellaneous water	1,150	37 (2 Unit)
	e		Water supply for high-rise miscellaneous water	600	30 (2 Unit)
Rainwater Filtration Pumps	f	1 Unit operation	Rainwater filtration and rainwater replenishment to miscellaneous water tank	300	7

*3) Appendix 3 shows the calculation conditions for the rainwater utilization equipment model.

Appendix 3 Calculation conditions and calculation formula for each water tank water level in the rainwater utilization evaluation model

Item	Symbol	Conditions	Calculation formula
Rainwater storage	$V_r(t)$	$V_r(t-1)+RC(t-1)-RW_r(t-1) \leq V_{r\,max}$	$V_r(t-1)+RC(t-1)-RW_r(t-1)$
		$V_r(t-1)+RC(t-1)-RW_r(t-1) > V_{r\,max}$	$V_{r\,max}$
Amount of water in the miscellaneous water tank	$V_m(t)$	$V_m(t-1)-WU_m(t-1) \leq V_{m\,start}$	$V_{m\,max}$
		$V_m(t-1)-WU_m(t-1) > V_{m\,start}$	$V_m(t-1)-WU_m(t-1)$
Replenishment water	$RW(t)$	$V_m(t)-V_m(t-1) \leq 0$	0
		$V_m(t)-V_m(t-1) > 0$	$70-V_m(t-1)+WU_m(t)$
Amount of tap water replenishment	$RW_d(t)$	$V_r(t-1) \geq V_{r\,cw}$	0
		$V_r(t-1) < V_{r\,cw}$	$RW(t)$
Amount of rainwater replenishment	$RW_r(t)$	$V_r(t-1) \geq V_{r\,cw}$	$RW(t)$
		$V_r(t-1) < V_{r\,cw}$	0
Amount of overflow	$OV(t)$	$V_r(t)+RC(t)-RW_r(t) \leq V_{r\,max}$	0
		$V_r(t)+RC(t)-RW_r(t) > V_{r\,max}$	$V_{r\,max} - (V_r(t)+RC(t)-RW_r(t))$

$RC(t)$: Rainwater catchment volume at time t [m³]

$V_{m\,start}$: Replenishment start capacity of miscellaneous water tank [m³]=40m³

$WU_m(t)$: Miscellaneous water use at time t [m³]

$V_{r\,cw}$: Replenishable Storage Volume of Rainwater storage tank [m³]=50m³

$V_{r\,max}$: Rainwater storage tank capacity [m³]

$V_{m\,max}$: Effective capacity of miscellaneous tank [m³]=70m³

t : Time（1 Time interval）

*4) Appendix Table 4 shows various calculation methods for rainwater.

Appendix 4 Various calculations of precipitation

Ground surface type	Precipitation conditions※	Calculation formula
Rainwater catchment surface	4mm/day <	WR $= R \times A_r / 1000$
Rainwater catchment surface	4mm/day $\geqq$	RC $= R \times A_r \times C_r / 1000$
Rainwater catchment surface	4mm/day $\geqq$	WR $= R \times A_r \times (1 - C_r) / 1000$
Other than rainwater catchment surface	4mm/day <	WR $= R \times \sum_{i=1}^{4} A_i \times C_i / 1000$
Other than rainwater catchment surface	4mm/day $\geqq$	RR $= R \times \sum_{i=1}^{4} A_i \times C_i / 1000$
Other than rainwater catchment surface	4mm/day $\geqq$	WR $= R \times \sum_{i=1}^{4} A_i \times (1 - C_i) / 1000$

WR	: Infiltration/Evapotranspiration	[m³/h]	R	: Precipitation	[mm/h]
A_r	: Rainwater catchment area	[m²]	C_r	: Roof runoff coefficient	[-]
RR	: Rainwater runoff	[m³/h]			

Refer to reference [6] for precipitation conditions.

*5) CO_2 emissions in the evaluation area were calculated using Equation 1.。

$$C_{all} = C_{T\,ws} + C_a + C_{b1} + C_{b2} + C_c + C_d + C_e + C_{T\,st} + C_{RU} + C_{RR} \tag{1}$$

C_{all}	: Annual CO_2 emissions during the operation phase of water supply and sewerage treatment systems	[kg-CO₂/yr]
$C_{T\,ws}$	: Annual CO_2 emissions associated with water supply at water supply facilities	[kg-CO₂/yr]
C_a	: Annual CO_2 emissions associated with drinking water supply for pump a	[kg-CO₂/yr]
C_{b1}	: Annual CO_2 emissions associated with drinking water supply for pump b	[kg-CO₂/ yr]
C_{b2}	: Annual CO_2 emissions associated with replenishment of cooling water for pump b	[kg-CO₂/ yr]
C_c	: Annual CO_2 emissions associated with rainwater filtration and replenishment of pump c	[kg-CO₂/ yr]
C_d	: Annual CO_2 emissions associated with miscellaneous water supply for pump d	[kg-CO₂/ yr]
C_e	: Annual CO_2 emissions associated with miscellaneous water supply for pump e	[kg-CO₂/ yr]
$C_{T\,st}$	: Annual CO_2 emissions associated with sewage treatment of used tap water	[kg-CO₂/ yr]
C_{RU}	: Annual CO_2 emissions associated with sewage treatment of used rainwater	[kg-CO₂/ yr]
C_{RR}	: Annual CO_2 emissions associated with sewage treatment of runoff rainwater	[kg-CO₂/ yr]

*6) CO_2 emissions from water supply and sewerage facilities were calculated using formulas 2, 3, 4, and 5. References [7, 8] were used as references for the CO_2 emission intensity related to water supply and wastewater treatment.

$$C_{T\,ws} = WS_i \times WU_T \tag{2}$$
$$C_{T\,st} = ST_i \times WU_T \tag{3}$$
$$C_{RU} = S_i \times RU \tag{4}$$
$$C_{RR} = S_i \times (OV + RR) \tag{5}$$

WS_i	: CO_2 emissions intensity of water supply facilities [7]	[kg-CO₂/m³]	ST_i	: CO_2 emissions intensity of sewerage facilities [8]	[kg-CO₂/m³]
WU_T	: Annual tap water use	[m³/yr]	RU	: Annual rainwater usage	[m³/yr]
OV	: Annual overflow volume	[m³/yr]	RR	: Annual rainwater runoff	[m³/yr]

*7) CO_2 emissions from building pumps were calculated using Equation 6. The values shown in Table 5 were used as CO_2 emission factors for electricity[9].

$$C_n = E_n \times C_o \tag{6}$$

C_n : Annual CO_2 emissions from pump operation　[kg-CO_2/yr]　　E_n : Power consumption due to pump operation　[kWh/yr]

C_c : CO_2 emission factor of electricity　[kg-CO_2/kWh]

Appendix 5 CO_2 emission factor of electricity consumption for calculation

Region	Power company	CO_2 emission factor of electricity consumption [kg-CO_2/kWh]
Tokyo	Tokyo Electric Power	0.505
Matsuyama City	Shikoku Electric Power	0.676
Fukuoka City	Kyushu Electric Power	0.584
Naha City	Okinawa Electric Power	0.816

*8) The power consumption of the pressurized water supply pump was calculated using Equation 7 with reference to literature [10]. For the water supply load flow rate, a value obtained by dividing the water supply amount for one hour by 60 [min/h] was used.

$$E_{n1} = q_{n1} \times ((q_{n1} / Q_o)^2 \times (H_o - H_{n1}) / 9.8 + H_{n1} / 9.8) / (6120 \times \eta_o \times \eta_{n1}) \tag{7}$$

E_{n1} : Power consumption of pressurized water supply pump　[kWh/min]　q_{n1} : Water supply load flow　[L/min]

Q_o : Rated wapply amount　[L/min]　H_o : Total pump head　[kPa]

H_{n1} : Total head at water supply q_{m1}　[kPa]　η_o : Highest efficiency pump　[-]

$\eta_o = -0.0145 (\log(Q_o))^2 + 0.2682 (\log(Q_o)) - 0.6018$

η_{n1} : Pressurized water pump efficiency　[-]

$\eta_o = -1.02073 (\log(q_n / Q_o))^2 + 1.99581 (\log(q_n / Q_o)) - 0.0369718$

*9) The power consumption of the filtration pump was calculated by Equation 8 with reference to literature [11]. The filtered water volume was obtained by dividing the hourly rainwater

$$E_{n2} = q_{n2}^2 \times H_o / (6120 \times Q_0 \times \eta_o) \tag{8}$$

E_{n2} : Power consumption of filtration pump　[kWh/min]　q_{n2} : Filtration water volume　[L/min]

*10) The ZWB achievement rate was calculated by Equation 9.

ZWB achievement rate $= (AW + WR) / (WU + RR + OV) \times 100 \tag{9}$

AW : Alternative water　[m^3]　WR : Water returned　[m^3]

WU : Water usage　[m^3]　RR : Rainwater runoff　[m^3]

OV : Overflow　[m^3]

6 References

[1] J. Oyagi and T.Nishikawa, Study on water balance and environmental performance evaluation in buildings- Part 2: Comparative evaluation of reclaimed water use and rainwater use, 2022 Symosium CIB W062 – Taichung, September 2022

[2] T.Nishikawa and J. Oyagi, Study on water balance and environmental performance evaluation in buildings- Part 1: Consideration of water balance and Net Zero Water Building, 2022 Symosium CIB W062 – Taichung, September 2022

[3] Kanto Regional Development Bureau, Ministry of Land, Infrastructure and Transport, Occurrence and frequency of drought, Viewed date：2023.6.28, URL：https://www.ktr.mlit.go.jp/river/bousai/river_bousai00000059.html

[4] Ministry of Land, Infrastructure and Transport, Japan Meteorological Agency, About the update of the climatological standard normal ~ The climatological standard normal（Statistics period 1991~2020）is created~ appendix（Data table of main new climatological standard normal）, Update date：2021.3.4, URL：https://www.jma.go.jp/jma/press/2103/24a/3_huroku.pdf

[5] Tokyo Metropolitan Government Bureau of Sewerage, Tokyo Metropolitan Government guidelines for drainage f acilities chapter 5 pivate road dainage facilities, Viewed date：2023.2.9, Update date：2022.3, p.128, URL：https://www.gesui.metro.tokyo.lg.jp/contractor/pdf/3_5_R3youkou.pdf

[6] The Society of Heating, Air-Conditioning and Sanitary Engineers of Japan：Practical Knowledge of Rainwater Utilization Design/Construction/Maintenance Manual（2011）, The Society of Heating, Air-Conditioning and Sanitary Engineers of Japan

[7] Keita Fukui, et al., Research on Greenhouse Gas Emissions from Water Supply Facilities, Summaries of technical papers of Annual Meeting Architectural Institute of Japan, 2020.9, pp.1685-1686

[8] Imai Masaki, et al., Actual Greenhouse Gas Emissions in Water Supply and Sewerage, Proceedings of the Annual Meeting of the Society of Heating, Air-Conditioning and Sanitary Engineers of Japan, 2020.9, pp.101-104

[9] Ministry of the Environment, Greenhouse Gas Emissions Accounting, Reporting and Disclosure System Emission factor by electricity supplier（For calculating greenhouse gas emissions of specified emitters）- Fiscal year 2014 Performance - , Viewed date：2023.6.20, Update date：2016 .7.12, URL：https://ghg-santeikohyo.env.go.jp/files/calc/h28_coefficient_rev2.pdf

[10] Iwao Hasegawa, et al., Research on the development of a simulation tool to calculate water and energy consumption in water supply systems - Development of a calculation system and study of its application using measured data -, Proceedings of the Society of Heating, Air-Conditioning and Sanitary Engineers of Japan, No.298, 2021.10

[11] Hiroyuki Kose, et al., Development of "BEST" Comprehensive Simulation Tool for Envelope/Frame and Facilities/Equipment（Part 36）Overview of Rainwater Utilization Program, Proceedings of the Annual Meeting of the Society of Heating, Air-Conditioning and Sanitary Engineers of Japan, 2008.8

7 Presentation of Author(s)

Jun Oyagi is a graduate student of Nishikawa Institute of Engineering University and a member of AIJ (Architectural Institute of Japan) and SHASE (The Society of Heating, Air-Conditioning and Sanitary Engineers of Japan). He is currently conducting research on the water environment in buildings.

Toyohiro Nishikawa is the Professor at School of Architecture, Kogakuin Univercity, Dr. Eng. He is a member of AIJ (Architectural Institute of Japan) and SHASE (The Society of Heating, Air-Conditioning and Sanitary Engineers of Japan). His current research interests are Performance verification if next generation air-conditioning systems, Development of highperformance outer wall, and Analysis of water environment in urban buildings.

Towards the Feasibility of Near-Zero Water Consumption Buildings

Sadahico Kawamura (1), Cheng-Li Cheng (2)

(1) sadahico@gmail.com

(2) CCL@mail.ntust.edu.tw

(1)(2) National Taiwan University of Science and Technology, Department of Architecture, Taiwan, R.O.C.

Abstract

According to the IPCC report (2022), the global water shortage remains a serious problem, and the increasing severity of global warming and climate change disasters is having a profound impact on Taiwan's water shortage problem. While water scarcity has been discussed, concrete actions have yet to be taken. Sustainable development of water resources and the establishment of water-saving buildings are key directions for addressing this issue. This study focuses on the feasibility of nearly zero water consumption buildings, with the aim of reducing dependence on water resources and lowering greenhouse gas emissions by improving building water efficiency .To achieve this goal, the study proposes a building water assessment system, which includes the establishment of assessment systems for residential and non-residential buildings, and the establishment of water-saving benchmarks and rating systems to increase water-saving awareness and achieve rational water use through measurement. To achieve a simplified and reliable building water assessment method, the study combines Taiwan's green building certification system with a water-saving technology carbon reduction assessment system. Additionally, the study investigated the actual water consumption data of various types of buildings in Taiwan, analyzed the water consumption intensity per unit area of buildings, and established rational and accurate water use benchmarks. Water consumption analysis was carried out to verify the theoretical water consumption estimation method. The results of this study are expected to provide important guidance and reference for achieving near zero water buildings. The results show that the design of near-zero water consumption buildings can be achieved by adopting technologies

and strategies such as integrated water management systems, such as water-saving appliances, and gray water recycling systems.

Keyword

Zero water building;Building water saving design;Recycling water;Renewable;Green building;Labeling.

1 Introduction

The increasing emphasis on zero-emission or near-zero-consumption architectural designs reflects the pressing global need to reduce greenhouse gas emissions and promote sustainable development, as manifested in the Sustainable Development Goals (SDGs) and Taiwan's 2050 net-zero emission policy. In 2022, the United Nations World Meteorological Organization highlighted that as early as 2018, a staggering 3.6 billion people worldwide experienced insufficient freshwater availability for at least one month annually (State of Global Climate 2022). Taiwan, characterized by its high population density and advanced economy, receives an average annual precipitation of approximately 2,500 millimeters, which surpasses the global average of 973 millimeters by a factor of 2.6. Nevertheless, due to the uneven distribution of rainfall, Taiwan faces water scarcity, with per capita rainfall amounting to less than one-fifth of the global average. The rise in temperatures has induced alterations in global and regional precipitation patterns, thereby affecting rainfall distribution and agricultural seasons, consequently exerting significant impacts on food security and human well-being. Hence, the availability of clean water resources assumes paramount importance for the future sustenance of humanity. The pursuit of zero-water-consumption buildings, as an ultimate objective, necessitates a preliminary approach towards near-zero water consumption. Consequently, the focal point should be placed on effective building water management, encompassing the establishment of a water grading system that facilitates a comprehensive understanding of the water usage status. Prioritizing water conservation measures and utilizing recycled water as supplementary resources can eventually culminate in achieving water balance at zero consumption. This study encompasses a wide range of building types, including residential and non-residential, as the water consumption varies based on usage patterns and building scales. To

evaluate building water usage, we have developed a simplified yet robust assessment methodology, which has undergone validation within the realm of architectural applications. The existing frameworks, such as the Building Water Resources Labeling Act, Building Water Intensity Index, U.S. Department of Energy (DOE) Building Energy Asset Rating, and Technological Potential Scale, have been utilized to establish a comprehensive building water consumption assessment system. The implementation of a grading and assessment framework not only serves as an active catalyst and encouragement for the effective utilization of building water resources but also sets a positive example for the public. This comprehensive approach not only raises public awareness regarding water scarcity issues but also educates individuals on how to maximize the utilization of the Earth's water resources and implement strategies for achieving near-zero water consumption in building designs. It represents a pragmatic response to the impending environmental challenges we face in the future.

2 Theories and review

2.1 Zero water building

Near-Zero Water Building (nZWB) refers to the adoption of both active and passive methods, namely water-saving and reclaimed water systems, in which water-saving methods should be the focus of its implementation. The concept of improving water efficiency is to first reduce your own water consumption and then use rainwater or reclaimed water to neutralize the amount of potable and non-potable water, including cleaning, rinsing and irrigation water accordingly, with the aim of completely offsetting the water demand, so almost Buildings with zero or zero water use in figure 1.
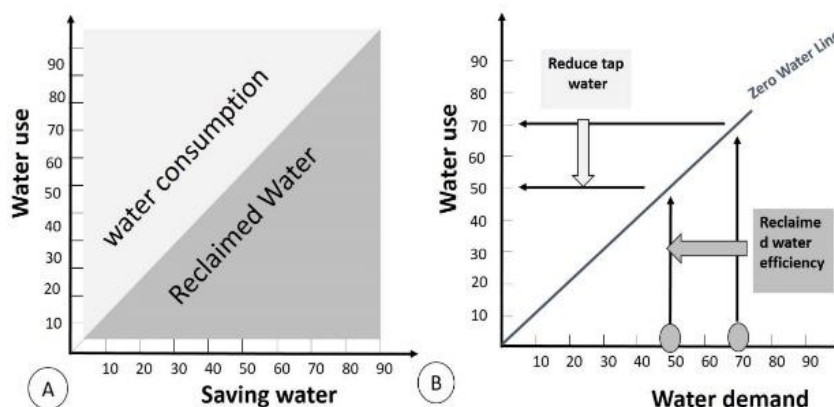

Figure 1－Conceptual drawing of nearly zero water buildings

2.2 International labels

Various countries around the world have begun establishing and implementing water efficiency rating schemes, particularly in water-stressed regions such as Germany, Nordic countries, the European Union, the United Kingdom, the United States, and Australia. These rating schemes serve as benchmarks for assessing building water usage. Taking Australia's Water Efficiency Labelling and Standards (WELS) as an example, the Australian government initiated the WELS program in 2005 to address long-term water resource scarcity. WELS is one of the most mature and successful rating schemes globally. The program mandates the regulation of devices including showers, toilets, washing machines, dishwashers, urinals, and taps, using flow control mechanisms. The scope of regulation has been expanded systematically to include evaporative cooling systems, hot water systems, hot water recirculation devices, and irrigation systems. The WELS rating scheme employs a six-star rating system to indicate water efficiency and water consumption or flow indicators. The more stars displayed on the label, the higher the water efficiency of the device, with a one-star rating indicating non-compliance with applicable standards. As a proponent of long-term sustainability, Singapore's national water agency, the Public Utilities Board (PUB), encourages water conservation as a way of life. Singapore is one of the countries with extremely limited water resources and has historically relied on purchasing water from Malaysia. Therefore, water efficiency is of paramount importance in Singapore, and the government launched the Water Efficiency Labeling Scheme in 2006 as a water-saving initiative. Since 2009, it has been mandatory to label all taps, flush valves for both large and small flow rates (including waterless types) and washing machines. The labeling scheme uses a three-tick rating system to indicate the overall water efficiency of products.

While many countries have used labeling schemes to assess the water-saving capabilities of products and equipment, the pace of water-saving technology and efficiency often lags water consumption rates. Therefore, the use of recycled water has become an inevitable trend. By combining water-saving technologies and incorporating plans for recycled water utilization, effective water usage can be achieved. Thus, it is necessary and urgent to assign a rating that combines water-saving and recycled water utilization for water efficiency in various types of buildings.
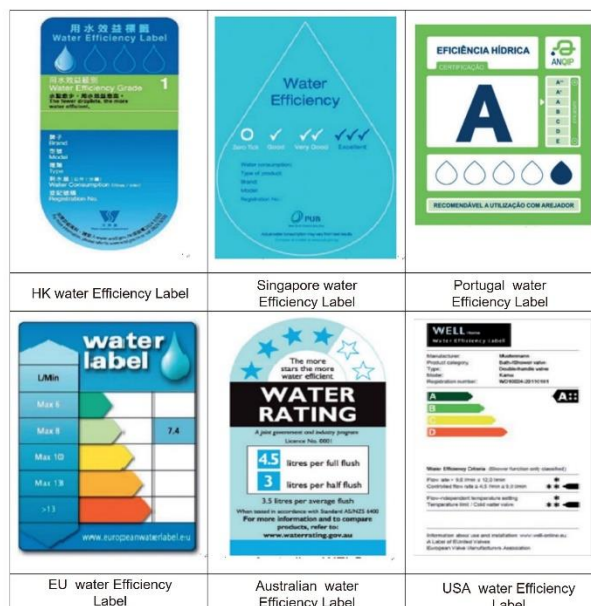
Figure 2－National and regional water use or water conservation assessment labels

2.3 Monte Carlo simulation method

Monte Carlo methods are based on the fundamental principle of iteratively generating random numbers to facilitate the simulation of outcomes. In practice, the probabilities associated with all possible outcomes are expressed as a probability density function (PDF), which is then aggregated with appropriate adjustments into a cumulative probability function (CPF). The CPF reaches a maximum value of 1, which serves as the basis for constructing numerical simulations of the standardized normal distribution. This normalized normal distribution faithfully reproduces the properties of probability, including the cumulative occurrence of all events with probability 1. Thus, it establishes a link between the simulation of practical problems and the utilization of random number sampling. The outcome of this study case is residential or non-residential, with an index close to 0 through 10,000 cases.

3   Methodology

3.1. Residential Buildings

The per capita annual water consumption benchmark for Water Use Intensity (WUIx) was determined through empirical estimation, as represented by formula (1). Based on this benchmark, the distribution of virtual water consumption and the corresponding grading labels for the evaluation system were established. The initial step in implementing the water consumption assessment model involved determining

the baseline model for individual cases and calculating various statistical measures such as median, maximum, minimum, deviation, and average values for each case. According to surveys, the average daily domestic water consumption per person in Taiwan over the past ten years was recorded as 0.19 m3/person. Day. This value served as a fundamental parameter for estimating the total annual water consumption for buildings, denoted as Qz, as shown in formula (2). Additionally, the impact of occupant intensity was considered as a calibrating weight factor for benchmark calculations. It was considered that the presence of the same number of occupants in a larger living space would result in a lower water consumption benchmark, while the opposite would be true for a smaller living space. Thus, a weight coefficient, rdi, was utilized to correct the evaluation consistency and prevent deviations and distortions in the grading label results, as indicated in formula (3).

$$\text{WUI}_x \;=\; Q_w \div A_f \times rd \qquad\qquad (1)$$

$$Q_z \;=\; 0.19 \times 365 \times np \qquad\qquad (2)$$

$$rd_i \;= P_{avf} \div P_f \qquad\qquad\qquad (3)$$

$$P_{avf} = A_{fi} \div N_{pi} \qquad\qquad\qquad (4)$$

$$P_f = K \times N_f \qquad\qquad\qquad\quad (5)$$

WUI_X : Benchmark of per capita annual water consumption (m³/m².year)

Q_Z: Annual water consumption (m³/year)

n_p: Number of residential persons

rd_i: Occupant intensity weighting factor

P_{avf} : Occupant intensity baseline in common dwelling units (person/m²)

P_f : Occupant intensity of evaluated object (person/m²)

A_{fi}: actual single household area (m²)

N_{pi}: total number of people (person)

K: fixed value (48.69)

N_f: actual number of people living in a single household (person)

In this study, Water Use Intensity (WUIxi) was used to evaluate residential buildings based on the annual per capita water consumption per unit area. The calculation of WUIxi, described in formula (6), considered the distribution of virtual water consumption and the corresponding grading scale. The study incorporated water

resource and water-saving assessment indicators from the green building evaluation system in Taiwan to account for water-saving design and facility planning. The evaluation focused on determining the reasonable water consumption of buildings, and the estimation of water consumption for residential buildings (Qzi) was obtained using formula (7). The primary calculation parameter was the green building water resource water-saving assessment coefficient RS8, with a maximum water-saving rate of 0.355 for residential buildings. If there were significant water-consuming elements such as garden irrigation equipment, landscape ponds, swimming pools, or rainwater recycling equipment, the estimated building would be given a weight and included in the calculation of the annual water consumption density, as shown in formula (8).

$$WUI_{xi} \;=\; (Q_{zi} \div A_f) + W_c - W_r \qquad (6)$$

$$Q_{zi} \;=\; 0.19 \times 365 \times np \times (1 - RS8 \div 8 \times S_{rc}) \qquad (7)$$

$$W_c \;=\; C_g + C_f + C_p \qquad (8)$$

WUI_{xi}: Annual water consumption intensity per unit area of the building (m³/m². year)

A_f : Effective floor area of the dwelling area (m²).

Q_{zi} : Estimated annual water consumption of the residential building (m³/year)

W_c : Annual water consumption of large water-consuming projects (m³/year)

W_r : Annual replacement water volume of rainwater or reclaimed water (m³/year)

n_p: Number of people living in the building

$RS8_n$: Water resource assessment indicator score of the Taiwan green building system

S_{rc}: Maximum water saving rate for residential buildings (0.355)

C_g : Water coefficient for garden irrigation

C_f : Landscape pond water use coefficient

C_p : Swimming pool water coefficient

3.2. *Non-residential Buildings*

When evaluating buildings other than residential ones, they are categorized as non-residential buildings. The estimation of annual per capita water consumption, WUI, per unit area for non-residential buildings follows the same concept as described in formula (6), represented by formula (9). However, the WUIs in formula (10) can be compared with the parameters provided in Table 2 and incorporated into the evaluation system formula for assessment. The maximum water-saving rate (Src) for the building can be referenced from the parameters in Table 2-4 and included in the respective formula. The calculation of estimated water consumption, Qnzi, for non-residential buildings is primarily influenced by the effective building area (Af), which encompasses the total

floor area of the building excluding non-utilized spaces such as parking lots, mechanical rooms, and warehouses. The floor area is determined based on the usable volume. In this study, the non-residential evaluation method is employed, and building types are evaluated by comparing construction type items outlined in the technical regulations.

$$WUI_{nx} \; = \; (Q_{nzi} \div A_f) + W_c - W_r \qquad\qquad (9)$$

$$Q_{nzi} \; = \; WUI_x \times Af \times (1 - RS8 \div 8 \times S_{rc}) \qquad\qquad (10)$$

WUI_{nx} ：Water Consumption Benchmark for Non-residential Buildings

A_f：Effective floor area of the dwelling area（m^2）。

Q_{nzi}：Estimated annual water consumption of the residential building (m^3/year)

$RS8$：Water resource assessment indicator score of the Taiwan green building system

S_{rc}：Maximum water saving rate for residential buildings

Table1－Standards for water use in non-residential buildings

Project	space code	Space Description	WUImin	WUImid	WUImax	Src
A-1	A12	Lecture halls, auditoriums, conference centers, religious assembly halls	0.00	2.87	6.29	38.6%
	A13	Performance halls, performance halls, gymnasiums dedicated to performing arts activities				
C-1	C23	Air-conditioned precision manufacturing area	0.00	1.99	5.35	47.1%
	C24	Air-conditioned clean production area				
D-1	D11	Gymnasium indoor area, sports venue space	0.00	3.25	6.99	38.9%
D-2	D12	Business-only SPA and sauna, hot spring bathhouse, indoor swimming pool	2.19	6.93	11.54	38.9%
D-3	D31	Classrooms for primary school children	0.00	1.78	4.28	38.6%
	D41	Classrooms for junior high school				
	D42	high school classroom space				
	D43	Classroom space for universities, and research institutes				
	D44	Ordinary classrooms and specialist classrooms required for courses				
F-1	F12	nursing home	0.00	2.40	6.49	39.5%
	F13	Orphanage, Nursery				
	F14	Safeguarding place				
G-1	G11	Office spaces	0.00	1.87	5.67	49.5%
	G12	conference, administration, research, experiment-related spaces				
H-1	H11	institutions, corporate dormitories	0.00	2.44	5.00	39.5%

To establish a building water consumption grading system, the range between WUImax and WUImin is used for scoring, and the scoring interval is 0 to 100 points. The final score WUIscore of building water consumption labeling will be the basis for grade labeling. A WUIscore baseline value of 60 is considered a qualified level, and the WUImin-WUI and WUI-WUImax intervals are divided into 1-100 points. In this study, 90-100 points above the baseline are taken as the level of near-zero water-consumption buildings (expressed as A level), and 100-60 is taken as B-D levels, and level D qualification standards. Divide the WUI-WUImax interval of 59-0 on the right into non-water-saving building grades E~G.

When WUI* ≤ WUImid

$$SCORE_w = 60 + 40 \times (WUI_{mid} - WUI) \div (WUI_{mid} - WUI_{min}) \tag{11}$$

When WUI* > WUImid

$$SCORE_w = 60 \times (WUI_{max} - WUI) \div (WUI_{max} - WUI_{mid}) \tag{12}$$

WUI*: Water resources and water consumption density indicators in the assessment case ($m^3/(m^2 \cdot yr)$)

WUI_{min}, WUI_{mid}, WUI_{max} : The minimum value, median value, and maximum value of the evaluation scale of the evaluation case.

$SCORE_w$：Building water consumption classification grade labelling score

4 Validation and Analysis

Residential buildings have the highest density among building types in Taiwan. In this study, the housing category serves as a benchmark within the evaluation framework. To establish reliable baseline values, minimum, median, maximum, and mean values were estimated based on 120 cases. In addition, Monte Carlo simulation methods were used to generate more cases, utilizing techniques borrowed from Mongolian. By using a Monte Carlo simulation method, the 120 cases can be extended to 12,500 cases, resulting in a more robust baseline value. The actual values for 120 cases and the simulated values from the Monte Carlo simulation for 12,500 cases are examined to explore their relationship. It turns out that the two sets of values are relatively close to each other, as shown in Figure 3. Therefore, the Monte Carlo simulation value is used as the evaluation benchmark.
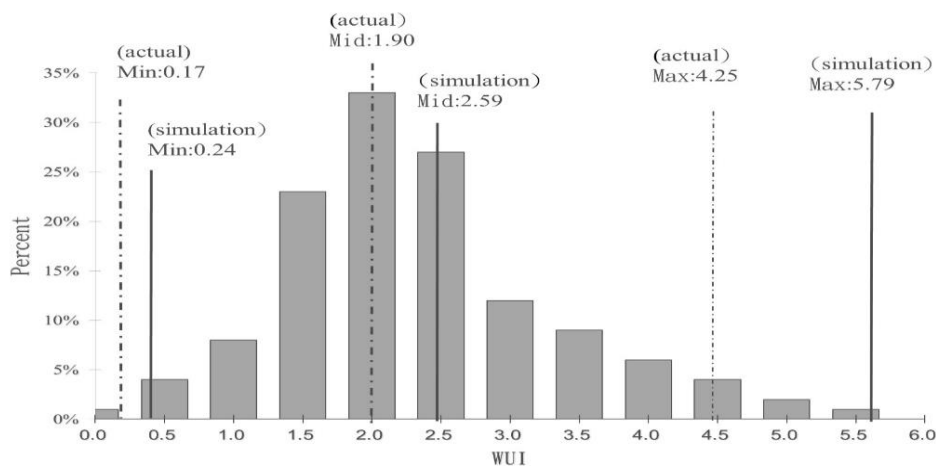
Figure 3－Comprehensive simulation analysis

The residential water use evaluation model calculates the water usage rate of residential buildings through evaluation calculations, scoring, labeling, and grading. Verifying the model's effectiveness by checking water bills for collective housing is challenging due to various factors such as diverse water use behaviors and privacy concerns. Skewed distribution in evaluation cases is expected and indicates the accuracy of the evaluation method. To validate the evaluation method in this study, building water consumption is estimated using the evaluation method and grading system. The scoring system assigns four grades: near-zero water consumption buildings, extremely water-saving buildings, water-saving benchmark buildings, and near-water-saving buildings receive scores from 100 to 60. Non-water-saving buildings, water-consuming buildings, and extremely water-consuming buildings receive scores from 59 to 0, indicating unqualified grades. The evaluation formula is applied to 120 collective housing cases in this study. Results show that 79% of the cases fall into the water-saving benchmark buildings category, while 21% fall into the extremely water-consuming buildings category. These results demonstrate a skewed distribution pattern, supporting the theory of skewness as shown in Figure 4.
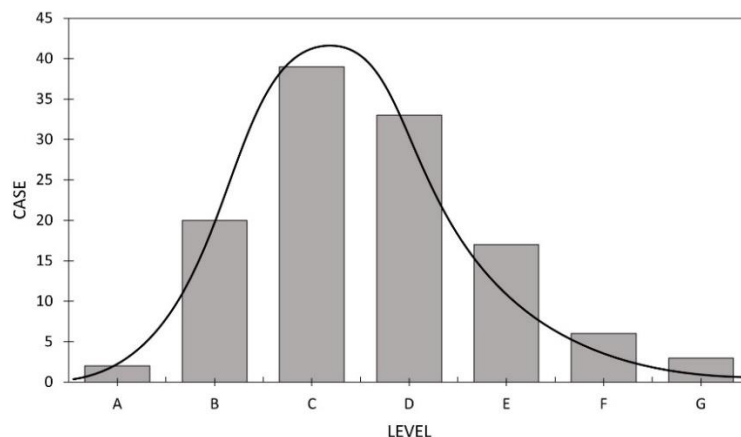
Figure 4－Residential building classification statistics and distribution of the evaluated cases.

The findings from the WUI_{xi} estimation model used in this study reveal a significant relationship between the assessment of water resources in green buildings and the distribution of buildings across different levels. Out of the 120 cases examined, it was observed that 2% of the buildings fell under the category of near-zero water usage (Level A), while 17% were classified as Extremely Water Efficient (Level B), 32% as Water Efficient (Level C), and 27% as Benchmark Water Efficient (Level D). These percentages indicate that these buildings successfully met the evaluation criteria. On the contrary, 14% of the buildings were categorized as not water-efficient (Level E), 5% as Water Consuming (Level F), and 3% as Extremely Water Consuming (Level G), indicating a failure to meet the established rating standards. Notably, Grade III water-saving benchmark buildings and Grade IV water-saving buildings accounted for 59% of the total cases, aligning with the original green building cases depicted in Figure 5.
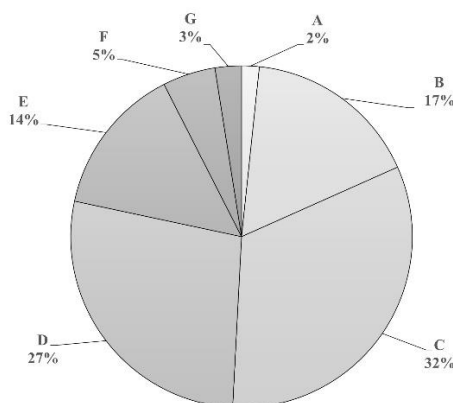

Figure 5－Residential building Evaluation result percentage

The results obtained from the estimated model WUI in this study were analyzed to evaluate 100 non-residential construction cases. The analysis is presented in the form of a histogram, as shown in Figure 6. The histograms showed a skewed distribution, confirming the accuracy and consistency of the evaluation method in this study with the underlying theory. Therefore, the non-residential evaluation method and grading system established in this study can effectively estimate the water density and grading results of any type of building. The relationship between scores and grades remains consistent, with a maximum score of 100. The grades include six categories: Level A is nearly zero water consumption buildings, Level B is extremely water-saving buildings, Level C is water-saving buildings, water-saving benchmark buildings are Level D, water-consuming buildings are Level E, and extremely water-consuming buildings are Level F, 59 points to 0 points are unqualified. It is worth noting that many of the evaluation cases focus on green buildings because the research is related to green building water projects. Among the 100 non-residential buildings evaluated, water-saving benchmark buildings belong to the largest number of Level III buildings, followed by Level IV non-water-saving buildings.
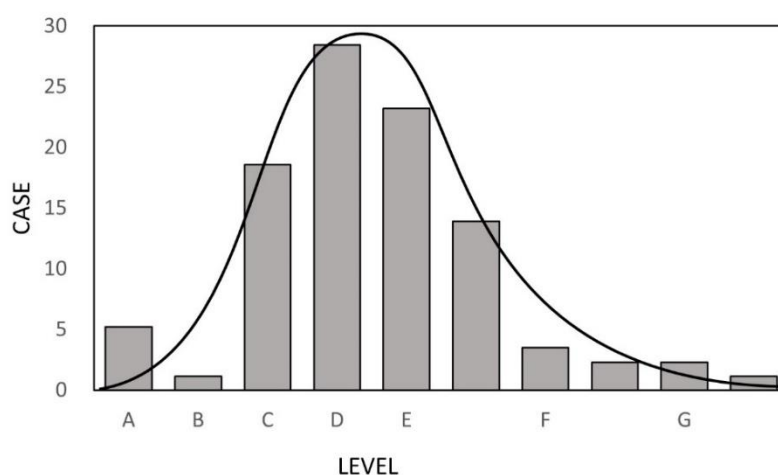

Figure 6－Non-Residential building classification statistics and distribution of the evaluated cases.

The calculation results of the WUI estimation model in this study show that there is a correlation between the water resource evaluation of green buildings and the

distribution of buildings at all levels. Of the 171 cases analyzed, 5% of the buildings were classified as having near-zero water use (Level A), 1% as Extremely Water Efficient (Level B), 19% as Water Efficient (Level C), and 28% as Benchmark Water Efficient (Level D), all of which meet the evaluation criteria. Conversely, 37% of buildings were classified as not water-efficient (Level E), 6% as Water Consuming (Level F), and 4% as Extremely Water Consuming (Level G), indicating that the rating failed. It is worth noting that Grade III water-saving benchmark buildings and Grade IV non-water-saving buildings accounted for 65% of the total cases, consistent with the original green building cases, as shown in Figure 7.
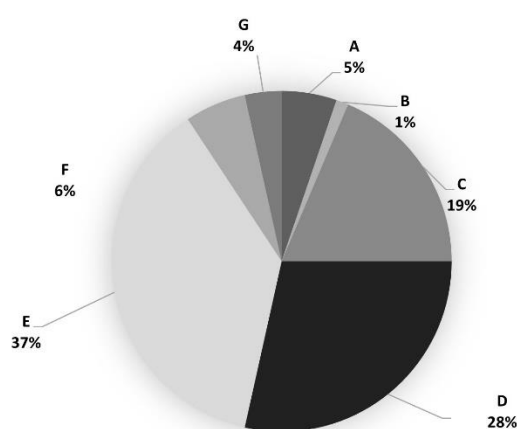
Figure 7－Non-Residential building Evaluation result percentage

5 Conclusion

Based on the analysis of the building WUI (Water Use Intensity) and the water efficiency of actual building cases, this study establishes water consumption benchmarks for both residential and non-residential buildings. The grading identification and evaluation system for building water use can encourage and promote the effective utilization of water resources by the public. In this research, we investigate the actual water consumption data from existing buildings in Taiwan, analyze the water use intensity per unit area across various building types, and determine a reasonable and accurate benchmark for building water consumption. We provide a summary of the annual average benchmark and a graded labeling system to assess water consumption. Additionally, this study integrates Taiwan's green building labeling system and carbon emission reduction evaluation system with water-saving technologies, marking the first step towards realizing near-zero water buildings.

References

Cheng Li Cheng, Sadahico Kawamura, Toward near-zero water consumption grade labelling and evaluation benchmarks for residential buildings. Journal of Asian Architecture and Building Engineering 2023.

State of Global Climate 2021 WMO provisional report, United Nations World Meteorological Organization, RMetS-General, https://www.rmets.org/news/wmo-provisional-report-state-global-climate-2021

Cheng, C.L.; Liao, W.J.; Liu, Y.C.; Tseng, Y.C.; Chen, H.J. Evaluation of CO_2 emission for saving water strategies. In Proceedings of the 38th International Symposium of CIB W062 on Water Supply and Drainage for Buildings, Edinburgh, UK, 28 August 2012.

C.L. Cheng, Study of the Interrelationship between Water Use and Energy Conservation for a Building, Energy and Buildings, UK 2002.

Presentation of Authors

Sadahico Kawamura is the Ph.D student at National Taiwan University of Science and Technology, Department of Architecture. His research is focus on energy conservation for green building.

Cheng-Li Cheng is the Professor at National Taiwan University of Science and Technology. He is a researcher and published widely on a range of water supply and drainage in building. He has published extensively on a range of sustainable issues, including the water and energy conservation for green building.

TECHNICAL SESSION 7 – LOW WATER CONSUMPTION BUILDINGS II

Economic feasibility of implementing rainwater harvesting systems for sustainable urban water management: A case study in Goiânia, Brazil.

L. M. Gonçalves (1) M. A. S. Campos (2)

(1) lanamarques.1@hotmail.com

(2) marcus_campos@ufg.br

(1) (2) School of Civil and Environmental Engineering, Federal University of Goiás, Goiânia, GO,.

Abstract

The search for sustainable cities is one of the premises of the early decades of the 21st century. Among these aspects, the use of rainwater emerges as an interesting alternative, both from the perspective of water saving and the reduction of drainage peak flows. Therefore, this study aims to evaluate the economic feasibility of implementing rainwater harvesting systems (RHS) on a large scale in a neighborhood located in Goiânia. Initially, this work sought to evaluate the current water management scenario in Brazil in the face of increasing demand, verifying that one way to improve it is by implementing this type of system. Furthermore, the study analyzed the possible advantages of this implementation, which, in addition to sustainability, could also bring about a reduction in urban drainage volume and financial savings. The methods used to determine feasibility were the Cost-Benefit Ratio and the Net Present Value. The 108 different scenarios analyzed, extending the analysis to the two localities with the highest and lowest water tariff in Brazil, showed that there is no economic viability in the case of private implementations without government subsidies. However, when studying the feasibility of implementation for the government, comparing this investment with the investment in urban drainage per inhabitant, it was noticed that there is a scenario among those analyzed in which the system becomes economically viable.

Keywords: ainwater harvesting, Particle Swarm optimization, reservoir sizing

1 Introduction

Water is a vital resource for human life, and its proper management is essential to meet the population's needs. Different human activities require different qualities of water, with urban water supply being an example that demands high standards. Factors such as

population growth, poverty reduction, economic expansion, rapid urbanization, and climate change drive the improvement of water management globally.

In Brazil, the National Water Resources Policy Law, enacted in 1997, establishes water as a public good and aims to ensure the availability of water with adequate quality for present and future generations. The water crisis that occurred in São Paulo in 2014 highlighted the importance of efficient water management, leading to measures such as water supply reduction and temporary water shortages (MARENGO, 2015).

A fundamental approach to avoid frequent supply crises is demand management, which seeks to reduce water consumption through measures such as efficient use in plumbing systems. Water conservation programs in buildings are important for controlling losses in hydraulic systems by establishing conservation policies, evaluating water usage, and monitoring the achieved results (SOUTO, PRADO, CAMPOS 2023).

Furthermore, investing in alternative water sources, such as greywater reuse and rainwater harvesting, is a measure to reduce the demand for potable water. Water reuse involves utilizing water from domestic and industrial wastewater for various applications, while rainwater harvesting consists of capturing and utilizing water from rainfall. These practices are encouraged by Brazilian legislation.

However, the implementation of these alternatives requires careful evaluation of costs, building structure, non-potable water demand, and regional impact. Cost-effectiveness and water quality should be considered, along with the effects of large-scale implementation of these systems in terms of reducing potable water consumption and stormwater effluents in the drainage network.

Given the challenges related to water in Brazil and the available alternatives, there is a justification for further exploring the subject in the present study. It is essential to seek economic and sustainable solutions to improve water management, considering the socio-environmental impact and implementing appropriate public policies.

The objective of this paper is to evaluate the economic feasibility of implementing rainwater harvesting systems (RHS) on a large scale in a brazilian neighborhood

2 Methods

This study was developed in the steps as presented in the following steps:

2.1 Choice of the region

Four criteria were used in selecting the neighborhood for studying the implementation of mass-implemented RWHS
- Being located in Goiânia;

- Having exclusively single-family buildings;
- Having fully constructed buildings;
- Having structurally similar buildings among themselves.

The neighborhood that met the aforementioned criteria belongs to the southeast region and is called Parque Atheneu. This neighborhood was developed in the 1980s. According to Souto (2019), it covers an area of 1.86 km² and has an estimated population of 14,068 inhabitants. In her work, data were collected regarding the lot areas, building coverage, permeable areas, and impermeable areas.

According to Souto; Prado; Campos (2023), who conducted statistical studies of the neighborhood under investigation in this research, a total of 3,584 residential lots were found. Furthermore, the author established three representative lot models for Parque Atheneu, differentiated by dimensions, which will be applied in this study. The characteristics of these three lots are shown in Table 1. Once the lots were characterized, the choice of RWHS to be used in the lots was made.

Table 1: Characterization of representative lots in Parque Atheneu.

	Lot 1	Lot 2	Lot 3
Number of lots	2551	857	176
Roof Area (m²)	151.24	208.75	967.52
Permeable area (m²)	23.71	66.71	61.33
Impervious area (m²)	66.11	106.93	411.82
Total area (m²)	241.06	382.40	1440.68

Fonte: Souto; Prado; Campos (2023)

2.2 Design of RWHS

RWHS used consisted of an underground reservoir and an upper reservoir. Since traditional Brazilian single-family homes already have an upper reservoir for potable water supply, the decision was made to indirectly supply rainwater as well.

Therefore, the system will store the collected water in the lower reservoir, which will supply the upper reservoir through a pump. After daily storage in the upper reservoir, it will gravity-feed the points of rainwater use.

For this study, it was decided to adopt four volumes for each type of lot. The first three volumes are the most common in the Brazilian market: 1, 5 and 10 m³. The fourth volume was calculated based on the lot, using the Netuno program (referred to as the optimal volume). This optimal volume is different for each of the standard lots used.

2.3 Demand determination

For both the simulation of lots and the definition of optimal volumes, it was necessary to define the demands of the three characteristic buildings. Based on the works of Pacheco (2016), Campos (2004), and NBR 15527 (2019), the following demands were determined:

• 6.8 liters/flush per resident, with a total of 6 discharges per day.
• 2.4 liters/square meter for gardening, with a frequency of 3 times per week (Monday, Wednesday, and Friday).
• External floor cleaning only occurs on Saturdays. On weekdays, cleaning is done with a cloth and bucket, totaling 0.5 liters/square meter. On Saturdays, cleaning is done with a broom, a squeegee, and a bucket, totaling 1.0 liter/square meter.
• Finally, external floor cleaning and gardening only occur in months with an average monthly precipitation below 200 mm. Thus, Tables 2 presents the demands considered for the typical year.

Table 2 : Rainwater Demand for a typical year

Months	Weekdays	Toilet Flushinga (L/person)	External floor cleaning (L/peron)			gardening (L/person)			Total (L/person)		
			L1	L2	L3	L1	L2	L3	L1	L2	L3
November to March	Sunday	40.80	0.00	0.00	0.00	0.00	0.00	0.00	40.80	40.80	40.80
	Monday	40.80	0.00	0.00	0.00	0.00	0.00	0.00	40.80	40.80	40.80
	Tuesday	40.80	0.00	0.00	0.00	0.00	0.00	0.00	40.80	40.80	40.80
	Wednesday	40.80	0.00	0.00	0.00	0.00	0.00	0.00	40.80	40.80	40.80
	Thursday	40.80	0.00	0.00	0.00	0.00	0.00	0.00	40.80	40.80	40.80
	Friday	40.80	0.00	0.00	0.00	0.00	0.00	0.00	40.80	40.80	40.80
	Saturday	40.80	0.00	0.00	0.00	0.00	0.00	0.00	40.80	40.80	40.80
April to October	Sunday	40.80	0.00	0.00	0.00	0.00	0.00	0.00	40.80	40.80	40.80
	Monday	40.80	5.87	7.58	8.48	7.74	14.16	20.42	54.41	62.54	69.71
	Tuesday	40.80	5.87	7.58	8.48	0.00	0.00	0.00	46.67	48.38	49.28
	Wednesday	40.80	5.87	7.58	8.48	7.74	14.16	20.42	54.41	62.54	69.71
	Thursday	40.80	5.87	7.58	8.48	0.00	0.00	0.00	46.67	48.38	49.28
	Friday	40.80	5.87	7.58	8.48	7.74	14.16	20.42	54.41	62.54	69.71
	Saturday	40.80	11.73	15.16	16.96	0.00	0.00	0.00	52.53	55.96	57.76

The usable volume for each of the analyzed systems was also determined. Table 3 presents these values to all the situations.

Table 3: Daily Usable Volume

	Tank´s volume (m³)											
	1			5			10			Ideal		
	Volume (L/day)											
	L1	L2	L3	L1	L2	L3	L1	L2	L3	L1	L2	L3
Jan	188.68	190.90	191.22	204.00	204.00	204.00	204.00	204.00	204.00	204.00	204.00	204.00
Feb	188.16	190.99	190.73	204.00	204.00	204.00	204.00	204.00	204.00	204.00	204.00	204.00

Mar	191.91	193.72	193.81	204.00	204.00	204.00	204.00	204.00	204.00	204.00	204.00	204.00
Apr	142.87	153.95	158.54	240.39	262.23	275.50	251.08	273.85	292.07	251.08	273.85	292.07
Mai	46.32	50.89	51.22	123.77	141.23	143.06	223.09	241.78	245.98	248.62	270.38	245.98
Jun	17.82	19.73	19.84	42.28	54.70	54.49	90.25	107.57	103.44	250.11	272.59	103.44
Jul	3.15	4.31	4.40	4.15	6.48	6.31	9.35	11.67	11.51	249.57	266.83	11.51
Aug	14.29	16.59	17.14	21.32	26.86	28.45	21.32	26.86	28.45	211.10	164.33	28.45
Sep	63.48	70.41	72.14	94.33	114.22	120.58	94.33	115.57	122.52	134.82	126.47	122.52
Oct	148.46	164.30	168.91	200.00	226.57	240.02	201.57	231.03	245.45	205.31	234.33	245.45
Nov	184.04	187.52	187.79	202.64	204.00	204.00	202.64	204.00	204.00	204.00	204.00	204.00
Dec	196.03	197.53	197.90	204.00	204.00	204.00	204.00	204.00	204.00	204.00	204.00	204.00

2.4 Economic evaluation

The evaluation of this system was based on two indicators: Net Present Value (NPV) and Benefit-Cost Ratio (BCR). To perform the evaluation, it was necessary to obtain the initial investment, revenue, and operational costs associated with the system.

The implementation costs were estimated using the National System of Prices and Indices for Civil Construction (SINAPI), [1]and in some cases, values were researched through surveys obtained from two different suppliers.

Additionally, to estimate the values of reinforced concrete reservoirs, an equation from Carvalho's work (2016) was used. The equation is represented by Equation 1 below.

$$C_{reservatório} = 3,200132254.10^{-6}.V^2 + 0,2908308367.V + 5996,358556 \quad \text{(EQ 1)}$$

where V is the volume of the reservoir in question.

For energy consumption, a daily operation of the pump for 6 hours was considered, and the adopted energy tariff was based on a residential kWh rate from the local energy utility (ENEL) in 2019, which was R$ 0.869.

The cleaning costs are related to the labor of a janitor, with the hourly wage obtained from SINAPI (2019) being R$ 9.84. Finally, the other values were estimated in the city of Goiânia in October 2019.

The economic return was calculated based on the savings generated from expenses on potable water (usable rainwater volume) versus water and sewage tariff. Three scenarios were used for the water tariff. The reference scenario was the price practiced in the city of Goiânia, and the other two were based on the tariffs of the cities of Maceió and Rio Branco, the highest and lowest tariffs, respectively, according to SNIS (2019). The corresponding values were R$ 11.52 and R$ 4.40. These values include the water tariff plus the collection, disposal, and treatment factors.

---

[1] From September of 2019

To determine the indicators, it was also necessary to define the adjustments for both the water tariff and the maintenance and operation costs. Three scenarios were used:

- Local utility for the water tariff and INCC (Brazilian National Civil Construction Index) for system operations and maintenance;
- IPCA for water, system operations, and maintenance;
- IGPM for water, system operations, and maintenance.

Historical data related to the indicated rates were obtained for the study of the three possibilities, as shown in Table 4.

Table 4: Adjustments of the adopted indexes

	2006	2007	2008	2009	2010	2011	2012	2013	2014	2015	2016	2017	2018	2019	**Média**
SANEAGO	-	3.4	4.4	6.4	3.0	5.8	8.2	3.4	5.7	2.3	44.7	6.3	3.4	5.8	**7.9**
IPGM	3.8	7.7	9.8	-1.7	11.3	5.1	7.8	5.5	3.7	10.5	7.2	-0.5	7.5	4.1	**5.8**
INCC	5.0	6.0	11.9	3.2	7.5	7.6	7.2	8.0	6.7	7.2	6.3	4.0	4.0	3.7	**6.3**
IPCA	3.1	4.4	5.9	4.3	5.9	6.5	5.8	5.9	6.4	10.7	6.3	2.9	3.7	2.5	**5.3**

Fontes: IBGE(2019); Portal Brasil (2019); SANEAGO (2019)

In addition to these, it was necessary to define the minimum attractive rate. Similarly to Carvalho (2017), three rates were used, thus considering variations in economic scenarios. The first rate was the long-term interest rate in Brazil (TJLP Brasileira). The second value considered was the current Brazilian TJLP, which is 5.95% per year. The third value was the Brazilian TJLP plus a risk premium of 5.4% due to the investment risk (BNDES, 2019). The fourth value used was the TJLP of Chile, an emerging country with a similar economic situation to Brazil, allowing for a comparison between both, equal to 3.0% per year (TRADING ECONOMICS, 2019).

Thus, to analyze the economic viability, a total of 108 scenarios were analyzed for the city of Goiânia, which consisted of combinations of the following variables

• Three scenarios of tariff value adjustments and system operations and maintenance;
• Four lower reservoir volumes;
• Three lot modeling for implementation;
• Three minimum attractive rates.

2.5 Results analysis

Once the indicators were obtained, it was possible to determine the investment viability both in terms of individual aspects and mass application. It should be noted that the entire analysis was based solely on the reduction of water consumption. Benefits from

the perspective of drainage reduction were not considered. This consideration of using only potable water reduces the obtained benefits and, consequently, reduces the economic viability of the system.

The analysis considered aspects related not only to individual use but also the benefits that the entire community would receive, even if not directly, such as increased water availability, reducing potential future supply failures.

4 Results

This item presents all the results obtained from the analyses carried out on lots 1, 2, and 3. This includes the entire design development , as well as all the sizing and budgeting associated with it, culminating in the verification of the final economic feasibility of this system under the considered assumptions.

4.1 Design developments

Certain construction characteristics were adopted for the sizing of the system, including:
• The ceiling height of the three residential typologies was set at 3 meters.
• The chosen roofing material was ceramic tiles, with a gable roof design inclined at 30% for lots 1 and 2, and 15% for lot 3.
•. Following the guidelines of NBR 10844 (ABNT, 1989), RWHS was sized.

In regards to the sizing of the rainwater distribution system, it was necessary, in addition to the pipes, which followed the NBR 5626/1998 standard, to incorporate a pump systemt. The sizing of the pump utilized data on estimated daily consumption per person for each month, obtained from Souto (2019), in order to size it for the month with the highest consumption.

Based on the performed sizings, it was possible to estimate the quantity of materials for the system per lot type, with unit costs obtained from the July 2019 data of the National System of Prices and Indices of Civil Construction (SINAPI), as well as private quotations made in October 2019. This budget, along with other variables necessary for the economic evaluation, is presented in the next item.

4.2 RWHS feasibility analysis

The first step in determining the economic feasibility of RWHS was the assessment of the initial investment. The assessment was conducted, as described in the methodology, through information obtained from SIAPE. Table 5 presents the summary of investment values, considering both each of the reservoirs in each of the lots, as well as the total investment considering the percentage of lot implementation.

Table 5: Total initial investment per lot and lower reservoir.

	UNITS	UNIT COSTS (R$)			
		1 m^3	5 m^3	10 m^3	Ideal Volume
LOT 1	2251	5,394.22	6,706.31	8,500.23	11,040.74
LOT 2	857	7,322.31	8,634.40	10.428.32	12,986.25
LOT 3	176	30,705.45	32,017.54	33,811.46	36,351.68
	TOTAL COSTS (R$)				
	10%	25%	50%	75%	100%
1 m^3	2,544,003.41	6,360,008.52	12,720,017.05	19,080,025.57	25,440,034.09
5 m^3	3,014,256.47	7,535,641.16	15,071,282.33	22,606,923.49	30,142,564.65
10 m^3	3,657,197.39	9,142,993.48	18,285,986.97	27,428,980.45	36,571,973.93
Ideal Volume	4,567,661.37	11,419,153.42	22,838,306.84	34,257,460.25	45,676,613.67

Based on the data of the usable volume and the water tariff value in the city of Goiânia, and additionally for Maceió (highest water tariff value in Brazil) and Rio Branco (lowest water tariff value in Brazil), the revenue values for the three lot typologies were obtained.

Based on the expenses and revenues for each system, it was possible to obtain the economic variables. As, an example Tables 6, present the economic feasibility of lots 1, with the minimum attractive rate of 1%

Table 6: Feasibility analysis – Lot 1

Initial investment	Volume (m³)	Adjustment	Minimmum atractive rate	BCR	NPV
R$ 5,394.22	1	1	3.00%	R$ 0.25	-R$ 8,828.35
R$ 5,394.22	1	2	3.00%	R$ 0.21	-R$ 8,789.91
R$ 5,394.22	1	3	3.00%	R$ 0.21	-R$ 8,838.29
R$ 6,706.31	5	1	3.00%	R$ 0.30	-R$ 9,872.50
R$ 6,706.31	5	2	3.00%	R$ 0.25	-R$ 9,855.14
R$ 6,706.31	5	3	3.00%	R$ 0.25	-R$ 9,900.00
R$ 8,500.23	10	1	3.00%	R$ 0.31	-R$ 11,540.51
R$ 8,500.23	10	2	3.00%	R$ 0.26	-R$ 11,533.06
R$ 8,500.23	10	3	3.00%	R$ 0.26	-R$ 11,576.27
R$ 11,040.74	Ideal	1	3.00%	R$ 0.39	-R$ 13,600.99
R$ 11,040.74	Ideal	2	3.00%	R$ 0.32	-R$ 13,631.30
R$ 11,040.74	Ideal	3	3.00%	R$ 0.33	-R$ 13,668.21

Analyzing the data shown above, it was found that the systems are not viable, regardless of the indicator considered. It is observed that the initial investment is responsible for the negative result presented. Therefore, it was decided to perform the analysis disregarding the initial investment. This situation serves to simulate how the behavior would be if there were a government incentive.

To verify the feasibility of application proportions (10%, 25%, 50%, and 100%), data related to scenario 1 were analyzed, with a minimum attractive rate of return equal to Brazil's TJLP. The results are shown in Table 7. The BCR (l Benefit-Cost Ratio) for all percentages obtained for the same parameter had the same values, hence its value is generalized and placed on the left.

Table 7: BCR and NPV in implementation percentages - Scenario 1

	BCR	10% NPV (R$)	25% NPV (R$)	50% NPV (R$)	75% NPV (R$)	100% NPV (R$)
				LOT 1		
1	0.23	- 1,757,985.94	- 4,394,964.86	- 8,789,929.72	- 13,184,894.57	- 17,579,859.43
5	0.27	- 2,062,056.80	- 5,155,142.00	- 10,310,283.99	- 15,465,425.99	- 20,620,567.99
10	0.27	- 2,505,137.76	- 6,262,844.39	- 12,525,688.79	- 18,788,533.18	- 25,051,377.58
Ideal	0.33	- 3,100,459.84	- 7,751,149.61	- 15,502,299.21	- 23,253,448.82	- 31,004,598.43
				LOT 2		
1	0.22	- 753,478.87	- 1,883,697.19	- 3,767,394.37	- 5,651,091.56	- 7,534,788.75
5	0.27	- 854,242.21	- 2,135,605.54	- 4,271,211.07	- 6,406,816.61	- 8,542,422.15
10	0.28	- 1,002,786.40	- 2,506,965.99	- 5,013,931.98	- 7,520,897.96	- 10,027,863.95
Ideal	0.33	- 1,204,145.96	- 3,010,364.89	- 6,020,729.79	- 9,031,094.68	- 12,041,459.58
				LOT 3		
1	0.12	- 566,213.52	- 1,415,533.81	- 2,831,067.62	- 4,246,601.44	- 5,662,135.25
5	0.15	- 586,779.65	- 1,466,949.13	- 2,933,898.27	- 4,400,847.40	- 5,867,796.53
10	0.15	- 617,254.05	- 1,543,135.13	- 3,086,270.26	- 4,629,405.38	- 6,172,540.51
Ideal	0.15	- 661,961.94	- 1,654,904.85	- 3,309,809.69	- 4,964,714.54	- 6,619,619.38

In this analysis, it was observed that to the BCR calculation, the change in water tariff had a greater influence on the return value. This can be explained by the equation itself, where revenue is updated with the attractiveness rate alone. Similarly, the limited impact of this change on the NPV can be explained by the equation as well. By discounting the initial investment, the change in water revenue becomes relatively small compared to the investment value in system implementation. Even in scenarios with higher possibilities of having a positive cash flow and potential economic viability over a 20-year lifespan, the cash flows were negative throughout the entire system's lifespan. This resulted in negative Net Present Values and a Benefit-Cost Ratio lower than one.

Based on the collected data and feasibility studies conducted, it was concluded that the system, under the considered conditions, does not have a viable economic implementation.

It was estimated the total consumption of potable water for the neighborhood to be 777,309.05 m³/year. For implementation cases of 10%, 25%, 50%, 75%, and 100%, the annual water consumption values in the city of Goiânia resulting from RWHS are presented in Table 8.

Tabela 82: Total Demand Volume and percentage of demand supplied by rainwater

	1 m³	5 m³	10 m³	Ideal
Volume (m³/year)	152,233.5	193168.2	211643.3	279201.1
10%	1.96%	2.49%	2.72%	3.59%
25%	4.90%	6.21%	6.81%	8.98%
50%	9.79%	12.43%	13.61%	17.96%
75%	14.69%	18.64%	20.42%	26.94%
100%	19.58%	24.85%	27.23%	35.92%

For the purpose of comparison, a search was conducted for the price per capita of water supply and drainage shares. It was found in Cruz ;Tucci (2008) where the authors took a survey from 2006 on the average cost of implementing the drainage network per additional inhabitant in the basin, which amounted to R$ 174.63. Updating this value based on the INCC for 2019, the government funding for the concession of reservoirs in 100% of the lots was compared with the implementation of urban drainage corresponding to the increase in a contingent of people responsible for demanding an annual amount of water equal to the annual savings of the RWHS. By considering the average daily demand per person, which is 49.42 liters, it was calculated the number of people and the savings obtained for the four reservoir typologies. These results are shown in Table 9.

Table 9 : Comparison of investment in RWHS and implementation of urban drainage

	Volume of lower reservoir			
	1 m³	5 m³	10 m³	Ideal
Equivalent in people	8439.83	10709.25	11733.51	15478.91
Urban drainage cost	R$ 3,310,729.88	R$ 4,200,965.42	R$ 4,602,756.47	R$ 6,071,981.29
Reservoir´s cost	R$ 1,285,616.64	R$ 5,988,147.20	R$ 12,417,556.48	R$ 21,522,751.03
Savings (%)	61.17%	-42.54%	-169.79%	-254.46%

As seen, for the 1 m³ typology, there was a savings of 61.17%, which becomes an interesting alternative in terms of governmental financial savings. However, if the government were to provide a portion of the total initial investment in the systems, it would contribute at most 36% of the total investment.

5 Conclusion

The analysis initially conducted at the beginning of this study refers to the viability of the system in terms of the financial return generated for the implementer, that is, in terms of directly measurable benefits. However, it is known that there are indirect benefits generated by the system, such as the reduction in drainable water volume in cities. This contribution, naturally, does not negate the need for improvement in the urban drainage systems of some Brazilian regions. However, it represents a short-term palliative measure and a long-term complementary approach.

In this regard, suggestions can be offered for alternative public subsidies to stimulate implementations, such as tax reductions, discounts on electricity bills, access to lower-interest financing options, among others. In the case of the possibility of public subsidies for the total initial investment, for example, it was found that the system is still unviable. However, the Net Present Value (NPV) values, as observed, remained in the range of R$ - 1000.00 per system.

Furthermore, with the latest analysis, it was observed that the total volume of water saved by the RWHS in the 1 m³ reservoir typology, with government donation of these reservoirs, when converted into urban drainable volume due to population growth in the neighborhood, would result in approximately 60% savings for the government, as the theoretical investment to be made in the drainage system is much higher than the investment in the neighborhood's RWHS. This represents economic viability for the government.

Therefore, a relevant analysis is as follows: are the methods of economic viability that are adopted to conclude unfeasibility truly effective when worked on independently? Individually, the NPV and BCR do not prove to be entirely effective methods for decision-making based solely on them, requiring a broader, indirect, and not solely numerical analysis. Being strictly numerical, they do not take into account the indirect (and largely positive) impacts generated by a mass implementation of this system, such as the reduction in the volume of water to be drained in cities and the achievement of sustainability, which is of great relevance.

Thus, there is a need to broaden the horizons of analysis for this type of system, linking and interacting it with other systems and factors, as mentioned earlier. Finally, this obtained feasibility reinforces the need to continue conducting more in-depth studies regarding the relationship among sequential RWHS implementations and long-term cost savings in the extension of urban drainage system implementations in cities.

6 References

ASSOCIAÇÃO BRASILEIRA DE NORMAS TECNICAS (BRAZILIAN ASSOCIATION OF TECHNICAL STANDARDS). NBR 10844: Stormwater Building systems.. Rio de Janeiro,. 1989 (in portuguese)

ASSOCIAÇÃO BRASILEIRA DE NORMAS TECNICAS. NBR 5626: Potable Water Building Service Rio de Janeiro. 1998 (in portuguese).

BNDES: BANCO NACIONAL DO DESENVOLVIMENTO. Long-Term Interest Rate: TJLP (Long-Term Interest Rate). Available em: https://www.bndes.gov.br/wps/portal/site/home/financiamento/guia/custos-financeiros/taxa-juros-longo-prazo-tjlp. Acess em: 24th of june de 2019

CARVALHO, L. P. Financial Analysis of Rainwater Harvesting Systems in Social Housing.. 2017. p. 184. Master´s Dissertation Master´s Program of Structure, Geotechinical and Civil Construction - Federal University of Goiás, Goiânia (GO), 2016. (in Portuguese).

CRUZ, M. A. S.; TUCCI, C. E. M. *Evaluation of Urban Drainage Planning Scenarios* Rio Grande do Sul, v. 13, n. 3, p. 59-71, set. 2008. (In portuguese)

IBGE: INSTITUTO BRASILEIRO DE GEOGRAFIA E ESTATÍSTICA. National Broad Consumer Price Index – IPCA . Available em: https://www.ibge.gov.br/estatisticas/economicas/precos-e-custos/9256-indice-nacional-de-precos-ao-consumidor-amplo.html?=&t=o-que-e. Acess em: Outubro de 2019. (in portuguese).

MARENGO, J. A.; ALVES, L. M. *Water Crisis in São Paulo in 2014: Drought and Deforestation. Geousp - Space and Time (Online)* v. 19, n. 3, p. 485-494, 2016. ISSN 2179-0892 (In portuguese)

PORTAL BRASIL. General Market Price Index - IGP-M. Available em: http://www.portalbrasil.net/igpm.htm. Acess em: Setembro de 2019. (in portuguese).

PORTAL BRASIL. National Construction Cost Index of the Market.. Available em: https://www.portalbrasil.net/incc.htm. Acess em: Setembro de 2019. (in portuguese).

SOUTO, S. L. Building Rainwater Harvesting System: Potential and Urban-Level Impact." Master´s Dissertation 2019.. Master´s Program of Structure, Geotechinical and Civil Construction. Federal University of Goiás Goiânia (GO), (in Portuguese).

SOUTO, Sara Lopes; REIS, Ricardo Prado Abreu; CAMPOS, Marcus André Siqueira. Impact of Installing Rainwater Harvesting System on Urban Water Management. *Water Resources Management*, v. 37, n. 2, p. 583–600, 2023.

SINAPI: NATIONAL SYSTEM OF PRICES AND INDICES OF CIVIL CONSTRUCTION – a partir Jul/2009 -GO. Available em: http://www.caixa.gov.br/site/Paginas/downloads.aspx#categoria_646. Acess em: Setembro de 2019. (in portuguese).

SNIS: NATIONAL SYSTEM OF INFORMATION ON SANITATION. Available em: http://snis.gov.br/. Acess em: 10 de outubro de 2019. (in portuguese).

TRADING ECONOMICS. Chile: Taxa de Juro, 2019. Available em: https://pt.tradingeconomics.com/chile/interest-rate. Acess em: 24 de junho de 2019.

6 Presentation of Author(s)

Lana Marques is a civil engineer and mathematician. .

Marcus André Siqueira Campos is professor at School of Civil and Environmental Engineer of University of Goiás and he is head of the Graduate Program of Structure, Geothecnical and Civil Construction. He is also father of Maria Luiza.

CO₂ Emissions from Water Supply Facilities and Rainwater Utilization Facilities in Japan

Ukyo Takeuchi (1)，Takehiko Mitsunaga (2)

(1) ce223041@meiji.ac.jp

(2) mitsunaga@meiji.ac.jp

(1)(2) Dep. of Architecture, School of Science & Technology, Meiji University, Japan

Abstract

In the background of global warming, the importance of efforts toward a decarbonized society is increasing. In Japan, the Law on the Promotion of Rainwater Utilization took effect in 2014, encouraging the promotion of rainwater utilization. Rainwater utilization are expected to reduce CO_2 emissions. Quantitative information on CO_2 emissions from water supply facilities, which can be used as a comparison, has only been studied on a regional basis. However, in Japan's water suppliers, water purification methods and other factors that affect CO_2 emissions vary by municipality. In order to substantially evaluate the CO_2 emissions reductions from rainwater utilization facilities, it is necessary to organize the CO_2 emissions intensity per unit of water volume for each water supply.

This study aims to identify trends among water suppliers that have a high advantage in rainwater utilization by calculating CO_2 emissions intensity for each water supplier, in order to quantitatively verify the effect of rainwater utilization on CO_2 emissions reduction. This study utilizes the 2018−2020 edition of "Water Supply Statistics" to calculate the CO_2 emissions intensity from water intake and conduction, water purification, and water delivery and distribution facilities for water supply. Then, CO_2 emissions intensity from water suppliers are compared with that by rainwater utilization. In consequence, we identify the CO_2 emissions intensity for each water suppliers throughout Japan, and these trends. And we examine the advantages of rainwater utilization.

Keywords

CO2 emission, Rainwater utilization, Water supply facility, Water purification method.

1 Introduction

In the background of global warming, the importance of efforts toward a decarbonized society is increasing. In Japan, the Law on the Promotion of Rainwater Utilization [1] took effect in 2014, encouraging the promotion of rainwater utilization. In FY2020, 177 new rainwater utilization facilities were installed, and at least 4,037 facilities [2] have been identified nationwide as of the end of FY2020. Rainwater utilization is expected to reduce the burden on sewage infrastructure through flood control and utilization, and reduce CO_2 emissions because of decreased water supply volume. Quantitative information on CO_2 emissions from water supply facilities, which can be used as a comparison, has only been studied on a regional basis [3]. However, in Japan's water suppliers, water purification methods and other factors that affect CO_2 emissions vary by municipality. The water supply are located in 1,312 locations throughout Japan's 47 prefectures [4], and the characteristics such as purification methods differ depending on water suppliers. Therefore, in order to practically evaluate the reduction of CO_2 emissions by rainwater utilization, it is necessary to organize the trends of water suppliers' CO_2 emissions intensity per unit of water volume, but the studies are limited to regional basis.

This study aims to identify trends among water suppliers that have a high advantage in rainwater utilization by calculating CO_2 emissions for each water supplier, in order to quantitatively verify the effect of rainwater utilization on CO_2 emissions reduction.

2 Survey method

2.1 Surveyed items

In this study, we selected 1,162 water suppliers for which three years of data were available and which were determined to be the same water suppliers based on the prefecture number and serial number listed in the 2018−2020 edition of "Water Supply Statistics" [4]−[6]. Water suppliers with an annual water purification volume of 0 m^3 were excluded from the analysis. Table 1 shows the surveyed items. Water suppliers in Japan have different CO_2 emissions intensity depending on the electricity company that supplies them with electricity.

<div align="center">

Table 1 – Surveyed items[4]−[6]

</div>

Purpose of use	Data items
Determination of main purification methods	Water purification volume by method ("Only disinfection"*, "Slow sand filtration", "Rapid sand filtration", "Membrane filtration")
Classification of water supply scale	Water supply volume
Primary energy consumption calculation	Electricity and fuel consumption
CO_2 emissions calculation	Contracted electricity company, Electricity and fuel consumption

*"Only disinfection" refers to water purification methods using chlorine disinfection, and includes cases where chlorine disinfection is used in combination with ultraviolet treatment, de-ironing, de-manganese removal, and other purification methods.

2.2 Water purification and supply volume

Figure 1 shows relationship between water purification and supply volume. Positive correlation was strong. Water supply volume was defined as the volume of water including diversion. Water purification volume is the total volume of water purified by "Only disinfection", "Slow sand filtration", "Rapid sand filtration", and "Membrane filtration".

As a result, water suppliers with higher water purification volumes tend to supply more water. "Water supply volume"> "water purification volume" indicates that a portion of the purified water is received from other facilities, while "water purification volume" > "water supply volume" indicates that a certain amount of water is taken and purified regardless of the water supply volume. There were 829 water suppliers where the greater of either water purification or water supply volume was within 1.5 times the lesser. After this, we included the 829 water suppliers described in Figure 1 to analyze the water suppliers that perform the series of processes from water intake to water distribution in proper quantities.
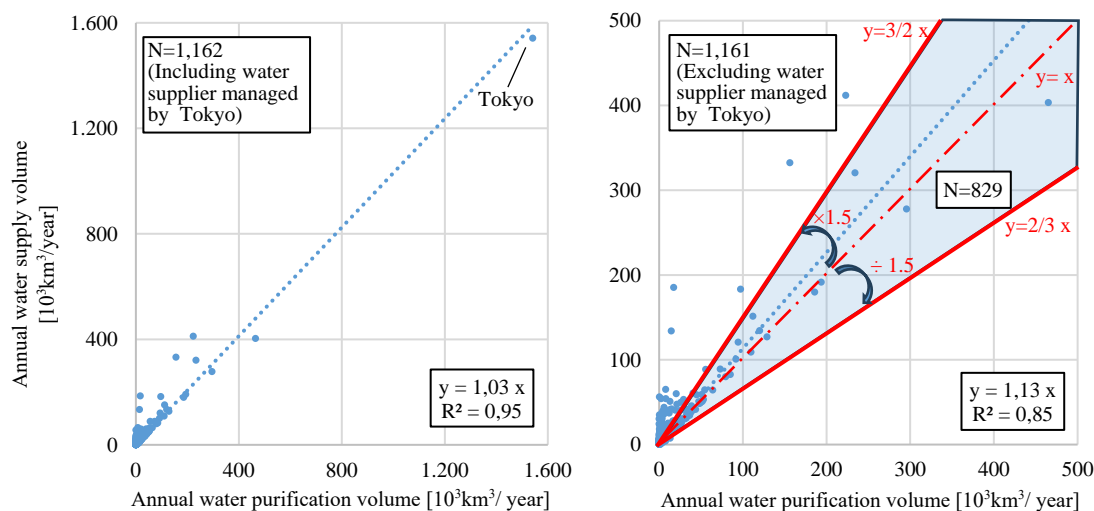
Figure 1 – Relationship between water purification and supply volume

2.3 Primary energy consumption and CO$_2$ emissions

Only major Japanese electricity companies were included in the analysis, and water suppliers that changed their contracted electricity companies over a three-year period were excluded from the analysis. Water suppliers with primary energy consumption intensity less than 1.0 were also excluded because of possible regional peculiarities. We also excluded outliers based on the Interquartile Range (IQR) method (outliers are values outside the range of 1.5×IQR (top 25%−bottom 25%) up from the top 25% and 1.5× IQR down from the bottom 25%).

2.3.1 Consumption of relevant items
・Electricity consumption
Electricity consumption for water intake and conduction, water purification, and water delivery and distribution facilities for water supply was calculated in total.

・Fuel consumption
The total amount of thermal coal, gasoline, city gas, kerosene, diesel oil, heavy oil A, heavy oil B and C, and LPG, LNG consumption was calculated in total.

2.3.2 Coefficient

Primary energy consumption and CO$_2$ emissions were calculated by multiplying the amount of each item used calculated above by the coefficients. Table 2 shows primary energy consumption intensity and CO$_2$ emissions intensity associated with electricity and fuel consumption, which are used as the coefficients [7][8]. The primary energy consumption intensity per unit of electricity consumption was used 8.64 MJ/kWh, the average for FY 2018−2020.

Table 2 –Primary energy consumption and CO$_2$ emissions intensity [7][8]

		Primary energy consumption intensity	CO$_2$ emissions intensity
Electricity Company	Hokkaido, Tohoku, Tokyo, Chubu, Hokuriku, Kansai, Chugoku, Sikoku, Kyusyu, and Okinawa	8.64 [MJ/kWh]	The respective coefficients are shown in Figure 2 below.
Fuel	Thermal coal	25.7 [MJ/kg]	2.33 [kg-CO$_2$/kg]
	Gasoline	34.6 [MJ/L]	2.32 [kg-CO$_2$/L]
	City gas	44.8 [MJ/Nm^3]	2.23 [kg-CO$_2$/Nm^3]
	Kerosene	36.7 [MJ/L]	2.49 [kg-CO$_2$/L]
	Diesel oil	37.7 [MJ/L]	2.58 [kg-CO$_2$/L]
	Heavy oil A	39.1 [MJ/L]	2.71 [kg-CO$_2$/L]
	Heavy oil B and C	41.9 [MJ/L]	3.00 [kg-CO$_2$/L]
	LPG (Liquefied petroleum gas)	50.8 [MJ/kg]	3.00 [kg-CO$_2$/L]
	LNG (Liquefied natural gas)	54.6 [MJ/kg]	2.70 [kg-CO$_2$/L]

Figure 2 shows the CO_2 emissions intensity per unit of electricity consumption for each electricity company. The CO_2 emissions intensity varies from year to year for each electricity company. Japan's major electricity companies are Hokkaido, Tohoku, Tokyo, Chubu, Hokuriku, Kansai, Chugoku, Shikoku, Kyushu, and Okinawa Electricity Company. The three-year average of CO_2 emissions intensity for each electricity company was the highest for "Okinawa Electricity Company" at 0.778 kg-CO2/kWh and the lowest for "Kyushu Electricity Company" at 0.343 kg-CO2/kWh.
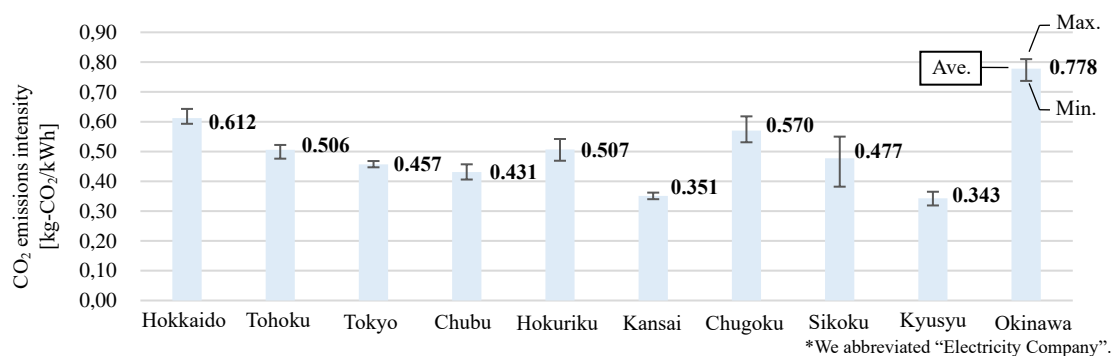
Figure 2 – CO_2 emissions intensity for each electricity company

3 CO_2 emissions from water suppliers in Japan

3.1 Main purification method for each water supply scale

Table 3 shows the number of water suppliers by main purification method for each water supply scale. The purification method with a purification volume exceeding 80% of the total water purification volume was considered the main purification method. "None" indicates that there is no main purification method. "Only disinfection" and "Rapid sand filtration" were relatively common, while "Slow sand filtration" and "Membrane filtration" were relatively few, at about the same level. The proportion of rapid "Rapid sand filtration" tended to increase with water supply scale.

Table 3 – Main purification method for each water supply scale

Water supply scale [km³/year]	The number of water suppliers(percentage)	Main purification method				
		Only Disinfection*	Slow sand filtration	Rapid sand filtration	Membrane filtration	None
−1000	144(100%)	49(33%)	8(6%)	40(28%)	7(5%)	40(28%)
1,001−5,000	545(100%)	199(37%)	16(3%)	144(26%)	15(3%)	171(31%)
5,001−10,000	201(100%)	66(33%)	3(1%)	67(34%)	6(3%)	59(29%)
10,001−50,000	235(100%)	66(28%)	5(2%)	96(41%)	2(1%)	66(28%)
50,001−	37(100%)	2(5%)	0(0%)	25(68%)	0(0%)	10(27%)
Total	1,162(100%)	382(32%)	32(3%)	372(32%)	30(3%)	346(30%)

3.2 Primary energy consumption and CO_2 emissions intensity

3.2.1 Relationship between water supply volume and primary energy consumption

Figure 3 shows relationship between water supply volume and primary energy consumption. Positive correlation was strong. It was found that the higher the water supply volume, the higher the primary energy consumption.
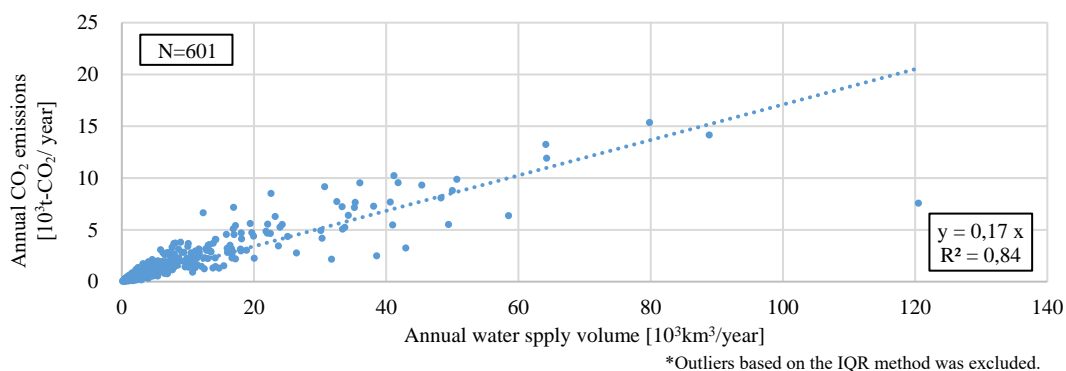

*Outliers based on the IQR method was excluded.
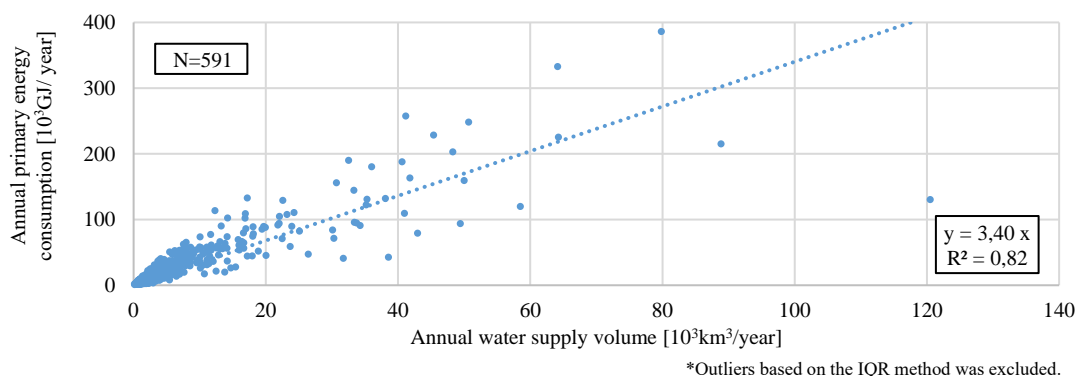
**Figure 3 – Relationship between water supply volume
and primary energy consumption**

3.2.2 Relationship between water supply volume and CO_2 emissions

Figure 4 shows relationship between water supply volume and CO_2 emissions. Positive correlation was strong. It was found that the higher the water supply volume, the higher the CO_2 emissions.

*Outliers based on the IQR method was excluded.

Figure 4 – Relationship between water supply volume and CO_2 emissions

3.2.3 Primary energy consumption and CO_2 emissions intensity

Table 4 shows primary energy consumption and CO_2 emissions intensity. The difference between the maximum and minimum values for both primary energy consumption and CO_2 emissions intensity was large. This seems to be because of differences in purification methods, water supply scale, and contracted electricity companies.

Table 4 – Primary energy consumption and CO_2 emissions intensity

	Primary energy consumption intensity ［MJ/m³］	CO_2 emissions intensity ［kg-CO_2/m³］
Maximum	10.33	0.550
Average	5.00	0.261
Median	4.86	0.245

*Water suppliers with primary energy consumption intensity less than 1.0 were excluded.

*Outliers based on the IQR method was excluded.

3.3 CO_2 emissions intensity for each purification method

Figure 5 shows CO_2 emissions intensity for each purification method. As a result, "Membrane filtration" has the largest CO_2 emissions intensity, with an average of 0.282 kg-CO_2/m³. This seems to be because "Membrane filtration" requires a large amount of pressure to be applied when water is allowed to permeate the membrane. Compared to the "Overall" average of 0.261 kg-CO_2/m³, the "Membrane filtration" was larger than the "Overall", while the other purification methods showed little difference.

Citing and calculating values from a report published by the Bureau of Waterworks of the Tokyo Metropolitan Government for 2018−2020 [9], the percentages of total electricity consumption for "Water intake and conduction processes", "Water purification processes", and "Water delivery and distribution processes" were respectively 4.4%, 34.2%, and 61.4% on average for the three years. Therefore, the impact of differences in purification method on CO_2 emissions intensity is expected to be small.
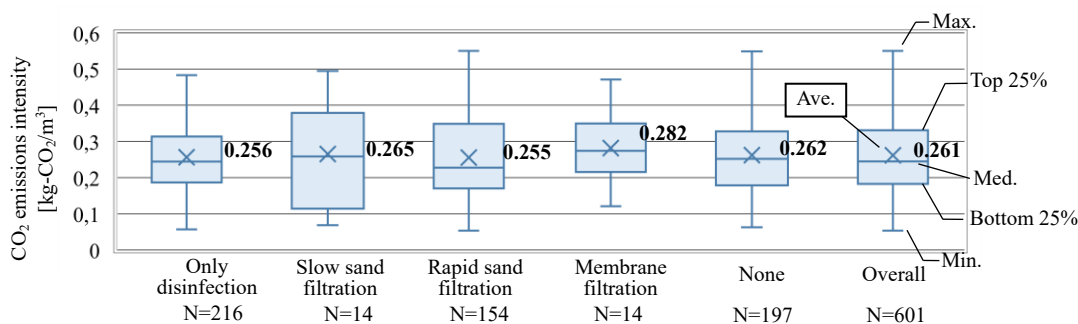
*"Only disinfection" refers to water purification methods using chlorine disinfection, and includes cases where chlorine disinfection is used in combination with ultraviolet treatment, de-ironing, de-manganese removal, and other purification methods.

*Outliers based on the IQR method was excluded.

Figure 5 – CO_2 emissions intensity for each purification method

3.4 CO₂ emissions intensity for each of water supply scale

Figure 6 shows CO_2 emissions intensity for each of water supply scale. As a result, "−1,000" category had the largest average value of 0.301 kg-CO_2/m³, while "50,001−" category had the smallest average value of 0.161 kg-CO_2/m³. It was found that it tended to be smaller for water suppliers with larger water supply volumes. Compared to "Overall", the trend was confirmed to be similar to that of "1,001−5,000" category. This seems to be because the fact that about half of "overall" respondents fall into "1,001−5,000" category when classified by water supply scale.
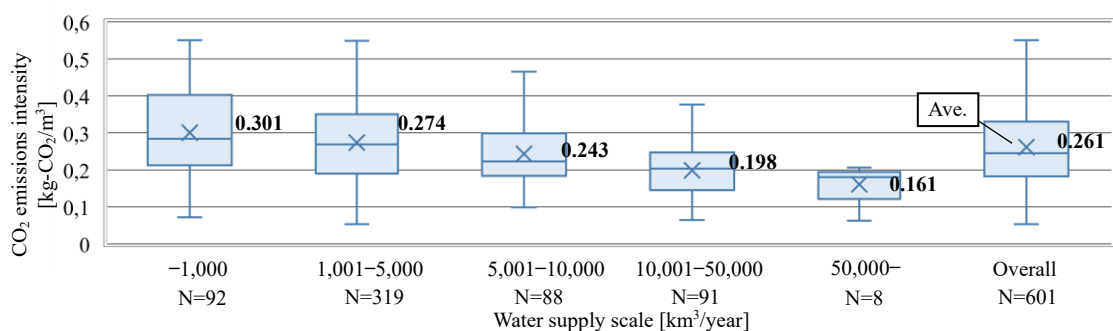
Figure 6 – CO₂ emissions intensity for each water supply scale

3.5 Distribution of water suppliers and CO₂ emissions intensity for each region

Figure 7 shows distribution of water suppliers in Japan and CO_2 emissions intensity for each region classified by Regional Planning Area, which is a grouping of the 47 prefectures of Japan with unity and commonality with respect to the 45 prefectures, excluding Hokkaido and Okinawa. Looking at the number of water suppliers by water supply scale for each region, there were many small water suppliers in "①Hokkaido," which has a small population density, and many large water suppliers in the "③ Metropolitan area," which has a large population density. Looking at CO_2 emissions intensity, "⑩Okinawa" had the largest average value of 0.444 kg-CO_2/m³, while "③ Metropolitan Area" had the smallest average value of 0.224 kg-CO_2/m³.

a) Distribution of water suppliers in Japan [10]

The authors processed the map based on maps from the Geospatial Information Authority of Japan.

*Outliers based on the IQR method was excluded.
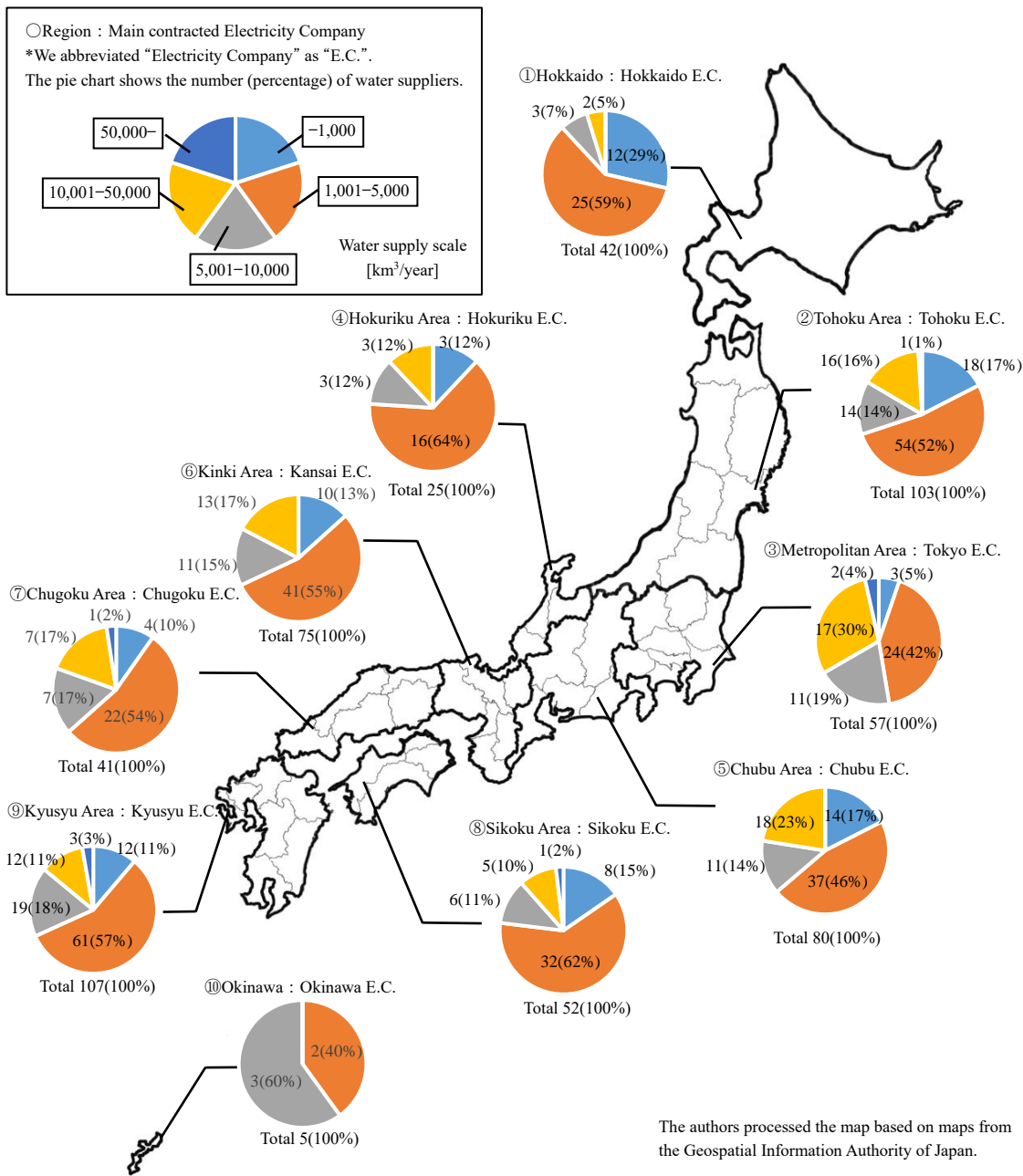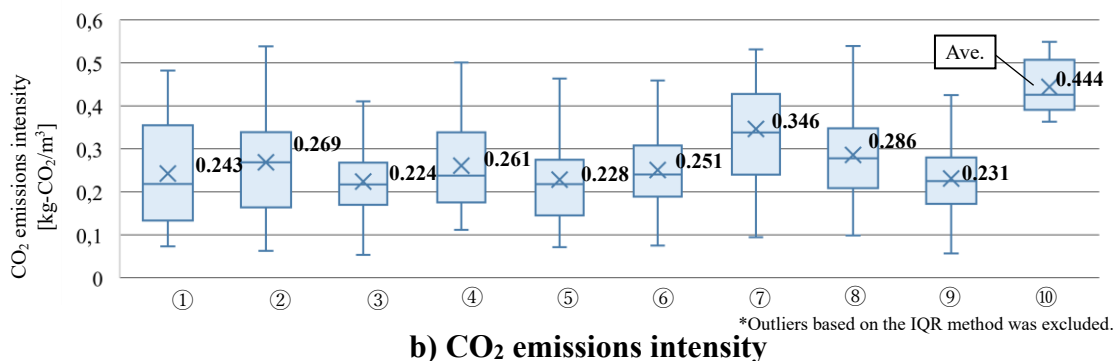
b) CO₂ emissions intensity

**Figure 7 – Distribution of water suppliers in Japan
and CO₂ emissions intensity for each region**

4 CO_2 emissions intensity from rainwater utilization facilities

We compared the CO_2 emissions intensity between water supply facilities and rainwater utilization facilities to verify the CO_2 emissions reduction effect of rainwater utilization.

4.1 Electricity consumption intensity

We calculated the electricity consumption intensity per unit of water volume from our research and partially reviewing rainwater utilization cases [11][12], the range was 0.119−0.337 kg-CO_2/m^3, with an average of 0.220 kg-CO_2/m^3.

4.2 Comparison with water supply facility

Figure 8 shows CO_2 emissions intensity from water supply facilities for each water supply scale and rainwater utilization facilities. When rainwater utilization facilities are installed in Japan, it is expected that contracted electricity companies will differ. CO_2 emissions intensity per unit of electricity consumption varies among electricity companies. Therefore, we calculated the CO_2 emissions intensity per unit of water volume from rainwater utilization by multiplying the electricity consumption intensity by the maximum (0.612 kg-CO_2/m^3), average (0.473 kg-CO_2/m^3), and minimum (0.343 kg-CO_2/m^3) CO_2 emissions intensity of the electricity companies. Note that we excluded "Okinawa Electricity Company", which is unique in that it is located on a remote island. As a result, the range of CO_2 emissions intensity from rainwater utilization was 0.041−0.206 kg-CO_2/m^3, with an average of 0.104 kg-CO_2/m^3, confirming that in most cases, rainwater utilization facilities' CO_2 emissions intensity is smaller than water supply facilities'.
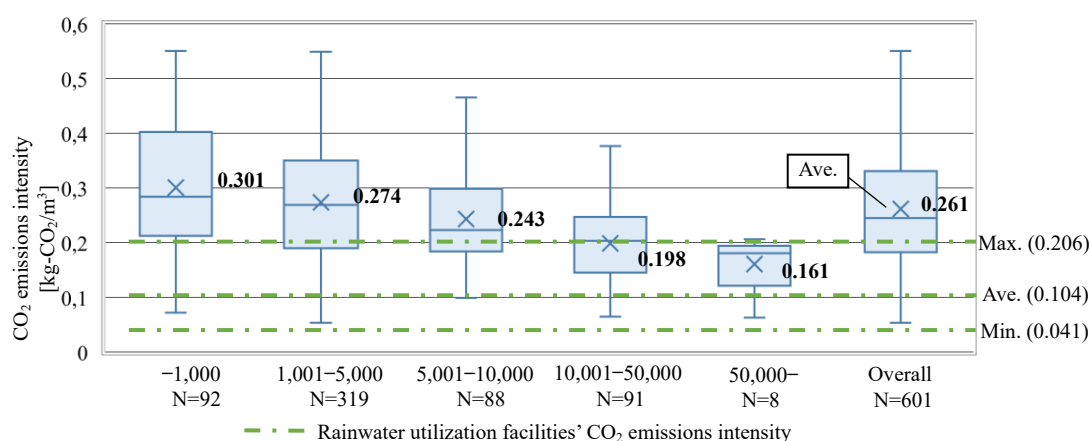
Figure 8 – CO_2 emissions intensity from water supply facilities for each supply scale and rainwater utilization facilities

5 Conclusion

In this study, we analyzed the CO_2 emissions intensity for each purification method, water supply scale, contracted electricity company, and region in order to identify trends for each water supplier. Then, we compared CO_2 emissions intensity from water supply facilities and rainwater utilization facilities to verify the CO_2 reduction effect of rainwater utilization. From the obtained results, the following points were clarified:

・The average CO_2 emissions intensity from water supply facilities in Japan is 0.261 kg-CO_2/m^3, which is greatly affected by the water supply scale and region.

・The range of CO_2 emissions intensity from rainwater utilization facilities is 0.041-0.206 kg-CO_2/m^3, with an average of 0.104 kg-CO_2/m^3. Compared to water supply facilities, most buildings can reduce CO_2 emissions. However, the effect may be small depending on the water supplier that supplies water with buildings, so care should be taken when installing the system.

Acknowledgments

6 References

[1] Architectural Institute of Japan Environmental Standards AIJES-B0002-2019 Guideline for Rainwater Harvesting Architecture, p.2, Mar.2019

[2] Ministry of Land, Infrastructure, Japan, Transport and Tourism: Rainwater utilization diffusion status, URL: https://www.mlit.go.jp/mizukokudo/mizsei/mizukokudo_mizsei_tk1_000055.html, (accessed June 20th, 2023)

[3] M. Iwai, K. Fukui, N. Maeda, S. Okada: Greenhouse Gas Emissions at Purification Plants and Sewage Treatment Plants, Technical paper of annual meeting SHASE, pp101−104, Sep.2020 (Online) (In Japanese)

[4] Japan Water Works Association: "Water Supply Statistics" Excel Version (FY2020), 2022

[5] Japan Water Works Association: "Water Supply Statistics" Excel Version (FY2018), 2020

[6] Japan Water Works Association: "Water Supply Statistics" Excel Version (FY2019), 2021

[7] Agency for Natural Resources and Energy, Ministry of Economy, Japan, Trade and Industry: FY2022 1st General Resources and Energy Investigation Committee, Document 4: Specific Theory of the Revised Law Concerning the Rational Use of Energy, etc, URL: https://www.meti.go.jp/shingikai/enecho/shoene_shinene/sho_energy/kojo_handan/2022_001.html, (accessed June 20th, 2023)

[8] Ministry of the Environment: Manuals and Tools for Formulation and Implementation, Japan, URL: https://www.env.go.jp/policy/local_keikaku/manual2.html, (accessed June 20th, 2023)

[9] Bureau of Waterworks Tokyo Metropolitan Government: Environmental Report, URL: https://www.waterworks.metro.tokyo.lg.jp/files/items/30854/File/2021-gaiyou-all.pdf, (accessed June 20th, 2023)

[10] Geospatial Information Authority of Japan, Ministry of Land, Infrastructure, Japan, Transport and Tourism: White Maps, URL: https://www.gsi.go.jp/kikakuchousei/kikakuchousei40182.html (accessed June 20th, 2023)

[11] J. Oyagi, T. Nishikawa: Study on water balance and environmental evaluation in buildings (Part2) Comparative evaluation of reclaimed water use and rainwater use, Technical paper of annual meeting SHASE, pp89−92, Sep.2022 (In Japanese)

[12] K. Fukui, S. Okada: Study on Carbon Dioxide Emissions of Rainwater Utilize Facilities, Proceedings of the Tohoku Section 10th Academic and Technical Report Meeting, pp17−20, Mar.2021 (Online) (In Japanese)

7 Presentation of Authors

Ukyo Takeuchi is a graduate student at Department of School of Science & Technology, Meiji University. His research is effective use of water resources.

Takehiko Mitsunaga (Ph.D) is a senior assistant professor at Department of Architecture, School of Science & Technology, Meiji University. His fields of specialization include water environment, building services engineering and plumbing system.

Navigating Modern Crises through Sustainable and Resilient Urban Development (How to do more with Less?)

Hana Nekrep (1), Matjaž Nekrep Perc (2), Tatjana Perc Nekrep (3)
1. hana.nekrep@gmail.com
2. matjaz.nekrep@um.si
3. tatjana.nekrep@gmail.com

(1) TU Wien, Faculty of Architecture and Planning, Austria
(2) Faculty of Civil Engineering, Transportation Engineering and Architecture, University of Maribor, Slovenia
(3) SGŠG Maribor, Slovenia

Abstract

In a world grappling with multiple challenges such as climate change, energy crises, inflation, migration, pandemics, and housing shortages, redefining housing and sanitation has become imperative for fostering open, caring, and communal living. As global warming and extreme weather events increasingly impact our built environment, adapting our knowledge of urban planning, construction, and living is crucial. With buildings contributing significantly to energy consumption and greenhouse gas emissions, there is an urgent need for sustainable building practices and climate-neutral cities. We must add "net zero water" to the net zero energy efforts and goals.

This paper explores the integration of green and blue infrastructure for urban resilience, highlighting their ecological, social, and economic benefits. By designing cities with green spaces, wetlands, green roofs, permeable pavements, and water-efficient fixtures, we can increase resilience to climate change impacts and improve overall community well-being. The presentation will discuss the application of these principles in a case study of a redesigned early 20th-century building, showcasing the potential for sustainable urban transformation.

Keywords: *climate change, built environment, net zero water, net zero energy*

1 Introduction

Climate change (Figure 1), energy crises, migration, pandemics, and housing shortages have plagued the 21st century. These crises require us to rethink housing and sanitation to promote open, caring, and communal living. Global warming and extreme weather events require a rethinking of urban planning, construction, and living. Sustainable building practices and climate-neutral cities are needed due to buildings' high energy use and greenhouse gas emissions. Net zero energy and water goals must be integrated.

Figure 1 Floods on May the 17th 2023, river Pesnica, Slovenija

This paper discusses green and blue infrastructure's ecological, social, and economic benefits for urban resilience. Green spaces, wetlands, green roofs, permeable pavements, and water-efficient fixtures can help cities withstand climate change and improve community well-being. A redesigned early 20th-century building will demonstrate sustainable urban transformation. This paper investigates sustainable and resilient urban development practices that let us do more with less. Innovative housing and sanitation solutions can solve our cities' biggest problems and create a more sustainable future.

2 Green Infrastructure for Urban Resilience

Growing in popularity, green infrastructure is being embraced as an effective approach to bolster urban resilience against climate change and other challenges. Comprising elements like parks, green roofs, wetlands, and urban forests, green infrastructure offers societal and environmental benefits and fosters sustainable urban development. Green infrastructure mitigates the environmental impact of urbanization. By providing green spaces within cities, it offsets the loss of biodiversity and ecosystem services brought about by urban development. These spaces also function as corridors for wildlife, enhancing biodiversity, and contribute to improved air quality by providing shade, capturing pollution, and releasing oxygen. The advantages of green infrastructure aren't solely environmental. Green spaces promote recreation, relaxation, and social interaction (Figure 2), contributing to better mental and physical health. They foster a sense of

community and make cities more attractive and liveable. Economically, green infrastructure boosts urban economies by raising property values and attracting businesses and tourists. Green roofs provide both insulation and cooling, offering cost savings to owners. Additionally, green spaces reduce stormwater runoff and flood risk, thus protecting infrastructure and saving resources. To realize its full potential, green infrastructure needs to be incorporated into urban planning and design, necessitating collaboration among city officials, planners, architects, and the community. Strategies should prioritize greening new developments, retrofitting existing structures, and utilizing nature-based stormwater management. Policies and regulations can also facilitate the adoption of green infrastructure. Green infrastructure addresses environmental, social, and economic concerns in urban development, contributing to urban resilience, sustainability, and community well-being. By creating sustainable and resilient urban ecosystems, green infrastructure enhances the quality of life for both present and future generations.

Figure 2 Simple but highly efficient element of Green Infrastructure in front of our faculty

3 Green Building Infrastructure

Buildings significantly influence the urban environment. The integration of green infrastructure in building design and construction is pivotal for enhancing sustainability and resilience in cities. This chapter delves into the multifaceted benefits and applications of green infrastructure within building constructs. Key elements of green building infrastructure encompass green roofs and walls, introducing vertical greenery to building exteriors. These components not only enhance thermal insulation and energy efficiency but also play a role in stormwater management and biodiversity promotion. They contribute to noise reduction while purifying both indoor and outdoor air. In the sphere

of water management, rainwater harvesting and greywater recycling form vital components of the green building strategy. By capturing rainwater runoff from roofs and recycling wastewater from household use, these systems not only conserve water but also alleviate the strain on municipal supplies and wastewater treatment facilities, underpinning sustainable water management. Energy efficiency is another crucial facet of green infrastructure. The inclusion of solar panels, wind turbines, geothermal systems, along with efficient lighting, insulation, and smart energy management, diminishes a building's environmental impact. Such systems pave the way for reduced energy consumption, lower greenhouse gas emissions, and increased urban energy resilience. Biophilic design strategies, employing natural elements and patterns, strengthen the human-nature connection. Utilizing features like atriums, vertical gardens, and indoor plants, biophilic design bolsters air quality, wellbeing, productivity, and stress relief, creating healthier and more pleasant building environments.

By weaving green infrastructure into building design and construction through the integration of green roofs and walls, effective water and energy management systems, and biophilic design urban sustainability and resilience can be markedly improved. This approach promotes the creation of sustainable, people-cantered cities, yielding far-reaching environmental, social, and economic benefits.

Figure 3 Green façade on the symmetrical house (position of sensors is marked with red dots)

Sustainable Renovation of 1903 Villa

Case study shows how green infrastructure may sustainably remodel a historic villa. The urban home was renovated and retrofitted with a green facade, retention pond, green roof (Figure 5), solar panels, a weather station, and temperature and humidity sensors. This case study shows how these aspects improve building sustainability and resilience. Climbing plants and vertical foliage complemented the villa's exterior.

Figure 4 Green façade through the year

The green facade adds beauty and benefits (Figure 4). It regulates summer temperatures and reduces heat gain, saving electricity and air conditioning. Plants filter air and reduce noise. The villa's retention pond manages stormwater runoff. The pond gently infiltrates precipitation into the ground, lowering drainage system load and flooding risk. Wildlife habitat and property aesthetics are provided by the retention pond. The villa's green roof turned underused space into a lush green space. In winter and summer, the green roof insulates the building. It absorbs and retains precipitation to reduce drainage system load.

Figure 5 Green roof

The green roof (Figure 5) enhances biodiversity, pollinator habitat, and building aesthetics. Solar Panels and Weather Station The villa's roof had solar panels for solar energy. Solar panels power the building and reduce carbon emissions. A roof-mounted weather station provides real-time temperature, humidity, and other meteorological data. This data can optimize building energy utilization. Advantages and Results The villa's green infrastructure has many benefits. Green facades, retention ponds, and roofs improve energy efficiency, stormwater runoff, biodiversity, and aesthetics. The renovated villa case study offers insights and recommendations for future sustainable building initiatives. To enhance sustainability and resilience, it emphasizes green infrastructure integration.

We compares facade temperatures of the green facade with the exposed area without vegetation over time. These data can reveal how the green facade affects building temperature and energy efficiency. Long-term weather parameter measurements assessed the building's microclimate. Temperature, humidity, wind speed, sun radiation, and rainfall are included. Weather sensors were carefully placed on the building to collect long-term data (Figure 3). The data reveals the local climate's seasonal changes. The study compares facade temperatures between the green facade and the uncovered part. We can evaluate the green facade's thermal performance and energy savings using temperature data. Long-term weather parameter observations reveal local climate patterns and fluctuations. Solar radiation, wind speed, and rainfall affect the building's microclimate. Comparing façade temperatures between the green facade area and the exposed section shows the thermal benefits of green infrastructure. Early investigation reveals that the green facade considerably affects building surface temperature. Vegetation lowers surface temperatures. Plant shadowing, evapotranspiration, and greenery insulation reduce warmth (Figure 6). These results show that green infrastructure can reduce heat gain and improve building comfort.
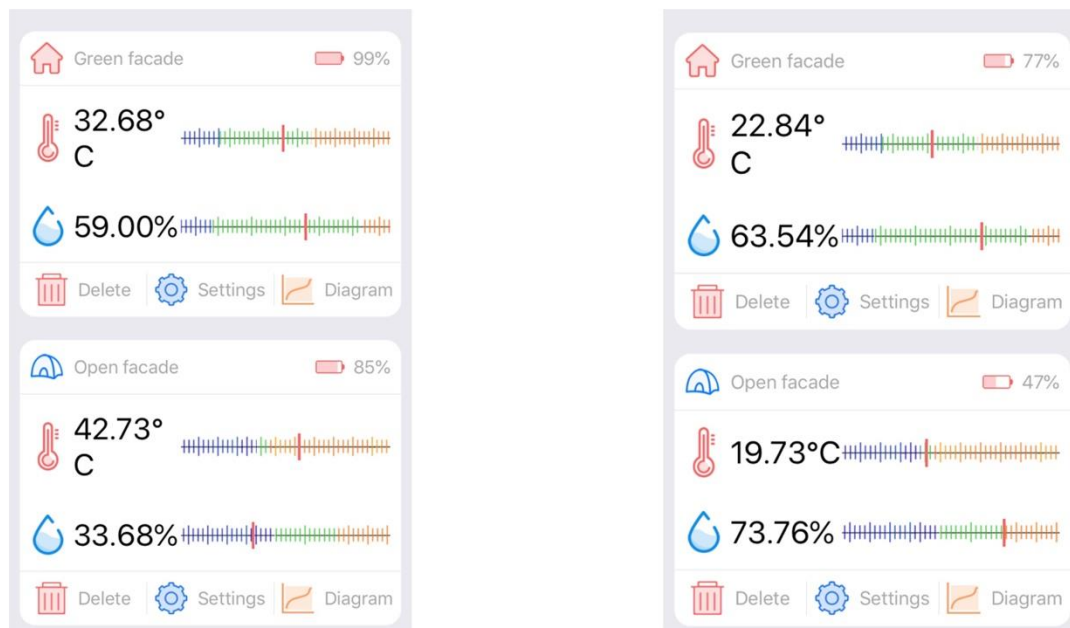
Figure 6 Less hot in the summer (left) and warmer in the winter (right)

Green infrastructure, like green facades, reduces cooling energy use, improves thermal comfort, and reduces the urban heat island effect. These findings can inform future building projects and promote green infrastructure for sustainable and resilient cities. Weather sensor data can also improve energy management systems. Building automation systems can dynamically modify energy use depending on weather data. This reduces energy waste and costs. Long-term weather data and façade temperature comparisons reveal the thermal performance and energy efficiency of green facade structures. The studies show that green infrastructure regulates temperature and saves energy. This understanding helps architects, urban planners, and building designers develop more sustainable and resilient buildings. Weather parameters, façade temperature, green facade, thermal performance, energy efficiency, sustainable building design, urban planning.

4 Conclusions

Green infrastructure's potential in fostering sustainable and resilient urban development has been explored in this study. Utilizing features such as green roofs, facades, and retention ponds can generate several ecological, social, and economic benefits. These elements serve not only to conserve biodiversity but also to manage energy and stormwater effectively, while enhancing the aesthetic appeal of urban areas. Specifically, the integration of water management approaches like rainfall harvesting and greywater recycling can significantly reduce reliance on municipal water supplies, offering a more sustainable approach to water usage. Complementing this, the incorporation of solar panels and smart building systems can substantially decrease energy consumption and carbon emissions, contributing to the broader objectives of sustainable urban development. Indoor green spaces represent another dimension of green infrastructure, offering benefits related to improved productivity, well-being, and air quality. They

exemplify the synergy between the natural and built environments, creating spaces that are not only functional but also conducive to healthier and more productive lifestyle.

Figure 7 Property with green infrastructure (retention pond, green roof and green façade)

Our case study of the 1903 villa upgrade brings these principles to life. The villa (Figure 7), an emblem of historical architecture, underwent an upgrade that involved the incorporation of several green infrastructure features. This integration resulted in enhanced energy efficiency, effective stormwater management, increased biodiversity, and an overall improvement in the villa's aesthetic appeal. This practical example underscores the real-world applicability and benefits of integrating green infrastructure into urban development and building design.

However, realizing the full potential of green infrastructure requires concerted effort across sectors. Governments, city planners, and developers need to prioritize the inclusion of green infrastructure elements in urban planning and building design. Furthermore, construction codes should promote the adoption of energy-efficient building solutions, rainwater harvesting, and greywater recycling.

The paper further advocates for increased collaboration and knowledge sharing among stakeholders in architecture, engineering, and environmental science. Disseminating green infrastructure best practices, lessons learned, and research findings can expedite the mainstreaming of these principles into urban development strategies. The growing urgency for sustainable and resilient urban development is being felt at all levels - individual, community, and societal. Green infrastructure measures have been shown to reduce construction emissions, increase urban resilience to climate change, and foster healthier, more livable cities. This can greatly enhance the quality of life for current residents and future generations. In conclusion, the role of green infrastructure in urban development and buildings is crucial to addressing the modern challenges of climate change, energy crises, and housing shortages. As demonstrated by the 1903 villa upgrade, green infrastructure elements such as green roofs, facades, and energy-efficient systems can result in resilient, eco-friendly, and people-centric urban environments. By embracing these principles, we can collaboratively address contemporary issues and create a sustainable future. The imperative is clear: let's commit to a future where our cities are in synergy with nature, resilient, and sustainable.

5. References

1. Rakhshandehroo, M. An Introduction to Green Building. *RMI Solut.* **2016**, 7–8, doi:10.13140/RG.2.1.5136.9049.
2. Baro, F.; Bugter, R. J. .; Gomez-Baggethun, E.; Hauck, J.; Kopperoinen, L.; Liquete, C.; Potschin, M. Green Infrastructure. In *Ecosystem Service Reference Book*; 2015; pp. 1–3.
3. Gledhill, D. *The names of plants*; Cambridge University Press, 2008; ISBN 9780521866453.
4. Vox, G.; Blanco, I.; Schettini, E. Green façades to control wall surface temperature in buildings. *Build. Environ.* **2018**, *129*, 154–166, doi:10.1016/j.buildenv.2017.12.002.

6 Presentation of Authors

Hana Nekrep is an Architect and Illustrator currently working on her PhD at Vienna University of Technology, Austria
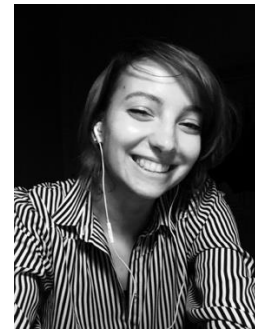
Matjaž Nekrep Perc is a Researcher and Senior Lecturer at the Faculty of Civil Engineering, Transportation Engineering and Architecture, University of Maribor, Slovenia

Tatjana Perc Nekrep is an High School teacher at SGŠG Maribor, Slovenia

TECHNICAL SESSION 8 – HEALTH & HYGIENE II

Study on Evaporation Phenomenon of Trap Seal Water

Part2 Indoor and outdoor evaporation rates by regions

Takehiko Mitsunaga(1)，Kyosuke Sakaue (2)

(1) mitsunaga@meiji.ac.jp

(2) sakaue@carrot.ocn.ne.jp

(1) Department of Architecture, School of Science & Technology, Meiji University, Japan

(2) Emeritus professor, Meiji University, Japan

Abstract

It is difficult to prevent evaporation of the trap seal water. If the device has not been used for many weeks and no wastewater flows through the trap, the seal will break. By predicting evaporation rate of trap seal water, it would be easier to plan refilling of the trap as part of maintenance. In the previous paper, evaporation rate calculation formula proposed, and the validity of this formula was confirmed. In addition, it was confirmed the air conditions on the trap outlet side that wind speed was almost 0 m/s, dry-bulb temperature was almost the same as indoors, and relative humidity was 80-90%. However, the evaporation at both ends of the outlet and inlet legs of the trap, and its rate considering the regional climate have not been studied.

The purpose of this report is to establish a method for predicting the evaporation rate of seal water in a trap. Evaporation rates of indoor and outdoor wash basins (P-trap) and floor drains (Bell-trap) in Tokyo and warm and cold regions of Japan are calculated. As a calculation method, using the evaporation rate calculation formula in the previous report and the one-hour value of the outdoor temperature and humidity for one year from the "Automated Meteorological Data Acquisition System". As a result, we show the difference in evaporation rate between indoors and outdoors for each region.

Keywords

Drainage trap; Seal water, Evaporation; Calculation formula; AMeDAS（Automated Meteorological Data Acquisition System）; Bell-trap.

1 Introduction

It is difficult to prevent the trap seal water from evaporating. If the trap is not used for a long period of time and the wastewater does not flow into the trap, the trap seal will eventually break, increasing the possibility of sewage gas odor entering the room. In 2003, a SARS (Severe Acute Respiratory Syndrome) outbreak at Amoy Gardens, a high-rise apartment building in Hong Kong [1], is a well-known case of bad effects caused by the breakage of the trap seal water. In order to prevent the breakage by evaporation, for floor drain traps, there is a method of changing the lid structure from a mesh grating shape to a closed shape, but it is necessary to change the floor cleaning method, because the wet floor type is changed to a dry floor type. And, the application of self-sealing traps [2] without seal water is expected not only for floor drains but also for drain traps for sanitary appliances. However, in SHASE-S 206 [3], which is the standard for plumbing and sanitary equipment in Japan, the structural standards for drainage traps for sanitary fixtures are based on the assumption that they are water-sealed, and building designers are hesitant to apply them.   Against this background, it is thought that water-sealed traps will continue to be generally used for some time to come. Therefore, it is important to predict the volume of seal water lost due to evaporation, and plan water replenishment especially for trap seals of sanitary appliances that are not normally used.

As a study on the prediction of the evaporation rate of the seal water in the trap, the previous report [4] investigated the natural convection field without considering the pressure fluctuation in the drain pipe. In that study, there was an experiment and a calculation formula for the evaporation rate using a cylindrical vessel, and the similarity of the evaporation rate between the cylindrical vessel and the water-sealed trap at the inlet leg was confirmed. A subsequent study [5] confirmed that the airflow conditions in the outlet leg were almost 0m/s in the absence of other drainage systems, the dry-bulb temperature was almost the same as indoors, and the relative humidity was 80-90%. However, no investigation has been made on seal water loss considering reduction of seal water level due to evaporation from both ends of the trap. In addition, the effects of changes in evaporation rate throughout the year, and differences in ambient temperature and humidity conditions have not been evaluated.

The purpose of this study is to establish a method for predicting the evaporation rate of seal water in traps. For this purpose, we calculated the evaporation rates of indoor and outdoor wash basins (P-trap) and floor drains (Bell-trap) in Tokyo, warm region, and cold region in Japan, and examined trends in evaporation rates.

2 Calculation methods

2.1 Calculation formula of evaporation rate for trap seal water

Table 1 shows the calculation formula of evaporation rate for trap seal water experimentally derived in previous study [4]. Evaporation rate is affected by diffusion, which is the movement of matter due to a density gradient, and convection, which occurs when water evaporates into the atmosphere. This calculation formula is in a natural convection field that does not consider the effects of external air flows, because the seal water is inside the drainage pipe. Evaporation rates are determined by hollow height h, inner diameter d, and water vapor pressure e.

Table 1 – Calculation formula for evaporation rate

$$\omega_t{'} = \alpha \cdot \omega_t$$

$$\omega_t = 0.59 \frac{(e_s - e)}{h^{1/4}}$$

$$\alpha = \frac{1}{(2h + 3.09)d^{-2.35}}$$

Where;

$\omega_t{'}$	: Evaporation rate (modified by experimental result[4]) [mg/(cm²·h·hPa)]		
ω_t	: Evaporation rate (theoretical formula [mg/(cm²·h·hPa)]	α	: Correction coefficient [-],
e_s	: Water vapor pressure on the water surface [hPa]	e	: Water vapor pressure of air [hPa]
h	: Hollow height [cm],	d	: Internal diameter [cm]

2.2 Trap and hollow height

Table 2 shows the types of traps used in the study. There are two types of traps: the P-trap (d:30mm) for the washbasin installed in the toilet space, and the Bell-trap for the floor drainage perforated plate commonly used in wet floor finishing.

Table 3 shows the hollow height conditions. Hollow height refers to the vertical distance from the upper end of the trap water seal to the air open end on the inlet leg side of the trap. Previous studies have shown that the evaporation rate varies with hollow height. There are four types of hollow height h, 5, 10, 20, and 30 cm, for both the P-trap and the Bell-trap.

Table 2 – Type of traps

Type of trap	Cross-sectional shape	Type of trap	Cross-sectional shape

P-trap
 	
【Inlet and outlet leg】
─Inter diameter 30mm
─Cross-sectional area 7.065cm^2
	Washbasin side
	Φ35
	Φ30
	100
	Φ30
	Φ35
	Drainage pipe side
	92.5
	51 100
		Bell-trap
		
		【Inlet leg】
		─Inter diameter
		  Outer circumference114.0mm
		  Inner circumference 90.2mm
		─Cross-sectional area 52.972cm^2
		【Outlet leg】
		─Inter diameter
		  Outer circumference 82.2mm
		  Inner circumference 60.0mm,
		─Cross-sectional area 24.781cm^2
			Floor side
			Φ140
			Φ132
			Φ82.2
			Φ60
			Φ50
			50 107 130
			25
			Φ50.75
			Φ60.35
			Drainage pipe side

Table 3 – Hollow height

Position in trap	Hollow height h	Remarks
Inlet leg	5cm 10cm 20cm 30cm	h Inlet leg side Outlet leg side
Outlet leg	10cm *	＊ A concept of hollow height h does not actually exist, because the outlet leg is connected to the drainage pipe and is not open to the atmosphere. Therefore, here we cite the finding that the theoretical value at a hollow height of 10 cm was close to the experimental value in the experimental verification of previous study [4].

2.3 Water vapor pressure

Table 4 shows the dry-bulb temperature and relative humidity conditions of the outdoor air observation points, trap inlet leg, outlet leg, and seal water surface, which are related to the water vapor pressure used in the calculation. The temperature and humidity data of outdoor air are taken from Tokyo (latitude 35.69177, longitude 139.74974）as the standard of Japanese air conditions, and Fukuoka (latitude 33.58628, longitude 130.37384) as a representative of warm regions, Sapporo (latitude 43.06280, longitude 141.32889) as a representative of cold regions, and hourly values for the year 2022 from AMeDAS (Automated Meteorological Data Acquisition System) are used. The effect of freezing of the sealed water due to low outdoor temperatures is ignored.

There are two types of toilet space: outdoor toilets and indoor toilets. The outdoor toilet is a restroom that assumes that the temperature and humidity of a regular toilet space are the same as the outdoor air, and it is assumed that it is greatly affected by the temperature and humidity of each region. The indoor toilet is a restroom in which part of the air from the

air-conditioned room flows into the toilet space to maintain the temperature and humidity, assuming a general office building, though not as much as in an air-conditioned room.

Specifically, according to the Environmental Sanitation Management Standard for Building [6], the cooling period (when air-conditioned) is 28°C/70%, and the heating period (when air-conditioned) is 18°C/40%. In addition, it is assumed that the temperature is slightly worse when the room is not air-conditioned than when it is air-conditioned, and the relative humidity does not change from the absolute humidity when air-conditioned. Based on that, the cooling period (when no air-conditioned) is 30°C/62.4%, and the heating period (when no air-conditioned) is 14°C/51.5%.

The temperature and humidity conditions on the inlet leg side are the same as those of the toilet space. On the outlet leg side, the temperature is the same as the toilet space, and the relative humidity is 80% according to previous studies. The temperature of the seal water surface is the same as those of toilet space, because its fixture drainage pipe is generally bare pipes not to install heat insulating materials. The temperature of the toilet space is assumed to be the same as the room temperature and the same value as the toilet space. The humidity of the water surface of the seal water is assumed to be 100% relative humidity [7], which is the saturated water vapor pressure.

Table 4 – Regions and air conditions of outdoor building and in trap

Region	Tokyo [Standard region] Lat. 35.69177, Lon. 139.74974	Fukuoka [Warm region] Lat. 33.58628, Lon. 130.37384	Sapporo [Cold region] Lat. 43.06280, Lon. 141.32889

Condition of dry bulb temperature and relative humidity

①Outdoor toilet space	Inlet leg : Outdoor temperature and humidity,
	Outlet leg : Outdoor temperature,　humidity 80%
	Seal water surface : Outdoor temperature,　humidity 100%
	[Note] Outdoor air condition date for the year 2022　from AMeDAS
②Indoor toilet space （in office building）	Inlet leg : Temperature and humidity assuming air inflow from an air-conditioned room
	Outlet leg : Temperature assuming air inflow from an air-conditioned room,　humidity 80%
	Seal water surface : Indoor temperature,　humidity 100%

[Indoor toilet air conditioning conditions]

1) Working hours are from 8:00 to 18:00, and the air conditioning is turned off outside working hours and on weekends.

2) The cooling period is from May 15th to Oct.15th in Tokyo and Fukuoka, and from Jun. 16th to Sep. 15th in Sapporo.
   The air conditions: in case of air-conditioned: 28°C/70%, in case of no air-conditioned: 30°C/62.4%

3) The heating period is from Nov. 1st to Apr. 30th in Tokyo and Fukuoka, and from Oct. 1st to May 31st in Sapporo.
   The air conditions: in case of air-conditioned: 18°C/40%, in case of no air-conditioned: 14°C/51.5%.

4) The outdoor air temperature and humidity are used during the non-air conditioning period, and the outside air temperature is higher than the air conditioning temperature even during the air conditioning period. If it is preferable, the outside air temperature is assumed to be introduced by opening and closing the window.

3 Evaporation of seal water

3.1 Evaporation rate of inlet and outlet legs

Figure 1 shows the evaporation rates of the inlet and outlet legs of an outdoor toilet space in Tokyo for each hollow height. Looking at the tendency of the evaporation rate, the inlet leg increases as the hollow height decreases, and the outlet leg is not affected by the hollow height because the height is constant. Looking at the whole year, the evaporation rate is high in summer around July, and low in winter around January. This is due to the high temperature and humidity in summer in Japan, which increases the vapor partial pressure of water in the outdoor air. The evaporation rate of the inlet leg was faster than that of the outlet leg at hollow heights of 5, 10, and 20 cm, but the outlet leg was faster at 30 cm.

(a)   Hollow height   5cm

(b)   Hollow height   10cm

(c)   Hollow height   20cm

(d)   Hollow height   30cm
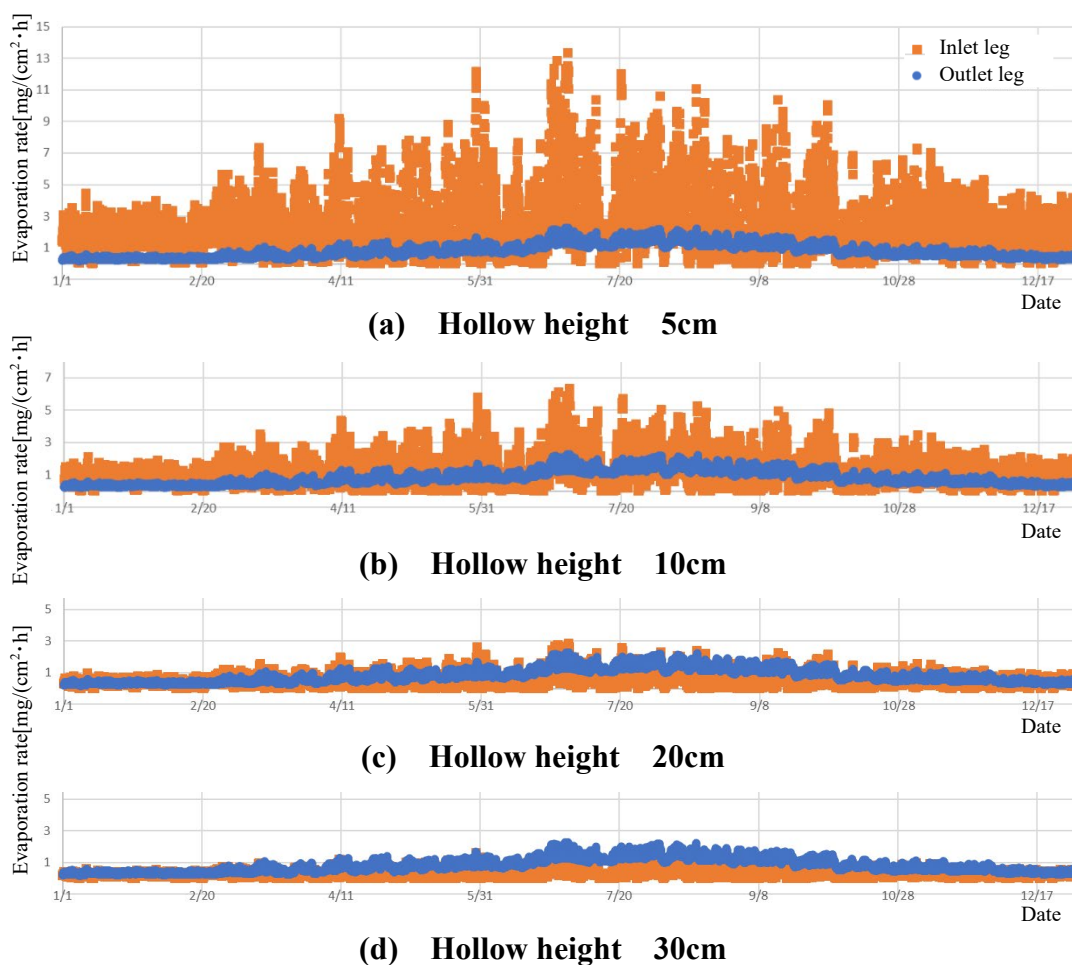
Leg	Hollow height	Max.	90%	80%	70%	60%	50%
Inlet	5cm	13.33	4.84	3.44	2.77	2.29	1.88
	10cm	6.35	2.31	1.64	1.32	1.09	0.90
	20cm	2.86	1.04	0.74	0.59	0..49	0.40
	30cm	1.77	0.64	0.46	0.37	0.30	0.25
Outlet	Common	2.27	1.39	1.17	0.99	0.79	0.66

Unit:〔mg/(cm²・h)〕

Figure 1 – Evaporation rate in case of P-trap in Tokyo under outdoor

3.2 Evaporation rate outdoors and indoors

Figure 2 shows the monthly trap seal loss due to evaporation in Tokyo. In the outdoor toilet space shown in Figure 2 (a), during the hot and humid months of July and August, when the hollow height is 5 cm, the seal water evaporates by approximately 18 cm per month. As the hollow height becomes smaller, the volume of seal water loss decreases, and when the hollow height is 30 cm, it is approximately 7 cm and the volume of evaporation decreases. Looking at the indoor toilets in Figure 2 (b), the monthly difference is small, because the outdoor air is treated by HVAC system. Around January, the vapor partial pressure of water tends to increase and the volume of evaporation tends to be larger than that of the outdoor toilet, because humidified air flows into the toilet. May and October are moderately hot and humid months in Japan, with no air-conditioning, therefore the results are similar to those of the outdoor toilet.

(a) Outdoor

(b) Indoor air conditions
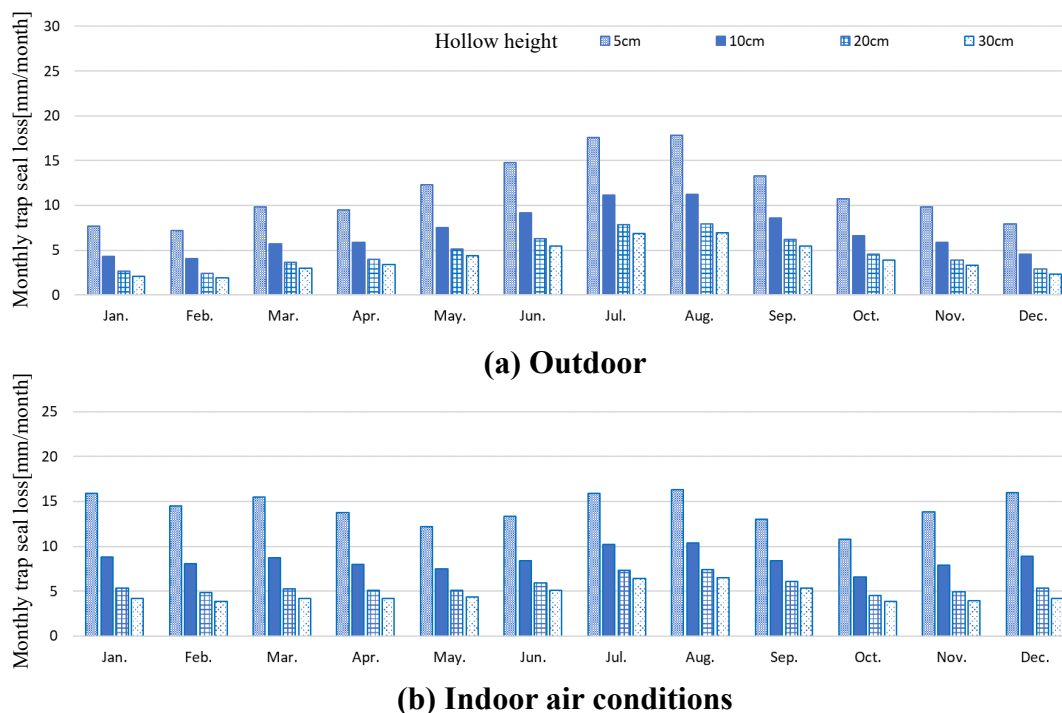
Figure 2 – Trap seal loss due to evaporation in case of P-trap in Tokyo

3.3 Evaporation rate by region

Figures 3 and 4 show the monthly trap seal losses due to evaporation in Sapporo and Fukuoka, respectively. Figures 3(a) and (b) show that when comparing outdoor and indoor region in Sapporo, the volume of seal water loss from November to March is significantly higher than outdoors. This is because Sapporo is a cold region and the outdoor air is dry, whereas the indoor air is humid, so the vapor partial pressure of water

increases. In addition, Comparing of Figure 3(a) and Figure 4(a) outdoor in Sapporo and Fukuoka in case of the hollow height 30 cm in July, the seal water loss is approximately 8
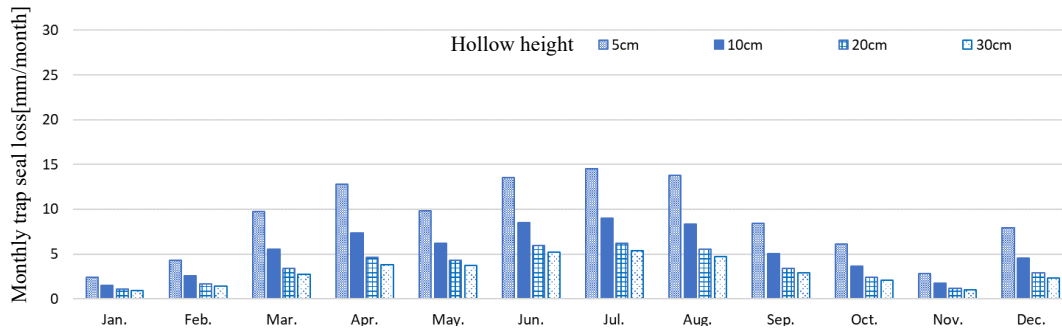
(a) Outdoor
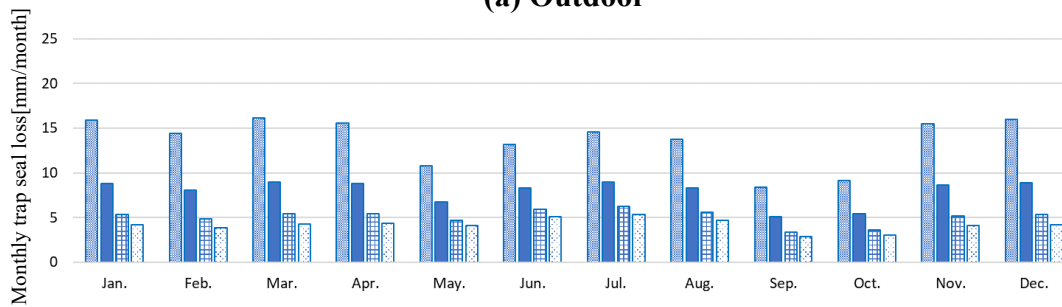
(b) Indoor air conditions

Figure 3 – Trap seal loss due to evaporation in case of P-trap in Sapporo
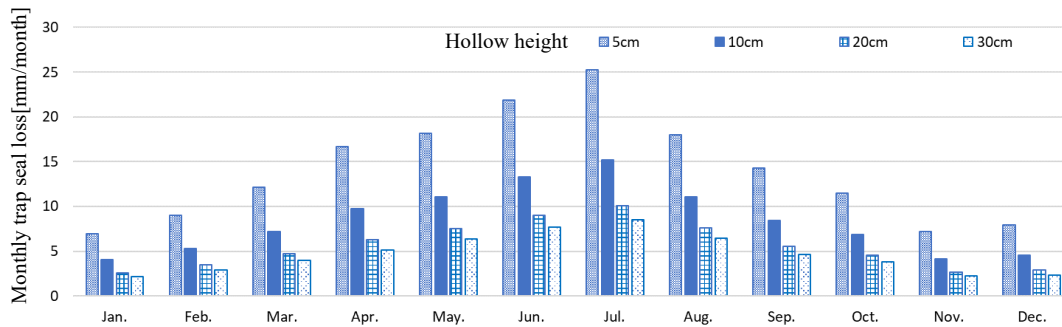
(a) Outdoors
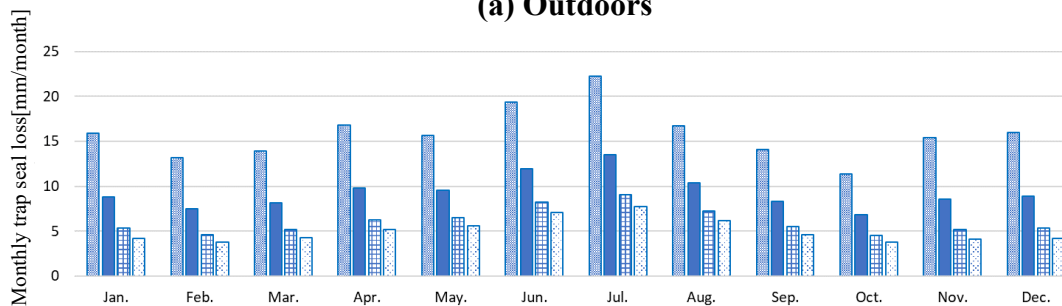
(b) Indoor air conditions

Figure 4 – Trap seal loss due to evaporation in case of P-trap in Fukuoka

cm in Fukuoka and approximately 5 cm in Sapporo. This is because Sapporo is a cold region, the outside temperature and absolute humidity are low throughout the year, and the vapor partial pressure of water is low. Comparing indoor and outdoor in Fukuoka in Figures 4(a) and (b), the volume of seal water loss in Indoor air conditions tends to be slightly smaller overall. This is because indoor air is dehumidified by air-conditioning, therefore the vapor partial pressure of water is low in contrast, to the high temperature and humidity of the outside air in summer.

3.4 Evaporation rate of Bell-trap

Figure 5 shows the calculation results of the evaporation rate in Tokyo for the Bell-trap, which is commonly used for floor drainage in wet toilet spaces. Compared to the results for the P-trap in Figure 2, there is no significant difference when the hollow height is 30 cm, but when the hollow height is 5 cm, the evaporation rate of the Bell-trap is approximately 3 times faster each month.

This is based on the experimental results of evaporation rates by diameter in the previous study [4], which showed that the inner diameter 3 cm (area 7.065 cm^2) and the inner diameter 5 cm (area 19.625 cm^2) had an area ratio of 1.0 : 2.8, in addition the evaporation rate ratio per unit area of 1.0 : 3.2. This is approximately 9 times the difference in the evaporation volume. The difference in evaporation rate is even more
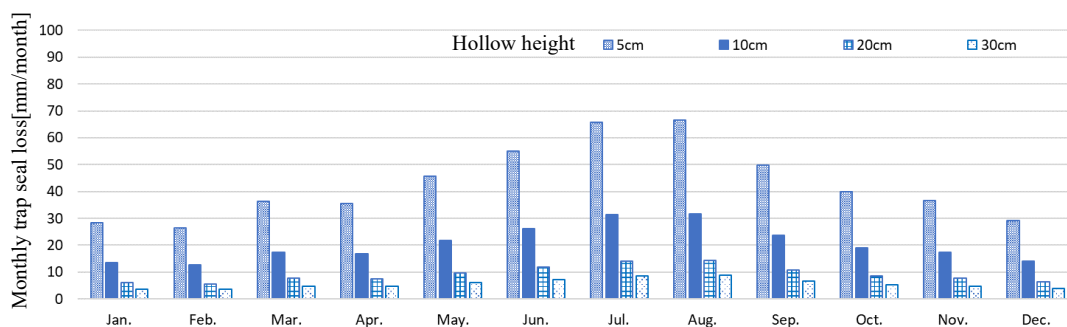
(a) Outdoors
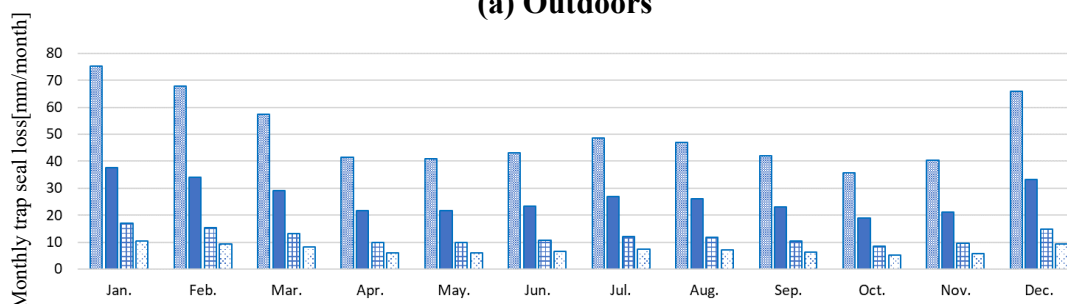
(b) Indoor air conditions

Figure 5 – Trap seal loss due to evaporation in case of Bell-trap in Tokyo

pronounced, because generally the hollow height of a P-trap is 30 cm, while that of a Bell-trap is 5 to 10 cm.

4 Conclusions

In this report, we calculated the difference in the evaporation rate between indoors and outdoors for each region using the calculation formula of evaporation rate, which was shown to be effective in the previous report [4]. For the meteorological data for each region, we used the hourly values of outdoor temperature and humidity for one year from the AMeDAS (Automated Meteorological Data Acquisition System) for three regions with different climates: Tokyo, Fukuoka, and Sapporo. As results, the trend of areas and seasons with high evaporation rates was shown.

Acknowledgments

5 References

[1] U Yanai：New impediment factor to health : biological contamination，Journal of the National Institute of Public Health, 63-4, pp.342-349, Apr.2018（in Japanese）

[2] K.Sakaue，T.Suruki，Y.Ito, T.Sasagawa: Studies on Performance Evaluation Method of Self-Sealing Trap Part1: Characteristics and Performance Evaluation Items of Trap, Proceedings of Society of Heating, Air-conditioning, and Sanitary Engineers of Japan, pp.137-140, Sep.2016（in Japanese）

[3] The Society of Heating, Air-Conditioning and Sanitary Engineers of Japan : SHASE-S206-2019 Plumbing Code, Jan.,2020（in Japanese）

[4] T.Kojima, K.Sakaue: A Study on Evaporation Phenomenon of Trap Seal Water, Proceedings of the 43rd CIB W062 International Symposium(Netherlands), pp.1-11, Aug.2017（in Japanese）

[5] T.Kojima, K.Sakaue: A Study on Evaporation Phenomenon of Trap Seal Water Part2 Experiment of Evaporation Rate in Traps and Measurement of Temperature, Humidity and Wind Velocity in Drain Pipe, Proceedings of Society of Heating, Air-conditioning, and Sanitary Engineers of Japan, pp.85-88, Sep.2018（in Japanese）

[6] Ministry of Health, Labor and Welfare, the Environmental Sanitation Management Standard for Building；https://www.mhlw.go.jp/bunya/kenkou/seikatsu-eisei10/

[7] M.Ueda: Humidity and evaporation – From Foundation to measurement technology, Corona publishing Co., Ltd., pp.123-126, Feb.2000（in Japanese）

6 Presentation of Authors

Takehiko Mitsunaga (Ph.D) is a senior assistant professor at Department of Architecture, School of Science & Technology, Meiji University. His fields of specialization include water environment, building services engineering and plumbing system.

Kyosuke Sakaue (Dr. Eng.) is a professor emeritus at Meiji University. His fields of specialization include water environment, building services engineering and plumbing system.

11/11

Improving the Environment of Toilet Spaces in Evacuation Centers
－Organizing the Problem of Evacuation Toilets based on Previous Studies and the Thermal Environment of Temporary Toilets－

H.Yamaguchi (1)

(1) haruy@kanto-gakuin.ac.jp

(1) College of Architecture and Environmental Design, Kanto Gakuin University, JAPAN

Abstract

In recent years, due to the effects of global warming, disasters have frequently occurred worldwide, and the damage caused by these disasters is severe. In Japan, if it is difficult to evacuate at home after these disasters, evacuees will have to spend time at evacuation centers, such as school facilities designated by the government. Various problems arise because many people stay here temporarily or for a long time. Sanitary management is essential for toilets. Existing toilets cannot be used at evacuation centers when water cannot drain, so portable toilets, simple toilets, and temporary toilets are used.

This research aims to improve the toilet environment at the evacuation center. This report summarizes the actual situation of toilets in evacuation centers during a large-scale disaster in Japan, how to deal with it, and the problems based on existing research.

In fact-finding surveys after the Great East Japan Earthquake (2011) and the Kumamoto Earthquake (2016), problems such as the condition of toilets at the evacuation centers, the hygiene of temporary toilets, odors, and dirt, and the lack of water for washing hands were raised. In addition, trial calculations of the number of temporary toilets required at evacuation centers and considered for odor. On the other hand, regarding the thermal environment of the sanitary spaces, which is a problem in houses, it is not taken up in the toilets of the evacuation center, and there is concern about the impact on health.

Following the actual measurement of the thermal environment of the toilet in the building in the previous report, we report the thermal environment of the temporary toilet installed outdoors.

Keywords

Evacuation Center; Disaster; Toilet Space; Thermal Environment

1 Introduction

In recent years, due to the effects of global warming and the like, disasters have frequently occurred worldwide, causing severe damage. If evacuating from home after a disaster is complex in Japan, evacuees must spend time at an evacuation center, such as a government-designated school facility. Many unspecified people stay in evacuation centers temporarily or for a long time, so various problems arise. Sanitary measures are significant for toilets. Existing toilets cannot be used at evacuation centers because they cannot drain water, so portable, simple, and temporary toilets are used.

The purpose of this research is to improve the toilet environment during disasters. In the previous report [1], to clarify the toilet space's actual situation, we measured the annual thermal environment of the toilet space of the university facility, which is used as an evacuation center, and evaluated the environment. This paper will first summarize the toilet situation in evacuation centers during a major disaster in Japan, how to deal with it, and the problems encountered based on previous research. Next, we report on the results of the measurements of temporary toilets' annual thermal environment and consider the issues of evacuation toilet spaces.

2 Standards and Previous Studies on Toilets in Evacuation Centers

2.1 Changes in the Number of Evacuation Centers and Evacuees during a Disaster

Figure 1 shows changes in the number of evacuation centers and evacuees after significant past earthquakes (the Great Hanshin-Awaji Earthquake in January 1995 and the Great East Japan Earthquake in March 2011) based on data from the Reconstruction Agency [2]. After the Great Hanshin-Awaji Earthquake, approximately 310,000 people lived in evacuation centers, and it took six months for the evacuation centers to close. After the Great East Japan Earthquake, about 410,000 people lived in evacuation centers in the three prefectures (Iwate, Miyagi, and Fukushima) that suffered the most damage (Iwate et al.), and about 470,000 people nationwide lived in evacuation centers, requiring seven months in Iwate Prefecture and nine months in Miyagi Prefecture. It was two years and nine months after the evacuation center closed, where people had evacuated to another prefecture due to the nuclear accident. When such disasters occur, life in centers can be long-term.
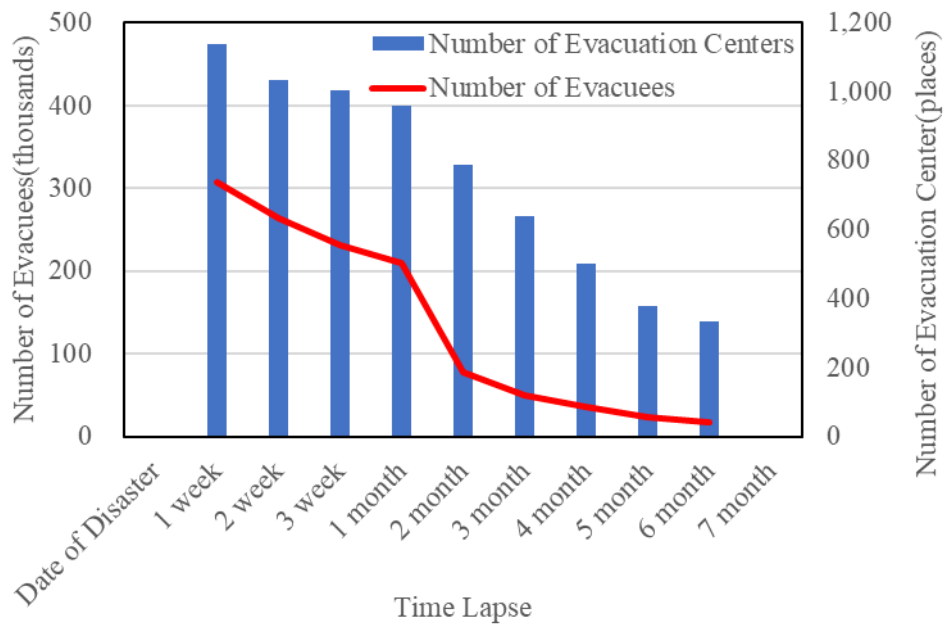
a) Great Hanshin-Awaji Earthquake
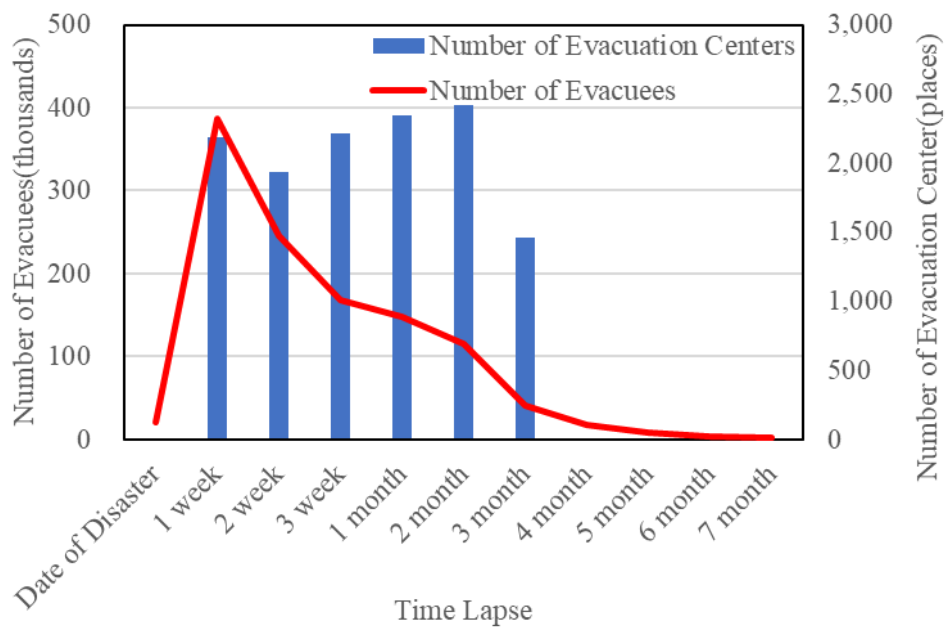
b) Great East Japan Earthquake

Figure 1. Changes in the number of evacuation centers and evacuees

2.2 Status of Disaster-Related Deaths

As shown in Figure 2, the percentage of disaster-related deaths [3] in people aged 70 and over was about 82% during the Great East Japan Earthquake and about 78% during the Kumamoto Earthquake (2016). "Physical and mental burden of evacuation life" and "Physical and mental burden due to disruption of lifelines" account for about 70% of the total.
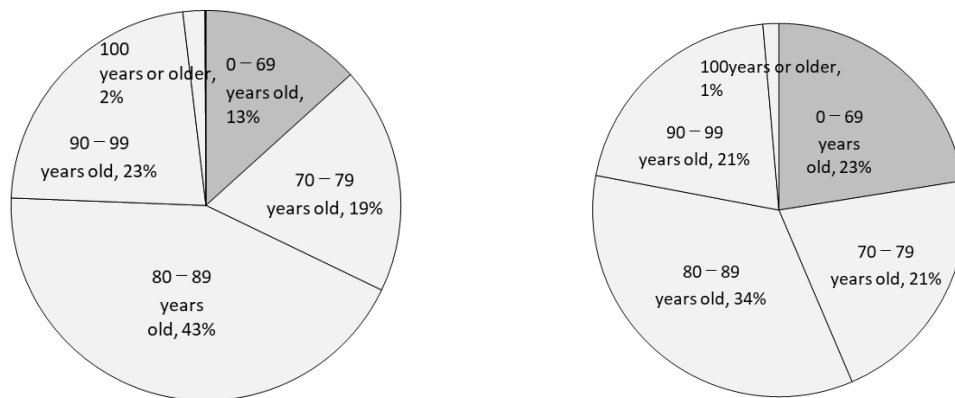
a) Great East Japan Earthquake (2011)   b) Kumamoto Earthquake(2016)
Figure 2. Disaster-Related Death by Age

2.3 Standards for Evacuation Center Toilets

Under these circumstances, the SPIER Standards include international standards for operating and managing evacuation centers and as a basis for support activities in the event of a disaster [4]. The Disaster Countermeasures Basic Act was revised in Japan, and the "Guidelines for Ensuring Good Living Environments at Evacuation Centers" (2013) were formulated. Based on these guidelines, the Cabinet Office has summarized disaster prevention and response in the "Evacuation Center Management Guidelines" [5].

Evacuation centers face various issues, including managing food and supplies, securing and managing toilets, improving beds, managing health, managing people who need special attention, including children, women, and senior citizens, and preventing crime. Among these, the suspension of toilet functions and the deterioration of the sanitary environment, resulting in infections and health impacts, are serious issues. The Cabinet Office has also summarized toilet items in the "Guidelines for Securing and Managing Toilets at Evacuation Centers" [6]. This guideline describes how to secure toilets, manage hygiene, and create a system. It also describes safety, hygiene/comfort, women/children, senior citizens/disabled, and foreigners as matters to be considered.

2.4 Previous Research on the Thermal Environment of the Senior Citizen and Vulnerable

Since senior citizen account for about 80% of the disaster-related deaths mentioned in the previous section, the environment of senior citizens at evacuation centers is essential. In the last report [7], we summarized previous research on residential plumbing spaces and the thermal environment of senior citizens. Characteristics of senior citizens include sluggish adaptation to thermal environments, sweating disorders, decreased metabolic rate, and vascular dysregulation. Regarding the relationship between room temperature and blood pressure, blood vessels constrict when a person is exposed to a cold space, and

blood pressure rises to suppress the heat released. High blood pressure causes arteriosclerosis, which gradually causes cerebral hemorrhage and cerebral infarction.

Systolic blood pressure on waking tends to increase with age and with lower room temperature, according to the indoor thermal environment and health survey conducted before and after insulation renovation in the Ministry of Land, Infrastructure, Transport, and Tourism's innovative smart wellness housing promotion project. In addition, it has been pointed out that the senior person, the more critical it is to raise the indoor temperature in winter [8].

The World Health Organization (WHO) has made indoor coldness and hotness recommendations for "public health" and to achieve the "making of a sustainable city." [9] Specifically, an 18°C indoor temperature is strongly recommended for warm and cold places to protect health. A room temperature of 18°C or higher is especially recommended for houses where senior citizens, children, or people with chronic diseases live.

The Architectural Institute of Japan's Research Group on Thermal Environments for Senior Citizens has proposed common temperature values for residential thermal environment evaluation according to room usage and activities, as shown in Table 1 [10]. For senior citizens, the winter reference value for toilets is 2°C higher than for the general public, and the allowable range is ±2°C. Furthermore, the summer reference value for disabled is 2°C lower than for senior citizens.

Table 1. Standard Values for Residential Thermal Environment Evaluation Considering the Senior Citizens and Disabled[10]

	Season	Living/Dining Gathering/Meals	Bedroom Sleep[※1]	Kitchen Housework[※2]	Corridor Move	Bath/Washroom Undressing	Toilet
General	Winter	21±3deg	18±3	18±3	18±3	24±2	**22±3**
	Middle	24±3	22±3	22±3	22±3	26±2	**24±2**
	Summer	27±2	26±2	26±2	26±2	28±2	**27±2**
Senior	Winter[※3]	23±2deg	20±2	22±2	22±2	25±2	**24±2**
	Middle	24±2	22±2	22±2	22±2	26±2	**24±2**
	Summer[※3]	25±2	25±2	26±2	26±2	28±2	**27±2**
Disabled	Winter	23±3deg	20±2	22±2	22±2	25±2	**24±2**
	Middle	24±3	22±2	22±2	22±2	26±2	**24±2**
	Summer[※4]	25±2	25±2	25±2	25±2	27±2	**25±2**

*Clothing amount: Summer 0.5-0.2clo, Middle 0.7-0.5clo, Winter 0.5-0.2clo
 The value is the globe temperature at 1.2m above the floor.
 Humidity was set at 30-50% in winter, 40-70% in mid-season, and 60-80% in summer.
 There is no characteristic radiant heat, airflow, or temperature distribution.
※1 Bedding (winter: futon + blanket ~ futon, summer: summer blanket + towel ~ none)
※2 General/Disabled: 3 met, Senior: 2 met
※3 Shading: Different from General
※4 Shading: Different from Senior

2.5 Previous Research on Toilets in Evacuation Centers

Previous research on toilet spaces in times of disaster includes fact-finding surveys on the Great East Japan Earthquake and the Kumamoto Earthquake. Also, problems such as the state of toilets in evacuation centers, the hygiene of temporary toilets, odors, dirt, and lack of water for washing hands have been raised [11)-15)]. Trial calculations of the number of temporary toilets required at evacuation centers [16), 17)], and measures against odors are also under consideration [18), 19)].

However, no previous research on the thermal environment of toilets in evacuation centers exists, and the Cabinet Office's guidelines for hygiene and comfort state that "measures against thickness, cold, rain, wind, and snow will be implemented."

The previous report [7)] research also indicates that senior citizens are blunted to thermal environments and more likely to suffer heatstroke and heat shock. Even in the indoor environment recommended for senior citizens, as mentioned in the previous section, a high-temperature environment in winter and a low-temperature setting in summer are proposed. Evacuation centers in the event of a disaster are placed in even harsher conditions, and there are concerns about health effects such as heatstroke and heat shock.
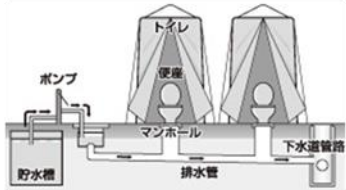
3 The Thermal Environment of Toilets in Evacuation Centers

3.1 Toilets during Disasters

The toilets shown in Table 2 are mainly used during a disaster. Simple and portable toilets are used indoors, while temporary and manhole toilets are used outdoors. In a previous report [1)], we measured the thermal environment of toilet spaces in school facilities, which are often designated as evacuation centers. The Toilet Space in the Building is affected by the corridor leading to the toilet and the external space. However, compared to the outdoor air temperature, the temperature of these toilets is generally lower in the summer and higher in the middle and winter. In addition, the private rooms and the washroom have almost no difference in temperature.

On the other hand, since temporary and manhole toilets are installed outdoors, these are more susceptible to the outdoor world than toilets in buildings.

Table 2. Types of Toilets for Evacuation

3.2 Thermal Environment of Temporary Toilets

3.2.1 Target Toilet

Materials used in general temporary toilets include polypropylene, high-precision polyethylene, and wood. Photo 1 and Fig. 3 show the outline of the target toilet in summer. For the toilet, as recommended by the Ministry of Land, Infrastructure, BS-KRY II Co., Ltd. B・S・K, floor area: 1.1 m2 [20], the material should be polypropylene. Ventilation louvers (0.015m2) are provided on the upper left and right walls (FL + 1800). The target toilet for winter is the specification model TU-V1FU, Grand Sangyo Co., Ltd., floor area: 0.85m2 [21], which has almost the exact dimensions of the summer toilets, and the material is high-precision polyethylene. Additionally, a ventilation louver (0.07m2) is provided above the front of the entrance door, and the ceiling is a translucent panel. These toilets are installed in a warm climate region in Yokohama.

Photo 1. Exterior and Interior of Temporary Toilet
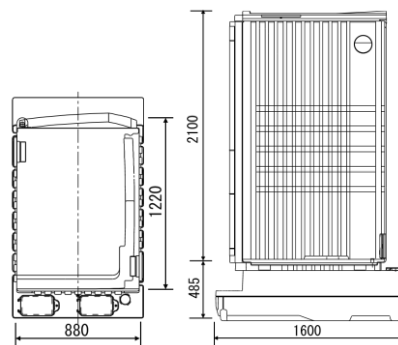
Figure 3. Plan and Elevation of Temporary Toilet

3.2.2 Outline of Measurement

The measurement periods are 24/8/2022–17/9/2022 (in the summer), 27/10/2022–30/11/2022 (in the fall), and 1/12/2022–28/2/2023 (in the winter). The measured items are the external conditions (outdoor temperature, horizontal solar radiation), the temperature inside the target toilet in the summer, the globe temperature, and the thermal image is taken from 12:00 to 12:30 on 24/8/2022. The winter temperature inside the target toilet twas measured. For the external conditions in winter, we used the central monitoring data of buildings during the measurement periods.

3.3 Measurement Results

3.3.1 External Conditions

These show the horizontal solar radiation and outdoor air temperature during the measurement periods. In summer, with an average of 25.8°C and a maximum of 34.0°C (14:20, 26/8/2022). The weather is generally sunny, and there are days when solar radiation exceeds 800 W/m2 during the day. In the fall, the average is 15.3°C, the maximum is 24.6°C, and the minimum is 8.2°C. The amount of solar radiation exceeds 600 W/m2 during the day. In the winter, the average temperature is 8.8°C, and the maximum is 19.3°C (12:30, 4/12/2022). Solar radiation exceeds 500 W/m2 during the daytime and is about 100 W/m2 on cloudy days.

a) Summer

b) Middle

c) Winter
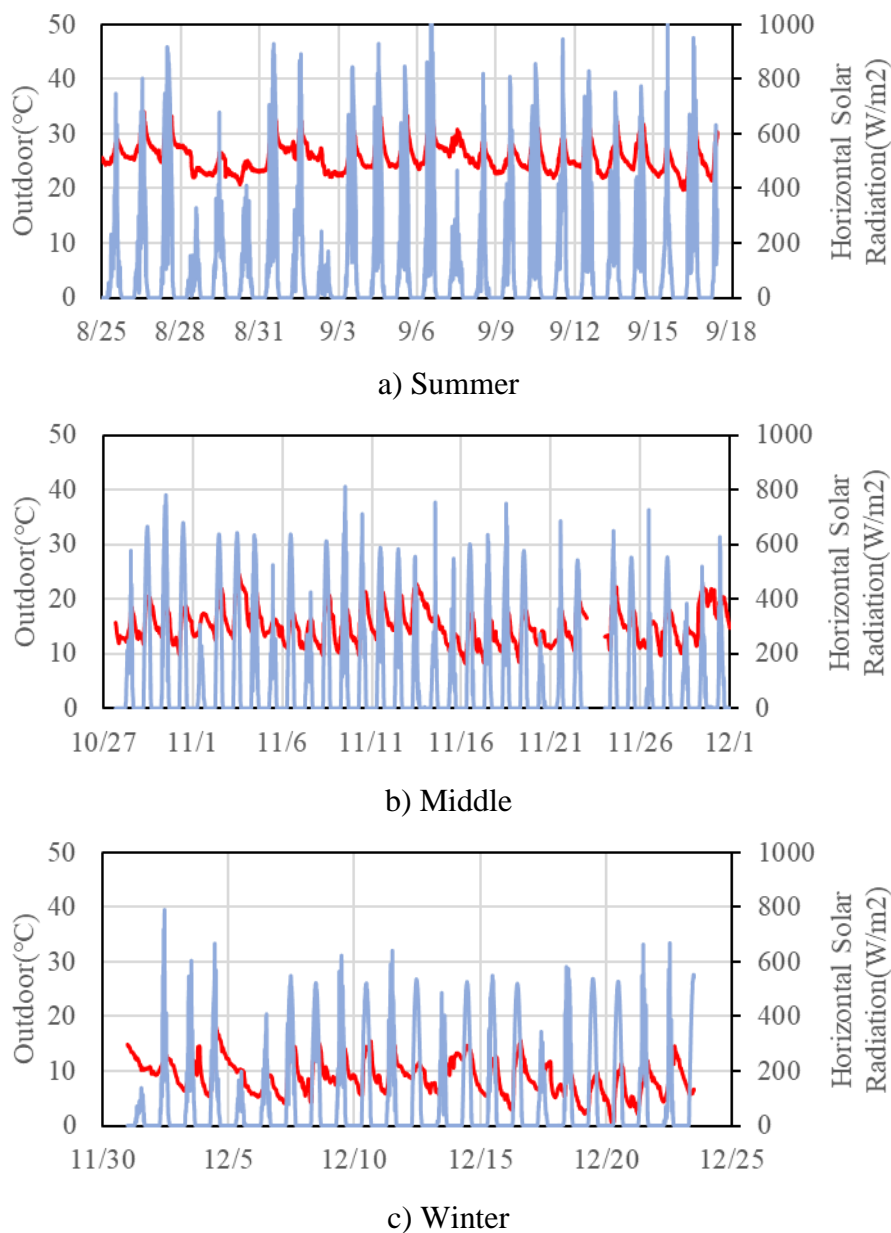
Figure 4. Horizontal Solar Radiation and Outdoor Air Temperature

3.3.2 Relation to the Outdoor Air Temperature

Figure 5 shows the relationship between the outdoor and toilet temperatures in each period. In the summer, the average toilet temperature is 26.9°C, and the maximum is 43.3°C. The toilet temperature is higher than the outdoor temperature, with a maximum difference of about 12°C. The globe temperature is the same as or higher than the toilet temperature. In the fall, the average temperature in the toilet is 16.0°C, the maximum is 35.2°C, and the minimum is 6.0°C. In the winter, the average temperature inside the toilet is 9.3°C, the maximum is 28.1°C during the day, and the minimum is -1.0°C. The maximum difference between the outdoor and internal temperatures during the day is 11.2°C on a sunny day. On cloudy days, the average difference is 1.1°C, almost unchanged. Overall, the toilet is always hotter than the outdoor air during the day, and the globe temperature is even higher in the summer, indicating a radiant heat impact.

a) Summer

b) Middle

c) Winter
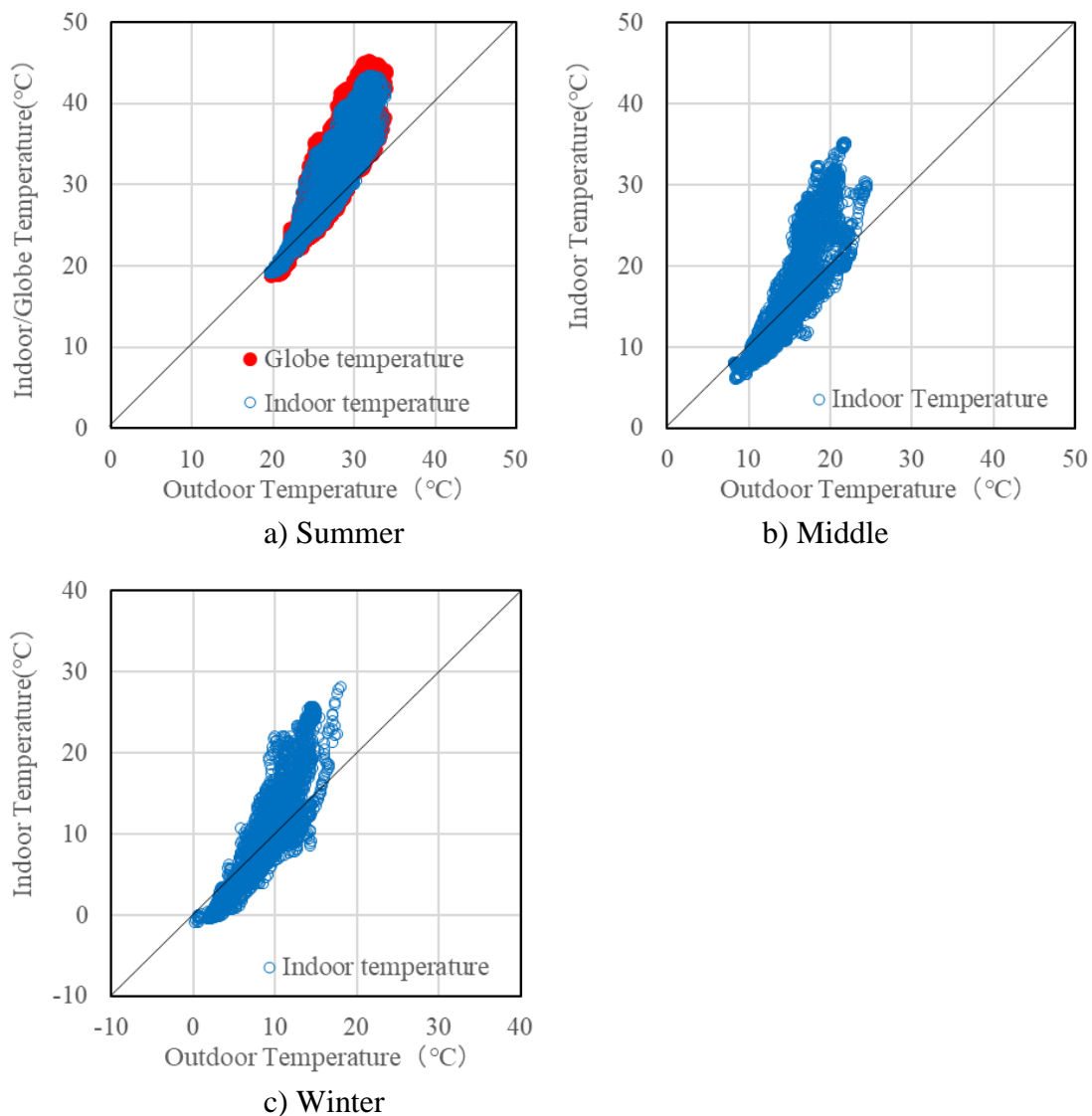
Figure 5. Outdoor and Indoor Temperature (Added Globe Temperature in Summer)

3.3.3 Surface Temperature and Thermal image (summer)
Figure 6 shows a thermal image of the inside of the toilet and the outer west wall (12:30,24/8/2022). Inside the toilet, the temperature of this wall is high, reaching a maximum of 47.2°C. Outdoor, the maximum temperature of the wall is 51.5°C in part exposed to the sun versus a minimum of 36.9°C in the part shaded by the surrounding trees, with a difference of about 15.0°C. Thus, blocking sunlight can suppress the surface temperature, effectively improving the thermal environment inside the toilet.
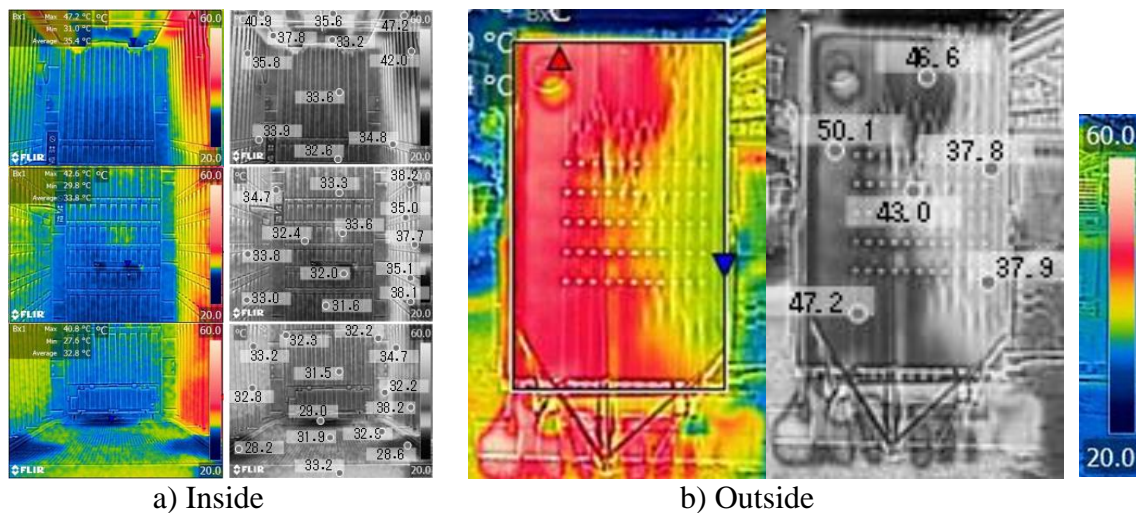
a) Inside   b) Outside
Figure 6. Thermal Image

3.4 Comparison with the Thermal Environment of the Building Toilet
Figure 7 shows the changes in temperature inside the building toilet and the temporary toilet. The toilet temperature was 27.0°C on average and 43.4°C at maximum (15:00, 4/9/2022), almost matching the outdoor temperature at night. The temperature transition from 4/8 to 11/8/2021, shown in the figure, is the summer temperature transition in building toilet 1). The outdoor temperature during the same period was almost the same as the actual measurement from 27/8 to 3/9/2022. Compared to the daytime temperature fluctuation range of 3.2°C in the building toilet, the measurement shows a significant fluctuation of 22.3°C, which is directly affected by the outdoor air.
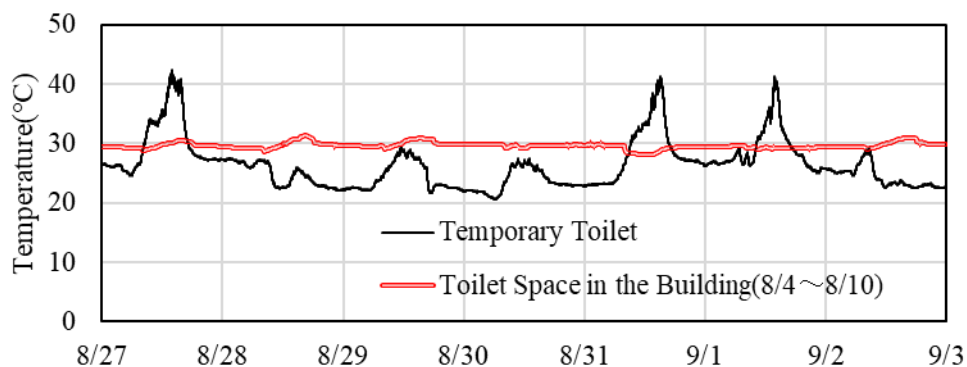

Figure 7. Temperature Transition of Toilet in the Building and the Temporary Toilet

4 Conclusions

After a disaster, survivors may stay in an evacuation center for a long time. Approximately 80% of disaster-related deaths are among senior citizens, and their burden is heavy. Senior citizens become dull in thermal environments. The indoor temperature should be higher in the winter and lower in the summer. Evacuation centers in the event of a disaster are placed in even harsher conditions, and there are concerns about health effects such as heatstroke and heat shock. In this report, we measured the thermal environment of temporary toilets. Regardless of the season, the inside of the toilet is hotter than the outdoor air during the day, and the globe temperature is even higher in the summer. By blocking the sunlight, the surface temperature can be controlled, effectively improving the thermal environment inside the toilet.

In the future, we will use simulations to examine the effects of cold regions and improvement measures.

Acknowledgments

5 References

1) Haru Yamaguchi; Annual Thermal Environment Evaluation of Toilet Space in University Facility, 2022 Symposium CIB W062, Technical Session 3 Provision and Sanitary Facilities, pp.209-221, 2022.10
2) Reconstruction Agency; Changes in the Number of Evacuation Centers and Residents Living in Evacuation Centers, 2011.10 (in Japanese)
3) Cabinet Office; About Disaster-Related Death Cases (Expanded Edition), 2021.4, 2023.5enlarged (in Japanese)
4) Sphere Standard; International Standards Operation of Shelters, for Management, Basis for Support Activities in Times of Disaster the Sphere Handbook Humanitarian Charter and Minimum Standards in Humanitarian Response Sphere2018, https://jqan.info/documents/sphere_handbook/
5) Cabinet Office; Shelter Management Guidelines, https://www.bousai.go.jp/taisaku/hinanjo/pdf/1604hinanjo_guideline.pdf, 2016.4
6) Cabinet Office; Guidelines for Securing and Managing Toilets at Evacuation Centers, https://www.bousai.go.jp/taisaku/hinanjo/pdf/1604hinanjo_toilet_guideline.pdf, 2016.4
7) Haru Yamaguchi; Consideration of the Thermal Environment in the Sanitary Space and the Senior Citizen's Thermal Sensation, 2021 Symposium CIB W062, SESSION C, 2021.10

8)   Wataru TANIMOTO; Current Problem of Odors Occurred in the Portable Toilet and Its Counter Measure in Future, Journal of Japan Association on Odor Environment, Vol.48, No.2, pp.106-113 (in Japanese)

9)   WHO Housing and Health guidelines; https://www.who.int/publications/i/item/9789 241550376, accessed 2018.11

10) Architectural Institute of Japan; For the Senior citizen to Live Comfortably, Gihodo, pp.66-73,2005.8.25(in Japanese)

11) Tomoko OKAYAMA; Distribution of temporary toilets and their use by evacuees of Kumamoto earthquake, Proceedings of the Annual Conference of Japan Society of Material Cycles and Waste Management, Vol.28, A14-4-O, 2017.11 (in Japanese)

12) Nobuharu MAEDA, Seishi OKADA, Keita FUKUI; Survey on the Toilets of Evacuation Centers at the Time of the Great East Japan Earthquake, Transactions of the Society of Heating, Air-conditioning and Sanitary Engineers of Japan, Vol.43, No.255, pp. 59-64 (in Japanese)

13) Masayuki OKADA, Shinji MAEDA, Keita FUKUI, Jun YASOGAWA; Investigative Research on Toilets in Shelters During Disasters, Summaries of Technical Papers of Annual Meeting of Architectural Institute of Japan, Vol.2018, pp.655-656, 2018.9 (in Japanese)

14) Masayuki OKADA, Shinji MAEDA, Keita FUKUI, Jun YASOGAWA; Fact-finding Survey of Toilet Installation in Designated Evacuation Shelters in the Event of a Disaster, Architectural Institute of Japan, Tohoku Branch Research Reports and Planning Division, No.82, pp.25-26, 2019.6 (in Japanese)

15) Masatsuna KARIYA, Kenji OKAZAKI, Chiho OCHIAI; A Study on Toilet Problem in Time of Disasters Focusing on Nakamachi District in Urayasu City, Chiba Prefecture, Reports of the City Planning Institute of Japan, Vol.14, No.4, pp.322-325, 2016.3 (in Japanese)

16) Tomoko OKAYAMA, Atsushi KATO; Research on the Procurement of the Temporary Toilets of the Local Government at the Time of The Disaster, Proceedings of the Annual Conference of Japan Society of Material Cycles and Waste Management, Vol.26, A11-4, 2015.10 (in Japanese)

17) Hideyuki ITO, Tomoko OKAYAMA; A Toilet in Shelter and From Preparation to Burning of Excrement, Proceedings of the Annual Conference of Japan Society of Material Cycles and Waste Management, Vol.24, A12-3, 2014.1 (in Japanese)

18) Wataru TANIMOTO; Current Problem of Odors Occurred in the Portable Toilet and Its Counter Measure in Future, Journal of Japan Association on Odor Environment, Vol.48, No.2, pp.106-113 (in Japanese)

19) Hiroshi SATO, Kumiko SIGEOKA; Research on Toilet Situation/Malodor in the Affected Areas at the Time of Kumamoto Earthquake, Journal of Japan Association on Odor Environment, Vol.48, No.2, pp.114-117, 2017.3 (in Japanese)

20) B・S・K Co., Ltd. HP; Simple Flush Temporary Toilet (BS-KRYII), https://www.b sk-net.co.jp/list.html, accessed 2022.3

21) Grand Industry Co., Ltd. HP; Pump Type Simple Flush Temporary Toilet (TU-V1FU), https://www.grand-s.co.jp/kt.html, accessed 2022.12

6 Presentation of Author

Haru Yamaguchi is a professor at the Faculty of Architecture and Environmental Design, Kanto Gakuin University. She has a doctoral degree in environmental design from Showa Women's University and is a certified architect (First Level). She is also an active member of the Architect Institute of Japan's association (AIJ) and (The Society of Heating, Air-Conditioning and Sanitary Engineers of Japan (SHASE).

Risk Assessment to Contaminant Spreading through Building Drainage System in Residential Building

Yen-Yu. Lin (1), Cheng-Li. Cheng (2)

(1) D11013011@mail.ntust.edu.tw

(2) CCL@mail.ntust.edu.tw

(1)(2) National Taiwan University of Science and Technology, Department of Architecture,

Taiwan, R.O.C.

Abstract

With the global outbreak of covid-19 in 2020, aerosol vector transmission in community houses has become a key research object of concern from all over the world. In order to clarify the risk of aerosol pathogen transmission in the building interior space through the drainage and ventilation system among the COVID-19 epidemic, this study analyzed the mechanism of the trap mechanism of the building drainage pipe and the main factors of the risk of aerosol pathogen transmission, combined with the failure mode theory establish a numerical risk evaluation index and evaluation system for aerosol vector transmission in drainage pipes. The building drainage system aerosol vector transmission risk assessment system structure is based on the combination of the risk factors causing trap failure and the factors that accelerate the spread of pollution. This study introduced a numerical risk assessment system based on failure mode and effect analysis. Based on computational simulation, it is determined that the possibility of water trap breaking is critical to the risk value. By analyzing 55 local cases, we discovered the potential high risk that the local area is facing, also identified the possible impact of the building custom to the risk value.

Keywords

Building Drainage System, Contaminant Controlling, Risk Assessment, Water Trap

1. Introduction

Drainage system plays a critical role in our daily life basis by transporting waste water away from our residential area, however, it is easily neglected since it is not usually visually exposed. Cases during SARS and Covid-19 nowadays have shown the possibility that neglected drainage system could become a potential virus spreading route. Simulations from previous studies show that unit with broken water trap would certainly be infected. Consequently, risk assessment highly associates with the probability of the situation where broken water trap was caused. The risk assessment this study developed will be based on such conception. As a result, we could examine real cases and determine how high the risk would be when a community infection occurred.

2. Material and Methods

Drainage system, putting in simple words, is series of pipe lines inside buildings that brings domestic wastewater down to the public sewage system. However, as simple as it may seemed, it plays not only a critical role in our daily life but also a great improvement monument of public health.[1][2][3]

Moreover, water trap is a stack of water that stay within the pipes that its main purpose is to divide the air between clean and contaminated. Breaking water seal is the situation where two sides of the trap are connected that could be caused by poor drainage system design, lack of maintenance, sudden pressure shift, or long-term misusage and eventually it could lead to contamination where foul gas and pathogen make their breach. With a proper system design and regularly maintenance, it can lower the chance of break seal.

Computational Fluid Dynamics is a powerful tool predicting fluid movements by computer calculation. With the help of CFD, previous studies[4] map out the concentration distribution and the movement of the contaminant among the drainage system under a 12-stories building model, shown as Figure 1. In conclusion, given an infinite time, broken water seal would certainly leads to the full infection all over the whole building eventually. Futhermore, under certain pressure, the contaminant spreads to the adjacent floors in the very first hour. As a result, we concluded that risk assessment to contaminant spreading through building drainage system could highly associate with the discussion about the possibility of whether the water trap will break.

Analyzing on the factors causing broken water seal, critical factors were selected due to their impact on the failure.[5][6][7] Besides reasons to broken water trap, indoor ventilation also shown its impact on accelerating contaminant movement and diluting indoor contaminant concentration. Thus, ventilation factor is also considered as a critical factor to the risk assessment system.
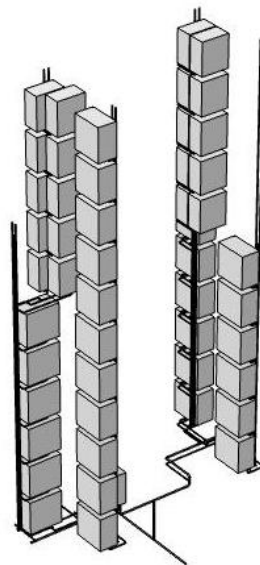

Figure 1 – Simulation model of a drainage system design

3. Risk Assessment

Drainage system failure could lead to foul gas or pathogen breach, and further contamination of the residential area. Besides, indoor ventilation could enhance the effect of virus diffusion. In order to determine the risk of such situation, a risk assessment system are introduced to this research.

$$R_{is} = T \times D \times M \times V \quad \text{................(1)}$$

where:

R_{is} : Risk value, $1 \leq R_{is} \leq 180$

T : Trap durability, $T \leq 10$

D: Drainage system, $D \leq 3$

M : Maintenance, $M \leq 3$

V: Ventilation, $V \leq 2$

Each factors are determined by the equipment used and local situation in the building. It could provide a more thorough overlook to the drainage system and verify the risk level of a building.

Trap Durability factor(T) is a critical factor that will directly cause the failure of the drainage system. Consequently, it is also a key factor of risk assessment to contaminant spreading. This factor mainly focuses on examining whether the usage behavior of such equipment has enough water supply to keep the trap functional and the precaution treatment has been taken before the trap dried out. Trap Durability(T) is determined by the following formula(2), where traps from different sanitary equipment will be examined.

$$\text{T} = \begin{cases} \prod_{i=1}^{8} T_i \,, otherwise \\ 10.0, \prod_{i=1}^{8} T_i \geq 10.0 \end{cases} \quad \text{............(2)}$$

Factor	Sanitary terminal	No trap	None installed	Rare Usage	Normal Usage	Special Treatment
T_1	Toilet	0	2.0	0.8	1.5	2.0
T_2	Urinal	0	2.0	0.8	1.5	2.0
T_3	Sink	0	2.0	0.8	1.5	2.0
T_4	Bathtub	0	2.0	0.8	1.5	2.0
T_5	Shower floor drain	0	2.0	0.8	1.5	2.0
T_6	Bathroom floor drain	0	2.0	0.8	1.5	2.0
T_7	Kitchen floor drain	0	2.0	0.8	1.5	2.0
T_8	Other equipment	0	1.0	0.8	1.5	2.0

Drainage system factor(D) is another important factor that included in risk assessment system. This factor describes the influence of the drainage system design and the height of the building on the water trap. The higher a building is, the higher pressure difference it causes among the pipes. However, the pressure gradient could be recovered by a well designed drainage system. Drainage system factor(D) is determined by the following formula(3).

$$\text{D} = \begin{cases} \prod_{i=1}^{3} D_i \,, otherwise \\ 3.0, \prod_{i=1}^{3} D_i \geq 3.0 \end{cases} \quad \text{............(3)}$$

Factor	Drainage system design		Floor height				
			Under 8F	8~15 F	16~29F	Over 29F	None
D_1	Single stack system	Normal joint	1.0	0.8	0.5	0	-
		Special joint	1.5	1.3	1.2	1.0	-
	Double stack system		1.5	1.3	1.2	1.0	-
D_2	Circuit ventilation		1.5	1.3	1.2	1.0	1.0
D_3	Equipment separates pipes				1.5		
	Waste/ Soiled water separates				1.3		
	Waste/ Soiled water converge				1.0		

Maintenance factor(M) means to detemine the importance of both the life cycle of the pipe system and the maintenance afterward. A long-used pipeline has a higher risk to induce breach and drainage system failure. However, a routine maintenance will be able to prevent such situation and futhermore discover malfunction before real damage was made. Maintenance factor(M) is determined by formula(4).

$$M = \begin{cases} M_l \times M_m, otherwise \\ 3.0, M_l \times M_m \geq 3.0 \end{cases} \cdots\cdots\cdots(4)$$

Factor	Examine	New	1-5years	6-10years	11-15years	16-20years	Over 20years
M_l	Sanitary equipment Life cycle	1.5	1.4	1.3	1.2	1.1	1.0

Factor	Examine	Great	Average	Poor
M_m	Maintenance Frequency & Quality	1.5	1.2	1.0

Ventilation factor(V) is introduced to determine the influence of indoor ventilation to the risk of contaminant spreading. Previous studies and cases shown that the air pressure caused by indoor mechanical ventilation system will accelerate the contaminant spreading due to the movement of the main carrier, air. However, the natural ventilation will replace polluted air with fresh air, lowering the risk of contaminant filling indoor environment. As a result, the competitive relationship is shown between natural ventilation and mechanical ventilation, thus, ventilation factor(V) is determined by formula(5).

$$V = \begin{cases} V_n/V_m\,, otherwise \\ 2.0,\, V_n/V_m \geq 2.0 \end{cases} \quad ....(5)$$

Factor	Ventilation system	Ventilation Quality				
V_n	Natural ventilation	Under 60% Floor area	60%-70% Floor area	70%-80% Floor area	80%-90% Floor area	90%-100% Floor area
V_m	Mechanical ventilation	No fresh air input	Below 50% fresh air input	Over 50% fresh air input	Fully fresh air input	Fresh air input through ventilation
		1.0	1.2	1.5	1.8	2.0

4. Experiment Preview and Discussion

55 cases were introduced to the risk assessment system. The result of the relationship between cumulating number of cases and R_{is} is shown in Figure 2, in which we could analyze risk distribution among local area. Futhermore, Figure 3 is the average score and standard deviation of each factor included in the assessment system. In which, we could determine the distribution of each factor.
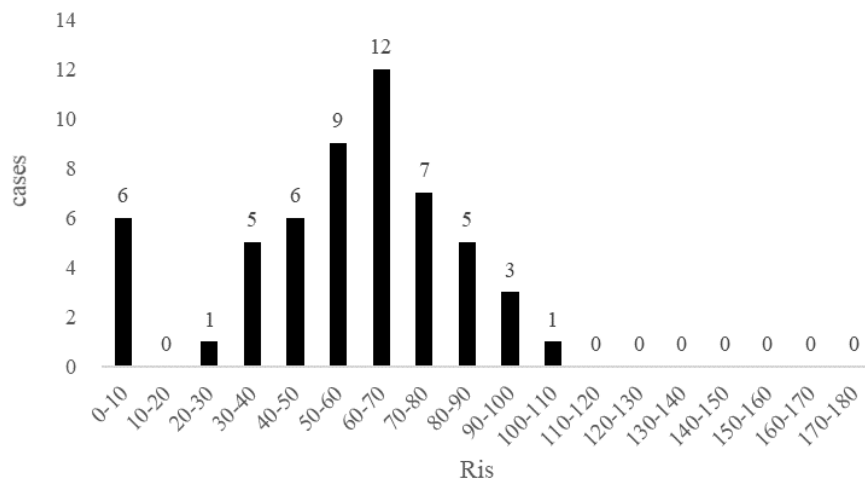
Figure 2 – Cumulating number of cases in different section R_{is} diagram

The risk assessment system shows the current risk score in the local area,and the average score of R_{is} is 55.91, and there are 6 failure cases which scores 0 due to their constant lacking of water trap. Based on Figure 2, chosen area is facing a high risk of contaminant spreading, since the cummulating numbers of cases mainly distribute in the lower score area. It is observed that the distribution mainly contributed by the vast number of cases that

equipped with seldom used bathroom and kitchen floor drain, which are building custom commonly found in the local area.

5. Conclusion

In this article, we introduced a numerical risk assessment system based on failure mode and effect analysis. Based on computational simulation, it is determined that the possibility of water trap breaking is critical to the risk value. By analyzing 55 local cases, we discovered the potential high risk that the local area is facing, also identified the possible impact of the building custom to the risk value. Future work will be including more cases to fit the distribution features of the local buildings, and also conducting an average risk value to the local area.

References

[1] CHENG Cheng-li et al.；Study on Pressure Distribution of Drainage Stack System in High-Rise Apartment Houses，CIB-W62 Symposium，1996.09. (Switzerland)

[2] Liao W.J., Mui K.W., Cheng C.L., Wong L.T., He K.C., Air Pressure Fluctuations of Drainage Stacks at a High-rise Office Building. Indoor and Built Environment. 2011;20(4):412-419.

[3] W.H. Lu, C.L. CHENG, M.D. Shen, K.C. Tu, Prediction method of air pressure distribution on vertical drainage stack for apartment house, CIB-W62 International Symposium, 2003, Ankra, Turkey.

[4] Cheng, C.-L.; Lin, Y.-Y. CFD Numerical Simulation in Building Drainage Stacks as an Infection Pathway of COVID-19. Int. J. Environ. Res. Public Health 2022, 19, 7475.

[5] Gormley M, Aspray TJ, Kelly DA, Rodriguez-Gil C (2017) Pathogen cross-transmission via building sanitary plumbing systems in a full scale pilot test-rig. PLoS ONE 12(2): e0171556.

[6] Cheng, C. L., Ho, K.C., Yen, C. J., Lu, W. H., Decision-making and assessment tool for design and construction of high-rise building drainage system, Automation in Construction, Vol 17, pp 897-906, 2008

[7] Cheng L Cheng, Wan J Liao, Chien S Lo, Jr J Peng, A tool for detecting and diagnosing faults in the drainage systems of existing buildings, Indoor and Built Environment, 2017, Vol. 26, 1: pp.108-118

Presentation of Authors

Lin, Yen-Yu is the PhD. student at National Taiwan University of Science and Technology, Department of Architecture. His research is focus on building water drainage system.

Cheng, Cheng-Li is the Professor at National Taiwan University of Science and Technology, Department of Architecture. He is a research scholar for water supply and drainage in building. He has published extensively on a range of sustainable issues, including the water and energy conservation for green building.

The Transport of a Model Viral Pathogen on Bioaerosols through a Full-Scale Building Drainage Test Rig under Realistic Conditions

T. Dight[1] & M. Gormley[2]
1. td17@hw.ac.uk
2. m.gormley@hw.ac.uk

1 & 2 School of Energy, Geoscience, Infrastructure and Society, Heriot-Watt University, Edinburgh, Scotland, UK.

Abstract

A number of post-factum studies of disease transmission in the field have identified the transportation of bioaerosols on air currents in drainage systems as a relevant method of disease transmission, involving both bacteria and viruses, notably in healthcare and high-rise residential buildings. Studies in the field and the laboratory have supported the transmission of aerosols, including viable bacterial bioaerosols, via this route, however existing results on the transmission of viral bioaerosols by this pathway have been inconclusive. We here address some of the difficulties which may have impeded the collection of evidence of viral bioaerosols via this pathway if present, including both the conditions within the model systems and the sampling technologies deployed. We further examine the use of PCR as an increasingly accessible tool for the detection of viruses, particularly in obviating the need to use viable virus, and allowing the detection of virus present at low concentrations. Building on previous work in our laboratory, this analysis was used to design a new programme of experiments targeting the detection of viral bioaerosols in the building drainage system. Although we have striven to optimise the conditions for bioaerosol detection in our model drainage system, the conditions for aerosol generation and transport are representative of those found in real buildings in the field. We demonstrate the detection of viral bioaerosols transmitted on air flows through the drainage test rig at Heriot-Watt University.

Keywords
PMMoV, Drainage, Disease Transmission, Bioaerosols, Aerodynamic Particle Sizing

1. Introduction

It is increasingly understood that pathogens can become aerosolised in a Building Drainage System (BDS) and these pathogens, including viruses, are easily amenable to aerosolization. (Gormley et al 2020a,b, Gormley et al 2021). There has also been credible evidence that there was inter-apartment cross-transmission during the early days of the COVID-19 pandemic (Kang *et al*, 2020).

The aerosolization of a virus often occurs at a different rate than that of bulk fluid, and the reasons behind this are intricate, not solely determined by the virion structure. This complexity makes it challenging to interpret results from the laboratory or disparate fields of research, particularly in the wastewater context. However, certain factors warrant attention in the wastewater context.

Research has widely demonstrated that virus survival varies with temperature and relative humidity (Verreault et al., 2008; Xagoraraki et al., 2014), and these factors interact with the influence of organic matter in the suspension fluid. For instance, Smither et al. (2020) found that the presence of artificial saliva affected the survival of aerosolized SARS-CoV-2 differently depending on the relative humidity. Moreover, Ijaz et al. (1985) observed that human rotavirus aerosolized from a human faecal suspension lost viability at a slower rate than the same virus in tryptic soy broth.

Once particles and aerosols are formed, they deviate from the path of the bulk fluid due to various influences, such as settling or buoyancy, inertial effects (which play a larger role in the motility of larger particles), and random walk effects like Brownian motion and turbophoresis (causing more mobility in smaller particles). Additionally, electrostatic effects exert a more significant influence on small particles relative to their mass. Furthermore, filtration is influenced by the physical obstruction of larger particles. Different sampling methods capture particles of varying sizes with different levels of efficiency due to the differing roles of these forces. The interaction of a particular aerosol with a specific sampler cannot be characterized solely by size, as factors like density, morphology, and electrical characteristics also impact their propensity to be sampled. Nonetheless, empirical results often indicate a trough at around 300 nm, at which neither inertia nor diffusion efficiently capture aerosols. Thus, efficiency at 300 nm is commonly used to quote filter efficiency and set standards (EN12341:2014 [European Committee for Standardisation, 2014]).

Verreault, Moineau, and Duchaine (2008) conducted a systematic review of viral bioaerosol sampling up to 2007, categorizing samplers as cyclones, liquid impingers, slit samplers, electrostatic precipitators, filters, and others, which included sample collection from existing air handling filters and plant and exposing animal hosts to putative aerosols. Pan, Lednicky & Wu (2019) classified samplers as impactors and cyclones, liquid impingers, filters, electrostatic precipitators, and water-based condensation devices. Due to the merits and weaknesses of different samplers, some authors explore chimeric devices that sequentially target different parts of the aerosol population.

In this paper we propose a method to evaluate the detection of aerosolised virus using 'safe to use' techniques which allow the transport of viruses to be established within the airstreams within premise BDS.

2. Methods
2.1 Laboratory setup

Figure 1 shows the arrangement used to carry out the experiments in the laboratory at Heriot-Watt University in Edinburgh. The system is essentially a physical model of a two-storey building with a single stack (primary ventilated stack) of 100mm diameter.
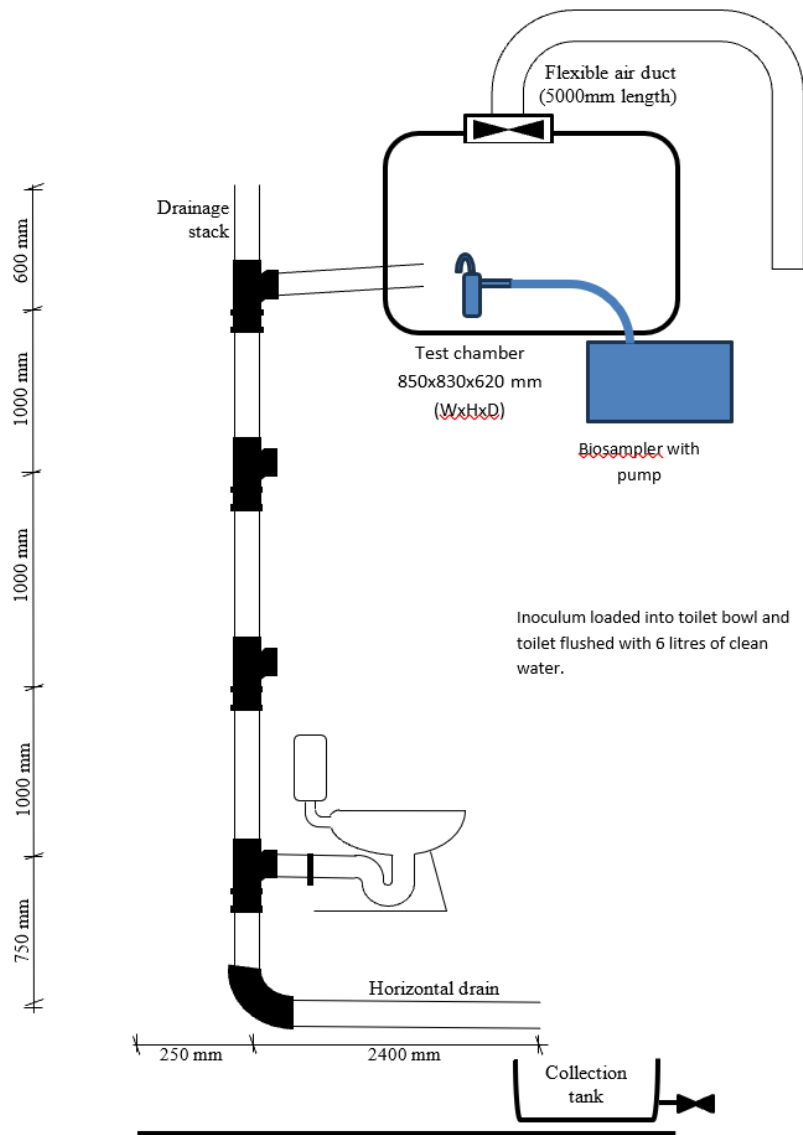

Figure 1 Bioaerosol test rig – system organisation and dimensions.

On the ground floor there is a WC connected to stack where the bowl can be contaminated with pathogenic material, or in this case, micro-organisms that act as surrogates for

pathogenic materials. The important criterion is that the organism physical act in similar manner to other more dangerous organisms which we want to establish system kinetics for. A photograph of the test rig is shown in Figure 2 (a) and a close-up photograph of the Biosampler with pump arrangement is shown in Figure 2(b). A gate valve to the left of the chamber in Figure 2(b) was opened and closed to vary levels of updraft air; this method was chosen in preference to opening the plenum chamber door as previously in order to maintain as strong as possible an updraught during flush events, and hence maximise aerosol generation.
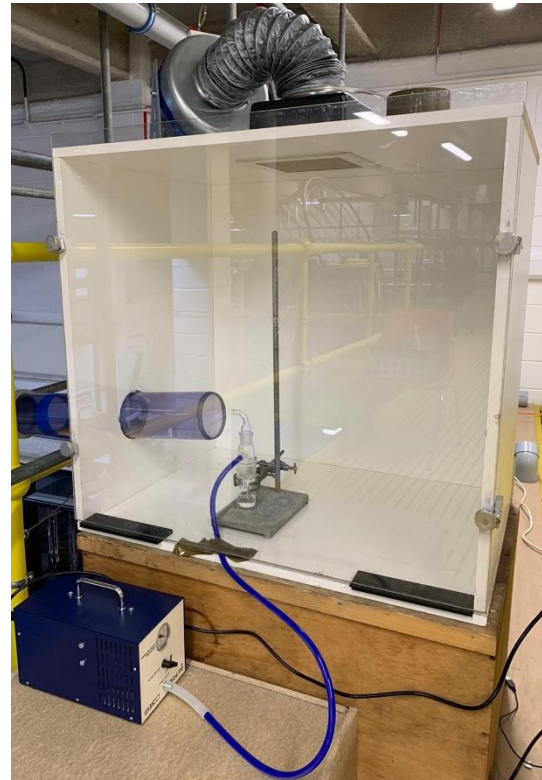
(a)   (b)

Figure 2 Photographic images of the laboratory setup. (a) shows the overall height of the test rig and (b) shows the setup of the Biosampler with pump in the chamber.

2.2 Surrogates

There are a number of surrogate micro-organisms which can be used in a building drainage context. Some are more difficult to use and detect. A few options were assessed before this research continued and one was selected on the basis that it was the safest and most appropriate. The options investigated were

1) *Pseudomonas putida.* This is a bacterium of approximate size 3-5μm. It can be useful for assessing the movement of bioaerosls within the system and is easy to use. It is also possible to obtain survivability and viability data for it and it is easily detected.

2) Porcine Respitory and Reproductive Virus Syndrome (PRRSv). This virus needs to be carefully deactivated before use since it is a real threat to the pig community. It therefore requires additional safety measures and since it is a virus, is not easily detectable nor is viability an option (since it is already deactivated by heat treatment). This is a difficult virus to acquire since it has to be grown in pig lung tissue – an additional issue being the media in which it needs to be stored causes issues when interacting with water.

3) Pepper Mild Mottled Virus (PMMoV). This is a plant virus and totally harmless. It is easily detectable with PCR but again viability is not possible. It is also available in large quantities from Tabasco sauce, making it easy to acquire.

Given that this research focussed on the transport of viruses rather than bacteria – PMMoV was chosen. It is described below.

2.3 PMMoV virus

Pepper mild mottle virus (PMMoV) was recently found to be the most abundant RNA virus in human faeces, and is a plant virus belonging to the genus Tobamovirus in the family Virgoviridae.

The occurrence and persistence of PMMoV in natural and engineered water systems means that it's presence can be an indicator of water quality.

It is a good candidate for a surrogate for viral presence in building wastewater systems.
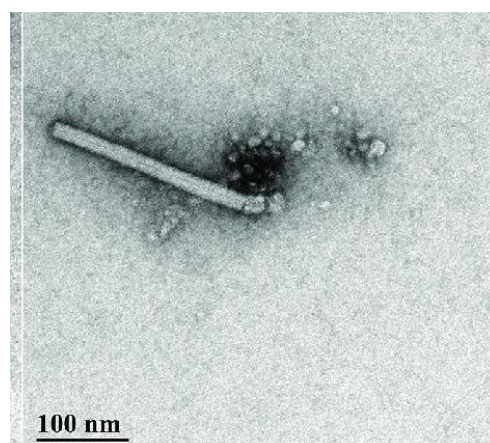
Figure 3 Electron microscopy of PMMoV

Figure 4 Tabasco sauce has a high concentration of PMMoV

PMMoV is found in high quantities in Tabasco sauce (and other hot sauces) at $10^{7\text{-}8}$ gc/millilitre. 4.7 l of Tabasco sauce was procured for these experiments, and let down with 1.3 l of tapwater in order to give a workable flush volume while retaining a high concentration to optimise the chances of detecting PMMoV bioaerosols. Nevertheless, the concentrations are representative of the higher concentrations found in WC wastewater (Gormley, 2020b).

2.4 Detection Protocol
PMMoV was detected and quantified by reverse transcriptase-quantitative polymerase chain reaction (RT-qPCR). Specifically, PMMoV RNA was extracted from wastewater samples using the Allprep PowerViral DNA/RNA extraction kit (Qiagen Ltd) as per the manufacturer's instructions. The extracted RNA eluted in 50 µl as recommended by the manufacturer to maximise concentration.

Extracted RNA was converted to cDNA, and the PMMoV target gene fragment amplified, using a one-step RT-qPCR protocol. Reaction mixes consisted of RNA template (2 µl), forward and reverse primers (0.8 µM), Taqman probe (0.2 µM) and 4x QuantiNova pathogen master mix (Qiagen Ltd). Reactions also contained QuantiNova IC Probe Assay and QuantiNova IC Control RNA. Primers and FAM/BHQ1 labelled probe were as previously reported (Haramoto et al., 2013).

Quantification standard was a 68-bp synthetic linear DNA fragment based on the relevant PMMoV genome sequence section (GenBank accession number M81413). The synthetic fragment diluted in DNase/RNase-free water to create a five-point calibration curve. All samples, controls and standards were analysed in duplicate.

RT-qPCR analysis was performed on a 2plex Rotor-Gene real-time system (Qiagen Ltd) programmed as follows: 50 °C for 10 mins, 95 °C for 2 mins followed by 45 cycles of 95 °C for 5 s and 60 °C for 30 s. The programme informed by Qiagen's standard protocol for the Pathogen + IC kit and information in the literature (Graham et al., 2021; Haramoto et al., 2013). Data capture was on the programme's combined annealing/elongation step.

3. Results and discussion
3.1 System Calibration
To inform the results some previously collected results are presented below to show the important aspects of the mechanisms involved. Figure 5 shows clearly the aerosols generated by a flushing toilet – as measured at the top of the stack. The background aerosol 'noise' can be clearly seen, as can the peak in number of particles emitted and the concentration of particles per cm^3. Figure 6 shows the range of aerodynamic sizes of the plume of aerosols generated. Note there are none above 5µm and a significant number are below 0.3 µm, which is the cut-off for sizing of the APS 3321 aerodynamic sampler, used in this research. Figure 7 shows the sensitivity of the process to water chemistry (particularly the presence of NaCl). Note the 1 log increase in peak particle count with the introduction of salt to the solution. These graphs were used to calibrate the virus experiments under consideration here.
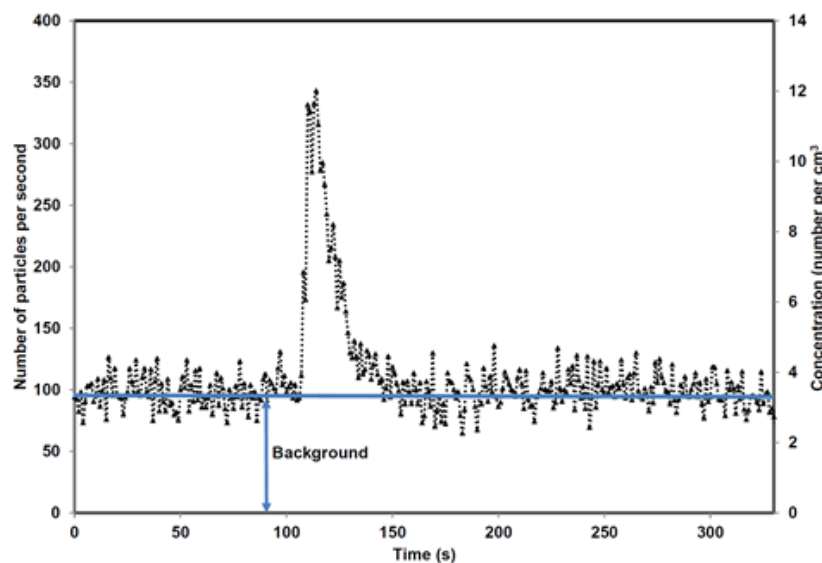
Figure 5 Typical aerosol spike inside drainage system from a toilet flush (source: Gormley et al 2021)
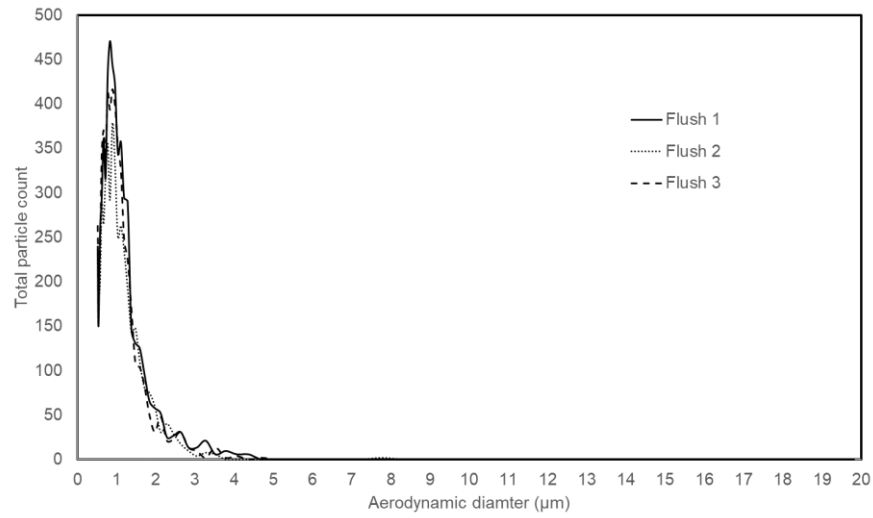
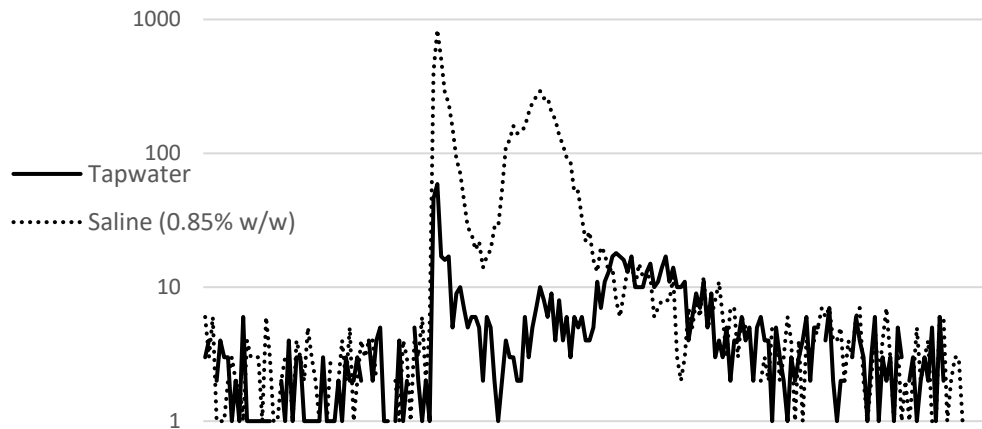**Figure 6 Size distribution of aerosol plume detected.**

Figure 7 Comparison of Particle Detection flushes with tap water and flushes with NaCl added to the water.

3.2 Typical Virus concentrations

Viral concentrations measured in wastewater in the field are typically in the range 10^3 - 10^5 gene copies/litre (gc/litre) and since this is typically flushed into a toilet and mixed with multiple litres of water it means that a higher concentration of raw virus is required to make a reasonably accurate viral load in the wastewater at discharge from the WC, typically 10^6 – 10^8 gc/litre. Producing this amount of virus for a single flush is challenging.

<div align="center">(a)   (b)</div>
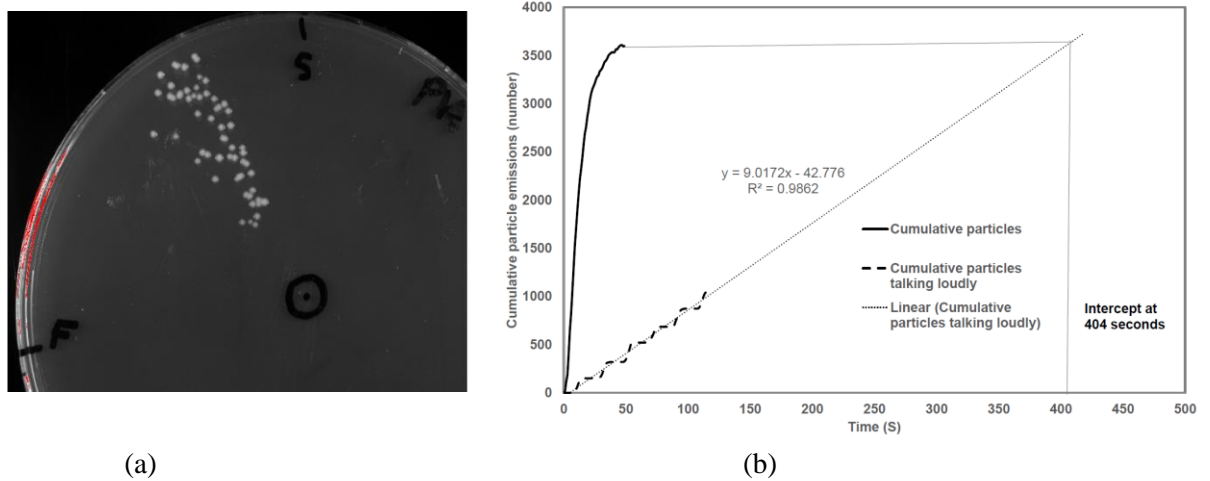
Figure 8 Emissions of pathogens from systems. Emission of particles follows similar pattern to toilet flush (a) A 6 l toilet flush produces the same number of particles as a person talking loudly for 6 and a half minutes (b). Note: Number of particles are proportional to the flush volume of the toilet. (Gormley *et al.*, 2017; Gormley, Aspray and Kelly, 2021)

Previous work using *p.putida* and aerosols showed that the kinetics of the microrganisms followed the profile of the toilet flush, as shown in Figure 8.

3.3 Virus detection results

The WC trap was filled with PMMoV inoculum with a concentration of approximately 10^9 gc/litre. These are indicated in the table of results below as 'stock'. Protocol as per section 2. above was followed with two samples being extracted from each sample presented. E.g. A00 has two entries below. This is for quality purposes and allows anomalies to be detected early. It can be seen that samples can have a wide variation – A00 was 4.37×10^6 and 1.29×10^8. This represents a 2 log difference between readings from the same sample. This highlights the difficulty of measuring such quantities. All results are shown below. The Cq values represent the number of cycles the PCR machine had to go through to get across the 'detectable' threshold. A high number (close to 40) represents a weak signal and a low number indicates a very strong signal with a lot of the virus. Notable is B02 with levels up to 10^{11}.

It's important to note that the virus was detected in relatively large quantities at the top of the stack when the inoculum was flushed through the toilet at the bottom (some 4m away). An updraught air was induced as follows:

> Experiment A ~ 2m/s
> Experiment B ~ 6 m/s
> Experiment C ~ 4 m/s
> Experiment D plenum door held open for comparison with previous results; nominal air flow rate 1-2 m/s.

Given the gap in the literature, the objective of these experiments was to investigate the presence and detection of viral bioaerosols, rather than how this varies with any given control variable. Previous results (previous conference papers & unpublished results) gathered using the APS suggested that there would be most particles in the detectable range under conditions of high

humidity; some of these experiments used saline solutions in the range 0.5%–2% m/m. The inoculum here comprised 4.7 l Tabasco sauce + 1.3 l water; this would give 1.3% NaCl m/m. Air was around 50% RH (not humidified).

The WC was 'flushed' by tipping the inoculum into the bowl (i.e. actual flush not used, in contrast with previous results). It was observed from the scoping results that the total particle counts (not necessarily the highest peak concentrations/total aerosols generated – but most aerosols detected – occurred at around 4 m/s – however, the pilot results did not include fine resolution in AFR so it was decided to conduct bioaerosol sampling experiments at three air flow rates in this region. Target air flow rates of 2, 4, and 6 m/s were used.

For each air flow rate, two tests were run with one flush event; one test was run with ten flush events in case the virus detection was marginal.

• Put 20ml distilled water into SKC Biosampler;
• Place Biosampler into the plenum chamber;
• Check extract fan air flow rate; adjust to target AFR;
• Turn on SKC pump;
• If single flush:
        o Tip inoculum down WC;
        o Run Biosampler for 120 seconds
• If multiple flushes:
        o Tip inoculum down WC;
        o Allow 90s to pass;
        o Switch off extract fan;
        o Transfer Tabasco sauce from the collection flask into a separate container to flush;
        o Repeat for a total of ten flushes
• Turn off SKC sampler;
• The investigator cleaned hands and forearms before decanting the contents of Biosampler into a sterile tube for transfer to the PCR lab.

The WC trap was filled with PMMoV inoculum with a concentration of approximately gc 10^9 per litre. These are indicated in the table of results below as 'stock'. The PCR protocol used is described in section 2 above, with two samples being extracted from each sample presented. E.g. A00 has two entries below. This is for quality purposes and allows anomalies to be detected early. It can be seen that samples can have a wide variation – A00 was 4.37×10^6 and 1.29×10^8 This represents a 2 log difference between readings from the same sample. This highlights the difficulty of measuring such quantities. All results are shown below. The Cq values represent the number of cycles the PCR machine had to go through to get across the 'detectable' threshold. A high number (close to 40) represents a weak signal, and values in excess of 40 are generally regarded as unreliable; low Cq values represent strong signals, i.e. a high concentration of virus. Here, note the exceptionally strong signal in sample B02, reaching 10^{11} copies/litre.

It's important to note that virus was detected in relatively large quantities at the top of the stack when the inoculum was flushed through the toilet at the bottom (some 4m away) with a variable updraft air whose velocity ranged from 0m/s to 6m/s (as per Gormley et al, 2017). Sample D, while incomplete still shows a weak positive signal with negligible updraft air.

Table 1 PCR Results from the Biosampler.

ID	Cq	gene copies / L
A00	35.54	4.37E+06
A00	31.12	1.29E+08
A01	29.19	5.70E+08
A01	35.74	3.74E+06
A02	*	
A02	31.98	6.69E+07
B00	33.91	1.52E+07
B00	35.42	4.79E+06
B01	29.36	5.00E+08
B01	23.56	4.28E+10
B02	26.32	5.15E+09
B02	22.24	1.18E+11
C00	29.38	4.91E+08
C00	31.16	1.25E+08
C01	35.72	3.80E+06
C01	36.38	2.28E+06
C02	28.74	8.06E+08
C02	34.02	1.40E+07
D	38.43	4.78E+05
D	*	
Stock	27.11	2.81E+09
Stock	26.41	4.82E+09

* note all samples were taken from the chamber at the top of the stack. A range of relative humidities were used but the analysis of these variables was not carried out in this instance.

4. Conclusions

1. The risk of cross contamination via building drainage sanitary plumbing systems is still a real threat although SARS-CoV-2 has not posed the risk once imagined, however other pathogens are still a threat.
2. It is challenging to measure and detect micro-organisms and aerosols in drainage systems.
3. Difference in wastewater properties (chemistry, salinity, RH and temp) change the likely detection of aerosols
4. Work using surrogate bacteria (*P. putida*) and viruses (PMMoV and PRRsV) have proved useful in showing transmission routes and determining the influence of water properties on transmission (and detection).
5. Viruses can be carried up through the drainage stack and can enter spaces above in relatively high concentrations in the air for a reasonable amount of time (~ 2-3 minutes from a WC flush).
6. Further work is planned using a wider range of PMMoV concentrations to establish links between quantities of virus detected against quantities of aerosols detected.

5. References

Agranovski, I.E., Safatov, A.S., Borodulin, A.I., Pyankov, O.V., Petrishchenko, V.A., Sergeev, A.N., Agafonov, A.P., Ignatiev, G.M., Sergeev, A.A., Agranovski, V. (2004). Inactivation of viruses in bubbling processes utilized for personal bioaerosol monitoring. Applied and environmental microbiology 70(12). doi: 10.1128/AEM.70.12.6963-6967.2004

Dight, T. and Gormley, M. (2022) 'The Influence of Air and Water Conditions on the Generation of Bioaerosols in the Building Drainage System', in *17th International Conference on Indoor Air Quality and Climate, INDOOR AIR 2022*. Available at: https://www.scopus.com/inward/record.uri?eid=2-s2.0-85159210059&partnerID=40&md5=297f689344d6060ca93fe2b0d72b6de0.

European Committee for Standardisation (2014). EN12341: Ambient air – Standard gravimetric measurement method for the determination of the PM10 or PM2.5 mass concentration of suspended particulate matter. Brussels, Belgium.

Gormley, M., Aspray, T. J. and Kelly, D. A. (2021) 'Aerosol and bioaerosol particle size and dynamics from defective sanitary plumbing systems', *Indoor Air*. John Wiley & Sons, Ltd,   doi: https://doi.org/10.1111/ina.12797.

Gormley, M., Aspray, T. J. and Kelly, D. A. (2020a) 'COVID-19: mitigating transmission via wastewater plumbing systems', *The Lancet Global Health*, 8(5), p. e643. doi: 10.1016/S2214-109X(20)30112-1

Gormley, M. (2020b) 'Wastewater systems in the time of Covid-19: surveillance, epidemiology and design', Proceedings of the Institution of Civil Engineers - Water Management. ICE Publishing, 173(6), pp. 271–273. doi: 10.1680/jwama.2020.173.6.271.

Gormley M, Aspray TJ, Kelly DA, Rodriguez-Gil C (2017) Pathogen cross-transmission via building sanitary plumbing systems in a full scale pilot test-rig. PLoS ONE 12(2): e0171556. https://doi.org/10.1371/journal.pone.0171556

Gormley, M., Kelly, D. A. and Aspray, T. J. (2014) 'Bio-aerosol cross-transmission via the building drainage system', in *Indoor Air 2014 - 13th International Conference on Indoor Air Quality and Climate*.

Graham, K. E., Loeb, S. K., Wolfe, M. K., Catoe, D., Sinnott-Armstrong, N., Kim, S., Yamahara, K. M., Sassoubre, L. M., Mendoza Grijalva, L. M., Roldan-Hernandez, L., Langenfeld, K., Wigginton, K. R., & Boehm, A. B. (2021). SARS-CoV-2 RNA in Wastewater Settled Solids Is Associated with COVID-19 Cases in a Large Urban Sewershed. Environmental science & technology, 55(1), 488–498. https://doi.org/10.1021/acs.est.0c06191

Hogan, C. J., Jr, Kettleson, E. M., Lee, M. H., Ramaswami, B., Angenent, L. T., & Biswas, P. (2005). Sampling methodologies and dosage assessment techniques for submicrometre and ultrafine virus aerosol particles. Journal of applied microbiology, 99(6), 1422–1434. doi: 10.1111/j.1365-2672.2005.02720.x

Ijaz, M. K., Sattar, S. A., Johnson-Lussenburg, C. M., Springthorpe, V. S., & Nair, R. C. (1985). Effect of relative humidity, atmospheric temperature, and suspending medium on the airborne survival of human rotavirus. Canadian journal of microbiology, 31(8), 681–685. https://doi.org/10.1139/m85-129

Haramoto E, Kitajima M, Kishida N, Konno Y, Katayama H, Asami M, Akiba M. Occurrence of pepper mild mottle virus in drinking water sources in Japan. Appl Environ Microbiol. 2013 Dec;79(23):7413-8. doi: 10.1128/AEM.02354-13. Epub 2013 Sep 20. PMID: 24056461; PMCID: PMC3837739.

Hogan, C. J., Jr, Kettleson, E. M., Lee, M. H., Ramaswami, B., Angenent, L. T., & Biswas, P. (2005). Sampling methodologies and dosage assessment techniques for submicrometre and ultrafine virus aerosol particles. Journal of applied microbiology, 99(6), 1422–1434. doi: 10.1111/j.1365-2672.2005.02720.x

Ijaz, M. K., Sattar, S. A., Johnson-Lussenburg, C. M., Springthorpe, V. S., & Nair, R. C. (1985). Effect of relative humidity, atmospheric temperature, and suspending medium on the airborne survival of human rotavirus. Canadian journal of microbiology, 31(8), 681–685. https://doi.org/10.1139/m85-129

Kang, M. ; Z. et al. (2020). Probable Evidence of Fecal-Respitory Transmission of SARS-CoV-2 in a high-rise building. Annals of Internal Medicine.

Pan, M., Lednicky, J. A., & Wu, C. Y. (2019). Collection, particle sizing and detection of airborne viruses. Journal of applied microbiology, 127(6), 1596–1611. https://doi.org/10.1111/jam.14278

Verreault, D., Moineau, S., & Duchaine, C. (2008). Methods for sampling of airborne viruses. Microbiology and molecular biology reviews : MMBR, 72(3), 413–444. doi: 10.1128/MMBR.00002-08

Xagoraraki I, Yin Z, Syambayev, Z. (2020). Fate of viruses in water systems. Journal of Environmental Engineering 140(1). doi: 10.1061/(ASCE)EE.1943-7870.0000827

6. Presentation of Authors

Thomas Dight is a PhD student at the Institute for Sustainable Building Design at Heriot-Watt University. His research focusses on the detection, modelling and fate of bio-aerosols as found in building drainage and vent systems.

Prof. Michael Gormley is Professor of Public Health and Environmental Engineering at the Institute for Sustainable Building Design at Heriot-Watt University. His research interests are pressure transient modelling and suppression in drainage systems, solid transport in above ground drainage systems and Pathogen identification and infection control in building drainage and ventilation systems

Trends in Studies, and Reviews Thereof, in Relation to Droplets on and around Toilets that Can Cause Infections

Ayaka Kimura (1), Masayuki Otsuka (2)

(1) aya.98pc@outlook.jp

(2) dmotsuka@kanto-gakuin.ac.jp

(1) M.Eng., former graduate school of engineering Kanto Gakuin University, Japan

(2) Prof. Dr.Eng, Department of Architecture and Environmental Design, College of Architecture and Environmental Design, Kanto Gakuin University, Japan

Abstract

There are high risks of becoming infected with E. coli O157, norovirus, etc., through activities in toilet spaces, such as excretion and poor hand washing. In addition, during the outbreak of SARS in 2003 and the outbreak of COVID-19 in 2019, there were reports indicating that the viruses entered broken traps of toilets and bathrooms of apartment houses and travelled through drainage stacks and vent stacks to cause the wide spread of the infections. These viruses are also found in human faeces and urine as well as in droplets (5μm or more) and aerosols (not more than 5μm) that are generated by flushing toilets. This suggests that contaminated droplets and aerosols could be responsible for faecal-oral transmission through which the viruses enter human bodies via the respiratory system, and research papers in this respect have been produced for hospitals and other medical institutions.

With these circumstances in mind, this report examines and evaluates research papers and information, produced both in and outside Japan, which relate to toilet plumes that are ejected and dispersed by flushes and the influence thereof. The report also summarises the outcomes of a related study which was conducted by the authors, and make a suggestion as to how hygienic and comfortable toilet spaces should be during the with-COVID-19 era and towards the post-COVID-19 era.

Keywords

COVID-19; toilet; infection control measures; plumbing system.

1. Necessity of infection control in and around toilet booths

In December 2019, coronavirus disease-2019 (COVID-19) was first identified in Wuhan, China, and in January 2020, the WHO declared that COVID-19 was a public health emergency of international concern. In Japan in March 2022, a large cluster of COVID-19 cases occurred on the Diamond Princess cruise liner docked in Yokohama, and it was reported that the results of collecting specimens from articles in 33 cabins, and parts of the cabins, which were occupied by those infected, indicated high detection rates of the viral RNA: toilet floors in bathrooms, i.e., wet spaces, (13 rooms) 39%; pillows 34%; telephones and desks 24%; and arms of chairs 12%1) (Fig. 1). In other cases reported outside Japan, in hospitals in particular, the COVID-19 RNA was found in more than half the excrement and urine samples collected from patients who were tested positive for COVID-19, as well as in the bathrooms and the toilets with seats which were used by the patients in their hospital rooms2), 3), 4) (Fig. 2). Accordingly, there is a concern that not only living spaces but toilet spaces and areas around sanitary fixtures could become sources of contact transmission and faecal-oral transmission.

In particular, it is pointed out that by flushing faeces and urine down toilets, virus-contaminated droplets with large diameters and small aerosols could be ejected from toilet bowls and dispersed in peripheral areas, and cause the spread of all kinds of infectious diseases. In Japan, few research cases have been reported where dispersion of droplets that are generated from sanitary fixtures are quantitatively determined, while a few such research cases have been reported in other countries.
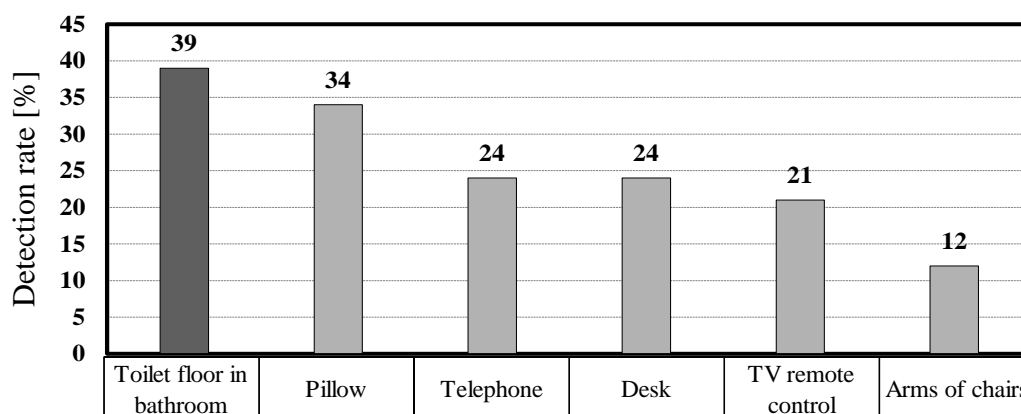

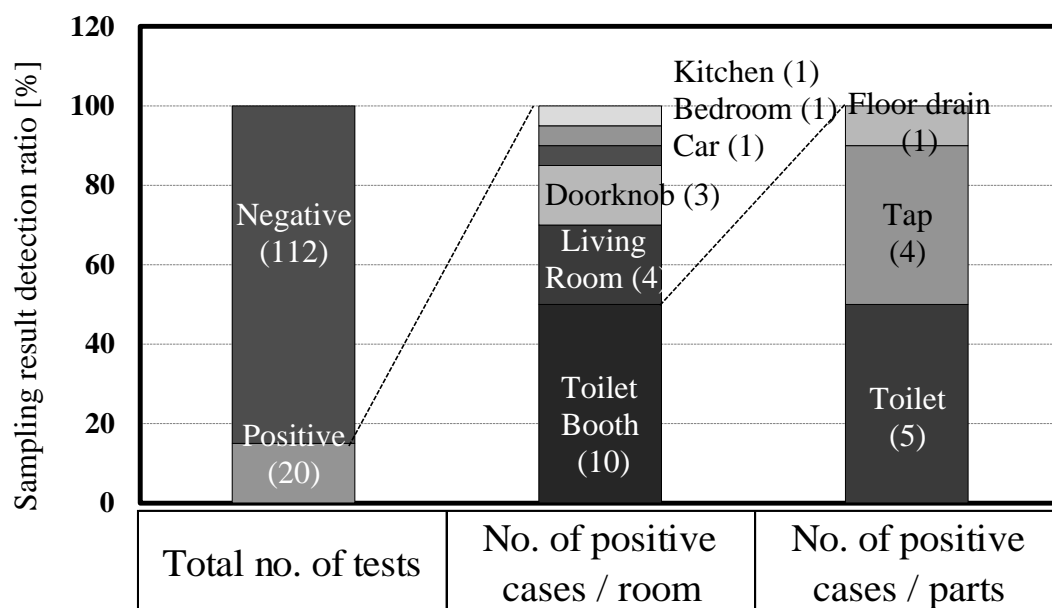**Fig. 1 Detection rates of SARS-CoV-2 RNA in cabins of Diamond Princess** created based on 1)

Fig. 2 Numbers and ratios of tested-positive specimens created based on4)
※**The figures in ( ) represent the numbers of tested-positive specimens**

2. Examination of methods for identifying toilet plumes dispersed by flushes, and issues to be addressed

There are measurement methods and simulation methods for ascertaining how toilet plumes are ejected and dispersed. The following major papers have been examined and issues to be addressed have been identified.

2.1 Examination of measurement methods

One such method was exemplarily conducted by Jesse H. Schreck et al.[5], who used a particle counter and other instruments to measure quantities of aerosols generated by toilet flushing at different heights from the surface of a toilet seat. Occurrence frequencies, etc., of aerosols having particle diameters of 0.3-25μm were quantitatively ascertained. The findings indicated that aerosols were detected at a height of 0.43m from the toilet seat, and although this height was only about a third of 1.22m, i.e., a height within a breathing range (respiratory height), the aerosols could have reached as high as 1.52m (Fig. 3). Meanwhile, Samantha D. Knowlton et al.[6] present measurements that were taken at a hospital, and it is inferred from the measurement results of toilet plume generation that aerosols having particle diameters of 0.3-3.9μm were increasingly generated immediately after a flush and relaxed a few minute later[6]. In their experiment, John P. Crimaldi et al.[7] counted numbers of dispersed droplets, using a particle counter

while irradiating the droplets with laser light so as to make droplet distributions visible. The measurement results also indicated that many aerosols were dispersed as high as approximately 1.5m within the breathing range.

However, one of the problems about these past studies is that the experimental toilets used for these studies were mainly of a wash-down type. It can be pointed out that these studies did not take into consideration fixture discharge characteristics, flushing methods, different toilet structures, etc., and the effects thereof, as they would if using more recent flushing systems. Another problem is that the evaluation of dispersion of aerosols with a particle diameter of approximately 5μm and the comprehensive ascertainment of dispersion of droplets, including relatively large and visible water particles, through visualisation and quantification are missing from these studies.
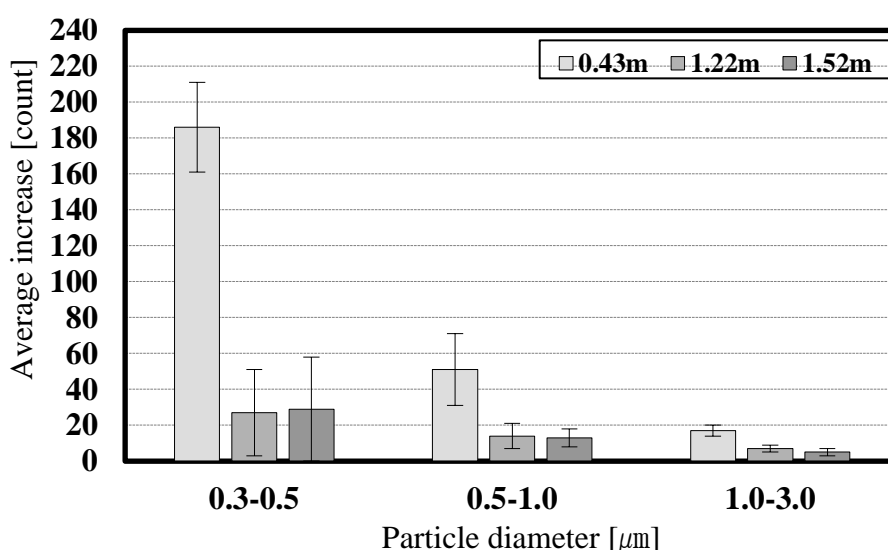
Fig. 3 Average increase of aerosol count per second [created from 5]

2.2 Analysis of toilet plume dispersion by simulation

In a simulation method, Computational Fluid Dynamics (CFD) is used for analysing how a toilet plume is ejected and dispersed into the air and how high it reaches. Yun-yun Li et al.[8] used a model simulating the shape of a toilet bowl and estimated heights that were reached by aerosols of a specific particle diameter. It was reported that when measured from the toilet seat, the maximum height reached 35 seconds after a flush was 53.5cm and it was 66.5cm 70 seconds after a flush. The rising rate of the particles was approximately 0.0037m/s. In their study, the experimental model was different in shape from a real toilet bowl and the analysis was carried out under limited conditions of aerosol particle diameter (8.6μm) and particle count (6,000). Meanwhile, Ji-Xiang Wang et al.[9] analysed changes in the state of aerosols, from the initial point at which they were generated by a flush in a toilet booth in a bathroom, in consideration of ventilation in the booth. In order to obtain simulation results that are more realistic, it is necessary to set

initial conditions (aerosol particle diameter, particle count, initial scattering rate (approx. 0.1-0.2m/s) etc.) on the basis of actual measurement results.

3. Adhesion of droplets to toilet lids and toilet seats when generated by flushing, and evaluation thereof

3.1 Guidelines of various countries

In order to suppress the ejection and dispersion of toilet plumes described above, various countries provide guidelines which recommend closing toilet lids before flushing (Table 1) [10] [11] [12] [13]. However, some reports say that aerosols were detected, though in small amounts, even when toilet seats were closed before flushing[6].

Meanwhile, in Japan, the guidelines for medical institutions[14] state advantages of providing toilet lids, which include prevention of heat from escaping from heated toilet seats and therefore saving energy, and prevention of airborne bacteria from spreading at the time of flushing. However, there are pros and cons to using toilet lids, in respect of causing contamination by opening and closing them by hand, for example.

Table 1 COVID-19 guidelines (concerning toilets) of various countries [created from 10) 11) 12) 13)]

REHVA (Europe)	Check water seals of drains and U-traps at least every three weeks, and add water if required.
	Flush toilets with lids closed to minimize the release of droplets.
IAPMO (USA)	Make sure that there are no dried-up traps.
	Make sure that solids are not being accumulated inside drainpipes and there is no pipe blockage at the time of flushing.
	When flushing toilets, make sure that lids are closed so as to prevent aerosols from being released.
SHASE (Japan)	Flush toilets with lids closed, and thoroughly disinfect and clean the backs of lids.
	Install automatic replenishing devices to traps in which water is likely to evaporate, or install non-water seal traps.

3.2 Adhesion of droplets to toilet lids and toilet seats, and evaluation thereof

In Japan, the Center of Better Living stipulates a quality housing component performance testing method for toilets, Methods of Testing Performance of Quality Housing Components, Water Closets [15], in accordance with which quantitative measurements of adhesion of droplets (adherent droplet count), due to flushing, to the backs of toilet lids and the surfaces of toilet seats are conducted. The method specifies that the allowable size and number of droplets adherent to the back of a toilet lid or the surfaces of a toilet seat per flush are at least 2mm in particle diameter and less than or equal to 25 droplets. [15]. In their past study conducted in an actual hospital, E.L. Best et al.[10] counted droplets when they were generated by flushing a toilet and adhered to the seat of the toilet. Past tests and studies do not clearly describe methods for counting droplets, and these methods are not quantitative measurement methods. It is therefore supposed that in other countries also, methods for evaluating amounts of adherent droplets are yet to be suggested.

On the basis of the above examination of past studies, the following are suggested as focal points and factors to consider for future studies:
(1) In respect of water supply, drainage and sanitation equipment, it is necessary to propose methods, applicable both in and outside Japan, for measuring and analysing ejection and dispersion of droplets (5μm or more in diameter) and aerosols (not more than 5μm) caused when flushing various types of water-saving toilets; examine results, discharge characteristics, and different conditions such as discharge volumes and the number of discharge ports; and discuss about methods of minimising toilet plumes.
(2) It is necessary to examine the effect of closing toilet lids as to minimising toilet plumes; discuss quantitative methods for ascertaining and evaluating amounts of adherent droplets on the backs of toilet lids, toilet seat surfaces and floor surfaces; and acquire knowledge conducive to cleaning methods and maintenance and management.

4. Focal points of study on toilet plumes

Taking into account the results of examining the aforementioned past papers, the authors of this report propose a method, as illustrated in Fig. 4, for comprehensively understanding and evaluating dispersion of toilet plumes generated by flushes, as well as the adhesion of droplets to toilet lids and seats, in consideration of influence factors.
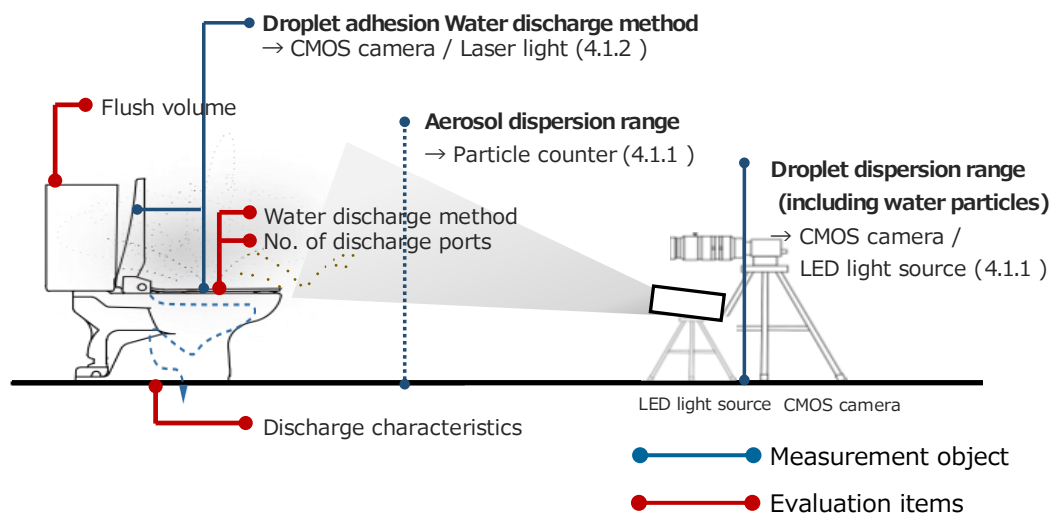

Fig. 4 Measurement objects and main analysis items for this study

4.1 Experimental apparatus overview

4.1.1 Identifying dispersion ranges of droplets (including water particles) and aerosols

This experimental apparatus uses an LED light source and a CMOS camera (by OMRON SENTECH CO., LTD.) together to identify, from captured images, distributions of relatively large droplets (including water particles) of 1mm or more in particle diameter. A particle counter is also used to identify vertical distributions each indicating the number of dispersed aerosols of not more than 5μm in particle diameter (Fig. 5 (1) and (2)).

4.2.2 Adhesion of droplets to toilet lid and toilet seat

The surfaces of the toilet lid and the toilet seat are irradiated with semiconductor laser light; the toilet is flushed with water containing fluorescent paint so that the CMOS camera can capture images of droplets that adhere to the toilet lid and seat surfaces; and the captured images of the adhesion surfaces are analysed using an image analysis software (Dipp Image by KATOKOKEN CO., LTD.) to obtain adhesion surface areas.
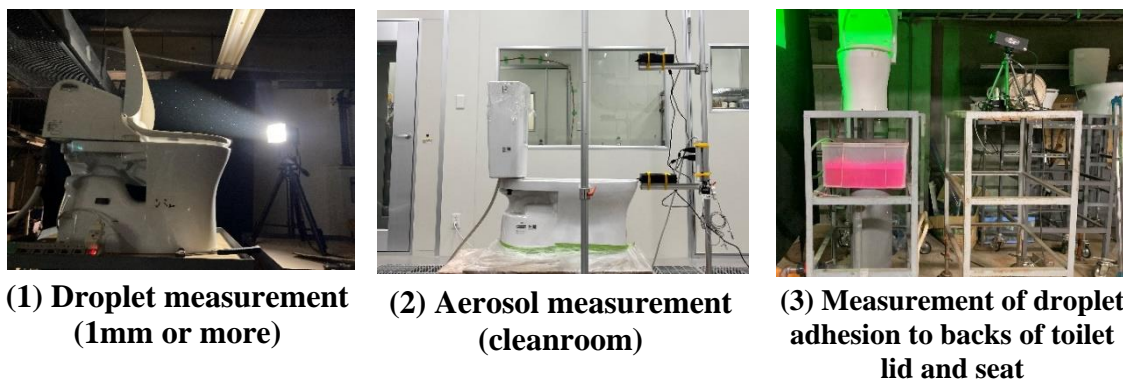
(1) Droplet measurement (1mm or more)

(2) Aerosol measurement (cleanroom)

(3) Measurement of droplet adhesion to backs of toilet lid and seat

Fig. 5 Experimental apparatus

4.2 Evaluation items

Table 2 lists the items to be evaluated during this study.

4.2.1 Droplets (including water particles) and aerosols

There are four evaluation items regarding droplets and aerosols: (A) fixture discharge characteristic (discharge volume, average fixture discharge flow rate, maximum discharge volume); (B) droplet dispersion range (water particles and aerosols); (C) aerosol count; and (D) water discharge structure (water discharge method, the number of discharge ports).

4.2.2 Adhesion of water particles to toilet lid and toilet seat

The adhesion of water particles (2mm or more in particle diameter) is evaluated after each flush in accordance with the number of water particles adherent to: (E) the back of the toilet lid; and (F) the surface of the toilet seat.

Table 2 Evaluation items

	Evaluation item			Evaluation method	Note
Droplets Aerosols	(A) Fixture discharge characteristics		Flush volume	Water volume used for flushing experimental toilet	Examination with reference to documents provided by manufacturers
			Average fixture discharge flow rate	SHASE-S220 Testing Methods of Discharge Characteristics for Plumbing Fixtures	
			Max. fixture discharge flow rate		
	(B) Droplet dispersion range		Water particles	Height reached from toilet seat surface when identified using LED light source and CMOS camera	
			Aerosols	Height at which particle counter is positioned	From toilet seat: 200mm, 400mm and 800mm upwards
	(C) Aerosol particle count			Particle count per height at which particle counter is positioned	From floor surface 1500mm upwards
	(D) Water discharge structure		Water discharge method	Tornado flush, rim-free	
			No. of discharge ports	No. of ports for discharging water into toilet bowl	
Water particle	(E) No. of droplets adherent to back of toilet lid			Allowable no, of water particles adherent to back of toilet lid and toilet seat surface when flushing ≦	
	(F) No. of droplets adherent to toilet seat surface				

4.3 Presenting experiment results

Following the description above, presented here are several experiment results which are noteworthy.

4.3.1 Droplet dispersion range

Fig. 6 shows how typically droplets were scattered from the experimental toilet. Toilet a is a siphon jet-type toilet with a flush volume of 6.0L and has three water discharge ports in the toilet bowl. Toilet b is also a siphon jet-type toilet with a flush volume of 5.0L and has one water discharge port. As indicated in the graphs, droplets ejected and dispersed from the toilet seats reached heights between about 100mm and 300mm, even when taking into consideration height variations due to the number of attempts, i.e., the minimum height of approximately 110mm and the maximum height of approximately 270mm.

Droplet dispersion range   Water discharge ports

(1) Toilet a (flush volume: 6.0L, water discharge ports: 3)

Droplet dispersion range   Water discharge ports

(2) Toilet a (flush volume: 5.0L, water discharge ports: 1)

Fig. 6 Dispersed states of droplets at the time of flushing
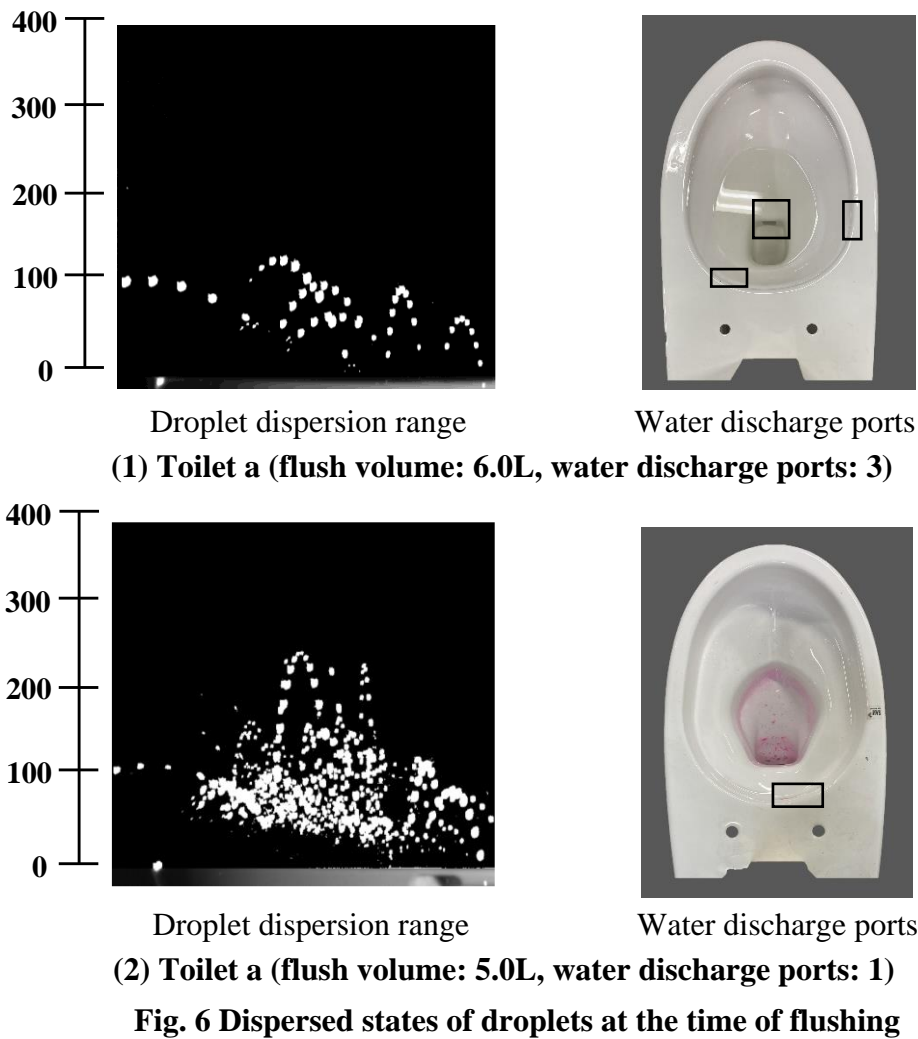
4.3.2 Aerosol dispersion

 Fig. 7 shows changes over time in quantities of aerosols generated by flushing Toilet b. The toilet was flushed 30 seconds after starting the measurement (0s). By flushing the toilet, aerosols of not more than 5μm in particle diameter were dispersed into the air. Aerosols were detected, reaching a height of 400mm or more, 5 seconds after the leading edge of the wave, and this suggests that the dispersion rate of aerosols is possibly around 0.08m/s, which is different from the result calculated using the simulation method in 2.2. Moreover, aerosols were detected, though in very small amounts, 30-60 seconds after the toilet was flushed, and it is suspected that these aerosols were detected for the second time after they were ejected and dispersed into the air and later came down.

(1) Floor surface ＋1500 ㎜

(2) Toilet seat surface ＋400 ㎜

(3) Toilet seat surface

‒‒‒‒0.3um ‒‒‒‒0.5um ‒‒‒‒0.7um ‒‒‒‒1.0um ‒‒‒‒2.0um
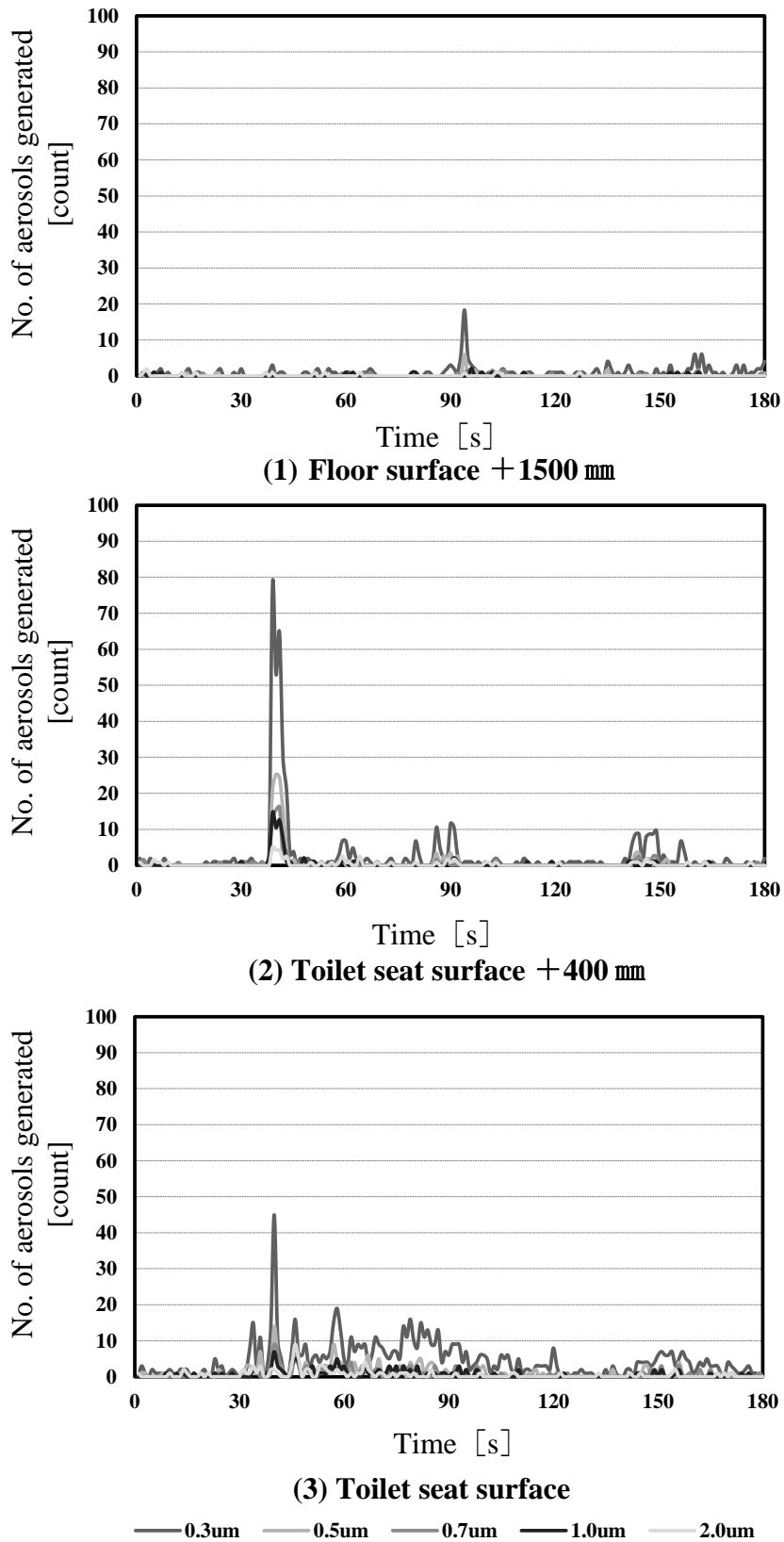
Fig. 7 Changes in no. of aerosols generated [count]

4.3.3 Droplet adhesion to toilet lid and toilet seat, and in vicinity

In line with the recommendation by guidelines, both in and outside Japan, the experimental toilets were flushed with clean water while the toilet lids were closed. Fig. 8 shows the adherent states of droplets on the backs of the toilet lids. The number of adherent droplets increases as flushing is repeated, and exceeds the reference value with the third flush and onwards. It can be observed that Toilet a with multiple discharge ports, from which flush water is discharged, has fewer droplets adhering to the back of the lid. Moreover, when evaluating in accordance with the evaluation standard set by the Center of Better Living, Methods of Testing Performance of Quality Housing Components, Water Closets[15], the requirements of the standard are met up to the second flush. Nonetheless, it is necessary to keep up with regular cleaning and hygiene when in use.
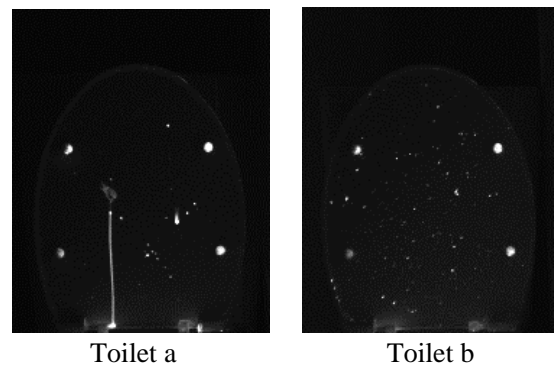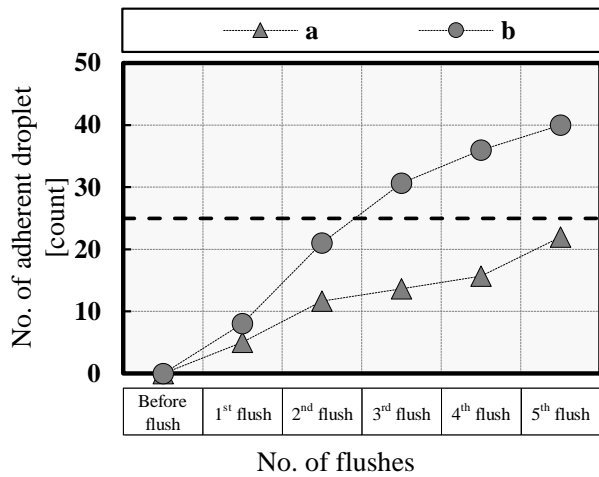
(1) No. of adherent droplets [count]

(2) Droplet adhesion on backs of lids with 5th flush - example

Fig. 8 Adherent states of droplets on backs of toilet lids

5. Summary of conclusions

(1)   Major studies and technical information, published both in and outside Japan, which relate to toilet plumes generated by toilet flushing and becoming a cause of faecal-oral transmission, have been sorted, and the following issues have been raised.

   1) It is necessary to present methods for measuring ejection and dispersion of droplets and aerosols that are generated when flushing water-saving toilets of various types, and to discuss about droplet/aerosol suppression methods in consideration of toilet-related conditions such as toilet structures.

   2) It is necessary to acquire knowledge conducive to quantitatively ascertaining and evaluating effects of minimising droplet dispersion by closing toilet lids, and amounts of droplets adhering to the backs of toilet lids and the surfaces of toilet seats.

(2)   In consideration of the issues surrounding the past studies, the authors of this report have presented a method for evaluating states of droplets (including water particles) and aerosols, using comprehensive evaluation items including fixture discharge characteristics and structures of toilets, droplet dispersion ranges, etc. The authors have also discussed a method for evaluating adhesion amounts of droplets.

(3)   In respect of a future aspect of toilet booths, it is important to provide them with hygiene, which is even better than the hygiene ensured by the existing infection control measures, by adopting technologies such as automatic opening/closing control for toilet lids when entering and leaving toilet booths, UV irradiation of toilet bowls and ejection of disinfectants thereinto, and plasmacluster ion technology, as shown in Fig. 9.
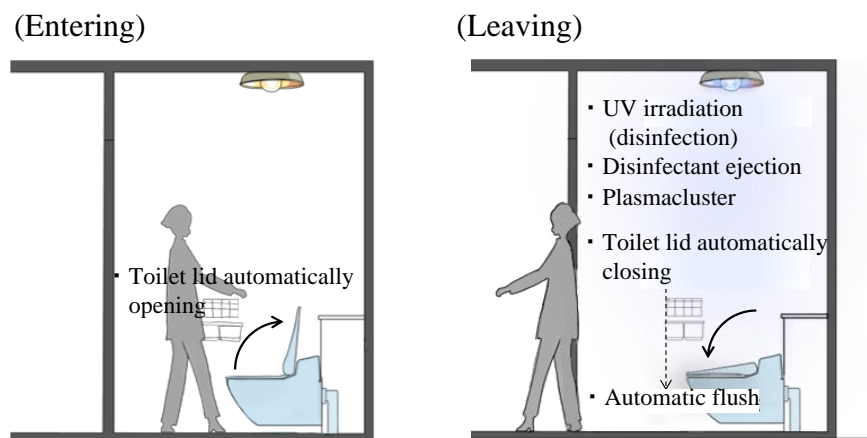
(Entering)   (Leaving)

Fig. 9 Considerations for infection control in toilet spaces [dimensional unit: mm]

6. Acknowledgements

7. References

(1) National Institute of Infectious Diseases (NIID); Report on Environmental Sampling for Coronavirus During a COVID-19 Outbreak on the Diamond Princess Cruise Ship (provisional title) 2020-8-30. https://www.niid.go.jp/niid/ja/diseases/ka/corona-virus/2019-ncov/2484-idsc/9849-covid19-19-2.html,（2023-01-14）

(2) Yongjian Wu, Cheng Guo, Lantian Tang, Zhongsi Hong, Jianhui Zhou, Xin Dong, Huan Yin, Qiang Xiao, Yanping Tang, Xiujuan Qu, Liangjian Kuang, Xiaomin Fang, Nischay Mishra, Jiahai Lu, Hong Shan, Guanmin Jiang, Xi Huang; Prolonged presence of SARS-CoV-2 viral RNA in faecal sample 2020-3-9.
https://www.ncbi.nlm.nih.gov/pmc/articles/PMC7158584/,(2023-01-30)

(3) Zhen Ding, Hua Qian, Bin Xu1, Ying Huang, Te Miao, Hui-LingYen, Shenglan Xiao, Lunbiao Cui, Xiaosong Wu, Wei Shao, Yan Song, LiSha, Lian Zhou1, Yan Xu, Baoli Zhu, Yuguo Li；Toilets dominate environmental detection of SARS-CoV-2virus in a hospital 2020-04-07.https://www.medrxiv.org/content/10.1101/2020.04.03.20052175v1.full.pdf,（2023-01-14）

(4) Lei Luo, Dan Liu, Hao Zhang, Zhihao Li, Ruonan Zhen, Xiru Zhang, Huaping Xie, Weiqi Song, Jie Liu, Qingmei Huang, Jingwen Liu, Xingfen Yang, Zongqiu Chen, Chen Mao ; Air and surface contamination in non-health care settings among 641 environmental specimens of 39 COVID-19 cases .https://pubmed.ncbi.nlm.nih.gov/33035211/（2023-01-19）

(5) Jesse H. Schreck, Masoud Jahandar Lashaki, Javad Hashemi, Manhar Dhanak, Siddhartha Verma et al.；Aerosol generation in public restrooms.2021-03-22.
https://aip.scitation.org/doi/10.1063/5.0040310 (2023-01-20)

(6) Samantha D. Knowlton, Corey L. Boles, Eli N. Perencevich, Daniel J. Diekema, Matthew W. Nonnenmann; Bioaerosol concentrations generated fromtoilet flushing in a hospital-based patient care setting.2018-07-16. https://pubmed.ncbi.nlm.nih.gov/29423191/,(2023-01-20)

(7) JohnP.Crimaldi, Aaron C. True, Kari G. Linden, Mark T. Hermandez, Lars T. Laeson and Anna K. Pauls; Commercial toilets emit energetic and rapidly spreading aerosol plumes, Scientific reports, 2022

(8) Yun-yun Li (李云云), Ji-Xiang Wang (王霁翔) and Xi Chen (陈希); Can a toilet promote virus transmission? From a fluid dynamics perspective. 2020-06-16.
https://aip.scitation.org/doi/10.1063/5.0013318,(2023-01-20)

(9) Ji-Xiang Wang a,b,* , Zhe Wu a , Hongmei Wang a , Mingliang Zhong c , Yufeng Mao c , Yunyun Li d , Mengxiao Wang e , Shuhuai Yao；Ventilation reconstruction in bathrooms for restraining hazardous plume: Mitigate COVID-19 and beyond, Journal of Hazardous Materials, 2022

(10) E.L. Best, J.A.T. Sandoe, M.H. Wilcox; Potential for aerosolization of Clostridium difficile after flushing toilets: the role of toilet lids in reducing environmental contamination risk. 2011-12-2. https://www.sciencedirect.com/science/article/abs/pii/S0195670111003392?via%3Dihub,(2023-01-20)

(11) Indian Society of Heating, Refrigerating & Air Conditioning Engineers (ISHRAE).ISHRAE

COVID-19 Guidance Document for Air Conditioning and Ventilation.2020-04-13. https://iisc.ac.in/wp-content/uploads/2020/05/AICTE_guidance-document-for-air-conditioning-and-ventilation.pdf

(12) REHVA. REHVA COVID-19 GUIDANCE version4. pp160. 2020-11-017. https://www.rehva.eu/fileadmin/user_upload/REHVA_COVID-19_guidance_document_V4_23112020_V2.pdf

(13) IAPMO. Tips and Recommendations for the Safe and Efficient Flushing of Plumbing Systems in Buildings https://www.iapmo.org/media/23921/flushing_stagnant_plumbing_systems.pdf (2023-01-22)

(14) The Society of Heating, Air-Conditioning, and Sanitary Engineers of Japan, Novel Coronavirus Measures Special Committee; Operation of Air-conditioning Equipment and Other Facilities as SARS-CoV-2 Infectious Disease Control (Revised 2nd Edition) 2020-09-07. http://www.shasej.org/recommendation/covid-19/2020.09.07%20covid19%20kaitei%20(2).pdf (2023-01-22)

(15) The Center for Better Living; Methods of Testing Performance of Quality Housing Components, Water Closets, 2018.7

8. Presentations of authors

Ayaka Kimura is a graduate of the Otsuka Laboratory at Kanto Gakuin University in Japan. During her studies, she was mainly involved in research on living space hygiene contributory to preventive measures against COVID-19.
She currently works for TEPCO Energy Partner, Inc., and is engaged in work in relation to power demand and energy conservation.

Masayuki Otsuka is a professor at the Faculty of Architecture and Environment, Kanto Gakuin University, Japan. He has been conducting a wide range of research on water supply, drainage and sanitary equipment. Otsuka is a member of AIJ (Architecture Institute of Japan). He also fulfilled his role as the Chairperson of SHASE (The Society of Heating, Air-Conditioning and Sanitary Engineers of Japan).

Vertical bioaerosol transmission in toilet environment

T.W. Tsang* (1), K.W. Mui (2), L.T. Wong (3), Y.S. Wong (4)

(1) hayley.tsang@polyu.edu.hk

(2) behorace@polyu.edu.hk

(3) beltw@polyu.edu.hk

(4) 21015186D@connect.polyu.hk

(1), (2), (3), (4) Department of Building Environment and Energy Engineering, The Hong Kong Polytechnic University, Hong Kong.

Abstract

Multiple COVID-19 outbreaks in high-rise residential buildings were found to be caused by the vertical spread of the virus along the building. Although such a transmission pathway was speculated to be one of the reasons for COVID-19 cases observed at top-floor residential units along a vertical column, empirical evidence and experimental results have yet to be obtained. To evaluate the effects of toilet ventilation on the spread of bathroom bioaerosols, a set of tracer gas experiments were conducted in a full-scale, 3-floor mock-up toilet experimental research facility. Using a novel IoT-enabled tracer gas sensing network, tracer gas dispersion from the lower floor toilet to the upper floor toilet and the roof under the 16 combinations of opening windows and exhaust fans was evaluated. Experimental results confirmed the potential vertical transmission pathway through toilet ventilation. Residents of both units are suggested to close the windows and switch on the exhaust fans of the toilet to minimize the risk of airborne infection via vertical transmission effectively.

Keywords

Vertical airborne transmission; bathroom bioaerosols; toilet ventilation; residential toilets; tracer gas experiment.

1 Introduction

The worldwide COVID-19 pandemic has caused severe economic losses and a global crisis. As of June 2023, there have been 767,750,853 confirmed cases of COVID-19, with 6,941,095 deaths reported to World Health Organization (WHO). The main symptoms of COVID-19 are fever, chills, cough, shortness of breath and fatigue, but some patients may develop gastrointestinal symptoms such as diarrhea and vomiting. Patients with respiratory symptoms may release the SARS-CoV-2 virus as droplets or aerosols, while viable viruses were also discovered in human faeces (Holshue et al., 2020).

The main routes of transmission of COVID-19 are direct contact with virus-laden droplets and indirect contact through contaminated inanimate surfaces. However, just like SARS-CoV-1, it was later found that airborne transmission was also feasible, contributing to numerous long-range transmissions and super spreading events through ventilation and drainage system. In particular, the vertical transmission of SARS-CoV-2 through toilet ventilation and poorly maintained drainage systems has been suspected as one of the possible causes of COVID-19 outbreaks in high-rise buildings. Solely in Hong Kong, over 50 outbreaks of COVID-19 in residential buildings were suspected to be caused by vertical transmission. In literature, several on-site investigations were carried out by researchers and experts responding to the super spreading events in residential buildings. For instance, in an outbreak that involved 3 families who lived in three vertically aligned flats connected by drainage pipes, the epidemiologic survey and tracer gas experiments found that cases of infection and the locations of positive environmental samples were consistent with the theory of the vertical spread of virus-laden aerosols via drainage stacks and vents (Kang et al., 2020).

While attention is put on vertical transmission by faecal aerosols through the drainage system, people often overlook the fact that toilet flushing and respiratory processes could also contribute to vertical transmission in bathroom environments. Coughing, breathing, or singing could generate virus-laden aerosols, which suspend in the air for a long time in a warm and humid toilet environment and exhaust the outdoor environment by toilet ventilation (Raines et al., 2020). Vertical super spreading events through toilet ventilation were suspected to be caused by the re-entrance of bathroom bioaerosols from a lower floor to an upper floor toilet propagated by outdoor wind and negative pressure induced by the toilet exhaust fan. In an outbreak in a residential building in South Korea, where all infected cases were found along two vertical lines of the building, researchers found that the spread of the virus could be caused by the stack effect created along the toilet air duct that was meant to improve toilet ventilation (Hwang et al. 2020).

It is apparent that airborne transmission through toilet ventilation among the top floors of the buildings is feasible but needs to be more appreciated. While current evidence and information are mainly from real-case epidemiologic surveys, experimental studies conducted under controlled conditions were rarely due to the lack of testing facilities

(Gormley et al., 2017). The potential vertical transmission pathways through toilet ventilation were investigated using a full-scale, 3-floor mock-up toilet experimental research facility. The dispersion of tracer gas from the lower floor toilet to the upper floor toilet and the roof was evaluated under the 16 combinations of opening windows and exhaust fans. This study presents the potential vertical transmission pathways through various toilet ventilation scenarios and summarizes the best strategy for minimizing infection risk.

2 Materials and Methods

2.1 Research facility

The study was conducted by The Research Platform of Sanitation Hygiene and Environment (RPSHE), a full-scale 3-floor mock-up toilet experimental research facility at The Hong Kong Polytechnic University. The RPSHE was constructed according to the design and the building of the bathroom of the single-person public housing flats in Hong Kong. Functional toilet facilities were installed, including water closets with drainage pipes, floor drains connected to the U-trap with water seal and the drainage pipes, 6-inch exhaust fans positioned on the panel wall behind the water closet with an air volume of 210m³/hr, openable windows of size 600 mm × 900 mm right under the exhaust fan, and sliding doors with a low-level louver of size about 150 mm × 300 mm. Figure 1 shows the schematic drawing and a photo of the RPSHE.
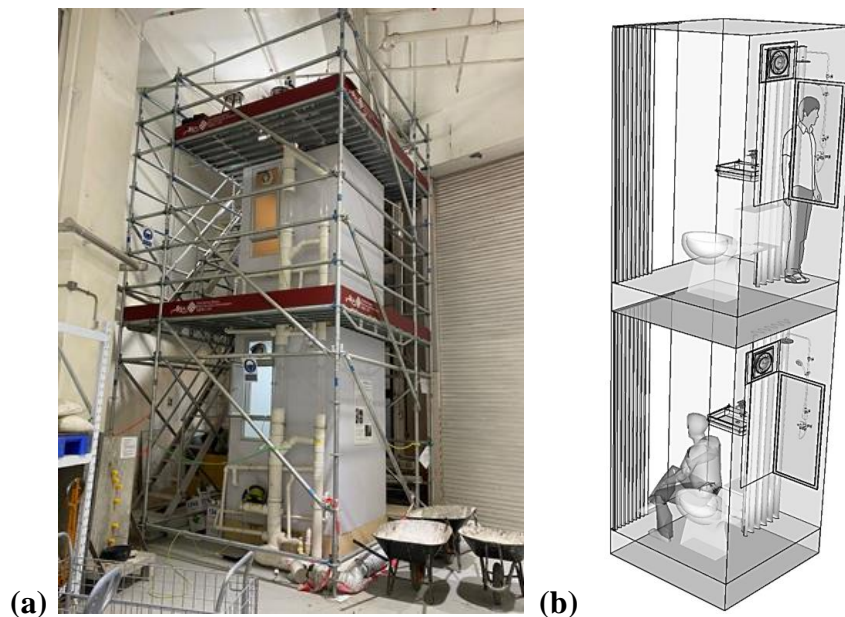

(a)　　　　　　　　　　　　　　(b)

Figure 1(a) – Photo of the Research Platform of Sanitation Hygiene and Environment (RPSHE); and (b) Schematic diagram illustrating the interior of the RPSHE.

2.2 Experimental setup

A sick patient who suffered from airborne diseases may experience respiratory symptoms such as coughing and sneezing, which can generate a certain amount of tiny respiratory droplets laden with the virus. It has been found that sneezing can cause up to 40,000 droplets at a velocity of 100 m/s during a sneeze (Cole and Cook, 1998) while coughing generate approximately 3,000 droplet nuclei (Fitzgerald and Haas, 2005). These actions, however, happen arbitrarily. On the other hand, breathing is vital and cannot be avoided. Aerosol exhaled during breathing are of the size between 0.2 and 0.6 μm, which contain mucus and surfactant that carry viruses from and remain suspended in the air for several hours (Scheuch, 2020). Tracer gas was adopted as a surrogate to simulate the movement of aerosol particles generated through breathing under the influence of toilet ventilation, as the aerodynamics of virus-laden aerosol are similar to those of a gas (Ai et al., 2020).

To simulate the release of virus-laden aerosols from the breathing action of an infected person sitting on the water closet, tracer gas was released on top of the water closet at the height of 1.2 m above the ground (i.e., the approximate height of the mouth of a sitting person) at a flow rate of 6 L/min for 8 min (i.e., the average breathing rate for humans (Pleil et al., 2021). A novel wireless tracer gas network was deployed to detect the concentration of tracer gas at eight different locations. Sampling locations included the inside of the toilets (G/F and 1/F), at floor level outside the door and the window of the toilet and at the roof. An increase in tracer gas concentration indicates the transportation of aerosol particles from the G/F toilet to other sampling points. The sensor locations and the tracer gas releasing point remained unchanged throughout the experiment. The toilet door was closed all the time. No entrance or exit was made throughout the investigation. The ventilation systems outside the facility were also switched off to ensure a controlled environment. Figure 2 displays the tracer gas releasing point and the sampling points.
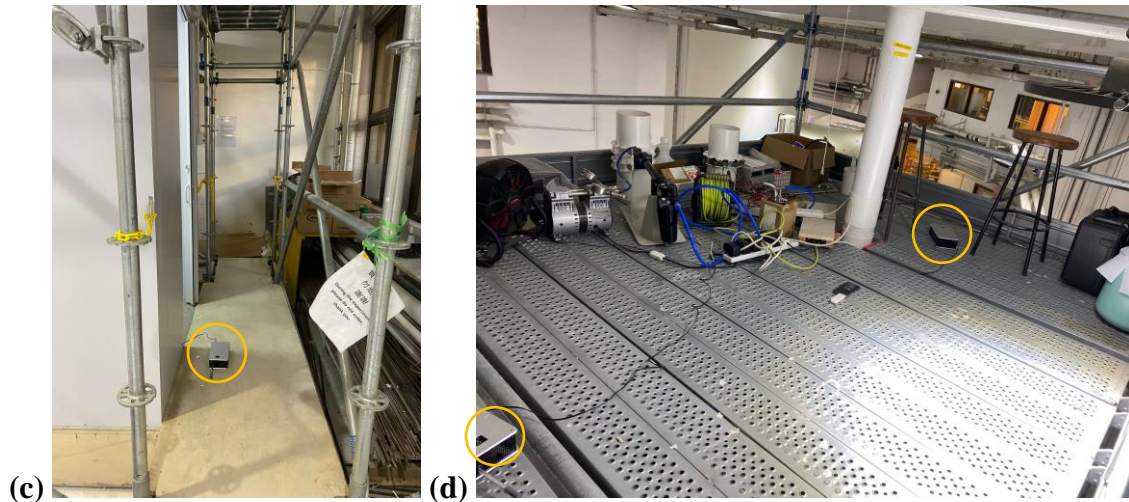

(a)   (b)

(c)

(d)
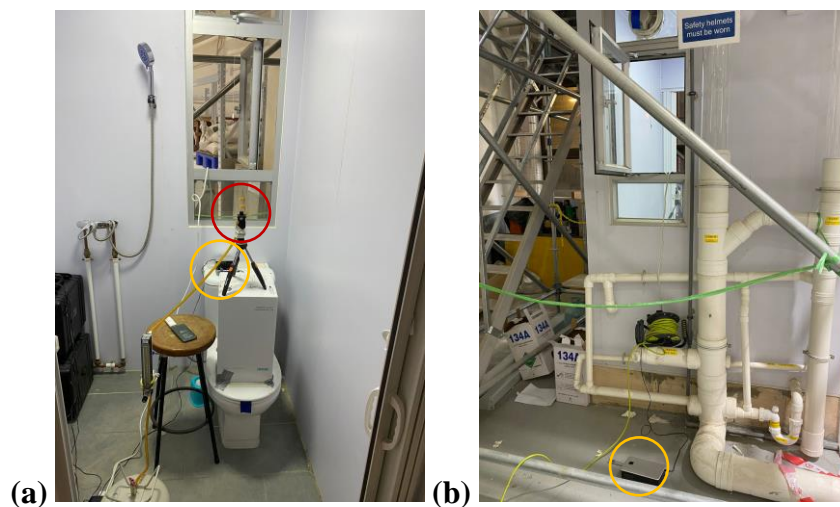
Figure 2(a) – The tracer gas releasing point in the G/F toilet (circled in red) and the sampling point inside both toilets (circled in yellow); (b) The sampling point near the window outside the toilets (circled in yellow); (c) The sampling point near the low-level louver of the door outside the toilets (circled in yellow); and (d) The sampling points at the roof (circled in yellow).

To evaluate the effects of toilet ventilation on the spread of bathroom bioaerosols from the infected person in the G/F toilet, a total of 16 scenarios with various combinations of the window opening and exhaust fan operation were tested. Table 1 shows the 16 scenarios.

Table 1 – Experiment Scenarios

Case	G/F Exhaust fan	G/F Window	1/F Exhaust fan	1/F Window
1	Off	Open	Off	Closed
2	Off	Closed	Off	Open
3	Off	Open	Off	Open
4	On	Open	Off	Closed
5	Off	Closed	Off	Closed
6	On	Open	On	Open
7	Off	Open	On	Closed
8	On	Open	Off	Open
9	On	Closed	On	Open
10	Off	Closed	On	Open
11	On	Closed	Off	Open
12	On	Closed	On	Closed
13	On	Open	On	Closed
14	On	Closed	Off	Closed
15	Off	Closed	On	Closed
16	Off	Open	On	Open

3 Results and Discussion

There are two potential situations in which infection risks may arise:1) among residents on the G/F after the infected person uses the washroom, and 2) among the residents of the 1/F. In the following section, the ventilation strategies that minimize airborne infection risks will be evaluated based on two criteria: the ability to remove aerosols from the G/F toilet and the extent to which it minimizes the re-entrance of aerosols into the 1/F toilet.

3.1 Removing the aerosols from the G/F toilet

To minimize the infection risks among residents in the G/F household, toilet ventilation strategies should be adequate to remove the virus-laden aerosols as soon as they are released from the source patient. Among all the case scenarios, Case 5 (both windows were closed; both exhaust fans were off) took up to 7 hr (the longest time in the investigation) to remove all the tracer gas from the G/F toilet. For cases with the G/F window closed and the exhaust fan off, opening the 1/F window (Case 2), switching on the 1/F exhaust fan (Case 15), or doing both (Case 10) reduced the tracer gas decay time at the G/F toilet to around 3 hr. Moreover, lower peaks at the G/F toilet were observed when the 1/F exhaust fan was operating. Figure 3(a) illustrates the movement of tracer gas under these case scenarios. A faster decay at the G/F toilet might be because these ventilation actions created a pathway for fresh air to enter the G/F toilet, which diluted the concentration of tracer gas and allowed it to be removed more quickly. In particular, the operation of the 1/F mechanical exhaust fan enhanced the ambient air movement in the area outside the toilet, which caused the tracer gas in the G/F toilet to disperse to the outdoor environment more quickly, resulting in lower peaks of tracer gas concentration in the G/F toilet. It is important to note that during the experiment, the use of ventilation in the 1/F toilet resulted in the entry of tracer gas through the gap in the door, as indicated in the red arrow in the figure. However, in a real-world scenario, the area outside the toilet door should be isolated from the G/F environment, ensuring that the air that enters is clean and free of any contaminants.

For cases with the G/F window open, opening the window of the 1/F toilet (Case 3) did not improve the decay rate at the G/F toilet, but switching on the exhaust fan at 1/F (Case 7) reduced the time by two-thirds compared to when the fan was off. This could be because the exhaust fan creating negative pressure in the 1/F toilet, which drew fresh air from the outside and promoted the removal of tracer gas from the G/F toilet. As displayed in Figure 3(b), switching on the 1/F exhaust fan and opening the window (Case 16) prevented the initial build-up of tracer gas. However, after around 10 min, the tracer gas concentration increased and decayed slowly over an hour. This might be because the open window and the exhaust fan create a pressure difference between the G/F and the 1/F toilet, allowing fresh air to enter the toilets and thus diluting the concentration of tracer gas in the G/F toilet. However, the opening of the G/F window also created airflows that

might cause the re-entrance of tracer gas from the ambient environment into the G/F toilet. The slow decay rate observed in this case suggested that the dilution effect of the open windows was not strong enough to counteract the re-entrance of tracer gas.
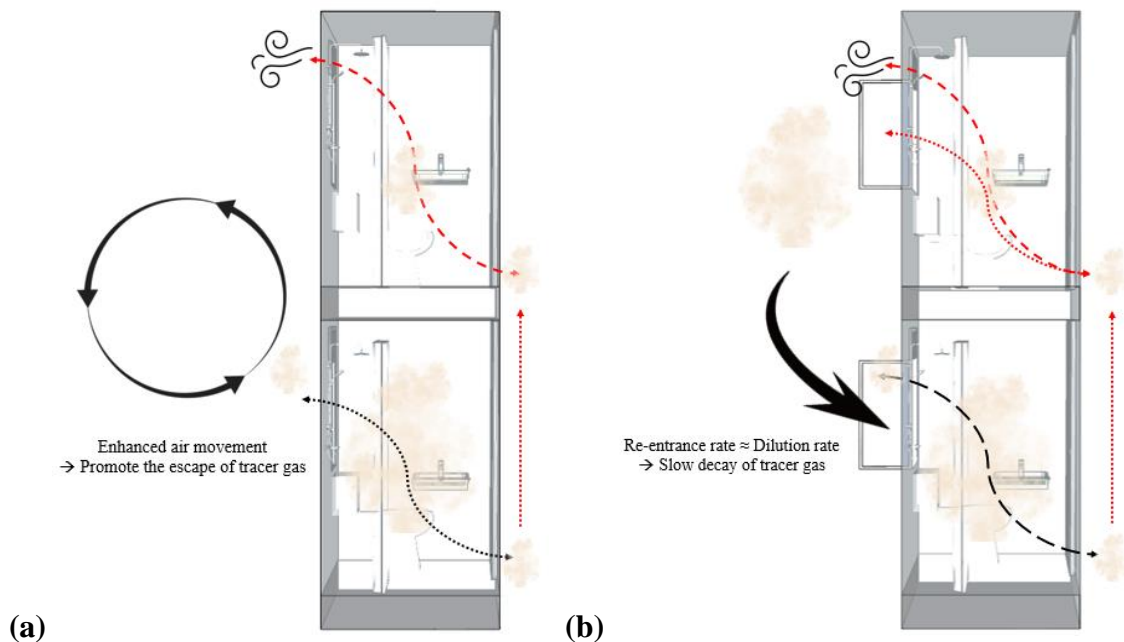

(a) **(b)**

Figure 3(a) – The use of ventilation strategies in the 1/F toilet to facilitate the escape of tracer gas (aerosols) from the G/F area; and (b) The re-entry of tracer gas due to an open window on the G/F.

When the exhaust fan at the G/F toilet was on in Cases 4, 6, 8, 9, 11–14, tracer gas at the G/F toilet was removed within 20 min or less for all cases. The best cases were Case 12 and Case 14, where only the G/F exhaust fan was on while both windows were closed. Operating an exhaust fan at the G/F toilet resulted in a negative pressure, which drew in fresh air from the outside and promotes the removal of tracer gas. Closing the G/F window ensured there was no short-circuit of the airflow and prevented the re-entrance of tracer gas from the outdoor environment.

3.2 Minimizing infection risks of the G/F residents

In several instances, elevated levels of tracer gas were detected outside the door of the G/F toilet within the first few minutes of tracer gas release. Although the concentration of the gas typically decreased rapidly within 20 minutes, this initial high level of tracer gas outside the toilet door still presented a potential risk to residents in the G/F household. In Case 5, where there was no ventilation in either the G/F or 1/F toilet, it took up to 43 min for tracer gas to decay, which was the longest time among all cases. Additionally,

not using any ventilation in the G/F toilet, such as in Case 10, also resulted in longer tracer gas removal time near the door outside the G/F toilet.

However, when both the G/F and 1/F exhaust fans were operating without opening any of the windows (Case 12), as shown in Figure 4(a), there was no increase in tracer gas levels near the door of the G/F toilet. This suggested that the gas was quickly removed from the G/F toilet to the outside of the window before it could reach the door, emphasizing the effectiveness of using exhaust fans for removing airborne particles.

(a)   **(b)**
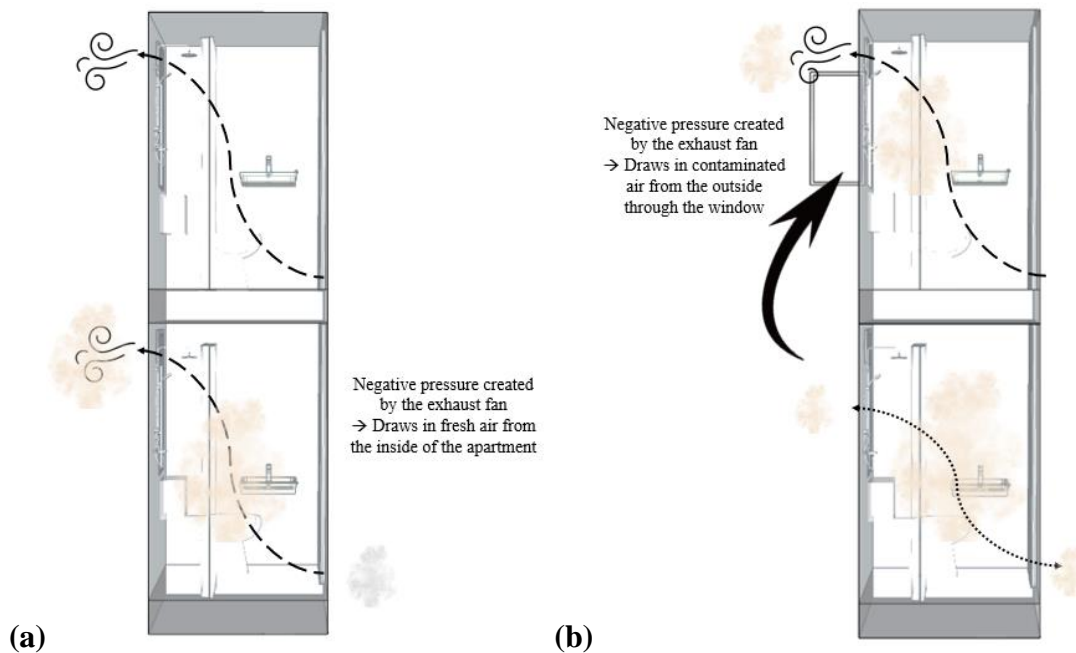
Figure 4(a) – The use of exhaust fans in both toilets to prevent cross-infection among G/F residents; and (b) The re-entry of tracer gas due to an open window and the operation of an exhaust fan on the 1/F.

Overall, these findings demonstrate the importance of proper ventilation in reducing the concentration of airborne particles. Effective ventilation strategies, especially the use of exhaust fans, can significantly reduce the risk of exposure to airborne infectious pathogens.

3.3 Minimizing the re-entrance of aerosols into the 1/F toilet

It is important to note that once virus-laden aerosols are removed from the G/F toilet and released into the outdoor environment, there is a possibility that they may move upwards and enter the 1/F toilet. Such vertical transmission could result in cross-infection.

Therefore, it is essential to consider the number of aerosols that may enter the 1/F toilet when selecting an appropriate ventilation strategy to minimize infection risk.

In Cases 4, 10, 15 and 16, relatively high levels of tracer gas were detected in the 1/F toilet, with the highest levels observed in Case 10. Specifically, in Case 10, where both the window and exhaust fans at the G/F toilet were closed and off while operating at the 1/F toilet, the peak tracer gas concentration recorded at the 1/F toilet was one-tenth of that at the G/F toilet. It took 24 minutes for the tracer gas concentration to drop back to background levels. Figure 4(b) demonstrates the transmission pathway in Case 10.

In Case 15, less tracer gas was able to enter the 1/F toilet through the closed window. However, the negative pressure generated by the mechanical exhaust fan drew in air from the nearby vicinity, which contained trace amounts of tracer gas, causing increased tracer gas levels inside the 1/F toilet. Similar situations were observed in Case 4 and Case 16, with elevated levels of tracer gas detected in the 1/F toilet. Notably, the sensor near the door louver of the 1/F toilet did not detect any significant increase in tracer gas concentration in these cases, but tracer gas was detected near the 1/F window. This suggested that the tracer gas likely entered the 1/F toilet through the window gap instead of the door louver.

3.4 Optimal ventilation strategy for minimizing the overall infection risks

By considering both the infection risk of the G/F and the 1/F residents, ventilation Case 12, as displayed in Figure 4(a), which utilized only the exhaust fan on both floors without opening the windows, was found to achieve the best tracer gas removal performance in the G/F toilet while preventing the aerosols from entering the 1/F toilet. It is important to note that when the exhaust fan is operating, the negative pressure created must be balanced by drawing fresh air from the nearby area. To ensure that the incoming air is fresh and not contaminated by virus-laden aerosols released from the G/F toilet, measures such as using a door gap or a door louver can ensure that fresh and clean air enters from the inside of the apartment rather than from the ambient air through window gaps.

4 Conclusion

Several COVID-19 outbreaks among top-floor residents in high-rise residential buildings have been attributed to the vertical spread of the virus along the building. Yet, experimental results had yet to be obtained to confirm this speculation. This study aimed to identify the optimal ventilation strategy to minimize the infection risks of residents in both top-floor units. Tracer gas experiments were conducted in a full-scale, three-floor mock-up toilet experimental research facility with various combinations of ventilation strategies. With a tracer gas sensing network, the tracer gas levels were evaluated at different points in the toilets and on the roof. Using an exhaust fan generally could achieve

good ventilation performance and remove the tracer gas from the G/F as soon as possible. Opening the window, however, might cause the re-entrance of tracer gas from the ambient environment into the G/F or the 1/F toilet. Overall, closing the window and switching on the exhaust fan at both the G/F and the 1/F toilet achieved the best ventilation performance while minimizing the infection risks of the upper-floor resident. These findings highlight the importance of carefully considering the overall ventilation strategy to minimize the risk of airborne transmission between floors. Appropriate measures shall be adopted to ensure the incoming air is clean and fresh.

Acknowledgments

5 Reference

Holshue, M. L., DeBolt, C., Lindquist, S., Lofy, K. H., Wiesman, J., Bruce, H., Spitters, C., Ericson, K., Wilkerson, S., Tural, A., Diaz, G., Cohn, A., Fox, L., Patel, A., Gerber, S. I., Kim, L., Tong, S., Lu, X., Lindstrom, S., Pallansch, M. A., … Washington State 2019-nCoV Case Investigation Team. (2020). First case of 2019 novel coronavirus in the United States. The New England Journal of Medicine, 382(10), 929–936. https://doi.org/10.1056/NEJMoa2001191

Kang, M., Wei, J., Yuan, J., Guo, J., Zhang, Y., Hang, J., Qu, Y., Qian, H., Zhuang, Y., Chen, X., Peng, X., Shi, T., Wang, J., Wu, J., Song, T., He, J., Li, Y., & Zhong, N. (2020). Probable evidence of fecal aerosol transmission of SARS-CoV-2 in a high-rise building. Annals of Internal Medicine, 173(12), 974–980. https://doi.org/10.7326/M20-0928

Raines, K. S., Doniach, S., & Bhanot, G. (2021). The transmission of SARS-CoV-2 is likely comodulated by temperature and by relative humidity. PLoS One, 16(7), e0255212. https://doi.org/10.1371/journal.pone.0255212

Hwang, S. E., Chang, J. H., Oh, B., & Heo, J. (2021). Possible aerosol transmission of COVID-19 associated with an outbreak in an apartment in Seoul, South Korea, 2020. International Journal of Infectious Diseases, 104, 73–76. https://doi.org/10.1016/j.ijid.2020.12.035

Gormley, M., Aspray, T. J., Kelly, D. A., & Rodriguez-Gil, C. (2017). Pathogen cross-transmission via building sanitary plumbing systems in a full-scale pilot test-rig. PLoS One, 12(2), e0171556. https://doi.org/10.1371/journal.pone.0171556

Cole, E. C., & Cook, C. E. (1998). Characterization of infectious aerosols in health care facilities: An aid to effective engineering controls and preventive strategies. American Journal of Infection Control, 26, 453–464. https://doi.org/10.1016/S0196-6553(98)70046-X

Fitzgerald, D., & Haas, D. (2005). Mycobacterium tuberculosis. In: Mandell GL, Bennett JE, Dolin R, editors. Principles and Practice of Infectious Diseases. 6th ed. Philadelphia (PA): Churchill Livingstone, 2852-86.

Scheuch, G. (2020). Breathing is enough: For the spread of influenza virus and SARS-CoV-2 by breathing only. Journal of Aerosol Medicine and Pulmonary Drug Delivery, 33(4), 230–234. https://doi.org/10.1089/jamp.2020.1616

Ai, Z., Mak, C. M., Gao, N., & Niu, J. (2020). Tracer gas is a suitable surrogate of exhaled droplet nuclei for studying airborne transmission in the built environment. Building Simulation, 13(3), 489–496. https://doi.org/10.1007/s12273-020-0614-5

Pleil, J. D., Ariel Geer Wallace, M., Davis, M. D., & Matty, C. M. (2021). The physics of human breathing: Flow, timing, volume, and pressure parameters for normal, on-demand, and ventilator respiration. Journal of Breath Research, 15(4), 10.1088/1752-7163/ac2589. https://doi.org/10.1088/1752-7163/ac2589

6 Presentation of author(s)

Dr. T.W. Tsang is a Postdoctoral Fellow at the Department of Building Environment and Energy Engineering at The Hong Kong Polytechnic University. Her research interests are focused on the critical areas of airborne infection in the built environment, indoor environmental quality, building ventilation, and carbon neutrality.

Prof. K.W. Mui is the Associate Head (Research) and a Professor at the Department of Building Environment and Energy Engineering, Associate Head of the College of Undergraduate Researchers and Innovators (CURI) at The Hong Kong Polytechnic University. Prof. Mui is a Chartered Engineer, a Fellow of HKIE, and a member of ASHRAE(USA), HKSMI, CIBSE and ISIAQ.

Dr. L.T. Wong is the Associate Head and an Associate Professor in the Department of Building Environment and Energy Engineering at The Hong Kong Polytechnic University. Dr. Wong is a Chartered Engineer and a member of HKIE and CIBSE. He also served as a court member in 2016-2021 and a council member in 2022-2023 for Hong Kong Baptist University.

Mr. Samson Wong recently graduated from The Hong Kong Polytechnic University, earning an honours degree in Building Environment and Energy Engineering. He is currently a building services consultant, specializing in piping and drainage systems for buildings.

TECHNICAL SESSION 9 − SIZING II

An international review of design requirements for the single stack drainage configuration

J. S. Lansing

john.lansing@pae-engineers.com
PAE, Portland, Oregon

Abstract

The single stack drainage system, also known as the primary ventilated stack, is a piping configuration that utilizes standard drainage fittings and the atmospheric opening at the top of the drainage stack termination as a means of stabilizing transient air pressure differentials throughout the piping system without a separate network of vent piping. Following extensive investigations at the Building Research Station in the 1950-1970s, variations of the single stack system have become widespread globally, resulting in regionally distinctive design and installation criteria. These variations are reflected in regional standards and are discussed in detail here, focusing on widely used configurations and configurations with unique requirements. Contrasting design and installation standards may be useful for developing generalized design and installation guidance for the single stack configuration as well as highlighting inconsistencies between regional characteristics to guide future investigations focusing on performance validation. The single stack drainage system in the following design and installation standards were chosen for review: BS EN 12056-2 (United Kingdom), DIN 1986-100 (Germany), NEN 3215 (Netherlands), DS 432 (Denmark), Byggvägledning 10 (Sweden), SANS 10252-2 (South Africa), GB 50015-2019 (People's Republic of China), SHASE-S 206-2019 (Japan), COPSSW (Singapore), AS/NZS 3500.2 (Australia & New Zealand), NBR 8160:1999 (Brazil), Philadelphia Plumbing Code, IPC and UPC (United States).

Keywords

Single stack drainage system, primary ventilated stack, drainage systems, plumbing codes, drainage standards, international standards

Definitions

Auxiliary vent: a drainage stack with a parallel vent to support greater airflow

Bypass stack: a separate drainage stack connecting upstream and downstream of the connection clearance zones of the main drainage stack the (Figure A1.7)

Bypass vent: vent piping that extends from the fixtures to the drainage stack (Figure A1.6)

Drainage branch: drainage piping carrying the flow from two or more fixture drains

Fixture drain: drainage piping between the trap and the drainage branch or drainage stack

Long sweep bend: a 90° bend with a radius equal to at least twice the drain diameter

Secondary vented stack: a drainage stack with a parallel vent to support greater airflow. Fixture drains and drainage branches may connect into the drainage stack unvented

Short sweep bend: a 90° bend with a radius less than twice the drain diameter

Square branch connection: a horizontal branch connection to the drainage stack with a centerline radius less than the diameter of the drain.

Stack base: where the stack transitions from vertical to horizontal (Figure A1.1)

Stack offset bypass: drainage and vent piping that extends from the lower drainage and the upper drainage stack (Figure A1.8)

Stack vent: extension of the drainage stack above the highest branch connection (Figure A1.1)

S-trap: A trap type similar to a P-trap except featuring a vertical segment immediately downstream of the trap outlet to direct the drainage downwards.

Swept branch connection: a horizontal branch connection to the drainage stack with a centerline radius at least twice the internal drain diameter

Unvented: a drain, whether vertical or horizontal, that is not connected to dedicated vent piping

Wye branch connection: a branch connection forming a 45° angle into the stack

Inspection chamber: point of access junction where two or more horizontal drains converge, located inside or outside (Figure A1.5)

1 Introduction

The water seal in fixture traps separates occupant spaces from foul air and aerosols within sanitary drainage piping in buildings. Traps typically have a water seal height of 50 mm (2 inches) or more, which allows a limited pressure differential within the drainage system without displacing water seals. As fixtures discharge into the drainage piping, air is drawn through the vent terminations to the exterior to stabilize the pressure differentials produced by the drainage flow. The sewer system outside of the building also allows for the stabilization of pressure differentials within the sanitary drainage system inside the building.

Trap seal loss events may be broken down into three categories: induced siphonage, self-siphonage and back pressure. Induced siphonage occurs when a trap seal is removed by negative pressure caused by drainage flow from an adjacent branch or drainage stack.

This form of siphonage is often addressed by providing an auxiliary vent stack with cross connections to the drainage stack to balance pressure differentials. Self-siphonage occurs when there is insufficient airflow downstream of an actively draining trap. Self-siphonage is most likely to occur in long, small diameter drains with flow high enough to fill the cross-sectional area of the drain. This is most often mitigated with an induvial trap vent, also known as an anti-siphon vent, but may also be addressed with a larger diameter drain to avoid hydraulic closure. Back pressure is another cause of water seal loss and occurs when the trap is subjected to positive pressure, in some cases, high enough to eject the water seal into the occupant space. All three trap seal loss scenarios may be addressed without a separate network of vent piping by extending the upper portion of the drainage stack to the exterior. This configuration, known as the single stack or primary ventilated stack, is the basis of many drainage design standards and achieved widespread use following the results of key investigations at the Building Research Station in the 1950s (Figure A1.1). Single stacks are ideally suited for conditions where fixtures are concentrated in close proximity and where stack offsets do not occur. Bathrooms in residential buildings and hotels are common applications for single stacks as well as remotely located fixtures such as kitchen sinks or washing machines.

Due to the complexity of the interactions within the stack, many design recommendations are based on regionally based investigations, trial and error, arbitrary judgements, and traditional practice within a given region. A review of existing design recommendations may provide valuable insight into the methods available for maintaining subjectively acceptable risk of trap seal failure with respect to system complexity and installation cost. The following review will assess recommendations based on peak drainage loads, height limitations, accommodations for fixtures near the stack base, branches and stack connections, and stack offsets while providing regional context. Many of the characteristics discussed in the regional context are not specific to the single stack drainage system but may influence aspects of the performance.

The information provided here is the culmination of reviews of design standards, industry journals, and interviews with subject matter experts, such as designers and standards specialists. Given the nature of this study, the literature review for each regional section is uneven due primarily to varying levels of guidance within the respective standards. Additional contributing factors to uneven discussion include varying availability for publications, challenges accessing information as well as language, social, and regional barriers. Subject matter experts for many of the regions discussed were consulted to increase accuracy and to provide greater context.

The modified single stack, also known as the secondary ventilated stack, is a configuration similar to the single stack system, except a parallel auxiliary vent stack is provided to allow for increased airflow. The auxiliary vent stack connects above the base of the stack and extends to the atmosphere, which may feature cross-connections between the vent and drainage stack and is most often used for stacks in high-rise buildings or stacks with offsets. Like the single stack, fixture branches and sanitary branches may connect to the drainage stack unvented. Branch-to-stack connections are assumed to use standard drainage fittings, such as the swept branch and wye unless noted otherwise.

Systems using special branch connection fittings, namely the Sovent system, which feature branch connection aerators, deaerator, or fittings with vanes to influence the movement of drainage flow within the stack are outside of the scope of this review. Similarly, single stack configurations with mechanical ventilation devices such as air admittance valves (AAV) or positive transient attenuators (PTA) are not considered in this review.

1.1 General comments on regional context

The historical adoption of vent piping to support the attenuation of airflow within sanitary drainage systems is varied. The transition away from individual vent piping in the United Kingdom begin as a result of post-war rebuilding efforts in the 1940s, leading A.F.E Wise of the Building Research Station (BRS) to perform testing of drainage systems with unvented drainage branches [1]. Wise's *One Pipe (Single Stack) Plumbing for Housing* 1952 publications [2] [3] demonstrated that unvented fixtures may discharge into a drainage stack while maintaining pressure differentials, provided that the upper portion of the stack was open to the atmosphere. In 1969, BRS introduced a methodology using the steady flow energy equation to calculate the maximum negative pressure developed within the single stack, taking into account both drainage flow and stack height, among other influencing factors [4]. These efforts were well-received and supported the adoption of the single stack internationally. In regions such as Germany and the Northeast United States however, similar configurations had been utilized prior to efforts at the BRS.

Some published drainage standards serve as a guide whereas others serve as a legal requirement or 'code' that may be legally enforced. Many standards are published as national standards intended to apply to a specific territory or region whereas other standards are intended for multinational usage.

The European Committee for Standardization (CEN) effort led to the publication of the 5 part harmonized drainage standard EN 12056 *Gravity drainage systems inside buildings* in 2000, part 2 of which contains a majority of the design guidance for sanitary drainage systems [5] While many regions of Europe continue to independently issue national design standards, the regional design and installation practices mostly fall within the four design categories described in Part 2 of EN 12056. Each of the design categories, designated as System I, II, III, and IV, feature separate values for calculating drainage loads, branch filling height, maximum drainage branch length, stack connection type, minimum gradient, minimum fixture drain diameter, and other specifications. The design and installation practices of System I reflect those of Germany, Switzerland, and Belgium and are most prevalent in Europe. System II reflects the design and installation practices of the Netherlands and to some extent Scandinavia, System III reflects those of the UK, and System IV reflects those of France [6]. The EN 12056 standard is republished by member nations of CEN as a national standard with a prefix identifying the associated national standards organization. All four System Type categories require a minimum trap seal of 50 mm (2 inches), effectively establishing a uniform minimum pressure performance criterion. EN 12056-2 features an equation for calculating the peak drainage

flow (Equation B1.1), using empirical discharge units based on the fixture type and a frequency factor to account for statistical usage criteria. The design loading basis for the single stack in EN 12056 is $1/6^{th}$ of the cross-sectional area and does not take into consideration stack airflow with respect to height [7].

1.2 General comments on stack height

When drainage flows from a branch into the stack, an annular flow forms around the interior wall, allowing a core of air to pass through the center. The shear force between the drainage and airflow generated by the 'no slip' condition draws air into the top of the stack to balance the developed negative pressure. Taller drainage stacks will generate greater negative pressures as the frictional resistances are greater due to the distance to the atmospheric termination [8]. Contrary to the assumptions that form the basis of many design standards, there is no simple relationship between airflow and drainage flow and many of the computational methods for determining negative pressure are complex and generally not considered suitable for routine design applications [9]. For this reason, many standards prescriptively indicate maximum height limits for single stacks, which are subject to greater pressure differentials due to the reduced airflow capacity compared to systems with dedicated vent piping. The use of DN 100 (4 inch) stacks in the single stack configuration is fairly standard for stacks serving residential bathrooms internationally while DN 150 (6 inch) stacks are sometimes used for taller buildings due to the increased airflow capabilities.

1.3 Stack base

Most standards require a connection clearance zone (Figure A1.2) extending a specified distance above and downstream of the stack base, where no drainage connections are permitted. The connection clearance zones account for the positive pressure waves due to the water curtain formation along the inner radius of the stack base transition from vertical to horizontal. While this requirement is often solely attributed to addressing the pneumatic effects of a hydraulic jump or suds production depending on the design standard, the clearance zone addresses a variety of performance issues to reduce the likelihood of pressure differentials exceeding established thresholds that will result in the failure of trap seals near the stack base. Due to the connection clearance zones at the stack base, the fixtures at the lowest floor are in many cases prohibited from connecting into the stack serving the floors above. Since single stacks do not have an auxiliary vent connecting shortly above the stack base, the single stack drainage system will generate larger pressures differentials, which may impact the water seals in traps unless countermeasures, such as connection clearance zones are implemented. Larger pressure differentials are associated with taller stacks due to the greater airflow needed to overcome the frictional resistance within the drainage stack as well as the style of fittings used for the stack base transition. Stack diameter, style of branch connection fitting to the stack, and vertical to horizontal arrangement at the stack base have a significant influence on the pressure differentials generated in the single stack [8].

2.4 Branches and stack connections

Fixture drains and drainage branches connecting into the single stack are often described as 'unvented' as they do not have individual vent piping installed. The design recommendations of the single stack are intended to provide adequate airflow to the unvented drainage branches to protect the water seals in traps, serving the same function as individual vent piping.

Unvented connections with small diameters may produce suction noise when draining at a high flow as well as produce siphonage that may compromise the water seal in the trap. The impact of self-siphonage tends to be greatest when draining a plugged basin[1] with a rounded bottom into an unvented drain or unvented S-trap configuration. In flat bottom fixtures such as a shower, bathtub or kitchen sink, the trailing discharge that occurs as the draining process is nearly complete has the tendency to refill any siphonage that may have occurred [10] [11].

The type of stack connection fitting from drainage branches and fixture drains may influence siphonage in unvented drainage branch. Wye fittings are more likely to create hydraulic closure conditions while swept and square branch fittings allow better airflow.

1.4 Stack offsets

Similar to the pressure conditions produced by the water curtain at the stack base, stack offsets create conditions for a second water curtain as the horizontal drain transitions to the vertical position of the lower stack. To protect the water seals in traps, the pressure differentials resulting from the second water curtain must be accounted for in the design and installation of the system with connection clearance zones (Figure A1.2).

1.5 Units of measure

Many standards specify maximum height limits for single stacks in values of 'floors of fixtures'. Where maximum stack height values are listed in meters or feet, values will be converted to equivalent floors, with 3 m (9.8 ft) being equal to one floor.

Drainage loads are generally determined using either units of flow to represent the peak drainage flow expected to occur or by using dimensionless values such as the drainage fixture unit (DFU). To simplify comparisons between methodologies, 'residential bathrooms' will be used as a unit of measurement for loading, since this is both somewhat uniform and translates directly into operating installations. While the typical arrangement of fixtures in a residential bathroom varies widely internationally, the chosen arrangement for the comparisons here consists of a flush tank water closet, a combination bathtub/shower, and a basin.

---

[1] Also known as a lavatory or handwash basin

2 United Kingdom   Primary ventilated stack

2.1 Regional context

With the introduction of BS EN 12056-2 in 2000 as the national drainage design standard, the term 'single stack' replaced with 'primary ventilated stack'. System III of EN 12056 reflects the traditional design and installation practices of the United Kingdom, with additional detail described in the appendices. System III requires unvented fixture drains to connect independently to the stack without grouping together into a common branch except under certain conditions where all fixtures are of the same type (e.g. groups of basins, groups of water closets). Accepted practice is to provide swept branch stack connections or wye branch connections. Design guidance is based on the branches achieving a filling degree of 100%, though this filling height is not reached in most observed installations. A minimum trap seal of 75 mm (3 inches) is required at basins to help mitigate issues with self-siphonage. Bottle traps and P-traps tend to be common at basins and washdown type water closets are prevalent. Drainage branches downstream of stacks may be designed for a filling height up to 75%, though 70% or 60% are also often used as a maximum design filling height. Additional guidance is given in Approved Document H [12] of the Building Regulations and in industry design publications such as *Guide G - Public health and plumbing engineering* [13] published by the Chartered Institution of Building Services Engineers (CIBSE) and *Plumbing Engineering Services Design Guide* [14] published by the Chartered Institute of Plumbing and Heating Engineering (CIPHE).

Under System III, fixture drains generally connect independently to the drainage stack. A typical bathroom, for example, would have three horizontal branch connections, one each for the WC, bathtub, and basin. The practice of joining the fixture drains together from basin and the water closet to make one stack connection has become more common. Swept connection fittings are used for branch connections to stacks. For the vertical to horizontal transition at the base of the stack, two 45° bends are recommended, with a single 90° long sweep fitting being acceptable as an alternative arrangement. Increasing the diameter at the bend is another alternative arrangement listed in Annex ND.

Prior to the introduction of BS EN 12056-2, the now withdrawn BS 5572 [15] standard set a maximum stack pressure differential of ±38 mm (1.5 inches) of water column, equivalent to ±375 Pa. BS 5572 indicates an association between 375 Pa (1.5 inches) and a water seal loss of 25 mm (1 inch) from a typical washdown water closet and 19 mm (0.75 inches) from a P-trap, with either a trap seal depth of 50 mm (2 inches) or 75 mm (3 inches).

2.2 Peak loads and height limitations

A DN 100 (4 inch) stack may flow up to 5.2 L/s (82 gpm), which is equivalent to 38 standard bathrooms or 19 stories with two bathrooms on each floor. While recommendations for height limits are missing from guidance documents, designers often

recommend limiting the single stack to somewhere between 15 and 20 levels [16]. DN 150 (6 inch) stacks are used less often for single stacks.

2.3 Stack base

For single stacks greater than 5 stories in height, National Annex ND of BS EN 12056-2 recommends fixtures at the lowest level connect downstream of the stack. This is typically accomplished utilizing the stub stack configuration (Figure A1.3). A stub stack is an unvented DN 100 (4 inch) stack that serves fixtures located on the same floor and is capped at the top rather than vented to the atmosphere. A maximum flow 5.0 L/s (79 gpm) is allowed and is limited to a height of 2.5 m (8.2 ft) between the invert level of the horizontal drain and highest fixture connection (S1 in Figure A1.3). The water closet must not be greater than 1.5 m (4.9 ft) above the invert level of the horizontal drain (S2 in Figure A1.3). The stub stack configuration is also often used for fixtures located on the floor above a stack offset [17]. Guide G recommends a connection clearance zone of at least 2 m (6.6 ft) downstream of the stack base (Figure A1.2) when serving more than 5 floors. BS EN 12056-2 also recommends separating the lowest 2 floors from the main stack when serving more than 20 floors. Given that stub stacks may only serve one level of fixtures, stacks extending more than 15 to 20 floors will typically be provided with an secondary vented stack, which may also serve as the stack vent extension for the stack serving the lower 2 floors. For stacks below 5 stories, a vertical connection clearance of 0.74 m (2.5 ft) is given (V1 in Figure A1.2).

2.4 Branches and stack connections

Swept or 45° wye fitting connections are used in traditional practice for branch connections to the stack to limit the negative pressure produced in the stack during a discharge. Branch connections to the stack that have a comparatively small diameter, such as those from a basin or bathtub, may connect without a swept or 45° wye fitting.

The height, length, and gradient limits for the drainage piping between the fixture trap and the stack are indicated in EN 12056 for different fixture types for System III. Many fixture types have no limits on the length. For basins, only horizontal piping is allowed between the trap and the stack connection whereas all other fixture types allow vertical piping up to 1.5 m (4.9 ft). The maximum length between the trap and stack for basins is 3 m (9.8 ft) at a gradient of 1.8% with a minimum diameter of DN 40 (1.5 inch). Steeper gradients have shorter allowable lengths, as indicated in Figure 2.1. No more than 2 bends are permitted if the 3 m (9.8 ft) limit or 1.8% gradient is utilized.
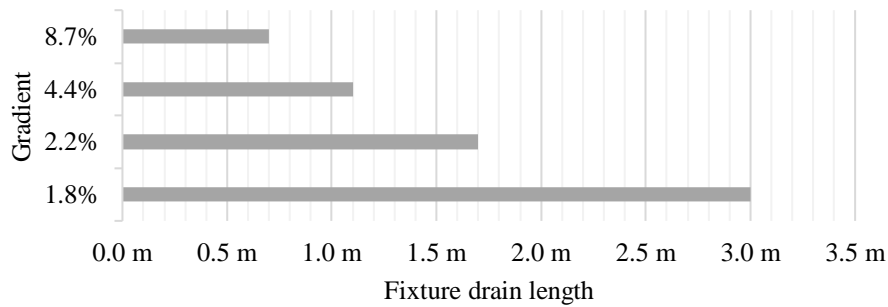
Figure 2.1 – Basin fixture drain length

No limit is indicated for bath/shower drains at DN 40 (1-1/2-inch), though a footnote in EN 12056-2 states that for drains longer than 3 m (9.8 ft), noisy discharges may result with an increased risk for blockages. The same footnote is indicated on kitchen sinks. Similarly, no limit is given for water closets, whether DN 80 (3 inch) or DN 100 (4 inch).

2.5 Stack offsets

A secondary vent stack is usually provided if fixtures connect to a stack below an offset. BS EN 12056-2 states that offsets less than 3 m (9.8 ft) can produce large pressure fluctuations.

3 Germany   Hauptlüftung

3.1 Regional context

System I of EN 12056-2 is used in Germany with additional provisions and requirements featured in DIN 1986-100 *Drainage systems on private ground* [18] published by Deutsches Institut für Normung with guidance published in *Gebäude- und Grundstücksentwässerung* [19] published by Beuth Verlag. The single stack is the standard drainage configuration used in Germany. Secondary vent stacks or special aerator fittings are typically only installed in applications where the single stack is not expected to provide acceptable performance. DIN 1986-100 states that pressures within the drainage system must be maintained to limit the maximum water seal loss to 25 mm (1 inch). No specific pressure limits are indicated. As for typical fixture installations, bottle traps are generally installed at basins and washdown type water closets are most common.

The first edition of DIN 1986 was published in 1928 [20]. Unlike many other drainage standards published in the first half of the 20th century, installing a separate network of vent piping for each fixture trap was not required in the DIN 1986 standard. The 1932 edition [21] stated that traps were required to be installed as close as possible to the drainage stack and be protected from siphonage. The 1942 edition [22] featured a graphic

showing a drainage stack for the water closet, a drainage stack for the bathtub, and a drainage stack shared between the sink and basin, with the only vent piping being the upper portion of the drainage stack where it terminates to the atmosphere above the roof. The current drainage values in DIN 1986-100 for stack loading match those in EN 12056. These values were informed by investigations at drainage testing facilities in Zürich in the 1980s and the original work of Wyly and Eaton [23] regarding drainage stack capacity [19].

3.2 Peak loads and height limitations

The DIN 1986-100 standard identifies limits on maximum drainage flow without specific reference to maximum stack height. Square branch connections are traditionally used in Germany, though swept branch connections are permitted as well and allow for higher maximum flow rates. The maximum drainage flow permitted for a DN 100 (4 inch) stack is 4.0 L/s (63 gpm), equivalent to 20 floors of residential bathrooms. If swept branch connection fittings are used, the maximum drainage flow is increased to 5.2 L/s (82 gpm) for a DN 100 (4 inch) stack, equivalent to 34 floors of bathrooms or 17 floors with two bathrooms per floor. A DN 150 (6 inch) stack may handle the load of 9.5 L/s (151 gpm), equivalent to 116 standard residential bathrooms. Due to the large negative pressures associated with tall stacks, the single stack is not often used for stacks greater than 100 m (328 ft), equivalent to 34 floors, though there is a lack of consensus and guidance on an appropriate maximum height.

The grouping together stack vents into a single header (Sammelhauptlüftung) is common for limiting the number of atmospheric terminations. The vent header size must have a cross-sectional area equal to at least half the total of the connected stacks. For example, a DN 150 (6 inch) stack has a cross sectional area equal to 167 cm² (26 in²), and may serve as a vent for up to four DN 100 (4 inch) stacks, each having a cross-sectional area of 72 cm² (11 in²).

3.3 Stack base

Fixtures on the lowest floor may connect to the drainage stack provided the stack is less than 10 m (33 ft) in height, equivalent to a stack serving 4 levels of fixtures. The height refers only to the drainage portion of the stack and not the vent extension. For stacks greater than 10 m (33 ft), fixtures at the lowest floor must connect at least 1 m (3.3 ft) downstream of the stack (H1 in Figure A1.2) and 1.5 m (4.9 ft) downstream of the stack for stacks taller than 22 m (72 ft), equivalent to a stack serving 8 floors of fixtures. Fixtures at the lowest floor may be provided with a bypass vent (Figure A1.6) or connect unvented to the horizontal drain downstream of the stack base clearance zone (Figure A1.4). In instances where there are no fixtures at the lowest level and the stack is greater than 22 m (72 ft), a bypass vent must still be provided, connecting between the drainage stack and horizontal drain. The vent connection to the drainage stack must also comply with the vertical clearance zone (V1 in Figure A1.2).

Table 3.1 – Connection clearance zone by stack height

Maximum Stack Height	Equivalent Floors	Minimum Connection Clearance Zone	
		V1	H1
10 m	≤ 4 levels	-	-
22 m	4 to 8 levels	2 m	1 m
≥ 22 m	≥ 9 levels	2 m	1.5 m

See Figure A1.2 for V1 and H1

The stack base transition is made with two 45° bends separated by a minimum of 0.25 m (0.8 ft) of diagonal drainage pipe. If the drainage stack is less than 22 m (72 ft) and the group of fixtures at the lowest floor are provided with a bypass vent, the 0.25 m (0.8 ft) separation between the 45° bends is not required. Stacks less than 10 m (33 ft) in height may use a single 90° bend for the vertical-to-horizontal transition, but this approach is not normally recommended due to lower acoustical and hydraulic performance.

3.4 Branches and stack connections

Unvented fixture drains and drainage branches DN 80 (3 inches) and larger must connect to the stack within 10 m (33 ft) of the furthest fixture. Unvented drainage branches less than DN 80 (3 inches) must connect to the stack within 4 m (13 ft) or to a drainage branch DN 80 (3 inches) or larger. The distance limitation accounts for both the horizontal distance and the vertical distance to the fixture (H and V in Figure A1.9). The vertical distance between the trap outlet and horizontal drainage branch must not exceed 1 m (3.2 ft). If the vertical distance is greater, the trap must be vented or provided with an AAV. DN 80 (3 inch) branches may be used to carry the drainage from both the WC, bathtub, and basin. The minimum slope for unvented branches is 1%.

3.5 Stack offsets

A connection clearance zone of 1 m (3.3 ft) must be maintained upstream and downstream of the horizontal-to-vertical transition of the stack offset (H2 and V2 in Figure A1.2). The horizontal-to-vertical transition must be made with two 45° bends. For stack offsets with a horizontal length less than 2 m (6.6 ft), fixtures must connect into a stack offset bypass (Figure A1.8) and connect at a minimum distance of 1 m (3.3 ft) below the horizontal-to-vertical transition. For stacks above 22 m (72 ft), a bypass vent is required regardless of whether fixtures are present at the lowest level.

4 Netherlands   Primaire ontspanningsleiding

4.1 Regional context

NEN 3215 *Drainage system inside and outside buildings within the property boundaries* [24] is the national building drainage standard published by Netherlands Standardization Institute (NEN). NTR 3216 *Sewerage inside buildings* [25] provides additional guidance and commentary on the application of NEN 3215. The single stack drainage system (primaire ontspanningsleiding) is the typical drainage configuration used the Netherlands. Where the conditions for a single stack are determined to be insufficient, a secondary vent stack (secundaire ontspannings leiding) is required. Horizontal drains are designed to a maximum filling height of 70%. Comparatively shallow gradients are utilized on horizontal branches, with a gradient between 0.5% and 2% being allowed for a DN 100 (4 inch) drain within a bathroom or downstream of a stack. The requirements outlined in NEN 3215 are based on a maximum pressure differential of 300 Pa (1.2 inches of water column) and a trap seal depth of 50 mm (2 inches). Water closets flushing with less than 6 L (1.6 gal) are not permitted due to reduced carrying capacity in the drainage piping.

4.2 Peak loads and height limitations

NTR 3216 indicates a maximum flow of 4.0 L/s (63 gpm) for DN 100 (4 inch) stacks and 9.0 L/s (143 gpm) for DN 150 (6 inch) stacks with a height between 10 m (33 ft) and 50 m (164 ft), equivalent to the drainage of 19 and 99 residential bathrooms respectively. NTR 3216 provides additional guidance on the drainage loads with respect to the stack height with the standard flow values above being based on stack heights between 10 m (33 ft) and 50 m (164 ft). Adjustment factors are provided in Table 4.1 to reduce the maximum recommended allowable drainage loading for stacks greater than 50 m (164 ft) up to 200 m (656 ft), equivalent to 19 to 67 levels respectively. No adjustment factors are needed below 50 m (164 ft), though an allowance of 40% additional drainage flow is given for stacks less than 10 m (33 ft) in height.

A DN 100 (4 inch) stack may carry the loading of up to 19 bathrooms, effectively limiting the stack to serving 21 floors of residential bathrooms, with the lower two floors being separated from the stack (see section 4.3 regarding connection clearance zones). A DN 150 (6 inch) stack may receive the drainage of up to 38 floors of residential bathrooms, taking into account the stack height adjustment factor. Interpolating the values shown in Table 4.1 produces an adjustment factor for a 113 m (371 ft) stack of 0.63, reducing the maximum recommended drainage load a DN 150 from 9.0 L/s (143 gpm) down to 5.67 L/s (90 gpm), approximately equal to 38 residential bathrooms.

Table 4.1 Maximum drainage flow for single stack drains in high-rise buildings

Stack Height	Equivalent Floors	Adjustment Factor	
		DN 100 (4 inch)	DN 150 (6 inch)
55 m (180 ft)	18	1.00	1.00
60 m (197 ft)	20	1.00	1.00
70 m (230 ft)	23	0.96	1.00
80 m (262 ft)	26	0.82	0.93
90 m (295 ft)	30	0.72	0.81
100 m (328 ft)	33	0.66	0.72
110 m (361 ft)	36	0.57	0.65
120 m (394 ft)	40	0.51	0.59
130 m (426 ft)	43	0.47	0.53
140 m (459 ft)	46	0.43	0.49
150 m (492 ft)	50	0.39	0.45
160 m (525 ft)	53	0.36	0.42
180 m (590 ft)	60	0.32	0.36
200 m (656 ft)	66	0.28	0.32

Stack height as defined in NTR 3216 extends from the stack base to atmospheric termination of the vent. Stack vent extensions may be combined together into a vent header (gecombineerde ontspanningsleiding) to limit the number of atmospheric terminations, provided the total length and height is taken into account. Depending on the airflow resistance imposed by the length of piping and fittings, vent header segments may be 1 or 2 nominal diameters larger than the horizontal drain receiving the drainage from the stack [26]. Formulas are provided in NTR 3216 for determining airflow losses in the vent piping.

4.3 Stack base

The connection clearance zones near the stack base are dependent on the stack height. Table 4.2 shows clearances zones ranging from 1 m (3.3 ft) to 9 m (30 ft). Fixtures at the lowest level may connect downstream of the stack base clearance zone unvented (Figure A1.4). For stacks less than 50 m (164 ft), a height equivalent to 16 levels, unvented fixtures at the lowest level may connect 3 m (9.8 ft) downstream of the stack base. For example, a DN 150 (6 inch) stack in a 38 floor building will separate the lower 3 floors from the stack using a bypass stack configuration (Figure A1.7). The vent from the top of the bypass stack may terminate into the drainage stack using a wye branch fitting and must connect at least 9 m (30 ft) above the stack base, as required for stacks greater than 80 m (262 ft).

---

[2] Stack height with respect to connection clearance zones refers to the distance between the stack base and highest drainage branch connection

to or less than 45° and not greater than 1.5 m (4.9 ft) in length, a clearance zone equal to 0.5 m (1.6 ft) must be maintained above the offset and 1 m (3.3 ft) below the offset.

5 Nordic region

5.1 Regional context

Harmonization efforts of the Nordic Committee for Building Regulations in the 1960s led to Sweden, Denmark, Finland, Norway and Iceland sharing a similar drainage design methodology, which are now independently issued as national standards with some regionally specific requirements. The single stack is the predominant drainage configuration used throughout the Nordic region. Many of the traditional design practices are reflected System II of EN 12056 though additional appendices are not provided for regional context on the Nordic approach. The EN 12056-2 standard is not widely used in Nordic region, instead utilizing regionally developed design standards. DS 432 [27] is used in Denmark and Byggvägledning 10 [28] is used in Sweden, both of which are the most predominantly used drainage standards in the Nordic region. When drafting EN 12056-2, Technical Committee CEN/165 Working Group 21 did not reflect the 50% branch filling height used in the Nordic region, instead indicating the 70% filling height used in the Netherlands, but managed to unify other criteria, such as many of the loading values for fixtures, branches and maximum branch length, under System II. A maximum pressure differential of ±400 Pa (1.6 inches of water column) is indicated in DS 432. Because the single stack system is assumed for design and installations, no name is given to differentiate the single stack from the secondary ventilated stack in either DS 432 or Byggvägledning 10. Air admittance valves (AAV) are common and bottle traps, P-traps, and S-traps are often used. Normflöde and summerade normflöden (standard flow and sum of standard flows) are used to determine peak drainage loads in units of flow using graphical charts. The equation and values for System II provided in EN 12056-2 achieve similar values. Basin drains often discharge into a common trap that also serves as a floor drain. Most water closets are dual flush, with the larger flush using 4 L (1.1 gal) and the smaller flush using 2 L (0.5 gal). A drainage branch gradient of 2% is typically used.

5.2 Peak loads and height limitations

DS 432 specifies a maximum stack loading equal to a cross-sectional area of 1/5th. This diverges from the 1/6th filling area that loosely formed the basis[3] for the values shown in EN 12056. DS 432 provides the Wyly Eaton stack formula along with roughness values to calculate the drainage capacity of the stack. In the case of the loading values for the DN 100 (4 inch) stack, this results in a loading of 4.2 L/s (67 gpm) if using cast-iron

---

[3]While 1/6th was agreed to serve as the basis for the values indicated in drainage loading Table 11 in EN 12056-2 for primary ventilated stack, the values arbitrarily diverge from the 1/6th in many instances to satisfy the recommendations of CEN Technical Committee 165 Working Group 21.

piping and 4.6 L/s (7.3 gpm) if using plastic or stainless-steel piping. From a drainage loading standpoint, a DN 100 (4 inch) stack receiving the drainage from residential bathrooms may serve up to 27 floors for cast-iron and 34 floors for plastic or stainless steel. The drainage allowance for a DN 150 (6 inch) stack is much higher than any realistic installation for a single stack, equivalent to the drainage of 300 residential bathrooms for cast-iron and over 600 residential bathrooms for plastic or stainless steel. No consideration is given to the effect of stack height with respect to maximum allowable drainage flow in DS 432 or Byggvägledning 10.

5.3 Stack base

DS 432 requires clearance zones upstream and downstream of the stack base of 1 m (3.3 ft) if one or more water closets is located more than 10 m (33 ft) above the stack base (V1 and H1 in Figure A1.2). The stack base transition is accomplished with two 45° bends or a long sweep 90° bend while a short sweep 90° bend may be used if the following specified conditions are met: If the stack does not contain more than 3 water closets, does not exceed 10 m (33 ft), and the V1 connection clearance zone (Figure A1.2) can be maintained for at least 2 m (6.6 ft), a short sweep 90° bend may be used for the stack base transition. Stacks with a height greater than 8 levels are provided with two 45° bends separated by a 0.3 m (1 ft) diagonal segment of piping at the stack base transition.

DS 432 features an unvented stack configuration (stående ikke-udluftede ledninger), similar to the stub stack, which is not often utilized since connection clearance zones are not required. A DN 100 (4 inch) unvented stack is limited to a height of 6 m (20 ft).

5.4 Branches and stack connections

While System II in EN 12056-2 allows for a filling height of 70%, DS 432 specifies that this is only applicable under circumstances where both sanitary drainage and storm drainage utilize the same piping. Under circumstances where only sanitary drainage loading is applied, a maximum filling height of 50% permitted. According to Byggvägledning 10, horizontal branch drains may be up to 10 m (33 ft) in length before connecting into the stack. In DS 432, maximum length limitations only apply for branches with a water closet with a flush volume less than 6 L (1.6 gal), in an effort to limit blockages (H in Figure A1.9). For WCs flushing with less than 6 L (1.6 gal), a maximum length of 10 m (33 ft) is allowed for branches (koblingsledninger) with a minimum gradient of 4% whereas branches with a minimum gradient of 2% are limited to a maximum distance of 3 m (9.8 ft). This requirement is unique in comparison to other design standards in that the steeper gradient is associated with a greater maximum length allowance rather than a shorter maximum length. In DS 432, DN 50 (2 inch) drains normally have a vertical drop allowance (V in Figure A1.9) of 2 m (6.6 ft) whereas DN 100 (4 inch) drains have a vertical drop allowance of 6 m (19.7 ft). In Byggvägledning 10, a maximum vertical drop of 2 m (6.6 ft) is allowed between the fixture and stack for DN 50 (2 inch) drains whereas 4 m (13 ft) is allowed for both DN 80 (3 inch) and DN

100 (4 inch) drains (V in Figure A1.9). DN 80 (3 inches) is the minimum diameter for a branch carrying the drainage of a water closet in DS 432 while Byggvägledning 10 requires a minimum of DN 100 (4 inches).

5.5 Stack offsets

For stacks with a height greater than 10 m (33 ft) in DS 432, equivalent to 3 levels, a 1 m (3.3 ft) connection clearance zone must be maintained for V1 and V2 (Figure A1.2). Two 45° bends are also required for the horizontal-to-vertical transition. No clearances are required for H2 or V2, unless a 90° short sweep bend is used, which may not contain more than one water closet and must maintain a clearance for H2 and V2 of 1 m (3.2 ft). Unvented fixtures and branches may connect below the horizontal-to-vertical transition as well as the horizontal section upstream, provided the connection clearance zones are observed.

6 South Africa   Single stack

6.1 Regional context

SANS 10252-2 *Drainage installations for buildings* [29] is the code of practice for sanitary drainage systems in South Africa and features commentary and guidance for design and installation. The single stack is common in residential applications in South Africa. SANS 10252-2 limits the maximum pressure differential is 38 mm (1.5 inches) water gauge, equal to 372 Pa (1.5 inches of water column). A water seal of 75 mm (3 inches) is required at all fixtures except for water closets, which may have a minimum seal have 50 mm (2 inches). Fixture units are used to represent the maximum allowable loading for sanitary drainage piping. SANS 10252-2 also features an empirical equation and chart for converting fixture units into units of flow (L/min), though units of flow are not featured in any of the drainage sizing tables.

6.2 Peak loads and height limitations

The single stack design is prescriptive in SANS 10252-2 and provides a table indicating the maximum number of floors that may be served by a DN 100 (4 inch) and DN 150 (6 inch) single stack. A DN 100 (4 inch) stack may serve up to 10 floors of fixtures in residential applications. The maximum stack height, specified by the number of floors, is the limiting factor whereas the allowable loading for a DN 100 (4 inch) stack would otherwise be suitable for 61 floors of residential bathrooms. Increasing the diameter of the stack to DN 150 (6 inch) allows the stack to serve up to 30 floors.

6.3 Stack base

A horizontal connection clearance zone of 2.5 m (8.2 ft) must be maintained downstream of the stack base (H1 in Figure A1.2). The vertical connection clearance zone (V1 in

Figure A1.2) for a single stack extending up to 5 levels must be a minimum of 0.75 m (2.5 ft). For a single stack serving more than 5 stories in height, the fixtures on the lowest floor are required to discharge separately from the stack. It is recommended that stacks serving more than 20 floors maintain a clearance zone equal to two floors.

Two 45° bends are recommended at the vertical-to-horizontal transition of the stack base. In the case where a long sweep bend is used, the drain size must be a minimum of DN 150 (6 inches) to comply with a 0.3 m (1 ft) minimum radius requirement. In instances where the drainage load allows for a DN 100 (4 inch) stack but is increased to a DN 150 (6 inch) drain at the base to comply with the 0.3 m radius requirement, the horizontal drain may transition back to a DN 100 (4 inch) drain using an eccentric transition at a distance of 2.5 m (8.2 ft) downstream of the stack base (Figure A1.10).

The stub stack configuration (Figure A1.3) is typically used at the lowest floor. The South African stub stack is similar to the British stub stack with a few key differences. SANS 10252-2 allows up to two floors to discharge into a stub stack. A minimum of 0.45 m (1.5 ft) vertical distance between the WC and invert elevation of the horizontal portion of the drain is required in SANS 10252-2 (S2 in Figure A1.3). The fixture drain from a basin draining into a stub stack must not have a gradient greater than 4.4%, be longer than 3 m (9.8 ft), or have more than 2 bends with a radius of 75 mm (3 inches).

6.4 Branches and stack connections

Fixture drains connect independently to the stack unless they are of the same fixture type. Basin drains must be at least DN 40 (1.5 inch), though the trap may be DN 32 (1.25 inch). Horizontal drains from WCs must have a minimum gradient of 2.5% and a maximum of gradient of 25% whereas other fixture drain gradients must be a minimum of 2.2% and a maximum of 8.7%.

6.5 Stack offsets

SANS 10252-2 recommends avoiding offsets wherever possible. Where the horizontal-to-vertical transition occurs in a stack offset, a connection clearance must be maintained 0.45 m (1.5 ft) upstream on the horizontal drain (H2 in Figure A1.2) and 0.6 m (2 ft) below on the vertical stack (V2 in Figure A1.2). Fixtures may connect unvented into the horizontal drain between the clearance zones and below the V2 connection clearance zone.

7 People's Republic of China 伸顶通气

7.1 Regional context

The design and installation standards in the People's Republic of China are featured in GB 50015-2019 *Building Water Supply and Drainage Design Standard* [30], also known as the Jiànshuǐ (建水). Additional guidance and commentary are featured in the *Design Manual for Building Water Supply and Drainage* (设计手册建筑给水排水) [31] published by the China Architectural Design and Research Institute.

The single stack, known as extension ventilation (伸顶通气), is frequently utilized in China and is typical in residential buildings. The drainage stack capacity was originally based on flowing at 15% full, or 50% less than that of a stack flowing at 7/24th full, using the Wyly-Eaton Formula. Early investigations in 1973 in the Qiansanmen district in Beijing found pressures in the stack were occurring as high as 500 Pa (2 inches of water column), prompting the development of new methodologies for design [32]. Recommendations on single stack drainage design are continually updated in GB 50015 to reflect current research and testing. Current drainage load recommendations are informed by experimental test towers constructed to simulate transient airflow in drainage stacks, including an Shangxi Xuanshi Tower at over 60 m (197 ft) and the Vanke Tower at over 122 m (400 ft). The testing procedures for the drainage stacks are outlined in CJJ/T 245-2016 *Standard for capacity test of vertical pipe of the domestic residential drainage system* [33]. The test includes two procedures, one reflecting an instantaneous or 'burst flow' into the stack and the other reflecting a constant or steady flow. Washdown type and siphon type water closets were tested and the recommended standards were based on the siphon type water closet, due to having a greater instantaneous drainage flow during flushing. The constant flow method tests drainage flows with characteristics similar to the drainage from a shower, draining bathtub, or a basin. CJJ/T245-2016 states that the test results show that a negative pressure of 318 Pa (1.3 inches of water column) will result in a trap seal loss of 25 mm (1 inch) when using the instantaneous method.

Discharging multiple stacks to a single horizontal drain is uncommon in residential buildings. The horizontal drainage piping downstream of the stack and the drainage piping serving the lowest floor fixtures often discharge independently into an outdoor inspection chamber (Figure A1.5) before draining into DN 300 (12 inch) drainage piping around the perimeter of the building [34].

Vent covers are common at the atmospheric termination of the stack and provide protection against wind interference. One unique alternative to terminating the vent through the roof is the self-circulating stack configuration. This configuration returns the stack vent down to the horizontal drain downstream of the stack base. This is however not a typical approach and is only used in unusual circumstances. Air admittance valves are also generally not used.

7.2 Peak loads and height limitations

GB 50015 indicates the maximum drainage flow for each stack diameter. While the maximum drainage flow values were informed by tall testing towers, maximum stack heights are not specified. The drainage loading is calculated using an empirical square root equation (Equation B1.2). A DN 100 (4 inch) stack has a maximum drainage loading of 4.0 L/s (63 gpm), allowing a DN 100 (4 inch) stack to serve 23 levels of residential bathrooms. For bathrooms with a shower instead of a bathtub, this limit is equal to 33 levels of residential bathrooms. A DN 150 (6 inch) stack has a maximum drainage capacity of 6.4 L/s (101 gpm), allowing a loading equal to 97 residential bathrooms. DN 150 (6 inch) stacks are not often used due to the space requirements of the larger diameter piping. In the prior edition of GB 50015, the single stack was not recommended for residential buildings 10 stories or more in height. Updated values were introduced in the 2019 edition after testing [35] [36].

7.3 Stack base

The lowest floor fixtures may be installed without vent piping. Drainage connections may not be made within 1.5 m (5 ft) downstream of the stack base. The length between the furthest unvented fixture and the horizontal drain connection may not be greater than 12 m (40 ft). Additional limitations are given on the quantity of unvented fixtures in non-residential buildings that can be connected into the horizontal drain and must not exceed more than 5 water closets.

The connection clearance zone at the base of the stack is dependent on the number of floors served by the stack. Table 7.1 indicates the stack base clearance zones for various stack heights. Fixtures at the lowest floor may not connect to the stack if serving more than 13 levels. For stacks with a height between 7 and 12 floors, a connection clearance of 1.2 m (3.9 ft) must be maintained above the stack base. Stacks less than 4 floors in height must maintain a connection clearance zone of 0.45 m (1.5 ft). GB 50015 also provides clearance zone requirements for stacks with secondary ventilation, which are much less than those provided for the single stack. If the clearances cannot be met or if there is a 90° bend within 1.5 m (4.9 ft) measured horizontally from the stack base, the lowest level is required to discharge separately to an inspection chamber. The *Design Manual for Building Water Supply and Drainage* recommends using two 45° bends at the stack base or using a single 90° long sweep bend as an alternative.

Table 7.1 – Minimum vertical clearance between

the stack base and lowest branch into the stack

Floors served by stack	Vertical connection clearance zone
	Extension ventilation
≤ 4	0.45 m (1.5 ft)
5 - 6	0.75 (2.5 ft)
7 – 12	1.20 (3.9 ft)
13 – 19	Lowest floor separate
>20	from drainage stack

Note: Refer to V1 in Figure A1.2

Another configuration for fixtures at the lowest floor is the bypass vent (Figure A1.6) for the group of fixtures at the lowest floor. The connects into the drainage stack with a wye branch fitting at least 2 m (6.6 ft) above the stack base (V1 in Figure A1.2). This bypass vent configuration is limited to use in residential buildings at the lowest floor.

7.4 Branches and stack connections

A swept branch connection to the stack is recommended over a wye branch connection. S-trap configurations from basins are acceptable. The minimum diameter of the drain from the WC is DN 100 (4 inches). DN 100 (4 inch) drainage branches have a minimum gradient of 1% but are typically installed at gradients equal to or greater than 2%. The intended peak filling height for drainage branches is 50%. There are no maximum length recommendations for drainage branches between the furthest fixture and the stack.

7.5 Stack offsets

Where a stack offset occurs, unvented drainage connections may be made below the horizontal-to-vertical transition provided a clearance zone of at least 0.6 m (2 ft) is maintained (V2 in Figure A1.2). No clearance zone is indicated for the horizontal-to-vertical transition (H2 in Figure A1.2).

8 Japan   伸頂通気

8.1 Regional context

SHASE-S 206-2019 *Plumbing Code* [37] is the plumbing standard used in Japan and published by The Society of Heating, Air-Conditioning and Sanitary Engineers of Japan. Additional design specifications for the single stack, known as extension ventilation（伸頂通気），are included in SHASE-S 218-2021 [38]. SHASE-S 206 was originally published as HASS 206-1967, which used a translation of the 1955 *American Standard National Plumbing Code* ASA-A40.8 [39] as a foundation. Subsequent editions included

updates based on national research and testing efforts to improve the standard. Single stack method was first published in the 1982 edition of HASS 206.

Special drainage stack branch fittings（特殊継手）are common for stacks in tall buildings that would otherwise not be suitable as a single stack using standard drainage fittings. A minimum water seal of 50 mm (2 inches) is required for traps along with a maximum pressure differential of ±400 Pa (1.6 inches of water column). SHASE-S 218-2021 indicates a correlation of -410 Pa (1.65 inches of water column) with a water seal loss of 25 mm (1 inch), equal to the maximum allowable water seal loss. Vent covers are common at the atmospheric termination, which add additional airflow resistance but limit the influence of wind on the trap seals. DN 80 (3 inch) stacks with an auxiliary vent stack are historically common for stacks serving restrooms in residential buildings up to 14 floors [40]. Single stack drainage flow is based on a cross-sectional filling area of 18%. Guidance is provided in SHASE standards to ensure that pressures do not exceed ±250 Pa (1 inch of water column) for stack discharges and ±100 Pa (0.4 inches if water column) for drainage branch discharges. A maximum filling height of 50% is recommended for the horizontal drainage piping downstream the stack base where the single stack configuration is used to ensure adequate airflow.

8.2 Peak loads and height limitations

The 1991 edition of SHASE-S 206 limited the maximum height of the single stack to 30 m (98 ft). Investigations revealed that taller stacks could still provide adequate performance and this restriction was removed in the 2000 edition provided that the design could be proved by testing [37]. SHASE-S218-2021 provides direction validated by testing for stacks with more than 10 levels. Empirical equations are provided based on the branch connection type indicating the reduction factor to be applied to the standard maximum drainage flows to account for the increased airflow in stacks. Drainage flow reduction factors are only required for stacks with a height above 10 floors.

Equation 8.1

$$y = 3.18x^{-0.52}$$

Equation 8.2

$$Q_{pm} = yQ_p$$

y = increase/decrease rate value

x = story number, one story approximately 3 m (9.8 ft)

Q_p = Allowable design flow rate value (L/s)

Q_{pm} = Allowable design flow rate value in consideration of increase/decrease rate (L/s)

For example, a DN 100 (4 inch) single stack is given a maximum drainage flow of 3.88 L/s (61 gpm). Using the equation for a swept branch connection (Equations 8.1 and 8.2), a stack serving 19 floors will require a reduction factor of y =0.69, reducing the maximum

drainage flow to 2.67 L/s (42 gpm), a flow with the drainage capacity for 19 residential bathrooms. A DN 150 (6 inch) single stack has a maximum flow of 11.4 L/s (181 gpm), allowing for 43 floors of residential units after applying the 0.521 reduction factor.

8.3 Stack base

The lowest floor fixtures are prohibited from connecting to the stack except where testing can prove the system will not result in the blowout of traps due to positive pressure. Fixtures may connect downstream of the stack base provided a connection clearance zone of 3 m (9.8 ft) is maintained (H1 in Figure A1.2). The horizontal drainage piping downstream of the stack base must continue straight for 3 m (9.8 ft) without bends to minimize hydraulic closure. Additional commentary is provided in SHASE-S 206 recommending a clearance zone of at least 10 m (33 ft) based on testing but acknowledges the impracticality of the additional horizontal piping required for compliance, deferring back to the 3 m (9.8 ft) clearance zone with a reasonable level of safety from water seal blowout from positive pressure.

8.4 Branches and stack connections

SHASE-S 206 suggests that the single stack configuration is best suited to applications where fixtures are in close proximity to the stack. Both swept branch fittings and wye branch fittings and are used for stack connections.

8.5 Stack offsets

Offsets are generally not permitted for single stacks unless vent piping is provided for the offset section or if there is minimal flow in the stack.

9 Singapore Single stack

9.1 Regional Context

Code of Practice on Sewerage and Sanitary Works (COPSSW) [41] is the national drainage standard in Singapore and is published by the National Water Agency (PUB). Most fixtures are required to discharge to a common trap from a floor drain (floor trap). These drainage connections occur in the vertical segment between the floor drain and the trap. The common trap has a minimum diameter of DN 100 (4 inches) with a minimum water seal of 50 mm (2 inches). Basins, showers, bathtubs, washing machines, and dishwashers discharge to common traps whereas kitchen sinks, urinals, and WC discharge to drainage piping connecting to the stack. A trap is still required at basins despite discharging into a common trap.

9.2 Peak loads and height limitations

The design approach for the single stack in COPSSW is comparatively prescriptive and limited in height by the number of floors served. DN 100 (4 inch) diameter stacks may be used only up to 4 floors, with the lowest floor connecting downstream of the stack base. DN 150 (6 inch) single stacks may serve up to 6 levels of residential bathrooms. Additional vent piping must be provided where installations cannot meet these requirements. Drainage flow is determined using the methodology outlined in EN 12056-2.

9.3 Stack base

Fixtures at the lowest floor are prohibited from connecting to the drainage stack. Both the horizontal drain downstream of the stack base and the drains from lowest floor fixtures discharge separately into an inspection chamber (Figure A1.5). The inspection chamber is provided with DN 100 (4 inch) vent piping and is vented to the atmosphere. The stack base transition is made using two 45° bends, separated by a diagonal segment with a length equal to 2 times the diameter of the stack e.g. 0.2 m (0.7 ft) for a DN 100 (4 inches).

9.4 Branches and stack connections

The maximum distance measured horizontally from the drainage stack is 2.5 m (8.2 ft). Swept branches or wye branches are suitable fittings for drainage stack connections. S-trap configurations are acceptable.

9.5 Vertical stack offsets

Vertical stack offsets are prohibited for single-stack configurations.

10 Australia & New Zealand　　Single stack

10.1 Regional context

AS/NZS 3500.2 *Plumbing and drainage Part 2: Sanitary plumbing and drainage* [42] is the standard used in Australia and New Zealand for the design and installation of sanitary drainage systems. Single stack configurations are not often used in residential applications in Australia and New Zealand though the configuration is available as an option within AS/NZS 3500.2. Sanitary drainage systems are designed to maintain a pressure differential within 375 Pa (1.5 inches of water column) of atmospheric pressure. Both P-traps and S-traps are common trap types at basins and washdown type water closets are used. The fixture unit methodology is used for estimating drainage load and determining drain diameter selections.

10.2 Peak loads and height limitations

A prescriptive approach is taken to the design of single stacks in AS/NZS 3500.2 and limitations are specified on the stack height, based on the number of floors served. For residential applications, DN 100 (4 inch) stacks are limited to 10 floors and DN 150 (6 inch) stacks are limited to 30 floors. The drainage loading allows for the equivalent of 43 residential bathrooms on a DN 100 (4 inch) stack and 130 residential bathrooms on a DN 150 (6 inch) stack.

10.3 Stack base

A connection clearance zone must be maintained at a minimum height of 0.6 m (2 ft) above the stack base (V1 in Figure A1.2). For stacks extending more than 5 floors in height, the clearance zone must be a minimum of 1 m (3.3 ft). For any stack where there is risk of excessive foaming of soap discharges from fixtures, the connection clearance zone must be a minimum of 2.5 m (8.2 ft). For stacks with 3 levels or more of fixtures, a 2.5 m (8.2 ft) clearance must be maintained downstream of the stack base (H1 in Figure A1.2). Stacks extending two stories or less must maintain a clearance zone of 0.5 m (1.6 ft) downstream of the stack base. Fixtures at the lowest floor may connect unvented into the horizontal drain downstream of the stack base, provided the connection clearance zones are observed.

The vertical to horizontal transition at the stack base is made with two 45° bends and a diagonal segment between the bends equal to twice the diameter of the horizontal drain in length (e.g. 200 mm (8 inches) for a DN 100 (4 inch) drain. A single 90° long sweep bend may be used alternatively provided the radius is at least 0.225 m (0.73 ft) for a DN 100 (4 inch) stack or smaller and at least 0.3 m (1 ft) for stacks larger than DN 100 (4 inches).

10.4 Branches and stack connections

Fixture drains connect either directly to the stack or through the common trap (4 way riser) of a floor drain (floor waste gully) without combining into a drainage branch. A shower or bathtub may omit a fixture trap if draining to a common trap within a length of 1.2 m (3.9 ft) from the fixture. A fixture trap is required at basins whether connecting into the drainage stack or a common trap. The length of drainage piping between a fixture trap and a common trap or stack must not exceed 2.5 m (8.2 ft) (H in Figure A1.9). Water closets may be installed up to 6 m (19.7 ft) from the stack if a DN 100 (4 inch) fixture drain is used, whereas water closets with a DN 80 (3 inch) fixture drain must be within the 2.5 m (8.2 ft) length requirement. The fixture drain from water closets must be installed at a gradient between 1.65% and 5% whereas the fixture drain from other fixtures must be installed at a gradient at least 2.5% to 5%. The maximum vertical drop from the fixture outlet must be within 1.5 m (4.9 ft) for basins and 2.5 m (8.2 ft) for other fixtures (V in Figure A1.9).

10.5 Stack offsets

Stack offsets must be separated by at least 2 m (6.6 ft) measured horizontally. A 0.9 m (3 ft) connection clearance zone is required above the stack base (V1 in Figure A1.2) or 2.5 m (8.2 ft) where foaming from soap is likely to occur and a 2.5 m (8.2 ft) connection clearance zone is required downstream of the stack base. For stacks with an offset, the total stack height may not exceed 10 levels and a maximum of 5 levels may be located above the stack offset. Only one offset may occur in the stack. The connection clearance zones for the horizontal-to-vertical transition are 0.45 m (1.5 ft) upstream (H2 in Figure A1.2) and 0.6 m (2 ft) downstream (V2 in Figure A1.2). Diagonal stack offsets at an angle of 45° or steeper require 0.6 m (2 ft) connection clearance zones above and below the offset for stacks up to 10 floors while stacks 5 floors or less may reduce the upper clearance zone to 0.45 m (1.5 ft).

11 Brazil   Ventilação Primária

11.1 Regional context

The single stack (ventilação primária) is not often utilized in Brazil, instead favoring drainage stacks with an auxiliary vent stack and at least one fixture trap being vented in group of fixtures. NBR 8160 *Building sanitary sewage systems -design and installation* [43] is the national design standard used in Brazil and features two methodologies for calculating drainage flow. The drainage fixture unit methodology is utilized with many of the loading values republished from the 1955 *American Standard National Plumbing Code ASA A40.8*. The Hydraulic Method (Método Hidráulico) is featured in NBR 8160 as an alternate approach which allows the time interval between use of fixtures and drainage duration to be independently selected for predicting peak drainage loads with binomial distribution tables. The design loading criteria for the single stack design methodology is based on the Hydraulic Method and is distinct from the prescriptive approaches used by many other design standards in that the approach is performance based. Limited guidance is provided in NBR 8160 on appropriate statistical values to use. The values used for comparison here are based on values in the 2016 study [44] at the Federal University of Rio Grande do Sul comparing the Unidades de Hunter approach with Método Hidráulico[4].

The single stack design methodology is outlined in Annex C of NBR 8160 and features a series of formulas which are used to assess the sufficiency of the drainage stack to balance pressure differentials. This methodology was first introduced by Moacyr Graça at Polytechnic School of the University of São Paulo in 1985. Graça's method introduces empirical formulas and coefficients generalized for design purposes. This methodology accounts for stack height, peak drainage flow, wind speed, outdoor air temperature, thermal drawing of air into the stack, water seal evaporation, type of branch connections,

---

[4]Assuming a drainage duration of 10 seconds for a WC, 30 seconds for a basin, and 500 seconds for a bathtub with 60 minutes between uses and a failure rate of 1%

trap types, airflow pressure losses in the stack, stack length, vent length and various other factors. The minimum allowable trap seal depth in NBR 8160 is 50 mm (2 inches).

11.2 Peak loads and height limitations

To ensure no more than 25 mm (1 inch) of water seal is lost due to negative stack pressure, equations in Annex C indicate that negative pressure must be kept below 485 Pa (1.9 inches of water column) and positive pressure be kept below 970 Pa (3.9 inches of water column). Taking these considerations into account, a DN 100 (4 inch) may carry the drainage of 14 residential bathrooms, equal to a drainage flow of 5.61 L/s (89 gpm), resulting in an airflow of 40 L/s (102 cfm). A DN 150 (6 inch) may carry the drainage of 25 levels of residential restrooms, equal to a drainage flow of 8.46 L/s (134 gpm) resulting in an airflow of 97 L/s (247 cfm).

11.3 Stack base

For installations where foaming from soap may occur, a connection clearance zone (Zonas de sobrepressão) must be maintained within 40 diameters above the stack base and 10 diameters downstream. For a DN 100 stack (4 inches), this is equivalent to a length of 4 m (13.3 ft) upstream of the stack base (V1 in Figure A1.2) and 1 m (3.3 ft) downstream (H1 in Figure A1.2).

11.4 Branches and stack connections

No limits are specified for the length of drainage branches between the fixtures and the stacks. Fixtures within the bathroom, with the exception of the WC, typically discharge directly into a common trap (caixa sifonada) rather than having independent traps at each fixture. The common trap usually features a grate at the top and also serves as a floor drain. Connections to the stack are often made with non-orthogonally placed horizontal piping to limit the amount of bends.

11.5 Stack offsets

No guidance is given with respect to stack offsets in Annex C.

12 United States   Single stack vent, Philadelphia single stack

12.1 Regional Context

Architect J. Pickering Putnam introduced the concept of a drainage stack with unvented fixture drains and branches at the AIA Convention in San Francisco in 1911 [45]. This configuration is installed in many buildings throughout Boston and Philadelphia built in

the early 20th century and remains a common method used in Philadelphia today. Detailed sizing guidance was introduced for the single stack in the 1961 Philadelphia Plumbing Code (PPC) [46], specifying height and drainage loading limits using the Drainage Fixture Unit method developed by Roy B. Hunter of the National Bureau of Standards. Design guidance remains substantially similar in the 2018 edition [47]. A variation of the Philadelphia single stack is also featured in the International Plumbing Code (IPC) [48] and the Uniform Plumbing Code (UPC) as the single stack vent system [49]. Fixture traps must be protected from pressure differentials exceeding 25 mm (1 inch) water column, equal to 250 Pa in the IPC, UPC and PPC. Siphonic type water closets represent a majority of water closet installations in the US and P-traps are the most common trap type at fixtures. S-traps are generally prohibited except in single stack installations.

Building traps are typically required in the PPC, effectively isolating pressure systems of the building drainage system from the sewer system. A vent is required at the upstream side of the trap for buildings 22 m (75 ft) in height or greater. The vent for the building trap must be at least DN 100 (4 inches). The UPC lists the single stack in the Appendix C, subjecting usage to discretionary approval in regions that have adopted UPC as the plumbing code.

12.2 Peak loads and height limitations

The single stack described in US plumbing codes indicate maximum drainage loads, measured in drainage fixture units (DFU), and stack height. Maximum DFU for various stack diameters and stack heights are indicated in a table featured in all three codes. Due loading limitations for DN 100 (4 inch) stacks above 23 m (75 ft), the single stack is effectively limited to serving 7 floors of residential bathrooms. DN 150 (6 inch) stacks greater than 23 m (75 ft) are practically limited only by the maximum DFU value indicated in a sizing table, allowing a stack to serve up to 45 floors of residential bathrooms. For stacks over 30 stories in height, velocity breakers, consisting of four 45° bends, are required along the drainage stack. Velocity breakers must be installed at intervals of 10 floors.

There is a general requirement to provide an auxiliary vent stack for stacks above 5 stories in the IPC and for stacks above 10 stories in the UPC, with no exception noted when utilizing the single stack drainage system, despite noting an exception for another drainage stack configuration in the IPC[5]. This may have been an unintentional omission in the IPC and UPC codes given the single stack in the PPC only requires a vent stack in instances where separate fixture venting is already required, and the stack is greater than 5 stories[6]. There is however disagreement on the verbiage regarding auxiliary vent stack requirements in the PPC leading some to interpret the requirement to apply to all stacks above 5 stories and not limited to stacks with fixtures that already have vent piping.

---

[5] Section 904.2, 2021 International Plumbing Code
[6] Section P-919.3.4, 2018 Philadelphia Plumbing Code

12.3 Stack base

A vertical clearance zone (V1 in Figure A1.2) at the stack base is not required for the single stack in the PPC and the lowest floor is typically connected to the drainage stack. In the IPC and UPC, stacks serving 3 or more floors must separate the lower two floors from the stack and connect at least 10 diameters downstream of the stack base (e.g. 1 m (3.3 ft) for a DN 100 (4 inch) stack). This requirement effectively limits the single stack to serving 2 floors, since the lower stack will require a stack vent which must have an atmospheric termination to the exterior, usually at the roof level. This requirement is revised in the 2024 UPC and allows a bypass vent for the lowest floor fixtures. Also included in the revision was the allowance of fixtures on the second level above the stack base to connect into the drainage stack, provided the stack is not greater than 22 m (75 ft) in height.

A single 90° long sweep bend is typically installed at the stack base while short sweep bends are also sometimes used. Two 45° bends are also used but are less common and not required. Records from City of Philadelphia indicate that two 45° bend-fittings were recommended at the stack base, however, this requirement was not explicitly stated in the historic or current PPC.

12.4 Branches and stack connections

Custom manifold branch fittings, known as Merion fittings and feature multiple inlets in one branch fitting, have traditionally been used with single stack installations in Philadelphia, though standard swept branch fittings and wye branch fittings are most common in current installations. Water closets must be installed within a horizontal length of 2.4 m (8 ft) from the drainage stack while other fixtures may be up to 3.7 m (12 ft) from the drainage stack. The S-trap is permitted in the Philadelphia single stack while the IPC and UPC version requires S-trap fixture drains with diameters less than DN 50 (2 inches) to increase in size at the vertical segment (V in Figure A1.9) to a minimum of DN 50 (2 inches), in an effort to reduce siphonage.

12.5 Stack offsets

Unvented fixtures may not connect downstream or below stack offsets for single stacks serving more than 3 floors.

13 Review

13.1   Peak loads and height limitations

DN 100 (4 inch) single stacks are not often recommended for buildings receiving the drainage from more than 20 stories. The maximum recommended height ranges from 4 floors in COPSSW (Singapore) to 21 floors in NTR 3216 (Netherlands) with most other

standards recommending limits between this range or featuring little guidance on the subject of stack height. The methods NTR 3216 and SHASE-S 218 (Japan) allow a DN 150 (6 inch) stack to serve 38 and 43 stories of residential bathrooms respectively while SANS 10252-2 and AS/NZS 3500.2 establish a prescriptive limit of 30 stories. Many other design standards and guides recommend either much shorter heights or recommend drainage loadings well beyond what would typically be considered acceptable if applied to a tall residential building serving one bathroom per floor.

Maximum allowable pressure differentials tend to fall between 250 Pa (1 inch of water column) to 400 Pa (1.6 inches of water column). A majority of the standards and recommendations reviewed here specify a water seal loss not to exceed 25 mm (1 inch) as a basis for performance of siphonage protection. There is disagreement between the reviewed standards on the pressure differentials associated with the loss of various trap seal heights. The precision of these specified values may not carry significance given that pressure differential testing is rarely conducted at the completion of new drainage installations in buildings and the actual failure rates are not well established.

13.2   Stack base

A variety of methods are used to protect the fixtures at the lowest floor from the pressure conditions near the stack base. An unvented stack may serve the lowest floor or lowest two floors of fixtures while a bypass vent connecting into the drainage stack from the group of fixtures is also a suitable configuration. Other methods consist of connecting unvented drains downstream of the stack base connection clearance zone. Providing a separate network of drainage piping serving only the lowest floor is also a strategy used. Some standards such as the Philadelphia Plumbing Code and DS 432 and Byggvägledning 10 allow connections near the base of the stack.

The characteristics of the stack base transition account for significant pressure differentials and are addressed with special restrictions in various standards. Some standards limit the allowable stack height when a single long sweep bend is used instead of two 45° bends separated with a short distance of piping. A majority of standards reviewed here recommend two 45° bends over a single 90° bend, with the US codes being an exception.

13.3   Branches and stack connections

Some standards such as BS EN 12056-2, AS/NZS 3500.2 and SANS 10252-2 generally recommend fixture drains connect independently to the drainage stack whereas other standards allow fixture drains to discharge into a drainage branch connecting into the drainage stack. A majority of standards allow the S-trap configuration from the basin while some such as BS EN 12056-2 require the fixture drain to connect horizontally to the stack without any vertical segments downstream of the trap. Many standards indicate

a maximum horizontal or vertical distance between the fixtures and stacks whereas others do not. Preferred stack connection fitting type vary depending on region.

13.4   Stack offsets

Many methods prohibit unvented connections at or below stack offsets or do not provide clear direction on accommodating pressure conditions, while some such as DIN 1986-100, NEN 3215, and SANS 10252-2 provide extensive detail on the subject of stack offsets.

13.5 Summary

While the recommendations provided in design standards do not provide conclusive insight into the complex interactions of airflow and drainage flow in single stack configurations, a review of various recommendations may stimulate discussion regarding existing guidance and support further research and testing procedures. Applying the principles of fluid mechanics to single stack design guidance remains a challenging undertaking but significant opportunities remain for optimization and improved performance.

References

[1] M. Gormley, "Myths and Legends: Developments towards modern sanitary engineering," in *CIB W062 International Symposium for Water Supply and Drainage for Buildings*, Brno, Czech Republic, 2007.

[2] A. F. E. Wise, "One-Pipe (Single Stack) Plumbing for Housing: (Part I)," Building Research Station Digest, London, 1952.

[3] A. F. E. Wise, "One-Pipe (Single Stack) Plumbing for Housing: Part II - Principles of Design," Building Research Station Digest, London, 1952.

[4]   M. S. T. Lillywhite and A. F. E. Wise, "Towards a general method for the design of drainage systems in large buildings," *Journal of the Institution of Public Health Engineers,* vol. Volume 68, no. no. 4, pp. 239-270, 1969.

[5]   BS EN 12056-2 - Gravity Drainage systems inside buildings, British Standards Institute, 2000.

[6]   R. Hanslin, "Toward a European harmonised code of practice for drainage installations inside buildings," in *CIB W062 International Symposium for Water Supply and Drainage for Buildings*, Brussels, 1991.

[7]   K. De Cuyper, "Toward a standardised code of practice for the drainage systems inside European buildings," in *CIB W062 International Symposium for Water Supply and Drainage for Buildings*, Porto, 1993.

[8]   J. Swaffield, Transient Airflow in Building Drainage Systems, London: Spon Press, 2010.

[9]   P. White, "Filling the gap in guidance on drainage in residential high-rise," 7 July 2008. [Online]. Available: https://www.building.co.uk/filling-the-gap-in-guidance-on-drainage-in-residential-high-rise/.

[10] J. French and H. Eaton, "Self-siphonage of Fixture Traps," National Bureau of Standards, Washington, D.C., 1951.

[11] J. A. Swaffield and A. F. E. Wise, Water, Sanitary and Waste Services for Buildings, 5th Edition, London: Routledge, 2002.

[12] Approved Document H - Drainage and waste disposal, London: The Building Regulations, 2010.

[13] Guide G - Public Health and Plumbing Engineering, London: The Chartered Institution of Building Services Engineers, 2014.

[14] Plumbing Engineering Design Services Design Guide, Hornchurch: Chartered Institute of Plumbing and Heating Engineering, 2002.

[15] BS 5572 - Code of practice for sanitary pipework, London: BSI, 1994.

[16] J. Daureeawo, "Performance Testing of Drainage Systems & Components," Vortex, London, 2020.

[17] J. Lansing, "A Comparison of British and American Plumbing Engineering Standards and Practices," World Plumbing Council, Zurich, 2020.

[18] DIN 1986-100 Entwässerungsanlagen für Gebäude und Grundstücke - Part 100: Provisions in conjunction with DIN EN 752 and DIN EN 12056, Berlin: Beuth Verlag, 2016.

[19] Gebäude- und Grundstücksentwässerung, Berlin: Beuth Verlag, 2016.

[20] DIN 1986 - Bau und Betrieb von Grundstücksentwässerungsanlagen, Berlin: Beuth-Verlag, 1928.

[21] Technische Vorschriften für den Bau und Betrieb von Grundstücksentwässerungsanlagen, Berlin: Beuth-Verlag, 1932.

[22] Technische Vorschriften für den Bau und Betrieb von Grundstücksentwässerungsanlagen, Berlin: Beuth-Vertrieb, 1942.

[23] R. S. Wyly and H. N. Eaton, "Capacity of stacks in sanitary drainage systems for buildings, Monograph 31," National Bureau of Standards, Washington, D.C., 1961.

[24] NEN 3215 - Drainage system inside and outside buildings, Delft: Nederlands Normalisatie Instituut, 2018.

[25] NTR 3216 Riolering van bouwwerken, Rotterdam: ISSO, 2019.

[26] N. Post, "Wijzigingen in NEN 3215 en NTR 3216," *TVVL Magazine,* pp. 30-33, 2019.

[27] "DS 432:2020 Wastewater Installations," Dansk Standard, Nordhavn, Denmark, 2020.

[28] Byggvägledning 10, Vatten och avlopp, Stockholm, Sweden: Svensk Byggtjänst, 2018.

[29] SANS 10252-2 Water supply and drainage for buildings Part 2: Drainage installations for buildings, Pretoria: The South African Bureau of Standards, 1993.

[30] GB 50015-2019 Standard for design of building water supply and drainage, Beijing: China Planning Press, 2019.

[31] Design Manual for Building Water Supply and Drainage, Beijing: China Architecture Design & Building Press, 2019.

[32] Z. Shiming, "Factors influencing stack capacities in single stack system," CIB W062 International Symposium for Water Supply and Drainage for Buildings, Yokohama, 1997.

[33] CJJ/T245-2016, Beijing: China Building Industry Press, 2016.

[34] H. Xiè, "Study on the American Building Water Supply and Drainage Design," *Building Water and Wastewater Engineering,* vol. 10, no. 4, pp. 41-47, 2022.

[35] J. Zhang, "建筑给水排水设计标准热点问题研讨," *Water Field,* vol. 6, no. 156, pp. 36-44, 2020.

[36] J. Zou and Q. Xie, "About the standard for design of building water supply and drainage(version 2019) - Discussion on the design of drainage system," *Building Water and Wastewater Engineering,* vol. 8, no. 4, pp. 87-91, 2019.

[37] SHASE-S 206-2019 Plumbing Code, Tokyo: The Society of Heating, Air-Conditioning and Sanitary Engineers of Japan, 2019.

[38] SHASE-S 218-2021 Testing Methods of Flow Capacity for Drainage Stack System, Tokyo, Japan: The Society of Heating, Air-Conditioning and Sanitary Engineers of Japan, 2021.

[39] ASA A40.8-1955 American Standard National Plumbing Code, New York City: American Society of, 1955.

[40] T. Abe, M. Otsuka, M. Itabashi and N. Ono, "Proposal of Drainage Performance Upgrading Method for Domestic Wastewater Drainage Stack Systems for High-Rise Apartment Housing Stocks," in *CIB W062 International Symposium for Water Supply and Drainage for Buildings*, Taichung, 2022.

[41] Code of Practice on Sewerage and Sanitary Works, Singapore: PUB, 2019.

[42] AS/NZS 3500.2:2021 Plumbing and drainage Part 2: sanitary plumbing and drainage, Standards New Zealand, Standards Australia, 2021.

[43] NBR 8160, Rio de Janeiro: Associação Brasileira de Normas Técnicas, Sistemas prediais de esgoto sanitário - Projeto e execução.

[44] D. S. Feloniuk, "Sistemas prediais de esgoto sanitário: estudo comparativo de dimensionamento pelos métodos hidráulico e das unidades de hunter de contribuição," Departamento de Engenharia Civil da Escola de Engenharia da Universidade Federal do Rio Grande do Sul, Porto Alegre, 2016.

[45] J. P. Putnam, Plumbing and household sanitation, Garden City: Doubleday, Page &, 1911.

[46] Rules and Regulations Relative to the Construction of Plumbing or House Drainage in the City of Philadelphia, Philadelphia: City of Philadelphia, 1961.

[47] Philadelphia Plumbing Code 2018, Country Club Hills: International Code Council, 2018.

[48] 2021 International Plumbing Code, Country Club Hills: International Code Council, 2020.

[49] 2021 Uniform Plumbing Code, Ontario: International Association of Plumbing and Mechanical Officials, 2020.
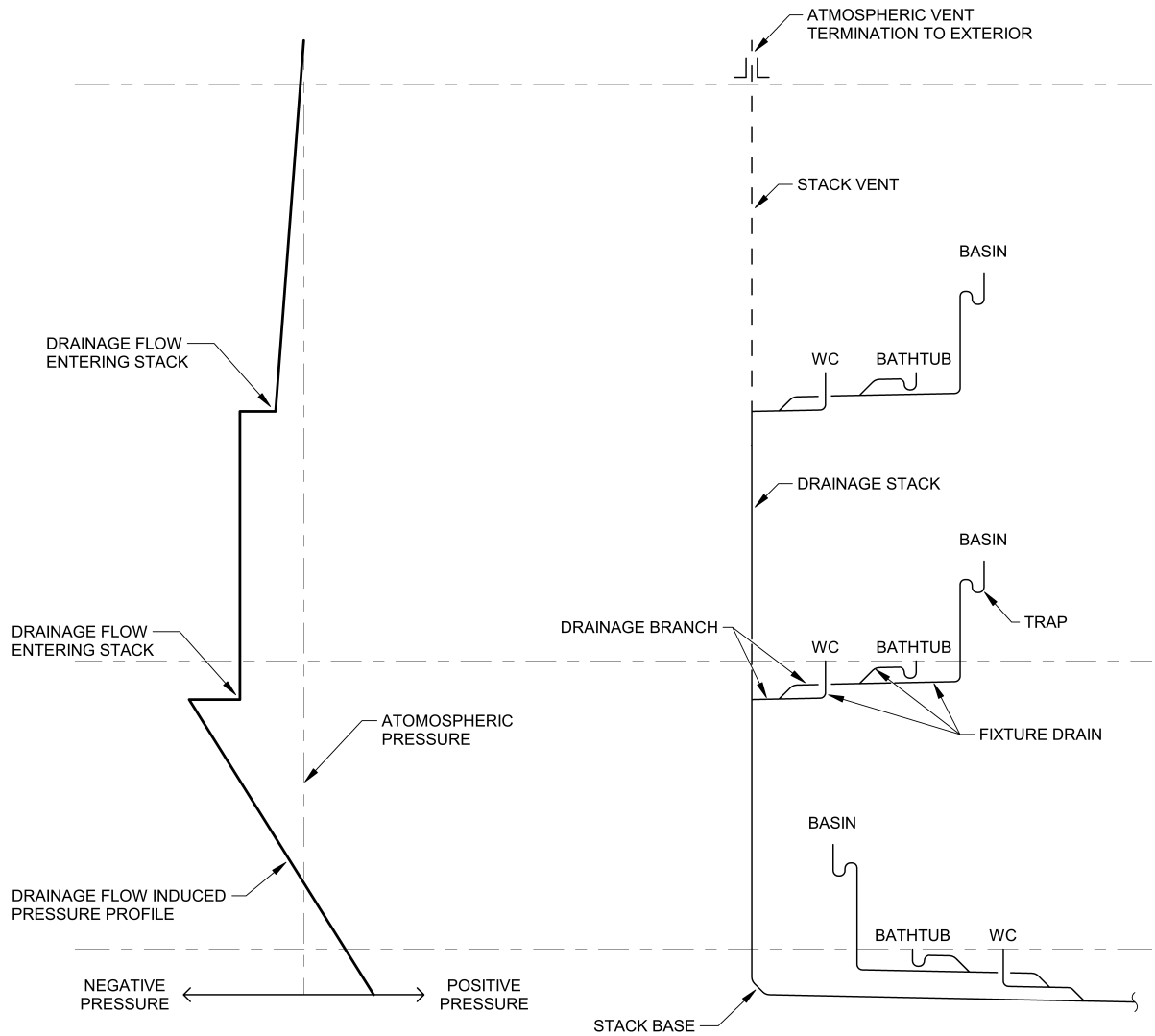
Appendix A – Supporting Figures

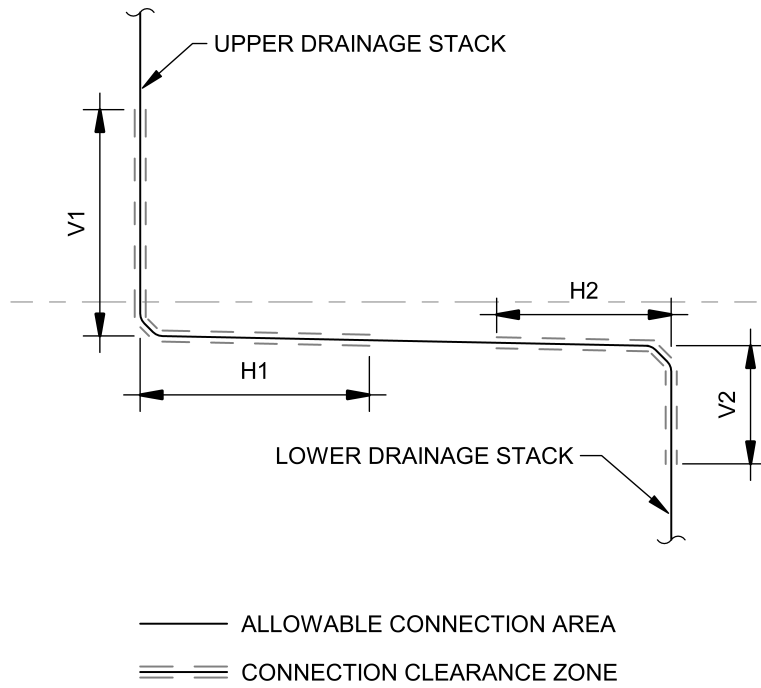**Figure A1.1 – Example of a single stack configuration and pressure profile**

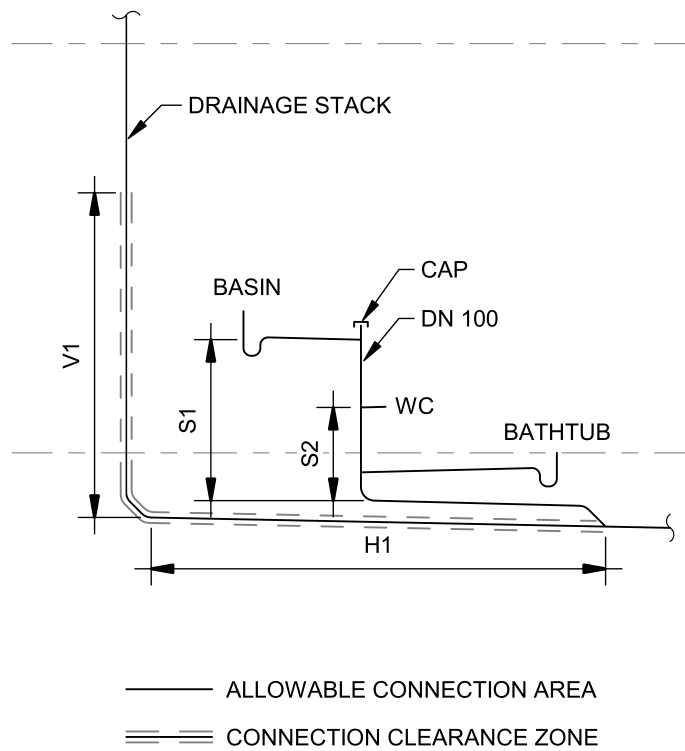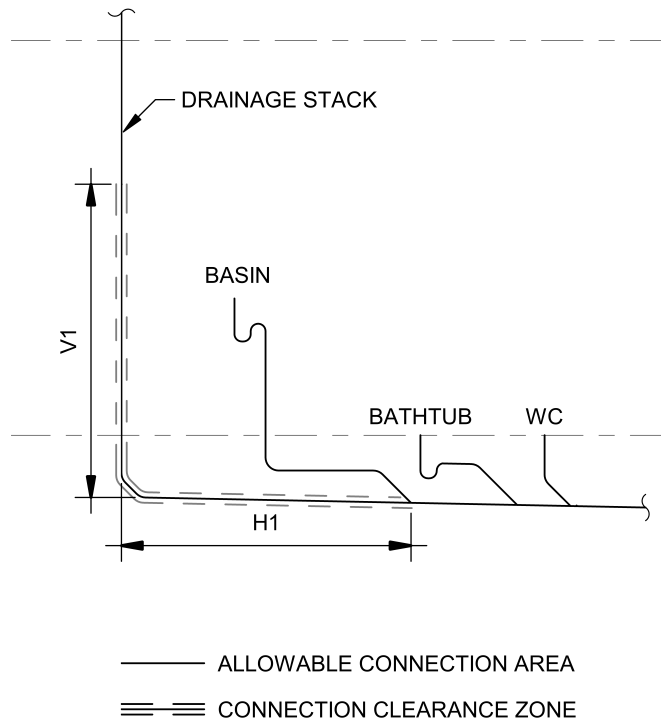**Figure A1.2 – Drainage stack connection clearance zones**

Figure A1.3 – Stub stack
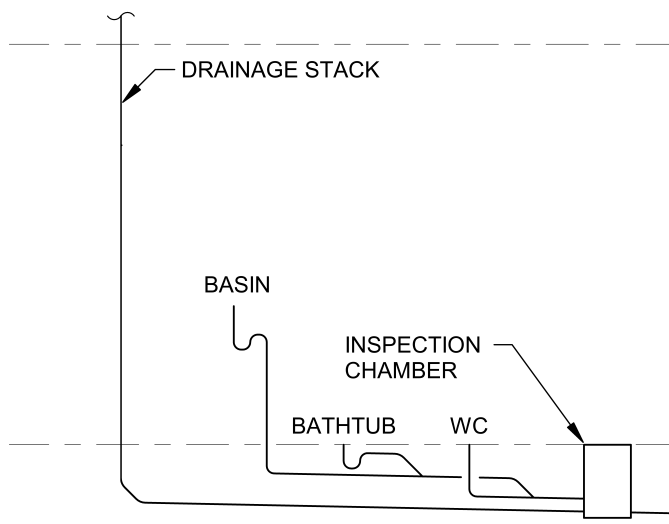
Figure A1.4 – Unvented fixtures at lowest floor

Figure A1.5 – Inspection chamber for lowest floor fixtures

DRAINAGE STACK

VENT FROM DRAINAGE PIPING
SERVING LOWEST FLOOR

VENT CONNECTION INTO
DRAINAGE STACK USING WYE

BASIN

V1

BATHTUB   WC

H1

——————— ALLOWABLE CONNECTION AREA
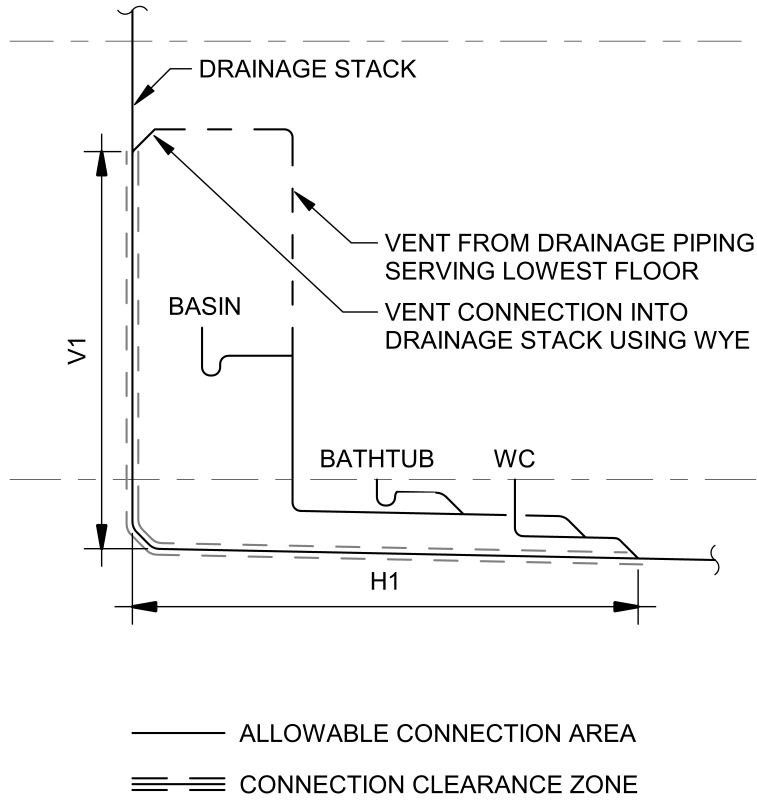
≡≡ ≡≡ CONNECTION CLEARANCE ZONE
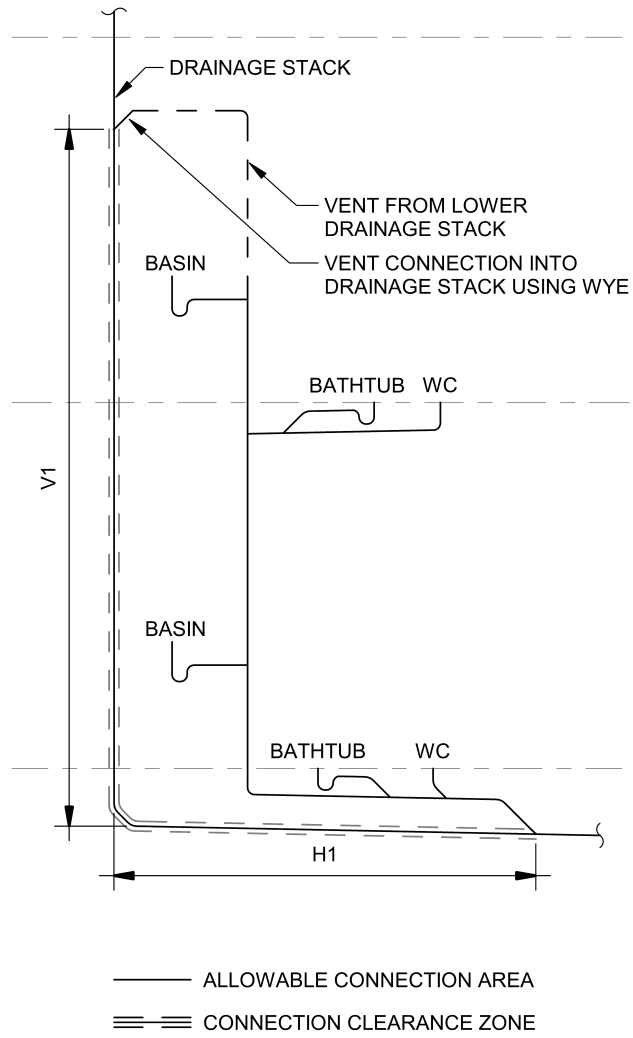
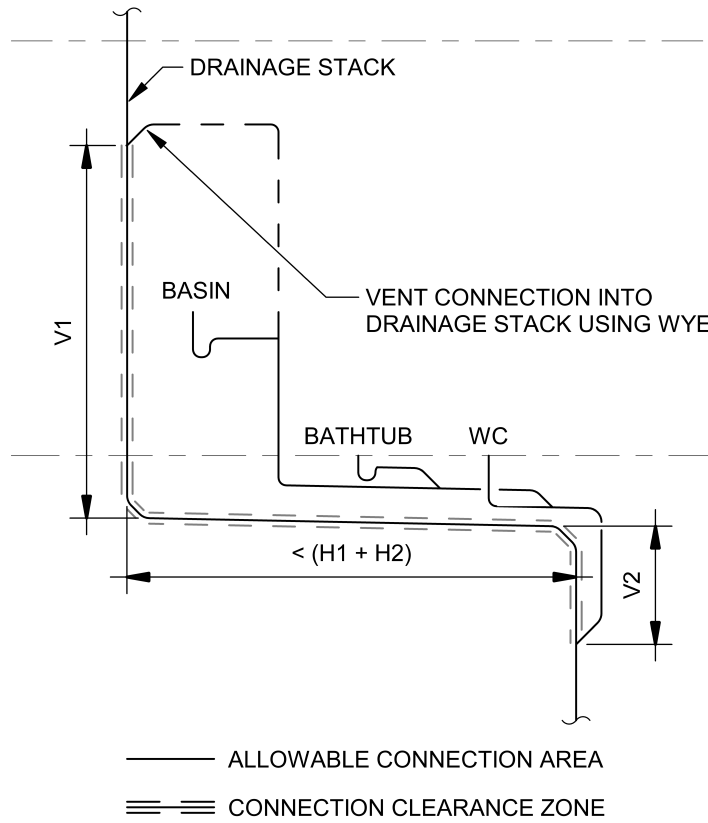**Figure A1.6 – Bypass vent**

Figure A1.7 – Bypass stack
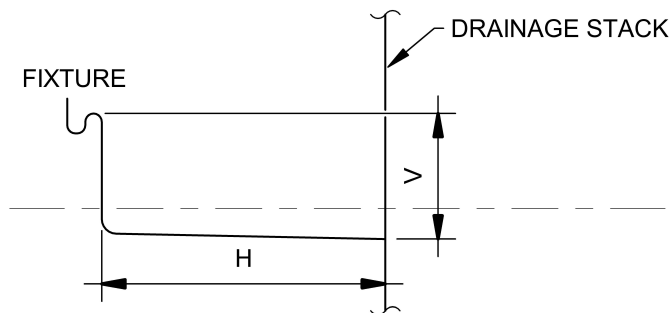
Figure A1.8 – Stack offset bypass

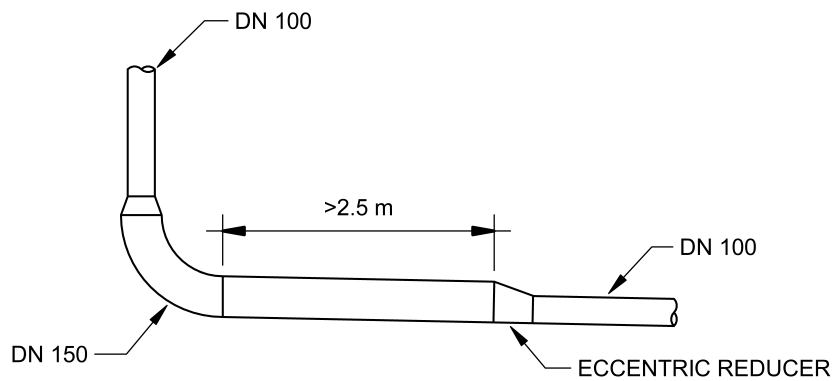**Figure A1.9 – Branch length and height limitations**

Figure A1.10 – Stack base long sweep configuration

Appendix B – Supporting Equations

Equation B1.1 – Loading calculation in EN 12056

$$Q_{ww} = K\sqrt{\Sigma DU}$$

Q_{ww} = waste water flowrate (L/s)

K = Frequency factor

ΣDU = Sum of discharge Units

Equation B1.2 – Loading calculation in GB 50015

$$q_p = 0.12a\sqrt{N_p} + q_{max}$$

q_p = Drainage design flowrate (L/s)

N_p = Sanitary appliance drainage equivalent value

a = Building type coefficient

Presentation of Author

John Lansing is a lead plumbing designer at PAE in Portland, Oregon. John specializes in applying sustainable solutions to plumbing systems and research on international engineering design guidance. He also serves on the technical committees for the IAPMO Water Efficiency and Sanitation Standard (WEStand) and the ICC 815 Standard for Sizing Water Distribution Sanitary Drainage and Vent Piping Systems.

Modeling Study of "Zero Water Building"

H. Kose (1)

(1) hkose@toyo.jp
(1) Professor, Faculty of Information Sciences and Arts, Toyo University, Japan

Abstract

Based on the research results of the "Subcommittee on Evaluation Method of Zero Water Building", which ended its four-year activities from 2019 to 2022 at the Architectural Institute of Japan, the two years of 2023 and 2024 "Subcommittee on modeling of Zero Water Building" has started its activities. This paper presents an overview of the research results of the "Subcommittee on Evaluation Method of Zero Water Building." It also summarizes information as a starting point for reaching consensus on the concept of "Zero Water Building", which is the activity goal of the "Subcommittee on modeling of Zero Water Building." Various conditions for building owners and designers to plan and design "Zero Water Building" (site area, green infrastructure, building area, roof area, building usage, total floor area, building personnel, potable water consumption, alternative water consumption, alternative water treatment amount, alternative water storage amount, rainfall amount, flood response, potable water outage response, etc.) and consider a method of displaying the results. Specifically, evaluation based on differences in building coverage ratios in buildings with the same total floor area, evaluation based on the infiltration coefficient of green infrastructure, evaluation based on building personnel, evaluation as "Zero Water Building" based on expanded use of alternative water, and evaluation of energy consumption. relationship, evaluation of water consumption by application in an emergency, and evaluation based on a combination of these evaluations.

Keywords

"Zero Water Building", trial evaluation, rainwater infiltration, potable water consumption, alternative water consumption.

1 Introduction

The U.S. Department of Energy's "Net Zero Water Strategy" [1] and the USGBC's LEED Zero project [2] started in 2018, with "water" positioned as one of the four zeros (Zero Carbon, Zero Energy, Zero Water, Zero Waste). As a result, interest in "Zero Water" is increasing in Japan as well. In Japan, the government and others are strongly promoting ZEB and ZEH, and the Energy Conservation Law for Buildings promulgated in 2015 has strengthened energy conservation standards for buildings [3]. On the other hand, about water, the water supply penetration rate will reach 98.2% [4] in 2021, and the sewage treatment population penetration rate will reach 92.6% [5]. regulations are not strict. Under these circumstances, in 2014, Water Cycle Basic Act [6] was promulgated and enforced as a basic law for the comprehensive implementation of measures by the government with the goal of maintaining or restoring a sound water cycle. In the same year, Act to Advance the Utilization of Rainwater [7] was enacted to promote the effective use of water resources and to contribute to the control of concentrated rainwater runoff into sewers and rivers.

Japan has much more rainfall than the world average of 880mm [8], with Tokyo's annual average rainfall of 1598.2mm from 1991 to 2020. However, there is a large monthly variation of 56.5mm in February and 234.8mm in October [9]. Water-related risks are higher in floods than in droughts. This is what I introduced in my 2019 paper [10]. On the other hand, due to the use of groundwater due to urbanization, the decline of groundwater level, ground subsidence, depletion of spring water, etc. became prominent in the 1960s in central Tokyo. As a result, in central Tokyo, there is currently a problem of floating underground structures due to rising groundwater levels.

Goal 6 of the SDGs (Sustainable Development Goals) is to "Ensure availability and sustainable management of water and sanitation for all." Target 6.4 states: "By 2030, substantially increase water-use efficiency across all sectors and ensure sustainable withdrawals and supply of freshwater to address water scarcity and substantially reduce the number of people suffering from water scarcity." Target 6.6 states, "By 2020, protect and restore water-related ecosystems, including mountains, forests, wetlands, rivers, aquifers and lakes." [11] Interest in zero water is gradually increasing as the desire to contribute to the achievement of the SDGs in organizations such as regions and companies is increasing.

Therefore, in this paper, I will report the outline of the research results of the "Subcommittee on Evaluation Method of Zero Water Building" from FY2019 to FY2022 at the Architectural Institute of Japan. In addition, the "Subcommittee on modeling of Zero Water Building" established from FY2023 to FY2024 aims to reach a consensus on the concept of "Zero Water Building". As a starting point, in this paper, I consider the conditions for achieving "Zero Water Building" by changing various conditions for building owners and designers to plan and design "Zero Water Building".

2 Methodology

In March 2023, the "Subcommittee on Evaluation Method of Zero Water Building" held the 46th Water Environment Symposium "Thinking about 'Zero Water Building' in Sustainable Community Development." At this symposium, five committee members prepared materials and gave presentations [12]. In this paper, I will introduce an overview and discuss matters to be considered in future "Zero Water".

Regarding the consideration of various conditions for achieving "zero water", I modified the Excel spreadsheet program in reference [13] presented at CIB W062 (Haarlem) in 2017. Using this, a case study of a small-scale apartment house and an office is conducted, and the results are presented and discussed.

3 Overview of the research results of the "Subcommittee on Evaluation Method of Zero Water Building"

Presentations at the symposium were based on the following five materials. Titles and their outlines are shown below.

3.1 Hiroyuki Kose (Toyo University): Explanation of purpose (issues surrounding the water environment of buildings in Japan)

This article introduced the current state of the water environment in Japan, where disaster and ecosystem risks are on the rise while pollution risks are on the decline. I also proposed a framework and evaluation of Japan's "Net Zero Water Building" considering disaster risk, based on research results at the 2017 CIB W062 International Symposium. Based on these results, future issues concerning the water environment of buildings in Japan were presented.

3.2 Tamio Nakano (Shizuoka University of Art and Culture): Overseas trends such as "Net Zero Water Strategy" and "LEED Zero Water"

He described the differences between the US "Zero Water Building Strategy" and Japan's "Zero Water Building" concept. In addition, he proposed a new scenario of zero water building that matches the actual situation in Japan, considering the contribution to disaster countermeasures (BCP, LCP) and energy reduction. He also introduced examples of overseas LEED Zero Water certification acquisition.

3.3 Toyohiro Nishikawa (Kogakuin University): Calculation of "Zero Water Building"

The water balance in the evaluation area was modeled in three parts, the amount of alternative water (AW), the amount of returned water (WR), and the amount of water used (WU). Using this model, he calculated a "Zero Water Building" using the management records and meteorological data of three buildings or campuses and presented the results of plotting the water balance.

3.4 Takeshi Aoi (Nikken Sekkei): Concept of "Zero Water Building" Design

From the perspective of a design company, six water issues (dependence on infrastructure, high domestic water consumption, low awareness of water conservation, deficit management of infrastructure, marine pollution, and BCP (flood damage)) were presented. He also explained the necessity of evaluating "Zero Water Building" from the three perspectives of water resources, BCP, and energy balance evaluation. In addition, he introduced two examples of planning, a research facility and a distribution warehouse,

and introduced planning matters that considered "zero water building" and matters related to energy conservation and BCP.

3.5 Michitaro Maki (LIXIL): "Zero Water" Product Trends

As a product that produces water, he introduced domestic and foreign products of water generators that generate drinking water from air. In addition, as a product that reuses water, he introduced examples of a portable water reclamation plant that can repeatedly use water without supplementary water, and a house based on the concept of self-sufficiency in water and electricity.

4 Examination of various conditions for achieving zero water building

4.1 Purpose

Quantitatively evaluate water use, energy consumption (in this study, evaluated by CO_2 emissions), regional precipitation, and water availability in the event of a disaster. Based on this result, the purpose is to clarify the considerations for the establishment of "Zero Water".

4.2 Calculation targets and conditions

I set two conditions, an apartment house (or detached housing complexes) and a small office building, and set conditions that facilitate comparison and study, and calculated annual water consumption and CO_2 emissions by use. In addition, the "Zero Water Index" was calculated based on the calculation conditions of "LEED Zero Water". Table 1 shows the building conditions, Table 2 shows the CO_2 emissions and water consumption per unit or rate, and Table 3 shows the trial calculation conditions for water consumption and water sources, water supply, hot water supply, wastewater, and water treatment by application.

This program is adapted from the one used in reference [13]. However, since the program at that time targeted detached houses and did not add rainwater infiltration to the site, it was added in this study. In addition, I added the condition of potable water supply water in the alternative water use. In addition, the use of water supply pumps was added for buildings with four or more floors. A direct connection booster water supply system was adopted for potable water supply, and an elevated water tank system was adopted for alternative water supply.

Regarding the basic housing conditions, the amount of water used for sanitary fixtures, hot water supply, and bathing is based on reference [14], and the facility conditions are based on case 4 of reference [13]. The amount of water used in the office was assumed for each use based on the unit water supply amount proposal in Reference [15] (10 to 20 L/person/day for potable water, 20 to 40 L/person/day for alternative water). Considering holidays, the number of working days for the office is set at 250 days.

In this program, priority is given to reused wastewater, and rainwater usage is calculated by overflowing and infiltrating surplus water collected from the roof. In addition, the trial calculations for rainwater utilization and rainwater infiltration are based on annual rainfall, and do not consider changes in rainfall or water storage. Taking these factors into account, the rainwater utilization rate is set at 0.6.

As for Case 5, which assumes an emergency, it is not suitable for annual calculations, but based on Reference [16], we calculated using the average water consumption for three weeks from the time of the disaster. From this, the effect of alternative water was grasped.

Table 1 - Building conditions

System	CO_2 Emission [kg-CO_2/m^3]	Basis for calculation
Potable Water	0.251	[17]
Non-Potable Water	0.063	[18]
Hot Water Supply	2.4 (Combined with solar water heater)	[19]
Sewage System	0.439	[20]
Septic System	1	[21]
Water Treatment	0.6	[22]
Potable Water Booster Pump	0.327 (Booster direct water supply system)	[23][24]
Non-Potable Water Pump	0.092 (Elevated tank water supply system)	[23][24]
Others		
Rainfall [mm/year]	1300 (Average rainfall in Kumagaya)	[25]
Hot Water Use Ratio	0.5	
Rate of Water Collection (Roof)	0.6 (or conditions to satisfy zero water)	
Rate of Water Filtration (Non-building area)	0.5 (or conditions to satisfy zero water)	

Table 2 - CO_2 emissions and water consumption per unit or rate

System	CO_2 Emission [kg-CO_2/m^3]	Basis for calculation
Potable Water	0.251	[16]
Non-Potable Water	0.063	[17]
Hot Water Supply	2.4 (Combined with solar water heater)	[18]
Sewage System	0.439	[19]
Septic System	1	[20]
Water Treatment	0.6	[21]
Potable Water Booster Pump	0.327 (Booster direct water supply system)	[22][23]
Non-Potable Water Pump	0.092 (Elevated tank water supply system)	[22][23]
Others		
Rainfall [mm/year]	1300 (Average rainfall in Kumagaya)	[24]
Hot Water Use Ratio	0.5	
Rate of Water Collection (Roof)	0.6 (or conditions to satisfy zero water)	
Rate of Water Filtration (Non-building area)	0.5 (or conditions to satisfy zero water)	

Table 3 - Trial calculation conditions for water consumption and water sources, water supply, hot water supply, wastewater, and water treatment by application

Apartment House

No.	Water Use	Case 1,2,3,5-2 U·T·P·D	Case 4 (Emergency) U·T·P·D	Case 5-1 (Use of All Collected Rainwater) U·T·P·D	Case 1 (Base Model) Source / Supply / Heating / Discharge / Treatment	Case 2,5 (Rainwater Harvesting)	Case 3 (Rainwater Harvesting and Greywater Reuse)	Case 4 (Emergency)
1	Kitchen Cooking & Washing	13 · 3 · 3 · 365		13 · 3 · 3 · 365	City Potable Water / Potable Water / Hot Water Supply / Black Water / Sewage System	City Potable Water / Potable Water / Hot Water Supply / Black Water / Sewage System	City Potable Water / Potable Water / Hot Water Supply / Black Water / Sewage System	
2	Hand & Face Washing	1.5 · 7 · 3 · 365		1.5 · 7 · 3 · 365	City Potable Water / Potable Water / Hot Water Supply / Black Water / Sewage System	City Potable Water / Potable Water / Hot Water Supply / Black Water / Sewage System	City Potable Water / Potable Water / Hot Water Supply / Grey Water / Water Treatment	
3	Bathtub	200 · 1 · 1 · 250		200 · 1 · 1 · 250	City Potable Water / Potable Water / Hot Water Supply / Black Water / Sewage System	City Potable Water / Potable Water / Hot Water Supply / Black Water / Sewage System	City Potable Water / Potable Water / Hot Water Supply / Grey Water / Water Treatment	
4	Bathroom Shower	25 · 1 · 3 · 365	25 · 1 · 3 · 365	25 · 1 · 3 · 365	City Potable Water / Potable Water / Hot Water Supply / Black Water / Sewage System	City Potable Water / Potable Water / Hot Water Supply / Black Water / Sewage System	City Potable Water / Potable Water / Hot Water Supply / Grey Water / Water Treatment	Rainwater+Grey Water / Non-Potable Water / Hot Water Supply / Grey Water / Water Treatment
5	Bidet	0.2 · 3 · 3 · 365		0.2 · 3 · 3 · 365	City Potable Water / Potable Water / Hot Water Supply / Black Water / Sewage System	City Potable Water / Potable Water / Hot Water Supply / Black Water / Sewage System	City Potable Water / Potable Water / Hot Water Supply / Black Water / Sewage System	
6	Washing Machine	40 · 1 · 3 · 300	20 · 1 · 3 · 300	40 · 1 · 3 · 300	City Potable Water / Potable Water / / Black Water / Sewage System	City Potable Water / Potable Water / / Black Water / Sewage System	City Potable Water / Potable Water / / Grey Water / Water Treatment	Rainwater+Grey Water / Non-Potable Water / / Grey Water / Water Treatment
8	Humidifying	1 · 1 · 1 · 100		1 · 1 · 1 · 100	City Potable Water / Potable Water	City Potable Water / Potable Water	City Potable Water / Potable Water	
11	Cleaning	5 · 1 · 3 · 180	5 · 1 · 3 · 180	5 · 1 · 3 · 180	City Potable Water / Potable Water / / Black Water / Sewage System	City Potable Water / Potable Water / / Black Water / Sewage System	City Potable Water / Potable Water / / Grey Water / Water Treatment	Rainwater+Grey Water / Non-Potable Water / / Grey Water / Water Treatment
12	Plumbing Fixtures	6 · 5 · 3 · 365	5 · 5 · 3 · 365	6 · 5 · 3 · 365	City Potable Water / Potable Water / / Black Water / Sewage System	Rainwater+Grey Water / Non-Potable Water / / Black Water / Sewage System	Rainwater+Grey Water / Non-Potable Water / / Black Water / Sewage System	Rainwater+Grey Water / Non-Potable Water / / Water Returned / Septic System
16	Irrigation	20 · 1 · 1 · 100		20 · 1 · 1 · 100	City Potable Water / Potable Water	Rainwater+Grey Water / Non-Potable Water	Rainwater+Grey Water / Non-Potable Water	
17	Landscape			118.3 · 1 · 1 · 365	Rainwater+Grey Water / Non-Potable Water			
	Total [L/day,person] or Zero Water Index [(Alternative Water Use + Water Returned) /	188.0	68.9	227.4	0.00	Case 2-1: 0.69, Case 2-2: 0.66 Case 2-3: 0.65, Case 2-4: 0.65 Case 2-6: 0.64, Case 2-8: 0.64 Case 5-1: 0.57, Case 5-2: 1.00	0.86	1.90

(U = Unit of Water Consumption [L/times], T = Times [times/day], P = Person(s) or Times, D = Number of Days Used)

Office

No.	Water Use	Case 1,2,3,5 U·T·P·D	Case 4 (Emergency) U·T·P·D	Case 1 (Base Model) Source / Supply / Heating-Cooling / Discharge-Recharge / Treatment	Case 2,5 (Rainwater Harvesting)	Case 3 (Rainwater Harvesting and Greywater Reuse)	Case 4 (Emergency)
1	Kitchen Cooking & Washing	5 · 2 · 120 · 250		City Potable Water / Potable Water / Hot Water Supply / Black Water / Sewage System	City Potable Water / Potable Water / Hot Water Supply / Black Water / Sewage System	City Potable Water / Potable Water / Hot Water Supply / Black Water / Sewage System	
2	Hand & Face Washing	1.5 · 4 · 120 · 250		City Potable Water / Potable Water / Hot Water Supply / Black Water / Sewage System	City Potable Water / Potable Water / Hot Water Supply / Black Water / Sewage System	City Potable Water / Potable Water / Hot Water Supply / Grey Water / Water Treatment	
5	Bidet	0.2 · 3 · 120 · 250		City Potable Water / Potable Water / Hot Water Supply / Black Water / Sewage System	City Potable Water / Potable Water / Hot Water Supply / Black Water / Sewage System	City Potable Water / Potable Water / Hot Water Supply / Black Water / Sewage System	
8	Humidifying	1 · 1 · 120 · 250		City Potable Water / Potable Water	City Potable Water / Potable Water	City Potable Water / Potable Water	
11	Cleaning	5 · 1 · 120 · 250	5 · 1 · 120 · 250	City Potable Water / Potable Water / / Black Water / Sewage System	City Potable Water / Potable Water / / Black Water / Sewage System	City Potable Water / Potable Water / / Grey Water / Water Treatment	Rainwater+Grey Water / Non-Potable Water / / Grey Water / Water Treatment
12	Plumbing Fixtures	6 · 4 · 120 · 250	5 · 4 · 120 · 250	City Potable Water / Potable Water / / Black Water / Sewage System	Rainwater+Grey Water / Non-Potable Water / / Black Water / Sewage System	Rainwater+Grey Water / Non-Potable Water / / Black Water / Sewage System	Rainwater+Grey Water / Non-Potable Water / / Water Returned / Septic System
16	Irrigation	100 · 1 · 1 · 365		City Potable Water / Potable Water	Rainwater+Grey Water / Non-Potable Water	Rainwater+Grey Water / Non-Potable Water	
	Total [L/day,person] or Zero Water Index [(Alternative Water Use + Water Returned) /	47.8	25.0	0.00	Case 2-1: 0.79, Case 2-2: 0.73 Case 2-3: 0.72 ,Case 2-4: 0.71 Case 2-6: 0.70 ,Case 2-8: 0.69 Case 5: 1.01	1.02	1.71

4.3 Trial calculation results for apartment house

Figure 1 shows the results of trial calculations for each case. Here, I used the following four graphs. "Pie chart showing the ratio of potable water and non-portable water in total water usage", "Bar graph showing the balance between water sources and alternative water usage", "Bar graph calculated showing CO_2 emissions related to water use for infrastructure and buildings", "Bar graph calculated for the balance between the total amount of water used and the amount of alternative water used + the amount of water returned for the evaluation of 'zero water'".
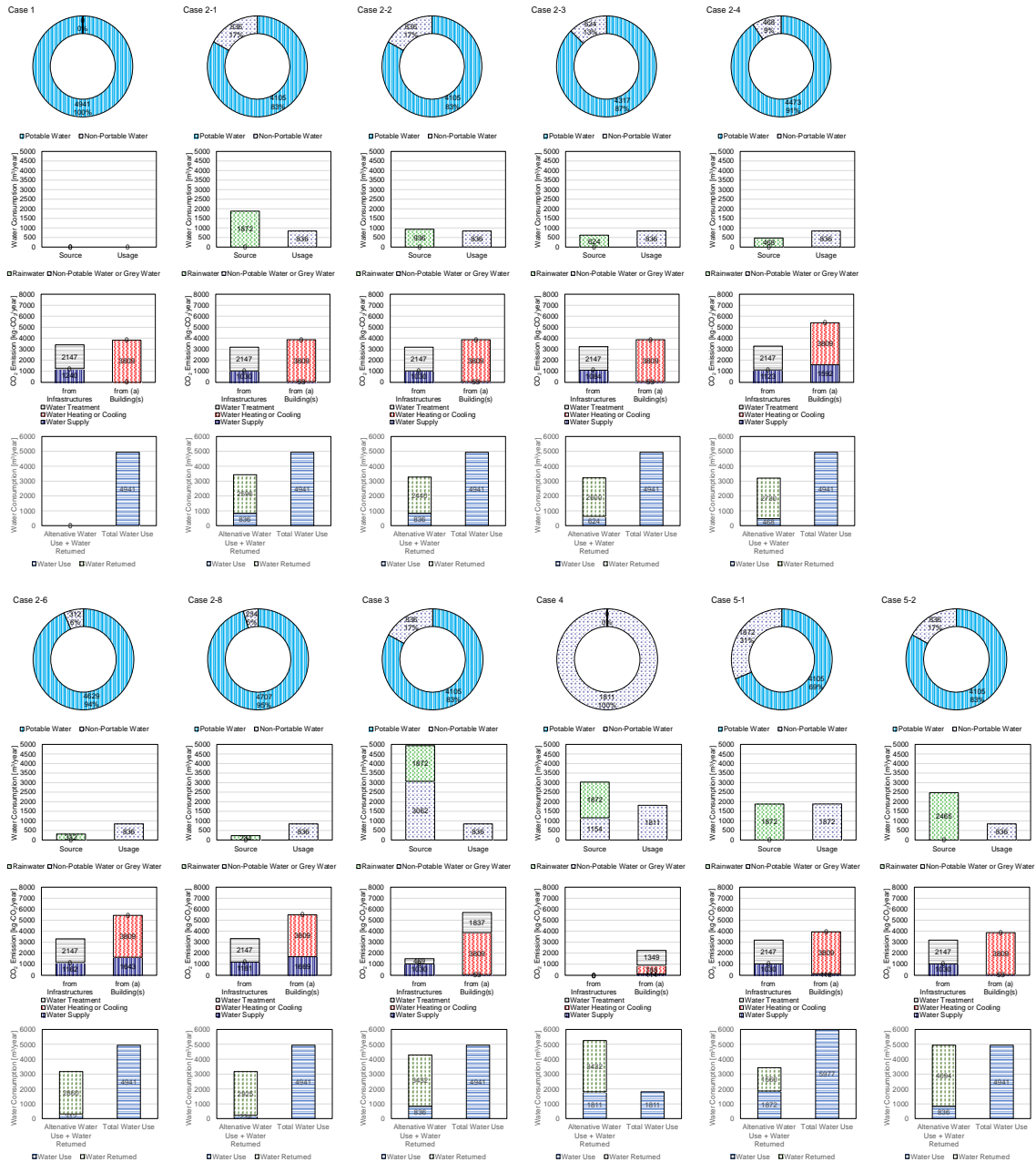
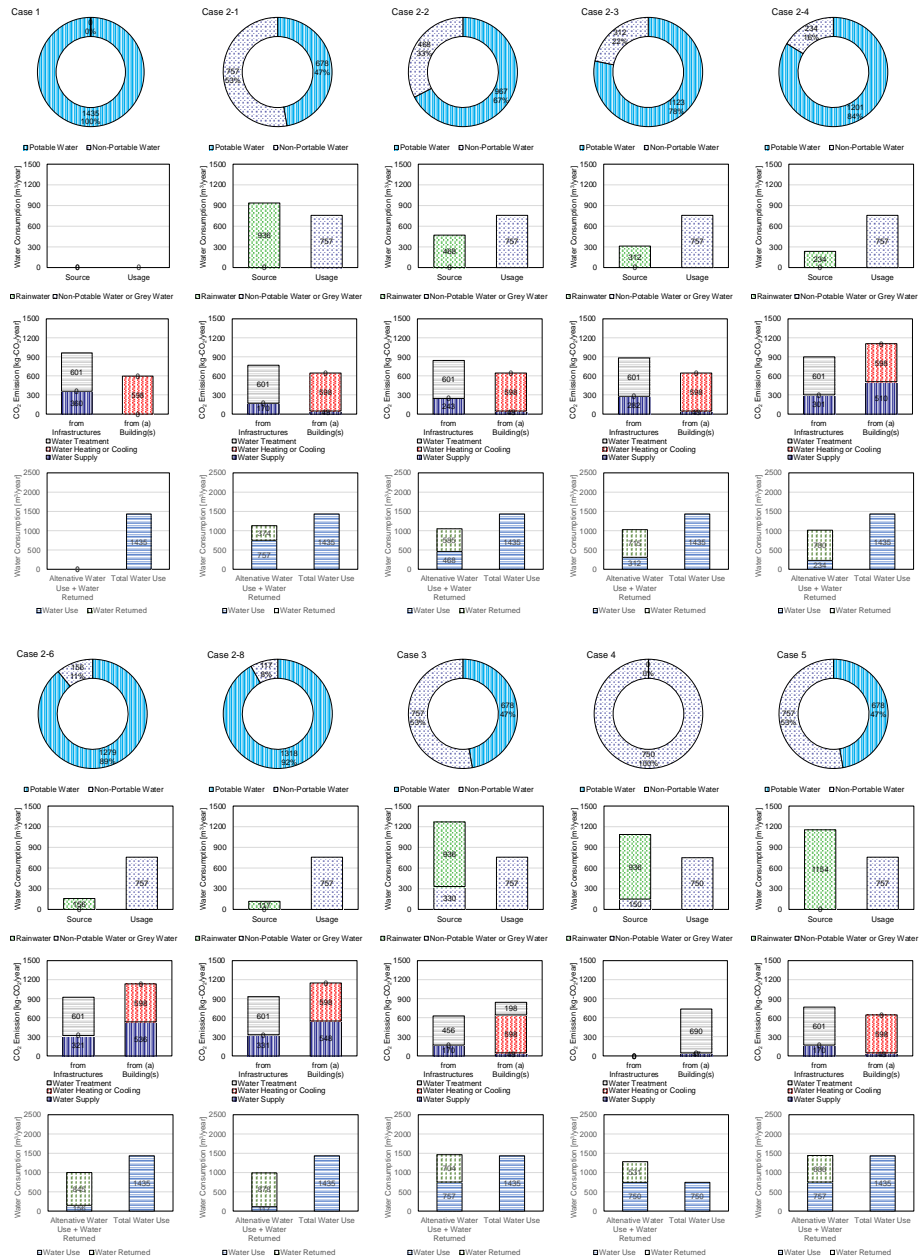**Figure 1 - Trial calculation results for apartment house**

Figure 2 - Trial calculation results at the office

If alternative water use is limited to flushing toilets, alternative water use accounts for up to 17% of total water use. The branch number in Case 2 represents the number of floors. In the case of the third floor and above, it is not possible to secure alternative water use only by using rainwater, so it is supplemented with potable water. On the 4th floor and above, the amount of CO_2 emitted from the water supply in the building has increased significantly, but this is due to the assumption that a direct booster water supply system will be used. On the other hand, rainwater is a big difference because it is assumed to be an elevated water tank system. From the perspective of decarbonization, low-rise buildings are advantageous in various ways.

Case 3 is calculated on the assumption that wastewater from washing hands, bathrooms, laundry, and cleaning is reused. In this case, grey water is sufficient as a water source, so rainwater can infiltrate the whole amount. Case 4 assumes that the water supply

is cut off during a disaster. If the system in the building can be operated normally, it is possible to secure alternative water. However, since rainfall is calculated based on annual rainfall here, a detailed study is required. Case 5-1 is a calculation of the conditions for using all the collected rainwater in the rainwater utilization conditions (Case 2). In this case, 118.3 L of water per household per day can be used for landscape use, or 138.3 L of water when combined with watering. If landscape water is used for microclimate and thermal mitigation, such as rain ponds and wall watering, it can contribute to the overall reduction of CO_2 emissions from the site and building. Case 5-2 is a trial calculation of the rainwater infiltration rate to satisfy "Zero Water" under the conditions of Case 2. In case 2, the roof rainwater utilization rate (excess water is infiltrated) is set at 0.6, and the site rainwater infiltration rate is set at 0.5. If these are set to 0.79, the condition of "Zero Water" is satisfied. To achieve "Zero Water", it is necessary to increase the rainwater infiltration rate as much as possible.

4.4 Trial calculation results at the office

Figure 2 shows the results of comparative calculations in the same way as for the apartment house. In the case of the office, the ratio of potable water to alternative water is 1:2, so effective use of rainwater is desirable. However, in Case 2, replenishment water from potable water is required on the second floor and above, and its effectiveness is limited. Case 3, which introduces a wastewater reuse system, is an effective means from the viewpoint of effective use of water. Under the calculation conditions of this time, the condition of "Zero Water" is satisfied. In Case 4, which assumes an emergency, if enough rainwater can be stored, water can be secured to meet the demand for alternative water. In case 2, as in the apartment house, the roof rainwater utilization rate (excess water is infiltrated) is set at 0.6, and the site rainwater infiltration rate is set at 0.5. Setting these to 0.74 satisfies the condition of "Zero Water" (Case 5).

5 Discussion

A low-rise building with a large roof area is desirable from the viewpoint of rainwater utilization and CO2 emissions. However, it is difficult to achieve "zero water" without increasing the rainwater infiltration rate in houses where water consumption per person is high. It is required that most of the site be used as a rainwater infiltration surface, and surplus water from roof rainwater can also permeate. On the other hand, in offices where water demand is low and the ratio of miscellaneous water is high, it is easier to satisfy the condition of "zero water" than in collective housing. Under the conditions of this trial calculation, it is possible to achieve zero water if the building coverage ratio is 60% (site area of 2,000m2). If a wastewater reuse system is introduced, it will be easier to achieve the condition of "zero water", but it is not realistic to introduce it in houses. However, from the viewpoint of securing water in an emergency, the introduction of a wastewater reuse system in collective housing is effective.

6 Conclusion

In this study, for the purpose of dissemination and enlightenment of "Zero Water Building", I reported the outline of the research results of "Subcommittee on Evaluation Method of Zero Water Building" of Architectural Institute of Japan. In addition, trial calculations were made using various conditions for building owners and designers to plan and design the "Zero Water Building" as parameters, and various conditions for achieving "Zero Water" were considered.

As a future task, I will continue trial calculations and case studies for the purpose of obtaining consensus on the concept of "Zero Water", which is the activity goal of the "Subcommittee on modeling of Zero Water Building." In addition, I will consider the possibility of introducing the concept of "Zero Water" such as water generators and systems that repeatedly use water, which were mentioned in previous committee results. Furthermore, I would like to examine the role that water should play in architecture, such as resilience and wellness, which are required for architecture, from a broad perspective.

7 Acknowledgments

8 References

[1] U.S. Department of Energy, "Net Zero Water Building Strategies", https://www.energy.gov/femp/net-zero-water-building-strategies, viewed on August 13, 2023

[2] U.S. Green Building Council, "LEED Zero", https://www.usgbc.org/programs/leed-zero, viewed on August 13, 2023

[3] Ministry of the Environment Government of Japan, "ZEB Portal", https://www.env.go.jp/earth/zeb/, viewed on August 13, 2023

[4] Ministry of Health, Labour and Welfare of Japan, "Basic water statistics", https://www.mhlw.go.jp/stf/seisakunitsuite/bunya/topics/bukyoku/kenkou/suido/database/kihon/index.html, viewed on August 13, 2023

[5] Ministry of Land, Infrastructure, Transport and Tourism of Japan, "About the sewage treatment population diffusion situation at the end of 2021", August 25, 2022

[6] Cabinet Office, Government of Japan, "Water Cycle Basic Act", https://www.cas.go.jp/jp/seisaku/mizu_junkan/about/basic_law.html, viewed on August 13, 2023

[7] Ministry of Land, Infrastructure, Transport and Tourism of Japan, "Act to Advance the Utilization of Rainwater",

https://www.mlit.go.jp/mizukokudo/mizsei/mizukokudo_mizsei_tk1_000068.html, viewed on August 13, 2023

[8] Ministry of Land, Infrastructure, Transport and Tourism of Japan, "Precipitation in Japan, twice the world average", https://www.mlit.go.jp/river/pamphlet_jirei/bousai/saigai/kiroku/suigai/suigai_3-1-1.html, viewed on August 13, 2023

[9] Japan Meteorological Agency, "Tokyo (Tokyo) Average yearly values (values for each year and month) Main elements", https://www.data.jma.go.jp/obd/stats/etrn/view/nml_sfc_ym.php?prec_no=44&block_no=47662, viewed on August 13, 2023

[10] Hiroyuki Kose, Tamio Nakano, Toyohiro Nishikawa, "Examination of "Net Zero Water Building" Evaluation Method in Japan", 45th International Symposium of CIB W062 (Melbourne, Australia), 1-12, September 2019

[11] United Nations Sustainable Development, "Water and Sanitation", https://www.un.org/sustainabledevelopment/water-and-sanitation/, viewed on August 13, 2023

[12] Subcommittee on Evaluation Method of Zero Water Building of AIJ, "Thinking about 'Zero Water Building' in Sustainable Community Development", March 2023

[13] Hiroyuki Kose, Tamio Nakao, Toyohiro Nishikawa, "Quantitative Evaluation Method of Resource and Energy Conservation in a Water Supply and Drainage System", CIB W062 2017 43rd International Symposium (Haarlem), 94-107, August 2017

[14] Bureau of Waterworks, Tokyo Metropolitan Government, "Skillful use of water | Living and Waterworks", https://www.waterworks.metro.tokyo.lg.jp/kurashi/shiyou/jouzu.html, viewed on July 14, 2017

[15] Kazuya Fujimura, Takehiko Mitsunaga, Minoru Uchiyama, Akihiro Doi, "New Water Supply Units for Specific Buildings Part 3 Water Supply Units for Office Buildings", Transactions of the Society of Heating, Air-conditioning and Sanitary Engineers of Japan, 306, 43-50, September 2022

[16] Saki Watari, Masayuki Otsuka, Takashi Matsuo, Toshihiro Sankai, "Plan of the Water Supply and Drainage Sanitation for Lifeline Disruptions such as at the time of Earthquake Disasters. -Part1 An Examination of a Water Supply Unit and Water Supply Tank Capacity and Drainage Tank Capacity-", Technical Papers of Annual Meeting, the Society of Heating, Air-Conditioning and Sanitary Engineers of Japan, B-23, Vol.1, 89-92, https://doi.org/10.18948/shasetaikai.2017.1.0_89, September 2017

[17] Tokyo Metropolitan Center for Climate Change Actions, "Environmental household account book input sheet", https://www.tokyo-co2down.jp/kakeibo/, viewed on July 14, 2017 (Not currently available)

[18] Keita Fukui, Nobuharu Maeda, Fumio Kanatsu, Seishi Okada, "Study on the Actual Situation of Environment Load of Rainwater Utilization Facilities", Transactions of the Society of Heating, Air-conditioning and Sanitary Engineers of Japan, 268, 27-32, https://doi.org/10.18948/shase.44.268_27, September 2019

[19] Nine Prefectures and Cities Summit Meeting Committee on Environmental Issues Special Subcommittee on Global Warming Countermeasures, "Comparative

survey report on hot water supply equipment in homes", http://www.tokenshi-kankyo.jp/images/report_pdf/report3-1.pdf, September 2010

[20] National Institute for Land and Infrastructure Management, "Current Status of Global Warming and Trends Concerning Carbon Neutrality", https://www.nilim.go.jp/lab/eag/pdf/20211008_2-4_ondanka.pdf, viewed on August 14, 2023

[21] Keiji Tezuka: "Septic Tank Engineering Chapter 5 Septic Tank and global environmental problems and overseas development Section 1 CO_2 emissions accompanying energy consumption in septic tanks", http://www.jsa02.or.jp/01jyokaso/02_3i.html, July 2011

[22] Ministry of Land, Infrastructure, Transport and Tourism of Japan, "Result of survey on CO_2 emissions related to the operation of regeneration/supply facilities - Expansion of samples of individual recycling facilities -", https://www.mlit.go.jp/common/000033103.pdf, viewed on August 14, 2023

[23] Shigekazu Okauchi, Kyosuke Sakaue, Makoto Fukuda, Guangzheng Wu, "Comparison of Power Consumption of Water Supply Pump by the water feeding system in an apartment house", Technical Papers of Annual Meeting, the Society of Heating, Air-Conditioning and Sanitary Engineers of Japan, G-9, Vol.1, 33-36, https://doi.org/10.18948/shasetaikai.2018.1.0_33, September 2018

[24] Ministry of the Environment of Japan, "List of Calculation Methods and Emission Factors - Emission factor by electric power company (for calculating greenhouse gas emissions of specified emitters) - 2021-year results -", https://ghg-santeikohyo.env.go.jp/files/calc/r05_coefficient_rev4.pdf, viewed on August 14, 2023

[25] Japan Meteorological Agency, "Kumagaya (Saitama) Average yearly values (values for each year and month) Main elements", https://www.data.jma.go.jp/stats/etrn/view/nml_sfc_ym.php?prec_no=43&block_no=47626&year=&month=&day=&view=, viewed on August 14, 2023

9 Presentation of Author

Hiroyuki Kose is the Professor at Toyo University, Faculty of Information sciences and arts from 2009. Special fields of study are water supply and drainage for buildings, water environment, reproduction of the agricultural and forestry industries by collaboration of citizens and an organization and community design for regional vitalization.

Comparison and Assessment of Building Drainage Design Codes for use in Tall Buildings

S. A. Mohammed (1), M. Gormley (2), C. Stewart (3) D.A. Kelly (4) and D.P Campbell (5)

1. sarwar.mohammed@hw.ac.uk
2. m.gormley@hw.ac.uk
3. colin.stewart@hw.ac.uk
4 d.a.kelly@hw.ac.uk
5. d.p.campbell@hw.ac.uk

(1-5) School of Energy, Geoscience, Infrastructure and Society, Heriot-Watt University, Edinburgh, Scotland, UK.

Abstract

Current design codes offer some valuable guidance on how to design drainage and vent systems, their application to high-rise buildings remains somewhat unclear. Moreover, different design codes may propose varying approaches for calculating the design flow rate, sizing the stack and vent pipe, and offering different configurations. Therefore, it is important for designers and researchers to have a comprehensive understanding of the current codes for building drainage systems (BDS), to gain an overview of each approach's limitations and strengths. In this research we investigate design codes BDS, specifically BS EN 12056 and its application for high-rise buildings. To achieve this, data was collected from a real-world physical model at the National Left Tower testing centre (NLT) in Northampton, UK, a 34 storey drainage test facility adaptable to many different scenarios. The system was tested under many different identifiable configurations, including single stack and with various ventilation options including different diameter ventilation pipework and a fully active ventilation system using positive air pressure transient attenuators (PAPA) and air admittance valves (AAV). In this study, the AIRNET model, a one-dimensional method of characteristics, finite difference computer model, developed over many years by Heriot-Watt University, was also applied to the given scenarios to validate its performance at height and to gain insight on design code methodologies. The real-time data from NLT was used to evaluate the effectiveness of different design codes for drainage systems and to confirm the applicability of the AIRNET model in simulating the system characteristics such as trap seal depletion, air pressure, and airflow regimes in tall building BDS. The paper highlights the significance of fluid mechanisms that relate specifically to tall buildings and provides a recommendation for their incorporation into drainage codes in the future. Such inclusion is crucial to ensuring public health and safety by improving the overall performance of BDS in high-rise buildings.

Keywords

Building drainage systems, drainage design codes, tall buildings, drainage system modelling.

1   Introduction

1.1 General

The main purpose of any Building Drainage System (BDS) is to ensure the safe and efficient disposal of human waste from a building, which protects public health by preventing potential cross-contamination with pathogens or viruses. Most design codes are primarily applicable to low-to-medium rise buildings, offering less, if any, guidance for high-rise buildings. Evidence suggests that most existing design codes have limitations in their applicability and are often unsuitable for high-rise building designs (Gormley *et al.*, 2021). While design guidelines may vary in the factors they consider when designing BDS, most of the codes primarily rely on flow rate to determine the appropriate BDS in terms of pipe size and system configurations. Estimating design flow rate, thus, can be considered as a paramount importance in all the design codes for BDS.

Most design codes implement the fixture unit (FU) or discharge unit (DU) method for designing flow rate for both water and drainage systems. This widely accepted method assigns fixture unit values to plumbing fixtures based on their load contribution to the plumbing system, providing a robust foundation for theoretical estimations of plumbing system loads and facilitating effective pipe sizing through mathematical computations. This methodology, initiated in the 1940s by Roy Hunter in the United States, used principles of probability. He developed Hunter's Curve and introduced the concept of "fixture units" to estimate flow rates. These numerical constants assist in determining water flow rates and, consequently, influence the sizing of pipes and storage capacities. A fixture unit, as defined by Hunter, accounts for the variable loads that a plumbing system must accommodate. This numerical metric, also known as a load factor, quantifies the load-producing impact of a specific plumbing fixture. The technique assigns a fixture unit weight to the plumbing fixtures and converts these weights into equivalent gallons per minute based on usage probability (Hunter, R, 1940). Initially formulated for residential buildings, this method has since found application in other types of buildings. It has been instrumental in designing water supply systems and sanitary drainage systems in buildings since its inception. Hunter's goal was to create a simple, standardised method that is grounded in scientific principles. The aim was to guarantee safe sanitary and cost-effective plumbing systems for all buildings, independent of the building's cost. This history underscores the significant role of codes and fixture units in shaping modern plumbing design and standardisation, contributing to the development of efficient and economical plumbing systems. Despite global acceptance, there are variations in design codes worldwide, particularly concerning the estimation of design flow rates and the sizing of drainage pipes.

A comprehensive review of current design codes, therefore, could provide valuable insights into the methods used to calculate flow rate and pipe size and could help identify potential limitations and inconsistencies. In this study, BS EN 12056 is explored as a well-used and well-understood standard in Europe, and is applied to buildings of various heights, focusing specifically on the design of vertical stacks and vent pipes, with the exclusion of discharge branch design. Additionally, the power of modelling system performance is explored and the computer model AIRNET applied to a range of designed configurations to allow for design evaluation beyond normal operating conditions which can highlight generalisations on the methodologies employed.

1.2 Historical development of codes

Historically, the design of building drainage systems has been based on an understanding of steady state flow within the system. While this has served the industry well in the past, the increasing height and complexity of buildings has made the engineering basis for this redundant. It must be recognised, that a significant aspect of the operation of building drainage wastewater and venting system is the management of air pressure transients resulting from changes in fluid flow in both the air and water domains. As stated above, the calculation of water flow rate is primarily due to the work of hunter in the USA in the 1940s. While attempts have been made to update these calculations (Omaghomi *et al.* 2020, Mohammed *et al.*, 2018), particularly in the water supply side they still rely on a steady flow premise and relate mainly to the supply of water to a building and not the discharge into the drain with its attendant transient nature. Discharges are due to collections of appliances on individual branches and lead to the sizing of vertical stack and ventilation pipes related entirely to the presumption that flow is steady.

The scientific basis for these relationships are due to work carried out, primarily in the UK by the Building Research Station (BRS now the BRE) and in the USA by the National Bureau of Standards (NBS – now NIST) Most of this seminal work was carried out in the 1950s – 1970s era (Wise&Croft 1954, Wise, 1954, Wyly and Eaton, 1961, Lilywhite &Wise, 1969, Verma et al, 1976, Wyly et al 1975). While there has been considerable work done since those publications, these publications were most influential in compiling the methodologies used in drainage pipe sizing design. Earlier work reported by Whipple (1924) and Hunter (1940) set the course of drainage design much earlier.

While this literature highlights the seminal research carried out to explain a methodology which could be easily applied by designers, all recognise the limitations of their work – from the height of the test systems used (often not more than 8 floors) to the instrumentation available at the time. Hunter states clearly that his definition of system loading was a work in progress and that further work was required to perfect the technique. Sadly, Hunter died before the additional work could be carried out and the initial findings were used for many years afterwards.

2   Application of BS EN 12056-2:2000

The scope of this European Standard (BS EN 12056 – 2:2000 Gravity drainage systems inside buildings – Sanitary pipework, layout and calculation) is one of the commonly used design code globally. This European Standard covers wastewater drainage systems that work by gravity and it is mandatory for implementation by national standards organizations of different countries across Europe. It is relevant for such systems inside residential, commercial, institutional, and industrial buildings. This code provides the characteristic of accommodating the differences in plumbing practices across Europe through the provision of multiple types of systems. While there may be differences in specific details within each system type, this code generally categorizes drainage systems into four distinct types that are used by different countries: System I: German, Swiss, Austrian Practice, System II: Scandinavian Practice, System III: UK Practice and System IV: French Practice (BS EN 12056-2, 2000).

The code has also classified each system into different configurations based on the requirement to regulate the pressure in the pipework to avoid the entry of foul air from the wastewater system into the building. The configuration includes primary ventilated stack, secondary ventilated stacks and air admittance valves. The code provides a wider range of discharge units (DU) in litres per second to calculate design flow rate. The DU is a specific numerical value assigned to an appliance, reflecting the correlation between the flow rate at its terminal fitting and its duration and frequency of usage, specific to the type and function of the building (often referred to as probable usage). Table (1) shows DUs for the sanitary appliances which are used in calculation of flow rate and pipe size in the system.

Table 1 Discharge units for appliances in BS EN 12056

Appliance	System I DU *l/s*	System II DU *l/s*	System III DU *l/s*	System IV DU *l/s*
Wash basin, bidet	0.5	0.3	0.3	0.3
Shower without plug	0.6	0.4	0.4	0.4
Shower with plug	0.8	0.5	1.3	0.5
Single urinal with cistern	0.8	0.5	0.4	0.5
Urinal with flushing valve	0.5	0.3	-	0.3
Slab urinal	0.2 *	0.2*	0.2*	0.2*
Bath	0.8	0.6	1.3	0.5
Kitchen sink	0.8	0.6	1.3	0.5
Dishwasher (household)	0.8	0.6	0.2	0.5
Washing machine up to 6 kg	0.8	0.6	0.6	0.5
Washing machine up to 12 kg	1.5	1.2	1.2	1.0
WC with 4,0 l cistern	**	1.8	**	**
WC with 6,0 l cistern	2.0	1.8	1.2 to 1.7 ***	2.0
WC with 7,5 l cistern	2.0	1.8	1.4 to 1.8 ***	2.0
WC with 9,0 l cistern	2.5	2.0	1.6 to 2.0 ***	2.5
Floor gully DN 50	0.8	0.9	-	0.6
Floor gully DN 70	1.5	0.9	-	1.0
Floor gully DN 100	2.0	1.2	-	1.3

* Per person
** Not permitted
*** Depending upon type (valid for WCs with siphon flush cistern only)
- Not used or not data

According to this code, wastewater flowrate (Q_{ww}) which is the expected flow rate in a part or in the whole drainage system can be calculated from equation (1). Total flowrate (Q_{tot}) can be used as a design flowrate in the system which is equal to the summation of waste water flowrate (Q_{ww}), continuous flowrate (Q_C), and pumped flowrate (Q_P), in a part or in the whole drainage system, equation (2).

Unlike other codes, BS EN 12056 provides more comprehensive guidelines for flow rate calculation and introduces a frequency factor, Table 2. This characteristic assists in differentiating buildings and estimating their flow rates based on their water usage. By calculating the total flow rate and selecting the system type and junction entry, designers can determine the appropriate stack size from Table 3. Therefore, along with discharge units, flow rates in litres per second are also required to choose the correct pipe size. This

important information provides designers with a comprehensive understanding of the entire system, thereby enabling more informed design decisions.

$$Q_{ww} = K\sqrt{\sum DU} \qquad ……………….\qquad \text{eq (1)}$$

Where:

Q_{ww} is waste water flowrate (l/s)
$\sum DU$ is sum of discharge units
K is frequency factor related to different usage of sanitary appliances given in Table (2)

$$Q_{tot} = Q_{ww} + Q_C + Q_P \qquad ……………….\qquad \text{eq (2)}$$

Table 2 Typical frequency factors (K)

No.	Usage of appliances	K
1	Intermittent use, e.g. in dwelling, guesthouse, office	0.5
2	Frequent use, e.g. in hospital, school, restaurant, hotel	0.7
3	Congested use, e.g. in toilets and/or showers open to public	1.0
4	Special use, e.g. laboratory	1.2

Table 3 Hydraulic capacity (Q_{max}) and nominal diameter (DN) in BS EN 12056

Stack and stack vent	Primary vented		Secondary vented		
	System I, II, III, IV Q_{max} (*l/s*)		Secondary vent	System I, II, III, IV Q_{max} (*l/s*)	
DN	Square entries	Swept entries	DN	Square entries	Swept entries
60	0.5	0.7	50	0.7	0.9
70	1.5	2.0	50	2.0	2.6
80*	2.0	2.6	50	2.6	3.4
90	2.7	3.5	50	3.5	4.6
100*	4.0	5.2	50	5.6	7.3
125	5.8	7.8	70	7.6	10.0
150	9.5	12.4	80	12.4	18.3
200	16.0	21.0	100	21.0	27.3

* Minimum size where WC's are connected in system II.
** Minimum size where WC's are connected in system I, II, IV.

3 Designing Drainage Systems for Buildings of Various Heights

3.1 Establishing number and types of sanitary appliances with Implementation of design codes

The methodology employed here is to design system configurations using the code and then use this in a validated model to draw generalisations. The case studies chosen span a wide range of building sizes, containing buildings from 10 to 100 stories high. To accurately simulate the drainage system requirements, a scenario with two apartments per floor has been assumed. The apartments include a hand washbasin, WC, bath, shower, kitchen sink, washing machine, and dishwasher. A schematic representation of the

standard floor plan along with the installed sanitary appliances can be seen in Figure 1. The categorization of height in 10 floor steps enables the observation of substantial changes in the system due to variations in the building height.

For each case, the computation of DU/FU was carried out in accordance with the guidelines provided by the four design codes. For an inclusive comparison of the design codes in terms of LU/FU and flow rate, specific guidelines and applications involving different LU/FU values were also considered. For instance, the approach of combining FU for a group of bathroom fixtures (like basin, bath, shower, and WC located in the same room) as recommended in AS/NZS was followed. Thus, for AS/NZS, the total value of FUs were calculated for both individual appliance and group appliance to ensure an impartial comparison across all design codes. Furthermore, to simplify the assessment when applying the BS EN 12056 standard, the analysis was conducted considering only swept entry inletsTable 6 outlines the per-floor discharge unit (DU) values, the cumulative total DU, and the associated design flow rates (in litres per second) for each case study building.
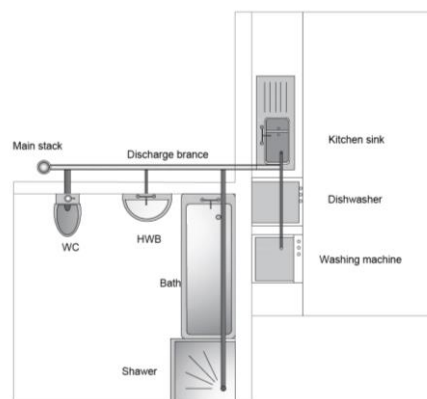

Figure 1 Typical sanitary appliance in a flat

3.2 Calculating design flow rate based on the design codes

After the calculation of DU/FU for a single floor, the total DU/DF for all case study buildings were determined, which then enabled the calculation of the design flow rate. For the BS EN12056 code, the design flow rate was determined from equation () with a frequency factor of k=0.5, under the assumption that the buildings are residential. However, the remaining codes, which provide FU in gallons per minute, the design flow rate was determined based on a conversion curve, commonly referred to as the Hunter curve. For comparison purposes, this was then converted to litres per second. The calculated design flow rates for all the case study buildings are displayed in Table 4.

Table 4 Discharge units and fixture unites for the case study buildings

Number of floors	Discharge Unite in *l/s*			
	I	II	III	IV
Hand wash basin (HWB)	0.5	0.3	0.3	0.3
Bath	0.8	0.6	1.3	0.5
Shower	0.6	0.4	0.4	0.4
WC	2	1.8	1.7	2
Kitchen sink	0.8	0.6	1.3	0.5
Washing machine	0.8	0.6	0.6	0.5
Dishwasher machine	0.8	0.6	0.2	0.5
Total per flat	**6.3**	**4.9**	**5.8**	**4.7**
Total per floor (2 flats)	**12.6**	**9.8**	**11.6**	**9.4**

In order to illustrate the discrepancies in the total flow rate as estimated by each design code, the results have been plotted in Figure 2. The results uncover that the design codes lead to different flow rates for the same building size, with the disparity becoming more pronounced as the size of the building increases. Essentially, as the height of the buildings increases, the divergence in flow rates calculated by the codes becomes increasingly noticeable. This suggests potential inconsistencies in how the codes account for the additional requirements imposed by the increasing building height. These results highlight the necessity for a critical evaluation and comparison of these codes in order to facilitate more accurate and efficient design of drainage systems in high-rise buildings.

Table 5 Calculated design flow rate based on the design code

Number of floors	Design flow rate *l/s*			
	I	II	III	IV
10	5.6	4.9	5.4	4.8
20	7.9	7.0	7.6	6.9
30	9.7	8.6	9.3	8.4
40	11.2	9.9	10.8	9.7
50	12.5	11.1	12.0	10.8

3.3 Determining drainage pipe size according to the design codes

All design codes provide essential information to correctly determine the size of the drainage pipe based on the LU/FU. However, each design code provides specific guidelines and considers different factors when determining the drainage pipes. In this analysis, the focus is solely on the main vertical pipes, excluding the discharge branches. The recommended pipe size for each case study building, keeping the same type and number of appliances, was then determined. Similar to the flow rate calculation, the assessment was undertaken for a range of building heights, spanning from 10 to 100 storey buildings. Table 8 presents the suggested pipe diameters (in millimetres) for various types of building drainage systems and different building heights, in accordance with the four plumbing codes i.e. BS EN 12056, AS/NZS, IPC, and UPC.
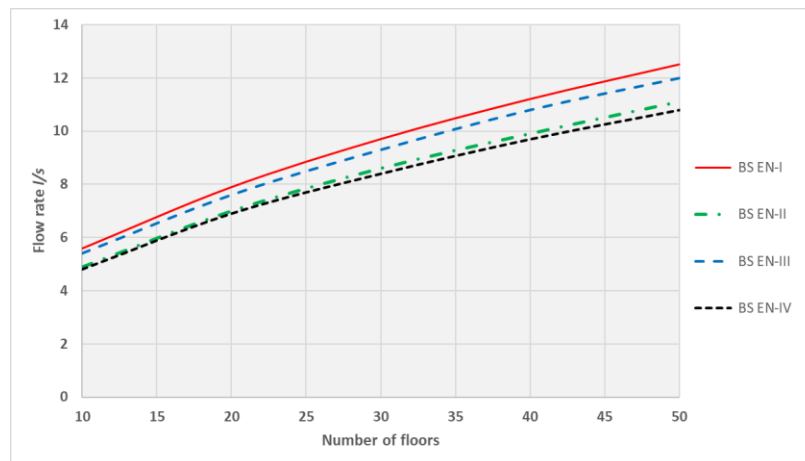
Figure 2 Design Flow Rates Calculated by Different Design Codes for Buildings of Various Heights

Overall, the results clearly indicate that the pipe sizes recommended by BS EN 12056 for multi-storey buildings differ considerably from those suggested by other codes. These differences can be attributed to three main unique features of the BS EN 12056 approach: Firstly, unlike other codes that recommend a separate vent pipe, BS EN 12056 also offers an option for a single stack. Secondly, it includes a frequency factor in calculating the flow rate, which generally results in a lower flow rate for residential buildings, the focus of this case. Lastly, it considers different types of entries - swept or square - which have an impact on the system's characteristics. It is also observable that within the same code (BS EN 12056), different results are achieved for the same building scale, depending on the type of system used. For example, for 10-storey buildings, the pipe sizes recommended are 100 mm for systems II and IV, and 125 mm in system I and III. This variability lessens when the pipe size increases, i.e., for 150 and 200 mm pipes.

The AS/NZS guidelines suggest incorporating a relief vent into any stack when there is at least one floor difference between the highest and lowest branch pipes linked to that stack. In addition, the UPC recommends the installation of a parallel vent pipe for every drainage system that extends ten meters or more above either the building drain or another horizontal drain. In the same way, the International Plumbing Code (IPC) of the United States specifies that in buildings where soil and waste stacks surpass ten branch intervals, it's necessary to install a relief vent at every tenth interval, commencing from the topmost floor. Thus, in the case of the modified one pipe (MOP) system or secondary vent, the main stack sizes determined by BS EN 12056 differ obviously from those recommended by all other codes. This difference often results in a main stack size that is at least one size smaller. The difference is more noticeable when it comes to vent pipe sizes, which are often half as small in some instances. Despite the fact that AS/NZS, UPC, and IPC all consider building height by choosing a vent pipe size based on the developed length of the vent pipe, they cover a broad range of developed lengths which necessitates further examination. For example, when using a 100mm vent pipe, the height range varies drastically from 5.5 meters to 299 meters, depending on total FUs and the size of the main stack. This suggests that the flow rate continues to exert significant influence on pipe size selection. In summary, there is a clear distinction between the various design codes, specifically between BS EN 12056 and all the other codes. This variation is particularly notable in how they handle the design and sizing of drainage systems. The results

presented provide a comparative overview, assisting in the selection of the most suitable drainage system design and pipe sizing. This is crucial to ensuring efficient performance in high-rise buildings.

Table 6 Drainage Pipe Sizes Based on Different Codes for Various Building Heights

Building height	Type of System	Stack /vent	Size of pipe DN in mm BS EN 12056			
			I	II	III	IV
10	SS	Stack	125	100	125	100
	MOP	Stack	100	100	100	100
		Vent	50	50	50	50
20	SS	Stack	150	125	150	125
	MOP	Stack	125	100	125	100
		Vent	70	50	70	50
30	SS	Stack	150	150	150	150
	MOP	Stack	125	125	125	125
		Vent	70	70	70	70
40	SS	Stack	150	150	150	150
	MOP	Stack	150	125	150	125
		Vent	80	70	80	70
50	SS	Stack	200	150	150	150
	MOP	Stack	150	150	150	150
		Vent	80	80	80	80

4 Investigation of Building Drainage Systems through Simulations

4.1 Application of AIRNET

The previous results thus far strongly emphasize that there are not universally accepted, comprehensive methodologies for designing BDS, especially when it comes to the complexities of high-rise buildings. The disparity in approaches is largely rooted in the complexities of the system and a lack of sufficient data that allows for the incorporation of all influencing factors during the design phase. Key characteristics of BDS operation include air pressure transients, the pattern and magnitude of airflow within the system, and the depletion of trap seals. These elements, integral to the system's functionality and efficiency, demand a nuanced understanding.

To overcome this limitation and to provide a more comprehensive insight into the behaviour of these systems, simulation tools such as AIRNET can be used. AIRNET is a 1-D finite difference, method of characteristics model specifically adapted to simulate Building Drainage Systems (BDS) in tall buildings, using the method of characteristics for its computations. This model allows for a more in-depth exploration of system behaviour under different conditions and can offer valuable insights into how different variables affect overall system performance. While a comprehensive exploration of AIRNET's functioning will not be provided here, as it has been discussed in previous

studies such as (Swaffield and Campbell, 1995; Swaffield, 2010; Gormley and Kelly, 2018; Gormley *et al.*, 2021) , interested readers can refer to a recent and more related discussion aligning with the current research in the study by (Gormley *et al.*, 2021).

4.2 Validation of AIRNET

The model AIRNET has been validated in general elsewhere as described above, however, following modification to incorporate specific algorithms for application to tall buildings, a re-validation exercise was carried out based on data from the NLT test facility.

Figure 3 shows the validation of a classical pressure profile for a set of flow conditions detailed in Figure 3 (a) whilst the measured against predicted profiles is shown in Figure 3 (b). It can be seen that agreement is close and therefore it can be taken that the model works for taller buildings.

| (a) | (b) | (c) |
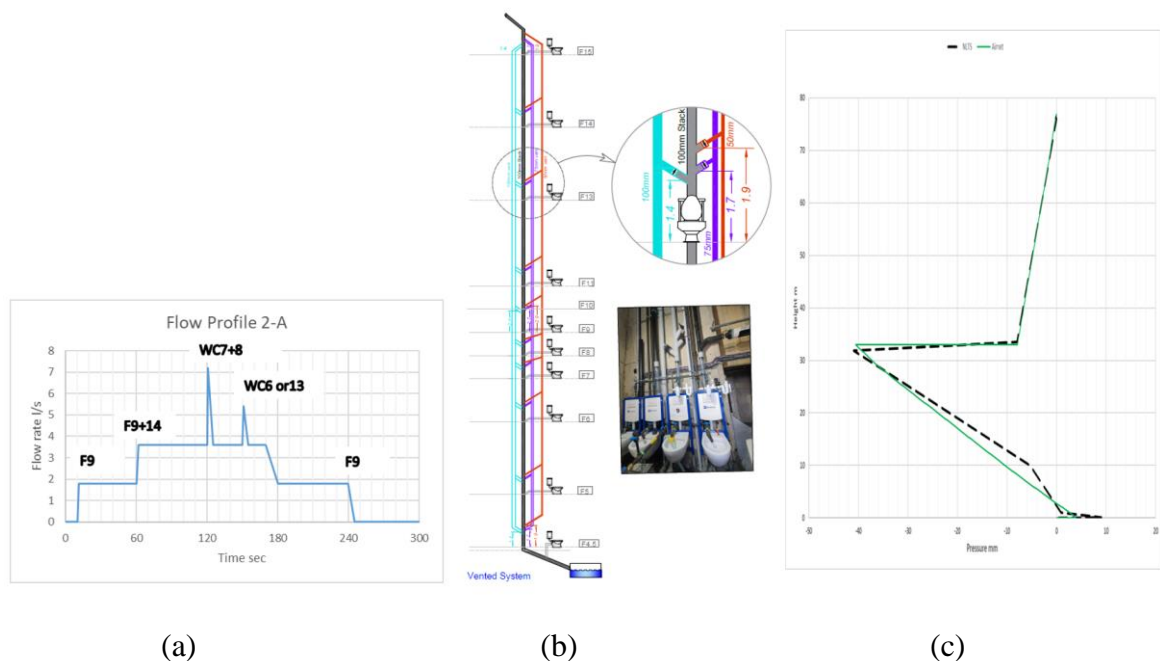
Figure 3. Validation setup at NLT. The water flow regime is shown in (a), a schematic of the system is shown in (b) and the measured vs predicted classical pressure profile is shown in (c).

4.3 Assessment of BDS for Buildings of Different Heights

Achieving real data and applying it using AIRNET can offer vital insights for assessing current design codes for drainage systems. Thus, the NLT was chosen as a case study to help determine the sizing of these systems based on the recommendations specified in these design codes. Then, an in-depth investigation of the system's characteristics was conducted to uncover its strengths and limitations using AIRNET simulation. We chose three scenarios to measure and model – Modified One Pipe, Single Stack and Fully Active.

Table 6 provides a comprehensive overview of how the design code recommends drainage pipe sizes for both Single Stack (SS) and Modified Open Pipe (MOP) systems. However, the code does not clearly address how building height is considered, as

increases in system size seem to be due to cumulative flow rates corresponding with an increased number of sanitary appliances. This implies that as the number of floors (and thus appliances) increases, the total flow rate also rises. To examine system characteristics at varying heights, AIRNET was applied to buildings ranging from 10 to 50 storeys. Assuming a flow rate of 5.2 l/s for a 10-storey building, the drainage system was simulated for various heights. It is important to note that, according to the design code (as shown in Table 3), the recommended pipe design for a flow rate of 5.2 l/s is a 100mm SS or a MOP with a 100mm main stack and a 50mm vent.

Figure 4 presents the effects of building height on system performance. Figure 4(a) shows the variation of pressure regimes with building height for both Single Stack (SS) and Modified Open Pipe (MOP) configurations. The results demonstrate a noticeable increase in both positive and negative pressures as the height of the building increases when using the SS configuration (represented by solid lines) without any vent pipe. Specifically, the positive pressure ascends from 45mm wg for a 10-storey building to 58mm wg in a 50-storey building, and the negative pressure rises from -24mm wg for a 10-storey building to -32mm wg for a 50-storey building. On the other hand, the air pressure change in MOP systems is relatively less significant; the positive pressure shifts from 38mm wg to 45mm wg, and the negative pressure modifies from -8mm wg to -10mm wg.

This lower pressure variation in the MOP system can be attributed to the mitigating effect of the 50mm vent pipe, which helps balance the pressure from the 5.2 l/s flow rate across the entire system. However, despite this less significant change in MOP systems, it should be noted that this difference might become more prominent with the increase in flow rate.
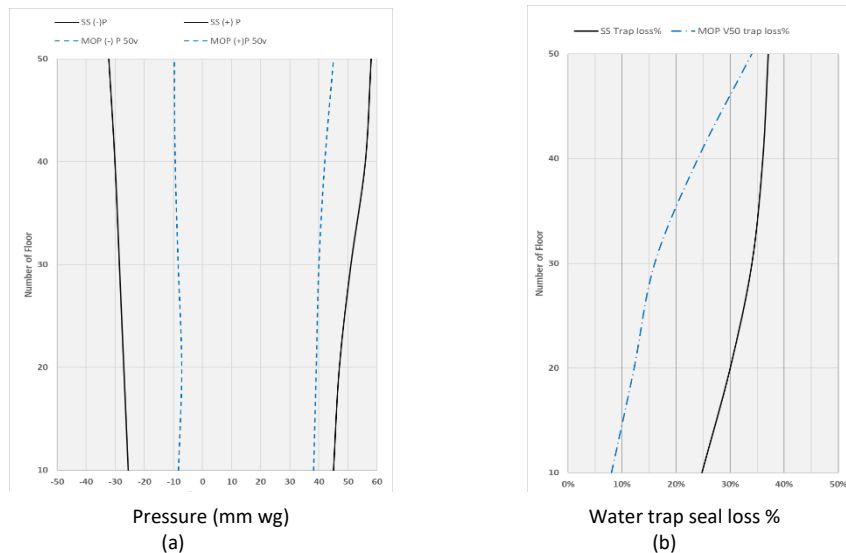

Figure 4 Effect of height on system performance. (a) Positive and Negative Pressures (max-min) in Buildings from 10 to 50 Storeys and (b) Percentage of water depth lost for various building heights.

To evaluate the impact of building height on the drainage system, particularly regarding trap seal depletion, data from AIRNET was used. This information was used to assess the retained water depth in a trap following an event throughout the system. Figure 4 (b) illustrates the percentage of the remaining water trap seal depth after a flow rate of 5.2 l/s is applied in buildings ranging from 10 to 50 storeys. The graph highlights trap seal loss

in both Single Stack (SS) and Modified Open Pipe (MOP) systems across varying building heights. Overall, results align with the pressure variations shown in Figure 3, indicating that both pressure and trap seal loss incrementally increase with building height.

For the SS system (represented by solid lines), trap seal loss starts at 25% for 10-storey buildings and increases to 37% for 50-storey buildings. It is important to note that trap seal loss ideally should not exceed 25%. Hence, even though a 100mm SS is recommended by the code, it proves to be an unsafe option for buildings rising above 50 storeys.

Conversely, the MOP system presents significantly less trap seal loss when the building height is limited – only 7% for a 10-storey building. However, the trap seal loss percentage markedly amplifies with increasing building height, reaching 34% for 50-storey buildings. This implies that the risk of trap seal loss intensifies considerably with the increase of building height.
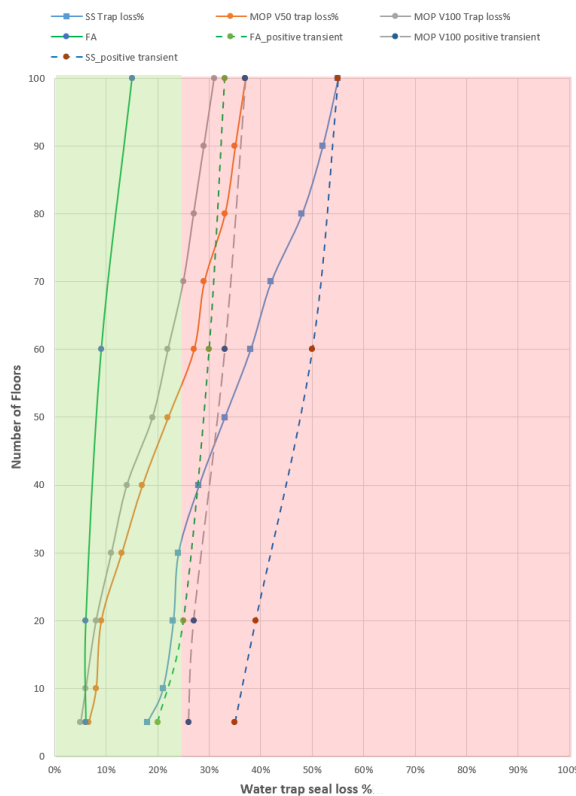
Figure 5. Full suite of configurations subjected to positive and negative pressure transients in a system of heights from 5 – 100 floors with same flow rate (5.2l/s) Green portion would pass and red portion would fail.

Figure 5 shows the full range of possible outcomes when increasing height from 5 floors to 100 floors. It can clearly be seen that all configurations perform worse with height, thus proving that building height requires additional attention in terms of design codes. Overall, the active ventilation options performs best since air and pressure relief is provided at the point of need, and therefore distributed across the height of the building.

5   Conclusions

It has become increasingly important to understand and optimize the design of BDS systems specifically for tall buildings.

Although the BS EN 12056 provides valuable recommendations for BDS, its application is somewhat limited when considering tall buildings. The research findings indicate that with an increase in building height, the risk of trap seal loss increases also, which can lead to cross-contamination, posing health hazards for the building's occupants.

Modelling offers an opportunity to draw conclusions over a greater range of building systems and configurations. In this research, AIRNET has been validated using real-world data from a comprehensive test facility in Northampton, UK. This has allowed the effects of height of building and pipe length to be incorporated into design code assessments for the first time.

Building height has been shown to be an important factor in the provision of safe sanitation in tall buildings. Current codes and standards do not adequately deal with this phenomenon and this should be rectified.

6   Acknowledgements

7   References

BS EN 12056-2 (2000) 'Gravity Drainage systems inside Buildings. Sanitary Pipework, Layout and Calculatioin', in. London: BSI.

Gormley, M. *et al.* (2021) 'Building Drainage System Design for Tall Buildings: Current Limitations and Public Health Implications', *Buildings*, 11(2), pp. 70-undefined. doi: 10.3390/buildings11020070.

Gormley, M. and Kelly, D. A. (2018) 'Pressure transient suppression in drainage systems of tall buildings', *Building Research and Information*. doi: 10.1080/09613218.2017.1412097.

Hunter, R.B. Methods of estimating loads in plumbing systems. US Department of Commerce, National Bureau of Standards. BMS 1940, 65, 17.

Lillywhite, M.S.T.; Wise, A.F.E. Towards a General Method for the Design of Drainage Systems in Large Buildings; Building Research Station Report (BRS): Watford, UK, 1969.

Mohammed, S.; Jack, L.B.; Patidar, S.; Kelly, D.A. Defining the oversizing problem and finding an optimal design approach for water supply systems for non-residential buildings in the UK. In Proceedings of the CIB W062 International Symposium on Water Supply and Drainage for Buildings, São Miguel, Portugal, 28–30 August 2018.

Omaghomi, T.; Buchberger, S.; Cole, D.; Hewitt, J.; Wolfe, T. Probability of water fixture use during peak hour in residential buildings. J. Water Resour. Plan. Manag. 2020, 146, 04020027. [

Swaffield, J. (2010) *Transient Airflow in Building Drainage Systems*. London: Spon.

Swaffield, J. A. and Campbell, D. P. (1995) 'The simulation of air pressure propagation in building drainage and vent systems', *Building and Environment*, 30(1), pp. 115–127. doi: 10.1016/0360-1323(93)E0006-Y.

Verma, N.K.; Chakrabarti, S.P.; Khanna, P. Modified one-pipe system of drainage for tall buildings. Build. Environ. 1976, 11,197–201.

Wise, A.F.E.; Croft, J. Investigation of single-stack drainage for multi-storey flats. J. R. Sanit. Inst. 1954, 74, 797–826.

Wise, A.F.E. Design factors for one-pipe drainage. J. R. Sanit. Inst. 1954, 74, 231–241.

Whipple, G.C.; Carson, H.Y.; Hanley, T.F.; Groeninger, W.C.; Gries, J.M.; Cartwright, F.P.; Hansen, A.E. Recommended Minimum Requirements for Plumbing in Dwellings and Similar Buildings: Final Report of Subcommittee on Plumbing of the Building Code Committee. US Department of Commerce, 3 July 1923. Available online: https://nvlpubs.nist.gov/nistpubs/Legacy/BH/nbsbuildinghousing2.pdf (accessed on 1 July 2023).

Wyly, R.S.; Eaton, H.N. Capacities of Stacks in Sanitary Drainage Systems for Buildings (No. 31); US Department of Commerce, National Bureau of Standards: Washington, DC, USA, 1961.

Wyly, R.S.; Parker, W.J.; Rorrer, D.E.; Shaver, J.R.; Sherlin, G.C.; Tryon, M. Review of Standards and Other Information on Thermoplastic Piping in Residential Plumbing; US Department of Commerce, National Bureau of Standards: Washington, DC, USA, 1975; Volume 68.

8   Authors

Dr Sarwar A Mohammed is a post-doctoral researcher in the Public Health and Environmental Engineering group at Heriot-Watt University, UK. His research focuses on Building Drainage Systems in high-rise buildings, as well as on water supply systems.

Michael Gormley is Professor of Public Health and Environmental Engineering at the School of Energy, Geoscience, Infrastructure and Society at Heriot-Watt University. His research specialisms are: mathematical modelling of air and water flows in building drainage systems, infection spread via bioaerosols and product development.

Dr. Colin Stewart is a Research Associate in the Public Health and Environmental Engineering group at Heriot-Watt University. He has a PhD fluid mechanics and has worked for many years in the fields of fluid mechanics in drainage systems, water systems and oil and gas systems.

Dr David Kelly is Associate Professor of Architectural Engineering and a member of the Public Health and Environmental Engineering group at Heriot-Watt University.His research interests include the monitoring and prevention of cross-contamination from building drainage systems. within buildings.

Dr. David Campbell has a BSc Biochemistry and PhD Mathematical Modelling. He is a member of the Public Health and Environmental Engineering group at Heriot-Watt University with continuous research activity in the field of water supply and drainage in the built environment.

DHW production for collective residential buildings: development of a sizing method

B. Poncelet (1), B. Bleys (2)

(1) benoit.poncelet@buildwise.be

(2) bart.bleys@buildwise.be

(1), (2) Buildwise (ex-Belgian Building Research Institute), Belgium.

Abstract

In a previous paper presented at the 2022 CIB Symposium[1] the Buildwise research team compared different sizing methods for DHW production for several multi-family residential buildings, commonly applied in Belgium. Considering the discrepancies between the results obtained by those methods, it was concluded that further research was needed to determine a unanimous sizing method.

This article presents the development of such a method, which consists in four steps:

1- Creation of demand profiles according to the number of apartments;
2- Creation of several dynamic simulation environments to calculate the thermal load necessary for the production of DHW to meet these maximum draw profiles. Each environment corresponds to an usual approach to produce DHW (instantaneous approach, semi-instantaneous, etc.);
3- Evaluation of the impact of the considered assumptions on the results by a sensitivity study.
4- Results and definition of typical power-volume curves (PV-Curves).

Keywords

Domestic hot water production, DHW sizing, draw profiles, dynamical simulations.

---

[1] . B. Poncelet, B. Bleys 'DHW production sizing: comparison of the results of different standards and methods.', 2022 Symposium CIB W062, 2022

1 Introduction

Quantitative and qualitative analysis of sizing methods for domestic hot water production in countries bordering Belgium has shown that the results are very different for a given building.

It is therefore difficult to establish which method would be the most accurate and adapted for determining the heat load required to prepare domestic hot water in multi-dwelling buildings in Belgium.

In order to avoid arbitrarily defining the best available approach, Buildwise has developed its own calculation method for defining this thermal load as a function of :

- typical drawing profiles based on hot water consumption measurement campaigns in Belgium;
- different hydraulic configurations.

This article presents the development of such a method, which consists in four steps:

1- Creation of demand profiles according to the number of apartments;
2- Creation of several dynamic simulation environments to calculate the thermal load necessary for the production of DHW to meet these maximum draw profiles. Each environment corresponds to an usual approach to produce DHW (instantaneous approach, semi-instantaneous, etc.);
3- Evaluation of the impact of the considered assumptions on the results by a sensitivity study.
4- Results and definition of typical power-volume curves (PV-Curves).

This method was developed as part of a research project called "OptiDim".

2 Demand profiles

The drawing profiles considered have a fundamental impact on the sizing of domestic hot water preparation systems:

- over-secure draw profiles lead to oversizing of the system, with the main consequence being increased energy consumption and reduced water quality due to insufficient renewal of the stored water.
- undervalued drawing profiles mean undersizing, which can lead to complaints about lack of comfort.

The draw-off profiles constructed were based on measurement campaigns carried out by Buildwise since 2011. To be sufficiently safe while avoiding oversizing the installations, it was decided to consider "maximum consecutive draw profiles". In concrete terms,

based on the measurement campaigns, the aim is to determine the maximum consecutive flow rates observed over a set period of time (= resolution).

This method is explained in more detail below.

2.1 Step 1

For each measurement campaign, the drawing profile is established day by day and according to a given time step. The hot water flow rate is converted into the energy required to create an energy/time graph.

For the OptiDim project, this time step was taken to be 1 minute.
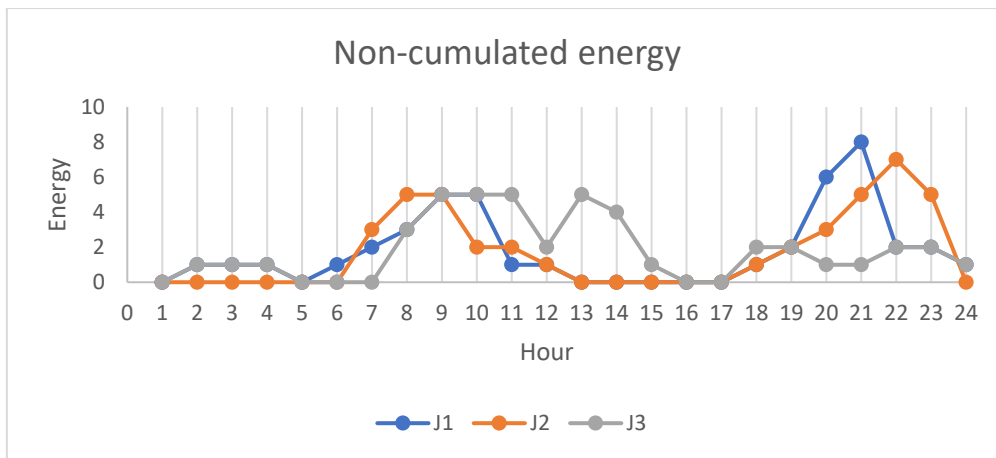
2.2 Step 2

For each day measured, it is then necessary to sum up the energy consumption required for different time resolutions. In other words, the sum is "sliding" until it covers a full day. This same operation is repeated for each day of the measurement campaign.

For the OptiDim project, the resolutions considered are 1,2,3,5,10,20,30,45,60,...,420, 435,1440 minutes.
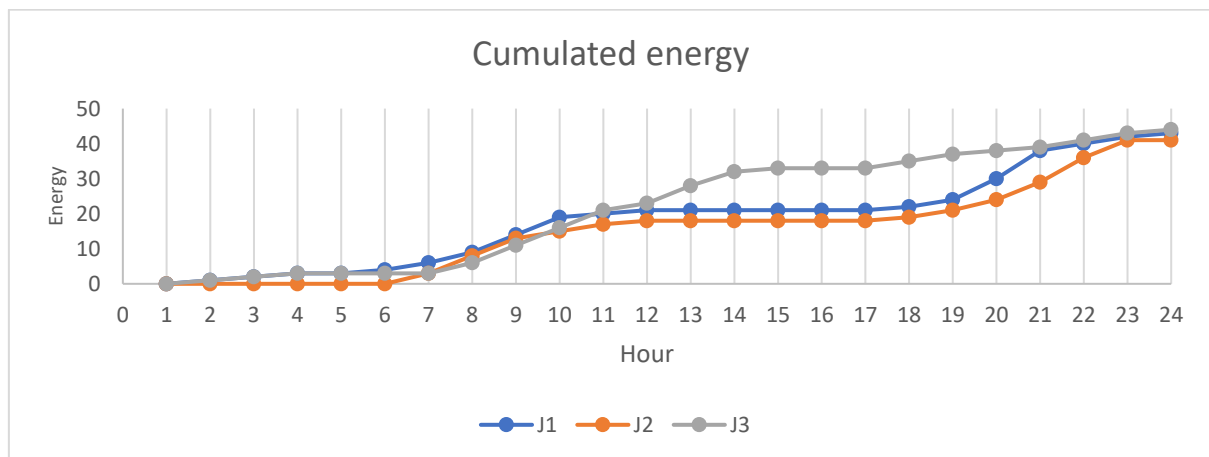
2.3 Step 3

The maximum energy consumption is determined for each day and for each resolution. Then, for each resolution, we consider the maximum energy consumption value of all the days measured. In this way, a fictitious day is reconstructed, with maximum energy consumption for the different resolutions considered.
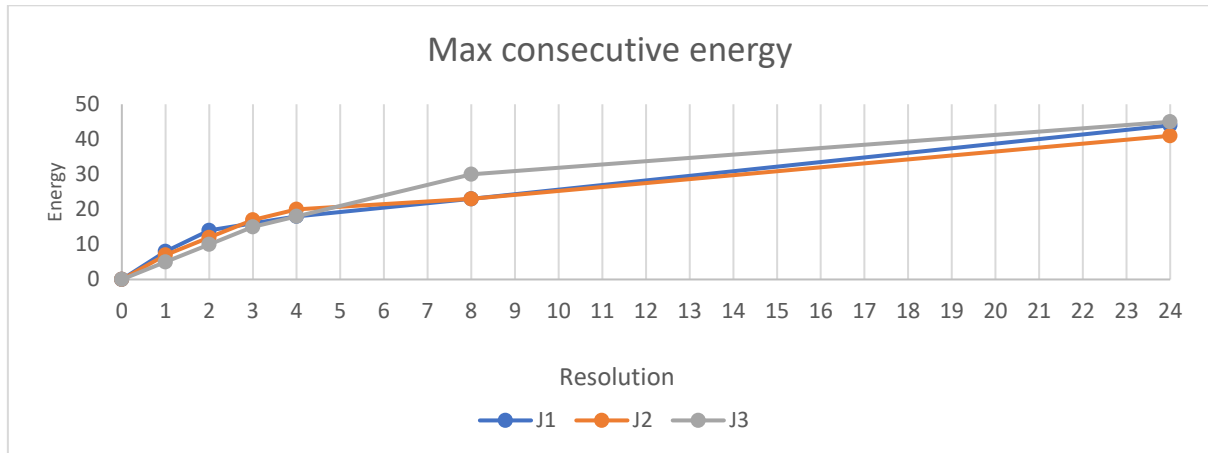
2.4 Step 4

We create a profile of maximum consecutive draws, corresponding to the maxima of all energy demands for each resolution. This curve reflects the most restrictive energy demands encountered during the measurement campaign, for all resolutions.
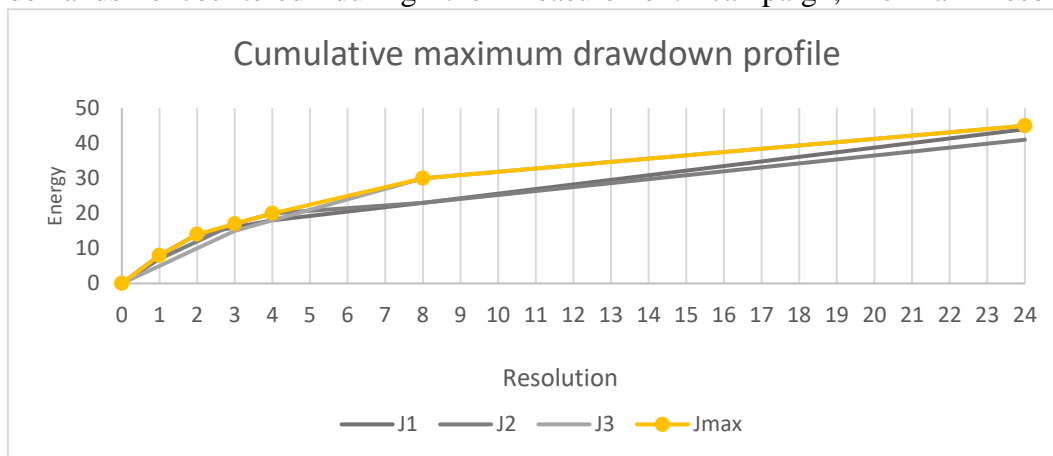
2.5 Step 5

Based on the cumulative maximum consecutive draw profile, a non-cumulative maximum consecutive draw profile is created. To do this, the following assumptions must be made:

- Definition of the duration of peak consumption over the day. This duration generally varies according to the number of dwellings. In the OptiDim project, the

duration of peak consumption was determined in accordance with DIN 4708, since it corresponded fairly well to that observed in the measurement campaigns.
- The start or end of the peak consumption period is determined arbitrarily. This definition has no bearing on the calculations, but it does enable us to construct a more illustrative graph.

Then, from the start of the peak consumption period, the energy consumption for each resolution is applied until the end of the peak consumption period.

Outside the peak consumption period, the remaining energy required for domestic hot water production is distributed evenly over the off-peak hours. Again, this assumption is purely arbitrary, but also has little impact on the results (since it is mainly the first peak consumption that is dimensional).
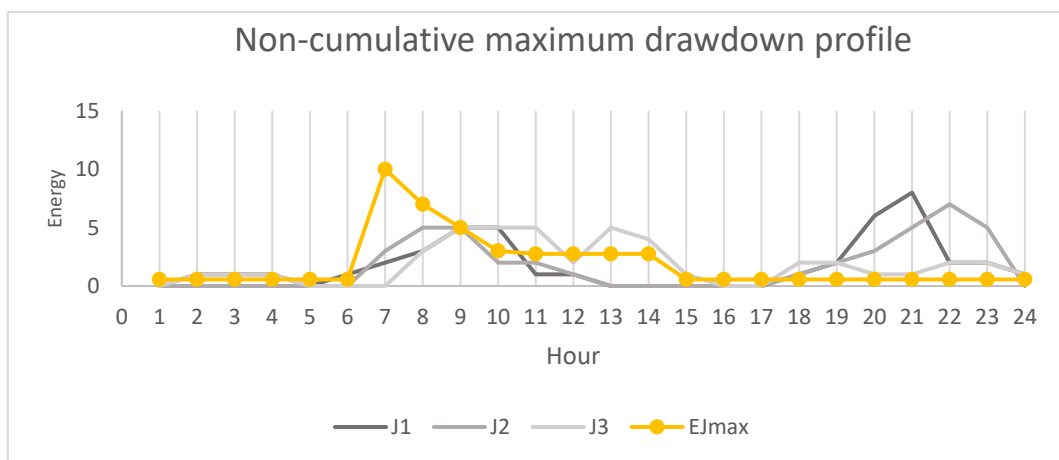
2.6 Step 6

The energy of each morning is added together to form a cumulative daily profile of maximum consecutive drawdown energies.
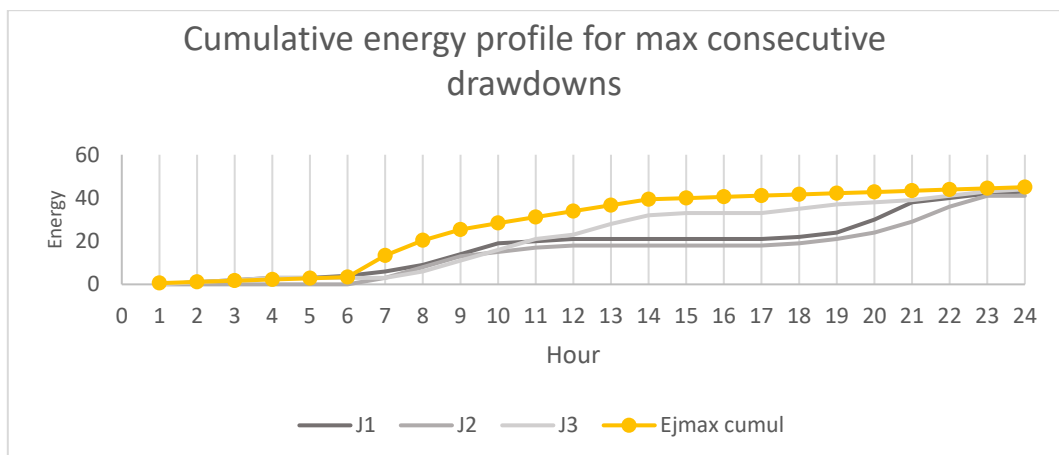
On this curve, we can see that :

- The slope of the yellow curve is steep enough to be safe. This slope is particularly important when sizing instantaneous systems;

- After 24 hours, the maximum energy demand for domestic hot water preparation is no higher than the profiles observed during the measurement campaigns. This value is particularly important for storage systems.

2.7 Step 7

In order to make these profiles as standard as possible, it is useful to take into account current statistical and normative data.

As part of the OptiDim project, it was decided to :

- Adapt the maximum flow rate measured so that it is identical to that provided by DIN 1988-300, since the measurement campaigns carried out gave maximum flow rates close to this standard.
- Adapt the volumes of hot water consumed per day according to statistical data on hot water consumption in Belgium (i.e. 35 l per day per person at 60°C).
  - If the daily volume supplied by the measurement campaign is lower than the standard daily volume, an increase in the daily volume is applied.
  - If the daily volume supplied by the measurement campaign is greater than the standard daily volume, no change is made..

3 Dynamic simulation environments

3.1 A dynamic calculation

Given the transient phenomena that characterize the production and consumption of domestic hot water, it is necessary to calculate the required thermal load dynamically. The time step must be short enough to take into account short-duration, large-scale draw-offs.

In the OptiDim project, this time step was set at one minute. This time step is relatively long, but acceptable given that the project is being carried out for collective installations with relatively high inertia (thanks, among other things, to the domestic hot water loop, which is almost always present in this type of building).

3.2 Several hydraulic configurations

Preliminary calculations and recent literature on the subject have shown that the sizing of a domestic hot water system also depends on the type of hydraulic configuration chosen by the designer.

It is therefore useful to develop as many dynamic models as the hydraulic design envisaged.

As part of the OptiDim project, a catalog of hydraulic diagrams was drawn up to illustrate the different ways in which domestic hot water can be produced in Belgium. In the end, some ten basic dynamic models were created:

| ID	Type
T10	Instantaneous production with plate heat exchanger
T21	Production with internal exchanger in a domestic hot water tank
T22	Production with internal exchanger in a technical water storage tank
T23	Production with internal exchanger in 2 domestic hot water tanks in series
T24	Production with internal heat exchanger in 2 hot water cylinders in parallel
T31	Production with external heat exchanger and domestic hot water cylinder
T32	Production with external heat exchanger and technical water cylinder
T33	Production with external heat exchanger and 2 hot water cylinders in series
T34	Production with external exchanger and 2 hot water cylinders in parallel
T40	Pure storage heating with internal heat exchanger
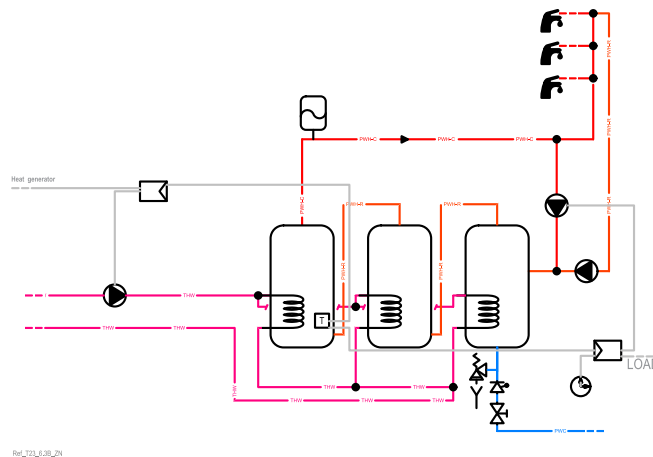
Figure 2: illustration of a proposed hydraulic design

3.3 Calibration

To validate these dynamic simulation models, it is generally recommended to perform calibrations. In concrete terms, this involves :

- Establishing a detailed measurement campaign using a series of sensors (temperature, flow and energy) on an existing installation;
- establishing a dynamic simulation model as close as possible to the existing installation;
- compare whether the physical quantities derived from the simulation model match those measured. If this is the case, we need to understand and/or adapt the model so that the evolution of the physical quantities corresponds to what has been measured.

As part of the OptiDim project, calibration focused on the thermal behavior of domestic hot water storage tanks, with or without internal heat exchangers. This is an important component of the system, which is complex to simulate. Dynamic simulations were carried out using TRNSYS software with the 534 type module (storage tank).
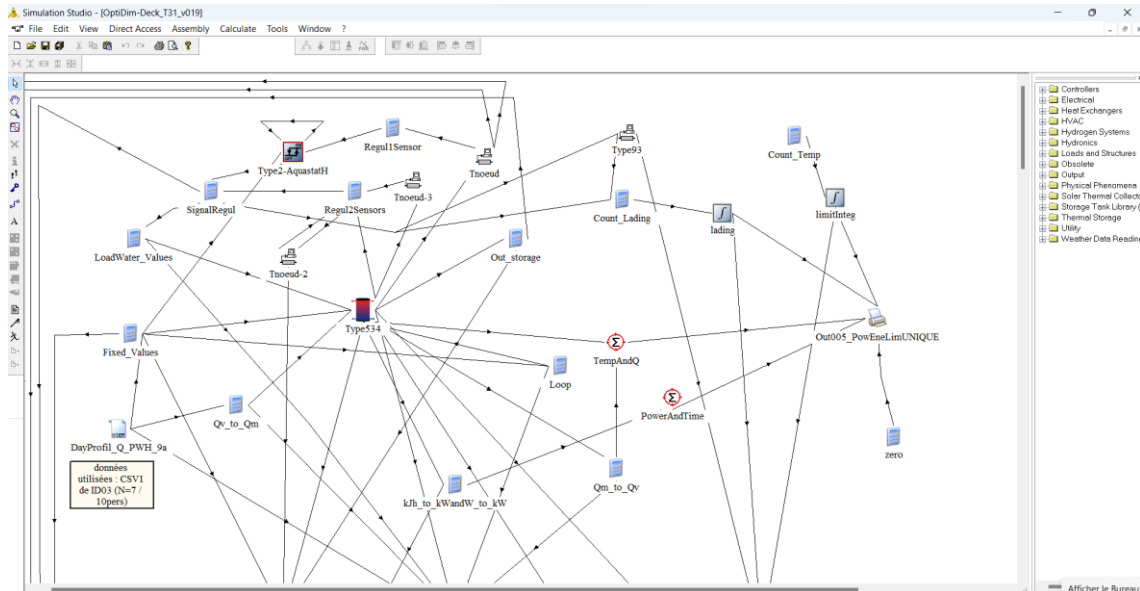

Figure 3: illustration of a dynamic model (TRNSYS).

4 Sensitivity study of the considered assumptions.

When creating the basic models for dynamic simulations, a series of assumptions were considered.

In the OptiDim project, for example, the following parameters were considered for an installation with a domestic hot water storage tank and an external heat exchanger:

- Storage tank volume
- Cold water temperature at heat exchanger inlet
- Domestic hot water loop flow rate
- Storage tank insulation
- Production reactivity (time difference between heat demand and arrival of technical hot water at exchanger inlet on primary side)
- Position of loop return in relation to storage tank (top, middle or bottom)
- Percentage of primary load nominal flow rate
- Number of sensors to control load start-up and shut-down
    - o If only one sensor:
        - ▪ Position of this probe (top, middle or bottom)
        - ▪ Hysteresis to define load ON/OFF

- o if 2 sensors:
  - ▪ temperature difference between the 2 sensors to define load ON/OFF
- Position of charge flow inlet in storage tank (top 2/3 of storage tank or top of storage tank).
- Charge pump operation: fixed, variable, continuous or intermittent flow.
- Charge flow temperature
- Setpoint temperature at primary heat exchanger inlet
- Heat exchanger temperature drop on primary side

The parameters are numerous, and so are the assumptions. Sensitivity studies are therefore extremely important, as they reveal, among other things:

- Which parameters have the greatest impact on the sizing of domestic hot water production;
- Possible encoding errors;
- The effectiveness or otherwise of certain control modes;
- The best way to design the system.

The optimum installation was defined as one that met four requirements:

- Maintain the required temperatures to ensure comfort and legionella control (60° at the storage tank outlet and 55° at all points in the system).
- Reduced energy consumption for domestic hot water production
- Reduced number of on/off cycles (minimum 15 min heat generator operation)
- Heat generator switch-off once a day (avoid continuous operation of the heat generator)

5 Results PV-Curves

To characterize the thermal load required for domestic hot water production, 3 types of results are provided:

- for instantaneous production systems: only the power is provided, as there is no energy storage
- for semi-instantaneous systems (with hot water storage or 2 techniques, with or without internal exchanger), power-volume curves have been used. This type of curve is explained in the IBC 2022 article "DHW production sizing: comparison of the results of different standards and methods". These curves allow designers to choose from a wide range of possibilities between power and volume.
- for pure storage systems: a single storage volume and a single power output.

The SWW2.0 research project has developed a computer application that allows anyone to obtain the above-mentioned results by answering a dozen simple questions. This application is freely available at the following link : https://waterdim.buildwise.be.

Each result is associated with a hydraulic diagram on which the user can receive information and advice by clicking on the various components of the installation.
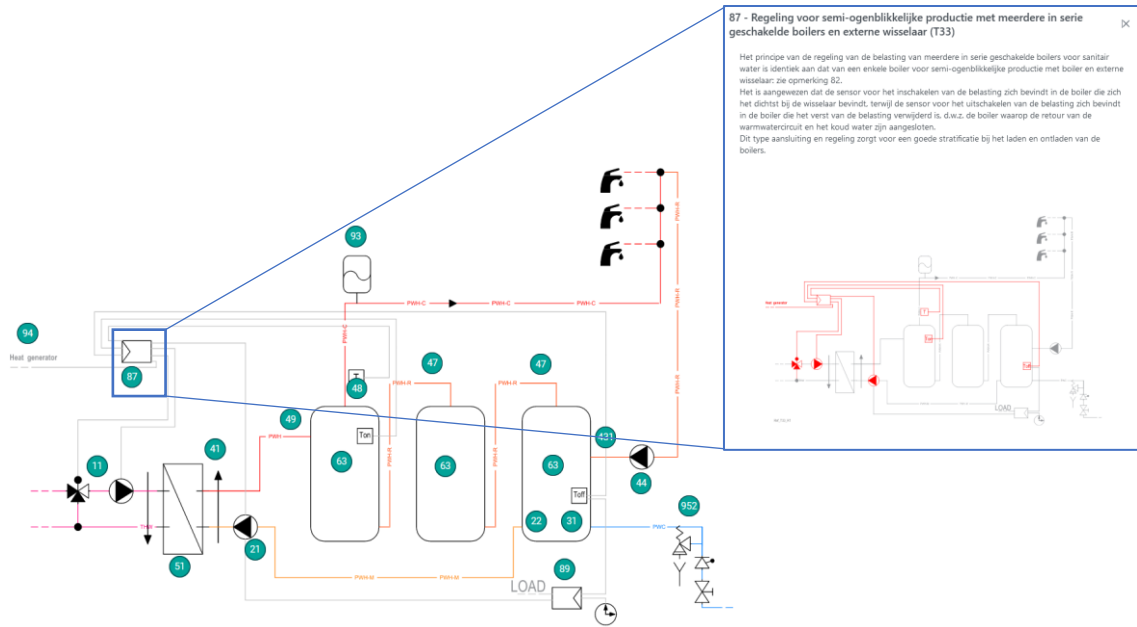
7 References

Assosiaction des ingénieurs 'Eau Chaude Sanitaire: concevoir les systèmes en climatique, ventilation et froid', 2004.

Cadoret Baeckeroot Georges & Jean-Michel 'Mode de calcul des installations d'eau chaude sanitaire', 2011.

COSTIC 'Guide technique: Les besoins d'eau chaude sanitaire en habitat individuel et collectif', 2016.

Deutsche Institut für normung 'Technische Regeln für Trinkwasser-Installationen - Teil 300: Ermittlung der Rohrdurchmesser; Technische Regel des DVGW',2012.

Deutsche Institut für normung 'Zentral Wassererwärmungsanlagen: Begriffe und Berechnungsgrundlagen', 1994.

Deutsche Institut für normung 'Zentrale Erwärmungsanlagen: Regeln zur Leistungsprüfung von Wassererwärmern für Wohngebäude', 1994.

Deutsche Institut für normun 'Zentrale wassererwärmungsanlagen: Regeln zur Ermittlung däs Wärmebedrafs zur Erwärmung von Trinkwasser in Wohngebäuden', 1994.

Kennisinstituut voor de installatiesector 'ISSO publicatie 55: Leidingswaterinstallaties voor woon- en utiliteitsgebouwen', 2013.

NBN 'Energy performarnce of buildings - Method for calculation of the design heat load - Part 3: Domestic hot water systems heat load and charachterisation of needs, Module M8-2, M8-3', 2017

A methodology to design Domestic Hot Water Production Systems Based on Tap Patterns, Y Verhaert - B Bleys - S Binnemans - E Janssen, ?

Guide au dimensionnement des appareils de production d'eau chaude sanitaire, Institut Wallon A.S.B.L., 2008

Presentation of Author(s)

Benoit Poncelet is engineer in architecture and project leader in the laboratory water technologies of the Belgian Building Research Institute (BBRI).

Bart Bleys is bioengineer and head of the laboratory water technologies of the Belgian Building Research Institute (BBRI).

The need for a new approach to the assessment of water demand loading, post-Covid, for office buildings

L.B. Jack (1), S. Fernandez (2), S. Dass (3) and C. Rogers (4)

(1) L.B.Jack@hw.ac.uk
(2) SF2000@hw.ac.uk
(3) S.Dass@hw.ac.uk
(4) CR99@hw.ac.uk

(1, 2, 4) Institute of Sustainable Built Environment, School of Energy, Geoscience, Infrastructure and Society, Heriot-Watt University, Edinburgh, UK.

(3) School of Mathematics and Computer Science, Heriot-Watt University, Malaysia

Abstract:

Many things have changed since the outbreak of Covid-19, and the impact that the pandemic has had on global society is wide-reaching. One key aspect of behaviour change that directly influences the determination of water demand loading figures for buildings is a shift in occupancy. This has the potential to directly impact the calculation of simultaneous design flow for a building.

This paper examines how a change in office occupancy might alter the resultant demand profile. Based on available literature, an assessment is made of how office occupancy has shifted as a result of the pandemic. These changes are then discussed within the context of loading unit calculations and corresponding simultaneous design flow estimates.

This paper shows the importance of having access to robust occupancy data alongside a meaningful estimate of the probability of use of fixtures. Furthermore, an accurate method of water demand estimation is also required; one that reflects volumetric consumption for fixtures. This paper articulates the challenges in representing a change in occupancy within the estimated design flow calculation. It shows how the number of factors for which robust information is required makes this estimation particularly difficult, especially given that we already know the extent of overestimation typically embedded in existing design codes. The paper hence makes the case for a new method based on machine learning techniques that will allow the flexibility to change parameters from a hypothetical perspective but for which validation can be attained through access to commonly available consumption data.

Keywords

Water demand, loading units, Covid-19, occupancy.

1   Introduction and background

The ability to be able to predict peak water demand within a building is one that has challenged design engineers for many decades. Understanding the diverse nature of the appliances fitted within a building and more so, the likelihood of their simultaneous use, has been the focus of attention for many research teams globally. More recently, this challenge has intensified as user behaviour has seen considerable change, alongside the introduction of a wide range of more water-efficient appliances (Pieterse-Quirijns et al, 2013, Kelly, 2015). With an evolving demographic and a continued push for water conservation, there is more need than ever before for an accurate and accessible prediction method.

The consequences of a lack of method, or of its accuracy, can be wide-reaching. It is known that current methods adopted globally tend to over-estimate the simultaneous design flow. This means that not only are systems over-sized (both pump provision and distribution pipework) but the space-take is also over-estimated; all with related energy and cost implications. Perhaps more significant though is the fact that this over-sizing can result in a degradation of water quality; in part through reduced velocity but also since this can result in temperature drift and the increased risk of Legionella (Pieterse-Quirijns et al, 2013, 2014).

The prediction of peak simultaneous demand is usually addressed within the context of either residential or non-residential settings. It will be appreciated that each has different diurnal usage patterns. In general, research in support of a prediction method for residential settings is more advanced (Jack, 2017) due in the main to the availability of more robust data on occupancy, usage patterns and fixture types. 'Non-residential' on the other hand is, by definition, more complex; often comprising multi-use units and with variable occupancy factors.

Having a good understanding of occupancy is important as this is a key factor in predicting the probability of usage of any given fixture. When discussing non-residential buildings, it can be seen that occupancy is highly dependent upon the intended use of the building. In addition, in a post-pandemic environment, we see some evidence of significant change in occupancy patterns that have been influenced by a new 'work-from-home' or hybrid work culture. While there is substantial anecdotal evidence of this shift, it remains difficult to establish definitive change across sectors.

Three questions thus arise. Firstly, does a change in occupancy, post-Covid19, mean that the overestimation of systems inherent within current design approaches is exacerbated? Secondly, is there a need to revisit the occupancy-derived probability factors supporting the development of new techniques for the prediction of peak flow? And thirdly, from a design perspective, can it be assumed that for new and retrofit projects, occupancy adjustments will be incorporated with the calculation of the number of fixtures required? To be able to answer these questions with any accuracy, a long-term study of building occupancy is required, alongside measurements of corresponding water consumption. Neither data set tends to be commonly available and/or accessible. This paper reviews the data available for a case study building for which post-Covid (daily) water consumption and occupancy figures are available.

2. Water demand estimation and occupancy

The onset of the Covid-19 pandemic in March 2020 saw unprecedented levels of lockdown and as a direct consequence, many were forced to work from home. Since this time, despite the lifting of restrictions globally, many work environments have experienced a seemingly permanent shift in employee preference, where home-working (or hybrid models) are now common [Williamson, 2020 and Manko, 2021]. In 2022, the ONS (Office of National Statistics) reported that 84% of those people who had to work from home during the peak of the pandemic, said that they preferred a future model that combined both working from home and from the office [ONS, 2022]. Additionally, this hybrid method of working was imbalanced insofar as survey respondents noted that they planned to spend most of their time at home. This view is echoed in a report for the Stanford Institute for Economic Policy Research where Bloom et al, 2020 present data from the USA that suggests that working from home will become the 'new normal' and that, as a result, some companies are considering downsizing their office space or perhaps moving to a new, smaller, building. Figure 1 presents an indication of the number of days of office working preferred by 2500 survey respondents and shows the proportion who expressed a preference to work from home and for how long.
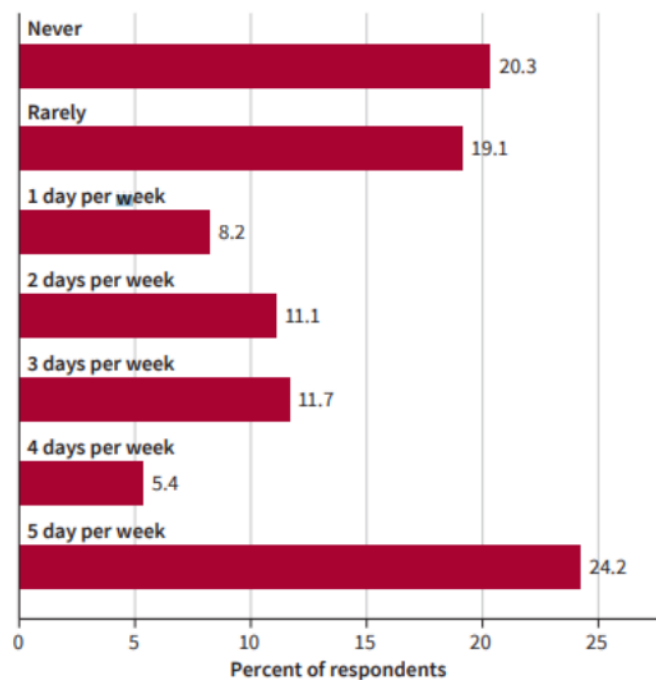

Figure 1 Percentage preference for office working [Bloom et al, 2020]

ONS data from the UK presents more recent information (for September 2022 to January 2023) and also breaks this down by age group, Figure 2 [ONS, 2022]. Overall, this data shows that during this five-month period, 16% of adults worked from home with a further 28% opting for a hybrid model that combined home and office-based working. There is,

of course, a direct correlation between this change in behaviour, building occupancy and corresponding water consumption.
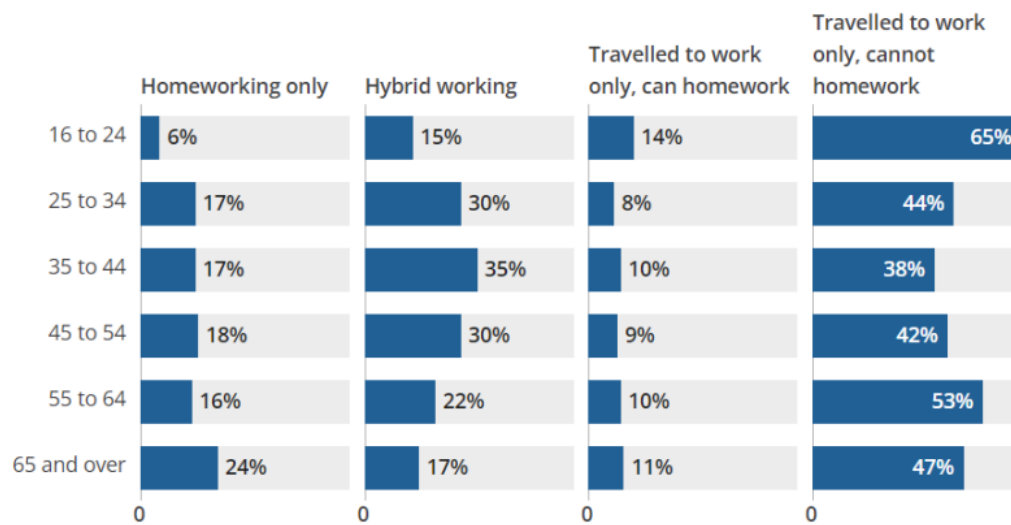

Figure 2 ONS data for working adults (UK) Sept 2022 to Jan 2023

3   Case study

The example discussed within this study is one of Heriot-Watt University's buildings for which occupancy and water consumption monitoring is ongoing. The building comprises six-storeys plus basement parking totalling just over 20,000m^2, Figure 3, and is located in Knowledge Park, Dubai, UAE. Internally, the layout combines large open-plan spaces for staff offices as well as a number of enclosed teaching spaces designed to serve almost 4000 students. Two cafés are included; one on the ground floor and one on the first floor; where consumption data for the former is recorded separately. In addition, the building includes a number of pantries/coffee bars on each level. It is also worth noting that given the nature of the programmes delivered by the University, the building requires a number of workshops; including those for structural engineering, chemical engineering and concrete technology. In addition, there are a number of fabrication workshops. Importantly, the campus building has been awarded LEED (Leadership in Energy and Environmental Design) Gold Status, part of which was supported by the use of water-efficient fixtures that resulted in a 46% reduction in use when compared to the LEED baseline.

An example of the layout of the building is shown in Figure 4. This is presented for the purposes of illustration only, to provide an indication of the type of spaces made available to occupants.

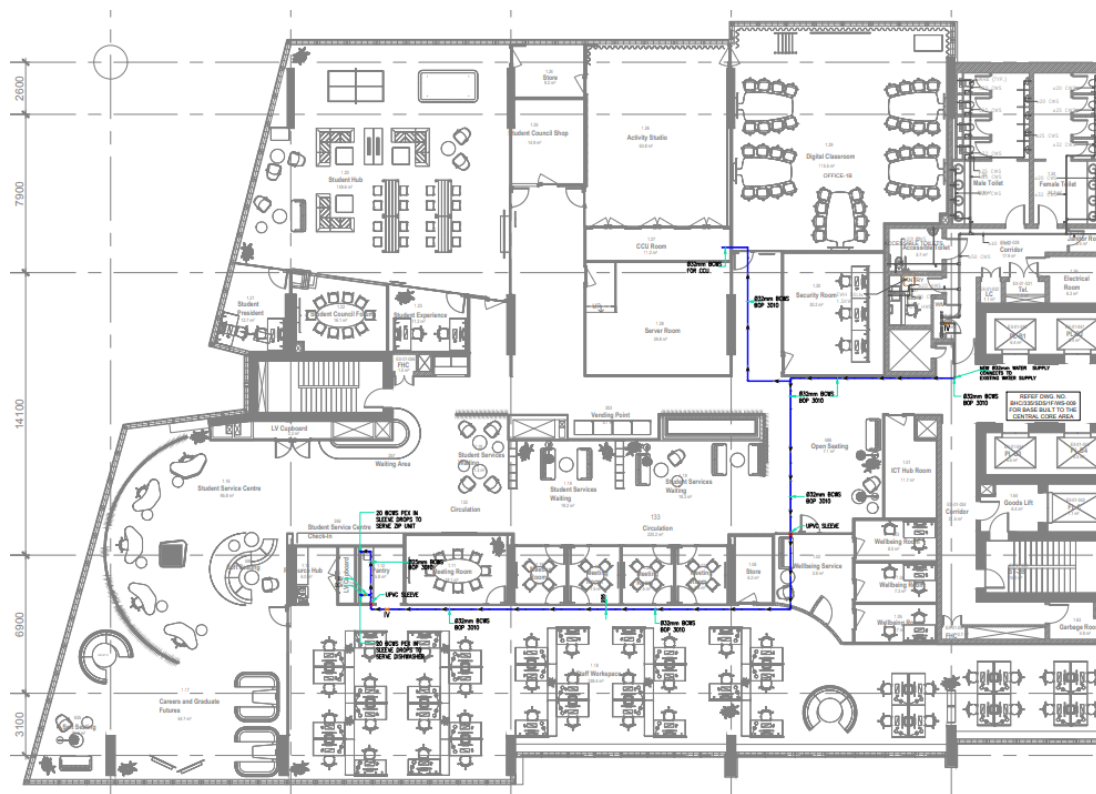**Figure 3 Heriot Watt University, Knowledge Park, Dubai, UAE**

Figure 4 Indicative layout, showing open-plan design

While the building does accommodate a number of academic staff, it can be seen that the space is also used predominantly for teaching. This means that a traditional 'workplace'

or 'office' category for space allocation cannot be used. Instead, we are guided by the fact that the building is designed to accommodate a maximum number of 4000 students.
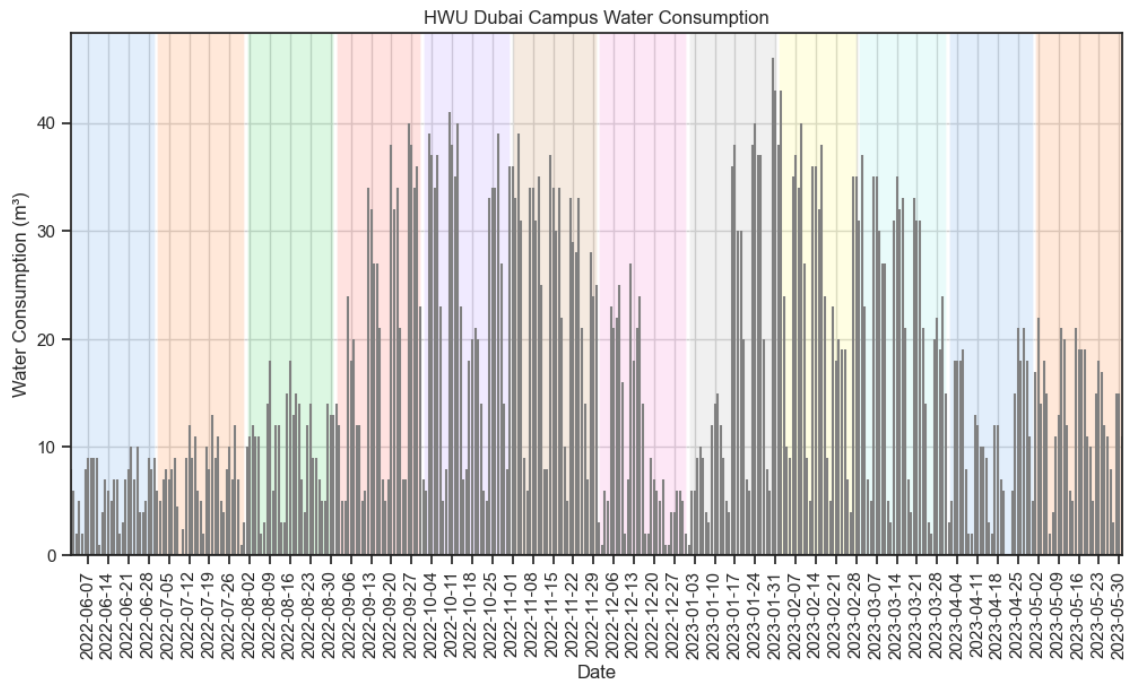

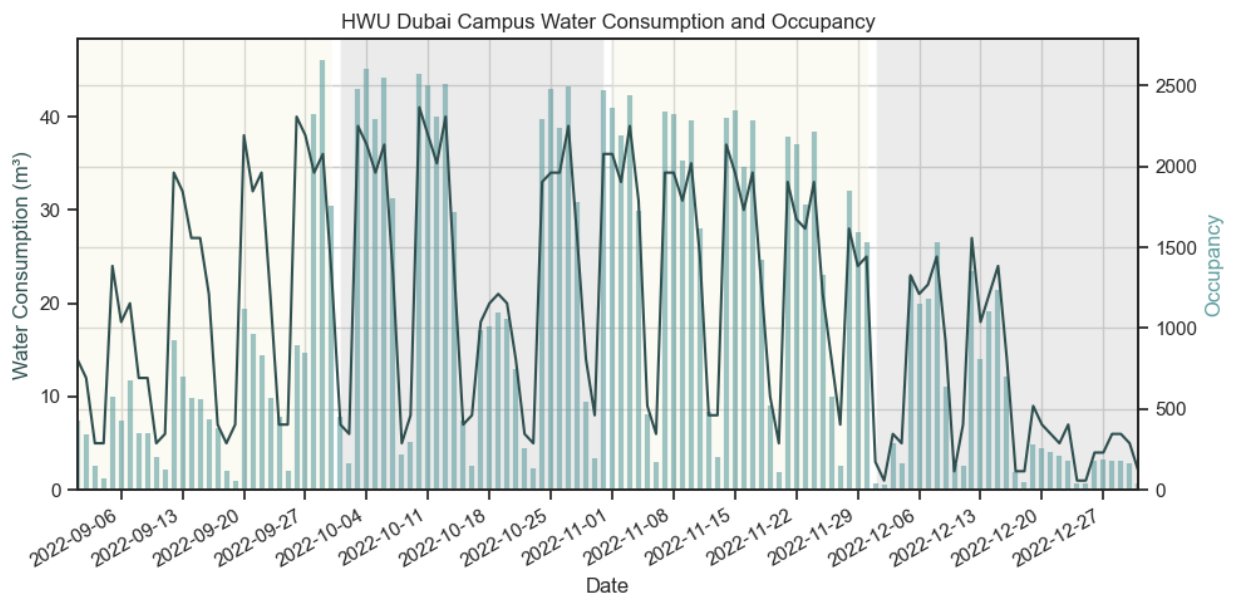**Figure 5 Water Consumption Data: May 2022-June 2023**

Figure 6 Occupancy data overlaid with water consumption data: Sept-Dec 2022

Figure 5 shows the daily water consumption profile for the campus for 12 months spanning June 2022 to May 2023. This shows clearly how the consumption increases during weekdays as opposed to weekends (when less teaching occurs), and also shows a significant uplift in consumption that can be mapped to our teaching semesters (September to December and January to April).

Occupancy data is available for a shorter period (September to December 2022) and is shown as an overlay on consumption data for the same period, Figure 6. This confirms the clear correlation between occupancy and consumption.

In accordance with the as-fitting drawings for the building, Table 1 shows the total number of fixtures per floor, while Table 2 shows the distribution across fixture type (for the whole building).

Table 1 Total number of fixtures per floor

Level	Total number of fixtures	Comments
Ground	24	*Includes engineering workshop and concrete lab*
Level 1	59	*Include main campus cafe*
Level 2	48	
Level 3	59	
Level 4	52	
Level 5	27	
Level 6	78	*Includes fabrication workshop and structures and chemical engineering laboratories*

Table 2 Number and types of appliances

Fixture Type	Count
Air Conditioning Unit	1
Bib tap	4
Centrifugal Pump	1
Coffee machine	3
Constant and falling head permeability	1
Dishwasher	1
Emergency Shower	1
Flexible cold, hot and vent sink	7
Fume cupboard	4
Gas Absorption Columns	2
Glass washer	2
Grinder	1
Heat Exchanger Service Units	2
Ice cuber	2
Ice flaker	1
Integrated Dishwasher	6
Mop sink	2
Separate cold and hot taps sink	3
Shower (mixer)	5
Sink	22
Urinal	55
Washbasin	104
Water filter	1
WC	102
Working Table Sink	6
Zip Unit (Zip hydro tap)	8

4   Design flow rate estimation

Despite its limitations, the most commonly used method, globally, for estimating design flow remains the application of Loading Units to fixtures. While the specifics of this method as adopted in different countries can vary, the underlying principle is the same.

As can be seen from Table 2, not all of the fixtures used in this case study building fall within the categorisation typically presented in commonly-adopted standards. This means that in some cases, this required the allocation of information that is specific to the fixture and its corresponding flowrate. Furthermore, the loading unit allocation for some non-

sanitary fixtures, for example, the gas absorption columns and the heat exchanger service units, was set to zero.

The simultaneous design flow for the building and appliances outlined above was estimated using British Standard BS8558 (2015). This standard covers non-residential buildings (where residential design flow can be estimated using BS806-3, 2006). This gave a resultant flow of 5.877 l/s.

The limitations of this Loading Unit method are clear, and this has prompted much work, globally, to yield improved predictions. Examples include the work by Blokker (2010), Murakawa et al (2021), and Omaghomi and Buchberger (2014). It is hence important to recognise the significant progress that has been made in the development of alternative techniques. However few, if any, of these methods have been able to directly inform design codes; with the exception of work developed by Blokker (2010). This means that outside the Netherlands, a more standard approach to the deployment of the Loading Unit Method remains common.

5   Discussion

We know from established literature that post-covid occupancy in office spaces is not only likely to see a marked decline but is also likely to introduce variability in occupancy profile throughout the working week. We know too that this will have a direct impact on the probability of use of fixtures in any given building and as a result, will introduce a reduction in peak simultaneous demand. In addition, it is important to bear in mind that, as is the case here, a building may also incorporate low flow fixtures, further stressing the need for an accurate prediction method.

Furthermore, it may seem that a change in occupancy might be the only lasting consequence of the pandemic. However, others may exist. For example, it is possible that handwashing has increased, as building occupants become more conscious of hygiene factors and the possibility of virus transition. Evidence of this is difficult to establish however, and is clearly more strongly linked to those times when many restrictions were in place. For example, Ahmed, K.O. et al. (2021) investigated how water consumption changed before and during the pandemic. They established that handwashing increased by 85.34%, and the duration that people spent washing their hands more than doubled. Understandably, there are a range of similar types of studies that apply within clinical and medical settings but that for the purposes of this review have not been assumed as indicative of change within a more traditional non-residential setting. There are, however, some studies that do indicate a broader uplift in water consumption post-pandemic [Sivakumar 2020 and Cooley, 2020].

While the literature presented herein may give an indication of the likely changes, it is not sufficiently definitive to establish a robust assessment of change in water usage. We know too that measuring occupancy can be exceptionally challenging. Techniques exist, usually counting devices installed at building entrances, but data is often unreliable and lacks the information needed to understand the implications for water use. It is, of course, possible to moderate the calculation of design flow to represent a lower building

occupancy. This can be done in the UK through reference to BS6465 (2009) whereby the number of fixtures required can be moderated. However, this only applies to new build or some refurbishment projects. It does not apply to existing buildings where the occupancy, especially that post-Covid, has changed in response to alternative (hybrid) working models. While a reduction in occupancy will understandably reduce the overall consumption of water (generally a good thing), it is clear that it also exacerbates the extent of 'oversizing'; an aspect that is known to be inherent within most sizing methods based on the application of Loading Units, or that rely on probability factors representative of higher occupancy and/or demand. Ideally, there would be a direct connection able to be made between building occupancy and the calculation of design flow. There would also be a robust method of design flow estimation, the data for which is populated readily by building information. Methods of predicting design flow are, however, still evolving.

This discussion presents an opportunity to develop data-driven methods and apply machine learning techniques to peak water demand estimation. The use of machine learning and neural networks has the potential to model a range of factors and variables with non-linear and complex relationships (in this case the building occupancy, water usage behaviour, and fixture usage probability) that cannot be easily modelled through equations. Occupancy estimation modelled through machine learning algorithms and neural networks has been widely researched in areas such as building energy and HVAC control (Zhao et al., 2022), and this can also be applied to building water demand analyses.

Data-driven methods offer more flexibility in terms of application to different contexts (building size, location, purpose of use) if there is sufficient data to make a generalised model. In addition, a data-driven model should be flexible enough to adapt not just to changing occupancy levels and occupant behaviour, but also to improved-efficiency fixtures.

6   References

Ahmed, K.O. Aziz, S.O. Hawez, D.M. Sabir, Z.L. (2021) 'Impact of COVID-19 Pandemic on Hand Washing Process and Water Consumption', Eurasion Journal of Science & Engineering, 7(1), pp. 228- 245.

Blokker, E. J. M. (2010) Stochastic water demand modelling for a better understanding of hydraulics in water distribution networks. Water Management Academic Press. doi: 10.1017/CBO9781107415324.004.

Bloom, N (2020) 'How working from home works out', Stanford Institute for Economic Policy Research (SIEPR).

BS 6465-1:2006+A1 (2009) Sanitary installations-Part 1: Code of practice for the design of sanitary facilities and scales of provision of sanitary and associated appliances. BSI 2009.

BS 8558 (2015) Guide to the design, installation, testing and maintenance of services supplying water for domestic use within buildings and their curtilages - Complementary guidance to BS EN 806. London: BSI 2015.

BS EN 806-3 (2006) Specification for installations inside buildings conveying water for human consumption — Pipe sizing- Simplified method. London: BSI 2006.
Cooley, H. et al. (2020) 'Water and the COVID-19 Pandemic – Impacts on Municipal Water Demand', Pacific Institute. Available at: Water and the COVID-19 Pandemic: Impacts on Municipal Water Demand - Pacific Institute (pacinst.org)

Jack, L. B. (2017) An Assessment of the Validity of the Loading Units Method for the Sizing of Domestic Hot and Cold Water Services. CIBSE

Kelly, D. A. (2015) 'Labelling and water conservation : A European perspective on a global challenge', Building Services Engineering Research & Technology, 36(6), pp. 643–657. doi: 10.1177/0143624415571758.

Manko, B. (2021). 'Considerations in the use of Work-From-Home (WFH) for Post-Pandemic Planning and Management' Management, 25(1), pp.118-140. DOI: 10.2478/manment-2019-0062.

Murakawa S., Ikeda D, Sakamoto K, Takata H, Verification on the dynamic calculation method for cold and hot water supply loads, and a simple calculation method for the instantaneous maximum flow rates. CIBW062 Water Supply and Drainage Symposium 2021.

Office for National Statistics (2022) 'Is hybrid working here to stay?' Available at: Is hybrid working here to stay? - Office for National Statistics (ons.gov.uk)

Omaghomi, T. and Buchberger, S. (2014) 'Estimating water demands in buildings', Procedia Engineering, 89, pp. 1013–1022. doi: 10.1016/j.proeng.2014.11.219.

Pieterse-Quirijns, E. J., Blokker, E. J. M., Van Der Blom, E. and Vreeburg, J. H. G. (2013) 'Non-residential water demand model validated with extensive measurements and surveys', Drinking Water Engineering and Science, 6(2), pp. 99–114. doi: 10.5194/dwes-6-99-2013.

Pieterse-Quirijns, E. J. et al. (2014) 'Validation of non-residential cold and hot water demand model assumptions', Procedia Engineering. Elsevier B.V., 70, pp. 1334–1343. doi: 10.1016/j.proeng.2014.02.147.

Sivakumar, B. (2020) 'COVID-19 and water' Stochastic Environmental Research and Risk Assessment, 35, pp. 531-534.

Williamson, S. Colley, L. Hanna-Osborne, S. (2020). 'Will working from home become the 'new normal' in the public sector?', Australian Journal of Public Administration, 79(4), pp. 601-607.

Zhao, L. et al. (2022) 'A State of Art Review on Methodologies of Occupancy Estimating in Buildings from 2011 to 2021', Electronics, 11(19). Available at: https://doi.org/10.3390/electronics11193173.

7   Presentation of Authors

Professor Lynne Jack is Director of the Institute of Sustainable
Built Environment at Heriot-Watt University's Malaysia
campus. Her research focuses on predicting simultaneous design
flow for water distribution networks and on the integration of
water efficient concepts within buildings. Lynne is Chair of the
CIBW062 Scientific Committee (for Water Supply and Drainage
for Buildings) and was also President of the Chartered Institution
of Buildings Services Engineers from 2019-2020; the
Institution's first female President.

Ms Sheena Fernandez is a postgraduate research student in the
Institute of Sustainable Built Environment at Heriot-Watt
University, Edinburgh. She holds an Erasmus Mundus Joint
Masters degree in Smart Cities and Communities awarded in
2022. Her research work is currently focused on developing data-
driven methods for estimating peak water demand in buildings.

Professor Sarat Dass is based in the School of Mathematical and
Computer Sciences (MACS) at Heriot-Watt University's
Malaysia campus. His research expertise is in areas of Bayesian
dynamical system modelling, inference and prediction, as well as
in data science and machine learning. A major component of his
research deals with collaborations with researchers from various
subject matter fields in developing Bayesian methods for these
application areas.

Ms Catherine (Kitty) Rogers is an undergraduate student studying
Architectural Engineering within the Institute of Sustainable Built
Environment at Heriot Watt University.